

ARO Report 79 - 2

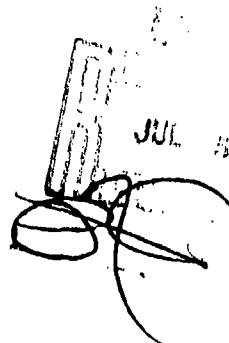
(2)

LEVEL

**PROCEEDINGS OF THE TWENTY-FOURTH
CONFERENCE ON THE DESIGN OF
EXPERIMENTS IN ARMY RESEARCH
DEVELOPMENT AND TESTING**

1473

DA 070840



Approved for public release; distribution unlimited.
The findings in this report are not to be construed
as an official Department of the Army position, un-
less so designated by other authorized documents.

DDC FILE COPY

Sponsored by
The Army Mathematics Steering Committee
on Behalf of

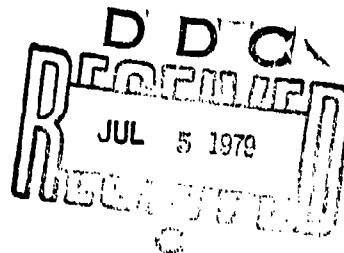
THE CHIEF OF RESEARCH, DEVELOPMENT AND ACQUISITION

U. S. Army Research Office

Report No. 79-2

June 1979

PROCEEDINGS OF THE TWENTY-FOURTH CONFERENCE
ON THE DESIGN OF EXPERIMENTS



Sponsored by the Army Mathematics Steering Committee

HOST

Mathematics Research Center
University of Wisconsin
Madison, Wisconsin

4-6 October 1978

Approved for public release; distribution unlimited.
The findings in this report are not to be construed
as an official Department of the Army position, un-
less so designated by other authorized documents.

U. S. Army Research Office
P. O. Box 12211
Research Triangle Park, North Carolina

FOREWORD

Over the years, scientists have developed many techniques for extracting and evaluating information from experimental data. One of the reasons for holding the design conferences is to develop, in Army scientists, an appreciation for and the necessary skills to handle these techniques. A special feature associated with the meeting this year was organized to help develop some of these skills. This was a basic tutorial seminar entitled, "Introduction to the Fundamentals of Experimental Design" given on 2-3 October 1978 by Dr. George E. P. Box, the Ronald Alymer Fisher Professor of Statistics at the University of Wisconsin and the Mathematics Research Center. This course was designed for engineers and other scientists with little or no formal training in statistics, and who are involved in generating physical measurements from experiments. It presented basic notions and statistical techniques which allows one to minimize data variance or variability, and hence ultimately enhances the opportunities for recovering data information in later analyses. The forty or so Army scientists attending this course were prepared to comprehend the papers given at the Twenty-fourth Conference on the Design of Experiments in Army Research, Development and Testing.

Members of the Program Committee for this conference were pleased to obtain the services of the following invited speakers to talk on topics of current interest to Army personnel.

<u>Speaker and Institute</u>	<u>Title of Address</u>
Professor Norman Draper University of Wisconsin-Madison	RIDGE REGRESSION
Professor Ralph Bradley Florida State University	STATISTICAL ANALYSIS OF WEATHER MODIFICATION EXPERIMENTS
Professor Grace Wahba University of Wisconsin-Madison	DESIGN PROBLEMS IN RECOVERING FUNCTIONS OF TWO OR SEVERAL VARIABLES

Professor Brian L. Joiner
University of Wisconsin-Madison

STATISTICAL CONSULTING

Professor Richard E. Barlow with
Bernard Davis
University of California-Berkeley

RECENT ADVANCES IN GRAPHICAL
TECHNIQUES FOR ANALYZING FAILURE
DATA

In addition to the invited addresses, there were nineteen contributed papers. Many of these informative talks covered areas associated with the theme of the conference, namely "Statistical Design and Analysis of Experiments." Titles of the technical sessions were: "Time Series and Stochastic Modeling"; "Analysis of Variance Models"; "Statistical Theory"; "Statistical Inference"; "Special Applications"; and "Material Reliability".

An important feature of these annual conferences is the awarding of the Samuel S. Wilks Memorial Medal. The 1978 award went to the distinguished scientist Dr. William H. Kruskal, Professor of Statistics at the University of Chicago. His contributions to the field of statistics have been truly outstanding.

The Army Mathematics Steering Committee (AMSC), an intra-Army committee, sponsors the design conferences on behalf of the Chief of Research, Development and Acquisition. Members of this committee appreciated the fact that the Mathematics Research Center (MRC) was willing to serve as host for the Twenty-Fourth Conference on the Design of Experiments. They would like to thank Professor Bernard Harris for serving as Chairman on Local Arrangements. He was ably assisted in this capacity by Mrs. Gladys G. Moran. Those in attendance appreciated the assistance these and other members of MRC gave them with the many problems that arose during the course of this meeting.

The AMSC has requested that these Proceedings be published and distributed Army-wide in order that the information contained therein will assist scientists with some of their statistical problems. Finally, committee

members would like to thank the Program Committee for all the work it did in putting together another successful scientific conference.

Program Committee

Gerald Andersen
Carl Bates
Larry Crow
Francis Dressel
Walter Foster

Bernard Harris
Clifford Maloney
Douglas Tang
Malcolm Taylor
Michael White

Frank Grubbs (Program Committee Chairman)
Robert Launer (Conference Secretary)
Herbert Solomon (Chairman of the Conference)

Accession For	
NTIS GRA&I	<input checked="" type="checkbox"/>
DDC TAB	<input type="checkbox"/>
Unannounced	<input type="checkbox"/>
Justification _____	
By _____	
Distribution _____	
Availability Codes	
Not	Airland/or Special
A	

TABLE OF CONTENTS

TITLE	PAGE
Foreword	iii
Table of Contents	vii
Agenda	ix
STATISTICAL ANALYSIS OF A WEATHER MODIFICATION EXPERIMENT	
Ralph A. Bradley	1
CANDIDATE SEQUENTIAL DESIGNS FOR OPTIMUM SEEKING	
Carl B. Bates	19
ENVIRONMENTAL AND WATER QUALITY OPERATIONAL STUDIES: EXPERIMENTAL DESIGN PROBLEMS ASSOCIATED WITH THE FISHERIES OF THE MISSISSIPPI RIVER	
Michael P. Farrell and A. Dale Magoun	43
RED NOISE IN THE POWER SPECTRUM OF ATMOSPHERIC TEMPERATURE DATA	
Oskar M. Essenwanger	51
SMALL SAMPLE BEHAVIOR OF SOME PROCEDURES USED IN TIME SERIES MODEL BUILDING AND FORECASTING	
Paul Newbold and Craig F. Ansley	63
STATISTICAL PROBLEMS ASSOCIATED WITH THE HORIZONTAL CHANNEL OF THE RAPID GEODETIC SURVEY SYSTEM (RGSS)	
H. Baussus von Luetzow.	81
ANALYSIS OF VARIANCE ON THE TRADE-OFF FUNCTION RELATING ACCURACY TO SPEED OF REACTION	
Walter D. Foster, John H. Wolcott and Terrence L. Kay	99
THE ANALYSIS OF PARTIALLY FACTORIAL EXPERIMENTS	
J. Robert Burge	107
STATISTICAL ANALYSIS OF EXPERIMENTS IN SORPTIVITY	
Richard N. Macnair and Edward W. Ross, Jr.	121
ON COMBINING PSEUDO-RANDOM NUMBER GENERATORS	
Mark Brown and Herbert Solomon	133
SIMPLIFIED POINT AND INTERVAL ESTIMATION FOR REMOVAL APPING	
Andrew P. Soms	143
REGRESSION FOR MARKOV BERNoulli RANDOM VARIABLES	
Edmond H. Inselmann	161

HOW TO SMOOTH CURVES AND SURFACES WITH SPLINES AND CROSS-VALIDATION Grace Wahba	167
METHODOLOGY FOR ACCEPTANCE CRITERIA FOR TARGET DISPERSION CHARACTERISTICS OF THE ARMOR PIERCING DISCARDING SABOT (APDS) ROUNDS Frank C. Hopkins	193
SEQUENTIAL ESTIMATION OF QUANTAL RESPONSE CURVES R. Srinivasan and R. M. Wharton	229
A MONTE CARLO SIMULATION OF A PROBABILITY RATIO SEQUENTIAL TEST (PRST) PLAN FROM MILITARY STANDARD 781C William J. Broemm	241
STATISTICAL CONSULTING OR THERE ARE NO STANDARD PROBLEMS, ONLY STANDARD SOLUTIONS Brian L. Joiner	261
LASER BEAM WAR GAMES: DESIGN, ANALYSIS AND MODELING CONSIDERATIONS W. S. Mallios, R. D. Batesole and D. R. Leal	287
DETERMINATION OF STRUCTURAL RELIABILITY USING A FLAW SIMULATION SCHEME Donald M. Neal and Donald S. Mason	311
PREDICTED MECHANICAL BEHAVIOR OF MATERIALS WHEN SUBJECTED TO WEAPON SETBACK FORCES Richard S. Simak	337
SUCCESSFUL APPLICATION OF STEWARTSON'S LIQUID INSTABILITY/STABILITY CRITERIA TO THE DESIGN OF ARTILLERY PROJECTILES John M. Ferriter	347
TOTAL TIME ON TEST PLOTS Richard E. Barlow and Bernard Davis	361
PITMAN-CLOSENESS EFFICIENCY OF ESTIMATORS OF RELIABILITY WITH APPLICATION TO THE EXPONENTIAL FAILURE MODEL Danny Dyer and Jerome P. Keating	381
LIST OF ATTENDEES.	411

AGENDA

THE TWENTY-FOURTH CONFERENCE ON THE DESIGN OF EXPERIMENTS IN
ARMY RESEARCH, DEVELOPMENT AND TESTING

4-6 October 1978

Host: The Mathematics Research Center

Held at: The Wisconsin Center, Lake and
London Streets, Madison, Wisconsin

***** Wednesday, 4 October *****

0815-0915 REGISTRATION -- First floor, The Wisconsin Center

0915-1030 GENERAL SESSION I -- Auditorium

CALLING OF THE CONFERENCE TO ORDER

Dr. Bernard Harris, Chairman of Local Arrangments,
Mathematics Research Center

WELCOMING REMARKS

Dr. Ben Noble, Director, Mathematics Research Center

CHAIRMAN OF SESSION I

Dr. Frank E. Grubbs, Program Committee Chairman, Aberdeen
Proving Ground, Maryland

RIDGE REGRESSION

Professor Norman Draper, Department of Statistics,
University of Wisconsin-Madison

1030-1100 BREAK

1100-1200 GENERAL SESSION I (continued)

SOME APPROACHES TO STATISTICAL ANALYSIS OF WEATHER
MODIFICATION EXPERIMENTS

Professors Ralph Bradley, Sushil S. Srivastava and
Adolph Lanzdorf, The Florida State University,
Tallahassee, Florida

1200-1330 LUNCH

1330-1500 CLINICAL SESSION A -- Room 210

CHAIRMAN

Dr. Douglas B. Tang, Walter Reed Army Institute of Research, Washington, DC

PANELISTS

Professor Ralph Bradley, The Florida State University, Tallahassee, Florida

Dr. Mark Brown, Memorial Sloan-Kettering Cancer Center, New York, New York

Professor Norman Draper, University of Wisconsin, Madison, Wisconsin

CANDIDATE SEQUENTIAL DESIGNS FOR OPTIMUM SEEKING

Mr. Carl B. Bates, US Army Concepts Analysis Agency, Bethesda, Maryland

ENVIRONMENTAL AND WATER QUALITY OPERATIONAL STUDIES

Drs. A. Dale Magoun and Michael P. Farrell, US Army Waterways Experiment Station, Vicksburg, Mississippi

1500-1530 BREAK

1530-1700 TECHNICAL SESSION I -- Room 210 -- TIME SERIES AND STOCHASTIC MODELING

CHAIRMAN

Dr. Edward Wegman, Office of Naval Research, Washington, DC

RED NOISE IN THE POWER SPECTRUM OF ATMOSPHERIC TEMPERATURE DATA

Dr. O. M. Essenwanger, US Army Missile Research and Development Command, Redstone Arsenal, Alabama

SMALL SAMPLE BEHAVIOR OF SOME PROCEDURES USED IN TIME SERIES MODEL BUILDING AND FORECASTING

Drs. Paul Newbold, Mathematics Research Center, University of Wisconsin-Madison, and C. F. Ansley, University of Chicago

STATISTICAL PROBLEMS ASSOCIATED WITH THE HORIZONTAL CHANNEL
OF THE RAPID GRAVITY SURVEY SYSTEM (RGSS)

Dr. H. Baussus von Luetzow, US Army Engineer Topographic
Laboratories, Ft. Belvoir, Virginia

1530-1700 TECHNICAL SESSION II -- Room 313 -- ANALYSIS OF VARIANCE MODELS

CHAIRMAN

Ms. Jill House, Ballistic Research Laboratory, Aberdeen
Proving Ground, Maryland

ANALYSIS OF VARIANCE ON THE TRADE-OFF FUNCTION RELATING
ACCURACY TO SPEED OF REACTION

Drs. Walter D. Foster, John H. Wolcott and Terrence L. Kay,
Armed Forces Institute of Pathology, Washington, DC

THE ANALYSIS OF PARTIALLY FACTORIAL EXPERIMENTS

Dr. John Robert Burge, Walter Reed Army Institute of Research,
Washington, DC

STATISTICAL ANALYSIS OF EXPERIMENTS IN SORPTIVITY

Dr. Edward W. Ross, US Army Natick Research and Development
Command, Natick, Massachusetts

1830 SOCIAL HOUR AND BANQUET

***** Thursday, 5 October *****

0900-1030 CLINICAL SESSION B -- Room 210

CHAIRMAN

Dr. O. M. Essenwanger, US Army Missile Research and
Development Command, Redstone Arsenal, Alabama

PANELISTS

Dr. Bernard Harris, Mathematics Research Center

Professor Brian L. Joiner, University of Wisconsin-Madison

Professor Grace Wahba, University of Wisconsin-Madison

ANALYSIS OF CENSORED REPAIRABLE SYSTEMS FAILURE DATA

Mr. Harold E. Ascher, Naval Research Laboratory,
Washington, DC

FRICITION OF RUBBER ON SNOW AND ICE

Mr. L. David Minsk, US Army Cold Regions Research and
Engineering Laboratory, Hanover, New Hampshire

0900-1030

TECHNICAL SESSION III -- Room 313 -- STATISTICAL THEORY

CHAIRMAN

Mr. Eugene Coppola, Watervliet Arsenal, Watervliet,
New York

ON COMBINING PSUEDO-RANDOM NUMBER GENERATORS

Dr. Mark Brown, Memorial Sloan-Kettering Cancer Center,
New York, New York and Dr. Herbert Solomon, Stanford
University, Stanford, California

SIMPLIFIED POINT AND INTERVAL ESTIMATION FOR REMOVAL TRAPPING

Dr. Andrew P. Soms, Mathematics Research Center, University
of Wisconsin-Madison

REGRESSION OF MARKOV DATA

Dr. Edmund H. Inselmann, US Army Combined Arms Combat
Developments Activity, Ft. Leavenworth, Kansas

1030-1100

BREAK

1100-1200

GENERAL SESSION II -- Auditorium

CHAIRMAN OF SESSION II

Dr. Bernard Harris, Mathematics Research Center,
University of Wisconsin-Madison

DESIGN PROBLEMS IN RECOVERING FUNCTIONS OF TWO OR
SEVERAL VARIABLES

Professor Grace Wahba, Department of Statistics, University
of Wisconsin-Madison

1200-1330

LUNCH

1330-1500

CLINICAL SESSION C -- Room 210

CHAIRMAN

Mr. Carl B. Bates, US Army Concepts Analysis Agency,
Bethesda, Maryland

PANELISTS

Dr. Frank E. Grubbs, Aberdeen Proving Ground, Maryland

Dr. Paul Newbold, Mathematics Research Center, University
of Wisconsin-Madison

Dr. Andrew P. Soms, Mathematics Research Center, University
of Wisconsin-Madison

**PROBLEMS OF GENERATING PREDICTION EQUATIONS BY MULTIVARIATE
ANALYSIS OF DATA DERIVED FROM COMPLEX SIMULATIONS**

Mr. Tom Kitchell, US Army Concepts Analysis Agency,
Bethesda, Maryland

1330-1500

TECHNICAL SESSION IV -- Room 313 -- STATISTICAL INFERENCE

CHAIRMAN

Mr. Lang Withers, US Army Operational Test and Evaluation
Agency, Falls Church, Virginia

**METHODOLOGY FOR ACCEPTANCE CRITERIA FOR TARGET DISPERSION
CHARACTERISTICS OF THE ARMOR PIERCING DISCARDING SABOT
(APDS) ROUNDS**

Mr. Frank Craig Hopkins, US Army Materiel Systems Analysis
Agency, Aberdeen Proving Ground, Maryland

**AN APPROACH TO THE SEQUENTIAL ESTIMATION OF QUANTAL
RESPONSE CURVES**

Professor R. Srinivasan, Temple University, Philadelphia,
Pennsylvania and Professor R. M. Wharton, Trenton State
College, Trenton, New Jersey

**A MONTE CARLO SIMULATION OF A PROBABILITY RATIO SEQUENTIAL
TEST (PRST) PLAN FROM MILITARY STANDARD 781C**

Mr. William Broemm, US Army Materiel Systems Analysis
Activity, Aberdeen Proving Ground, Maryland

1500-1530

BREAK

1530-1630

GENERAL SESSION II (continued)

STATISTICAL CONSULTING

Professor Brian L. Joiner, Department of Statistics,
University of Wisconsin-Madison

***** Friday, 6 October *****

0900-1030

TECHNICAL SESSION V -- Room 210 -- SPECIAL APPLICATIONS

CHAIRMAN

Dr. Edward Ross, US Army Natick Research and Development
Command, Natick, Massachusetts

LASER BEAM WAR GAMES: DESIGN AND ANALYSIS CONSIDERATIONS

Mr. William S. Mallios, BDM Corporation, Ft. Ord,
California

STAR SIGNATURE MODELS

Dr. John W. Bond, US Army MERADCOM, Ft. Belvoir, Virginia

0900-1030

TECHNICAL SESSION VI -- Room 313 -- MATERIAL RELIABILITY

CHAIRMAN

Mr. William S. Agee, White Sands Missile Range, New Mexico

DETERMINATION OF STRUCTURAL RELIABILITY USING A FLAW
SIMULATION SCHEME

Drs. Joseph I. Bluhm, Donald M. Neal, and Donald S. Mason,
US Army Materials & Mechanics Research Center, Watertown,
Massachusetts

PREDICTED MECHANICAL BEHAVIOR OF MATERIALS WHEN SUBJECTTED
TO SETBACK FORCES

Dr. Richard S. Simak, Chemical Systems Laboratory, Aberdeen
Proving Ground, Maryland

SUCCESSFUL APPLICATION OF STEWARTSON'S LIQUID INSTABILITY-
STABILITY CRITERIA TO THE DESIGN OF MUNITIONS

Dr. John M. Ferriter, Chemical Systems Laboratory, Aberdeen
Proving Ground, Maryland

1030-1100 BREAK

1100-1130 GENERAL SESSION III -- Auditorium

 CHAIRMAN OF GENERAL SESSION III

 Dr. Frank Grubbs, Aberdeen Proving Ground, Maryland

 OPEN MEETING OF THE AMSC SUBCOMMITTEE ON PROBABILITY
 AND STATISTICS

 Dr. Douglas B. Tang, Department of Biostatistics and
 Applied Mathematics, Division of Biometrics and Medical
 Information Processing, Walter Reed Army Institute of
 Research, Washington, DC

1130-1230 RECENT ADVANCES IN GRAPHICAL TECHNIQUES FOR ANALYZING
 FAILURE DATA

 Professor Richard E. Barlow and Bernard Davis, Operations
 Research Center, University of California-Berkeley,
 Berkeley, California (Address to be presented by Bernard
 Davis)

1230- ADJOURN

STATISTICAL ANALYSES OF A WEATHER
MODIFICATION EXPERIMENT*

Ralph A. Bradley

Department of Statistics
Florida State University
Tallahassee, Florida

I. INTRODUCTION AND SUMMARY

This article is a summary of a manuscript [4] prepared for inclusion in a special issue on weather modification of the referenced journal. The subject area is one of national importance as emphasized in the recent reports [12,13] of the Weather Modification Advisory Board.

Phase I of the Santa Barbara Convective Seeding Test Program was conducted by North American Weather Consultants (NAWC) in the Santa Barbara area of California from 1967 through 1971. Details of this research were reported in [5,9], with the first report using augmented raingage data. Initial data analysis was reported by NAWC and additional exploratory analyses are summarized here, in [2,4], and in technical reports [1,3,10], the second giving additional detail. We are indebted to NAWC for their courtesy

*A summary of research supported by the U.S. Office of Naval Research under Contract No. N00014-76-C-0394. Reproduction in whole or in part is permitted for any purpose of the United States Government.

in providing data tapes to us. The Phase I experimentation was followed by Phase II research with some experimental design changes. Only Phase I data are considered here.

The exploratory statistical analyses reported are parametric and intended to lead to insights that may be checked with Phase II data. There are problems of validity of parametric assumptions and issues of experimental design, multiplicity of analyses, and possible need for randomization analyses raised in [12].

We review the Phase I Santa Barbara experiment and data available. An experimental unit is a single "seedable" convective band occurring in a winter storm that may have one or more such convective bands. The choice of experimental unit has the advantage of increasing the number of available experimental units in a season and the possible disadvantages of serial correlation and persistence of seeding effects from unit to unit. Raingage data are available for both a Target and a Control Area; concomitant cloud physics data were recorded and, after summarization by Gleeson [10], used in trial covariance analyses.

The problem of data summarization is addressed first. It is found that use of response-surface methods is not advantageous. Use of concomitant variables for the reduction of experimental errors in analyses reduces also the apparent effect of cloud seeding. When storm effects are included as components of a parametric model, they are found to be totally or partially confounded with seeding and again the apparent effect of seeding is reduced. Some brief comments are included on some multivariate analyses. The effect of our analyses is to leave some doubt as to the efficacy of cloud seeding in the Phase I Santa Barbara experiment.

II. The Phase I Santa Barbara Experiment

The geographical setting of the Phase I Santa Barbara Experiment is shown in Figure 1. Control and Target or Test Areas were designated; rainfall was measured through series of raingages, some of which are shown in the figure. While the objective of the experiment was not precisely defined, it can best be described as an

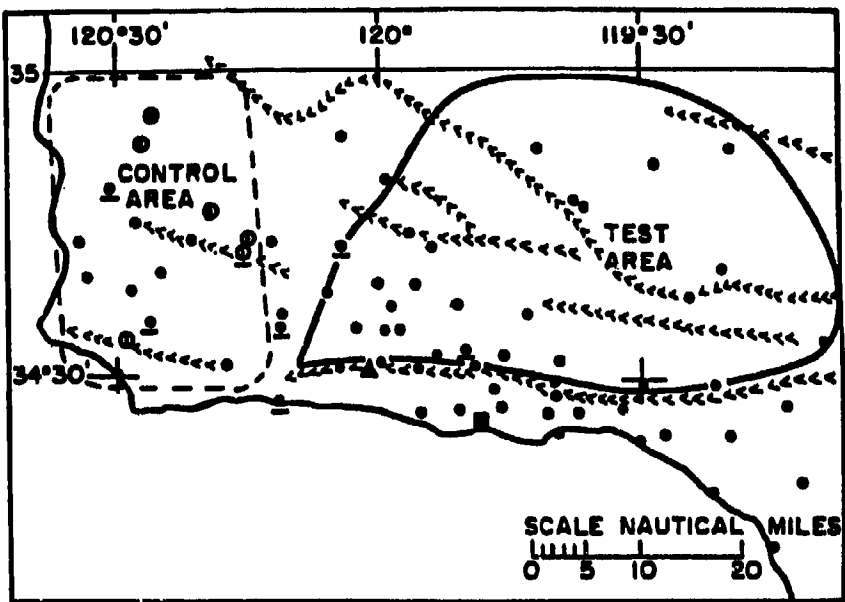


FIG. 1. Santa Barbara Pyrotechnic Seeding and Control Test Areas.
 Source: Figure 2, Elliott, St. Amand, and Thompson [7]. Rain-gage sites are designated by solid or open circles, telemetered gages underlined. The seeding and radar site is indicated by a solid triangle and Santa Barbara Airport by a solid square.

investigation of whether cloud seeding can enhance precipitation within a rather large target area.

The experimental unit was a suitable convective band in a winter storm that might contain one or more such bands in a sequence. The seeding decision was randomized effectively and care was taken that the decision was not known to the meteorological analyst determining raingage band passage times and precipitations. Criteria for determination of seedable convective bands were specified but some operational difficulties were encountered.

Band precipitation data were obtained from all raingages in control and target areas operational for a band. Air-mass characteristics of each band were determined from radiosonde observations at Santa Barbara Airport, occasionally replaced by Vandenberg Air Force Base observations. Gleeson [10] defined and summarized data for each band on the following variables: X_1 - Mixing Ratio, X_2 - 700mb Wind Speed, X_3 - 700mb Wind Direction, X_4 - Mean Wind Speed, X_5 - Direction Avg. Vector Wind, X_6 - 500mb Temperature, X_7 - Stability Class, X_8 - Showalter Index, X_9 - Stability Wind Speed, X_{10} - Direction Stability Wind, X_{11} - Instability Transport, X_{12} - Band Passage Time (Seeding Site). The data array for the Phase I experimentation may be viewed as a data matrix with N rows or bands, the first N_1 rows for unseeded bands and the second N_2 rows for seeded bands, $N = 107$, $N_1 = 51$, $N_2 = 56$, and with columns containing precipitation responses at individual raingages, possibly grouped by locations, and values of the concomitant variables, X_1 to X_{12} . The data are not without problems. Raingage precipitation responses are correlated, data are missing for many raingages, rows may not be independent observation vectors, and there may be a persistence effect of seeding.

The main NAWC approach to data analysis was on a raingage station-by-station basis. Single and double ratio indices of precipitation were calculated and contour plots based on these

ratios over control and target areas were given in various reports. Let y_{ia} denote precipitation at station i for band a , $a = 1, \dots, N$. Let $\gamma_a(i) = 1$ or 0 as station i was or was not operable for band a and let $\delta_a(i) = 1$ or 0 as band a was or was not seeded. Then $\sum_a \gamma_a(i) = N(i)$ and $\sum_a \delta_a(i) \gamma_a(i) = N_s(i)$, respectively the number of observations and the number of seeded bands recorded at station i . The number of unseeded bands at station i is $N_{ns}(i) = N(i) - N_s(i)$. Then

$$\bar{T}_s(i) = \sum_a \delta_a(i) \gamma_a(i) y_{ia} / N_s(i)$$

and

$$\bar{T}_{ns}(i) = \sum_a [1 - \delta_a(i)] \gamma_a(i) y_{ia} / N_{ns}(i)$$

are precipitation averages at station i for seeded and unseeded bands. Six control-area detection stations were used, stations circled in Figure 1. If k indexes these control stations, define,

$$\bar{C}_s = \sum_k \bar{T}_s(k) / 6$$

and

$$\bar{C}_{ns} = \sum_k \bar{T}_{ns}(k) / 6.$$

The double ratio of NAWC at station i is

$$DR(i) = [\bar{T}_s(i) / \bar{C}_s] / [\bar{T}_{ns}(i) / \bar{C}_{ns}]$$

and the single ratio is

$$SR(i) = \bar{T}_s(i) / \bar{T}_{ns}(i).$$

Much the same contour plots were obtained from both ratios. Use of the double ratio represents a use of control area precipitation as a covariate.

The Wilcoxon-Mann-Whitney, two-sample, rank test was used also by NAWC to assess the significances of double and single ratios for each raingage station. The method of application is

not clear in reports but is understood as follows. For the single ratio, y_{ia} was used; the precipitation themselves were grouped into two samples, seeded and unseeded, and the rank test applied. For the double ratio, y_{ia}/\bar{C}_a was calculated for each band a at station i , \bar{C}_a being the average of the six control area detection stations for band a , and these indices were grouped into two samples as before.

NAWC was aware that these significance tests were open to possible criticisms, particularly dependencies from station to station. A limited Monte Carlo study was conducted and reported by Elliott and Brown [6]. They state: "At the 0.05 significance level for all bands, 29 stations in the original test sample were found to show a positive difference between seeded and not-seeded cases (bands); and three Monte Carlo runs (out of 50) were found to have as high or higher counts of stations with a positive difference at this significance level."

III. DATA SUMMARIZATION

A more direct approach to analysis of the experiment is through summary measures of precipitation for each experimental unit over designated response areas.

Bradley, Srivastava and Lanzdorf [1,2] defined response areas as in Table I that may be located in Figure 1. The numbers of raingage stations and the data used for Target Areas (i)-(iv) are those of the Bureau of Reclamation study [5] and those for Target Area (v) are those of the Naval Weapons Center study [9] with minor modifications noted in [3,4].

TABLE I
Definitions of Response Areas

Response Area	Ranges in Degrees		Number of Stations
	Latitude	Longitude	
(i)	34.0-35.25	118.0-120.02	107
(ii)	34.4-35.0	119.51-120.02	26
(iii)	34.0-35.0	118.0-119.51	72
(iv)	Areas (ii) + (iii)		98
(v)	All Stations in the Naval Weapons Center Reports East of Seeding Site, long. 120.02		61
Control*	34.4-35.25	120.02-120.60	34

*The Control Area for the Naval Weapons Center study consists of all 39 stations West of the seeding site.

Use of a simple average over stations is the most direct method of data summarization for a convective band. Overall precipitation means are reported in Table II. Note that the Control Area mean is higher for seeded bands suggesting that seeding may have had some effect in the Control Area or misfortune in the randomized choice of bands to be seeded.

TABLE II
Precipitation Means in Inches

Response Areas	(i)	(ii)	(iii)	(iv)	(v)	Control
Seeded Bands	0.257	0.329	0.249	0.271	0.267	0.234
Unseeded Bands	0.178	0.229	0.172	0.187	0.190	0.203

With a view to improved data summarization, Briley, Srivastava and Lanzdorf [1,2] fitted response surfaces separately for the Control Area and Target Area (i) with the coordinates of latitude and longitude of raingage stations as independent variables and raingage precipitation as the dependent variable. General

two-dimensional cubic response models were necessary to represent responses adequately. Separate response surfaces were found for each convective band. Precipitation volumes and their variances were calculated over the designated target areas and Control Area. Figure 2 is typical of results obtained; the region where the surfaces is negative is off-shore.

The response surface approach was successful as a method of data summarization in that some 70% of the inherent variation in responses among raingages within a band and response area was explained by the independent variables. It was not successful in improvement of data summarization in comparison with use of the means of raingages within response areas for a convective band in that correlations between precipitation volumes calculated from the response surfaces and precipitation means ranged from 0.97 to 0.99 for Target Areas (i)-(iv) and the correlation was 0.89 for the Control Area. Thus, the use of volumes cannot be expected to yield new insights.

Scott [10] used a multivariate approach to data summarization. He found, with some difficulty and innovation, principal components among raingage responses in both Target Area (i) and the Control Area. The first three principal components were interpretable approximately as a mean response, a coastal versus inland contrast, and an East-West contrast. Percentages of variation explained by these components were respectively 71.3, 6.7 and 5.9 in Target Area (i) and 76.1, 6.7 and 4.7 in the Control Area. The correlations of the first component with the band mean were 0.997 for Target Area (i) and 0.985 for the Control Area. Scott is engaged in the use of these results in examination of the effects of seeding; it seems unlikely that much additional information will be forthcoming.

In the following section, we show some parametric analyses for Target Area (i). Although Bradley, Srivastava and Lanzdorf [3] followed through with analyses on precipitation volumes as well as means, we report only on the use of means. All Target Areas

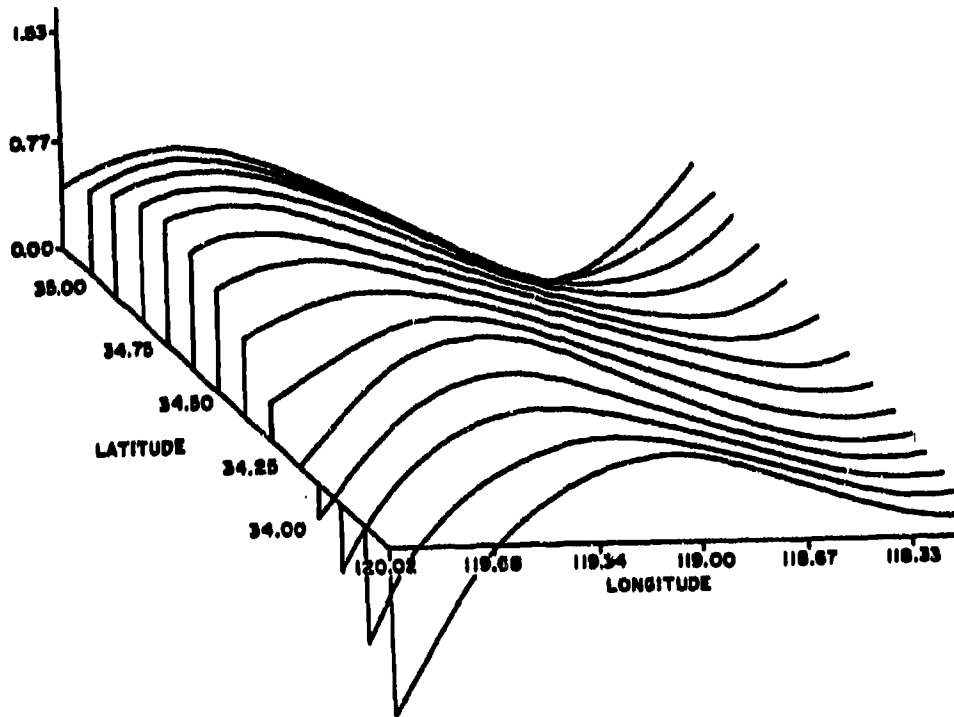


FIG. 2. Graph of Cubic Response Surface: Band 96 (Seeded), Target Area (i). Source: Figure 2, Bradley, Srivastava, and Lanzdorf [1]. Vertical axis is 2.3 times precipitation in inches.

of Table I gave similar results.

IV. SOME PARAMETRIC ANALYSES

Weather modification experiments are conducted necessarily in a natural environment involving much variability. The use of covariates in analyses, as summarized by Gleeson [10], for the reduction of experimental error appeared to be the best means to improved experimental design.

Initial covariance analyses were reported in [3]. (Some later analyses are summarized below). Regression models used were of the form.

$$U = \beta_0 + \sum_{i=1}^p \beta_i V_i + \delta Z + \epsilon,$$

where U is a precipitation response variable for a target area, V_i is the i -th covariate, $Z = 1$ or 0 as the convective band was or was not seeded, the β 's and δ are regression parameters, and ϵ is a random error. The data matrix has rows, $(U_\alpha, V_{1\alpha}, \dots, V_{p\alpha}, Z_\alpha)$, $\alpha = 1, \dots, N$. The regression parameters were estimated by weighted least squares through minimization of

$$\sum_{\alpha=1}^N w_\alpha (U_\alpha - \beta_0 - \sum_{i=1}^p \beta_i V_{i\alpha} - \delta Z_\alpha)^2.$$

In [3], use of the listed set of covariates and their interactions with seeding, along with X_C , a measure of Control Area precipitation, was explored. In analysis of variance tables in [3] and below, sources of variation, when included in models, were ordered: covariates, covariate by seeding interactions after adjustment for covariates, and seeding after adjustment for covariates and interactions.

The use of covariates was effective in reducing experimental error but less so was the use of covariate by seeding interactions. Preliminary analyses and redundancy considerations suggested reduction from 12 covariates to 7: X_2 , X_3 , X_6 , X_7 , X_8 , X_{11} and X_{12} , along with X_C , Control Area mean precipitation. There is concern about use of X_C because Elliott and Thompson [8] suggest the possibility of an up-wind effect of seeding west of the seeding site attributable not to westward seeding contamination but to a seeding-caused blocking of the air-mass flow leading to up-wind convection development. This may have affected X_{12} , band passage time at the seeding site, also. Two choices of weighting were used, $w_a = 1$ (unweighted) and $w_a = n_a / s_a^2$ when U was target area mean precipitation, where n_a was the number of observations contributing to the precipitation mean for band a and s_a^2 was the variance among those observations. Weighted analyses with $w_a = n_a / s_a^2$ were less satisfactory than unweighted analyses. This difficulty arose because standard deviations are proportional to means and very high weights were associated with convective bands with low precipitations. The two best covariates were X_C and X_{12} . The use of covariates reduced the apparent effect of seeding. In these analyses and those below, $N = 106$ when covariates are used because covariate data were missing for Band 73.

Analyses were redone in [4] with responses transformed logarithmically to stabilize variances. The transformed variate z has the form, $\log(1+ay)$, where Y is a target area precipitation observation. For Target Area (i), U is now the target area mean of z , and $w_a = n_a$. The regression analyses are similar to those described above. Models with and without X_C and X_{12} were used because it has been suggested that they may have been affected by seeding. Six models were used as follows:

Model	Identification of v_1, \dots, v_p
(1)	No covariates.
(2)	$x_C, x_2, x_3, x_6, x_7, x_8, x_{11}, x_{12}$
(3)	Model (2) less x_C .
(4)	Model (2) less x_{12} .
(5)	Model (2) less x_C, x_{12} .
(6)	Model (2) plus $x_2z, x_3z, x_6z,$ $x_7z, x_8z, x_{11}z, x_{12}z$.

Mean squares, values of F, and values of R^2 , the coefficient of determination, for these models are shown in Table III.

We comment on the analyses of Table III. The transformation was shown to be effective in stabilizing variances except for small values of U, values for convective bands that may not have been acceptable "seedable" bands. Examination of residuals about regression models for the transformed data suggests that transformation improved symmetry and approximate normality of their distributions. Slightly larger values of R^2 were obtained from the transformed data than in [3]. Results for model (5) show that R^2 is reduced considerably when x_C and x_{12} are omitted as covariates. Results for model (6) show that interaction terms contribute little.

There is little indication for models (2)-(6) in Table III of any effect of seeding. For Model (1), the one-sided significance level is 0.06, consistent with the randomization analysis reported in Section II. The covariates may be affected by seeding. We have commented on this in regard to x_C and x_{12} . Gleeson [10] saw small but consistent differences in covariates for seeded and unseeded bands. The other covariates were based on radiosonde data taken at Santa Barbara Airport, well into the target area.

TABLE III

Analyses of Variance, Transformed Data,
Target Area (i), Models (1)-(6)

Model	(1)			(2)			(3)		
Source of Variation	d.f.	M.S.	F	d.f.	M.S.	F	d.f.	M.S.	F
Seeding	1	110.3	2.77	1	0.6	.05	1	0.0	.00
Interactions	-	-	-	-	-	-	-	-	-
Covariates	-	-	-	8	382.5	30.79	7	374.4	22.24
Error	104	39.8	-	96	12.4	-	97	16.8	-
R^2	-	-	0.03	-	-	0.72	-	-	0.62

Model	(4)			(5)			(6)		
Source of Variation	d.f.	M.S.	F	d.f.	M.S.	F	d.f.	M.S.	F
Seeding	1	11.6	.78	1	44.7	1.46	1	1.6	.13
Interactions	-	-	-	-	-	-	7	17.0	1.41
Covariates	7	398.6	26.64	6	200.4	6.53	8	382.5	31.73
Error	97	15.0	-	98	30.7	-	89	12.1	-
R^2	-	-	0.66	-	-	0.29	-	-	0.75

Some other sources of variation have not been considered yet. Convective bands occur within winter storms with one or more bands. Therefore there is a total or partial confounding of storm effects with seeding. If covariates are omitted and the effect of seeding is considered after adjustments for storms, we have the analysis of Table IV. It is seen that $R^2 = 0.54$, comparable to values of R^2 in Table III; more degrees of freedom are expended.

TABLE IV

Analysis of Variance, Target Area (i), Transformed
Data, Storm Effects in Model

Source of Variation	d.f.	M.S.	F
Seeding	1	24.0	0.82
Storms	37	61.1	2.08
Error	67	29.4	-
R ²	-	-	0.54

But the apparent effect of seeding has disappeared again. In future similar experimentation, use of storms for blocking should be considered, perhaps as suggested in [12], with randomization within storms rather than over all convective bands as done in the Phase I Santa Barbara experiment for which the analyses reported in Section II and in Table III for model (1) seem appropriate.

In further exploratory analyses, we considered as additional sources of variation position of the band within a storm and a possible first-order carry-over effect of seeding from a seeded band to the following band if in the same storm. No real effects for position or carry-over were found.

The analyses of this section are open to technical concerns, but parametric methods provide the best means of exploratory analysis if not for the exact determination of significance levels. The possible persistence effect of seeding raises questions about the independence of experimental units that may be subject also to serial correlation. Normality assumptions are not valid for individual raingage observations but may be appropriate for target area

means. Some variance heterogeneity is present after transformation of the data. Choice of weights, $w_a = n_a$, for analyses with transformed data is only strictly appropriate if raingage observations are independent. Covariates in regression models are subject to experimental errors.

V. REMARKS

Some remarks and recommendations can be made after analysis of the Phase I Santa Barbara experiment. We are in near agreement with the conclusion of Elliott and Brown [6]: "Even when those bands not as receptive to seeding were included in the sample, the seeded to not-seeded precipitation increases were greater than 50%." The means of Table II show increases near to 50% and the analysis of Table III for Model (1) suggests significance near to the 0.05 level.

Improved experimental design is needed but not easy to achieve. Use of convective bands as experimental units increases the number of available units per season but raises other problems. Some improvements are needed:

- (i) Improved detection and determination of "seedable" bands.
- (ii) More uniform dispersement of raingages over regions of interest.
- (iii) Improved determination and measurement of precipitations attributed to particular convective bands.
- (iv) Better determination and measurement of covariates free from possible seeding effects.
- (v) Allowance for blocking by storms for further control of variation. Concerns may remain in regard to dependencies among experimental units, data transformation, variance heterogeneity and persistence effects of seeding, some of which may be met through use of randomization analyses. Further meteorological and statistical research is needed.

REFERENCES

- [1] Bradley, R. A., Srivastava, S.S. and Lanzdorf, A. (1977). Data Summarization in a Weather Modification Experiment: I. A Response Surface Approach, Tech. Report M417, Department of Statistics, Florida State University, Tallahassee, Fl.
- [2] Bradley, R. A., Srivastava, S.S. and Lanzdorf, A. (1977). "Summarization of Precipitation Data for a Weather Modification Experiment", Fifth Conf. Prob. and Statist., Preprint Vol., 201-205, Amer. Meteor. Soc., Boston, Ma.
- [3] Bradley, R. A., Srivastava, S.S. and Lanzdorf, A. (1978). An Examination of the Effects of Cloud Seeding in Phase I of the Santa Barbara Convective Band Seeding Test Program, Tech. Report M467, Department of Statistics, Florida State University, Tallahassee, Fl.
- [4] Bradley, R. A., Srivastava, S.S. and Lanzdorf, A. (1978). "Some Approaches to Statistical Analysis of a Weather Modification Experiment", prepared for Communications in Statistics; Theory and Methods.
- [5] Brown, K. J., Thompson, J. R. and Elliott, R. D. (1975). Large Scale Effects of Cloud Seeding, Final Report, 1970-74 Seasons, Tech. Report 75-2, Aerometric Research Inc., Goleta, Ca.
- [6] Elliott, R. D. and Brown, K. J. (1971). "The Santa Barbara II Project - Downwind Effects", Int. Conf. on Weather Mod., Preprint Vol., 179-184, Canberra, Sept. 6-11, 1971.
- [7] Elliott, R. D., St. Amand, P. and Thompson, J.R. (1971). "Santa Barbara Pyrotechnic Cloud Seeding Results 1967-70", J. Applied Meteorology 10, 785-795.
- [8] Elliott, R. D. and Thompson, J. R. (1969). Santa Barbara Pyrotechnic Seeding Device Program, 1967-68 and 1968-69 Seasons, Tech. Publ. 4816, Naval Weapons Center, China Lake, Ca.
- [9] Elliott, R. D. and Thompson, J. R. (1972). Santa Barbara Convective Seeding Test Program, 1970-71 Season and 1967-71 Summary, Tech. Publ. 5308, Naval Weapons Center, China Lake, Ca.

- [10] Gleeson, T. A. (1977). Data Summarization in a Weather Modification Experiment: II Concomitant Variables, Tech. Report M419, Department of Statistics, Florida State University, Tallahassee, Fl.
- [11] Scott, E. (1978). Data Summarization in a Weather Modification Experiment: III. A Multivariate Analysis, Tech. Report M442, Department of Statistics, Florida State University, Tallahassee, Fl.
- [12] Statistical Task Force to the Weather Modification Advisory Board (1978). The Management of Weather Resources, Volume II: The Role of Statistics, Report to the Secretary of Commerce, Washington, U.S. Government Printing Office.
- [13] Weather Modification Advisory Board (1978). The Management of Weather Resources. Volume I: Proposals for a National Policy and Program, Report to the Secretary of Commerce, Washington, U.S. Government Printing Office.

Key Words & Phrases: weather modification; cloud seeding; data analysis; summarization of data; transformations; covariance analysis; applied regression; multivariate analysis.

CANDIDATE SEQUENTIAL DESIGNS FOR
OPTIMUM SEEKING

Carl B. Bates
US Army Concepts Analysis Agency
Bethesda, Maryland

ABSTRACT. Phase I of the Target Acquisition Systems Force Mix Evaluation Analysis (TASFMA) Study is the development of a methodology for evaluating the combat effectiveness of mixes of systems within a functional area. The methodology requires a division combat simulation model whose outcome is sensitive to changes in the quality and quantity of sensor systems deployed. DIVOPS, a division-level combined arms engagement model, is the primary candidate for the combat simulation model. The model will simulate multiple quantities of up to 15 different sensor types. Because the DIVOPS Model can represent 15 sensor systems, the developed methodology must be capable of accommodating 15 system types. Additionally, it is desired that three quantities be examined for each of the 15 sensor types. Although DIVOPS is a relatively fast running model, all 3^{15} runs are impossible. Consequently, a method is needed for constructing a manageable sized subset of the total 3^{15} input combinations. This paper presents candidate sequential designs for the study and search of the optimum sensor mix. Two two-level designs are presented, a resolution III design which requires 16 runs and a resolution V design which requires 256 runs. Then two three-level designs are presented, a "Minimum Number of Points" design requiring 136 runs and a 3^{k-p} fractional factorial design requiring 243 runs. Advantages and disadvantages of the designs are discussed.

1. **INTRODUCTION.** The Target Acquisition Systems Force Mix Evaluation Analysis (TASFMA) Study consists of two phases. Phase I is the development of a methodology for evaluating the combat effectiveness of mixes of systems within a functional area. Phase II is the demonstration of the usefulness of the methodology. The following sequential designs are proposed for incorporation into the developed methodology.

The methodology requires a division combat simulation whose combat outcome is sensitive to changes in the quality and quantity of sensor systems deployed. DIVOPS is the primary candidate for the combat simulation. DIVOPS is a two-sided, deterministic, division-level ground combat model. The model will simulate multiple quantities of up to 15 different sensor types. The model documentation is in Reference 1.

2. **PROBLEM DESCRIPTION AND BACKGROUND.** Because the DIVOPS Model can represent 15 sensor types, the developed methodology must also be capable of accommodating 15 system types. Additionally, because sensor

influence may be nonlinear, it is essential that more than just two quantities (say, a low and a high number) of sensors be examined for each of the different types. It is desired that three quantities be examined for each of the 15 sensor types. Although DIVOPS is a relatively fast running model, all 3^{15} input combinations cannot be run since $3^{15} > 14,000,000$. Moreover, neither could the model be exercised for all 2^{15} input combinations, if desired, since $2^{15} = 32,768$. Consequently, a method is needed for constructing a manageable size subset of the totality of the 3^{15} input combinations, hereafter referred to as design points. The purpose of this paper is to present proposed sequential designs for the above described optimization problem.

3. METHODOLOGY RATIONALE. The methodology presupposes little or no a priori information about the functional relationship between model input variables and model output variables. The model input variables and output variables are considered to be continuous variables. For the purpose of this paper, it is assumed that the three quantities, hereafter termed levels, of sensors or systems are known for each system under investigation. That is, the proposed procedure is not for determining what the levels should be. Rather, it is for identifying the combinations of existing levels which should be employed in the search for the optimum systems mix.

Although interest is in three levels of each of the input variables, because of the magnitude of 3^k it is felt that the examination process must be sequential in nature. That is, the search should start with a 2^k design and proceed to a 3^k design where $k' \leq k$. This approach employs some of the screening concepts of experimental designs and response surface fitting.

4. TWO-LEVEL DESIGNS

a. General. Let $x_i, i = 1, 2, \dots, k$ be the model input variables, where $k = 15$. Denote the extreme two of the three levels of each of the variables by "0" and "1," respectively. If k were three, the eight design points would be as shown in Table 1 and are geometrically illustrated in Figure 1.

If the full factorial experiment were performed and a dependent variable y were measured or observed at each of the eight independent variable combinations, the full model shown as Equation [1] could be fitted.

$$\begin{aligned} y = & b_{000} + b_{100}x_1 + b_{010}x_2 + b_{001}x_3 + b_{110}x_1x_2 \\ & + b_{101}x_1x_3 + b_{011}x_2x_3 + b_{111}x_1x_2x_3 \end{aligned} \quad [1]$$

Table 1. 2^3 Design Matrix

x_1	x_2	x_3
0	0	0
1	0	0
0	1	0
0	0	1
1	1	0
1	0	1
0	1	1
1	1	1

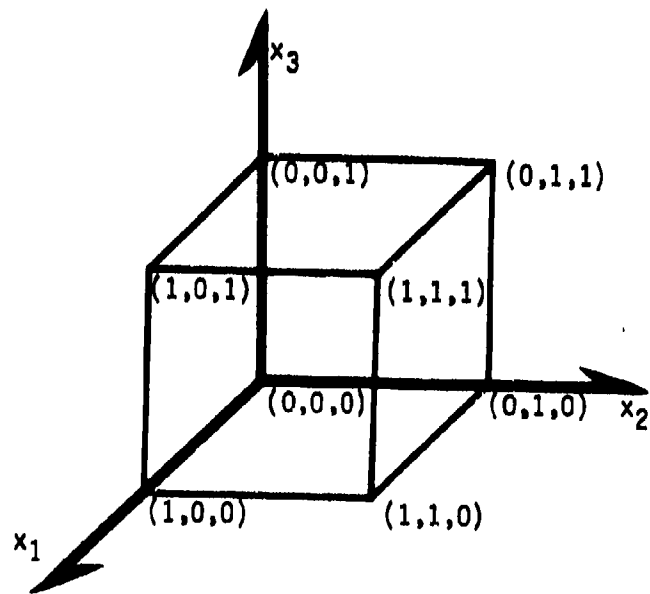


Figure 1. Full 2^3 Factorial

The general full 2^k design permits the fitting of the following 2^{k-1} terms plus the intercept, b_0 .

k	single-variable terms
$k(k-1)/2$	two-variable terms
$k(k-1)(k-2)/2x3$	three-variable terms
•	
•	
•	

Because a full 2^{15} experiment is impossible for the TASFMA optimization problem, two alternative $(1/2)^P$ fractional designs, 2^{k-P} , are presented. The first design permits fitting the 15 single-variable terms only. The second design permits fitting the 15 single-variable terms and the $(15 \times 14)/2 = 105$ two-variable terms.

b. Resolution III Design. Resolution III designs are available which require $k+1$ runs to study k variables, where $k+1$ is a multiple of four. In Reference 2, Box and Hunter give the following definition of resolution III designs:

"No main effect is confounded with any other main effect, but main effects are confounded with two-factor interactions and two-factor interactions with one another."

The design is first illustrated for a seven-variable experiment. Consider a $(1/2)^4$ of a complete 2^7 factorial, a 2^{7-4} design. Construction of the design matrix starts with the design matrix in Table 1, a full 2^3 . Four additional columns are generated from the three original columns. Treat a "0" as a "-1" and a "1" as a "+1" and product the three pairs of columns and the one triple. That is, generate columns 4, 5, 6, and 7 as follows:

```
column 4 = column 1 times column 2
column 5 = column 1 times column 3
column 6 = column 2 times column 3
column 7 = column 1 times column 2 times column 3
```

The resulting design matrix is shown in Table 2 and permits fitting the seven-dimensional plane given in Equation [2].

Table 2. 2^{7-4} Design Matrix

x_1	x_2	x_3	x_4	x_5	x_6	x_7
0	0	0	1	1	1	0
1	0	0	0	0	1	1
0	1	0	0	1	0	1
0	0	1	1	0	0	1
1	1	0	1	0	0	0
1	0	1	0	1	0	0
0	1	1	0	0	1	0
1	1	1	1	1	1	1

$$y = b_0 + b_1x_1 + b_2x_2 + b_3x_3 \\ + b_4x_4 + b_5x_5 + b_6x_6 + b_7x_7 \quad [2]$$

Applying the technique described in the previous paragraph to the 15 variables of the TASFMA Study gives the design matrix in Table 3. The first four columns constitute the design for a full 2^4 factorial. Columns 5 through 10 are pairwise products of the first four columns. Columns 11 through 14 are the four triple products, and column 15 is the product of all four columns. The products are indicated under the column heading in the table. Exercising the computer simulation model for each of the 16 input variable combinations identified in Table 3 would permit fitting a 15-dimensional plane for each output variable under study. For each output variable, this would give a function in terms of each of the 15 input variables, Equation [3].

$$y = b_0 + b_1x_1 + b_2x_2 + \dots + b_{14}x_{14} + b_{15}x_{15} \quad [3]$$

The regression coefficients b_1, b_2, \dots, b_{15} are the slopes of the plane in the respective dimensions. The slopes can be analyzed to assess the effect each of the 15 input variables has upon the particular output variable and also to refine the space which will be further examined with a three-level design.

Table 3. 2^{15-11} Resolution III Design

Run	Column														
	1	2	3	4	5	6	7	8	9	10	11	12	13	14	15
1.	0	0	0	0	1	1	1	1	1	0	0	0	0	0	1
2.	1	0	0	0	0	0	0	1	1	1	1	1	0	0	0
3.	0	1	0	0	0	1	1	0	0	1	1	0	1	0	0
4.	1	1	0	0	1	0	0	0	0	1	0	0	1	1	1
5.	0	0	1	0	1	0	1	0	1	0	1	0	1	1	0
6.	1	0	1	0	0	1	0	0	1	0	0	1	0	1	1
7.	0	1	1	0	0	0	1	1	0	0	0	1	1	0	1
8.	1	1	1	0	1	1	1	0	1	0	0	0	0	0	0
9.	0	0	0	1	1	1	0	1	0	0	0	1	1	0	0
10.	1	0	0	1	0	0	1	1	0	0	1	0	0	1	1
11.	0	1	0	1	0	1	0	0	1	0	1	0	1	0	1
12.	1	1	0	1	1	0	1	0	1	0	0	1	0	0	0
13.	0	0	1	1	1	1	0	0	0	0	1	1	0	0	1
14.	1	0	1	1	0	1	1	0	0	0	1	1	0	0	0
15.	0	1	1	1	1	0	0	0	1	1	0	0	0	1	0
16.	1	1	1	1	1	1	1	1	1	1	1	1	1	1	1

The assessment will give the direction of the maximum response as well as an ordering of the relative contribution of each of the 15 sensor types. If some of the 15 contribute very little as compared to the others, then the low contributors can be fixed at either their upper or constraining levels for the follow-on three-level examination.

The above "cheap" experiment is not without risk. Naturally, a sacrifice has to be made for a design with such a small number (16) of design points. If two input variables, x_i and x_j , significantly interact and neither x_i nor x_j individually significantly contribute, the variables would not be recognized as being sufficiently important for inclusion in the follow-on three-level investigation. If this risk is considered too great and a design is required which will permit the testing of all of the two-variable interactions, then the price of many more computer simulation model runs must be made. In any case, the resolution III design should be conducted first because it requires so few runs.

c. Resolution V Design. Resolution V designs are defined by Box and Hunter in Reference 2 as:

"No main effect or two-factor interaction is confounded with any other main effect or two-factor interaction, but two-factor interactions are confounded with three-factor interactions."

Box and Hunter discuss resolution V designs and their construction in Reference 3. This is the type of 2^{k-p} fractional factorial designs conventionally introduced in experimental design texts, such as References 4, 5, 6, 7, 8, and 9. The construction of resolution V 2^{k-p} designs is not the purpose of this paper and will not be discussed here. Their construction can be found in the above references.

A 15-variable experiment has $k = 15$ main effects and $k(k-1)/2 = 105$ two-variable interaction effects. The smallest resolution V design for a 2^{15} experiment has 256 design points. Using the 15 letters A, B, ..., P (excluding I) to represent the 15 input variables x_1, x_2, \dots, x_{15} and the identifying contrast shown in Table 4, gives the 2^{15-7} design given in Table 5. From the 256-run simulation model experiment we can fit the model in Equation [4].

$$\begin{aligned} y = & b_0 + b_1 x_1 + b_2 x_2 + \dots + b_{15} x_{15} + b_{1,2} x_1 x_2 + \dots \\ & + b_{14,15} x_{14} x_{15} \end{aligned} \quad [4]$$

Table 4. Identifying Contrast for a $(1/2)^7 \times 2^{15}$ Experiment^a

Factors: A, B, C, D, E, F, G, H, J, K, L, M, N, O, P.
$I = ABE\bar{G}N = ACEFNP = BC\bar{F}HP = DEFGO = AB\bar{D}ENO = AC\bar{D}GNOP = BCDEOP = ADHKO$
$= BDEGHKNO = CDEFHKNO = ABCDFGHKOP = AEFGHK = BFHKN = CGHKNP$
$= ABCFEHKP = BC\bar{H}JN\bar{O}P = ACE\bar{H}JOP = ABEPHJ\bar{O} = F\bar{H}JNO = BCDEFGHJNP = ACDFHJ\bar{P}$
$= ABDGHJ = DEHIN = ABCD\bar{V}INP = CD\bar{E}GJKP = BDE\bar{F}JK = AD\bar{F}GJKN = ABCFGJKN$
$= CFJKOP = BC\bar{J}KO = AE\bar{J}KNO = ABKLOP = EGKLN\bar{O}P = BCEFKLN\bar{O} = ACP\bar{E}KL\bar{O}$
$= ABDEFGKLP = DFKLNP = BDGKLN = ACDEKL\bar{I} = BDHLP = ADEGHLNP = ABCDEFLIN$
$= CD\bar{F}GHL = BEFGH\bar{L}OP = AFH\bar{L}N\bar{O}P = ABCGHLNO = CEH\bar{L}O = ACH\bar{J}KL\bar{N} = BCEGH\bar{J}KL$
$= EFH\bar{J}KL\bar{P} = ABPH\bar{J}KL\bar{N}P = ACD\bar{E}F\bar{G}H\bar{J}KL\bar{N}O = EDFH\bar{J}KL\bar{O} = DGH\bar{J}KL\bar{O}P$
$= ABDEH\bar{J}KL\bar{N}\bar{O}P = CD\bar{J}LNO = ABC\bar{D}EG\bar{J}L\bar{O} = ADEFJL\bar{O}P = BDF\bar{G}JLN\bar{O}P = CEF\bar{G}JLN$
$= ABCP\bar{J}L = AG\bar{J}LP = BE\bar{J}LNP = CD\bar{G}H\bar{J}M\bar{A}O = ABCDEH\bar{J}M\bar{N}O = ADEF\bar{G}H\bar{J}M\bar{N}OP$
$= BD\bar{F}H\bar{J}MOP = CEF\bar{H}JM = ABC\bar{F}GH\bar{J}MN = AH\bar{J}M\bar{N}P = BE\bar{G}H\bar{J}MP = AC\bar{G}J\bar{K}M = BCE\bar{J}K\bar{M}N$
$= EP\bar{L}J\bar{K}M\bar{N}P = AB\bar{F}J\bar{K}MP = ACDEF\bar{J}KM\bar{O} = BCDF\bar{G}J\bar{K}M\bar{N}O = DJ\bar{K}M\bar{N}OP = ABDE\bar{G}J\bar{K}M\bar{O}P$
$= BD\bar{G}M\bar{A}P = ADE\bar{M}P = ABCDEF\bar{U}M = CD\bar{F}M\bar{A}N = BE\bar{F}M\bar{N}OP = AFG\bar{M}OP = ABC\bar{M}O$
$= CE\bar{A}M\bar{N}O = ABGH\bar{K}M\bar{N}OP = EH\bar{K}M\bar{O}P = BCE\bar{F}G\bar{H}K\bar{M}O = AC\bar{F}H\bar{K}M\bar{N}O = ABDEF\bar{H}K\bar{M}R\bar{P}$
$= DP\bar{E}H\bar{K}M\bar{A}P = BC\bar{D}H\bar{K}M = ACDE\bar{G}H\bar{K}M\bar{N} = ABCD\bar{G}H\bar{J}K\bar{L}MP = CDE\bar{H}J\bar{K}LM\bar{N}P$
$= BDE\bar{F}G\bar{H}\bar{J}K\bar{L}MN = AD\bar{F}H\bar{J}K\bar{L}M = ABCE\bar{F}H\bar{J}K\bar{L}MOP = CP\bar{G}H\bar{J}K\bar{L}M\bar{N}OP = BH\bar{J}K\bar{L}M\bar{N}O$
$= A\bar{E}G\bar{H}J\bar{K}L\bar{M}O = BC\bar{G}J\bar{L}M\bar{O}P = ACE\bar{J}LM\bar{N}OP = AB\bar{E}J\bar{L}M\bar{N}O = BCDEF\bar{J}L\bar{A}MP$
$= ACD\bar{F}G\bar{J}LM\bar{N}P = AB\bar{D}J\bar{L}M\bar{N} = DE\bar{G}J\bar{L}M = AD\bar{E}K\bar{L}M\bar{N}O = BDE\bar{K}L\bar{M}O = CDEF\bar{G}K\bar{L}M\bar{O}P$
$= ABCD\bar{F}K\bar{L}M\bar{N}OP = AEF\bar{K}LM\bar{N} = BF\bar{G}K\bar{L}M\bar{N} = CK\bar{L}MP = ABC\bar{E}G\bar{K}L\bar{M}N\bar{P} = GH\bar{L}MN$
$= ARE\bar{H}LM = ACE\bar{F}G\bar{H}LM\bar{P} = BC\bar{F}H\bar{L}M\bar{N}P = DEF\bar{H}LM\bar{N}O = ABDF\bar{G}H\bar{L}M\bar{O} = ACD\bar{H}LM\bar{O}P$
$= BCDE\bar{H}LM\bar{N}OP.$

^aPlan 128.15.8 in Reference 10.

Table 5. 2¹⁵⁻⁷ Resolution V Design
(Page 1 of 3 pages)

1	0000000000000000	2	0101010101010101	3	1001100110010011
4	1010100001010111	5	0101010101010111	6	0101010101010111
7	1101010101010101	8	1010001101010101	9	1010001101010101
10	1001111010101010	11	0101010101010101	12	0000000101010101
13	1000101010101010	14	1110000010101010	15	0011000010101010
16	0101101010101010	17	1010101010101010	18	1010101010101010
19	0010111011011011	20	0000000101010101	21	1010000001010101
22	1101010101010101	23	0101010101010101	24	0101010101010101
34	1100110121010101	35	0111011010101010	36	0101000010101011
37	1001011101110101	38	1011101010101010	39	0001010101010101
46	0001010101010101	47	1011100010101010	48	1010101010101010
49	0010011010101010	50	0101010101010101	51	1010101010101010
52	1110010101010101	53	0101010101010101	54	0101010101010101
55	1010010101010101	56	1101010101010101	57	1101010101010101
58	1011010101010101	59	0111100010101010	60	0101010101010101
61	1001101000000100	62	1011101010101010	63	0001010101010101
64	0001011101010101	65	1011101010101010	66	0101010101010101
67	1011101010101010	68	1011101010101010	69	1011101010101010
70	0110000000000000	71	1010000000000000	72	1101010101010101
73	1011101010101010	74	1011101010101010	75	0101010101010101
76	0010000011110001	77	1101010101010101	78	1101010101010101
79	0110011001110001	80	0010111001110001	81	1011101010101010
82	1011010000101000	83	0001010101010101	84	0101111101010101
85	1101111101010101	86	0110010101010101	87	0110101010101010

Table 5. 2^{15-7} Resolution V Design
 (Page 2 of 3 pages)

83	010111100011101	89	0010101010001000	1000	90	0000011101101001
91	101101110011011	92	1001110101100111	93	0101110000001011	
94	011100091111110	95	100000011010001	96	1110110001011011	
97	1100101110000000	99	11100110111100	99	0101011010100111	
100	01111010101111	101	1011101011001010	102	1001000011011011	
103	00100000011001100	0000110110001	105	0111100001000001		
106	01010110101100107	11100101111011	108	1001000001111111		
109	0000111010101010	110	0010011010101010	111	1011001101100111	
112	1011110100001111	113	0111100110100000	114	0101010011010001	
115	11100100000011116	116	11001001111111	117	0000111010101011	
118	0010001011010110	119	1001010100100101	120	1011110110101011	
121	11010101110000	122	1110011101011010	123	0101011010101011	
124	0111101010111111	125	1011110100111010	126	1001000111010101	
127	0010000111010011	128	0000111010001101	129	0001001001010101	
130	00111111101001131	131	1000111111101010	132	1010001001010101	
133	01001001101111134	0100101010101011	135	1111001011110101		
136	11010101000000137	101000100010001	138	1000110011110001		
139	00111101010110140	0001001010101010	141	1101011110111111		
142	111111010110111143	0100101010101100	144	011001111000001		
145	101000000111101146	100011010100101	147	0111010101010101		
148	0001000001011010149	10101110111111	150	11111011000101110101		
151	0100101111010110152	01100111001000	153	0010011101010101		
154	00111110011001155	1000111100010101	156	1010001111101011		
157	01100101010111158	0100100110011111	159	11111000101011001		
160	1101010101110000161	1110010100111101	162	110111111000011		
163	01010111100110164	0100010100110010	165	1000010101010111		
166	10101001010101167	0001100100010100	168	001101001110001		
169	010000010111101170	01101100100001	171	1011110101101101		
172	111100001001010173	0011011111111111	174	0001101001010111		

Table 5. 2¹⁵-7 Resolution V Design
 (Page 3 of 3 pages)

175	10001010010000	176	10000111010000	177	0000000011101101
178	01001010010001	179	10011010010000	180	1111010010000011
181	00101100010011	182	00101100010010	183	1101101001001011
184	10001100010000	185	1111010010001011	186	1001101001000011
187	01101100010010	188	0100110001001001	189	1101101001001001
190	10101100010011	191	0001101001001101	192	0101101001001101
193	0001101001001011	194	0101010010010101	195	1101010010010101
196	1001010010010101	197	0101010010010101	198	1101010010010101
199	1101010010010101	200	0111010010010101	201	1001010010010101
202	1101010010010101	203	0111010010010101	204	1001010010010101
205	1111010010010101	206	0111010010010101	207	0101010010010101
208	0101010010010101	209	1101010010010101	210	0101010010010101
211	0010110001001101	212	0101010010010101	213	1101010010010101
214	1010100111011101	215	0101010010010101	216	1101010010010101
217	0011001001011101	218	0010101001011101	219	1101010010010101
220	1001000100010101	221	0101000100010101	222	0101000100010101
223	1101010010010101	224	0101000100010101	225	1101010010010101
226	1111010010010101	227	0101000100010101	228	1101010010010101
229	10101010101010101	230	1000000000000000	231	1111010010010101
232	0001111100000000	233	0111010010010101	234	1111010010010101
235	1111010010010101	236	0111010010010101	237	1111010010010101
238	0101010010010101	239	1100000000000000	240	1111010010010101
241	0101010010010101	242	0101010010010101	243	1111010010010101
244	1111010010010101	245	0101010010010101	246	1111010010010101
247	0000000000000000	248	1101010010010101	249	1111010010010101
250	1111010010010101	251	0100000000000000	252	1111010010010101
253	1010111001111111	254	1000000000000000	255	0011110000000000

Equation [4] has the 15 single-variable terms that are in equation [3] plus 105 two-variable terms. That is, 120 degrees of freedom of the total 255 degrees of freedom are used for fitting. The remaining 135 can be used for significance testing. Testing significance of the regression coefficients can be accomplished as illustrated in the ANOVA table, Table 6. The testing will identify those coefficients which are not significantly different from zero. The corresponding variables can then be fixed in the manner discussed in paragraph b above, and the investigation can proceed to the three-level follow-on investigation.

Table 6. ANOVA for 2^{15-7} Design

Source	DF	SS	MS	F-ratio
b_1	1	$SS(b_1)$	$MS(b_1)$	$MS(b_1)/MS(LOF)$
b_2	1	$SS(b_2)$	$MS(b_2)$	$MS(b_2)/MS(LOF)$
.
.
.
b_{15}	1	$SS(b_{15})$	$MS(b_{15})$	$MS(b_{15})/MS(LOF)$
$b_{1,2}$	1	$SS(b_{1,2})$	$MS(b_{1,2})$	$MS(b_{1,2})/MS(LOF)$
.
.
.
$b_{14,15}$	1	$SS(b_{14,15})$	$MS(b_{14,15})$	$MS(b_{14,15})/MS(LOF)$
<u>Lack of Fit</u>	<u>135</u>	<u>$SS(LOF)$</u>	<u>$MS(LOF)$</u>	
Total	255	SS(Total)		

The obvious disadvantage of the above design is the large number of simulation model runs required. This cannot be avoided when so many (120) coefficients are to be estimated and tested. Care must also be taken when assessing interaction significance. Since the interaction of each variable with each of the other 14 variables is being tested, an alpha-percent of the interactions would be expected to be statistically significant due to random chance.

5. THREE-LEVEL DESIGNS

a. General. As with the two-level designs, two candidate three-level designs are proposed. One design may be applied to all 15 input variables if necessary; the other design presupposes that the previous screening process reduces the number of input variables so that $k' \leq 10$.

First, the notation is changed from that used in the previous section. Now, denote the three levels--low, middle, and high--by "0", "1", and "2", respectively. If k' were three, the 27 design points of a full 3^3 experiment would be as given in Table 7. The full design is illustrated geometrically in Figure 2.

If the full design were executed, the following model of Equation [5] could be fitted. Equation [5] has 27 terms.

$$\begin{aligned} y = & b_{000} + b_{100}x_1 + b_{010}x_2 + b_{001}x_3 \\ & + b_{200}x_1^2 + b_{020}x_2^2 + b_{002}x_3^2 \\ & + b_{110}x_1x_2 + b_{101}x_1x_3 + b_{011}x_2x_3 \\ & + b_{120}x_1x_2^2 + \dots + b_{222}x_1^2x_2^2x_3^2 \end{aligned} \quad [5]$$

The general full $3^{k'}$ design permits fitting $3^{k'}$ terms, including the intercept. In practice, however, even for moderate k' , all possible 3^k terms are seldom fitted. Usually they are not even desired. Two candidate three-level designs are proposed which require considerably less than 3^k design points. The first is the "Minimum Number of Points" design. The second design is the conventional 3^{k-p} fractional factorial design.

Table 7. 3^3 Design Matrix

x_1	x_2	x_3
0	0	0
1	0	0
2	0	0
0	1	0
1	1	0
2	1	0
0	2	0
1	2	0
2	2	0
0	0	1
1	0	1
2	0	1
0	1	1
1	1	1
2	1	1
0	2	1
1	2	1
2	2	1
0	0	2
1	0	2
2	0	2
0	1	2
1	1	2
2	1	2
0	2	2
1	2	2
2	2	2

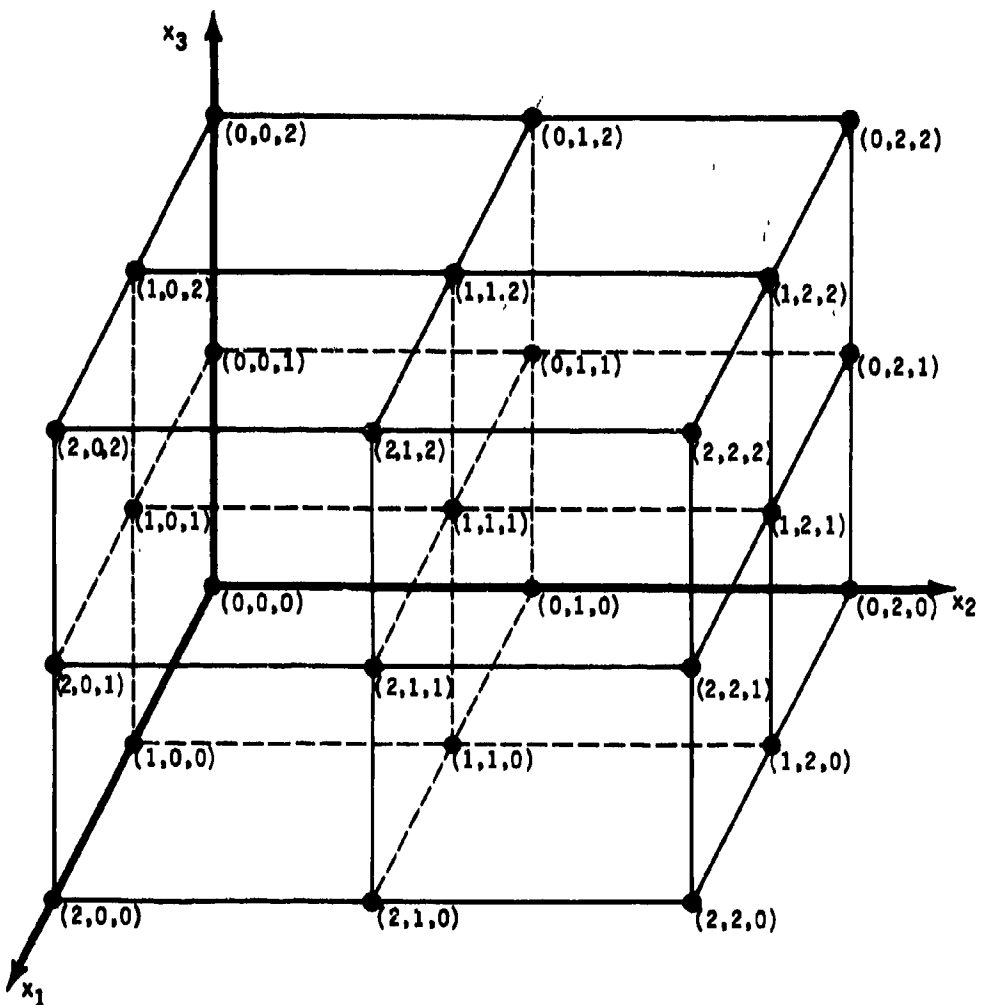


Figure 2. Full 3^3 Factorial

b. "Minimum Number of Points" Design.* The "Minimum Number of Points (MNOP)" design contains the same number of design points as there are terms in the fitted function, including the intercept. The design permits fitting all first and second order terms.

First, the design is illustrated for $k' = 3$. The design matrix for $k' = 3$ is shown in Table 8. The ten design points are illustrated in Figure 3 and will permit fitting Equation [6].

Table 8. Minimum Number of Points Design Matrix for $k' = 3$

x_1	x_2	x_3
0	0	0
1	0	0
0	1	0
0	0	1
2	0	0
0	2	0
0	0	2
1	1	0
1	0	1
0	1	1

$$\begin{aligned}
 y = & b_{000} + b_{100}x_1 + b_{010}x_2 + b_{001}x_3 \\
 & + b_{200}x_1^2 + b_{020}x_2^2 + b_{002}x_3^2 \\
 & + b_{110}x_1x_2 + b_{101}x_1x_3 + b_{011}x_2x_3
 \end{aligned} \quad [6]$$

To show the pattern more clearly before presenting the MNOP design for $k' = 15$, the design is also illustrated for five variables. Table 9 contains the design for $k' = 5$. Note that k' rows have a single "1", k' rows have a single "2", and $k'(k'-1)/2$ rows have two "1's". Although the model that can be fitted is obvious, it is given in Equation [7] for completeness. Subscript notation is changed from that previously used to conserve space.

*The design was brought to the attention of the author by Dr. George Box in a personal communication during May 1978.

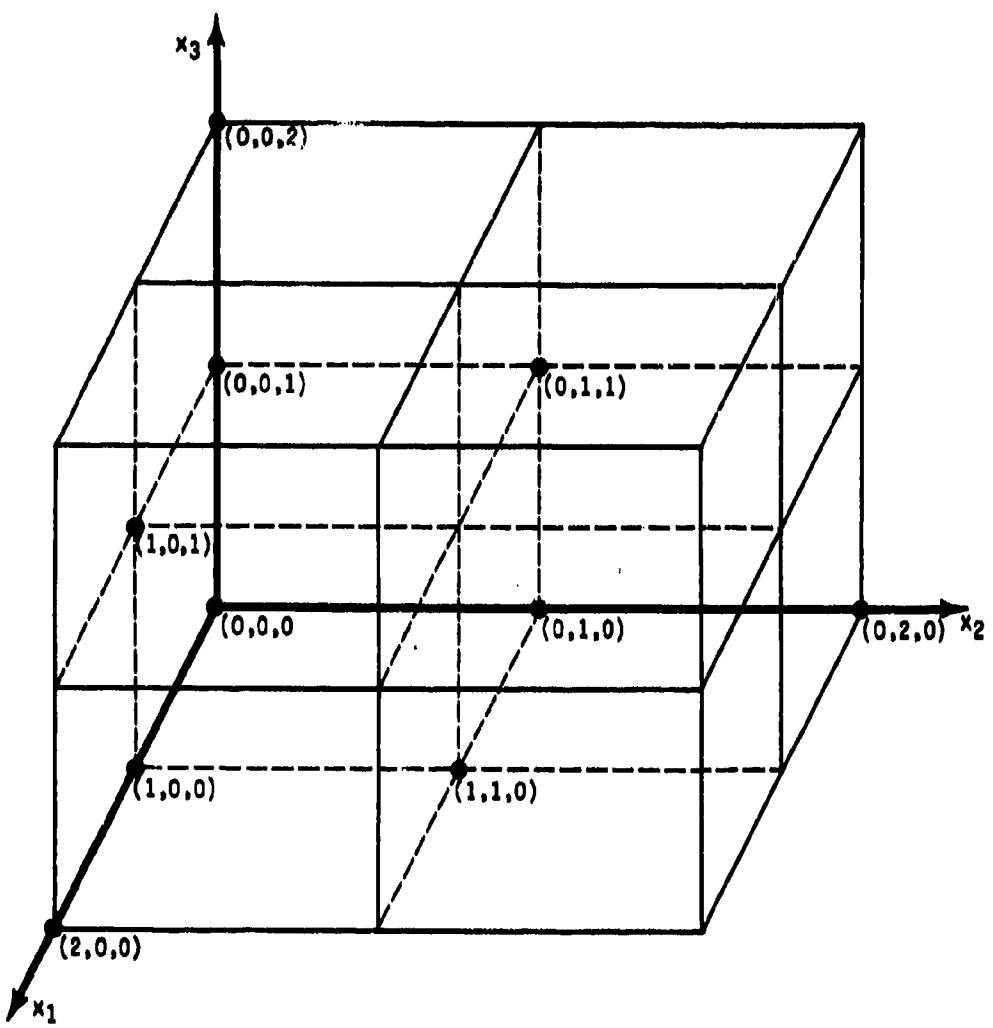


Figure 3. MNOP Design for Three Variables

Table 9. MNOP Design Matrix for $k' = 5$

x_1	x_2	x_3	x_4	x_5
0	0	0	0	0
1	0	0	0	0
0	1	0	0	0
0	0	1	0	0
0	0	0	1	0
2	0	0	0	0
0	2	0	0	0
0	0	2	0	0
0	0	0	2	0
1	1	0	0	0
1	0	1	0	0
1	0	0	1	0
1	0	0	0	1
0	1	1	0	0
0	1	0	1	0
0	0	1	1	0
0	0	1	0	1
0	0	0	1	1

$$\begin{aligned}
 y = & b_0 + b_1x_1 + b_2x_2 + b_3x_3 + b_4x_4 + b_5x_5 \\
 & + b_{11}x_1^2 + b_{22}x_2^2 + b_{33}x_3^2 \\
 & + b_{44}x_4^2 + b_{55}x_5^2 + b_{12}x_1x_2 \\
 & + b_{13}x_1x_3 + b_{14}x_1x_4 + b_{15}x_1x_5 \\
 & + b_{23}x_2x_3 + b_{24}x_2x_4 + b_{25}x_2x_5 \\
 & + b_{34}x_3x_4 + b_{35}x_3x_5 \\
 & + b_{45}x_4x_5
 \end{aligned}$$

[7]

Construction of the MNOP design for 15 variables should be obvious from the above illustrations. The design has 15 rows with a single "1", 15 rows with a single "2", and 105 rows with two "1's", and one row of all "0's", giving a total of 136 design points. The design matrix is shown in Table 10. The columns denote the 15 variables x_1 through x_{15} . If a computer model simulation experiment were conducted using the MNOP design, the model given in equation [8] could be fitted for each dependent variable under investigation. Each fitted function could then be studied to determine the optimum systems mix for each measure of effectiveness.

$$\begin{aligned}
 y = & b_0 + b_1x_1 + b_2x_2 + \dots + b_{15}x_{15} \\
 & + b_{11}x_1^2 + b_{22}x_2^2 + \dots + b_{15,15}x_{15}^2 \\
 & + b_{12}x_1x_2 + b_{13}x_1x_3 + \dots + b_{14,15}x_{14}x_{15}
 \end{aligned} \quad [8]$$

If, however, the MNOP design is considered inadequate and the prior two-level examination has resulted in a screening of the original 15 input variables down to not more than 10 variables, a fractional factorial design can be applied.

c. $3^{k'-p}$ Fractional Factorial. If $k' \leq 10$, a fractional factorial experiment can be designed which has 243 design points. Theoretical background on $3^{k'-p}$ fractional factorial designs can be found in References 4, 5, 6, 7, 8, and 9.

The design is illustrated for $k' = 10$. The design is a $1/3^5 \times 3^{10}$, i.e., a 3^{10-5} fractional factorial. As in paragraph 4c above, the ten letters A, B, ..., K (excluding I) are used to represent the ten k' input variables x_1, x_2, \dots, x_{10} . Using the identifying contrast shown in Table 11 yields the design matrix given in Table 12.

Table 10. "Minimum Number of Points" Design Matrix
for 15 Variables

1	00000000000000	46	01100000000000	91	0000010000000001
2	10000000000000	47	01010000000000	92	0000011000000000
3	01000000000000	48	01001000000000	93	0000010100000000
4	00100000000000	49	01000100000000	94	0000010010000000
5	00010000000000	50	01000010000000	95	0000010001000000
6	00001000000000	51	01000001000000	96	0000010000100000
7	00000100000000	52	01000000100000	97	0000010000010000
8	00000010000000	53	01000000010000	98	0000010000001000
9	00000001000000	54	01000000001000	99	0000010000000100
10	00000000100000	55	01000000000100	100	0000010000000001
11	00000000010000	56	01000000000010	101	0000001100000000
12	00000000001000	57	010000000000010	102	0000000101000000
13	00000000000100	58	010000000000001	103	0000000100100000
14	00000000000010	59	001100000000000	104	0000000100010000
15	000000000000010	60	001010000000000	105	00000001000001000
16	000000000000001	61	001001000000000	106	00000001000000100
17	20000000000000	62	001000100000000	107	00000001000000010
18	02000000000000	63	001000010000000	108	00000001000000001
19	00200000000000	64	001000001000000	109	0000000011000000
20	00020000000000	65	001000000100000	110	0000000010100000
21	00002000000000	66	001000000010000	111	0000000010010000
22	00000200000000	67	001000000001000	112	0000000010001000
23	00000020000000	68	001000000000100	113	0000000010000100
24	00000002000000	69	001000000000010	114	0000000010000010
25	00000000200000	70	001000000000001	115	0000000010000001
26	00000000020000	71	000110000000000	116	0000000001100000
27	00000000002000	72	000101000000000	117	0000000001010000
28	00000000000200	73	000100100000000	118	0000000001001000
29	000000000000200	74	000100010000000	119	0000000001000100
30	000000000000020	75	000100001000000	120	0000000001000010
31	000000000000002	76	000100000100000	121	0000000001000001
32	11000000000000	77	000100000010000	122	0000000000110000
33	10100000000000	78	000100000001000	123	0000000000101000
34	10010000000000	79	000100000000100	124	0000000000100100
35	10001000000000	80	000100000000010	125	0000000000100010
36	10000100000000	81	000100000000001	126	0000000000100001
37	10000010000000	82	000011000000000	127	0000000000011000
38	10000001000000	83	000010100000000	128	0000000000010100
39	10000000100000	84	000010010000000	129	0000000000010010
40	100000000100000	85	000010001000000	130	00000000000010001
41	100000000010000	86	000001000010000	131	0000000000001100
42	100000000001000	87	000001000001000	132	0000000000001010
43	100000000000100	88	000001000000100	133	0000000000001001
44	100000000000010	89	0000010000000100	134	0000000000000110
45	100000000000001	90	0000010000000010	135	00000000000000101
				136	00000000000000011

Table 11. Identifying Contrast for a $(1/3)^5 \times 3^{10}$ Experiment^a

Factors: A, B, C, D, E, F, G, H, I, K

$I = \overline{BCDEFG} - \overline{ACDEFHIK} = \overline{ABCDEFHIK} - \overline{ABCEFGHIK} = \overline{ABCEFGHIK} - \overline{ABCDEFHIK}$

$= \overline{ABCDEF} \overline{FGHIK} - \overline{BDEFHIK} = \overline{ACDEFI} \overline{GH} - \overline{BCDFGHI} = \overline{ACDEFI} \overline{GH} - \overline{ABCDFGHI}$

$= \overline{ABDEF} \overline{GHIK} - \overline{ABCDEFH} = \overline{ABCD} \overline{EFHIK} - \overline{ABCDEFH} = \overline{ABCD} \overline{EFHIK} - \overline{ABCDEFH}$

$= \overline{CDGHJ} = \overline{ACD} \overline{EFH} - \overline{BDFGJ} = \overline{ACD} \overline{EFH} - \overline{ABC} \overline{FGHJ} = \overline{ACD} \overline{EFH} - \overline{ABC} \overline{FGHJ}$

$= \overline{CDEFH} - \overline{DEFCH} = \overline{ACGHI} - \overline{CDEIJ} = \overline{ACGHI} - \overline{ABC} \overline{EIJ} = \overline{ACGHI} - \overline{ABC} \overline{EIJ}$

$= \overline{ABC} \overline{CDGHI} - \overline{ABCDEFIJ} = \overline{ABC} \overline{CDGHI} - \overline{ABC} \overline{DEFIJ} = \overline{ABC} \overline{CDGHI} - \overline{ABC} \overline{DEFIJ}$

$= \overline{ADEF} \overline{GJK} = \overline{ABDEHK} - \overline{ACT} \overline{GHIK} - \overline{BDFGJK} = \overline{ABDEHK} - \overline{ACT} \overline{GHIK} - \overline{BDFGJK}$

$= \overline{ACEFGHK} - \overline{BDFGJK} - \overline{ABFGHK} = \overline{ACEFGHK} - \overline{BDFGJK} - \overline{ABFGHK}$

$= \overline{ACDEFGHK} - \overline{ABCDEFHK} - \overline{CDEFHK} - \overline{BEGHK} = \overline{ACDEFGHK} - \overline{ABCDEFHK} - \overline{CDEFHK}$

$= \overline{ABC} \overline{DEFHK} - \overline{ABCDEFHK} - \overline{ABC} \overline{EFHK} - \overline{ABC} \overline{EFHK} = \overline{ABC} \overline{DEFHK} - \overline{ABC} \overline{EFHK}$

$= \overline{CD} \overline{EFGHIK} = \overline{BCD} \overline{FGIK} = \overline{ABCD} \overline{EFHK} = \overline{ABC} \overline{CETFGHK} = \overline{ABC} \overline{CETFGHK}$

$= \overline{ACDEFGJK} - \overline{ABCDEFHK} - \overline{ACDEFHJK} = \overline{ACDEFGJK} - \overline{ABCDEFHK} - \overline{ACDEFHJK}$

$= \overline{BCD} \overline{EFGHK} = \overline{ABCDEFHK} - \overline{BCEFHK} = \overline{BCD} \overline{EFGHK} - \overline{BCEFHK}$

$= \overline{BCD} \overline{EJK} = \overline{CDEFGJK} = \overline{ABCDEFHK} - \overline{AEGHK} = \overline{ACDEFGJK} - \overline{ABCDEFHK}$

$= \overline{ACDEFHJK} = \overline{AEGHK} = \overline{ADFIJK} = \overline{ABCDEFGJK} - \overline{ACDEFHJK} = \overline{ABCDEFGJK} - \overline{ACDEFHJK}$

$= \overline{BDEFGHIK} = \overline{ABCDEFHK} - \overline{BCEFHK} = \overline{BCD} \overline{EFGHK} - \overline{BCEFHK}$

$= \overline{AEGHK} = \overline{ABCDEFHK} - \overline{BCEFHK} = \overline{ABCDEFHK} - \overline{BCEFHK} = \overline{ABCDEFHK} - \overline{BCEFHK}$

$= \overline{BCE} \overline{FGHIK} = \overline{ABC} \overline{DGFHK} = \overline{ABC} \overline{DGFHK} - \overline{ABC} \overline{EFGHK} = \overline{ABC} \overline{DGFHK} - \overline{ABC} \overline{EFGHK}$

aplan 243.10.9 in Reference 11.

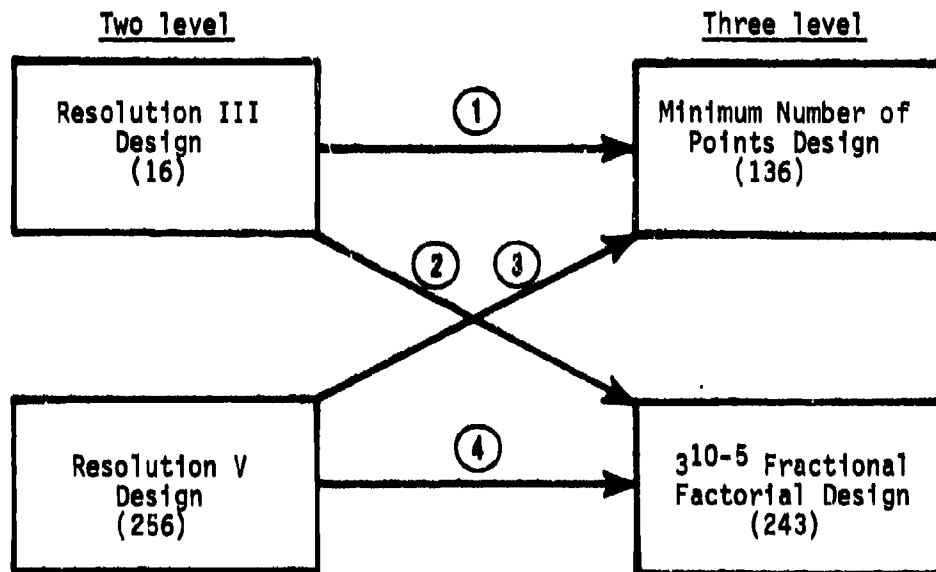
Table 12. 3^{10-5} Fractional Factorial Design Matrix

1	2	3	4	5
0000000000	0002112020	0001221010	0101010022	0100122012
2120012020	2122121010	2121200000	2221022012	2220101002
1210021010	1212100000	1211212020	1011001002	1010110022
0112110912	0111222202	0110001222	0210120201	0212202231
2202122202	2201201222	2200010212	2000102231	2002211211
1022101222	1021210212	1020022202	1120111211	1122220201
0221220121	0220009111	0222111101	0022200110	0021012100
2011902111	2010011101	2012120121	2112212100	2111021120
1101211101	1100020121	1102102111	1202221120	1201000110
6	7	8	9	10
0102001002	0200000011	0201102001	0200011021	0102120100
222210022	2022002001	2021111021	2020220011	2222102120
1012222012	1112011021	1111120011	1110202001	1012111110
0211011211	0011100220	0010212210	0012021200	0211200012
2001020201	2101112210	2100221200	2102000220	2001212002
1121002221	1221121200	1220200220	1222012210	1121221022
0020121120	0120210102	0122022122	0121101112	0020010221
2110100110	2210222122	2212001112	2211110102	2110022211
1200112100	1000201112	1002101021	1001122122	1200001201
11	12	13	14	15
0101202120	0100011110	0200100122	0302212112	0201021102
2221111110	2220020100	2020112112	2022221102	2081000122
1011220100	1010003190	1110121102	1112200122	1111012112
0210012002	0212121022	0012210001	0011022021	0010101011
2000021022	2000100012	2102222021	2101001011	2100110001
1122000012	1122112002	1222201011	1221010001	1220122021
0022122211	0021201201	0121020210	0120102200	0122211220
2112101201	2111210221	2211002200	2210111220	2212220210
1202110221	1201222211	1001102120	1000120210	1002202200
16	17	18	19	20
0001110111	0000222101	0002001121	C201210300	0200022220
2121122101	2120201121	2122010111	2021222220	2020001210
1211101121	1210210111	1212022101	1111201210	1110010200
0110220020	0112003010	0111110000	0010020112	0012102102
2200202010	2202011000	2201120020	2100002102	2102111222
1020211000	1022020020	1021102010	1220011122	1222120112
022200202	0221112222	0220221212	0122100021	0121212011
2012012222	2011212122	2010200202	2212112011	2211221001
1102021212	1101100202	1100212222	1002121001	1001200021
21	22	23	24	
0202101210	0002220222	0001002212	0000111202	
2022110200	2122202212	2121011202	2120120222	
1112122220	1212211202	1211020222	1210102212	
0011211122	0111000101	0110112121	0112221111	
2101220112	2201012121	2200121111	2202200101	
1221202102	1021021111	1020100101	1022212121	
0120021001	0220110010	0222222000	0221001020	
2210000021	2010122000	2012201020	2011010010	
1000012011	1100101020	1102210010	1101022000	
25	26	27		
0100200211	0102012201	0101121221		
2220212201	2222021221	2221100211		
1010221221	1012002111	1011112201		
0212010120	0211122110	0210201100		
2002022110	2001101100	2000210120		
1122001100	1121110120	1120222110		
0021120002	0020202022	0022011012		
2111102022	2110211012	2112020002		
1201111012	1200220002	1202002022		

The design permits fitting and testing 20 single-variable terms and 180 interaction terms. The 20 single-variable terms are the 10 linear terms x_1, x_2, \dots, x_{10} and the 10 quadratic terms $x_1^2, x_2^2, \dots, x_{10}^2$. Each of the $(10 \times 9)/2 = 45$ interaction effects have four terms, $x_1x_2, x_1x_3, x_1x_4, x_1x_5, x_2x_3, x_2x_4, \dots, x_8x_9$, giving a total of 180 two-variable terms. This leaves 42 degrees of freedom for Lack of Fit which can be used for testing. The fitted function of each measure of effectiveness can then be studied to determine the optimum systems mix in the same manner explained in the previous section.

6. SUMMARY. Four candidate experimental designs have been proposed for the Target Acquisition Systems Force Mix Evaluation Analysis methodology development. The designs, two two-level designs and two three-level designs, are recommended for sequential application. The resolution III and resolution V two-level designs contain 16 and 256 design points, respectively. The MNOP and the 3^{10-5} fractional factorial three-level designs contain 136 and 243 design points, respectively. Therefore, four candidate combinations of 2^m and 3^n sequential designs are available. The total number of computer model simulation runs range from $16 + 136 = 152$ to $256 + 243 = 499$. The sequential designs and the required numbers of model runs are shown in Table 13. The number of model runs is shown in parentheses.

Table 13. Candidate Sequential 2^m and 3^n Designs



REFERENCES

1. BDM Service Company, "DIVOPS: A Division-Level Combined Arms Engagement Model (Version 3)," Leavenworth, KS, October 1975.
2. Box, G. E. P. and Hunter, J. S., The 2^{k-p} Fractional Factorial Designs, Part I, Technometrics, Vol. 3, No. 3, pp. 311-351, 1961.
3. Box, G. E. P. and Hunter, J. S., The 2^{k-p} Fractional Factorial Designs, Part II, Technometrics, Vol. 3, No. 4, pp. 449-458, 1961.
4. Cochran, W. G. and Cox, G. M., Experimental Designs, John Wiley and Sons, Inc., New York, 1957.
5. Davies, C. L. (Ed.), Design and Analysis of Industrial Experiments, Hafner Publishing Company, New York, 1960.
6. Winer, B. J., Statistical Principles in Experimental Design, McGraw-Hill Book Company, Inc., New York, 1962.
7. Hicks, C. R., Fundamental Concepts in the Design of Experiments, Holt, Rinehart, and Winston, Inc., New York, 1964.
8. Kirk, R. E., Experimental Design: Procedures for the Behavioral Sciences, Brooks/Cole Publishing Company, California, 1968.
9. Anderson, V. L. and McLean, R. A., Design of Experiments: A Realistic Approach, Marcel Dekker, Inc., New York, 1974.
10. Connor, W. S. and Zelen, M., Fractional Factorial Experiment Designs for Factors at Two Levels, NBS Applied Mathematics Series 48, US Government Printing Office, Washington, DC, 1957.
11. Connor, W. S. and Zelen, M., Fractional Factorial Experiment Designs for Factors at Three Levels, NBS Applied Mathematics Series 54, US Government Printing Office, Washington, DC, 1959.

**Environmental and Water Quality Operational
Studies: Experimental Design Problems
Associated with the Fisheries of the
Mississippi River**

**Michael P. Farrell,
A. Dale Magoun,**

**Environmental Laboratory
Waterways Experiment Station
Vicksburg, Mississippi**

Introduction

The Waterways Experiment Station is conducting a six-year, nationwide program of applied research to investigate selected high priority environmental quality problems associated with the Civil Works activities of the Corps of Engineers (CE). The study is being conducted for the Office, Chief of Engineers, and is entitled the Environmental and Water Quality Operational Studies (EWQOS).

The principle goal of EWQOS is to provide new or improved methodologies and technology for the planning, design, construction, and operation of CE projects to meet environmental quality objectives in a manner compatible with project purposes. A key element of EWQOS is the use of extensive field studies to evaluate and document the utility of new or improved methodologies and technology developed within the program.

During the early planning phase of EWQOS, visits by WES personnel were made to each CONUS Corps Division office to identify and assess the magnitude of environmental quality problems. The nature and extent of environmental quality problems being experienced by Corps field offices was used as a basis for planning research to address these problems. One major problem area identified as being of high priority was the environmental impacts of project activities on waterways. Specifically, it was determined that EWQOS research should develop field office guidance to address environmental and water quality aspects of dikes and revetments. Such structures are common in waterways in many parts of the United States, but most commonly occur along the Mississippi River and its tributaries.

Based on this problem identification phase, a project was established within EWQOS to conduct a comprehensive field study of dikes and revetments associated with CE waterway navigation projects. This field study is being undertaken within a 50 mile reach of the Lower Mississippi River between Lake Providence, Louisiana, and Greenville, Mississippi. This site was selected after an intensive survey of CE waterways navigation projects and after discussions with knowledgeable CE field personnel. Site selection was based on the existence of an extensive hydraulic and hydrologic data base, the presence of a representative variety of dike and revetment structure design, and optimum diversity of characteristic floodplain and riverine aquatic macrohabitats, and plans by the Vicksburg District to conduct potamology studies in the reach during the time frame of EWQOS, and to synthesize in a report the existing hydraulic and sediment data.

Goals and Objectives

The goal of the long-term waterway field study of dikes and revetments is to assess the relative ecological importance of channel alignment and bank stabilization structures in the riverine ecosystem, and

to provide data to formulate environmental quality guidelines for use by CE districts in designing and planning new structures and modifying existing ones.

The specific objectives are based on a macrohabitat approach in which revetted banks and dike fields are considered as aquatic habitats within the river system.

(1) Quantitatively define riverine macrohabitats of the study reach including relative size, current velocity, sediment type, materials composing the dikes and revetments and associated riparian vegetation at various river stages and times of year.

(2) Quantitatively describe the physicochemical characteristics of the water and sediments in riverine macrohabitats at various river stages and times of year and how these variables relate to the distribution and abundance of aquatic organisms.

(3) Quantitatively describe the composition of the particulate organic matter, including phytoplankton, zooplankton, and detritus, in riverine macrohabitats at various river stages and times of year.

(4) Quantitatively describe the species diversity, abundance distribution and production of benthic macroinvertebrates in riverine macrohabitats, including the use of these habitats as spawning, nursery, and feeding areas.

(5) Quantitatively describe the species diversity, abundance distribution and production of fishes in riverine macrohabitats, including the use of these habitats as spawning, nursery and feeding areas.

General Background

Dikes have been placed in rivers by the CE for many years for the purpose of aligning and contracting river channels. The lower Mississippi, middle Mississippi, Missouri, and Arkansas are examples of rivers that have extensive amounts of dike structures. In navigation projects, the principle use of dikes is in adjusting channel width, depth, and alignment and to close secondary channels and chutes. Dike structures are probably the most effective means of channel alignment and contraction in use today.

Dikes are structures constructed of permeable wooden piles or, more typically in present times, of relatively impermeable stone riprap. Dikes may be singular or placed one after another along a bank forming a dike field. Generally dikes are of the transverse type which extend from the bank perpendicularly into the river channel past the point of highest current velocities. An extension or L-head may be placed at the off-shore end of a dike parallel to the main axis of the dike to retard scouring and turbulence. Vane dikes which are placed in the channel parallel to the bank line are also used.

Water is shunted by a dike toward the opposite river bank and, if this bank is stable, the resulting narrower channel is deepened by scouring in order that the river's discharge may be carried. Dikes are typically placed on the convex side or point bar in a bendway or in straight reaches to achieve some degree of channel sinuosity and resulting contraction. Concurrent with channel contraction, suspended sediments are deposited downstream of individual dikes due to the reduction of current velocities caused by the structure. In dike fields sediment accretion may be appreciable, and these accumulated sediments, which may in some instances form fast land or a bar, further serve to confine the flow of water. Slackwater pools may be found downstream of transverse dikes at low river stages in cases where sediment accretion has not completely filled in these areas. Since, ecologically, slackwater areas are thought to be important in a river system, notches have been put in transverse dikes to prevent sediment buildup on the downstream side of dikes.

In the lower Mississippi River there are presently 393 dikes totaling approximately 875,000 linear feet (Table 1). The number of dikes diminishes downstream in lower Mississippi River, with no dikes being present in the river within the confines of the New Orleans District. However, many new structures are planned within the next two decades in the lower river.

Despite the large number of dikes present in many of the major river systems of the United States, the ecological effects of these structures are poorly known. Dike fields and individual dikes are distinct habitats within river systems where these structures are numerous. Data on this environmental quality characteristics of these structures and methods for designing and modifying dikes to enhance their value as aquatic habitat is needed by CE districts and divisions in designing and operating waterway navigation projects.

Revetments are installed along river banks to prevent bank caving and erosion. These structures are of many types, but generally consist of erosion-resistance materials which are placed upon a pregraded bank from the top of the bank line to the toe of the channel. In navigation and flood control projects revetments are often located on the concave bank in bendways and crossings in association with dike fields on the opposite bank to contract the river channel and to retard meandering. They are also placed in areas where erosion threatens levees.

Bank revetments are of many different types including stone riprap and articulated concrete mattresses (ACM). ACM with stone riprap placed on the upper portions of the bank as paving is the most common type of revetment presently being installed in the lower Mississippi River. In the past, asphalt and willow mats were used instead of riprap for bank paving. Approximately 3.9 million linear feet of bank revetment works have been constructed in the lower Mississippi River. In the Missouri River, revetments constructed of stone riprap are used extensively.

When river banks are revetted, much of their natural character is

Table 1

Dike and Revetment Structures in the Lower Mississippi River¹

Linear Ft. of Revet.	1,758,515	1,202,610	930,721	3,891,846	ln ft
Linear Ft. of Dikes	583,498	292,229	0	875,727	ln ft
No./Types	pile (wood)	31	8		
	pile & stonefill	68	24		
	stone	137	90		
	stone trail	6	5		
	stone vane	8	15		
	car body		1		
Total No. Dikes	250	143	0		

¹

Source of information. George Kerr, MRC, 327. (As of 30 September 1977).

altered. However, the environmental quality of the habitat formed by the revetment structures is unknown. Older revetment structures which have become extensively vegetated with willow and cottonwood trees and a variety of sedges, grasses, and shrubs may have different value as aquatic habitat than new revetments. Thus age is a variable of importance in evaluating environmental effects of revetments. The type of material composing the revetment may also be an important variable in determining the biological productivity and habitat value of revetment structures. For example, stone riprap is probably a more productive substrate for fish food organisms than asphalt. Another factor is the sinuosity of the bank line upon which revetment is placed. A sinuous bank would tend to have relatively lower velocities caused by eddies and upstream flow than would a straight bank line, and would, therefore, be expected to constitute more productive fish habitat.

The large magnitude of revetted banks in many river systems make investigation of the environmental effects of these structures of value to CE districts and divisions for use in impact assessments, and the planning, design, and construction of new structures. At present there exists very little environmental data on revetment structures regarding their productivity as compared to "natural" banks.

The distribution and abundance of organisms in a large river system are fundamentally determined by river geomorphology, flow, and sediment load for it is these factors which interact to produce distinct environments or macrohabitats for riverine biota. Undoubtedly, water quality, temperature sediment type and other factors are important determinants of the distribution and abundance of aquatic species in a given river but these are secondary to the more basic geomorphology and hydraulic features of the stream. Land use practices, terrestrial vegetation patterns, and edaphic characteristics in the drainage basin, also contribute importantly to the environmental conditions of the river, but these factors mainly impose conditions upon the macrohabitats formed by the rivers' shape, flow, and sediment load. For example, a broad, shallow braided river has different proportions and types of macrohabitats than a stream with a deep, narrow well-defined channel, irrespective of water quality.

The channel alignment and bank stabilization structures placed in rivers by the Corps for achieving flood control and navigation objectives can modify to different degrees geomorphology, stage and discharge relationships, and sediment movements within the stream. These changes in the river's characteristics, plus the presence of the structures themselves as a substrate for organisms, result in shifts in the types, sizes and variety of aquatic macrohabitats. Such alterations in riverine habitats effected by the installation of structures may or may not produce positive impacts on the ecology of the system. For example, certain "natural" macrohabitats may be reduced in size and quality by training and stabilization structures, while habitats created by the installed structures, such as dike fields or revetted banks, may become commonplace. The primary goal of this research is to determine the ecological importance or value of the

macrohabitats formed in the river by dike fields and revetted banks as compared to "natural" habitats, and to formulate environmental quality guidelines for use in designing and planning new structures and modifying existing ones.

The general approach to the dike and revetment study in the lower Mississippi River will be from a macrohabitat point of view, wherein the length of river to be investigated will be subdivided into its macrohabitats which will be characterized as to both biotic and abiotic variables. Dike fields and revetted banks will be treated as macrohabitats, although man-made, together with other distinct biological habitats such as the main channel, natural steep banks, towheads, chutes, river borders, point bar cutoffs, and old river channels. The ecological importance of each macrohabitat will be evaluated according to its basic water quality, production of benthic organisms used as fish food, abundance of fishes, use as spawning, nursery and feeding areas for fishes, and production of suspended particulate organic matter. The function and relative value as aquatic habitats of dike fields and revetted banks within the river ecosystem will be defined based on this information. The habitat evaluation will be related to various key river stages and times of year.

The dike and revetment study will be initiated by preparing a quantitative map of aquatic macrohabitats in the 50 mile reach of lower Mississippi River selected for study. These data will form the basis of the field investigations. The map will be prepared using existing hydraulic and topographic survey data and aerial photographs belonging to the Vicksburg District as a basis. Habitats will be initially delineated at a low water stage, defined as 0 ft Low Water Reference Plane, using as criteria primarily depth and information from aerial photographs as to the location of sandbars and other features. This map will be refined as to the definition of habitats with data on currents, sediments, and biota collected during the pilot survey. The map will be redefined for bank full and over-bank river stages.

The first efforts in the field will be a series of pilot surveys designed to provide additional data for the habitat map, for developing and testing sampling equipment and techniques, selecting representative habitats for intensive study, and developing an experimental design for the habitat surveys and detailed ecological studies. The pilot survey will be conducted from April through September, 1978.

Following completion of the pilot survey and formulation of experimental designs, at least two representatives of each habitat type will be selected for comparative study. Dike fields and revetments will be included in the category of habitats. Selected habitats will be surveyed intensively four times each year, beginning in the fall of 1978. Data on biota, water and sediment chemistry and physical variables will be collected in a manner amenable to detailed statistical comparisons. The four yearly samples will be related to distinctive river stages and seasons.

Detailed ecological studies will be carried out in a few selected habitats to investigate specific phenomena of interest. In general, these studies will require collection of samples at short time intervals during particular years, seasons, or river events such as flooding, and will be directed towards answering specific questions. Examples of these types of studies include particulate organic matter composition and distribution studies, determination of fish spawning periods and locations, fish movements studies, studies of stream macroinvertebrate drift, secondary production estimates for organisms growing upon the stone riprap and other materials of which dike and revetment structures are constructed, and fish food habit studies.

RED NOISE IN THE POWER SPECTRUM OF ATMOSPHERIC TEMPERATURE DATA

Oskar M. Essenwanger
Research Directorate
Technology Laboratory
US Army Missile R&D Command
Redstone Arsenal, AL 35809

ABSTRACT. It is well known that persistence generates red noise in power spectra of meteorological time series. In fact, significance of spectral peaks is checked against the background of white or red noise, although other criteria have been suggested in the literature.

Several types of red noise exist. In atmospheric science the most common type is the exponential model which is identical with the first order Markov chain. This type is easy to recognize and can be readily calculated from the correlogram.

Today power spectra are mostly produced with the algorithm of the Fast Fourier Transform (FFT) rather than based on the autocorrelogram. Consequently, calculation of the exponential red noise is difficult unless the first lag correlation is included in the computer processing.

Two questions have been pursued in this paper. What is the effect on the exponential red noise pattern if any periodicity, significant or not, is removed from the power spectrum? Can true periodicities with low wave numbers be distinguished from red noise?

The influence of "quasiperiodicity" on red noise, the power spectrum and Fourier components is analyzed for atmospheric temperature data. Finally, the utilization of discrete spectral filters will be discussed and a separation of the time series into cycles, quasicycles and red noise is delineated.

I. INTRODUCTION. The question of the reality of meteorological cycles has been raised at various times in the past (e.g., Bartels, 1943; Brier et al., 1964; Craddock, 1965; Shapiro, 1975; etc.) and has not been completely settled. The physical mechanism behind the annual and daily cycle in meteorological time series leaves no doubt about their reality, but most other periodicities are accepted by some authors and rejected by others. Although significance criteria have been developed in statistical analysis, the subjectivity in the adoption of a significance threshold leaves some ambiguity.

In addition, many criteria are based on the postulation that the data are independent and/or Gaussian distributed which is not applicable to many atmospheric elements. It is well known that most atmospheric time series show varying degrees of persistence. This persistence is usually taken into account by testing time series data, e.g., power spectra, against "red noise" which is generated by persistence. An added difficulty is the appearance of the "quasiperiodicity" where apparent cycles prevail during a limited time only.

It is well known that red noise is related to the first lag correlation coefficient but the modification of this coefficient by the presence of a cycle is neglected in most references. It will be shown that the construction of red noise is not independent of the presence of cycles, and it is not trivial to select a red noise test background.

Time series data of atmospheric temperature serve as an example for a mixture of cycles and red noise pattern. An attempt is made to separate these two components. It proved that the power spectrum has the advantages of disclosing significant cycles in concentrated form and of responding better to quasiperiodicity than the Fourier analysis. The Fourier analysis is the most appropriate tool to provide quickly amplitude and phase angle for spectral filters. The periodogram analysis reveals quasiperiodicity best and permits us to pinpoint the exact cycle length.

II. THE EXPONENTIAL RED NOISE MODEL. Different types of red noise patterns have been discussed by the author (1977), and only the equations for the exponential model will be presented here.

The most common red noise in meteorology follows a plain exponential sequence:

$$\rho_t = \exp(-bt) \quad (1)$$

with

$$t \geq 0, b > 0.$$

This exponential series is also obtained from a first order Markov chain:

$$\rho_k = \rho^k. \quad (2)$$

It is trivial that $t = k$, $b = -\ln \rho$, and $0 < \rho < 1.0$. In the first order Markov chain $\rho = \rho_1$. The constant b in the exponential noise can be calculated from:

$$b = -\ln \rho_1 \quad (3a)$$

We must also keep in mind that by eqn. (1) the ρ_t follows the exponential distribution (see Essenwanger, 1976, p. 113). Consequently:

$$\sum_t \rho_t = 1/b_1 \quad (3b)$$

Because in practical applications the summation is truncated after m terms, $b \neq b_1$, and some discrepancies between eqn. (3a) and (3b) may arise.

A suitable equation for the power spectrum has been deduced by Gilman et al. (1963). They cast:

$$L_1 = [(1 - \rho^2)/(1 - \rho^2 - 2\rho \cos k\pi/m)]/m \quad (4)$$

In our case $\rho \equiv \rho_1$.

Other models and their differences have been analyzed by the author (1977). It becomes evident that ρ_1 is a crucial parameter in red noise analysis. Eqns. (1) and (4) are related by:

$$\rho_t = \sum_{k=1}^m L_k \cos(k\pi/m) \quad (5)$$

III. RED NOISE MIXTURE WITH CYCLES. The general meteorological time series may comprise a mixture of red noise and periodicities. This fact was previously exemplified with the aid of three-hourly temperature data at Huntsville, Alabama for a time period from 6 November 1958 through 14 March 1959 with $N = 1024$ (see Essenwanger, 1977). In this article the author has illustrated that an appropriate combination for the structure of the autocorrelation function is:

$$\rho_i = w_1 \rho_{R_i} + \sum_{j=2}^n w_j \rho_{ji} \quad (6)$$

where:

$$\sum_1^n w_i = 1 \quad (6a)$$

and ρ_{R_i} denotes the red noise, ρ_{ji} the correlation of the respective cycle L_j . (The consideration is for data without a trend). This simple linear (weighted) combination of correlation coefficients works better than Fisher's z function which is suggested for the combination of correlations by various authors. A numerical example which confirmed eqn. (6) was given by the author (1977).

Let us assume that $\omega_1 = 0.5$ and $\omega_2 = 0.5$. The first lag correlation coefficient for red noise could be $\rho_{R_1} = 0.6$ and $\rho_{2,1} = 0.4$ from a cycle. Then the first lag correlation of the data series is $\rho_1 = 0.5 (0.6 + 0.4) = 0.5$ which is less than ρ_{R_1} . In this case the correct size of the first lag correlation for red noise is not identical with the first lag correlation of the data series.

IV. POWER SPECTRUM, QUASIPERIODICITY AND FOURIER ANALYSIS. Three different statistical tools are available for the analysis of meteorological time series data: power spectrum, Fourier series and periodogram. These three individual techniques serve different purposes. Consequently, we must expect that different characteristics are enhanced by the analysis of the same data sample with different methods although the meteorological characteristics do not vary.

A set of 8-hourly data (one year from 1 September 1959) was subjected to a Fourier analysis. Today this task is rapidly performed by application of the FFT, the fast Fourier Transform (see Cooley and Tukey, 1965). The FFT, conveniently performed for a basic period of $1024 = 2^{10}$, shows a first significant cycle of 341.3 days, the annual period.

The 24^{h} cycle is not a period of an integer divisor, and is spread over the wave numbers 339-345. A more sophisticated computer program was utilized for the FFT, which does not require that the basic period can be expressed as a power of 2. This Fourier analysis was established with a basic period of 365 days. In this analysis the day is an integer wave number, and a sharp peak appears alone at 24^{h} , i.e., wave number 365, without spilling over to the adjacent classes.

This fact confirms results by Rikiishi (1976), and illustrates some fundamental characteristics of power spectrum, FFT and Fourier analysis. If an existing cycle is not precisely the length governed by an integer wave number the cycle is "smear" over the neighboring frequencies. One solution is the use of a "filter band" (or band filter) whose width is determined by the spreading. If one particular cycle exists, the precise length can be found by a periodogram analysis (see Essenwanger, 1976, p. 234).

The utilization of a filter band for the representation of a cycle has some added benefits. A peak in the power spectrum may indicate quasi-periodicity. This expression may comprise two phenomena. First, the cycle length may fluctuate, e.g., in our case between 5 to 6 days (or even 4 to 7 days). Second, the cycle may be repetitive over a few periods, and then suddenly either disappear or become longer or shorter. The power

spectrum or Fourier analysis reflects the closest mathematical fitting, resembling an average cycle (see Essenwanger, 1951). Quasiperiodicity is weakening the amplitude over the total data length, and the significance of quasiperiodicity is difficult to prove by statistical tests because of the resemblance to random cycles. Indeed, some authors consider quasiperiodicity by and large as a totally random product. It must be interjected, however, that in atmospheric science a physical background for quasiperiodicity can sometimes be found. E.g., a cycle of 5-6 days can be generated by the development of sets of cyclones, so-called families of cyclones. The length of this development fluctuates but the fact of its existence cannot be denied.

The explanation of a 5-6 day cycle as related with the development of cyclone families is also supported by an examination of the FFT for the winter 1976/77 with predominantly meridional circulation. In this "cold winter" at Huntsville, Alabama, the 5-6 day "quasiperiodicity" was absent, and was replaced by an 8-9 day quasicycle.

V. EXAMPLE OF SEPARATING RED NOISE FROM CYCLES. After the utilization of filter bands has been explained we return to the analysis of two data sets: the time series of 6-hourly temperature observations from 15 July 1959 to 10 July 1960 and 15 July 1961 to 10 July 1962. The truncation of 5 days from the year simplified the computational efforts for the application of the FFT and its relationship with the power spectrum. Later one full year of data was utilized but the results from the full year differed only by 0.1% from the truncated series.

The elimination of cycles (quasicycles) was performed in three steps (see Figures 1a and b). First, the spectrum of the original data series was obtained. Then the annual and daily cycles were removed. The remaining data were subjected to the FFT again. A series of "quasicycles" or "quasiperiodicities" were identified and subtracted. Afterwards, the spectrum of the remaining data series displayed only insignificant deviation from the recalculated red noise series thus leaving the "noise" or random fluctuations with persistence. The cycles and quasicycles with their percentage share are exhibited in Table 1.

At first glance we may find it peculiar that the annual cycle is listed as a filter band from the wave numbers 1-7. One would think that the truncation of 5 days from the year should not make a significant difference. In reality a peak appeared at 360 days with a side lobe at 90 days length. It was convenient to eliminate the total series of waves from 1-6 or 1-7. The appearance of this filter band may be caused by the asymmetric behavior of the annual cycle.

Table 1. Separation of Temperature Time Series Data into Cycles (Quasicycles) and Red Noise

1961				1959			
Wave Number		%	Wave Number		%		
1 - 7	Annual	67.0	1 - 6	Annual	71.3		
12 - 15	24 - 30 days	1.5	13 - 23	16 - 28 days	4.9		
20 - 28	13 - 18 days	3.9	28 - 33	11 - 13 days	1.7		
33 - 41	9 - 11 days	3.3	43 - 52	7 - 8 days	1.5		
51 - 53	7 days	0.8	61 - 70	5 - 6 days	0.8		
73 - 86	4 - 5 days	2.1	-	-	-		
359 - 361	daily	10.2	359 - 361	daily	8.6		
720	semi-daily	0.5	710	semi-daily	0.4		
Red Noise		10.7	Red Noise		10.8		

A distinct peak at wave number 360 appeared which signifies the daily cycle. The adjacent classes 359 and 361 displayed an amplitude more than 10 times as large as the adjacent waves (350 to 358 or 362 to 369). In order to eliminate a remaining peak at the daily cycle in the power spectrum of the red noise series the band from 359 to 361 was removed.

It is evident from Table 1 that the "quasicycles" fluctuate from year to year which should be expected. These quasiperiodicities vary in amplitude, phase angle and duration. As pointed out some authors consider them equivalent to random fluctuations. The red noise series and displayed power spectrum after removal of cycles (middle of Figures 1a and b) illustrate that additional cycles (i.e., quasicycles) should be subtracted to achieve a better agreement (see right hand side of Figures 1a and b).

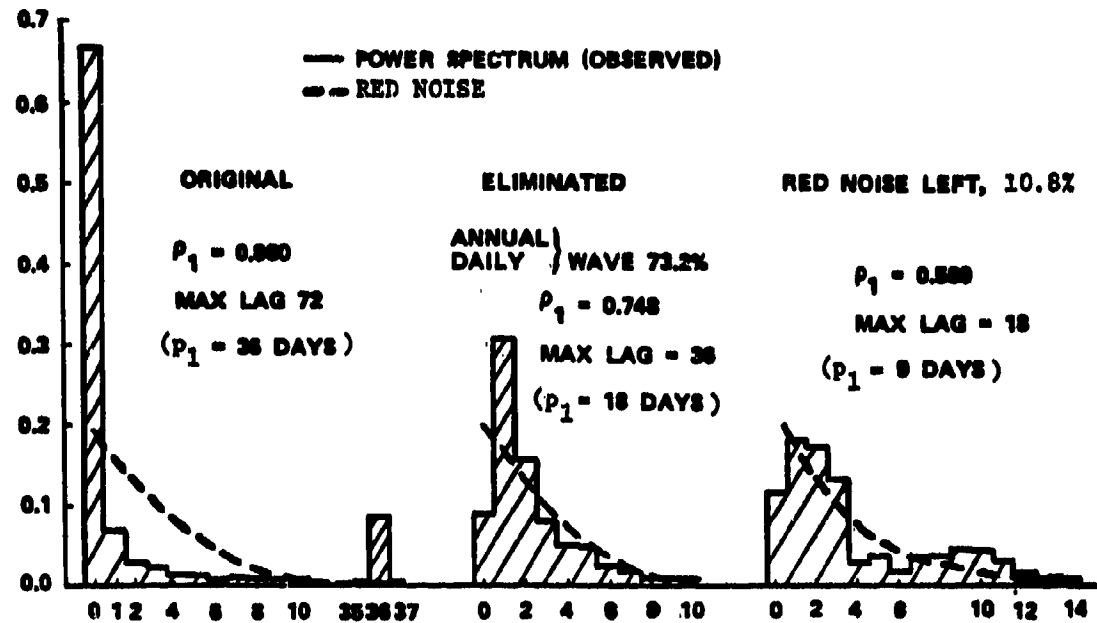
Thus, the time series of the two sets of data samples can be expressed by 3 cycles (annual, daily and semi-daily) with about 78 to 80% of the variance, 4 or 5 (for 1959 and 1961, respectively) quasicycles with an added 9 to 11%, and a remaining red noise component of about 11%. The proper red noise influence is then:

$$\rho_{R_1} = \left[\rho_1 - \sum_{j=2}^n \omega_j \rho_{j1} \right] / \omega_1 \quad (7)$$

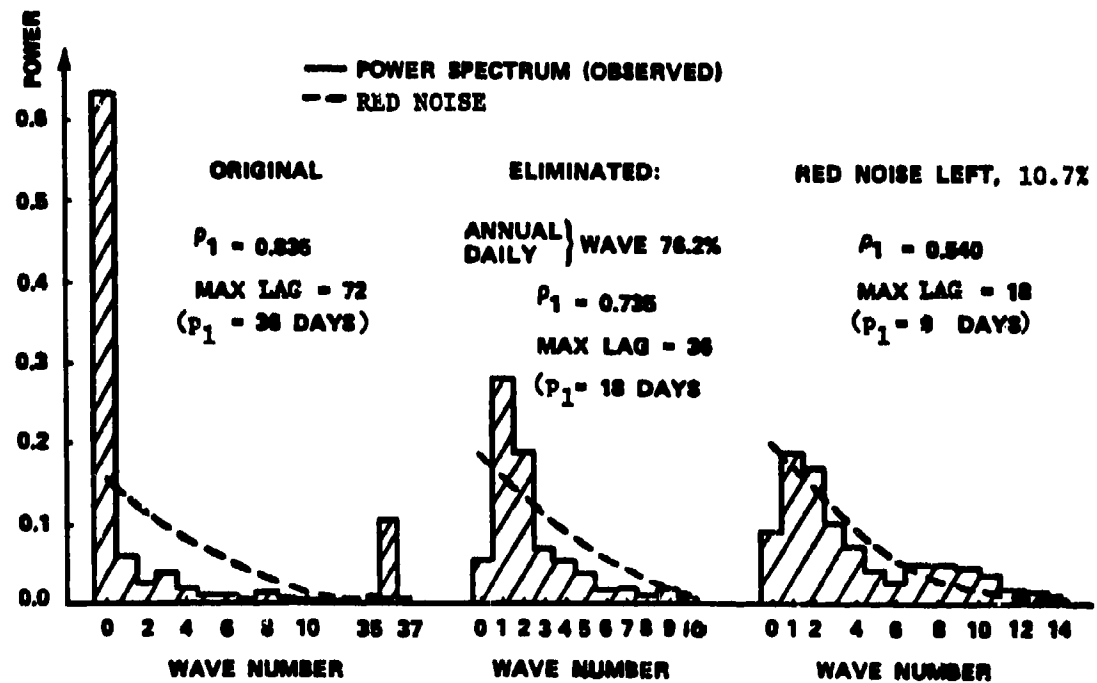
where $\rho_1 = 0.86$ for the 1959/60 data set, $n = 7$, and $\rho_{R_1} = 0.59$. The respective numbers for the data set 1961/62 can be found from Figure 1b and Table 1. It is evident that the true red noise first lag correlation is different from ρ_1 .

FIGURE 1. SIX-HOURLY TEMPERATURE DATA

HUNTSVILLE, ALABAMA,
 (a) 15 JULY 1959 - 10 JULY 1960



(b) 15 JULY 1961 TO 10 JULY 1962



We can safely deduce that the red noise pattern cannot be obtained in a trivial way in the presence of cycles. Furthermore, the first lag coefficient ρ_1 in the autocorrelation is not automatically the one which provides the proper red noise entry. How does this result affect significance testing of the power spectrum against the statistical background of red noise? The answer is not simple and depends on the goal.

If we only intend to find whether the power spectrum is produced by red noise, the pattern based on the first lag coefficient may suffice. If our goal is the separation of the data series into cycles and red noise, a formalistic application of the first lag correlation is not realistic unless we find no cycles.

A similar composite pattern to the autocorrelation can be developed for the power spectrum. We deduce:

$$L_j = \omega_1 L_{R_j} + \sum \omega_k F_k(L_j) \quad (8)$$

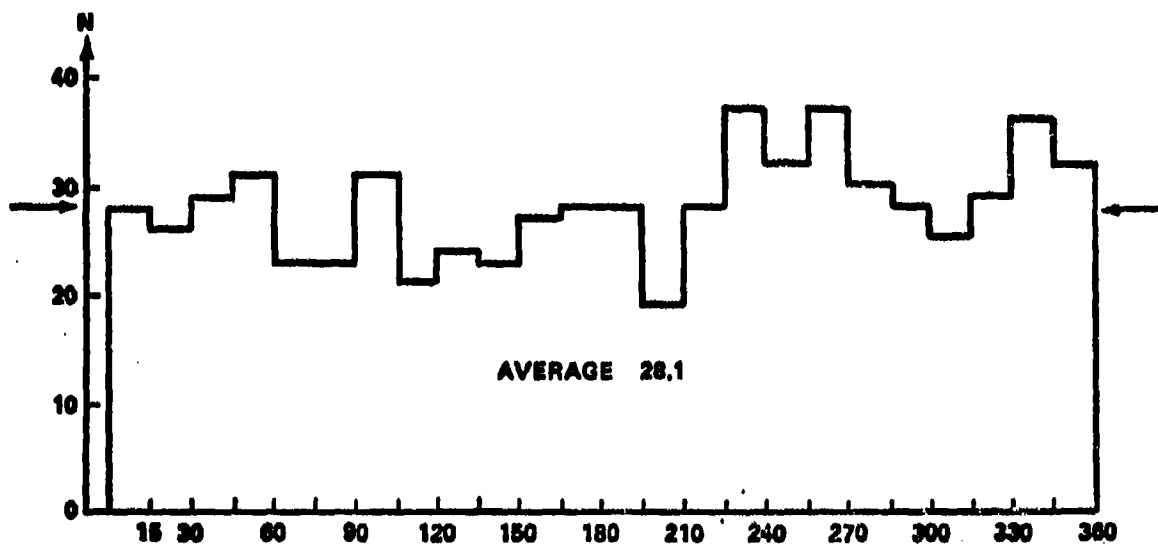
where $F_k(L_j)$ stands for the spectrum of the filters.

The reconstruction of the red noise component in the data series is not trivial because the phase angles for the Fourier terms must be known. One way to obtain these is by eliminating the filter bands from the data series, and subjecting the remainder to a FFT. This method is not difficult to develop once it is known which cycles (quasicycles) must be removed. Furthermore, random fluctuations will produce randomness of the phase angles for the red noise waves. We can check whether the remaining phase angles display randomness because it requires a rectangular distribution of the angles. The result is disclosed in Figures 2a and b. The deviation from the average number of occurrence, 28.1 or 28.2, was tested for statistical significance by applying the Kolmogorov-Smirnov test for the cumulative distribution. None of the deviations proved to be high enough to reject the hypothesis that the displayed histogram has a rectangular distribution as statistical background. We find confirmation that the remaining data series behaves like red noise in amplitude, and now in phase angles.

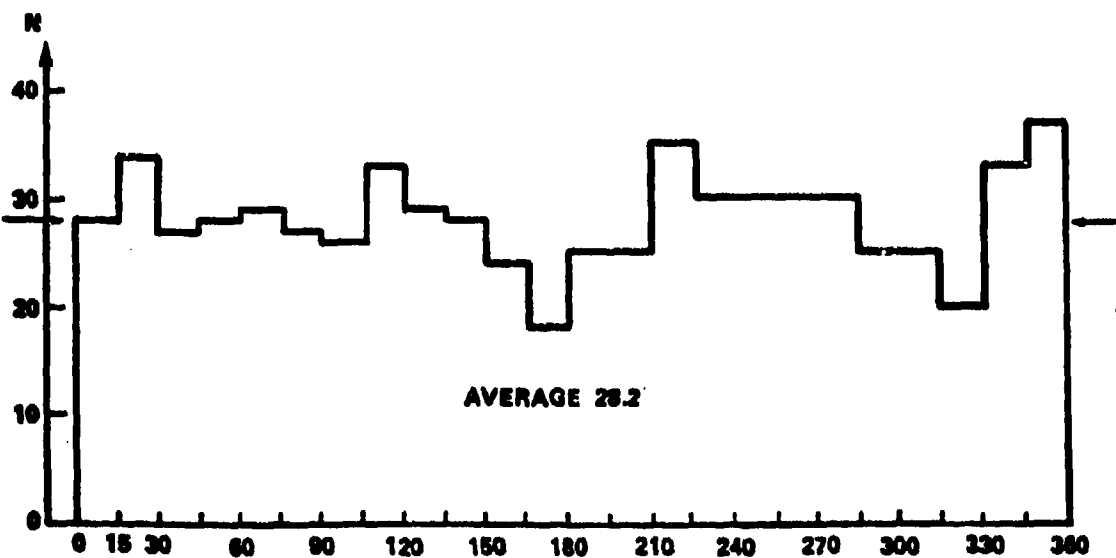
VI. CONCLUSION. The background of red noise in meteorological time series has been examined for temperature data at Huntsville, Alabama. Of special interest was the question whether significant cycles influence the determination of the red noise pattern from autocorrelogram or spectral analysis. As illustrated, the presence of long time periodicities tends to increase the first lag correlation. In fact, any existing cycle may modify it. Therefore, the judgment of red noise from the first lag correlation alone may be insufficient in many cases.

**FIGURE 2. FREQUENCY DISTRIBUTION OF PHASE ANGLE
(RED NOISE)**

(a) 59-07-15



(b) 61-07-15



This result is important in the evaluation of an existing time series, but it may be of little consequence for the testing of cycles against red noise background. However, the drawing of conclusions from one test curve alone may not always be advisable. A sequence of testing such as the 3 steps illustrated in Figures 1a and b may be more appropriate.

A separation of the data series into red noise and cycles was delineated (Figures 1a and b). This method resembles Craddock's (1965) suggestion of filtering insofar as certain significant cycles are filtered out. Two significant deviations from Craddock's scheme must be emphasized. First, the filtered cycles are subtracted from the total data series after the cycles have been determined from the power spectrum. Second, the remaining data series is a red noise spectrum. These differences are produced by the dissimilarities in the analysis goals between Craddock's method and the technique of this study.

The red noise contribution to the variance of the two sets of data of 3 hourly observation for about one year is approximately 11%, i.e., this percentage can be associated with random noise with persistence while the remaining fluctuations are produced by cycles or quasicycles. About 80% represent the diurnal, semi-diurnal and annual cycle which can be considered as a simple and predictive part. Quasicycles impose some restrictions to the predictability because they vary from year to year, and the red noise fluctuations are predictive only with respect to their statistical properties. The determination of the contribution of red noise in meteorological time series may thus be important information.

VII. REFERENCES CITED.

- Bartels, J., 1943. Gesetz und Zufall in der Geophysik, Naturw., 31, 421-435.
Brier, G.W., Shapiro, R., and MacDonald, N.J., 1964. A Test for the Period of 18 Cycles per Year in Rainfall Data. J. Appl. Meteor., Vol. 3, 53-57.
Cooley, J. W. and Tukey, J.W., 1965. An Algorithm for the Machine Calculation of Complex Fourier Series. Math. Comput., 19, 297-301.
Craddock, J. M., 1965. The Analysis of Meteorological Time Series for Use in Forecasting. The Statistician, 15, 167-190.
Essenwanger, O. M., 1951. Beiträge zur Statistik mittellanger Luftdruckwellen in Mitteleuropa. Ber. Dt. Wetterd. in US Zone, Nr. 20, pp 19.
Essenwanger, O.M., 1976. Applied Statistics in Atmospheric Science, Part A. Frequencies and Curve Fitting. Elsevier, Amsterdam, pp 412.
Essenwanger, O.M., 1977. Red Noise Analysis in Autocorrelogram and Power Spectrum of Atmospheric Temperature. Preprint Volume, 5th Conf. Prob. Stat., Nov 15-18, 1977, published by Am. Meteor. Soc., 1977.

- Gilman, D. L., Fuglister, F. J., and Mitchell, J. M. Jr., 1963.
J. Atmosph. Sciences, 20, 182-184.
- Rikiishi, F., 1976. Methods of Computing the Power Spectrum for
Equally Spaced Time Series of Finite Length. J. Appl. Meteor.,
15, 1102-1110.
- Shapiro, R., 1975. The Variance Spectrum of Monthly Mean Central
England Temperatures. Qu. J. Roy. Meteor. Soc., 101, 679-681.
- Taubenheim, J., 1969. Statistische Auswertung geophysikalischer und
meteoreologischer Daten. Akadem. Verlagsgesellschaft, Leipzig,
pp 386.

ACKNOWLEDGMENT: The author wishes to express his sincere thanks to Dr. Dorothy A. Stewart for her critical review of the manuscript. Mrs. Clara Brooks deserves credit for her diligent efforts of expeditiously typing and assembling the manuscript.

SMALL SAMPLE BEHAVIOR OF SOME PROCEDURES USED
IN TIME SERIES MODEL BUILDING AND FORECASTING

Paul Newbold
Mathematics Research Center, University of Wisconsin
Craig F. Ansley
Graduate School of Business, University of Chicago

ABSTRACT. This paper summarizes the results of a very large simulation study of some procedures commonly used in time series model building and forecasting. Theoretical results available in this area are generally asymptotic and exact finite sample results are readily obtainable only for a few over-simplified cases.

Often (particularly in business and economic applications) analysis of relatively short time series, in the neighborhood of 50-100 observations, is required. We examine, by simulation, the behavior of various procedures for such sample sizes.

Specifically, we examine the properties of three estimators of the coefficients of autoregressive-moving average models, two procedures for testing the adequacy of representation of such models and the usual estimates of error variances when these models are projected ahead for forecasting.

I. INTRODUCTION. Suppose that the available data consists of n observations X_1, X_2, \dots, X_n on a stationary time series. (In practice it is often necessary to difference the original data to induce stationarity). Such data can generally be well represented by a low order autoregressive-moving average, ARMA(p,q), model

$$(1 - \phi_1 B - \dots - \phi_p B^p)X_t = (1 - \theta_1 B - \dots - \theta_q B^q)a_t \quad (1)$$

where B is a back-shift operator on the index of the time series defined so that $B^j X_t = X_{t-j}$, and a_t is white noise, i.e., $E(a_t) = 0$, $E(a_t^2) = \sigma_a^2$ for all t and $E(a_t a_s) = 0$ for all $t \neq s$. Stationarity of the model (1) is guaranteed by requiring that the roots of the polynomial equation in B , $(1 - \phi_1 B - \dots - \phi_p B^p) = 0$, all have modulus greater than unity. It is also convenient to impose the invertibility condition, that the roots of $(1 - \theta_1 B - \dots - \theta_q B^q) = 0$ all have modulus greater than unity. This ensures uniqueness of representation of the model. A constant term can be added to (1) to account for non-zero series mean.

For seasonal time series of period s (so that $s = 4$ for quarterly and 12 for monthly data) the model (1) can be elaborated to give the multiplicative seasonal model

$$\begin{aligned} & (1 - \phi_1 B - \dots - \phi_p B^p)(1 - \phi_{1,s} B^{s^1} - \dots - \phi_{p_s, s} B^{s^p})X_t \\ & = (1 - \theta_1 B - \dots - \theta_q B^q)(1 - \theta_{1,s} B^{s^1} - \dots - \theta_{q_s, s} B^{s^q})a_t \end{aligned} \quad (2)$$

Stationarity and invertibility conditions for this model are obvious extensions of those for (1).

Following the principles set out in (1), the fitting of models of the form (1) or (2) to data involves an iterative cycle of identification, estimation and diagnostic checking. At the identification stage, based on statistics calculated from the data, a particular model is selected, that is specific values for P, P_s, Q and Q_s in (2) are chosen. The parameters of this model are then estimated by asymptotically efficient statistical methods. Finally checks are made on the adequacy of representation of the chosen model to the given data. Any inadequacies revealed at this stage may suggest an alternative specification, and the cycle is iterated until a satisfactory model is found. The model eventually obtained may then be projected forward to obtain forecasts of future values of the time series.

Details of the model building and forecasting methodologies are given in the books (1), (2) and (3) and more briefly in the paper (4). In the remainder of this section we describe only those procedures whose properties are investigated in the present study.

Consider, first, the problem of estimating the vector β of unknown parameters in (1) or (2), under the additional assumption that a_t is normally distributed. The likelihood function can then be written

$$L(\beta, \sigma_a^2 | X_n) \propto (\sigma_a^2)^{-n/2} f(\beta) \exp.[-S(\beta, X_n)/2\sigma_a^2] \quad (3)$$

where $X_n' = (X_1, X_2, \dots, X_n)$ and $f(\beta)$ involves the parameters but not the data. Analytic expressions for $f(\beta)$ and $S(\beta, X_n)$ are given in (5), and an alternative form which can lead to great computational savings is given in (6). Maximum likelihood (M.L.) estimates of β are then obtained as those values which maximize

$$L_n(\beta | X_n) = f(\beta) [S(\beta, X_n)]^{-n/2} \quad (4)$$

Now, clearly, as sample size increases (4) is dominated by its final term. If $f(\beta)$ is treated as roughly constant, then, this suggests use of the exact least squares (E.L.S.) estimator which involves minimizing $S(\beta, X_n)$. This has computational advantages over M.L., particularly if one adopts the approximation involving "back-forecasting" proposed in (1). The name "exact least squares" derives from the fact that $S(\beta, X_n)$ can be written as a sum of squares.

An estimator of greater computational simplicity is obtained by writing, for example, (1) as

$$a_t = x_t - \phi_1 x_{t-1} - \dots - \phi_p x_{t-p} + \theta_1 a_{t-1} + \dots + \theta_q a_{t-q} \quad (5)$$

If a_{p+1-j} ($j = 1, 2, \dots, q$) are set to their expected values, zero, a_{p+j} ($j = 1, \dots, n-p$) can then be calculated recursively from (5) as functions of the ϕ_i and θ_j , and these parameters estimated by minimizing the sum of

squares $\sum_{t=p+1}^n a_t^2$. This is the conditional least squares (C.L.S.) estimator.

All three estimators are calculated by numerical function minimization and for very large sample sizes they are virtually identical. However, in small samples there are important differences and these are investigated in the next section of this paper.

Now let $\hat{\beta}$ denote the coefficient estimates and \hat{a}_t the residuals from the fitted model. Since, if the model is correctly specified, the \hat{a}_t should be white noise, it is natural in assessing model adequacy to examine the residual autocorrelations.

$$\hat{r}_k = \sum_{t=k+1}^n \hat{a}_t \hat{a}_{t-k} / \sum_{t=1}^n \hat{a}_t^2 \quad (k = 1, 2, \dots) \quad (6)$$

These quantities are studied in (7) and (8), where it is shown that, if the model is correctly specified, they are asymptotically normally distributed with zero means and variances which we write as $V_k(\hat{\beta})$. Unfortunately, $V_k(\hat{\beta})$ is unknown, but can be estimated by $\hat{V}_k(\hat{\beta})$, so that the distribution of

$$t_k = \hat{r}_k / (\hat{V}_k(\hat{\beta}))^{1/2} \quad (k = 1, 2, \dots) \quad (7)$$

should be close to a standard normal. Clearly, if this distributional approximation is valid, then large absolute values of the statistics (7) will indicate probable model inadequacy.

Also in (7) a "portmanteau test" of model inadequacy involving the first m residual autocorrelations is proposed. It is shown that, if the model is correctly specified the statistic

$$Q = n \sum_{k=1}^m \hat{r}_k^2 \quad (8)$$

is asymptotically distributed as chi-squared with $(m - k)$ degrees of freedom, where k is the number of estimated coefficients, provided m is sufficiently large (values of $m \geq 20$ are commonly used).

In fact the available evidence (see (9) and (10)) suggests that in finite samples a closer approximation to the asymptotic distributions is likely to be obtained by replacing \hat{r}_k in (7) and (8) by

$$\hat{r}_k^* = [(n + 2)/(n - k)]^{1/2} \hat{r}_k \quad (k = 1, 2, \dots) \quad (9)$$

giving the statistics t_k^* and Q^* . In section 3 of this paper we examine the empirical distributions of these statistics.

Suppose now that the coefficients of (1) or (2) are known. Setting $t = n + h$, these equations may be written in the form

$$x_{n+h} = (a_{n+h} + \psi_1 a_{n+h-1} + \dots + \psi_{h-1} a_{n+1}) + (\psi_h a_n + \psi_{h+1} a_{n-1} + \dots) \quad (10)$$

where the ψ_j are known functions of the ϕ_i and θ_j . It is then well known that, given $x_n, x_{n-1}, x_{n-2}, \dots$, the minimum mean squared error predictor of x_{n+h} linear in $x_{n-j} (j = 0, 1, 2, \dots)$ is the second bracketed expression on the R.H.S. of (10). The other bracketed term is then the forecast error, so that the optimum predictor has error variance

$$V(h) = \sigma_a^2 (1 + \sum_{j=1}^{h-1} \psi_j^2) \quad (11)$$

Now, in practice there are two reasons why (11) constitutes an understatement of the best attainable forecast error variance. First, even if the model parameters were known, given only a finite realization of the time series the $a_{n-j} (j = 0, 1, 2, \dots)$ required to compute the optimal predictor would be unknown and would have to be estimated from data. Second, the model parameters themselves have to be estimated, and sampling variability in the parameter estimates naturally leads to an increase in forecast error variance (see, for example, (11)). Thus the best attainable $V(h)$ in fact depends on the method of parameter estimation employed, and comparisons will be made amongst estimators in this way in the following section. More details on these points are given in (12).

In practice forecast error variance is estimated by substituting estimates of σ_a^2 and of the model coefficients to calculate estimates of the ψ_j in (11). This implies the possibility of further bias in the resulting estimator $V(h)$ and the quality of this as an estimator of forecast error variance is examined in section 4 of the paper.

The results presented in the remainder of this paper summarize an extensive simulation study covering a wide range of non-seasonal and seasonal time series models. While we will discuss our findings in general, specific results will be quoted for just two models. These are the ARMA(1,1) model

$$x_t - \phi x_{t-1} = a_t - \theta a_{t-1} \quad (12)$$

and the first order multiplicative moving average quarterly seasonal model

$$x_t = (1 - \theta_1 B)(1 - \theta_4 B^4)a_t \quad (13)$$

More detailed results are contained in (12), (13) and (14).

II. COMPARISON OF ESTIMATORS. In evaluating the performances of the M.L., E.L.S. and C.L.S. estimators we generated data from a range of models of the form (1) and (2), taking the a_t to be standard normal deviates. The estimates were compared in terms of bias, mean squared error and the quality of the forecasts resulting from their use. In general our finding was that, if a single estimator is to be recommended for all-purpose use, M.L. is preferable, as there are circumstances where each of the others has undesirable features. It is not the case that M.L. is invariably best by any of our criteria, but it is rarely out-performed to any great extent.

To illustrate, Tables 1 and 2 contain results for the ARMA(1,1) model (12) with 50 observations. Clearly for this sample size the C.L.S. estimator can be very badly biased with unacceptably large mean squared errors for large values of $|\theta|$ or when ϕ and θ are close to one another in value. On the other

hand, the E.L.S. estimator compares rather well with M.L. in terms of bias and mean squared error. However, use of this estimator rather than M.L. would lead to slightly inferior performance in terms of forecast error variance, except in the extreme case $|\theta| = 1$.

Tables 3 and 4 contain similar results for the quarterly seasonal model (13). The performance of the C.L.S. estimator for this model is rather poor for moderate and large values of $|\theta_4|$, where it is badly biased towards zero. On the other hand E.L.S. is badly biased away from zero for small and moderately large values of $|\theta_4|$. These characteristics are reflected in poor forecast performances of these two estimators. Indeed, by this criterion, M.L. seems clearly preferable except in extreme cases where one or other of the parameters is on the boundary of the invertibility region. Here E.L.S. shows up rather well. However, its doing so is in fact a reflection of a very undesirable characteristic of this estimator. Even when the true values are inside the boundaries of the parameter region, E.L.S. estimators are quite likely to fall on these boundaries. This point is illustrated for our two models in Tables 5 and 6.

Clearly, as would be expected, the problem is more severe for a sample of 50 observations than for one of 100 observations. Nevertheless it is by no means negligible for the larger sample size. The importance of the problem lies in the fact that, if the E.L.S. estimator were used, the analyst could frequently be led to erroneous conclusions about the appropriate degree of differencing for the data.

The results presented in this section are a small subset of those contained in (13). From this larger study it emerged that the greatest differences between the estimators arise in models with moving average terms. In that case there can be problems in small samples with the use of either of the least squares estimators. If the true parameter values are not quite far from the boundary of the invertibility region, C.L.S. estimates can be badly biased to the center of that region, with large mean squared errors and an associated poor forecasting performance. On the other hand, when the true parameter values are some distance from the boundary, the E.L.S. estimates can be biased towards the boundary with rather large mean squared errors, resulting on occasions in poor forecasts. Moreover, this estimator has a disturbing tendency to produce estimates on the boundary of the invertibility region, even when the true parameter values are well inside.

III. STATISTICS BASED ON RESIDUAL AUTOCORRELATIONS. We assume now that a time series model has been fitted to data, the coefficients having been estimated by maximum likelihood. In checking model adequacy it is natural to look at the residual autocorrelations for the first one or two lags and at low multiples of the seasonal period. The statistics t_k^* , based on (7) and (9) could then be used to suggest possible model inadequacies. However, it is first necessary to inquire whether, for correctly specified models, the distribution of these statistics is sufficiently close to standard normal. In (14) it is shown that, for first order autoregressive and moving average models, even for samples of only 50 observations, the distributional agreement in the tail areas is quite close. However, for two parameter models the situation is rather less clear, as can be seen from Table 7.

For the ARMA(1,1) model the empirical significance levels agree very well with the asymptotic levels for $k > 1$, even for sample size 50. However, for this sample size, a test based on the first residual autocorrelation would

reject the hypothesis of correct specification too frequently when the true parameter values are fairly small. The situation improves markedly, however, as the sample size increases to 100. The only case which gives difficulty here is the model

$$x_t - 0.5x_{t-1} = a_t - 0.4a_{t-1} \quad (14)$$

which again would be rejected far too often by a test based on the first residual autocorrelation. In fact this is not alarming as, for such a small sample size, it would rarely be fitted since in practice it would be virtually indistinguishable from the simplex hypothesis that $x_t = a_t$, i.e. that the data is white noise.

This is typical of the results found in (14) for non-seasonal models. The test statistics behave very much like the corresponding asymptotic distributions except in cases of near-overparameterization (which would be unlikely to be identified in practice). In these circumstances the test statistic based on the first residual autocorrelation tends to give too many large values.

For seasonal time series models it is natural to check not only the low order residual autocorrelations, but also those at small multiples of the seasonal period. For the quarterly moving average model (13) some results are shown in Table 8. Of course, it is almost invariably the case that the agreement between empirical and asymptotic distributions improves as sample size increases. Nevertheless, the improvement from sample size 50 to 100 here is remarkable. For the larger sample size the empirical significance levels are generally quite close to the asymptotic levels, suggesting that for this sample size interpretation of the statistics is straightforward. On the other hand, for the smaller sample size the empirical significance levels are frequently too high, particularly at those lags associated with the seasonal frequency. These results are typical of those reported in (14).

We now consider the portmanteau statistic Q^* , based on (8) and (9). Although this statistic is almost invariably calculated in practical time series studies, published evidence of its empirical distribution is sparse, the prime exception being in (10), where just the simple first order autoregressive model is examined. Tables 9 and 10 show empirical significance levels for the models (12) and (13). The evidence in these tables certainly reflects variability between models and also variability between parameter values within the same model. However, it is quite clear (and this is confirmed by further evidence in (14)) that the empirical significance levels are generally "too high". This observation accords with a prediction made from theoretical considerations in (9). Generally speaking, the discrepancies between the empirical and asymptotic distributions are likely to be largest for small sample sizes, for seasonal models, and in the extreme tail areas of the distributions. However, it is clear from the tables that even for samples of 100 observations, for such relatively simple two parameter models, use of the Q^* statistic can lead to rejection of a correctly specified model far more often than reference to the asymptotic significance levels would indicate.

An additional consideration when using any test statistic, of course, concerns its power. Some evidence on the frequency with which the portmanteau test detects model misspecifications of varying degrees of severity is contained in (15), where it was found that, unless the sample size is large, the test can have disturbingly low power.

IV. ESTIMATION OF FORECAST ERROR VARIANCE. When a fitted time series model is projected forward to obtain forecasts, it is usual to estimate the error variance by substituting estimates of the unknown parameters in (11). The ψ_j in that expression are estimated in an obvious way from the coefficient estimates $\hat{\phi}_j$ and $\hat{\theta}_j$. If, as will be assumed in this section, the model is estimated by maximum likelihood, it follows from (3) that the innovation variance σ_a^2 is estimated by

$$\hat{\sigma}_a^2 = S(\hat{\beta}, X_n)/n \quad (15)$$

where $\hat{\beta}$ is the vector of maximum likelihood coefficient estimates. With these substitutions, we denote the estimate of $V(h)$ of (11) as $\hat{V}(h)$.

In fact, as we have already noted, the minimum attainable forecast error variance, $V_*(h)$, will be greater than $V(h)$. This is so, since the expression (11) takes no account of sampling variability in the parameter estimates or of the fact that only the finite past of a time series is available for the computation of forecasts. It is likely then that $\hat{V}(h)$ will be a biased estimator of $V_*(h)$. In this section we examine the extent of that bias. It should be emphasized that our results are specific to the case where parameter estimation is by maximum likelihood. In particular circumstances, rather different conclusions can hold for alternative estimators, as illustrated in (12).

Tables 11 and 12 contain values of $(E(\hat{V}(h)) - V_*(h))/V_*(h)$ estimated by simulation for the models (12) and (13). The general picture emerging from these tables is of a moderate downward bias in $\hat{V}(h)$. For one step ahead prediction in the ARMA(1,1) model this is in the neighborhood of 5-10% of the true variance for sample size 50, and 3-6% for samples of 100 observations. For the seasonal model the corresponding figures are slightly higher. Perhaps the outstanding feature of the tables concerns prediction 10 steps ahead for ARMA(1,1) models with the higher autoregressive parameter value. Here the bias can be around 20% of the true variance for 50 observations and around 12% for twice that sample size.

Although, with this latter exception, the tables suggest some uniformity in the proportionate bias, the causes of that bias differ substantially between models and parameter values. We suggested previously four potential causes of bias in the usual estimator of forecast error variance. It is of interest, now, to examine these factors in a little more detail.

Suppose, for now, that the parameter values are given. It is still the case that, if the model contains moving average terms and only the finite past is available to compute forecasts, the minimum attainable forecast error variance will be somewhat higher than (11). This factor is only of practical significance when the moving average coefficients are on or very close to the boundary of the invertibility region. Even then, for the kind of sample sizes considered here, it is relatively unimportant for simple non-seasonal models. For example, for the ARMA(1,1) models of Table 11 for sample size 50 it accounts for an addition of at most 2% (when $\theta = -1$) to one step ahead prediction error variance, and less for prediction further ahead. On the other hand, for seasonal moving average models, in small samples this factor can be more substantial. For example, for the multiplicative first order moving average quarterly model, in the extreme case $\theta_1 = 1, \theta_4 = 1$, the minimum attainable one-step forecast error variance is 13.4% higher than (11) for sample size 50 and 6.9% higher for sample

size 100. However, the effect quickly dies out as the parameters move away from the boundary. For example, for $\theta_1 = 0.85$, $\theta_4 = 0.85$ the inflation factor for one step ahead prediction is only 0.5% for sample size 50.

The necessity to estimate the model parameters inflates forecast error variance by a proportion in the neighborhood of K/n , where K is the number of estimated coefficients. There is, of course, some variability here. A particular case is in forecasting several steps ahead when the optimal predictor is dominated by a relatively low autoregressive term. In this case the influence of estimation error can be very slight. For example, for the ARMA(1,1) model for $\phi = 0.5$, $\theta = -0.4$, $h = 10$, estimation error in the parameters adds only 0.1% to (11). This factor is discussed in more detail for non-seasonal models in (11) and (16).

For maximum likelihood estimation, the estimate (15) of residual variance tends to be slightly biased downwards. An exception is the case where moving average coefficients are on or very close to the boundary of the invertibility region, when the bias is upwards. In this latter case some of the effects of the inflation caused by only having the finite past to calculate forecasts are cancelled out, and this explains why the estimates of error variance when moving average terms are on the boundary of the invertibility region do not have a more severe downward bias. For example, for the multiplicative first order moving average quarterly model with $\sigma_a^2 = 1$ and $n = 50$, for $\theta_1 = 0.85$, $\theta_4 = 0.85$, $E(\hat{\sigma}_a^2) = 0.92$, while for $\theta_1 = 1$, $\theta_4 = 1$, $E(\hat{\sigma}_a^2) = 1.05$.

Finally, the term $\sum_{j=1}^{h-1} \psi_j^2$ in (11) is generally well estimated by substitution of the parameter estimates, except for moderately large h in models containing autoregressive factors close to the stationarity boundary. This is the reason for the serious under-estimation of forecast error variance in the ARMA(1,1) model for $\phi = 0.95$, $h = 10$ noted in Table 11.

These factors are all discussed in more detail for a wider range of models in (12).

Table 1: Estimated coefficient biases for ARMA(1,1) process
 (n = 50; 1,000 replications)

ϕ	θ	Bias $\hat{\phi}$			Bias $\hat{\theta}$		
		M.L.	E.L.S.	C.L.S.	M.L.	E.L.S.	C.L.S.
-0.95	-1.00	0.172	0.096	0.505	0.112	0.042	0.468
-0.95	-0.85	0.090	0.067	0.298	0.074	0.050	0.286
-0.95	-0.40	0.039	0.017	0.046	0.026	0.006*	0.029
-0.95	0.40	0.028	0.012	0.033	0.015	0.033	0.017
-0.95	0.85	0.027	0.009	0.024	0.025	0.053	-0.012
-0.95	1.00	0.026	0.007	0.023	-0.028	-0.008	-0.098
-0.50	-1.00	0.064	0.054	0.184	0.041	0.011	0.180
-0.50	-0.85	0.061	0.053	0.191	0.001*	-0.017	0.143
-0.50	-0.40	0.119	0.064	0.191	0.114	0.047	0.178
-0.50	0.40	0.038	0.031	0.016	0.032	0.040	0.018
-0.50	0.85	0.007*	0.004*	-0.001*	0.025	0.056	-0.016
-0.50	1.00	0.005*	-0.008	-0.026	-0.032	-0.008	-0.105
0.50	-1.00	-0.013	0.006*	0.010	0.027	0.007	0.105
0.50	-0.85	-0.020	-0.010	0.007*	-0.021	-0.057	0.018
0.50	-0.40	-0.033	-0.020	-0.016	-0.036	-0.034	-0.013
0.50	0.40	-0.120	-0.064	-0.181	-0.114	-0.056	-0.164
0.50	0.85	-0.072	-0.046	-0.183	-0.009*	0.025	-0.128
0.50	1.00	-0.064	-0.055	-0.182	-0.040	-0.011	-0.181
0.95	-1.00	-0.028	-0.004	-0.024	0.030	0.008	0.105
0.95	-0.85	-0.026	-0.010	-0.025	-0.020	-0.056	0.019
0.95	-0.40	-0.030	-0.007	-0.035	-0.010	-0.028	-0.018
0.95	0.40	-0.046	-0.017	-0.047	-0.03	-0.012*	-0.015*
0.95	0.85	-0.096	-0.050	-0.281	-0.07	-0.028	-0.264
0.95	1.00	-0.168	-0.103	-0.526	-0.110	-0.051	-0.500

*Bias is not statistically significant at 5% level.

Table 2: Estimated coefficient mean squared errors and forecast error variances
for ARMA(1,1) process [n = 50; 1,000 replications]

ϕ	θ	M.S.E. $\hat{\phi}$ ($\times 10^3$)			M.S.E. $\hat{\theta}$ ($\times 10^3$)			V(1)		
		M.L.	E.L.S.	C.L.S.	M.L.	E.L.S.	C.L.S.	M.L.	E.L.S.	C.L.S.
-0.95	-1.00	90.5	28.1	502	63.8	23.2	510	1.054	1.050	1.065
-0.95	-0.85	52.0	50.7	298	70.8	86.2	320	1.036	1.058	1.057
-0.95	-0.40	9.41	7.09	13.2	33.4	34.3	36.8	1.037	1.053	1.048
-0.95	0.40	4.78	4.85	5.54	22.7	30.2	23.6	1.043	1.051	1.049
-0.95	0.85	4.40	3.86	4.36	9.04	12.5	10.1	1.039	1.063	1.047
-0.95	1.00	3.91	3.20	5.19	3.11	1.12	17.8	1.055	1.050	1.101
-0.50	-1.00	29.0	20.9	91.7	9.60	2.09	104	1.059	1.053	1.114
-0.50	-0.85	57.6	59.2	122	38.6	40.1	121	1.041	1.059	1.053
-0.50	-0.40	234	214	283	287	255	323	1.044	1.047	1.045
-0.50	0.40	34.1	35.4	29.5	40.8	43.0	40.3	1.049	1.049	1.050
-0.50	0.85	17.1	17.1	18.1	11.1	12.9	12.6	1.047	1.061	1.054
-0.50	1.00	14.4	14.7	18.4	4.18	0.95	20.0	1.066	1.047	1.100
0.50	-1.00	13.8	13.8	20.1	3.46	0.82	20.8	1.055	1.046	1.095
0.50	-0.85	19.5	17.6	17.8	10.5	13.7	12.5	1.045	1.068	1.058
0.50	-0.40	31.9	31.3	30.0	40.8	45.0	42.9	1.046	1.053	1.051
0.50	0.40	241	199	282	294	253	329	1.043	1.044	1.046
0.50	0.85	60.9	54.8	118	40.4	38.2	104	1.046	1.062	1.059
0.50	1.00	30.1	24.8	90.3	9.36	4.76	96.9	1.059	1.054	1.104
0.95	-1.00	3.71	3.08	4.08	3.72	1.10	20.3	1.056	1.049	1.101
0.95	-0.85	3.64	4.06	4.76	10.1	12.6	11.6	1.039	1.065	1.046
0.95	-0.40	5.16	4.12	6.02	23.8	23.4	23.9	1.039	1.051	1.044
0.95	0.40	14.0	9.91	13.2	38.4	38.9	38.6	1.042	1.060	1.054
0.95	0.85	67.4	39.9	258	87.6	71.7	276	1.041	1.070	1.051
0.95	1.00	93.9	42.4	520	68.6	36.6	547	1.048	1.050	1.060

Table 3: Estimated coefficient biases for multiplicative first order moving average quarterly models [n = 50; 600 replications]

		Bias $\hat{\theta}_1$			Bias $\hat{\theta}_4$		
θ_1	θ_4	M.L.	E.L.S.	C.L.S.	M.L.	E.L.S.	C.L.S.
-1.00	-1.00	0.030	0.011	0.085	0.083	0*	0.257
-1.00	-0.85	0.035	0.010	0.089	-0.020	-0.133	0.128
-1.00	-0.40	0.031	0.009	0.091	0.005*	-0.056	0.010*
-1.00	0.40	0.039	0.006	0.171	0.046	0.149	-0.006
-1.00	0.85	0.048	0.004	0.256	0.033	0.142	-0.164
-1.00	1.00	0.042	0.001	0.264	-0.064	0*	-0.287
-0.85	-1.00	-0.012	-0.038	0.004*	0.082	0*	0.245
-0.85	-0.85	-0.018	-0.045	0.013	-0.014	-0.132	0.122
-0.85	-0.40	-0.022	-0.049	0.005*	-0.007*	-0.075	0.007*
-0.85	0.40	-0.018	-0.054	0.062	0.030	0.105	0.000*
-0.85	0.85	-0.025	-0.094	0.141	0.010*	0.141	-0.156
-0.85	1.00	-0.029	-0.103	0.147	-0.074	0*	-0.278
-0.40	-1.00	-0.006*	-0.010*	-0.010*	0.076	0*	0.241
-0.40	-0.85	-0.003*	-0.013	0.002*	-0.022	-0.130	0.117
-0.40	-0.40	-0.017	-0.015	-0.014	-0.008*	-0.079	-0.007*
-0.40	0.40	0.003*	-0.025	-0.001*	0.017	0.084	-0.009*
-0.40	0.85	-0.019	-0.044	0.005*	0.007*	0.137	-0.119
-0.40	1.00	-0.007*	-0.032	0.007*	-0.080	0	-0.249

*Bias is not statistically significant at 5% level.

Table 4: Estimated coefficient mean squared errors and forecast error variances for multiplicative first order quarterly moving average models [n = 50; 600 replications]

<u>θ_1</u>	<u>θ_4</u>	M.S.E. $\hat{\theta}_1$ ($\times 10^3$)			M.S.E. $\hat{\theta}_4$ ($\times 10^3$)			V(1)		
		M.L.	E.L.S.	C.L.S.	M.L.	E.L.S.	C.L.S.	M.L.	E.L.S.	C.L.S.
-1.00	-1.00	2.83	1.46	13.2	17.4	0	80.1	1.149	1.113	1.471
-1.00	-0.85	4.30	1.13	13.7	14.9	22.4	31.1	1.077	1.055	1.250
-1.00	-0.40	3.79	1.09	15.3	23.0	49.8	23.8	1.072	1.089	1.189
-1.00	0.40	6.42	1.09	44.4	29.6	80.1	26.9	1.066	1.133	1.272
-1.00	0.85	6.67	0.92	84.5	14.1	22.5	41.1	1.092	1.070	1.425
-1.00	1.00	6.26	0.24	90.7	13.5	0	95.7	1.182	1.134	1.503
-0.85	-1.00	7.79	12.9	9.59	17.2	0	74.1	1.126	1.124	1.410
-0.85	-0.85	8.06	12.0	9.90	16.3	23.2	28.8	1.051	1.065	1.192
-0.85	-0.40	9.39	12.9	9.38	26.9	53.6	24.5	1.051	1.108	1.140
-0.85	0.40	11.3	13.5	16.1	32.1	63.1	23.9	1.052	1.113	1.076
-0.85	0.85	11.8	18.2	39.3	18.2	22.6	38.5	1.057	1.068	1.178
-0.85	1.00	9.19	19.1	42.9	15.3	0	89.9	1.130	1.124	1.383
-0.40	-1.00	15.8	20.0	22.6	17.0	0	70.0	1.127	1.102	1.205
-0.40	-0.85	18.9	24.8	21.3	17.8	22.5	25.2	1.047	1.056	1.087
-0.40	-0.40	25.9	24.3	24.0	27.9	52.0	23.6	1.057	1.088	1.065
-0.40	0.40	21.7	25.5	21.1	26.6	56.3	23.9	1.045	1.106	1.048
-0.40	0.85	22.7	36.2	26.7	19.7	22.7	26.7	1.052	1.074	1.092
-0.40	1.00	19.5	33.4	25.3	17.8	0	73.9	1.128	1.121	1.218

Table 5: Percentage times an E.L.S. parameter estimate is on the boundary of the stationarity or invertibility region for ARMA(1,1) process [1,000 replications, n=50; 600 replications, n=100]

<u>ϕ</u>	<u>θ</u>	<u>n=50</u>	<u>n=100</u>	<u>ϕ</u>	<u>θ</u>	<u>n=50</u>	<u>n=100</u>
0.50	-0.85	46.7	8.7	0.95	-0.85	47.4	17.3
0.50	-0.40	1.4	0	0.95	-0.40	10.8	0.3
0.50	0.40	15.2	5.5	0.95	0.40	19.8	0.8
0.50	0.85	53.0	26.8	0.95	0.85	54.0	19.8

Table 6: Percentage times an E.L.S. parameter estimate is on the boundary of the invertibility region for multiplicative first order moving average quarterly models [600 replications]

<u>θ_1</u>	<u>θ_4</u>	<u>n=50</u>	<u>n=100</u>	<u>θ_1</u>	<u>θ_4</u>	<u>n=50</u>	<u>n=100</u>
0.40	0.40	9.3	0.2	0.85	0.40	57.3	22.2
0.40	0.85	92.3	73.7	0.85	0.85	98.0	78.3

Table 7: Empirical significance levels of the statistic t_k^* for ARMA(1,1) models [1,000 replications, n = 50; 600 replications, n = 100]

ϕ	θ	K	<u>n = 50</u>		<u>n = 100</u>	
			0.05 level	0.10 level	0.05 level	0.10 level
0.50	-0.85	1	0.111	0.186	0.072	0.128
		2	0.063	0.109	0.040	0.095
		3	0.052	0.112	0.055	0.103
0.50	-0.40	1	0.184	0.257	0.068	0.130
		2	0.050	0.105	0.055	0.100
		3	0.045	0.099	0.057	0.112
0.50	0.40	1	0.147	0.195	0.197	0.248
		2	0.055	0.107	0.095	0.143
		3	0.051	0.103	0.047	0.097
0.50	0.85	1	0.072	0.141	0.058	0.108
		2	0.052	0.112	0.058	0.098
		3	0.049	0.092	0.042	0.100
0.95	-0.85	1	0.066	0.133	0.053	0.100
		2	0.059	0.099	0.043	0.112
		3	0.065	0.110	0.058	0.110
0.95	-0.40	1	0.101	0.157	0.063	0.120
		2	0.065	0.116	0.077	0.130
		3	0.052	0.114	0.053	0.083
0.95	0.40	1	0.113	0.175	0.078	0.122
		2	0.060	0.102	0.045	0.093
		3	0.041	0.086	0.062	0.120
0.95	0.85	1	0.068	0.130	0.055	0.130
		2	0.058	0.133	0.062	0.110
		3	0.057	0.109	0.055	0.090

Table 8: Empirical significance levels of the statistic t_k^* for multiplicative first order moving average quarterly models [600 replications]

<u>θ_1</u>	<u>θ_4</u>	<u>K</u>	<u>n = 50</u>		<u>n = 100</u>	
			<u>0.05 level</u>	<u>0.10 level</u>	<u>0.05 level</u>	<u>0.10 level</u>
0.40	0.40	1	0.060	0.100	0.053	0.102
		2	0.040	0.080	0.038	0.097
		4	0.067	0.125	0.047	0.102
		8	0.057	0.105	0.045	0.093
0.40	0.85	1	0.105	0.152	0.063	0.133
		2	0.050	0.087	0.055	0.107
		4	0.085	0.150	0.050	0.107
		8	0.085	0.120	0.073	0.135
0.85	0.40	1	0.052	0.100	0.050	0.093
		2	0.048	0.102	0.047	0.108
		4	0.107	0.163	0.058	0.122
		8	0.072	0.135	0.052	0.095
0.85	0.85	1	0.048	0.108	0.052	0.125
		2	0.042	0.093	0.050	0.093
		4	0.093	0.162	0.045	0.087
		8	0.097	0.165	0.057	0.128

Table 9: Empirical significance levels of the statistic Q^* for ARMA(1,1) models
 $[m = 20; 1,000$ replications, $n = 50$; 600 replications, $n = 100]$

ϕ	θ	n = 50			n = 100		
		0.05 level	0.10 level	0.20 level	0.05 level	0.10 level	0.20 level
0.50	-0.85	0.104	0.169	0.267	0.053	0.112	0.212
0.50	-0.40	0.069	0.106	0.198	0.068	0.110	0.208
0.50	0.40	0.080	0.132	0.224	0.072	0.123	0.200
0.50	0.85	0.100	0.152	0.243	0.068	0.112	0.212
0.95	-0.85	0.102	0.153	0.267	0.065	0.132	0.228
0.95	-0.40	0.092	0.146	0.256	0.072	0.128	0.208
0.95	0.40	0.078	0.123	0.218	0.077	0.138	0.248
0.95	0.85	0.106	0.179	0.272	0.105	0.167	0.275

Table 10: Empirical significance levels of the statistic Q^* for multiplicative first order moving average quarterly models [$m = 24$; 600 replications]

θ_1	θ_4	n = 50			n = 100		
		0.05 level	0.10 level	0.20 level	0.05 level	0.10 level	0.20 level
0.40	0.40	0.065	0.123	0.210	0.050	0.100	0.212
0.40	0.85	0.135	0.223	0.330	0.088	0.157	0.245
0.85	0.40	0.105	0.143	0.253	0.077	0.133	0.213
0.85	0.85	0.168	0.235	0.338	0.095	0.160	0.255

Table 11: Estimates of $(E(\hat{V}(h)) - V_*(h))/V_*(h)$ for ARMA(1,1) models
 [1,000 replications, n=50; 600 replications, n = 100]

ϕ	θ	n=50			n=100		
		<u>h=1</u>	<u>h=2</u>	<u>h=10</u>	<u>h=1</u>	<u>h=2</u>	<u>h=10</u>
0.50	-1.00	-0.058	-0.060	-0.009	-0.036	-0.038	-0.010
0.50	-0.85	-0.097	-0.077	-0.013	-0.060	-0.049	-0.027
0.50	-0.40	-0.087	-0.067	-0.004	-0.038	-0.029	0.005
0.50	0.40	-0.079	-0.036	-0.005	-0.040	-0.024	-0.012
0.50	0.85	-0.077	0.007	0.022	-0.053	-0.011	-0.003
0.50	1.00	-0.068	0.009	0.005	-0.033	0.002	-0.002
0.95	-1.00	-0.062	-0.083	-0.194	-0.033	-0.045	-0.119
0.95	-0.85	-0.080	-0.076	-0.178	-0.047	-0.048	-0.136
0.95	-0.40	-0.071	-0.069	-0.180	-0.037	-0.040	-0.118
0.95	0.40	-0.098	-0.100	-0.204	-0.039	-0.046	-0.126
0.95	0.85	-0.081	-0.064	-0.067	-0.036	-0.027	-0.019
0.95	1.00	-0.069	-0.034	0.002	-0.033	-0.019	0.003

Table 12: Estimates of $(E(\hat{V}(h)) - V_*(h))/V_*(h)$ for multiplicative first order moving average quarterly models [600 replications]

<u>θ_1</u>	<u>θ_4</u>	n=50			n=100		
		<u>h=1</u>	<u>h=2</u>	<u>h=4</u>	<u>h=1</u>	<u>h=2</u>	<u>h=4</u>
0.40	0.40	-0.087	-0.028	-0.026	-0.046	-0.023	-0.023
0.40	0.85	-0.121	-0.078	-0.084	-0.073	-0.050	-0.048
0.40	1.00	-0.086	-0.052	-0.056	-0.052	-0.031	-0.034
0.85	0.40	-0.101	-0.064	-0.060	-0.058	-0.036	-0.032
0.85	0.85	-0.138	-0.096	-0.092	-0.068	-0.042	-0.043
0.85	1.00	-0.106	-0.066	-0.057	-0.052	-0.018	-0.018
1.00	0.40	-0.072	-0.061	-0.062	-0.041	-0.036	-0.036
1.00	0.85	-0.106	-0.087	-0.090	-0.066	-0.061	-0.062
1.00	1.00	-0.105	-0.071	-0.071	-0.040	-0.028	-0.032

REFERENCES

- (1) Box, G.E.P. and Jenkins, G.M. (1970). Time Series Analysis, Forecasting and Control. Holden Day, San Francisco.
- (2) Nelson, C.R. (1973). Applied Time Series Analysis for Managerial Forecasting. Holden Day, San Francisco.
- (3) Granger, C.W.J. and Newbold, P. (1977). Forecasting Economic Time Series. Academic Press, New York.
- (4) Newbold, P. (1975). The principles of the Box-Jenkins approach. Operational Research Quarterly, 26, 397-412.
- (5) Newbold, P. (1974). The exact likelihood function for a mixed autoregressive-moving average process. Biometrika, 61, 423-426.
- (6) Ansley, C.F. (1979). An algorithm for the exact likelihood of an auto-regressive-moving average process. Biometrika, 66 (forthcoming).
- (7) Box, G.E.P. and Pierce, D.A. (1970). Distribution of residual autocorrelations in autoregressive integrated moving average time series models. Journal of American Statistical Association, 65, 1509-1526.
- (8) McLeod, A.I. (1977). On the distribution and applications of residual autocorrelations in Box-Jenkins models. Department of Statistics, University of Waterloo.
- (9) Davies, N., Triggs, C.M. and Newbold, P. (1977). Significance levels of the Box-Pierce portmanteau statistic in finite samples. Biometrika, 64, 517-522.
- (10) Ljung, G.M. and Box, G.E.P. (1978). On a measure of lack of fit in time series models. Biometrika, 65.
- (11) Yamamoto, T. (1976). Asymptotic mean square prediction error for an auto-regressive model with estimated coefficients. Applied Statistics, 25, 123-127.
- (12) Ansley, C.F. and Newbold, P. (1979). On the bias in estimates of forecast error variance. Graduate School of Business, University of Chicago.
- (13) Ansley, C.F. and Newbold, P. (1979). Finite sample properties of estimators for autoregressive-moving average models. Graduate School of Business, University of Chicago.
- (14) Ansley, C.F. and Newbold, P. (1979). On the finite sample distribution of residual autocorrelations in autoregressive-moving average models. Graduate School of Business, University of Chicago.
- (15) Davies, N. and Newbold, P. (1979). Some power studies of a portmanteau test of time series model specification. Biometrika, 66 (forthcoming).
- (16) Yamamoto, T. (1977). Prediction error of parametric time series models with estimated coefficients. Department of Economics, Soka University, Tokyo.

STATISTICAL PROBLEMS ASSOCIATED WITH THE HORIZONTAL CHANNEL
OF THE RAPID GEODETIC SURVEY SYSTEM (RGSS)

H. Baussus von Luetzow
U.S. Army Engineer Topographic Laboratories
Fort Belvoir, Virginia

ABSTRACT

The paper discusses the estimation of deflections of the vertical along with horizontal gyro biases from a set of given and measured data as a statistical adjustment problem. In conjunction herewith, it presents a quasi-optimal estimation method and necessary covariance functions. It further outlines the estimation of gridded deflections from RGSS data and improved stochastic position error control.

1. INTRODUCTION

The involvement of the U.S. Army Engineer Topographic Laboratories (ETL) in the field of inertial surveying and, subsequently, in inertial geodesy, can be characterized by three phases. Phase I comprised the development of a Position and Azimuth Determining System (PADS) primarily in support of U.S. Army artillery and was completed in 1972. Phase II was concerned with the installation of a higher-accuracy vertical accelerometer for improved vertical positioning and the inclusion of software and a data storage unit for the determination of gravity anomalies and deflections of the vertical components ξ and η under consideration of initial and terminal gravity vector components. The modified PADS operates as an optimal local-level system in the Inertial Positioning System (IPS) mode and as a quasi-local-level system in the Rapid Geodetic Survey System (RGSS) mode. The RGSS mode without Kalman platform tilt corrections has advantages concerning gyro bias estimations and thus for the determination of ξ and η . Phase II was essentially completed after ETL tests at White Sands Missile Range in 1976. These tests established an RGSS capability of determining gravity anomalies and deflection components with average rms errors of 2 mgal and 2 arcsec, respectively for 50 km runs in comparison with unreduced rms values of 35 mgal and 5 arcsec. Phase III concentrates essentially

on additional RGSS testing in the vicinity of Washington, D.C., the development of improved methods for the determination of ξ and n and their implementation, improved stochastic error control for positioning, and desirable hardware improvements, notably the installation of two Al1000 accelerometers in the horizontal channel. With sufficient funding, it could be completed in 1981 and should permit ξ , n -determinations with a mean standard error between 0.5 and 1.0 arcsec without repetitions, and improved positioning. Promising RGSS applications are:

- *Rapid Δg , ξ , n -determinations along solitary courses of about 60 km length.
- *Establishment of regional Δg , ξ , n -grid information networks suitable for use in a gravity-programmed inertial positioning system and for analytical continuation in space in the case of flat or moderate terrain.
- *Improved point positioning approaching classical surveying accuracy.
- *Flood plain profiling and mapping under consideration of the underlying geoidal structure.
- *Geophysical prospecting.

Section 2 of this paper describes quasi-optimal and suboptimal methods for the determination of ξ and n by means of RGSS and auxiliary data. Section 3 gives a short overview as to required auto-correlation functions. Section 4 outlines the construction of regular ξ , n -grid networks from solitary course data. Finally, section 5 addresses essentially improved stochastic position error control which would be particularly valuable in the context of local surveying within a radius of about 20 km from the starting point.

2. Optimal and Suboptimal Post-Mission ξ , η -Estimation.

The error differential equations of interest, applicable to horizontal motion, are for the RGSS:

$$\frac{d}{dt} \hat{x} = -\frac{1}{R} \dot{x} \quad (1)$$

$$\frac{d}{dt} \hat{y} = -\frac{1}{R} \dot{y} \quad (2)$$

$$\frac{d}{dt} \dot{x} = s_N \phi_Z - g \phi_N + g \eta + a_E \quad (3)$$

$$\frac{d}{dt} \dot{y} = -s_E \phi_Z + g \phi_E - g \xi + a_N \quad (4)$$

$$\frac{d}{dt} \phi_Z = \tan \phi \frac{\dot{x}}{R} - (\Omega_N + p_N \sec^2 \phi) \hat{y} + \omega_N \phi_E + \alpha \quad (5)$$

$$\frac{d}{dt} \phi_N = \frac{\dot{x}}{R} + \omega_Z \phi_E + \beta \quad (6)$$

$$\frac{d}{dt} \phi_E = -\frac{\dot{y}}{R} + \omega_Z \phi_N - \omega_N \phi_Z + \gamma \quad (7)$$

For simplicity, the symbol δ in front of the dependent variables has been omitted. The applicable coordinate system is evident from Figure 1.

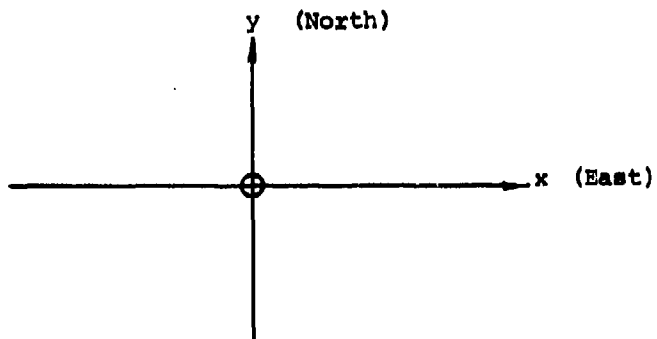


Figure 1

Applicable Coordinate System

Symbols used in the foregoing local level equations are:

- \hat{x} east angular position error
- \hat{y} north angular position error
- \dot{x} east velocity error
- \dot{y} north velocity error
- α azimuth axis angular drift rate error¹
- β north axis angular drift rate error¹
- γ east axis angular drift rate error¹
- g normal gravity
- ϕ geographic latitude
- R mean earth radius
- $\hat{\phi}_z$ azimuth platform attitude error
- $\hat{\phi}_N$ platform tilt error about north axis
- $\hat{\phi}_E$ platform tilt error about east axis
- $g_T = \frac{\partial T}{\partial y}$ product of g and deflection component²
- $g_t = -\frac{\partial T}{\partial x}$ product of g and deflection component²
- $a_N = \frac{dv_N}{dt}$ north acceleration of survey vehicle
- $a_E = \frac{dv_E}{dt}$ east acceleration of survey vehicle
- a_x correlated east accelerometer error
- a_y correlated north accelerometer error

¹ $\alpha = \bar{\alpha} + (\alpha - \bar{\alpha})$, $\beta = \bar{\beta} + (\beta - \bar{\beta})$, $\gamma = \bar{\gamma} + (\gamma - \bar{\gamma})$ where the bar symbol indicates constant bias and the terms in parentheses are correlated random errors.

² T is the earth's anomalous gravity potential. The derivatives $\frac{\partial}{\partial x}$ and $\frac{\partial}{\partial y}$ are taken along the level horizon in the eastern and northern direction, respectively.

$$\Omega_N = \Omega \cos \phi \text{ north earth rate}$$

$$\rho_N = V_E/R \text{ north angular rate}^3$$

$$\omega_N = \Omega_N + \rho_N = \Omega \cos \phi + V_E/R \text{ north spatial rate}$$

$$\omega_E = \rho_E = -V_N/R \text{ east spatial rate}$$

$$\omega_Z = \Omega_Z + \rho_Z = \Omega \sin \phi + V_E/R \cdot \tan \phi \text{ vertical spatial rate}$$

In inertial land navigation, terms involving ω_E in equations (5) and (6) are neglected in Litton's Kalman error controller. The initial conditions at time $t_0 = 0$ are $\phi_Z^{(0)} = 0$, $\phi_N^{(0)} = \eta_0$, $\phi_E^{(0)} = \xi_0$, $\dot{x}^{(0)} = \dot{y}^{(0)} = x^{(0)} = y^{(0)} = 0$.

The system (5)-(7) can be approximately solved in closed form for constant gyro biases \bar{a} , $\bar{\beta}$, $\bar{\gamma}$. The solution is, with $\omega_N = \Omega_N$ and $\omega_Z = \Omega_Z$,

$$\begin{aligned} \bar{\phi}_Z(t) &= \bar{\gamma} \cos \phi \cdot \Omega^{-1} (1 - \cos \Omega t) + \bar{\beta} \sin \phi \cos \Omega t - \Omega^{-1} \sin \Omega t \\ &\quad + \bar{a} (\sin^2 \phi \cdot t + \cos^2 \phi \cdot \Omega^{-1} \sin \Omega t) \end{aligned} \quad (8)$$

$$\begin{aligned} \bar{\phi}_N(t) &= \bar{\gamma} \sin \phi \cdot \Omega^{-1} (\cos \Omega t - 1) + \bar{\beta} (\cos^2 \phi \cdot t + \sin^2 \phi \cdot \Omega^{-1} \sin \Omega t) \\ &\quad + \bar{a} \sin \phi \cos \phi (t - \Omega^{-1} \sin \Omega t) \end{aligned} \quad (9)$$

$$\begin{aligned} \bar{\phi}_E(t) &= \bar{\gamma} \Omega^{-1} \sin \Omega t \\ &\quad + \bar{\beta} \sin \phi \Omega^{-1} (1 - \cos \Omega t) \\ &\quad + \bar{a} \cos \phi \Omega^{-1} (\cos \Omega t - 1) \end{aligned} \quad (10)$$

The substitution of $\bar{\phi}_Z(t)$, $\bar{\phi}_N(t)$, and $\bar{\phi}_E(t)$, respectively in equations (3) and (4) permits the direct assessment of gyro bias effects on y and x .

In order to provide for quasi-continuous time integration for intervals λ between stops, successive representative ξ 's and η 's for constant time

³ In the error equations, normal and meridional radii with respect to the reference ellipsoid may be replaced by R for $|v| < 100 \text{ km h}^{-1}$.

intervals Δt are designated by a subscript v . Subsequently, numerical integration with respect to time yields the following solution structure for the first interval between stops, identified by $\lambda = 1$:

$$\begin{aligned} \Sigma A_{1v} \xi_v + \Sigma B_{1v} n_v + C_1 \bar{\alpha} + D_1 \bar{\beta} + E_1 \bar{\gamma} + \Sigma a_{1v} (\alpha - \bar{\alpha}) + \Sigma b_{1v} (\beta - \bar{\beta}) + c_{1v} (\gamma - \bar{\gamma}) \\ + \Sigma A_{1v} a_{Nv} + \Sigma B_{1v} a_{Ev} = \dot{x}_1 + \phi_1(\xi_0, n_0, \xi_e, n_e) \end{aligned} \quad (11)$$

$$\begin{aligned} \Sigma G_{1v} \xi_v + \Sigma H_{1v} n_v + J_1 \bar{\alpha} + K_1 \bar{\beta} + L_1 \bar{\gamma} + \Sigma d_{1v} (\alpha - \bar{\alpha}) + \Sigma e_{1v} (\beta - \bar{\beta}) + f_{1v} (\gamma - \bar{\gamma}) \\ + \Sigma G_{1v} a_{Nv} + \Sigma H_{1v} a_{Ev} = \dot{y}_1 + \psi_1(\xi_0, n_0, \xi_e, n_e) \end{aligned} \quad (12)$$

The terms involving α_v , β_v , γ_v and stochastic accelerometer-induced errors are only used for the computation of error covariance matrices which are necessary for the establishment of a priori weights in a least-squares solution. The terms ϕ_1 and ψ_1 represent known linear functions. The small terms $S_N \phi_Z$ and $S_E \phi_Z$ in equations (3) and (4), respectively are omitted prior to the determination of constant gyro biases and may be considered in an iterative scheme.

The variables ξ_v and n_v except ξ_0 , ξ_e , n_0 , n_e as given initial and terminal values are estimated by means of statistical collocation by suitably spaced $\hat{\xi}_i$ and \hat{n}_i the number of which should be chosen to achieve sufficient degrees of freedom in a post-mission adjustment. Accordingly, under consideration of representative $\xi_v = \xi_v[x(t), y(t)]$, $n_v = n_v[x(t), y(t)]$,

$$\xi_v = \sum m_{vi} \hat{\xi}_i \quad (13)$$

$$n_v = \sum n_{vi} \hat{n}_i \quad (14)$$

under consideration of $\xi_0 = \hat{\xi}_0$, $n_0 = \hat{n}_0$, $\xi_e = \hat{\xi}_e$, $n_e = \hat{n}_e$.

For short distances no advantage is gained from estimating ξ_v and n_v in equations (13) and (14) by additional terms containing \hat{n}_i and $\hat{\xi}_i$, respectively.

Substitution of $\hat{\xi}_v$ and \hat{n}_v estimates (13) and (14) in λ equations of the form (11) and (12) yields the final observational equations:

$$F_\lambda^{(1)} = \sum M_{\lambda i} \hat{\xi}_i + \sum N_{\lambda i} \hat{n}_i + C_\lambda \bar{u} + D_\lambda \bar{B} + E_\lambda \bar{Y} \quad (15)$$

$$- (\dot{x}_\lambda + \hat{a}_\lambda \hat{\xi}_0 + \hat{b}_\lambda \hat{n}_0 + \hat{c}_\lambda \hat{\xi}_e + \hat{d}_\lambda \hat{n}_e) = 0$$

$$F_\lambda^{(2)} = \sum P_{\lambda i} \hat{\xi}_i + \sum Q_{\lambda i} \hat{n}_i + H_\lambda \bar{u} + J_\lambda \bar{B} + K_\lambda \bar{Y} \quad (16)$$

$$- (\dot{y}_\lambda + \hat{e}_\lambda \hat{\xi}_0 + \hat{f}_\lambda \hat{n}_0 + \hat{g}_\lambda \hat{\xi}_e + \hat{h}_\lambda \hat{n}_e) = 0$$

A weighted least-squares solution yields quasi-optimal deflections of the vertical together with gyro biases and also makes it possible to provide error estimates thereof. Approximate constant survey vehicle velocities between stops and standard vehicle acceleration and deceleration would simplify the analyses and contribute to greater accuracy.

The geometrical considerations relating to equations (11) - (14) are evident from Figure 2.

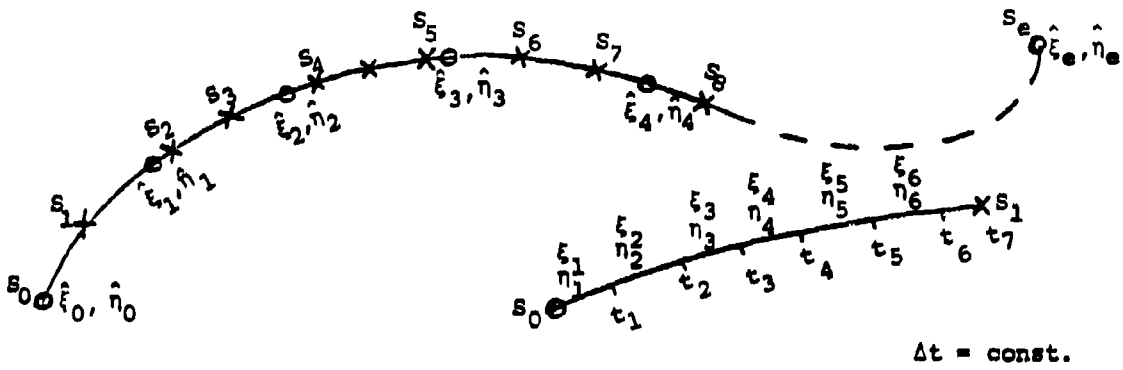


Figure 2

Traverse with Stops s_λ and Point Estimates ξ_i, η_i and Segment s_0, s_1

For the computation of m_{vi} and n_{vi} it is necessary to record t, x, y , to tabulate these data together with stop and point estimation coordinates $x_\lambda, y_\lambda, \hat{x}, \hat{y}$, to compute distance and correlation matrices $[r_{vi}]$ and $[p_{vi}]$, and finally to determine m_{vi} and n_{vi} -regression coefficients under restriction to five appropriate $\hat{\xi}_i$ or $\hat{\eta}_i$ -estimators. In a strict solution, corresponding m_{vi} 's and n_{vi} 's differ from each other. In practice, it may be possible to use isotropic correlation functions for both ξ and η because of short distances involved (see section 3). Due to the small correlation between ξ and η for short distances no advantage is gained by estimating ξ_v and η_v in equations (13) and (14) by additional terms containing $\hat{\eta}_i$ and $\hat{\xi}_i$, respectively.

The present quasi-optimal method is illustrated by the following: The observable acceleration error at the first vehicle stop is

$$\ddot{y}_1 = g\phi_{E1} - g(\xi_1 - \xi_o) + a_{N1} \quad (17)$$

under consideration of the initial deflection component ξ_o . The tilt error ϕ_{E1} is then estimated by means of the observable velocity errors \dot{x}_1 and \dot{y}_1 according to the linear regression equation

$$\hat{\phi}_{E1} = \alpha_1 \dot{x}_1 + \beta_1 \dot{y}_1 \quad (18)$$

The accelerometer is then biased according to

$$\ddot{y}_{B1} = \ddot{y}_1 - g\hat{\phi}_{E1} \quad (19)$$

The deflection difference of interest is then estimated as

$$\hat{\xi}_1 - \xi_o = -\frac{\ddot{y}_{B1}}{g} - \frac{DN_1}{g} \quad (20)$$

With respect to the second stop interval it is

$$\ddot{y}_2 = g(\phi_{E1} - \hat{\phi}_{E1}) + g\delta\phi_{E2} - g(\xi_2 - \xi_o) + a_{N2} \quad (21)$$

where $\delta\phi_{E2}$ is estimated in the form

$$\hat{\delta\phi}_{E2} = \alpha_2 \dot{x}_2 + \beta_2 \dot{y}_2 \quad (22)$$

Subsequently,

$$\ddot{y}_{B2} = \ddot{y}_2 - g\hat{\delta\phi}_{E2}$$

The second deflection change estimate is then

$$\hat{\xi}_2 - \xi_o = -\frac{\ddot{y}_{B2}}{g} = -\frac{DN_2}{g} \quad (23)$$

The accuracy of deflection determination is thus dependent on the accelerometer error, gyro bias error, and the cumulative tilt estimation error.

With $\hat{\xi}_\lambda - \xi_0 = \Delta_\lambda^1$ as initial estimates, it is

$$\xi_1^{(1)} = \xi_0 + \Delta_\lambda^1, \xi_2^{(1)} = \xi_1 + \Delta_\lambda^2 - \Delta_\lambda^1, \dots, \xi_n^{(1)} = \xi_{n-1}^{(1)} + \Delta_\lambda^n - \Delta_\lambda^{n-1} \quad (24)$$

Following estimation of ξ_e^1 and n_e^1 , the closing errors $\xi_e - \xi_e^1$ and $n_e - n_e^1$ are available for the approximate determination of average gyro biases $\bar{\alpha}$, $\bar{\beta}$, $\bar{\gamma}$. However, at least one additional intermediate ξ or n is required for a unique bias calculation. Finally, bias corrections to the initial deflection components $\xi_\lambda^{(1)}$ can be applied as

$$\delta\xi_\lambda = (\phi_{E\lambda} - \hat{\phi}_{E\lambda}) \text{Bias} \quad (25)$$

In contrast to the above procedure, the prior quasi-optimal method for the determination of $\hat{\xi}_i$ and \hat{n}_i -data contains sufficient degrees of freedom for the simultaneous estimation of gyro biases. It is, however, of significance that \dot{x}_λ and \dot{y}_λ of the general optimization method and $\dot{x}_{L\lambda}$ and $\dot{y}_{L\lambda}$ of the present RGSS mechanization are different because of implemented Kalman "corrections" $\delta\hat{\phi}_{E\lambda}$ and $\delta\hat{\phi}_{N\lambda}$. It is, e.g.,

$$\dot{y}_\lambda = \dot{y}_{L\lambda} + g \sum_{i=1}^{i=\lambda-1} \delta\hat{\phi}_{Ei} (t_i - t_{i-1}) \quad (26)$$

with $\lambda > 2$. While the identified accelerometer "corrections" permit an improvement in stochastic position determination, they are not beneficial with respect to optimal ξ , n -determinations.

The present suboptimization method is due to Huddle [1977] while the quasi-optimization concept was originally formulated by Baussus von Luetzow [1977].

3. Necessary Covariance Functions

Useful and consistent covariance functions, including cross-covariances, pertaining to Δg , ξ and n are those developed by Jordan [1972]. The covariance functions are:

$$\Phi_{gg}(r) = \sigma_g^2 \Phi_{gg} = \sigma_g^2 (1 + \frac{r}{D} - \frac{r^2}{2D^2}) e^{-r/D} \quad (27)$$

$$\phi_{\xi\xi}(r, \theta) = \sigma_{\xi\xi}^2 = \sigma_{\xi}^2 (1 + \frac{r}{D} - \frac{r^2}{D^2} \cos^2 \theta) e^{-r/D} \quad (28)$$

$$\phi_{nn}(r, \theta) = \sigma_{nn}^2 = \sigma_n^2 (1 + \frac{r}{D} - \frac{r^2}{D^2} \sin^2 \theta) e^{-r/D} \quad (29)$$

Suitable constant parameters are

$$\sigma_g = \sigma_{\Delta g} = 35 \text{ mgal}, \sigma_{\xi} = \sigma_n = 5 \text{ arcsec}, D=37 \text{ km.}$$

Cross-covariance functions, although available and includable in the general optimization method outlined in section 1, are not shown here. For short distances, cross-correlations tend to be small, and they become hardly significant for longer distances. The assumption of (approximate) homogeneity applies to all covariance functions. The geometry relating to an arbitrary 2 point-correlation is evident from Figure 3.

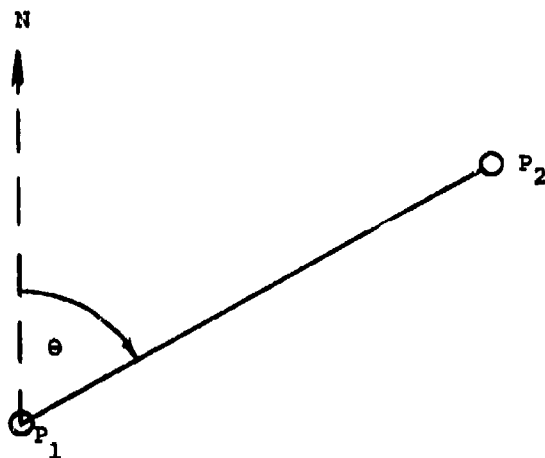


Figure 3
2 Point-Correlation Geometry

Basic, direction-independent correlation functions $\phi_{gg}(r, \theta)$ and $\phi_{nn}(r, \theta)$ are shown in Figure 4.

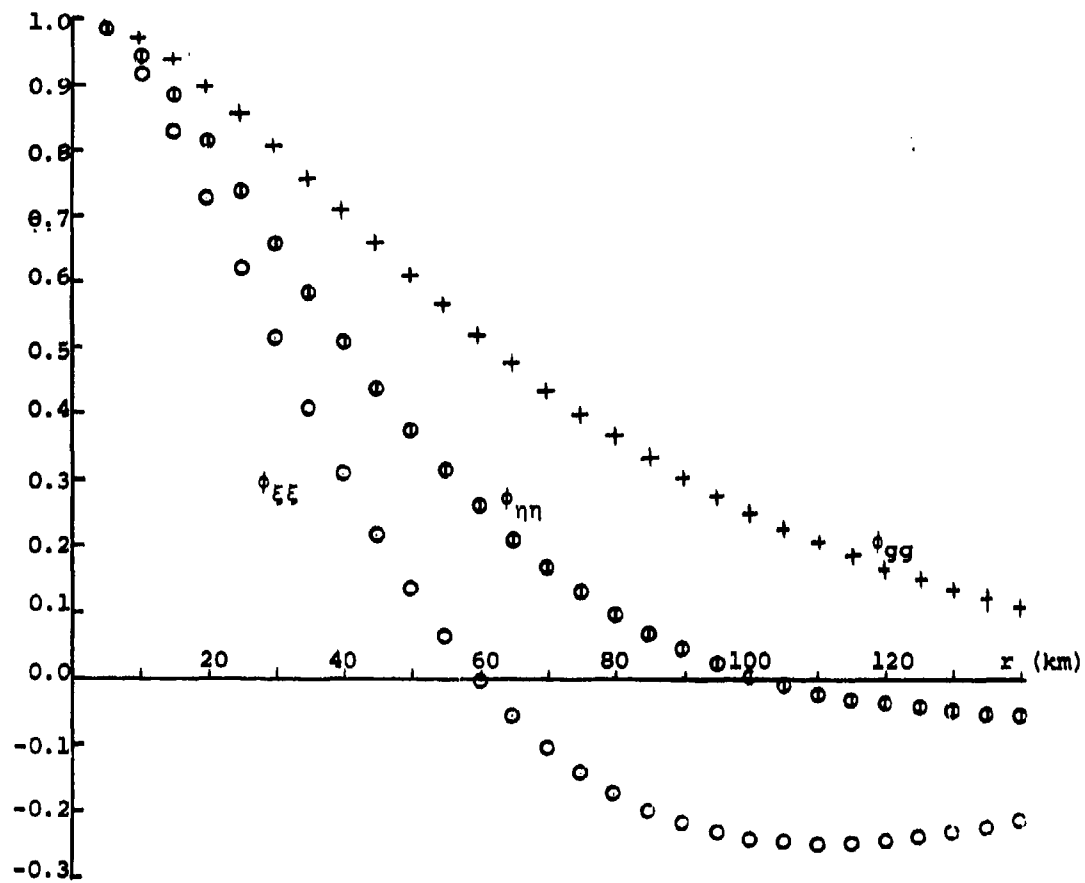


Figure 4

- +---Δg-Correlation Function $\phi_{gg}^{(r)}$
- n -Correlation Function $\phi_{nn}^{(r)}$ for $e=0$
- e -Correlation Function $\phi_{ee}^{(r)}$ for $e=0$

covariance functions pertaining to correlated gyro drift errors and correlated accelerometer errors are approximated by $A \cdot e^{-\frac{t}{\tau}}$. Parameters to be used are $\sigma_G = 0.002^\circ/\text{hr}$ and $\tau_G = 2 \text{ hr}$ in connection with Litton's G200 gyroscopes, and $10 \mu\text{gal}$ and $\tau_A = 40 \text{ min}$ in the case of Litton's A200 accelerometers.

4. Estimation of Gridded $\hat{\xi}$, $\hat{\eta}$ -Data from Discrete RGSS-Determined ξ , η -Information

For a mathematically satisfactory solution of the estimation problem in question, error covariances $\bar{e}(t_i) \bar{e}(t_k) = \bar{e}_{ik}$ should be computed from time-dependent linear aggregates of correlated gyro and accelerometer errors. In general, it is sufficient to estimate $\hat{\xi}$, $\hat{\eta}$ -data from about 20 corresponding ξ , η -values, obtained by means of the RGSS. Otherwise, the computational load as to matrix inversion becomes too great. Under utilization of Figure 5, $\hat{\xi}$ -estimation at P_{33} may be formulated as

$$\begin{aligned} \hat{\xi}_{33} &= \hat{\xi} = \\ &= a_{11}(\xi_{11} + e_{11}) + \dots + a_{15}(\xi_{15} + e_{15}) \\ &\quad + a_{22}(\xi_{22} + e_{22}) + \dots + a_{26}(\xi_{26} + e_{26}) \\ &\quad + a_{33}(\xi_{33} + e_{33}) + \dots + a_{36}(\xi_{36} + e_{36}) \\ &\quad + a_{42}(\xi_{42} + e_{42}) + \dots + a_{46}(\xi_{46} + e_{46}) \\ &\quad + a_{54}(\xi_{54} + e_{54}) + \dots + a_{56}(\xi_{56} + e_{56}) \\ &\quad + a_{73}(\xi_{73} + e_{73}) + \dots + a_{76}(\xi_{76} + e_{76}) \end{aligned} \tag{30}$$

with regression coefficients a_{11} , etc. The first line of the resulting covariance matrix is then

$$\begin{aligned} \bar{\xi} \bar{\xi}_{11} &= \\ &= a_{11}(\text{var}\xi + \bar{e}_{11}) + \dots + a_{15}(\bar{\xi}_{11} \bar{\xi}_{15} + \bar{e}_{15}) \\ &\quad + a_{22} \bar{\xi}_{22} \bar{\xi}_{11} + \dots + a_{26} \bar{\xi}_{26} \bar{\xi}_{11} \\ &\quad + a_{33} \bar{\xi}_{33} \bar{\xi}_{11} + \dots + a_{36} \bar{\xi}_{36} \bar{\xi}_{11} \quad (\text{con't}) \end{aligned}$$

$$+ a_{42} \overline{\xi_{42}} \overline{\xi_{11}} + \dots + a_{46} \overline{\xi_{46}} \overline{\xi_{11}}$$

$$+ a_{54} \overline{\xi_{54}} \overline{\xi}_{11} + \dots + a_{56} \overline{\xi_{56}} \overline{\xi}_{11}$$

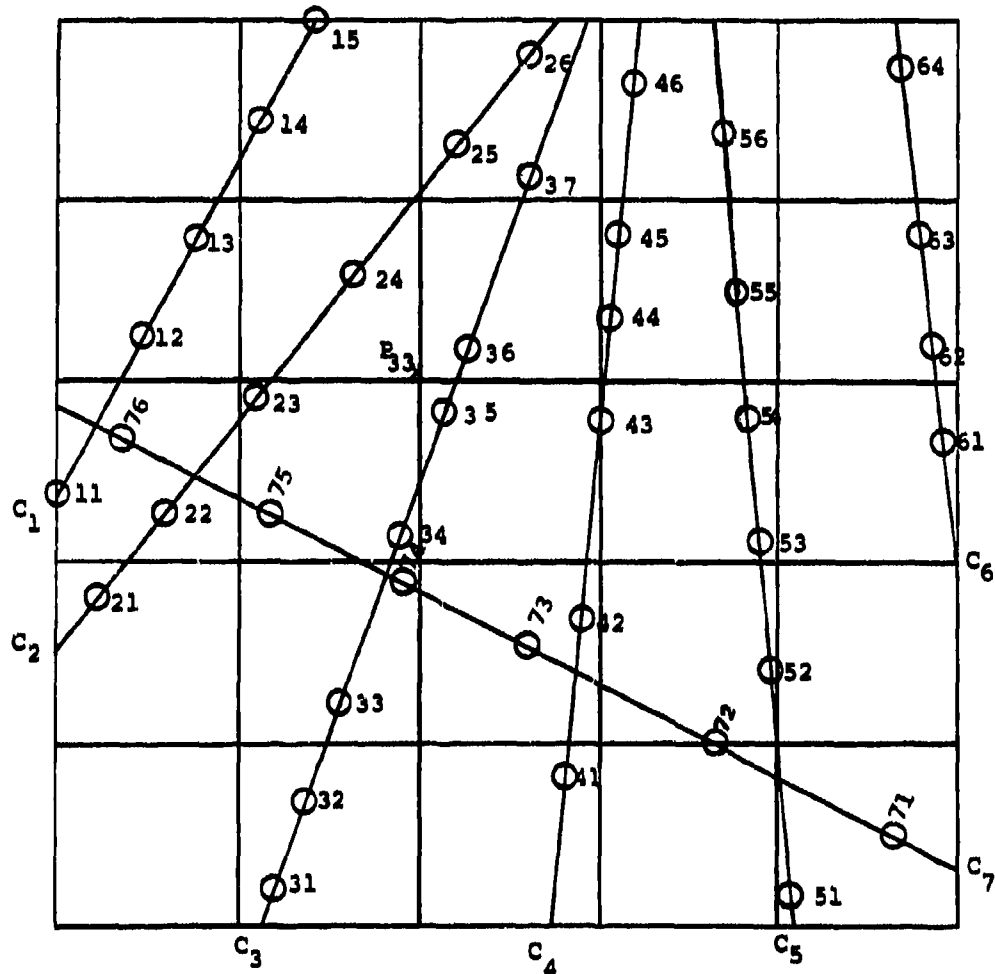


Figure 5

RGSS Solitary Courses C_m with Discrete ξ_{mn} , η_{mn} -Data Crossing

a Regular Grid with Estimated $\hat{\epsilon}_{ik}$, \hat{n}_{ik} -Data

Of significance is that "noise" covariances may be neglected as to data from different runs. The computation of respective covariances by means of equations (23) and (24) and the inversion of the covariance matrix presents no computational difficulties. Simplifications as to the inclusion of variable noise covariances may be potentially possible.

It should be noted that the midpoint Δg -estimation from Δg -data measured at two points separated by a distance of 3 km has a mean error of 0.32 mgal which corresponds to 0.05 arcsec. Although this theoretical estimate appears to be optimistic, the indications are that gravity anomalies and deflection components can be well-interpolated in non-mountainous terrain for grid intervals $\Delta x = \Delta y \leq 5$ km.

5. Improved Stochastic Position Error Control

The determination of gyro biases along with that of deflections of the vertical under availability of initial and terminal deflection components ξ_0, n_0, ξ_e, n_e , makes it also possible to compute position corrections $\delta x_B(t_\lambda), \delta y_B(t_\lambda)$. Terminal position closure errors $\delta x_e, \delta y_e$ may thereafter be attributed to accelerometer scale factors, and these closure errors are then linearly allocated as additional position corrections. A linear allocation appears, moreover, to be beneficial if gyro biases corrections are not explicitly available.

The geometrical framework for terrestrial inertial navigation is the applicable reference ellipsoid. If the initial deflection components ξ_0, n_0 are known, leveling of the platform at the start of the survey mission results in the terms $g(n-n_0)$ and $-g(\xi-\xi_0)$ instead of gn and $-g\xi$ in equations (3) and (4). For the computation of $\text{var } \dot{x}(t_\lambda), \text{var } x(t_\lambda), \text{cov } (\dot{x}, x)(t_\lambda)$, etc., ξ and n

are considered as random variables and ξ_0 and η_0 as unknown biases with $\text{var } \xi$ and $\text{var } \eta$, respectively. As an illustration, the variance contribution due to $-g(\xi - \xi_0)$ in the computation of $\text{var } \dot{y}(t_\lambda)$ is then in simplified form

$$\text{var } \dot{y}_\xi^{(1)}(t_\lambda) = g^2 \overline{\left(\int_{t_{\lambda-1}}^{t_\lambda} \xi dt \right)^2} + g^2 \text{var } \xi(t_\lambda - t_{\lambda-1})^2 \quad (32)$$

Actually, ξ and ξ_0 are correlated random variables, and the correct computation would read

$$\text{var } \dot{y}_\xi^{(2)}(t_\lambda) = \text{var } \dot{y}_\xi^{(1)}(t_\lambda) - 2g^2(t_\lambda - t_{\lambda-1}) \overline{\int_{t_{\lambda-1}}^{t_\lambda} \xi_0 \xi dt} \quad (33)$$

The implications of eq. (33) and of corresponding correct $\text{var } \dot{y}^{(2)}$ and $\text{cov}^{(2)}(\dot{y}, y)$ -terms are the following:

- *For short distances, i.e., for local surveys within a radius of 30 km from the initial departure point, the incremental position variances and the total position variance are significantly reduced.

- *For short distances, Kalman filter-computed regression coefficients for position determination are not optimally computed.

- *It is beneficial for vertical positioning to facilitate initial $\Delta g - \Delta g_0$ elimination by appropriate calibration under consideration of a measured g_0 .

The above conclusions are consistent with encouraging good RGSS positioning results.

Identified correction terms involve the consideration of $\text{cov}(\xi, \xi_0)$ and $\text{cov}(\eta, \eta_0)$ -computations and thus require to record the coordinates $X(t)$, $Y(t)$ in addition to $X(0)$, $Y(0)$. The existing computer capacity would

have to be moderately increased. Improved stochastic position error control would be particularly effective in conjunction with the use of improved accelerometers, gyroscopes and velocity quantizers and then approximately achieve classical survey accuracies.

6. Conclusions

Quasi-optimal determination of deflections of the vertical under simultaneous consideration of all measured velocity component errors at vehicle stops is feasible and computer-programmable. It has inherent advantages over the present estimation technique and can be generalized to a fully optimal method by the inclusion of the whole set of observed accelerometer errors at stops. Solutions involving covariances between ξ , n , Δg are neither promising nor economic. The construction of gridded ξ , n -data from RGSS-determined estimations under consideration of non-stationary errors is possible and does not necessarily require longitudinal and traverse surveys. Actual position errors are smaller than Kalman-estimated position errors, particularly for distances below 30 km. The computation of improved regression coefficients for position determination is possible and can be facilitated without expensive complexity. Further theoretical research and testing and the implementation of RGSS hardware improvements are expected to achieve highly promising results in position and gravity component determination for various military and non-military applications.

7. Acknowledgments

The author would like to thank his colleagues Dr. J. Huddle from Litton Guidance and Control Systems, Dr. W. Heller from The Analytical Sciences Corporation, Professor Dr. E. Grafarend from the German Armed Forces University, Munich, and the U.S. Army Engineer Topographic Laboratories

for direct or indirect support of this paper. In addition, he feels indebted to Mr. M. Todd and Mrs. C. Gradick for the preparation of graphical presentations and for the typing of the manuscript, respectively.

REFERENCES

Baussus von Luetzow, H. 1977. A Review of Past, Present and Future USAETL Inertial/Gradiometric Geodesy Activities and Programs. Proc. 1st Int'l Symp. on Inertial Technology for Surveying and Geodesy, Ottawa, Canada, October 1977.

Huddle, J., 1977. The Measurement of the Change in the Deflection of the Vertical with a Schuler-Tuned North-Slaved Inertial System. Litton Guidance and Control Systems, Woodland Hills, CA.

Jordan, S., 1972. Self-Consistent Statistical Models for the Gravity Anomaly, Vertical Deflections, and Modulation of the Geoid. J. Geoph. Research, Vol. 77, No. 20.

ANALYSIS OF VARIANCE ON THE TRADE-OFF FUNCTION
RELATING ACCURACY TO SPEED OF REACTION

Walter D. Foster, AFIP
John H. Wolcott, AFIP, Lt. Col., USAF, BSC
Terrence L. Kay, AFIP
Washington, D.C. 20306

ABSTRACT. The customary variable in the analysis of variance is a single, continuous variable, presumed to possess the usual assumptions. In contrast, the variable of analysis here is a function,

$$\ln[P/(1-P)] = A + BT, \text{ where}$$

P is the proportion of correct responses, T is the response time, and A and B are parameters to be estimated from the data. This response (or trade-off) function was derived from observations on P vs. T as human subjects were asked to operate a simple right or left-hand response to a light signal at different levels of an altitude chamber and mood as determined by a psychological scale.

The analysis of variance of the trade-off function took the following form:

<u>Source</u>	<u>df</u>
Mean	2
Subjects	2(s-1)
Altitudes	2(a-1)
Moods	2(m-1)
AxM	2(a-1)(m-1)
Exp Error	2(s-1)(am-1)
Pooled Devs	ams(n-2)
TOTAL	ams

to ascertain if altitude or mood affected the trade-off function.

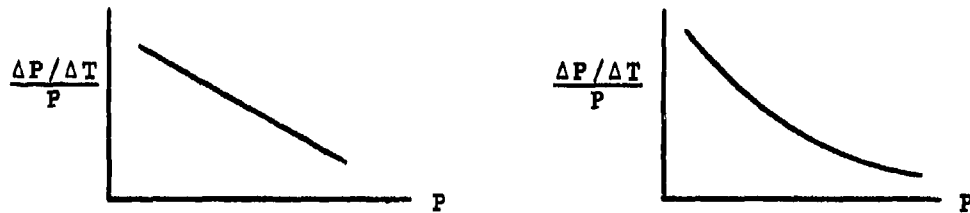
I. INTRODUCTION. Factors affecting aircraft pilots have been extensively chronicled in the literature on aircraft safety. To a dismaying degree, these factors are difficult both to define and to measure. A highly bally-hooed factor currently enjoying a most lucrative existence is biorhythm whose effect on pilots involved in aircraft accidents has been scientifically demonstrated to be wholly fallacious (Wolcott 1977 a,b). Our report is concerned with two factors, altitude and mood, their definition and measurement, and their possible effect on reaction time. Emphasis is placed on a novel statistical analysis, the analysis of variance of a function (Foster 1962).

The opinions or assertions contained herein are the private views of the authors and are not to be construed as official or as reflecting the views of the Department of the Army, Department of the Air Force, or the Department of Defence.

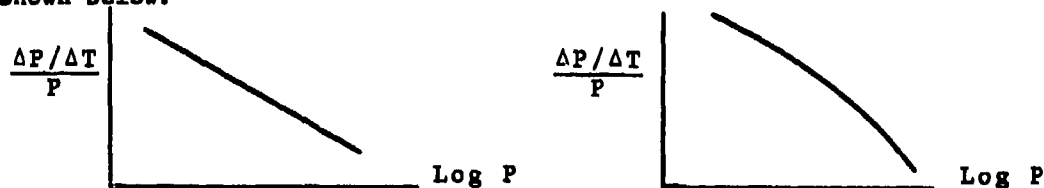
The laboratory experiment consisted of measuring the reaction time of a human subject responding to two lights. If the right light would flash, the subject should depress the right-hand button within a specified length of time for a correct response, and similarly for the left. An incorrect response would consist of depressing the wrong button or exceeding the time limit. Time limits were 275, 240, 215, 180 milli seconds. The time limits were balanced and randomized in their order of presentation to preclude an order effect. At each time limit, the subject was challenged with 100 flashes. Simulated heights in the altitude chamber went from 0 to 12,000 feet in 2,000 foot intervals. While measured on a continuous psychological scale mood was condensed for analysis here to the three levels of high, middle and low. The seven altitudes were condensed to low, middle, and high for this analysis, thus creating a three-by-three factorial design for treatments. There were eight volunteers, each having at least one trial in each of the three by three factorial to provide a completely balanced design.

The variable of analysis is defined to be the function relating the proportion of correct responses to reaction time. Because accuracy generally decreases as response time is decreased--a trade-off between accuracy and time, the function relating these two is customarily called the trade-off function.

II. DERIVATION OF THE TRADE-OFF FUNCTION. A variety of models have been used in similar experimentation by other researchers. A good review of these is given by Wood (1976) and Lappin (1977). None of these was found to be outstandingly successful. The procedure followed here was to elicit a model from consideration of the basic data. It seemed to us after trying many approaches that a plot of successive differences in the percent correct when divided by change in time and by percent correct answers and then plotted against performance--this plot was linear for most trials and when not, it tended to be concave to the right, as shown in the following diagram:



When this dependent variable was plotted versus log performance, the plots were occasionally linear but usually concave to the left as shown below.



The physical meaning of these plots was interpreted to be as follows: Improvement rate related to performance fell off at a constant rate as performance increased. Thus,

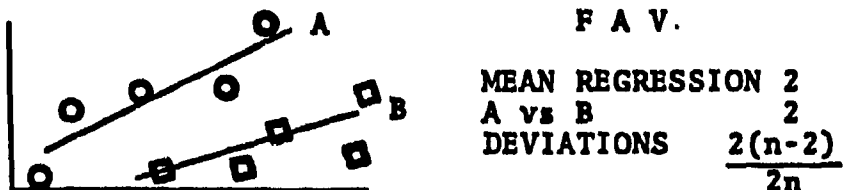
$$\frac{\Delta P / \Delta T}{P} = A - BP$$

The derivation of the trade-off function was accomplished by approximating the differences by differentials, separating variables to give $\frac{dp}{(A-BP)P} = dt$, and integrating by partial fractions to give the following model:

$$P = \frac{A/B}{1 + k \exp(-AT)}$$

which is recognizable as a 3-parameter logistic function. Plots on logistic paper, i.e. a 2-parameter logistic by placing $A/B = 1$, were generally linear. Some typical examples of these plots are given in Figure 1. Therefore, the model $\ln[p/(1-P)] = a + bT$ was adopted.

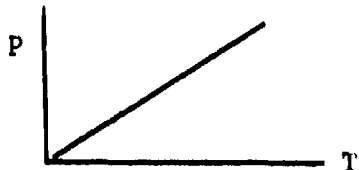
III. FUNCTION ANALYSIS OF VARIANCE (FAV). What is FAV? Perhaps it is best exemplified in an analogy to the typical analysis of variance. Note that the net sum of squares for an effect can be computed by subtracting a correction term: $\sum (treatment\ totals)^2/r - (Grand\ total)^2/rt$ to center the data at the mean. In the corresponding FAV on linear regression, the moments are taken about the origin so that not one degree of freedom but two are allocated. However, the average regression through all the points is used as the correction term when distinguishing between two or more linear regressions representing groups or treatments, as illustrated below:



The complete analysis of variance of the trade-off function is shown in Table 1 in which the degrees of freedom are allocated as indicated above; tests of the effects of altitude, mood, and the AXM interaction are seen to be not statistically different. However, the graphs of these effects (in Figure 2) show a distinct ordering of the effects as expected if the effects are real.

Low altitude is taken as the reference or ground level compared to which the curves for the higher altitudes are displaced downward reflecting a depressed performance. Similarly with respect to a good mood (as reference) poorer moods are associated with curves with downward displacement. That both mood and altitude should have the ordering as discussed above under the null hypothesis has a significance probability of 1/36 as shown at the bottom of Table 1.

IV. COMPARISON OF FAV TO AN ALTERNATE ANALYSIS ON EFFICIENCY.
Efficiency was defined as the proportion correct divided by the average reaction time. This definition is able to be compared to the trade-off function by considering the following plot in which proportion of correct answers is plotted against time.



Assuming a linear model to be appropriate with intercept at the origin, efficiency can be seen to be the slope of this plot. Recall that the logistic model plotted the logarithm [percent correct/percent wrong] versus time but the line was not forced through the origin.

For efficiency, the alternate analysis consisted of a multiple regression in which efficiency as the dependent variable was related linearly to altitude and mood both in the original scales. In that analysis, both altitude and mood were found to be statistically significant, primarily because of a larger number of trials and about double the number of subjects. However, the multiple correlation coefficient was found to be less than .45 and R^2 usually less than .20. Thus, less than 20% of the variation in efficiency was accountable by mood or altitude. Because of the presumed advantage of the trade-off function and its putative sophistry, it was something of a surprise to have it perform not as well as the simple efficiency approach. To pursue the question further, the intercept of the trade-off function was plotted against slope for each of the 72 individual regressions in the FAV analysis. Because these 72 points were incredibly linear, it was concluded that a very large experimental (not statistical) correlation existed between intercept and slope. It is clear from this very high correlation that virtually all of the information in the FAV analysis was contained either in the intercept or the slope parameter, but certainly not both. Thus no advantage was derived from a two-paramter model for these data.

REFERENCES

- Wolcott, John H., Robert R. McMeakin, Robert E. Burgin, Robert E. Yanowitch,
"Correlation of General Aviation Accidents with the Biorhythm Theory."
Human Factors, 1977, 19(3), 283-93.
- Wolcott, John H., Robert R. McMeakin, Robert E. Burgin, Robert E. Yanowitch,
"Correlation of Occurrence of Aircraft Accidents with Biorhythmic
Criticality and Cycle Phase in U.S. Air Force, U.S. Army and Civil
Aviation Pilots." Aviat. Space Environ. Med. 48(10) 976-83, 1977.
- Foster, Walter D., "Analysis of a Function in Collaborative Experimentation."
Proc. of 8th Conf. on Design of Experiments in Army R, D, & T.
ARO-D Report 63-2. 1963.
- Wood, Charles C., and J. Richard Jennings, "Speed-accuracy Trade-off Functions
in Reaction Time." Perception and Psychophysics, Vol. 19(1), 92-101,
1976.

TABLE 1. FAV ON TRADE-OFF FUNCTION

<u>Source</u>	<u>df</u>	<u>SS</u>	<u>MS</u>	<u>F</u>
MEAN	2	1700.8420		
SUBJECTS	14	492.2826	35.1630	
ALTITUDES	4	8.1274	2.0318	1.17
MOODS	4	8.1038	2.0259	1.16
A x M	8	6.6508	.8313	
EXP ERROR	112	195.2660	1.7434	
DEVIATIONS	<u>432</u>	<u>398.6270</u>	.9227	
	576	2803.8996		

ALTERNATIVE APPROACH TO SIGNIFICANCE PROBABILITY

1. MOOD: Number of ways of ordering results = 6

Number of ways if effect exists = 1

 $P(\text{Observed result}) = 1/6$

2. ALTITUDE: Same as above.

3. JOINT PROBABILITY: $1/6 \times 1/6 = 1/36$

FIGURE 1. LOGIT (CORRECT) VS REACTION TIME, M-SECS: NINE TRIALS

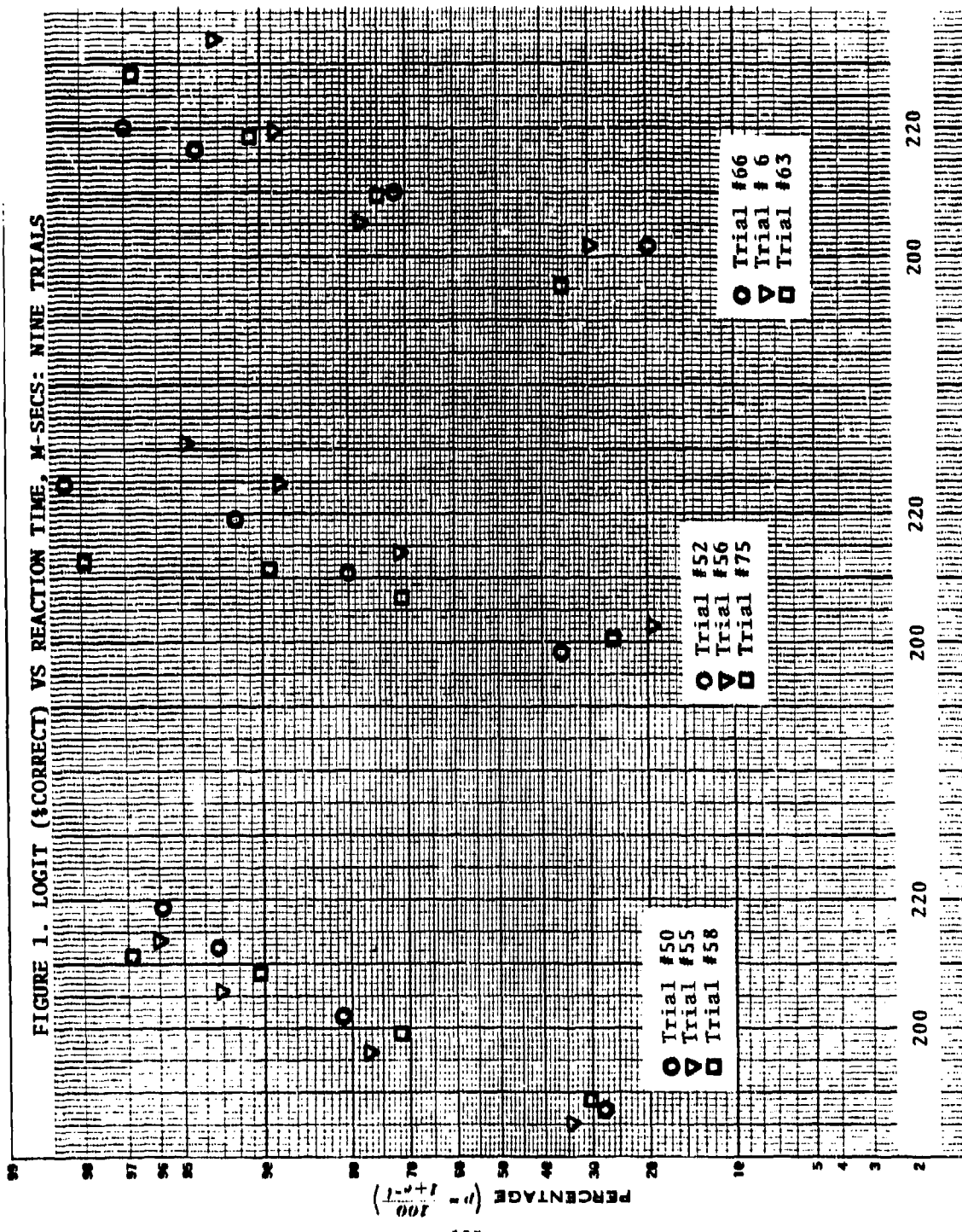
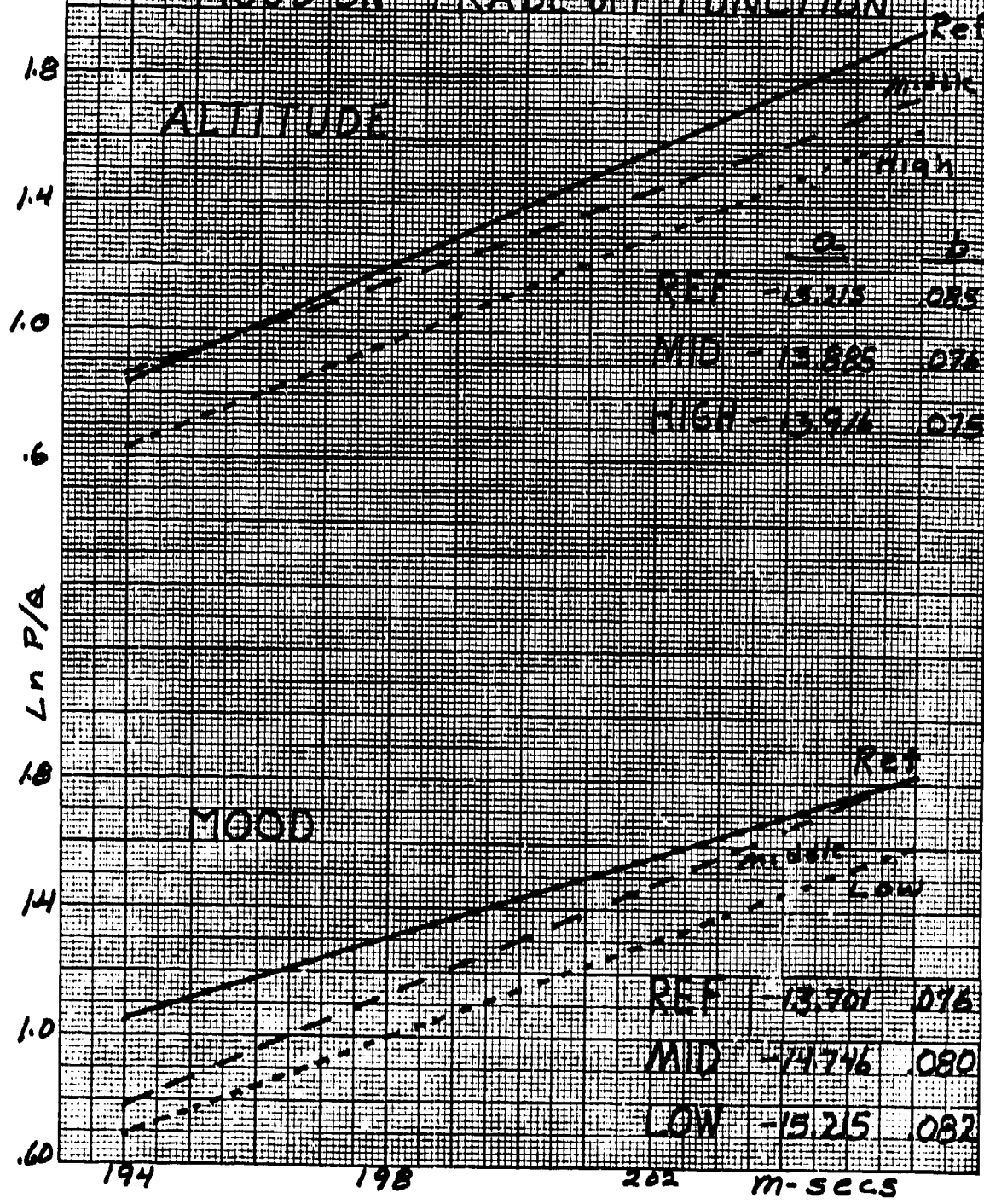


FIG 2. HEIGHT OF ALTITUDE AND
MOOD ON TRADE-OFF FUNCTION



THE ANALYSIS OF PARTIALLY FACTORIAL EXPERIMENTS

J. Robert Burge
Walter Reed Army Institute of Research

I. INTRODUCTION.

It frequently happens in factorial experiments that one or more of the factors is of such a nature that certain treatment combinations are identical. To illustrate this point, a problem commonly encountered by blood banks involved in platelet transfusion therapy has been selected (Table 1). The two variables of interest affect the integrity and function of platelets. One of the factors involves two different methods of storing blood. The other consists of three different times of storage (including fresh blood or NO storage), so there will be no differences between storage methods at the ZERO level of time.

TABLE 1
Relationship Between Storage Time and
Storage Method on Platelet Integrity

<u>Stored For</u>	<u>Concentrates Stored At</u>	
	<u>Room Temperature.</u>	<u>Frozen</u>
0 hours	y_{11}	y_{12}
24 hours	y_{21}	y_{22}
48 hours	y_{31}	y_{32}

This experiment falls into a class of experiments in which the treatment combinations have an appearance of consisting of a full set of factorial combinations when in fact this is not so. Under such circumstances, when testing different types of storage, the storage method is irrelevant when a zero amount of storage time is administered. Consequently, there will be additional degrees of freedom for error arising from comparisons between identical combinations and correspondingly fewer treatment degrees of freedom. The partition of the treatment degrees of freedom into their separate components will also be different.

Computing the Analysis of Variance Table for Experiments Involving Qualitative Factors and Zero Amounts of Quantitative Factors:

A short summary of this type of analysis is given by Addelman (1974).

Let factor A (holding time) represent the quantitative factor and factor B (storage method) denote the qualitative factor. If we assume that the first level of factor A is the zero amount, the appropriate AOV table is given below (Table 2) where factor A has a levels and factor B has b levels:

TABLE 2
AOV for an $a \times b$ Partially Factorial Experiment
(one observation per cell)

Source of Variation	df	SS
Factor A (Time)	$a-1$	$\sum_{i=1}^a \frac{y_{i..}^2}{b} - \frac{y_{..}^2}{ab}$
Factor B (Method)	$b-1$	$\sum_{j=1}^b \frac{\sum_{i=2}^a (y_{ij})^2}{a-1} - \frac{\sum_{i=2}^a \sum_{j=1}^b y_{ij}}{(a-1)b}^2$
A X B	$(a-2)(b-1)$	$\sum_{i=2}^a \sum_{j=1}^b y_{ij}^2 - \sum_{i=2}^a \frac{y_{i..}^2}{b} - \frac{\sum_{j=1}^b (\sum_{i=2}^a y_{ij})^2}{a-1}$ $+ \frac{\sum_{i=2}^a \sum_{j=1}^b y_{ij}}{(a-1)b}^2$
Controls (Exp. Error)	$b-1$	$\sum_{j=1}^b y_{1j}^2 - \frac{y_{1..}^2}{b}$
Total	$ab-1$	$\sum_{i=1}^a \sum_{j=1}^b y_{ij}^2 - \frac{y_{..}^2}{ab}$

Note that the SS due to factor B is computed only for the nonzero amounts of factor A. Similarly, the SS due to interaction of the two factors is utilizing only the nonzero amounts of the quantitative factor A.

It may be helpful to illustrate the Addelman algorithm with an example (artificial data):

EXAMPLE ONE

TABLE 3

Storage Method

	s_1	s_2	Row Totals	
Holding Time	T_0	49.5	61	110.5
	T_{24}	18	41	59.
	T_{48}	29	23.5	52.5
Column Totals	47*	64.5*	111.5*	

$$\sum_{i=1}^3 \sum_{j=1}^2 y_{ij} = 222.$$

Source	df	SS	
T_A	2	$(110.5^2 + 59^2 + 52.5^2)/2 - \frac{(222)^2}{6}$	= 1,009.75
S_B	1	$(47^2 + 64.5^2)/2 - \frac{(111.5)^2}{4}$	= 76.5625
$T_A \times S_B$	1	$18^2 + 41^2 + 29^2 + 23.5^2 - \frac{59^2 + 52.5^2}{2} - \frac{47^2 + 64.5^2}{2} + \frac{115.5^2}{4}$	= 203.0625
Error	1	$61^2 + 49.5^2 - \frac{(110.5)^2}{2}$	= 66.125
Total	5	$49.5^2 + 61^2 + 18^2 + 41^2 + 29^2 + 23.5^2 - \frac{(222)^2}{6}$	= 1,355.1

* (An asterisk was utilized to indicate that the totals involve only the nonzero amounts of the quantitative factor - holding time.)

II. REGRESSION APPROACH (An Alternative Method).

The standard analysis of variance model for the two-way classification considered in Section 1 is:

$$E[Y_{ij}] = \mu + \alpha_1 + \beta_j + \delta_{ij}$$

$$\text{Where } \alpha_1 + \alpha_2 + \alpha_3 = 0$$

$$\delta_{21} + \delta_{22} = 0$$

$$\beta_1 + \beta_2 = 0$$

$$\delta_{31} + \delta_{32} = 0$$

$$\delta_{21} + \delta_{31} = 0$$

$$\delta_{22} + \delta_{32} = 0$$

Thus if μ , α_1 , α_2 , β_1 , and δ_{21} are known or estimated, all other parameters or their estimates can be found from the restrictions. We can write the regression model:

$$E[Y_{ij}] = \mu + \alpha_1 x_1 + \alpha_2 x_2 + \beta_1 x_3 + \delta_{21} x_4 \quad \text{or } E[\mathbf{Y}] = \mathbf{X}\boldsymbol{\beta}$$

Where:

$$\mathbf{Y} = \begin{bmatrix} Y_{11} \\ Y_{12} \\ Y_{21} \\ Y_{22} \\ Y_{31} \\ Y_{32} \end{bmatrix}; \quad \mathbf{X} = \begin{bmatrix} 1 & 1 & 0 & 0 & 0 \\ 1 & 1 & 0 & 0 & 0 \\ 1 & 0 & 1 & 1 & 1 \\ 1 & 0 & 1 & -1 & -1 \\ 1 & -1 & -1 & 1 & -1 \\ 1 & -1 & -1 & -1 & 1 \end{bmatrix} \quad \text{and } \boldsymbol{\beta} = \begin{bmatrix} \mu \\ \alpha_1 \\ \alpha_2 \\ \beta_1 \\ \delta_{21} \end{bmatrix}.$$

One should note the following:

(i) For all observations belonging to the zero level
 $x_2 = x_3 = x_4 = 0$

(ii) The elements of the δ_{21} column are obtained as a product of the corresponding elements of the a_2 and β_1 columns.

(iii) Because of the orthogonality in X , we can obtain separate orthogonal sums of squares which are additive for the estimates of μ , a_1 , and a_2 , β_1 , and δ_{21} . These will be the usual sums of squares for the mean, rows, columns, and interaction.

(iv) Two column vectors, a and β , are orthogonal if and only if their inner product is zero (i.e., $a^T \beta = 0$).

Using the $R()$ - notation for reductions in sum of squares when fitting linear models:

A more complete summary of $R()$ - notation is given in Searle(1971).

The $R()$ - notation is defined by denoting as $R(b)$ the reduction in sum of squares due to fitting the familiar linear model

$$E[y] = X b \quad (1)$$

Let b^0 be any solution to the normal equations

$$X'Xb^0 = X'y \quad (2)$$

$$\text{say } b^0 = (X'X)^{-} X'y \quad (3)$$

where $(X'X)^{-}$ is a generalized inverse of $X'X$, meaning that it is a matrix satisfying $X'X(X'X)^{-} X'X = X'X$, then

$$R(b) = b^0 X'y. \quad (4)$$

It can also be expressed as

$$R(b) = Y'X(X'X)^{-} X'y \quad (5)$$

We take (4) and (5) as our formal definition of $R(b)$.

Now suppose b is partitioned into two vectors b_1 and b_2 so that the model is (full model)

$$E[Y] = X_1 b_1 + X_2 b_2 \quad (6)$$

The reduction in sum of squares for fitting this is denoted by:

$$R(b_1, b_2) = Y'(X_1 X_2) \begin{bmatrix} X'_1 X_1 & X'_1 X_2 \\ X'_2 X_1 & X'_2 X_2 \end{bmatrix}^{-1} \begin{bmatrix} X'_1 \\ X'_2 \end{bmatrix} Y, \quad (7)$$

This being the direct analogue of:

$$R(b) = Y'X (X'X)^{-1} X'Y$$

In connection with (6) consider the submodel (reduced model):

$$E[Y] = X_1 b_1 \quad (8)$$

For the fitting of this model:

$$R(b_1) = Y'X_1 (X_1 X_1)^{-1} X'_1 Y \quad (9)$$

Differences between reductions in sums of squares are also accommodated by the notation:

$$R(b_2 | b_1) = R(b_1, b_2) - R(b_1) \quad (10)$$

This indicates the reduction in sums of squares due to fitting the full model over and above that due to fitting the reduced model.

The $R()$ - notation is quite general and can be used for regression models, for familiar linear models involving main effects and interactions, and for combinations of the two.

In order to demonstrate this notation, it has been applied to the data given in Table 3 and summarized in Table 4.

TABLE 4
AOV for a 3x2 Partially Factorial Experiment
(One Observation/Cell)

Source of Variation	df	SS	R() - Notation
μ	1	8,214.00	$R(\mu)$
Factor A (Time)	2	1,009.75	$R(\alpha_1, \alpha_2 \mu, \beta_1, \delta_{21}) = R(\alpha_1, \alpha_2)$
Factor B (Method)	1	76.56	$R(\beta_1 \mu, \alpha_1, \alpha_2, \delta_{21}) = R(\beta_1)$
A X B	1	203.06	$R(\delta_{21} \mu, \alpha_1, \alpha_2, \beta_1) = R(\delta_{21})$
Full Model	5	9,503.375	$R(\mu, \alpha_1, \alpha_2, \beta_1, \delta_{21})$
Error	1	66.125	$Y'Y - R(\mu, \alpha_1, \alpha_2, \beta_1, \delta_{21})$
Total	6	9,569.5	$Y'Y$

III. PARTIAL FACTORIAL EXPERIMENTS WITH MORE THAN ONE OBSERVATION PER CELL.

A. BALANCED CASE

Whenever the experimental plan involves one observation in each subclass, Addelmann's article applies. The following example illustrates how to treat a 3×2 partial factorial experiment when cell frequencies exceed one. Specifically, the zero treatment has been replicated 4 times. All of the other subclass frequencies equal 3.

EXAMPLE TWO
(Cell Frequencies Greater Than One)

Storage Time	Storage Method		Row Totals
	S_1	S_2	
T_0 : 0 hours	63 61	49.5 47	$220.5 = Y_{1..}$
T_1 : 24 hours	23 13 18 $\frac{54}{54} = Y_{11..}$	40 41 42 $\frac{123}{123} = Y_{12..}$	$177 = Y_{2..}$
T_2 : 48 hours	40 18 $\frac{29}{87} = Y_{21..}$	22 23.5 $\frac{70.5}{70.5} = Y_{22..}$	$157.5 = Y_{3..}$
Column Totals	$141 = Y_{*1..}$		$334.5 = Y_{*..}$
			$555 = Y_{...}$

Analysis of Variance Computations:

$$\text{Factor A} \\ SS(T) = \frac{220.5^2}{4} + \frac{177^2}{6} + \frac{157.5^2}{6} - \frac{(555)^2}{16} = 2,259.375$$

$$\text{Factor B} \\ SS(S) = \frac{141^2 + 193.5^2}{6} - \frac{(334.5)^2}{12} = 229.6875$$

$$\begin{aligned}
 \text{Interaction SS(TxS)} &= \frac{54^2 + 87^2 + 123^2 + 70.5^2}{3} - \frac{177^2 + 157.5^2}{6} - \frac{141^2 + 193.5^2}{6} \\
 &\quad + \frac{(334.5)^2}{12} = 609.1875 \\
 \text{Error} &= 63^2 + 61^2 + 49.5^2 + 47^2 - \frac{(220.5)^2}{4} + \dots + 22^2 + 23.5^2 + 25^2 \\
 &\quad - \frac{(70.5)^2}{3} = 492.6875 \\
 \text{Mean} &= \frac{(555)^2}{16} = 19,251.5625 \\
 \text{Total} &= 63^2 + \dots + 25^2 = 22,842.50
 \end{aligned}$$

TABLE 5
AOV for an 3x2 Partially Factorial Experiment
(Cell Frequencies Exceed One)

Source of Variation	df	SS	R() - Notation
μ	1	19,251.562	$R(\mu)$
Factor A (Time)	2	2,259.375	$R(a_1, a_2 \mu, \beta_1, \delta_{21}) = R(a_1, a_2 \mu) \neq R(a_1, a_2)$
Factor B (Method)	1	229.6875	$R(\beta_1 \mu, a_1, a_2, \delta_{21}) = R(\beta_1)$
AxB	1	609.1875	$R(\delta_{21} \mu, a_1, a_2, \beta_1) = R(\delta_{21})$
Full Model	5	22,349.812	$R(\mu, a_1, a_2, \beta_1, \delta_{21})$
Error	11	492.6875	$\mathbf{Y}'\mathbf{Y} - R(\mu, a_1, a_2, \beta_1, \delta_{21})$
Total	16	22,842.50	$\mathbf{Y}'\mathbf{Y}$

B. UNBALANCED CASE

The analysis of variance (AOV) table has been used to summarize the results from the analyses performed up to this point. The results from an analysis of balanced data are frequently summarized in this way because researchers automatically associate each sum of squares (SS) line item in the table with testing a particular hypothesis in the linear model.

In the $a \times b$ partially factorial experiment with one observation per cell, the regression approach offers a computationally convenient alternative for generating the various entries in the AOV table. This situation is analogous to balanced data (equal subclass frequencies), so there is no confusion as to what is being tested in each line item of the table. However, when the cell frequencies exceed one, as they did in example two, a complication ensues (viz., $R(a_1, a_2) \neq R(a_1, a_2 | \mu)$ as the result of an emerging non-zero off-diagonal element in the $X'X$ matrix). The situation becomes more complicated when further unbalance arises through missing observations. With unbalanced data hypotheses tested under such headings as row, column, and interaction effects cannot be uniquely presented by paralleling (merely extending) the methods of analysis for balanced data.

In order to illustrate these points consider the following example:

EXAMPLE THREE

Missing Observations

Storage Time	Storage Method	
	S1	S2
T ₀ 0 hours	61 49.5	
T ₁ 24 hours	23 13	41 (41)†
T ₂ 48 hours	(40)† 18	22 25

† The two numbers in parentheses will be treated as missing observations.

We can write the regression model $E[Y] = X\beta$

As

$$\begin{aligned} Y &= \begin{bmatrix} 61 \\ 49.5 \\ 23 \\ 13 \\ .41 \\ (41) \\ (40) \\ 18 \\ 22 \\ 25 \end{bmatrix}; \quad X = \begin{bmatrix} 1 & 1 & 0 & 0 & 0 \\ 1 & 1 & 0 & 0 & 0 \\ 1 & 0 & 1 & 1 & 1 \\ 1 & 0 & 1 & 1 & 1 \\ 1 & 0 & 1 & -1 & -1 \\ 1 & 0 & 1 & -1 & -1 \\ 1 & -1 & -1 & 1 & 1 \\ 1 & -1 & -1 & 1 & -1 \\ 1 & -1 & -1 & -1 & 1 \\ 1 & -1 & -1 & -1 & 1 \end{bmatrix} \text{ and } \beta = \begin{bmatrix} \mu \\ \alpha_1 \\ \alpha_2 \\ \beta_1 \\ \beta_{21} \end{bmatrix} \end{aligned}$$

In the situation with unbalance created through missing observations, the two rows of the X matrix corresponding to the missing observations (lines drawn across them) will be deleted.

The upper triangular $X'X$ matrix based on all 10 observations is:

$$X'X(10) = \begin{array}{ccccc} \mu & \alpha_1 & \alpha_2 & \beta_1 & \beta_{21} \\ \hline 10 & 2 & 0 & 0 & 0 \\ & 6 & 4 & 0 & 0 \\ & & 8 & 0 & 0 \\ & & & 8 & 0 \\ & & & & 8 \end{array}$$

While in the case of 2 missing observations we have:

$$X'X(8) = \begin{array}{ccccc} 8 & -1 & 0 & 0 & 2 \\ 5 & 3 & 1 & -1 & \\ 6 & 2 & 0 & & \\ 6 & 0 & & & 6 \end{array}$$

In general, for a 3×2 partially factorial experiment with the following cell frequencies:

Stored For	Storage Method		Row Totals
	s_1	s_2	
T_0	f_0		f_0
T_1	f_{11}	f_{12}	$f_{1.}$
T_2	f_{21}	f_{22}	$f_{2.}$
Column Totals	$f_{.1}$	$f_{.2}$	

$X'X$ will have the following structure:

μ	a_1	a_2	β_1	δ_{21}
N	$f_0 - f_{.2}$	$f_{.1} - f_{.2}$	$f_{1.} - f_{2.}$	$f_{11} - f_{12}$ $-f_{21} + f_{22}$
	$f_0 + f_{.2}$	$f_{.2}$	$f_{22} - f_{12}$	$f_{12} - f_{22}$
		$f_{..}$	$f_{11} - f_{12}$ $-f_{21} + f_{22}$	$f_{1.} - f_{2.}$
			$f_{..}$	$f_{.1} - f_{.2}$
				$f_{..}$

$$\text{where } N = f_0 + f_{1.} + f_{2.}$$

$$\text{and } f_{..} = f_{1.} + f_{2.}$$

The effect of unequal subclass frequencies produces sum of squares that are not orthogonal. Thus, the influence of missing observations can be readily observed by examination of the off-diagonal terms in the above generalized $X'X$ matrix for a reparameterized 3x2 partially factorial experiment.

Table 6 allows one to examine the various reductions in sums of squares that are easily generated as a result of the $R()$ -notation. The problem now becomes one of relating the associated sums of squares to the testing of "appropriate" hypotheses about the parameters in the model. Obviously, care must be taken so as not to incorrectly describe what is being tested. To better understand how this can be achieved, has prompted a number of articles in the recent statistical literature. However, it is recommended that you turn first to Speed, Hocking, and Hackney (1978).

TABLE 6
AOV Table for 3x2 Partially Factorial Experiment
With Missing Observations (Unequal Subclass Frequencies)

Source of Variation	df	SS(N=10)	Line	SS(N=8)	df	R() - Notation
Mean	1	11,122.225	1	7,969.5313	1	R(μ)
Factor A (Time)	2	1,220.15	2	1,520.2604	2	R($\alpha_1, \alpha_2 \mu$)
Factor B (Method)	1	153.125	3	192.6667	1	R(β_1)
A x B	1	405.125	4	<u>278.3210</u>	1	R(δ_{21})
Sum		<u>12,901.625</u>	5	<u>9,960.7794</u>		
Full Model	5	12,901.625	6	9,862.625	5	R($\mu, \alpha_1, \alpha_2, \beta_1, \delta_{21}$)
Error	5	362.625	7	120.625	3	$Y'Y - R(\mu, \alpha_1, \alpha_2, \beta_1, \delta_{21})$
Total	10	13,264.25	8	9,983.25	8	$Y'Y$

For N = 8

$$\begin{aligned}
 R(\alpha_1, \alpha_2) &= 469.7857 & 192.6667 - R(\beta_1) - R(\delta_{21} | \mu) \\
 R(\alpha_1, \alpha_2 | \mu, \beta) &= 1,598.3437 & \text{and} & 270.75 = R(\beta_1 | \mu, \alpha_1, \alpha_2) \\
 R(\alpha_1, \alpha_2 | \mu, \beta_1, \delta_{21}) &= 1,422.10601 & 270.75 = R(\beta_1 | \mu, \alpha_1, \alpha_2, \delta_{21}) \\
 \end{aligned}$$

and

$$278.3210 = R(\delta_{21} | \mu) \neq R(\delta_{21} | \mu, \alpha_1, \alpha_2, \beta_1) = 102.0833$$

REFERENCES

- Addelman, S., Computing the AOV Table for Experiments Involving Qualitative Factors and Zero Amounts of Quantitative Factors, The American Statistician, Feb 1974, Vol. 28, No. 1, p. 21-22.
- Kempthorne, O., The Design and Analysis of Experiments, Wiley, New York (1952).
- Kutner, M. H., Hypothesis Testing in Linear Models, The American Statistician, August 1974, Vol. 28, No. 3, p. 98-100.
- Searle, S. R., Linear Models, John Wiley & Sons, Inc., New York (1971).
- Speed, F. M. and Hocking, R. R., The Use of the R() Notation With Unbalanced Data, The American Statistician, February 1976, Vol. 30, No. 1, p. 30-33.
- Speed, F. M., Hocking, R. R., and Hackney, O. P., Methods of Analysis of Linear Models With Unbalanced Data, Journal of the American Statistical Association, March 1978, Vol. 73, No. 361, p. 105-112.

STATISTICAL ANALYSIS OF EXPERIMENTS IN SORPTIVITY

Richard N. Macnair

Edward W. Ross, Jr.

U. S. Army Natick Research and Development Command
Natick, Massachusetts 01760

Abstract. This paper describes several experiments about the apparatus and procedure used in testing materials from which chemical-protective clothing is made. The purpose of the work is ultimately to reduce the variability and cost of such testing by clearer understanding of the processes involved. The design and analysis of three experiments are outlined, and some tentative conclusions are stated.

I. Introduction. This paper has to do with the military problem of defending a soldier against attack by chemical agents (usually poison vapor). This defense takes the form of special, protective clothing which absorbs large quantities of the agent. For this purpose large rolls of material from which the clothing is made are purchased and samples from these rolls are tested for their sorptivity, i.e. their absorbing power. This testing is slow, expensive and somewhat unreliable. The present paper is a study of the test-methodology (apparatus and procedure) with the objective of improving the process, in the sense of obtaining greater reliability or lower cost.

Specifically, a certain standard test procedure and apparatus has been used in the past. Recently, a simpler apparatus of the same general type has been tried and found to give acceptable results in a shorter time than the standard method. However, the results were irregular enough to raise questions

about the entire process, so it was thought desirable to conduct the more systematic tests described here.

II. Background. The two apparatuses, sketched schematically in Figure 1, are generally similar. Instead of a toxic agent CCL_4 is used as a representative vapor in these tests. A calibrated mixture of this vapor and an inert gas flows through the sample at a standard rate, and a test for detection of CCL_4 is done on the downstream side of the sample. The result of each test is the length of time (in minutes) before detectable CCL_4 appears, i.e. before "breakthrough". The sorptivity or amount absorbed at breakthrough is then calculated.

The two vapor-penetrations apparatuses, which we describe as standard (std) and simplified (sim), respectively, differ in the following respects:

(a) Nitrogen (N_2) is used as the inert gas in the std and air in the sim.

(b) On the upstream side of the sample the gas is heated to $32^{\circ}C$ in std but maintained at ambient (usually $20^{\circ}C$) in the sim. The tests are both conducted in a room with coarse temperature control but no humidity regulation.

(c) The methods of detecting CCL_4 on the downstream side of the sample are notably different, but both involve a human observer. In std the gas is pyrolyzed and bubbled through a tube containing a starch-potassium iodide solution, which turns blue when products of CCL_4 are present. In sim the gas flows over a copper disc in the flame of a propane torch, and the flame turns green in the presence of CCL_4 .

(d) The human operators observe the color changes in the two apparatuses. For std, the observer records the time at which the liquid in the bubbler tube

first shows blue. For sim, he records the time at which the flame-color is perceptibly "more green" than a comparison flame located near the test flame but not in the flow-stream. An additional complication is the following: it is thought (based on previous experience) that the std tends to give false-positive readings. The operators are, therefore, instructed to replace the bubbler tube, when the first blue color is observed, with a fresh bubbler tube. The time is recorded only if the fresh bubbler tube shows blue within two minutes. Otherwise, the fresh bubbler tube is left in place until it shows blue. This process is repeated as many times as necessary until a blue color is obtained within two minutes. No analogous routine is applied to the sim.

III. Objectives: We would like to answer the following questions about these test methods:

- (1) Do the apparatuses give the same results?
- (2) Is there an effect due to the initial concentration of the agent CCL₄?
- (3) Do the operators have an effect on the results?
- (4) What other factors are important?

Concerning (1) and (2), if the apparatuses and concentrations have an effect, then we want to know whether some combination of sim and concentrations gives results that can be reliably used in place of the std at its traditional concentration. Concerning (4), some other factors that may have effects are material properties, ambient conditions and the treatment of the material samples prior to testing.

IV. Variables. The variables in the tests are as follows:

A, apparatus, takes on values (1) sim, and (2) std.

C, concentrations takes on values (1), low or 5 mg/l, and
(2), high or 15 mg/l.

D, day of test 1 to 4.

G, sample group, (1) and (2).

O, operator, (1) and (2).

R, repetition number, 1 to 12.

W, week of test, 1 to 2 or 3.

V. Design of Tests. Three different tests in all were run.

Test 1: In this test each operator remained with the same apparatus throughout the experiment. To minimize the effects of material variability, samples were re-used over and over again. In order to restore samples as nearly as possible to their original condition, they were heated overnight in an oven at 50°C prior to each day's tests (including the first day's). We surmised that this cycle of heating and testing might affect sorptivity, so the test plan involved periodic repetition of tests in order to find and eliminate any trend.

Twenty-four samples were taken as close together as possible from a large roll of material and divided into two groups of twelve samples each. The groups are labelled 1 and 2 and chosen in the irregular, but not random, sample-pattern shown in the sketch.

1	2	1	2	1	2
2	1	2	1	2	1
2	1	2	1	2	1
1	2	1	2	1	2

The test plan for each week is as follows:

D	G	A	C
---	---	---	---

1	calibration, no tests		
---	-----------------------	--	--

heat overnight (16 hrs)

2	{	1	1	2
		2	2	2

heat overnight

3	{	1	1	1
		2	2	1

heat overnight

4	{	1	2	2
		2	1	2

heat overnight

5	{	1	2	1
		2	1	1

This test was run for two weeks, then, after a lapse of about a month, for a third week.

Test 2: This was nearly a repetition of Test 1. The only differences were:

- (i) A different set of 24 samples was used from the large roll.
- (ii) The test lasted only two weeks.

Test 3: This differed substantially from the two preceding tests. Samples were not re-used, and the effect of operator was specifically investigated. The samples, 96 in all, were obtained from two sheets of the same large roll used

in Tests 1 and 2. Each sheet was divided into 6 rectangular sets, and 8 samples were taken from each set. From each of these 12 sets, one sample at a time was randomly chosen, and these 12 samples formed a group. In this way 8 groups of 12 samples each were obtained and tested according to a plan that was identical with that of Test 1 except that the variable O replaced the variable G.

Test 3 differed from Tests 1 and 2 in one other important respect. Since the samples were not re-used, there was no need to heat them overnight. Consequently, they were simply kept at 65% relative-humidity for several days prior to test. This is a much higher humidity (about 600%) than that of the samples heated in the oven prior to test, which was about 10%.

VI. Results and Discussion. The statistical analyses of the data were done using principally the routines of the Statistical Package for the Social Sciences (SPSS), edition 2. The main results are shown in Figures 2 and 3 as graphs of sorptivity, y, versus various variables.

Figure 2 shows graphs of the daily averages of the results for Experiments 1 and 2. The main reason for studying these is to see whether there is any overall trend in the tests where samples were re-used. No significant quadratic effects were found. Weak but significant (95% level), and nearly equal, downward linear trends were found in the data from Test 2 and the first two weeks of Test 1, labelled (1¹) in Figure 2. When the third week's data was appended to Test 1, the trend disappeared.

Since about a month elapsed between the second and third weeks of Test 1, it is not clear how to interpret the trend. The most plausible

explanation is that re-heating has an effect, but that effect was washed out by the simple passage of time between weeks 2 and 3. In any case the trends are rather weak, and no further effort was made to correct for them.

Figure 3 shows the effect of apparatus, A, and concentration, C, on the sorptivity in the form of estimated means and 95% confidence limits for the three different tests.

Figure 3(i) shows that the three tests gave inherently different results. Tests 1 and 2 differed only slightly, but Test 3 gave lower and more variable results. Possibly these differences are due to both material variability and the different pre-conditioning of the samples in Test 3.

Figure 3(ii) and 3(iii) show the main effects of A and C on sorptivity. Clearly, the std A produces higher readings than the sim A, the size of the difference being much greater in Test 3 than in the others. The effect of C is less clear. Tests 1 and 2 show no difference, but Test 3 suggests that higher C gives lower sorptivity.

Figure 3(iv) exhibits the interaction between the effects of A and C. These are somewhat confusing. First, we notice that in Test 1 there was no effect of A at low C, i.e. the overall effect of A was due entirely to the effect at high C. Related to this is the fact that in Tests 1 and 2, the result of increasing C is to increase the sorptivity measured by std A and decrease that by sim A. This effect is not observed in Test 3, and is not always significant in Tests 1 and 2.

An ANOVA of Test 3 showed that there was no main effect of operator.

However, operator 1 gave consistently higher readings on the std A and operator 2 on the sim A.

Most of the statistical tests (F-tests, t-tests) are based on assumed normality of the data. Some rough estimates of departure from normality (skewness and kurtosis) were made for the three sets of data. The data of Test 1 were not perceptibly non-normal; Tests 2 and 3 were less satisfactory but not outrageously non-normal.

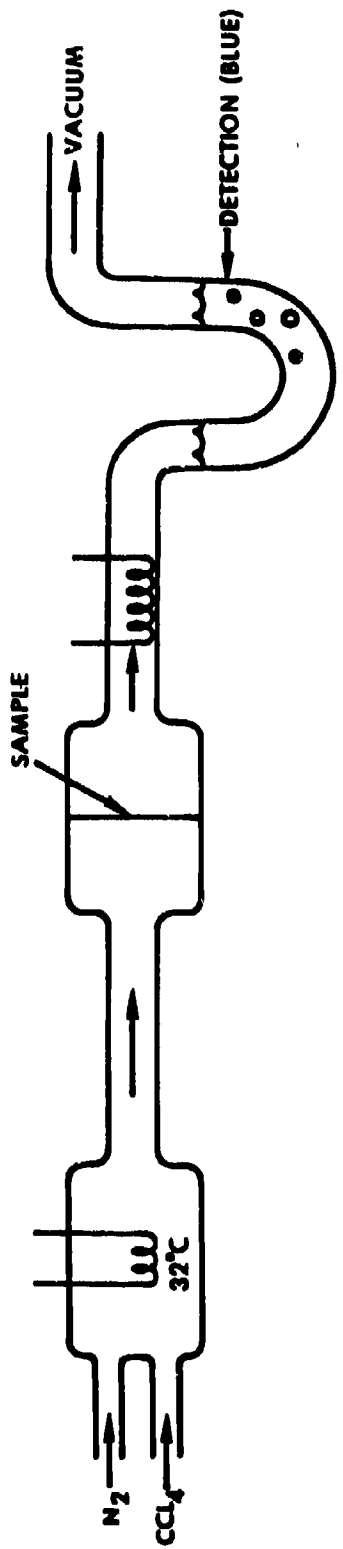
It was thought that there might be some effect of the time of the day on the results, but a plot of the overall means for each repetition number showed no effect that could not be attributed to randomness.

VII. Conclusions.

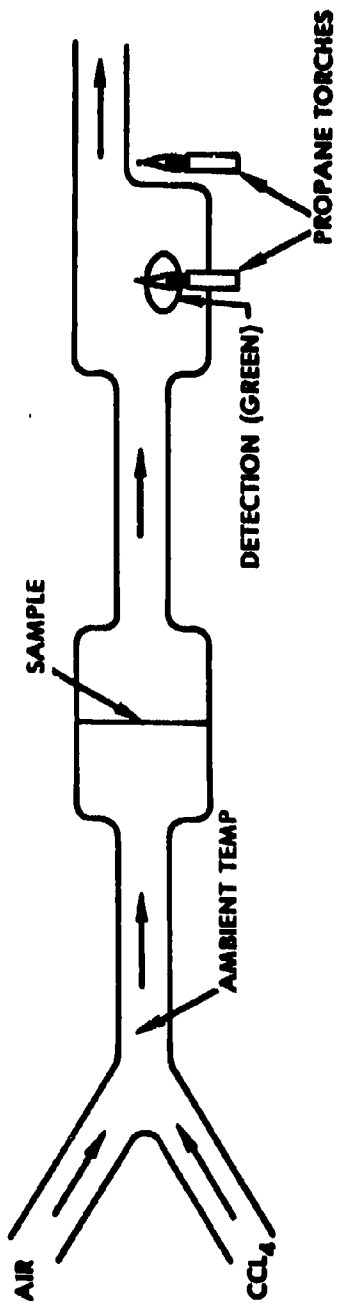
The results of these tests are somewhat fragmentary and suggest that our understanding of the process is incomplete. One thing which emerges is that the effect of sample pre-conditioning is very important. Generally, the std A gives higher results than the sim A, the size of the difference being much affected by C and by the preconditioning. The std A gives somewhat more stable values than the sim A.

Tests in which one tries to observe the first non-zero value of a continuous variable are notoriously unreliable. Some of the present difficulties might be avoided by using comparisons with standard color cards, or some spectral analysis. Obviously much remains to be done in this area.

Schematic Sketch of Vapor-penetration Apparatuses.



STANDARD APPARATUS



SIMPLIFIED APPARATUS

FIGURE 1

Daily averages of sorptivity, y , versus day of test in Experiments 1 and 2. —— • —— denotes Test 1 data; - - + - - - denotes Test 2 data. The linear approximation is —— and - - - for Tests 1 and 2.

The line (1') is the first two weeks only of Test 1.

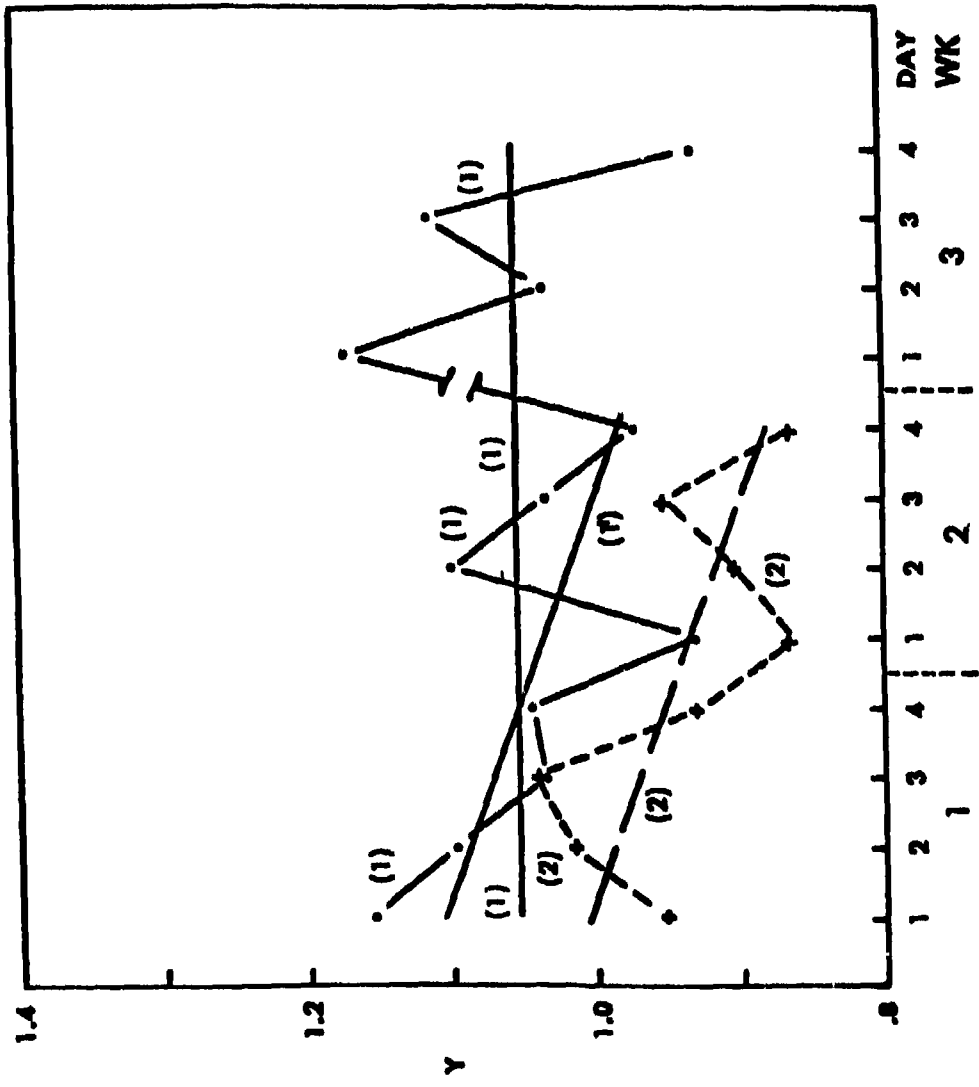


FIGURE 2

Effects of Apparatus (A) and Concentration (C) on
the sorptivity, y . Means and 95% confidence limits
are shown for Experiments 1, 2 and 3.

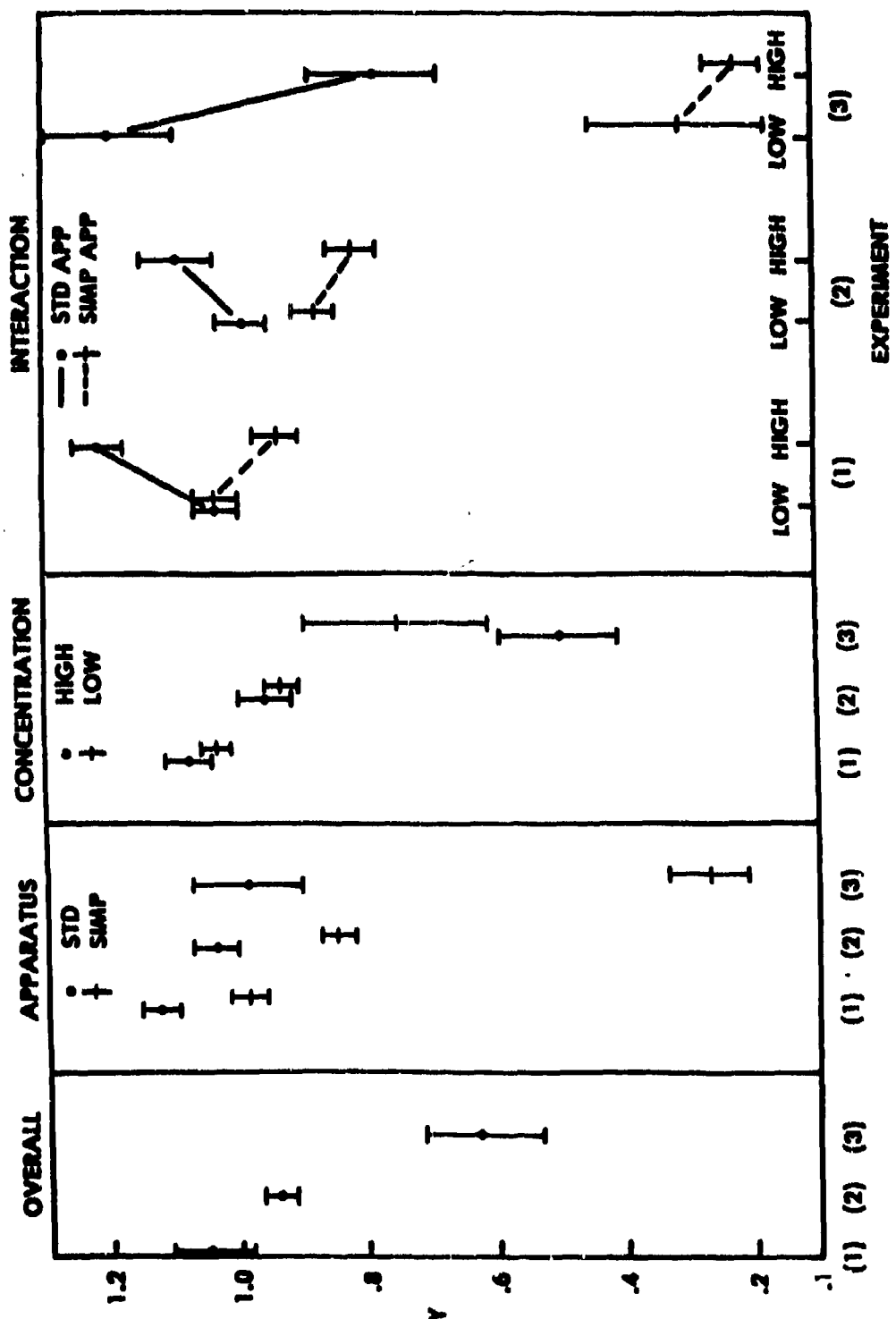


FIGURE 3

ON COMBINING PSEUDO-RANDOM NUMBER GENERATORS

Mark Brown⁽¹⁾ and Herbert Solomon⁽²⁾

SUMMARY

A technique used in pseudo-random number generation is to combine two or more different generators with the goal of producing a new generator with improved randomness properties. We study such a class of generators and show that in a strong sense the combined generator does offer improvement. Our approach applies results from majorization theory.

AMS 1970 subject classification. Primary 65C10; Secondary 68A55.

Key words and phrases. Pseudo-random number generators, Monte Carlo simulation, majorization, uniform distribution, Markov chains.

- (1) Department of Mathematics, City College, CUNY, and Biostatistics Laboratory, Memorial Sloan-Kettering Cancer Center.
- (2) Department of Statistics, Stanford University, Stanford California.

Research supported by Contract N0014-67-A-0012-000.

The following paper appeared in the Annals of Statistics, Volume 7, Number 3, May 1979. The authors thank Dr. Rupert G. Miller, Jr., editor of the Annals of Statistics, for permission to include this paper in the conference proceedings.

On Combining Pseudo-Random Number Generators

Mark Brown and Herbert Solomon

1. Introduction.

Many methods have been proposed, tested and employed for generating pseudo-random numbers ([2], [3], [4], [5], [8], [9], [11], [12], [14], [16], [18], [19]). The goal is to produce strings of numbers which behave like independent uniform [0,1] random variables. The generators yield integers in the set $\{0, 1, \dots, m-1\}$, which are then transformed to $[0, 1]$ by division by m . Suppose that X_1, X_2, \dots and Y_1, Y_2, \dots are strings of numbers generated by two separate generators. Various suggestions have been made for combining the two strings to produce a new string Z_1, Z_2, \dots which hopefully improves upon X and Y . One method, discussed in Knuth [8], p. 26-27, is to set $Z_1 = X_1 + Y_1 \pmod{m}$. Another, due to Maclaren and Marsaglia [11], which Knuth reports to be excellent ([8], p. 31), uses the Y string to randomly permute the X string.

For the additive generator $Z_1 = X_1 + Y_1 \pmod{m}$ we obtain the following result (Corollary 2). For any k and corresponding choice of indices $i_1 < i_2 < \dots < i_k$ consider the vectors $X_A = (X_{i_1}, \dots, X_{i_k})$, $Y_A = (Y_{i_1}, \dots, Y_{i_k})$ and $Z_A = (Z_{i_1}, \dots, Z_{i_k})$. Let p_A , q_A and s_A denote the respective distributions of X_A , Y_A and Z_A ; p_A , q_A and s_A are probability distributions on \mathbb{M}^k where $\mathbb{M} = \{0, 1, \dots, m-1\}$. Define r_k to be the uniform distribution over \mathbb{M}^k ; r_k is a vector of m^k components each equal to m^{-k} . Let $\|\cdot\|$ be an arbitrary symmetric norm on \mathbb{R}^{m^k} ($\|x\| = \|Jx\|$ where Jx is any permutation of x). Then $\|s_A - r_k\| \leq \min(\|p_A - r_k\|, \|q_A - r_k\|)$.

For the generator suggested by Maclaren and Marsaglia a similar but weaker result is obtained. Using Y to shuffle (X_1, \dots, X_m) results in improvement for the joint distribution of X_1, \dots, X_m but not necessarily for the marginal distributions of subsets.

The potential value of our approach is that it can provide additional justification for some generators currently in use, and perhaps suggest new generators which would then be analyzed by traditional methods.

In our analysis we treat the strings X and Y as independent random vectors. In practice X and Y are deterministic strings of numbers. This creates a problem in the strict application of our results to pseudo-random number generation.

2. Majorization.

By definition ([6] p. 45) an n -vector a is said to be majorized by an n -vector b if upon reordering to achieve $a_1 \geq a_2 \geq \dots \geq a_n$ and $b_1 \geq b_2 \geq \dots \geq b_n$ it follows that $\sum_1^k a_i \leq \sum_1^k b_i$ for $k = 1, \dots, n-1$ and $\sum_1^n a_i = \sum_1^n b_i$. A function ψ , $R^n + R$, is defined to be Schur convex ([13] p. 1189) if whenever a is majorized by b , $\psi(a) \leq \psi(b)$. Schur convex functions include symmetric convex functions which in turn include symmetric gauge functions and symmetric norms ([1], p. 229). By a symmetric norm on R^n we mean a function $\|\cdot\|$, $R^n \rightarrow R$, satisfying:
 $\|x\| \geq 0$ for all $x \in R^n$ with equality if and only if $x = 0$,
 $\|\alpha x\| = |\alpha| \|x\|$ for all $\alpha \in R$, $x \in R^n$, $\|x+y\| \leq \|x\| + \|y\|$ for all $x, y \in R^n$, and $\|x\| = \|P_x\|$ for all $x \in R^n$ and for all permutations P_x of x . We note that if r is the uniform distribution over $\{1, 2, \dots, n\}$ ($r(i) = \frac{1}{n}$, $i = 1, \dots, n$) and $\|\cdot\|$ is a symmetric norm on R^n , then $g(x) = \|x-r\|$ is a symmetric convex function and is thus Schur convex. Some references for majorization are [1], [6], [13], and [17].

Lemma 1 below contains four equivalent statements relating to majorization. The equivalence between (i) and (ii) is due to Hardy, Littlewood and Polya ([6] p. 49); the fact that (ii) implies (iii) is found in [1] p. 183 and (iii) \Rightarrow (ii) in [1] p. 181; the fact that (i) \Rightarrow (iv) is the definition of Schur convexity and (iv) \Rightarrow (i) because $\psi(x_1, \dots, x_n) = \sum_1^j x_{(1)}$, where $x_{(1)}$ is the i^{th} largest component of x , is symmetric and convex, and therefore Schur convex.

Lemma 1. The following statements are equivalent:

- (i) a is majorized by b
- (ii) $a = Pb$ where P is doubly stochastic
- (iii) a is a mixture of permutations of b , i.e., $a = \sum p_i(\Pi_i b)$ where (p_1, \dots, p_n) is a probability vector and each $\Pi_i b$ is a permutation of b .
- (iv) $\psi(a) \leq \psi(b)$ for all Schur convex functions ψ .

Theorem 1. Suppose that X is a discrete random variable taking values in the set $\mathcal{X} = (x_1, \dots, x_n)$ with probability distribution $p = (p_1, \dots, p_n)$, where $p_i = P(X_i)$, and Y is a random variable, independent of X , taking values in the set \mathcal{Y} . For each $y \in \mathcal{Y}$ let T_y be a 1-1 transformation of \mathcal{X} onto itself. Define $Z = T_Y X$ and let s be the distribution of Z . Then s is majorized by p .

Proof. Since T_y is 1-1 and onto the distribution of $T_Y X$ is a permutation of p . Thus s is a mixture of permutations of p . By lemma 1 s is majorized by p . ||

3. Applications to pseudo-random number generation.

Suppose that $X = (X_1, \dots, X_N)$ and Y are independent random vectors, with each X_i assuming values in $\mathcal{M} = \{0, 1, \dots, m-1\}$. Consider a subset of k indices $A = \{1 \leq i_1 < i_2 < \dots < i_k \leq N\}$. Define p_A to be the distribution of $X_A = (X_{i_1}, \dots, X_{i_k})$; p_A is a probability distribution on \mathcal{M}^k . For each y in the support of Y let T_y be a 1-1 transformation of \mathcal{M}^k onto \mathcal{M}^k , and let s_A denote the distribution of $T_y X$. Define r_k to be the uniform distribution over \mathcal{M}^k ($r_k(x) = m^{-k}$ for each $x \in \mathcal{M}^k$).

Corollary 1. Let s_A and p_A be as defined above. Then s_A is majorized by p_A . Thus $\psi(s_A) \leq \psi(p_A)$ for all Schur convex functions ψ , and in particular $\|s_A - r_k\| \leq \|p_A - r_k\|$ for any symmetric norm, $\|\cdot\|$, on \mathcal{R}^{m^k} .

Proof. The majorization of s_A by p_A follows from lemma 2 with $n = m^k$ and $\mathcal{Z} = \mathcal{M}^k$. The other statements are consequences of majorization (see lemma 1 and our remarks on Schur convex functions).

Remark 1. Consider $Z_i = X_i + Y_i \pmod{m}$ $i = 1, 2, \dots, N$, where X_i and Y_i both assume values in $\mathcal{M} = \{0, 1, \dots, m-1\}$. In this case X and Y play symmetric roles. It follows from corollary 1 that if q_A denotes the distribution of $Y_A = (Y_{i_1}, \dots, Y_{i_k})$ then s_A is majorized by q_A . Thus $\psi(s_A) \leq \min(\psi(p_A), \psi(q_A))$ for all Schur convex functions. Also note that this conclusion applies to any subset A of the index set. Thus for all $k \leq N$, all k dimensional marginal distributions of Z are at least as uniform, in the sense we described, as are the corresponding distributions of X and Y .

Remark 2. If $\underline{T}_Y \underline{X}$ is of the form $(T_{Y_1} X_1, \dots, T_{Y_N} X_N)$ where each $T_{Y_i} X_i$ is a mixture of 1-1 onto transformations and X and Y are independent, then the conclusion of corollary 1 will hold for all A . In addition if we have an $m \times m$ matrix B with rows labeled $0, \dots, m-1$ and columns $0, \dots, m-1$, with each row and column containing each of the numbers $0, \dots, m-1$ exactly once (an $m \times m$ Latin square) then defining $T_{Y_1} X_1 = B(X_1, Y_1)$ leads to $\psi(s_A) \leq \min(\psi(p_A), \psi(q_A))$ for all A . The additive generator, $Z_1 = X_1 + Y_1 \pmod{m}$, is of this form.

Remark 3. We briefly consider a generator proposed by Maclarin and Marsaglia [11], and discussed in Knuth [8], p. 30-31. Knuth remarks that the method produces sequences with excellent randomness properties and is quite efficient in terms of computer time usage. Under this method the first k elements of \underline{X} are used to form a table. We observe Y_1 which tells us which element of the table to choose as Z_1 . We replace this element by X_{k+1} . The process is then repeatedly applied to generate the string. Suppose that a string of n numbers Z_1, \dots, Z_n , is generated by this method. We artificially enlarge this set to size $n+k$ by setting Z_{n+1} equal to the entry which sits in the i -th place in the table after the string of n numbers has been generated. The new string (Z_1, \dots, Z_{n+k}) is thus a random permutation of (X_1, \dots, X_{n+k}) , induced by \underline{Y} . Since a permutation of coordinates is a 1-1 onto transformation, $\pi^{n+k} \rightarrow \pi^{n+k}$, theorem 1 applies. Thus s , the distribution of (Z_1, \dots, Z_{n+k}) is at least as uniform in our sense as is that of (X_1, \dots, X_{n+k}) .

In general, improving the uniformity of a joint distribution does not necessarily improve the uniformity of marginals. For example let

$p(0,0) = p(1,0) = .1$ and $p(0,1) = p(1,1) = .4$, $\Pr(Y=0) = \Pr(Y=1) = .5$, $T_0(i,j) = (i,j)$, $T_1(i,j) = (j,i)$, $(Z_1, Z_2) = T_Y(X_1, X_2)$. Then $s(0,0) = .1$, $s(1,1) = .4$ and $s(1,0) = s(0,1) = .25$. Then s is majorized by p and the joint distribution of (Z_1, Z_2) is more uniform on $[0,1] \times [0,1]$ than that of (X_1, X_2) . Nevertheless X_1 is perfectly uniformly distributed while Z_1 is not.

Remark 4. In theorem 1 we show that $\psi(s_A) \leq \psi(p_A)$ for all Schur convex ψ . The Schur convex functions of greatest interest to us are distances from r_k under symmetric norms. There are other relevant Schur functions which arise from information theory considerations. If a is a probability distribution over \mathbb{N}^k then $g(a, r_k) = \sum_{\alpha \in \mathbb{N}^k} a(\alpha) \log(m^k a(\alpha))$, the Kullback-Leibler information number for discriminating between a and r_k when a is true, is Schur convex; $g(a, r_k) \geq 0$ with equality if and only if $a = r_k$, and in interesting ways can be interpreted as a measure of discrepancy between a and r_k (Kullback [10]). Similarly $g(r_k, a) = \sum_{\alpha \in \mathbb{N}^k} m^{-k} \log(m^{-k} / a(\alpha))$, the Kullback-Leibler information number for discriminating between a and r_k when r_k is true, is Schur convex, as is $g(a, r_k) + g(r_k, a)$, the divergence between a and r_k . Substituting these Schur convex functions into the inequality $\psi(s_A) \leq \psi(p_A)$, derived in corollary 1, strengthens the assertion that s is as least as uniform as p .

4. Combining several generators.

Suppose we have a sequence of independent random vectors $X_1, X_2, \dots, X_n, \dots$. We combine $X_{1,A}$ and $X_{2,A}$ to form a vector $Z_{2,A}$, then combine $Z_{2,A}$ and X_3 to form $Z_{3,A}$, etc. Assume that at each stage the transformation is of the form $Z_{n,A} = T_{n,X_n}(Z_{n-1,A})$, a mixture of 1-1 transformations of \mathbb{N}^k .

onto \mathcal{M}^k . Represent the transition from stage $n-1$ to stage n by the matrix P_n , where $P_n(\alpha, \beta) = \Pr(Z_{n,A}=\beta | Z_{n-1,A}=\alpha)$, for $\alpha, \beta \in \mathcal{M}^k$. Define $s_{n,A}$ to be the distribution of $Z_{n,A}$. Then $s_{n-1,A}P_n = s_{n,A}$ and $s_{n,A}$ is majorized by $s_{n-1,A}$ by theorem 1; thus by lemma 1 P_n is doubly stochastic. The process $(Z_{n,A}, n=1, 2, \dots)$ is thus a non time homogeneous doubly stochastic Markov chain on the state space \mathcal{M}^k . Also assume that $\min_{\alpha, \beta} P_{n,\alpha, \beta} = \Delta_n \geq \Delta > 0$ for all n . Define $M_n = \max_{\alpha} s_n(\alpha)$, and $m_n = \min_{\alpha} s_n(\alpha)$. We will show that $M_n - m_n \leq (1-m^k \Delta)^n$ which implies that $\max_{\alpha} |s_n(\alpha) - m^k|$ goes to zero at a geometric rate. The method employed below is well known in the theory of Markov chains. Now:

$$(1) \quad M_n \leq M_{n-1}(1-(m^k - 1)\Delta_n) + \Delta_n(1-M_{n-1}) \\ = M_{n-1}(1-m^k \Delta_n) + \Delta_n$$

$$(2) \quad m_n \geq m_{n-1}(1-(m^k - 1)\Delta_n) + \Delta_n(1-m_{n-1}) \\ = m_{n-1}(1-m^k \Delta_n) + \Delta_n.$$

Thus by (1) and (2), $M_n - m_n \leq (M_{n-1} - m_{n-1})(1-m^k \Delta)$ and thus by iteration $M_n - m_n \leq (1-m^k \Delta)^n$, which prove the result.

Under the weaker condition $\sum_1^\infty \Delta_i = \infty$ we get $\lim_{n \rightarrow \infty} (M_n - m_n) = 0$ but the convergence need not be geometric. The condition $\sum \Delta_i = \infty$ is not necessary for convergence of $M_n - m_n$ to zero (and thus of $s_{n,A}$ to r_k). For example if $\Delta_i = m^{-k}$ for any i then $s_{n,A} = r_k$ for all $n \geq i$.

References

- [1] Berge, C. (1963). Topological Spaces, MacMillan, New York.
- [2] Beyer, W.A., Roof, R.B. and Williamson, D. (1971), "The lattice structure of multiplicative congruential pseudo-random vectors," Mathematics of Computation, 25, 345-63.
- [3] Coveyou, R. R. (1960), "Serial correlation in the generator of pseudo-random numbers," J. Assoc. Comp., 72-74.
- [4] Dieter, U. (1972), "Statistical interdependence of pseudo-random numbers generated by the linear congruential method," Applications of Number Theory to Numerical Analysis, S.K. Zaremba, Ed., Academic Press.
- [5] Greenberger, M. (1961), "On a priori determination of serial correlation in computer generated random numbers," Math. of Comp., 15, 383-89.
- [6] Hardy, G.H., Littlewood, J.E. and Polya, G. (1952), Inequalities, (2nd ed.). Cambridge University Press, Cambridge.
- [7] Hull, T.E. and Dobell, A.R. (1962), "Random number generators," SIAM Review, 4, 230-54.
- [8] Knuth, Donald E. (1969), The Art of Computer Programming, Volume II; Seminumerical Algorithms, Addison-Wesley, Reading, Massachusetts.
- [9] Kuipers, L. and Niederreiter, H. (1974), Uniform Distribution of Sequences, John Wiley and Sons Inc New York.
- [10] Kullback, S. (1959), Information Theory and Statistics, John Wiley and Sons, Inc. New York.
- [11] MacLaren, M.D. and Marsaglia, G. (1965), "Uniform random number generators," J. Assoc. Comp. Mach., 12, 83-89.
- [12] Marsaglia, G. (1972), "The structure of linear congruential sequences," in S. K. Zaremba, Ed., (as in [4] above).
- [13] Marshall, A.W., and Olkin, I. (1977), "Majorization in multivariate distributions," Annals of Statistics, 2, 1189-1200.
- [14] Meyer, H.A., Editor (1956), "Symposium on Monte Carlo Methods," John Wiley and Sons, Inc. New York.
- [15] Monte Carlo Methods (1951), N.B.S. Applied Mathematics Series No. 12, U.S. Government Printing Office.

- [16] Niederreiter, H. (1976), "On the distribution of pseudo-random numbers generated by the linear congruential method. III," Mathematics of Computation, 30, 571-97.
- [17] Proschan, F. and Sethuraman, J. (1977), "Schur functions in statistics, I. The preservation theorem," Annals of Statistics, 5, 256-62.
- [18] Rotenberg, A. (1960), "A new pseudo-random number generator," J. Assoc. Comp. Mach., 7, 75-77.
- [19] Strawderman, W.E. (1971), "Generation and testing of pseudo-random numbers," Technical Report No. 171, Department of Statistics, Stanford University.

SIMPLIFIED POINT AND INTERVAL ESTIMATION
FOR REMOVAL TRAPPING

Andrew P. Soms[†]

Abstract

A regression technique, based on the limiting normal distribution of the multinomial, is given for point and interval estimation of the parameters in the removal trapping method of determining animal and insect populations. Pooling is described for using the method even when the individual catches are small and a simulation approach to the calculation of bias is described. Two examples of estimating spider populations are given.

[†]University of Wisconsin-Milwaukee, Wisconsin 53201. The author would like to thank Joan Jass of the Milwaukee Public Museum for pointing out this problem.

Sponsored by: The United States Army under Contract No. DAAG29-75-C-0024. The University of Wisconsin-Milwaukee.

Key Words: Removal Method; Regression Estimation; Asymptotic Confidence Intervals.

1. Introduction

A thorough discussion of the removal trapping method of estimating animal and insect populations, together with limitations, is given in [7], pp. 182-6. It is pointed out in [5] that this method is particularly suited for insect populations. Briefly, there are assumed to be m organisms in some fixed area, k trapping or sweeping periods, $k \geq 2$, and each organism is assumed to have a constant probability p of being captured in any of the k periods, independent of the other organisms (the organisms are not released when captured). If the trapping probability is p , $0 < p < 1$, then, as pointed out by Moran [6], p. 308, the joint density of the n_i , $1 \leq i \leq k$, the number of organisms trapped in each of the periods, is

$$\begin{aligned} P[n_i = s_i, \sum_1^k s_i \leq m, 1 \leq i \leq k] &= \frac{m!}{s_1! \dots s_k! (m - \sum_1^k s_i)!} p^{s_1} (p(1-p))^{s_2} \dots \\ &\cdot (p(1-p)^{k-1})^{s_k} ((1-p)^k)^{m - \sum_1^k s_i} \cdot \frac{m!}{s_1! \dots s_k! (m - \sum_1^k s_i)!} \\ &\cdot p^{\sum_1^k s_i} (1-p)^{\sum_1^k (i-1)s_i + k(m - \sum_1^k s_i)}. \end{aligned}$$

The above is seen to be a multinomial distribution, with $k+1$ categories, and parameters m and $p_i = p(1-p)^{i-1}$, $1 \leq i \leq k$, and $p_{k+1} = (1-p)^k = 1 - \sum_1^k p_i = 1 - \sum_1^k p(1-p)^{i-1}$. It is desired to estimate m and p and give asymptotically exact confidence intervals. A Bayesian approach has been considered by Carle and Strub [2]. Here an attempt will be made to remedy some of the problems in [6]

in which a method based on maximum likelihood is proposed, which is elaborated upon by Zippin [8]. In addition to replacing $m!$ by Stirling's approximation, the effect of which is not clear, both Moran [6] and Zippin [8] state that the usual regularity conditions for the joint asymptotic normality of the maximum likelihood estimators are not satisfied in this case (in addition to other assumptions, it is assumed that the parameters being estimated, m and p , remain constant, which is not true here, since the asymptotic behavior is for fixed p as $m \rightarrow \infty$), and then they proceed in the hope that somehow a justification may be produced without giving it. Further, even if these difficulties are neglected, the estimating equations are either implicit, requiring iteration, or after some approximations, require charts. Here a theoretically justifiable intuitive method is discussed, based on the limiting distribution of the multinomial, which gives the estimates explicitly as functions of n_1, \dots, n_k .

The author was introduced to this problem by Joan Jass of the Milwaukee Public Museum, who, as a part of her Master's thesis wanted to estimate spider populations. She found the existing literature somewhat complicated and confusing and wondered whether there was a simpler and more intuitive approach available. The subsequent sections are an attempt to do this.

2. The Modified Moment Estimates for Two Trapping Periods

Sometimes the n_i are so small as to cast doubt on the validity of the asymptotic method to be described. Alternatively, it may be desired to produce quick and simple estimates and to determine

whether biases exist (this will be discussed later). With this objective in mind, we will assume that there are $2t$ trapping periods and divide them into two groups consisting of the first t and second t . Then the assumptions of the removal method are met with 2 periods, $n_1 = \#$ caught in first t periods, $n_2 = \#$ caught in second t , and

$$p = 1 - (1-p_0)^t , \quad (2.1)$$

where p_0 is the original trapping probability. Hence estimates and confidence intervals for p can be immediately converted to those for p_0 and this will be done after obtaining estimates for m and p .

Note that $E n_1 = mp$ and $E n_2 = mp(1-p)$, hence a ratio estimate \hat{q} of $q = 1-p$ is

$$\hat{q} = n_2/n_1 \quad (2.2)$$

and a moment estimate \hat{m} of m is

$$\hat{m} = \frac{n_1 + n_2}{1 - \hat{q}^2} . \quad (2.3)$$

It is readily seen that if n_1 and n_2 are replaced by their expected values in \hat{q} and \hat{m} , q and m are obtained ($E(n_1 + n_2) = mp + mp(1-p) = m(1-q^2)$), hence the name "modified moment estimates". Let \hat{p} be the natural estimator of p , $\hat{p} = 1 - \hat{q}$ here and throughout.

The limiting distribution of \hat{p} and \hat{q} will be now obtained. The reader who is not mathematically inclined can jump to the results, but it must be pointed out that the derivations are straightforward and can be checked by anyone with a modest background in statistics.

Consider the problem of asymptotically exact confidence intervals — a reasonable assumption is that p and k stay constant and $m \rightarrow \infty$. Note that in [2], p. 626, it is required that also $k \rightarrow \infty$. For later use, instead of two trapping periods, k will be considered and then specialized to two. The asymptotic distributions of \hat{p} and \hat{m} will be obtained by using two results — the joint asymptotic normality of $\tilde{n} = (n_1, \dots, n_k)$ and a result given in Anderson [1], pp. 76-7. It is well known that as (p_1, \dots, p_k) stays constant and $m \rightarrow \infty$ for a multinomial distribution,

$$\left[\sqrt{m} \left(\frac{n_i}{m(p_i q_i)^{\frac{1}{k}}} - \left(\frac{p_i}{q_i} \right)^{\frac{1}{k}} \right), 1 \leq i \leq k \right] \xrightarrow{w} \left[\frac{n_i - mp_i}{(mp_i q_i)^{\frac{1}{k}}}, 1 \leq i \leq k \right] \xrightarrow{w} N(\bar{0}, R), \quad (2.4)$$

(" \xrightarrow{w} " means convergence in distribution), where $\bar{0}$ is a k -tuple of 0's, $\bar{0} = (0, 0, \dots, 0)$, $R = [r_{ij}]$, $r_{ii} = 1$ and for $i \neq j$, $r_{ij} = -(p_i p_j / (q_i q_j))^{\frac{1}{k}}$ (see, e.g. Johnson and Kotz [4], p. 284) — recall that here $p_i = p(1-p)^{i-1}$, $1 \leq i \leq k$ (also for notational convenience always $p_1 = p$, $q_1 = 1 - p_1 = q$), and hence it suffices to keep p constant. The result cited in Anderson is: Let $f(\tilde{x})$ be a function of $\tilde{x} = (x_1, \dots, x_k)$ with continuous first and second derivatives existing in a neighborhood of $\tilde{x} = \tilde{b}$, $\tilde{b} = (b_1, \dots, b_k)$ a fixed vector, and suppose $\sqrt{n} (\tilde{U}(n) - \tilde{b}) \xrightarrow{w} N(\bar{0}, T)$. Then

$$\sqrt{n} [f(\tilde{U}(n)) - f(\tilde{b})] \xrightarrow{w} N(0, \Phi_{\tilde{b}}^T \Phi_{\tilde{b}}^{-1}), \quad (2.5)$$

where $\Phi_{\tilde{b}} = (\frac{\partial f}{\partial x_1}, \dots, \frac{\partial f}{\partial x_k})_{\tilde{b}}$. In all that follows, $\tilde{b} = [(p_1/q_1)^{\frac{1}{k}}, \dots, (p_k/q_k)^{\frac{1}{k}}]$, and $\tilde{U}(n) = (n_1/m(p_1 q_1)^{\frac{1}{k}}, \dots, n_k/m(p_k q_k)^{\frac{1}{k}})$. Let us now assume that $k = 2$ and take $f(\tilde{x})$ to be

$$f(\tilde{x}) = \frac{x_2 \sqrt{p_2 q_2}}{x_1 \sqrt{p_1 q_1}}. \quad (2.6)$$

Note that for $k=2$, $f(\tilde{b}) = \frac{n_2}{n_1^2}$. the estimator of \hat{q} . Using (2.5),

$$\sqrt{m} \left(\frac{n_2}{n_1^2} - q \right) \xrightarrow{w} N(0, q \left(\frac{1+q}{p} \right)) = N(0, \sigma_p^2) ,$$

since

$$\left(\frac{\partial f}{\partial x_1} \right)_{\tilde{b}} = -q(q/p)^{\frac{1}{2}} ,$$

$$\left(\frac{\partial f}{\partial x_2} \right)_{\tilde{b}} = q[(1-pq)/(pq)]^{\frac{1}{2}} ,$$

and $\Phi_{\tilde{b}} \approx \Phi_b^1 = \sigma_p^2$. Therefore also

$$\sqrt{m} (\hat{p}-p) \xrightarrow{w} N(0, \sigma_p^2) , \quad (2.7)$$

or, equivalently, $\hat{p}-p$ is asymptotically $N(0, \sigma_p^2/m)$. Using the same technique on \hat{m} , let

$$g(\tilde{x}) = \frac{x_1(p_1 q_1)^{\frac{1}{2}} + x_2(p_2 q_2)^{\frac{1}{2}}}{1 - f(\tilde{x})^2} , \quad (2.8)$$

with $f(\tilde{x})$ given by (2.6). It can be seen that for $k=2$, $g(\tilde{U}(n)) = \hat{m}/m$ and $C(\tilde{b}) = 1$. Then

$$\left(\frac{\partial g(\tilde{x})}{\partial x_1} \right)_{\tilde{b}} = \frac{(p_1 q_1)^{\frac{1}{2}} - 2(q_1/p_1)^{\frac{1}{2}} q^2}{1-q^2} ,$$

$$\left(\frac{\partial g(\tilde{x})}{\partial x_2} \right)_{\tilde{b}} = \frac{(p_2 q_2)^{\frac{1}{2}} + 2(q_2/p_2)^{\frac{1}{2}} q^2}{1-q^2}$$

and

$$\Phi_{\tilde{b}} \approx \Phi_b^1 = \sigma_m^2 = \frac{q^2}{1-q^2} \left[1 + \frac{4q}{p^2} \right] ,$$

and so by (2.2),

$$\sqrt{m} \left(\frac{\hat{m}}{m} - 1 \right) \xrightarrow{w} N(0, \sigma_m^2) ,$$

or equivalently $\hat{m} - m$ is asymptotically $N(0, m\sigma_m^2)$. Since $\hat{p} \rightarrow p$ and $\hat{m} \rightarrow m$ in probability, $\hat{\sigma}_p^2$ and $\hat{\sigma}_m^2$ converge to σ_p^2 and σ_m^2 , respectively, in probability ($\hat{\sigma}_p^2$ and $\hat{\sigma}_m^2$ are obtained from σ_p^2 and σ_m^2 by replacing p by \hat{p} and q by \hat{q}), and so the limiting distribution of both $(\hat{p} - p)/(\hat{\sigma}_p^2/\hat{m})^{1/2}$ and $(\hat{m} - m)/(\hat{\sigma}_m^2/\hat{m})^{1/2}$ is the standardized normal. Hence asymptotically exact (marginal) $1-\alpha$ confidence intervals for p and m are

$$\hat{p} \pm z_{\alpha/2} (\hat{\sigma}_p^2/\hat{m})^{1/2} \quad (2.9)$$

and

$$\hat{m} \pm z_{\alpha/2} (\hat{m} \hat{\sigma}_m^2)^{1/2}, \quad (2.10)$$

where z_α is the upper 100α th percentile of the standardized normal.

Simulation results indicate that for \hat{p} the asymptotic distribution is attained faster than for \hat{m} . An alternative approach to obtaining accurate 95% confidence intervals for m (coverage probability close to but bigger than .95 even when m is small) is to use an actual standard deviation obtained by simulation. In this approach \hat{p} and \hat{m} are regarded as the true values and a large number (say 1000) of samples is drawn and the sample standard deviation and bias calculated. This is, in fact, recommended in any case, since the comparison of the two standard deviations (the limiting and the simulation) will indicate whether it is safe to use the asymptotic theory. In addition, \hat{m} can be corrected for bias. This point will also be discussed in subsequent sections.

In order to convert the estimate and confidence interval for p to p_0 , note that $p = 1 - (1-p_0)^t$ and hence $\hat{q}_c = \hat{q}^{1/t}$. Also, if the confidence interval for p is (a, b) , then the corresponding interval for p_0 is $(1 - (1-a)^{1/t}, 1 - (1-b)^{1/t})$.

The lack of fit discussion will be given after the general estimates are obtained, since it will be seen that the \hat{p} and \hat{m} here are a special case when $k=2$.

3. Regression Estimates for Arbitrary k

While the method discussed in 2. is useful when the catches in the individual periods are small, it is often desirable to use the original data if, e.g., all $\hat{m}\hat{p}_i \geq 5$, where $\hat{p}_i = \hat{p}q^{i-1}$ and \hat{p} and \hat{m} are suitable estimates of p and m . An estimate of p , the regression estimate, can be obtained as follows. It is suggested in [5] that a simple graphical check of the validity of assumptions is to plot n_i against i on semi-log paper and check whether the plot approximates a straight line. It is pointed out in [6] that the $\log E n_i = \log \mu_i = \log mp(1-p)^{i-1}$ lie on the straight line

$$\log \mu_i = i \log(1-p) - \log(1-p) + \log p + \log m , \quad (3.1)$$

but this method is then dismissed by saying that the usual assumptions of regression theory are not satisfied. Here a different approach is taken — namely, the point estimator of p suggested by regression theory is used but then, in place of the usual regression theory, the limiting distribution is obtained from (2.5). The regression equation suggested by (3.1) is

$$\log n_i = i\beta + \alpha + \epsilon_i , \quad 1 \leq i \leq k ,$$

where $\beta = \log(1-p)$ (to any base), α a constant, and ϵ_i the error term which will be of no interest here. The least squares estimate $\hat{\beta}$ of β is

$$\hat{\beta} = \frac{k}{1} \left\{ (\log n_i) \left(i - \frac{k+1}{2} \right) \right\} / \sum_{i=1}^k \left(i - \frac{k+1}{2} \right)^2 .$$

Since $\sum_1^k i^2 = (k)(k+1)(2k+1)/6$,

$$\hat{p} = \sum_1^k (\log n_i) \left(i - \frac{k+1}{2} \right) / (k(k^2-1)/12).$$

Then the corresponding estimator $\hat{q} = 1 - \hat{p}$ of $q = 1 - p$ is

$$\hat{q} = 1 - \hat{p} = \sum_1^k n_i c_i, \quad (3.2)$$

where $c_i = (i - (k+1)/2) / (k(k^2-1)/12)$. Note that replacement of n_i by $E n_i$ in (3.2) gives q . In order to show that (3.2) is consistent for p and to obtain its asymptotic variance, it is just as easy to consider general estimates of $1-p$ of the form (3.2) with the c_i arbitrary and to determine the conditions on c_i needed for consistency. Let

$$h(\tilde{x}) = \sum_1^k (x_i (p_i q_i)^{\frac{1}{k}})^{c_i}. \quad (3.3)$$

Then, using (2.5) and $p_i = p(1-p)^{i-1}$,

$$\sqrt{m} \left(\sum_1^k n_i c_i / m^{\frac{1}{k}} - \sum_1^k p_i c_i \right) = \sqrt{m} \left(\sum_1^k n_i c_i / m^{\frac{1}{k}} - p \sum_1^k (1-p)^{\frac{1}{k}} (i-1) c_i \right).$$

Therefore a sufficient condition for consistency is

$$\sum_1^k c_i = 0 \quad \text{and} \quad \sum_1^k i c_i = 1 \quad (3.4)$$

and in this case

$$\sqrt{m} \left(\sum_1^k n_i c_i - (1-p) \right) \xrightarrow{w} N(0, \sigma_p^2),$$

where σ_p^2 is determined in the usual way from (3.3) using (2.5).

It is noted that for $c_i = (i - (k+1)/2) / (k(k^2-1)/12)$ (3.4) is satisfied, since clearly $\sum_1^k c_i = 0$ and, letting $c = k(k^2-1)/12$,

$$\sum_{i=1}^k i c_i = \sum_{i=1}^k i(i - \frac{k+1}{2})/c = \left[\frac{(k)(k+1)(2k+1)}{6} - \frac{k(k+1)^2}{4} \right] / c = 1.$$

So, for any choice of c_i satisfying (3.4), $\sigma_p^2 = \Phi_b^{-T} \Phi_b^1$,
 $\Phi_b = (\frac{\partial h(\tilde{x})}{\partial x_1}, \dots, \frac{\partial h(\tilde{x})}{\partial x_k})_b$ and since

$$\frac{\partial h(\tilde{x})}{\partial x_i} = (c_i/x_i) \prod_{j=1}^k (x_j (p_j q_j)^{\frac{1}{2}})^{c_j},$$

we have that

$$(\frac{\partial h(\tilde{x})}{\partial x_i})_b = c_i (q_i/p_i)^{\frac{1}{2}} q_i. \quad (3.5)$$

Therefore, after some short algebra,

$$\sigma_p^2 = q^2 \sum_{i=1}^k c_i^2 / p_i. \quad (3.6)$$

A satisfactory estimator of \hat{m} is obtained by the same argument as for the moment estimator, namely,

$$\hat{m} = \sum_{i=1}^k n_i / (1 - \hat{q}^k), \quad (3.7)$$

where \hat{q} is given by (3.2), with the c_i arbitrary and satisfying (3.4). It is seen that replacement of random variables by their expectations in (3.6) gives m . As before, let

$$g(\tilde{x}) = \sum_{i=1}^k x_i \sqrt{p_i q_i} / (1 - (\sum_{i=1}^k (x_i \sqrt{p_i q_i})^{c_i})^k). \quad (3.8)$$

Then, by (2.5),

$$\sqrt{m} (\frac{\hat{m}}{m} - 1) \xrightarrow{w} N(0, \sigma_m^2),$$

where $\sigma_m^2 = \Phi_b^{-T} \Phi_b^1$, $\Phi_b = (\frac{\partial g}{\partial x_1}, \dots, \frac{\partial g}{\partial x_k})_b$ and

$$(\frac{\partial g}{\partial x_i})_b = \frac{(p_i q_i)^{\frac{1}{2}} + k c_i (q_i/p_i)^{\frac{1}{2}} (1-p)^k}{1-q^k}. \quad (3.9)$$

Using (3.9), after some simple algebra,

$$\sigma_m^2 = \frac{q^k}{1-q^k} \left[1 + \frac{k^2 q^k}{1-q^k} \sum_1^k \frac{c_i^2}{p_i} \right]. \quad (3.10)$$

The regression estimates \hat{q} and \hat{m} are obtained from (3.2) and (3.7) by choosing $c_i = (i-(k+1)/2)/(k(k^2-1)/12)$, and their variances from (3.6) and (3.10). It then follows, exactly as in 2., that asymptotically exact $1-\alpha$ confidence intervals for \hat{p} and \hat{m} are

$$\hat{p} \pm z_{\alpha/2} (\hat{\sigma}_p^2 / \hat{m}) \quad (3.11)$$

and

$$\hat{m} \pm z_{\alpha/2} (\hat{m} \hat{\sigma}_m^2)^{1/2}, \quad (3.12)$$

where $\hat{\sigma}_p^2$ and $\hat{\sigma}_m^2$ are obtained from σ_p^2 and σ_m^2 by replacing p by \hat{p} .

It is interesting to note that if $k=2$, the estimates given here coincide with those in 2.

It should also be pointed out that there is an alternate way of estimating m from (3.1), namely by equating the estimate of the constant term with what it estimates. Without going into the details, the resulting estimator \hat{m} is

$$\hat{m} = \frac{\left(\prod_{i=1}^k n_i \right)^{1/k}}{\hat{p} \hat{q}^{1/(k-1)}} \quad (3.13)$$

and the asymptotic variance σ_m^2 of $\sqrt{\hat{m}} (\frac{\hat{m}}{m} - 1)$ is

$$\sigma_m^2 = \sum_1^k \frac{1}{p_i} \left[\frac{1}{k} + c_i \frac{q-(k-1)p/2}{p} \right], \quad (3.14)$$

where c_i correspond to the regression estimator of q . The estimator given by (3.13) has an interesting form - it is the ratio of the geometric mean of the n_i to the geometric mean of

the \hat{p}_i . If random variables are replaced by their expectations in (3.13), m results. The asymptotic variance (3.14) is very close to (3.10) with the regression c_i . Simulation studies indicate, however, that (3.13) has a substantially bigger bias and sample variance than (3.7), which is the preferred estimator.

4. Lack of Fit

Having estimated the parameters, using the regression method as in 3. (recall 2. is a special case), it is natural to ask how good the fit is. The customary statistic used to test the adequacy of the model is $Z = \sum_1^k (n_i - \hat{m}\hat{p}_i)^2 / (\hat{m}\hat{p}_i)$, where $\hat{p}_i = p(1-p)^{i-1}$. It is not at all clear, in this or, of course, the maximum likelihood case, that Z has an asymptotic (p and k fixed, $m \rightarrow \infty$) χ^2 distribution with $k-2$ degrees of freedom (d.f.), since the usual regularity conditions (see [3], pp. 500-1, 506) are not satisfied. The empirical approach given here consists of using (2.5) to obtain the expected value of the limiting distribution of Z and then to fit a χ^2 distribution (as is done with good results in fitting the distribution of sums of χ^2 random variables) by estimating the d.f. from the parameter estimates. The observed value of Z is then compared to the upper $100\alpha^{th}$ percentile of the fitted χ^2 (using interpolation of the d.f., since in general the fitted d.f. will not be integral). Specifically, consider

$$f_i(\tilde{x}) = x_i(p_i q_i)^{\frac{1}{2}} - g(\tilde{x})(1-f(\tilde{x}))(f(\tilde{x}))^{1-1},$$

where $f(\tilde{x})$ and $g(\tilde{x})$ are given by (3.3) and (3.8), respectively.

Note that $f_i(\tilde{b}) = 0$ and thus from (2.5),

$$\sqrt{m} f_i(n_i/(m(p_1 q_1)^{\frac{1}{2}}), \dots, n_k/(m(p_k q_k)^{\frac{1}{2}}))$$

$$= \sqrt{m} ((n_i - \hat{m} \hat{p} \hat{q}^{i-1})/m) \xrightarrow{w} N(0, \sigma_i^2), \quad (4.1)$$

where $\sigma_i^2 = \Phi_{ib}^{-1} \Phi_{ib}$, $\Phi_{ib} = (\frac{\partial f_i(\tilde{x})}{\partial x_1}, \dots, \frac{\partial f_i(\tilde{x})}{\partial x_k})_{\tilde{b}}$.

Using (3.5) and (3.9) and the chain rule, $(\frac{\partial f_i(\tilde{x})}{\partial x_j})_{\tilde{b}}$ is

$$(\frac{\partial f_i(\tilde{x})}{\partial x_j})_{\tilde{b}} = -(\frac{\partial g(\tilde{x})}{\partial x_j})_{\tilde{b}} p_i - (i-1)p p_i (\frac{\partial f(\tilde{x})}{\partial x_j})_{\tilde{b}} + q^{i-1} (\frac{\partial f(\tilde{x})}{\partial x_j})_{\tilde{b}}, \quad (4.2)$$

if $i \neq j$, and $(p_i q_i)^{\frac{1}{2}}$ is added to (4.2) if $i = j$. From this, σ_i^2 can be computed. By (2.5), since $(\hat{m}/m)^{\frac{1}{2}} \rightarrow 1$ and $\hat{p}_i \rightarrow p$ in probability, it follows from (2.5) and (4.1) that

$$(n_i - \hat{m} \hat{p} \hat{q}^{i-1})/(\hat{m} \hat{p}_i)^{\frac{1}{2}} \xrightarrow{w} N(0, \sigma_i^2/p_i)$$

and therefore the asymptotic mean of $Z = \sum_{i=1}^k (n_i - \hat{m} \hat{p} \hat{q}^{i-1})^2/(\hat{m} \hat{p}_i)$ is $\mu = \sum_i \sigma_i^2/p_i$. Replacing the parameters p_i and q_i by their estimates \hat{p}_i , \hat{q}_i in μ gives the estimated d.f. of the distribution of Z , and using these d.f. a cut-off point for the adequacy of fit test can be obtained from tables. Even though explicit expressions do not appear practical, the σ_i^2 and μ are easily evaluated by means of a short computer program.

5. Numerical Examples

We illustrate the preceding theory by two data sets of thomisid (crab) spiders furnished by Joan Jass. The first set has $k=5$ and $(n_1, n_2, n_3, n_4, n_5) = (37, 29, 17, 15, 12)$ and the second $k=6$ and $(n_1, n_2, n_3, n_4, n_5, n_6) = (46, 29, 36, 22, 26, 23)$. The results, using the regression estimators, are in Table 1.

Table 1

	<u>1st Data Set</u>	<u>2nd Data Set</u>
\hat{p}	.253	.115
s.d.	.056	.040
\hat{m}	143	350
s.d.	17.4	88.2
	<u>Test of Fit</u>	
Z	.71	4.06
d.f.	3.14	4.04

It might be guessed that because of the small value of \hat{p} in the 2nd set there would be a serious bias in the estimate. A simulation was done, for both data sets, using 4000 samples and the estimates in Table 1 as the true values, conditional on $1-\hat{q}^k$ being equal to or bigger than .001 - while this value is arbitrary, the bias was not sensitive to it. As expected, the bias in \hat{p} was negligible for both sets. The bias in \hat{m} was 5.7 for the first set and 60 for the second. Thus while it is satisfactory to subtract 5.7 from \hat{m} in the first set to obtain 137 as an estimate and use this in the confidence interval procedures, it is clearly desirable to pool the intervals in the 2nd set. After this was done, using $k=2$, the estimate of m was 308, with s.d. 66.5, quite close to what would have been obtained by subtracting the bias from the original estimate. The actual sampling variance of \hat{m} was 340.1 as compared to the theoretical limit of 88.2. For the reduced set the two values were 212.5 and 66.4, indicating that

the confidence intervals based on the limiting distribution should be viewed with caution. For the first set the sampling variance was 24.6 and the limiting value 17.23.

Simulation studies support the view that if the bias is not large (equivalently if p is not close to 0), replacement of the limiting variance by the sampling variance yields realistic (in fact, slightly conservative) 95% confidence intervals, even when m is as small as 100.

The listings of the two short computer programs used for the above analysis, the estimation and simulation, are available on request from the author.

6. Summary and Concluding Remarks

For ease of use, we list the estimation and confidence interval formulas in 2. and 3. If $k=2$, then

$$\hat{q} = n_2/n_1, \quad \hat{p} = 1 - \hat{q}, \quad \hat{m} = (n_1+n_2)/(1-\hat{q}^2)$$

and

$$s_p^2 = \hat{\sigma}_p^2/\hat{m} = \frac{\hat{q}(1+\hat{q})}{\hat{p}\hat{m}}, \quad s_m^2 = \hat{m}\hat{\sigma}_m^2 = \frac{\hat{m}\hat{q}^2}{1-\hat{q}^2} \left(1 + \frac{4\hat{q}}{\hat{p}^2}\right),$$

and asymptotic $100(1-\alpha)\%$ confidence intervals for p and m are

$$\hat{p} \pm z_{\alpha/2} s_p \quad \text{and} \quad \hat{m} \pm z_{\alpha/2} s_m,$$

where $z_{\alpha/2}$ is the $100\alpha/2$ upper percentile of the standard normal.

If $k \geq 3$

$$\hat{q} = \frac{k}{\sum_i n_i} c_i, \quad \hat{p} = 1 - \hat{q}, \quad \hat{m} = \frac{\sum_i n_i}{(1-\hat{q}^k)},$$

where $c_i = (i - \frac{k+1}{2})/(k(k^2-1)/12)$, and

$$s_p^2 = (\hat{q}^2/\hat{m}) \sum_1^k c_i^2/\hat{p}_i, \quad s_m^2 = \frac{\hat{m}\hat{q}^k}{1-\hat{q}^k} \left[1 + \frac{k^2\hat{q}^k}{1-\hat{q}^k} \sum_1^k \frac{c_i^2}{\hat{p}_i} \right],$$

and asymptotic $100(1-\alpha)\%$ confidence intervals for p and m are

$$\hat{p} \pm z_{\alpha/2} s_p \quad \text{and} \quad \hat{m} \pm z_{\alpha/2} s_m,$$

with $z_{\alpha/2}$ as before. To calculate the lack of fit statistic and its d.f., it is simplest to use the short computer program referred to above.

In summary, the purpose of this paper has been to give a statistically justifiable and conceptually and computationally simple method, the regression, as an alternative to the maximum likelihood approach which suffers from three deficiencies: the standard regularity conditions for the joint asymptotic normality of the maximum likelihood estimators are not satisfied, the estimating equations are either implicit or require the use of charts, and it is complicated appearing to non-specialists.

The methods discussed here should also be useful in other cases where the data is multinomial and the standard maximum likelihood regularity conditions are not satisfied.

REFERENCES

- [1] Anderson, T. W., An Introduction to Multivariate Analysis, New York: John Wiley and Sons, Inc., 1958.
- [2] Carle, F. L., and Strub, M. R., Biometrics, 34 (December 1978), 621-30.
- [3] Cramer, H., Mathematical Methods of Statistics, Princeton: Princeton University Press, 1946.
- [4] Johnson, N. L., and Kotz, S., Discrete Distributions, Boston: Houghton Mifflin, 1969.
- [5] Menhinick, E. F., Estimation of Insect Population Density in Herbaceous Vegetation with Emphasis on Removal Sweeping, Ecology, 44 (Summer 1963), 617-21.
- [6] Moran, P.A.P., A Mathematical Theory of Animal Trapping, Biometrika, 38, Parts 3 and 4 (1951), 307-11.
- [7] Southwood, T.R.E., Ecological Methods with Particular Reference to the Study of Insect Populations, London: Chapman and Hall, 1966.
- [8] Zippin, C., An Evaluation of the Removal Method of Estimating Animal Populations, Biometrics, 12 (June 1956), 163-89.

REGRESSION FOR MARKOV BERNOULLI RANDOM VARIABLES

Edmond H. Inselmann
US Army Combined Arms Combat Development Activity
Fort Leavenworth, Kansas

1. INTRODUCTION. The problem studied was that of regression on Bernoulli random variables in the case where some of the random variables were dependent. The interest in this case arose from a problem of trying to fit probability of hit curves to data generated by repeated missile simulations performed at US Army Material Systems Analysis Activity using tracking data from the Antitank Missile Test (ATMT). Hit/miss data were generated one second apart. Because overlapping tracking data were used, successive shots were dependent. This caused problems that seemed insurmountable until the author became aware of Klotz's papers (1) (2). In these papers the parameters of a sequence of Bernoulli dependent random variables satisfy the Markov chain property. In the case of successive shots, the assumption of Markov chain seemed reasonable and was used to solve the problem. Klotz's technique was extended to the regression problem.

2. PRELIMINARIES. In the generated data the following occurred: for several different ranges, a number of gunners (the number was not the same for all ranges) fired a sequence of shots (not all the same sequence length). The shots were fired a second apart. Let $X(I,J,R)$ be the results of the I th shot of the J th gunner at range R . A hit caused X to be 1 and a miss caused it to be 0. The notation that is now introduced is that of Klotz but modified to the needs of the problem under consideration. The first probability of hit is:

$$P(R) = \Pr \{X_{1JR}\} = b_0 + b_1 R + b_2 R^2 \quad \text{Eq 1}$$

which, as shown in the above equation, is taken to be a second degree polynomial in R . Next, the probability of a hit given that the previous shot was a hit, is:

$$P_{11}(R) = \lambda(R) = \Pr \{X_{1JR} = 1 | X_{1-1 JR} = 1\} = a_0 + a_1 R + a_2 R^2 \quad \text{Eq 2}$$

which is also taken as a second degree polynomial in R and which is the lower right hand term in the transition matrix. Clearly, equations 1 and 2 hold only when the sequences are stationary, which was a reasonable assumption for the problem considered. The remaining three terms of the transition matrix are:

$$P_{01}(R) = 1 - \lambda(R) = \Pr \{X_{1JR} = 0 | X_{1-1 JR} = 1\} \quad \text{Eq 3}$$

$$P_{10}(R) = \frac{P(R)[1 - \lambda(R)]}{1 - P(R)} = \Pr \left\{ X_{1jR} = 1 | X_{i-1,jR} = 0 \right\} \quad \text{Eq 4}$$

$$P_{00}(R) = 1 - P_{10}(R) = \Pr \left\{ X_{1jR} = 0 | X_{i-1,jR} = 0 \right\} \quad \text{Eq 5}$$

3. LIKELIHOOD. Having the above machinery, the joint probability of the data is:

$$\begin{aligned} \Pr \left\{ X_{1jR} \text{'s} \right\} &= \prod_{j=1}^{N_R} P_{11}(R)^{X_{1jR}} [1 - P(R)]^{1 - X_{1jR}} \\ &\times \prod_{j=2}^{n_{jR}} P_{11}(R)^{X_{1jR}} X_{i-1,jR} P_{10}(R)^{X_{1jR}} (1 - X_{i-1,jR}) \\ &\times P_{01}(R)^{(1 - X_{1jR})} X_{i-1,jR} P_{00}(R)^{(1 - X_{1jR})(1 - X_{i-1,jR})} \end{aligned} \quad \text{Eq 6}$$

where:

N_R = number of gunners firing at range R

n_{jR} = number of shots by the jth gunner at the Rth range.

Substituting r_{jR} , s_{jR} , and t_{jR} as described in equations 8 through 10, equation 6 becomes:

$$\Pr \left\{ X_{1jR} \text{'s} \right\} = \pi \prod_{R=1}^{N_R} \left\{ \lambda(R) r_{jR} (1 - \lambda(R))^{2(s_{jR} - r_{jR}) - t_{jR}} \right. \\ \left[1 - 2p(R) + \lambda(R)p(R) \right]^{(n_{jR} - 1 - 2s_{jR} + r_{jR} + t_{jR})} \\ p(R)^{(s_{jR} - r_{jR})} \left[1 - p(R) \right]^{-(n_{jR} - 2 - s_{jR} + t_{jR})} \right\}$$

Eq 7

Where:

$$r_{jR} = \sum_{i=1}^{n_{jR}} x_{1-i,jR} x_{ijR} \quad \text{Eq 8}$$

$$s_{jR} = \sum_{j=1}^{n_{jR}} x_{ijR} \quad \text{Eq 9}$$

$$t_{jR} = x_{1jR} + x_{n_{jR},jR} \quad \text{Eq 10}$$

Then the likelihood function is:

$$\begin{aligned}
 L = \sum_{R} \sum_{j=1}^{N(R)} & \left\{ r_{jR} \ln \lambda(R) + [2(s_{jR} - r_{jR}) - t_{jR}] \ln (1 - \lambda(R)) \right. \\
 & + (n_{jR} - 1 - 2s_{jR} + r_{jR} + t_{jR}) \ln (1 - 2P(R) + \lambda(R)P(R)) \\
 & + (s_{jR} - r_{jR}) \ln P(R) \\
 & \left. - (n_{jR} - 2 - s_{jR} + t_{jR}) \ln (1 - P(R)) \right\}
 \end{aligned} \tag{Eq 11}$$

Now, substituting $\lambda(R)$ and $P_{11}(R)$ in the likelihood function one has:

$$\begin{aligned}
 L = \sum_{R} \sum_{j=1}^{N(R)} & \left\{ r_{jR} \ln \left(\sum_{k=0}^2 a_k R^k \right) \right. \\
 & + [2(s_{jR} - r_{jR}) - t_{jR}] \ln \left(1 - \sum_{k=0}^2 a_k R^k \right) \\
 & + [n_{jR} - 1 - 2s_{jR} + r_{jR} + t_{jR}] \\
 & \quad \ln \left(1 - 2 \sum_{q=0}^2 b_q R^q + \sum_{q=0}^2 b_q R^q \sum_{k=0}^2 a_k R^k \right) \\
 & + (s_{jR} - r_{jR}) \ln \left(\sum_{q=0}^2 b_q R^q \right) \\
 & \left. - (n_{jR} - 2 - s_{jR} + t_{jR}) \ln \left(1 - \sum_{q=0}^2 b_q R^q \right) \right\}
 \end{aligned} \tag{Eq 12}$$

To find the maximum likelihood estimates of the regression coefficients, partial derivatives of the likelihood function with respect to the a's and b's are required. These partials are:

$$\frac{\partial L}{\partial a_m} = \sum_R \sum_{j=1}^{N(R)} \left\{ \frac{r_{jR} R^m}{\sum_{k=0}^2 a_k R^k} - \frac{[2(s_{jR} - r_{jR}) - t_{jR}] R^m}{1 - \sum_{k=0}^2 a_k R^k} \right.$$

Eq 13

$$+ \frac{(n_{jR} - 1 - 2s_{jR} + t_{jR}) R^m}{1 - 2 \sum_{q=0}^2 b_q R^q + \sum_{q=0}^2 b_q R^q \sum_{k=0}^2 a_k R^k} \left. \sum_{q=0}^2 b_q R^q \right\}$$

and

$$\frac{\partial L}{\partial b_n} = \sum_R \sum_{j=1}^{N(R)} \left\{ \frac{(n_{jR} - 1 - 2s_{jR} + r_{jR} + t_{jR})(-2R^n + R^n \sum_{k=0}^2 a_k R^k)}{1 - 2 \sum_{q=0}^2 b_q R^q + \sum_{q=0}^2 b_q R^q \sum_{k=0}^2 a_k R^k} \right.$$

Eq 14

$$+ \frac{(s_{jR} - r_{jR}) R^n}{\sum_{q=0}^2 b_q R^q} + \frac{(n_{jR} - 2 - s_{jR} + t_{jR}) R^n}{1 - \sum_{q=0}^2 b_q R^q} \left. \right\}$$

These expressions are set to zero and solved for the a's and b's. It is clear that the solutions must be obtained by iterative methods. A program was written to do this using the Newton Raphson method (3).

4. CONCLUSION. Recall that the problem discussed in the introduction was the problem of fitting probability of hit curves to data generated by repeated missile simulations. The curves were assumed to be quadratic functions of R expressed as follows:

$$P(R) = b_0 + b_1R + b_2R^2 \quad \text{Eq 1}$$

$$P_{11}(R) = a_0 + a_1R + a_2R^2 \quad \text{Eq 2}$$

Hence, utilization of the maximum likelihood technique, given by equations 11 through 14 above, and subsequent solution by the Newton Raphson method, provides the values of the coefficients, a's and b's, necessary to achieving a maximum likelihood "best fit" of equations 1 and 2 to their respective data points.

REFERENCES

1. Klotz, Jerome. Markov Chain Clustering of Births by Sex. Proceedings of the Sixth Berkeley Symposium on Mathematical Statistics and Probability, Volume IV: Biology and Health. University of California Press, 1972.
2. . Statistical Inference in Bernoulli Trials with Dependence. The Annals of Statistics, Volume 1, Number 2, pp. 373-379, 1973.
3. Ralston, Anthony. International Series in Pure and Applied Mathematics. A First Course in Numerical Analysis. McGraw-Hill Book Company, 1965, pp. 332, 334, 337, 343-344, 349-350, 373-376.

How to Smooth Curves and Surfaces With Splines and Cross-Validation

Grace Wahba
Department of Statistics
University of Wisconsin-Madison
Madison, Wisconsin 53706

ABSTRACT

We briefly review the use of smoothing splines and the method of generalized cross validation (GCV) for smoothing discrete noisy data from an unknown but smooth curve. Then we describe the use of "plaqué mince" or Laplacian smoothing splines with GCV for smoothing discrete noisy data from an unknown but smooth surface. A numerical algorithm for this (non-trivial!) computational problem is described, and an example from a Monte Carlo study is presented to show how the method works on simulated data. The results are extremely promising. Some design problems are briefly mentioned. Some conjectures are made concerning optimality properties of Laplacian smoothing splines and Laplacian histosplines.

Note: This report was written for the Proceedings of the 24th Design of Experiments Conference, held at Madison, Wisconsin, May 3-5, 1978, and sponsored by the U.S. Army Research Office.

TYPIST: Mary E. Arthur

This work was sponsored in part by the U.S. Army under Contract No. DAAG29-77-G-0207 and in part by the Office of Naval Research under Grant No. N00014-77-C-0675.

How to Smooth Curves and Surfaces With Splines and Cross-Validation

1. Introduction

In the conference talk we considered four problems. The first two had to do with estimating curves when they are observed discreetly and with error. The model is

$$y_i = f(t_i) + \epsilon_i, \quad i = 1, 2, \dots, n$$

where $f(t)$, $t \in [0,1]$ is an unknown curve, only known to be "smooth", $0 \leq t_1 \leq \dots \leq t_n \leq 1$, and ϵ_i are independent zero mean random variables with a common unknown variance σ^2 . The $\{y_i\}$ are observed. The first problem is: How should f be estimated nonparametrically from $y = (y_1, \dots, y_n)'$? The second (or design) problem is: How should the points $\{t_i\}$ be chosen so that the estimate of f is as good as possible? The third and fourth problems have to do with estimating surfaces. The model is

$$z_i = u(x_i, y_i) + \epsilon_i, \quad i = 1, 2, \dots, n,$$

where $u(x, y)$, $(x, y) \in$ some region in the plane, is only known to be "smooth". (x_i, y_i) , $i = 1, 2, \dots, n$ are n points in this region, the ϵ_i are zero mean independent random variables with common unknown variance σ^2 , and $z = (z_1, \dots, z_n)'$ is observed. The third problem is: How should u be estimated nonparametrically from z . The fourth (or design) problem is: How should the points (x_i, y_i) , $i = 1, 2, \dots, n$ be chosen so that the estimate of u is as good as possible. We will not discuss the design problems here. The design work mentioned in the talk has appeared in Athavale and Wahba (1978) and Wahba (1971, 1974, 1976, 1978c). That work (and the work of others, mentioned there) represents only some first steps in design problems for

nonparametric curve and surface fitting. There are many open problems.

Very good and relatively complete results for the first (curve estimation) problem are available (Craven and Wahba (1979), (CW) and Golub, Heath and Wahba (1977) (GHW), and transportable code is available from at least three sources Fleisher, (1979), Merz (1978a), and Paihua (1978). We will briefly summarize those results, because they will aid in understanding our discussion of the third problem, that is, surface smoothing. The remainder of this paper will then be devoted to the problem of smoothing of surface data non-parametrically. Some very nice theoretical results are available, and we have turned them into a computer program which delivers very pleasing pictures. The development of the program is the work of Mr. James Wendelberger, and it and other results will appear in his Ph.D. thesis.

2. Curve Smoothing

For curve smoothing, we recommend that f be estimated by the solution $f_{n,m,\lambda}$ of the minimization problem: Find $f \in H^m = \{f: f, f', \dots, f^{(m-1)}$ abs. cont., $f^{(m)} \in L_2[0,1]\}$ to minimize

$$\frac{1}{n} \sum_{i=1}^n (f(t_i) - y_i)^2 + \lambda \int_0^1 (f^{(m)}(u))^2 du . \quad (1)$$

The first term represents infidelity of f to the data, and the second term represents "roughness" of the solution. The parameter λ represents the tradeoff between the two. $m=2$ represents "psychological" smoothness (we think!) and is frequently used, and gives good results. We briefly discuss the determination of m from the data later. The solution $f_{n,m,\lambda}$ is known to be a polynomial spline of degree $2m-1$. The parameter λ is chosen from the data by the method of generalized cross-validation (GCV). GCV is derived from CV ("ordinary" cross validation). CV goes as follows: Let $f_{n,m,\lambda}^{(k)}$

be the solution of the minimization problem of (1) with the k th data point omitted. The value λ will be a good choice if $f_{n,m,\lambda}^{(k)}(t_k)$ comes close, on the average, to y_k . We measure this by the "ordinary" cross validation function $V_0(\lambda) = V_0^m(\lambda)$,

$$V_0(\lambda) = \frac{1}{n} \sum_{k=1}^n (f_{n,m,\lambda}^{(k)}(t_k) - y_k)^2.$$

For fixed m the parameter λ is chosen by minimizing $V_0^m(\lambda)$. For technical reasons involving convergence proofs, we replace $V_0(\lambda)$ by the generalized cross validation function

$$V(\lambda) = \frac{1}{n} \sum_{k=1}^n (f_{n,m,\lambda}^{(k)}(t_k) - y_k)^2 w_k(\lambda)$$

where the $(w_k(\lambda))$ are certain weights to reflect unequally spaced data, end effects, etc. Details are given in CW and GHW. It turns out that $V(\lambda)$ is much easier to compute than $V_0(\lambda)$, and $V(\lambda)$ has the representation

$$V(\lambda) = \frac{\frac{1}{n} \| (I - A(\lambda)) v \|^2}{\left(\frac{1}{n} \text{Trace}(I - A(\lambda)) \right)^2}$$

where $A(\lambda)$ is the $n \times n$ matrix which is uniquely determined by

$$\begin{pmatrix} f_{n,m,\lambda}(t_1) \\ \vdots \\ f_{n,m,\lambda}(t_n) \end{pmatrix} = A(\lambda) v.$$

Pleasing results have been obtained using smoothing splines with GCV in both Monte Carlo studies and various applications, Benedetti (1977), CW, GHW, Merz (1978a, 1978b), Stutzle (1977), Utreras (1978a), Welch (1979). These results are not surprising in the light of the following theoretical result (CW, GHW). Let $R(\lambda) = \frac{1}{n} \sum_{j=1}^n (f_{n,m,\lambda}(t_j) - f(t_j))^2$. $R(\lambda)$ is the "true mean square error" averaged over the data points. Before data are observed both $R(\lambda)$ and $V(\lambda)$

can be considered functions of the unknown f and random functions of the $\{\epsilon_j\}$. Let λ^* be the minimizer of $ER(\lambda)$ and $\tilde{\lambda}$ be the minimizer of $EV(\lambda)$. We have under rather general circumstances (see CW, GHW)

$$\lim_{n \rightarrow \infty} \frac{ER(\tilde{\lambda})}{ER(\lambda^*)} \downarrow 1. \quad (2)$$

Thus (very loosely), the mean square error with the estimated λ tends to the minimum mean square error achievable with any λ . Let $\hat{\lambda}$ be the minimizer of $V(\lambda)$. Numerical results based on Monte Carlo studies with $m=2$ reported in CW, with $n=50$ and equally spaced data points, show the achieved inefficiency $R(\hat{\lambda})/\min_{\lambda} R(\lambda)$ in the range 1.01 to 1.42.

Some numerical experiments to assess the effectiveness of choosing m by GCV have been done. (Lucas, 1978). One obtains $V^m(\hat{\lambda})$ for each m and minimizes $V^m(\hat{\lambda})$ over m . The results indicate that this procedure does a good job of picking out the m and $\hat{\lambda}$ which minimize $R(\lambda) = R^m(\lambda)$, and that there are classes of f 's for which it is worthwhile to do this, that is, $\min_{\lambda} R^m(\lambda)$ is usefully less than $\min_{\lambda} R^2(\lambda)$ for some $m \neq 2$. Efficient transportable code is not presently available, however. Depending on f , reduction in inefficiency of several percent can be obtained.

3. Surface Smoothing

We now turn to the third problem, that of recovering smooth surfaces. We recommend that u be estimated by the solution $u_{n,m,\lambda}$ of the minimization problem: Find $u \in H$ (an appropriate space, to be described) to minimize

$$\frac{1}{n} \sum_{j=1}^n (u(x_j, y_j) - z_j)^2 + \lambda \sum_{j=1}^m \iint (\frac{\partial^m u}{\partial x^j \partial y^{m-j}})^2 dx dy. \quad (3)$$

and that λ (and possibly m) be estimated by GCV. We now describe how to do this. For mathematical convenience the limits on the double integral in

(3) are taken to be $-\infty$ and ∞ . H is taken as $H = H^m(\mathbb{R}^2) = \{u: u \in D,$
 $\frac{\partial^m u}{\partial x^j \partial y^{m-j}} \in L_2(\mathbb{R}_2), j = 0, 1, \dots, m\}$. (D' is the dual of the Schwartz space D of
infinitely differentiable functions with compact support, this need not concern
us here, see Meinguet (1978, 1979), Schwartz (1966).)

Theorem: Let $t_j = (x_j, y_j)$, $t = (x, y)$ and $|t - t_j| = ((x - x_j)^2 + (y - y_j)^2)^{1/2}$.

Let $m \geq 2$ and $n \geq M = \binom{m+1}{2}$. The solution $u_{n,m,\lambda}$ to the problem: Find
 $u \in H$ to minimize

$$\frac{1}{n} \sum_{i=1}^n (u(t_i) - z_i)^2 + \lambda \iint \sum_{j=0}^m \binom{m}{j} \left(\frac{\partial^m u}{\partial x^j \partial y^{m-j}} \right)^2 dx dy, \quad (4)$$

is given by

$$u_{n,m,\lambda}(t) = \sum_{j=1}^n c_j E_m(t, t_j) + \sum_{v=1}^M d_v \phi_v(t), \quad (5)$$

where

$$E_m(s, t) = \theta_m |s-t|^{2m-2} \log |s-t|, \quad \theta_m = (2^{2m-1} \pi [(m-1)!]^2)^{-1}$$

$$\phi_v(t) = x^\alpha y^\beta \quad v = 1, 2, \dots, M$$

where α, β run over all the M combinations of non-negative integers with
 $\alpha + \beta \leq m-1$, provided the $n \times M$ matrix T with iv^{th} entry $\phi_v(t_i)$ is of rank M .

The coefficients $\underline{c} = (c_1, \dots, c_n)'$ and $\underline{d} = (d_1, \dots, d_M)'$ are determined by

$$(K + \rho I) \underline{c} + T \underline{d} = \underline{z} \quad (6)$$

$$T' \underline{c} = 0 \quad (7)$$

where K is the $n \times n$ matrix with jk^{th} entry $E_m(t_j, t_k)$, and $\rho = n\lambda$.

This theorem is essentially due to Duchon (1976a, 1976b). Meinguet (1978) has also proved very similar results in a reproducing kernel Hilbert space setting. For completeness, in the Appendix we outline a proof which roughly follows Meinguet's argument. By putting the minimization problems of (1) and (4) in a reproducing kernel Hilbert space setting, $f_{n,m,\lambda}$ and $u_{n,m,\lambda}$ can be

shown to be Bayes estimates with a certain (partially improper) prior on f or u , see Wahba (1978a).

4. An Algorithm for Computation of the Smoothing Surface

We now want to compute $\hat{u}_{n,m,\lambda}$ efficiently, and choose λ (and possibly m) by GCV. Our algorithm below has benefited from the algorithmic work of Paitua (1978). However it is different and seems especially well adapted to determining the generalized cross validation function $V(\lambda)$ for this case. We next derive the equations behind our computational approach.

Let R be any $n \times (n-M)$ dimensional matrix of rank $n-M$ satisfying $R'T = 0_{(n-M) \times M^*}$. Subscripts indicate the dimensions of the subscripted matrix. Since $T'c = 0$, we have

$$\hat{c} = Ry \quad (8)$$

for y a unique $n-M$ dimensional vector. Left multiplying (6) by R' and substituting (8) into (6) gives

$$R'(K+\rho I)Ry = R'z \quad (9)$$

$$y = (R'(K+\rho I)R)^{-1}R'z \quad (10)$$

$$\hat{c} = R(R'KR+\rho R'R)^{-1}R'z . \quad (11)$$

The vector d is then given by $d = (T'T)^{-1}T'(z-Kc)$, obtained by left multiplying (6) by T' . To estimate λ (equivalently ρ) by GCV, we want to choose λ to minimize

$$V(\lambda) = \frac{\frac{1}{n} | | (I-A(\lambda))z | |^2}{\left(\frac{1}{n} \text{Trace}(I-A(\lambda)) \right)^2} .$$

where $A(\lambda)$ is the $n \times n$ matrix determined by

$$\begin{pmatrix} u_{n,m,\lambda}(t_1) \\ \vdots \\ u_{n,m,\lambda}(t_n) \end{pmatrix} = A(\lambda) \underline{z} .$$

To talk about good properties of GCV here, we suppose the $\{t_i\}$ will be in a bounded region of the plane R_2 (even though the minimization is over functions in R_2). The basic property (2) of GCV can then be shown to hold as the t_i become dense in this region - the proof (CW, GHW) is independent of the nature of the region.

To obtain a convenient representation for $A(\lambda)$, we see from (5) that

$$\underline{z} - \begin{pmatrix} u_{n,m,\lambda}(t_1) \\ \vdots \\ u_{n,m,\lambda}(t_n) \end{pmatrix} = \underline{z} - K\underline{c} - T\underline{d} . \quad (11)$$

From (6), we have

$$\underline{z} - T\underline{d} = (K + \rho I)\underline{c}$$

so that the right hand side of (11) equals \underline{c} . Thus,

$$(I - A(\lambda))\underline{z} = \underline{c} = \rho R(R'KR + \rho R'R)^{-1}R'\underline{z} \quad (12)$$

We need to compute \underline{c} , $\| (I - A(\lambda))\underline{z} \|^2$, and $\text{Tr}(I - A(\lambda))$. Any $R_{n \times (n-M)}$ will have a singular value decomposition

$$R = U_{n \times (n-M)} D_{(n-M) \times (n-M)} V_{(n-M) \times (n-M)}^T \quad (13)$$

where $U^T U = V^T V = I_{n-M}$ and D is diagonal. Then

$$\begin{aligned} R(R'KR + \rho R'R)^{-1}R^T &= UDV^T(VDU^T KUDV^T + \rho VDDV^T)^{-1}VDU^T \\ &= U(U^T K U + \rho I)^{-1}U^T \end{aligned} \quad (14)$$

Define

$$B_{(n-M) \times (n-M)} = U^T K U$$

and define Γ and δ by

$$B = \Gamma \delta \Gamma'$$

where Γ and δ are the orthogonal and diagonal matrices in the eigenvalue decomposition of B . Then the right hand side of (14) becomes

$$U(\Gamma \delta \Gamma' + \rho)^{-1} U' \quad (15)$$

$$= U \Gamma' (\delta + \rho I)^{-1} \Gamma U' \quad (16)$$

$$= U \Gamma' \begin{pmatrix} \frac{1}{b_1 + \rho} & & 0 \\ & \ddots & \\ 0 & & \frac{1}{b_{n-M} + \rho} \end{pmatrix} \Gamma U' \quad (17)$$

where b_1, \dots, b_{n-M} are the diagonal entries in δ (i.e. the eigenvalues of B).

Given $U \Gamma'$, $\{b_i\}$ we compute

$$\underline{z} = U \Gamma' \begin{pmatrix} \frac{1}{b_1 + \rho} & & 0 \\ & \ddots & \\ 0 & & \frac{1}{b_{n-M} + \rho} \end{pmatrix} \Gamma U' \underline{z} ,$$

$$||(I - A(\lambda))\underline{z}||^2 = \rho^2 ||(\delta + \rho I)^{-1} \Gamma U' \underline{z}||^2$$

and

$$(\frac{1}{n} \text{Tr}(I - A(\lambda))^2 = (\frac{1}{n} \sum_{i=1}^{n-M} \frac{\rho}{b_i + \rho})^2 .$$

We now discuss the determination of U . It can be seen that U is any matrix whose $n-M$ columns are orthonormal and perpendicular to the M columns of T . $U_{(n-M) \times n}^T T = 0_{(n-M) \times M}$. We obtained U as follows. Let

$$I - T(T^T T)^{-1} T^T = \tilde{U} \Delta \tilde{U}' . \quad (18)$$

where \tilde{U} is orthogonal and Δ is diagonal. Since $I - T(T^T T)^{-1} T^T$ is a projection matrix of rank $n-M$, Δ is a matrix with M zeroes and $n-M$ ones on the diagonal. We used EISPACK (Smith et al. (1976)) to perform the eigenvalue decomposition $\tilde{U} \Delta \tilde{U}'$ and the $n-M$ columns of U are taken as the columns of \tilde{U} corresponding to the $n-M$ ones in Δ . Each such vector is perpendicular to the columns of T ,

as can be seen by right multiplying (18) by T. The EISPACK computation of the entries of Δ was good to seven figures. Given U, B is computed and T and S are also computed using the eigenvalue decomposition routines in EISPACK.

5. Numerical Results

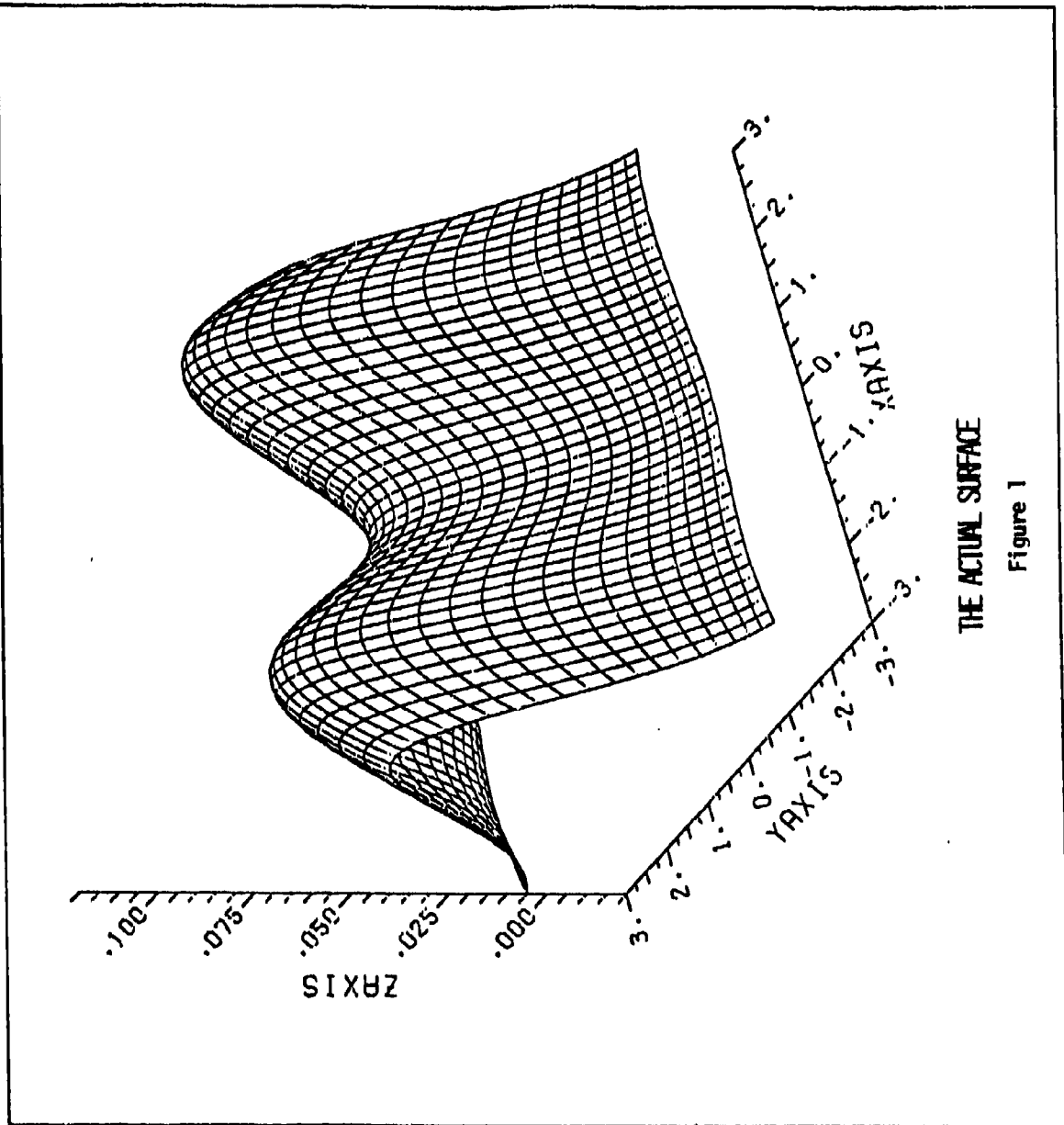
We present the results of a single Monte Carlo experiment, with $m=2$. Figure 1 gives a picture of the true function u that was the subject of the first experiment,

$$u(x,y) = \frac{1}{2\pi(1.3)^2} \left[e^{-\frac{1}{2(1.3)^2}((x-2)^2+y^2)} + e^{-\frac{1}{2(1.3)^2}((x+2)^2+y^2)} \right]$$

A regular 7×7 square array of 49 points t_i , $i = 1, 2, \dots, 49$ was selected, with the middle point being $(0,0)$ and the point spacing being 1.0. Data y_i were generated as

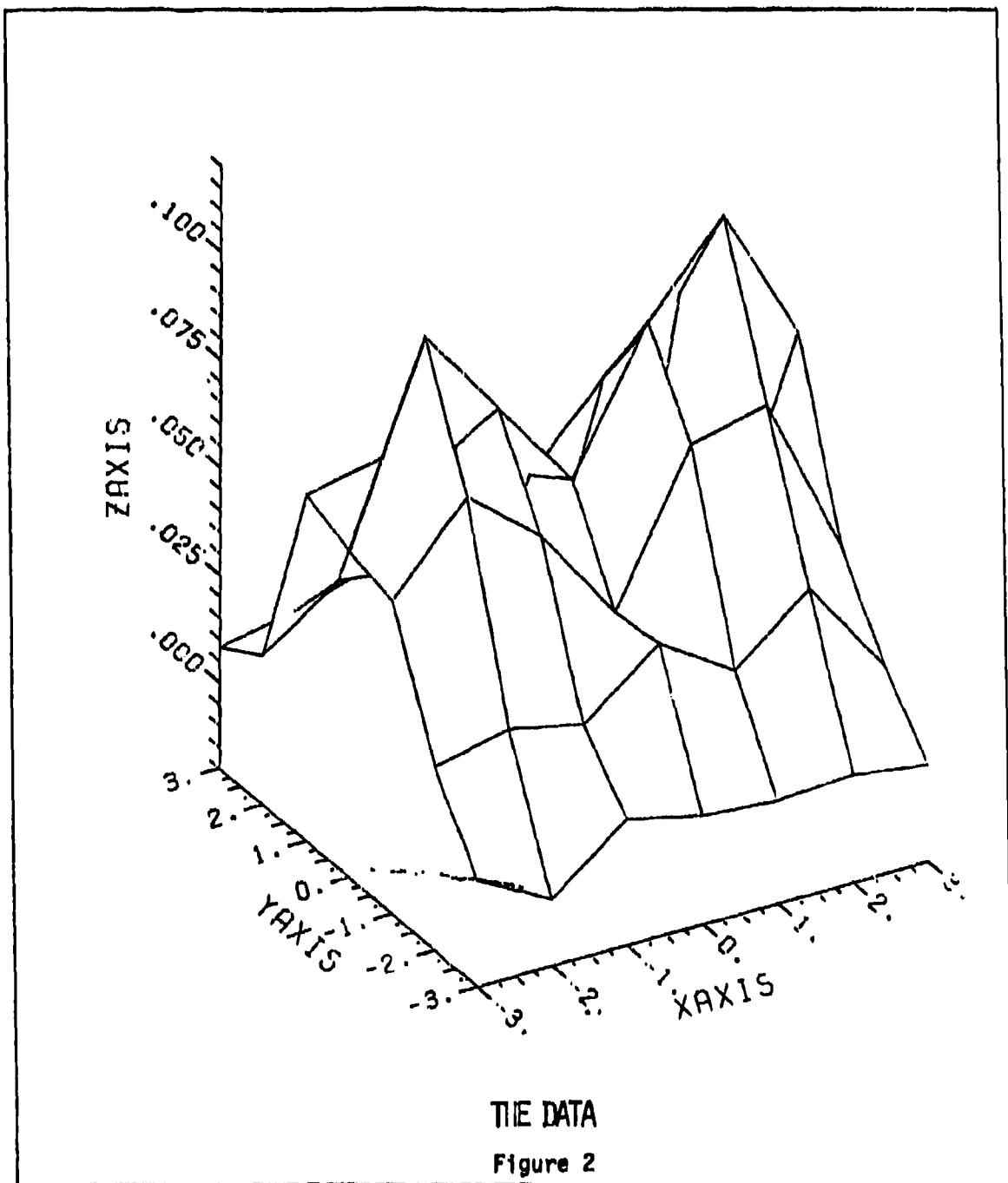
$$y_i = u(t_i) + \epsilon_i, \quad t_i = (x_i, y_i), \quad i = 1, 2, \dots, 49$$

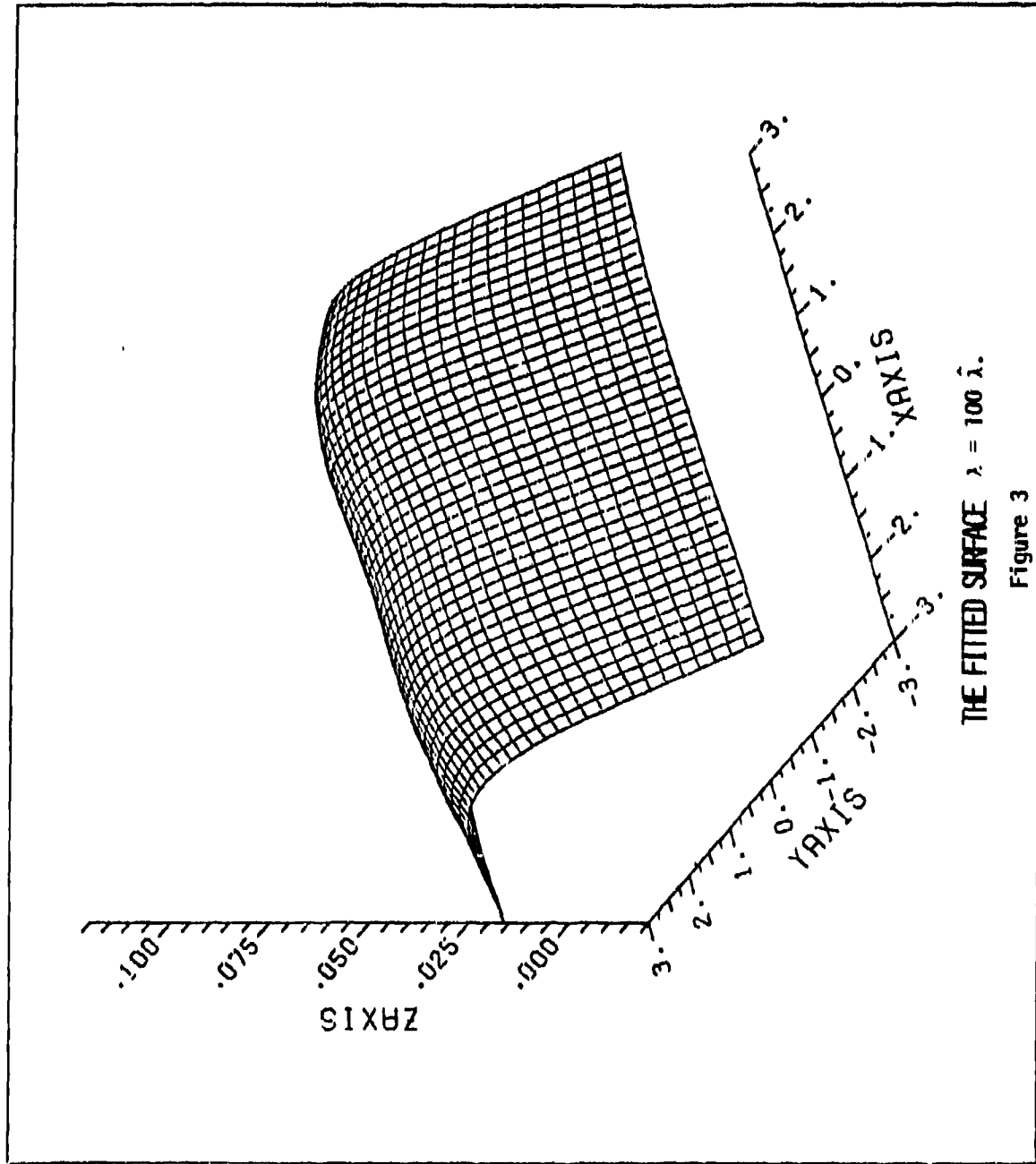
where the ϵ_i were pseudorandom $N(0, \sigma^2)$ random variables with $\sigma = .01$. σ is about 1/8 of the maximum height of u . Figure 2 presents a picture of the data points, which have been joined by straight lines. Figures 3 and 4 give $u_{n,2,\lambda}$ for two values of λ , in Figure 3, λ is too large, and in Figure 4, λ is too small. Figure 5 gives $u_{n,2,\hat{\lambda}}$, where $\hat{\lambda}$ is the minimizer of $V(\lambda)$. Figure 6 gives a plot of $R(\lambda)$ and $V(\lambda)$ against $\log \lambda$. It is seen that, in the neighborhood of the minimizer of $R(\lambda)$, $V(\lambda)$ roughly follows $R(\lambda)$. Theoretically, we have $\min_{\lambda} EV(\lambda) \approx \min_{\lambda} ER(\lambda) + \sigma^2$, for large n , see CW, and this relationship is roughly approximated here. The achieved inefficiency, defined by $R(\hat{\lambda})/\min_{\lambda} R(\lambda)$, where $\hat{\lambda}$ is the minimizer of $V(\lambda)$, was 1.54. Note that $\min_{\lambda} R(\lambda) = .25 \sigma^2$. If we were fitting a surface which is known to be a linear combination of given functions by regression we would expect the mean square error to be proportional to $\frac{\sigma^2}{n}$. Here numerical and theoretical results in the one



THE ACTUAL SURFACE

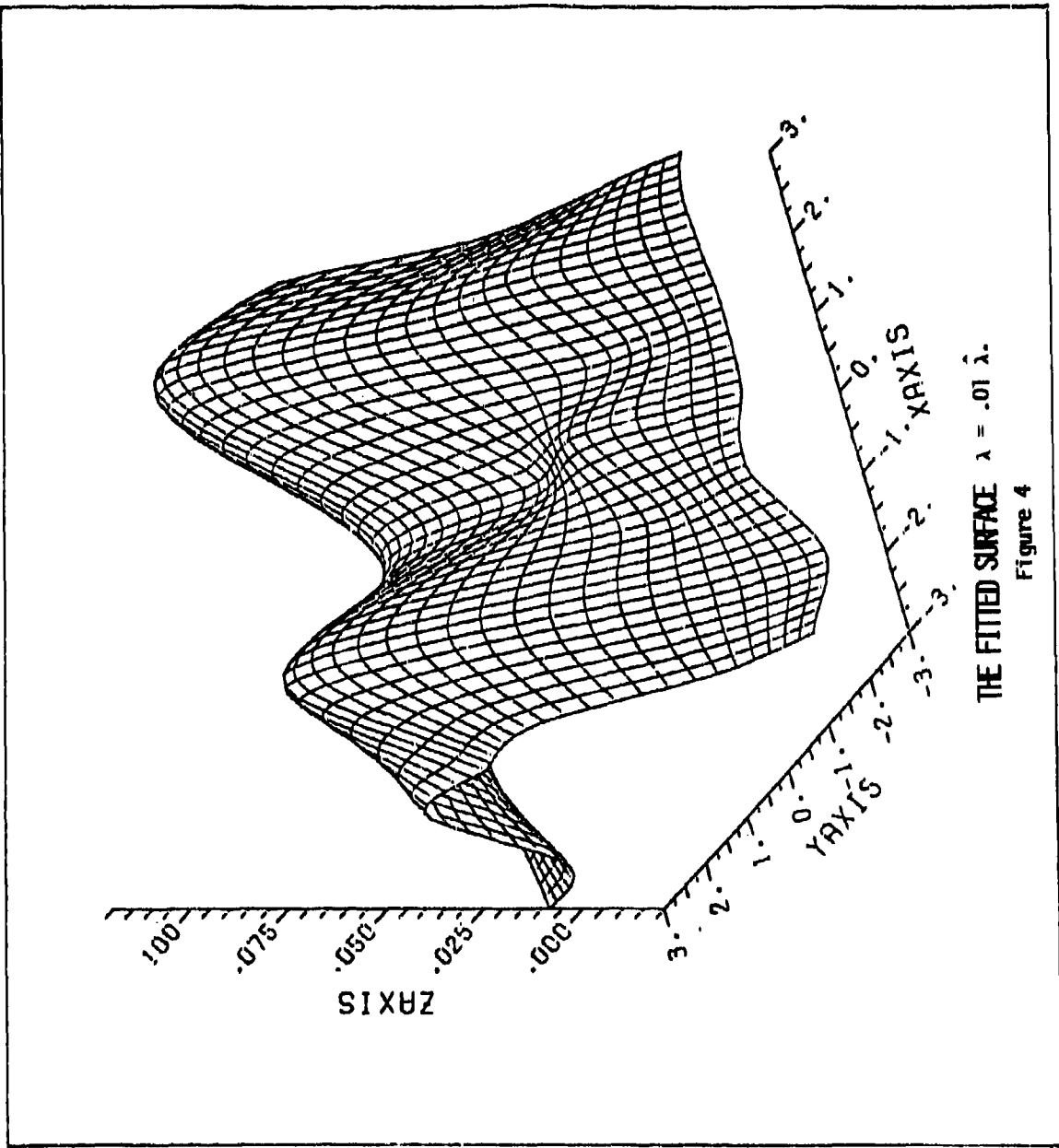
Figure 1





THE FITTED SURFACE $\lambda = 100 \hat{i}$.

Figure 3



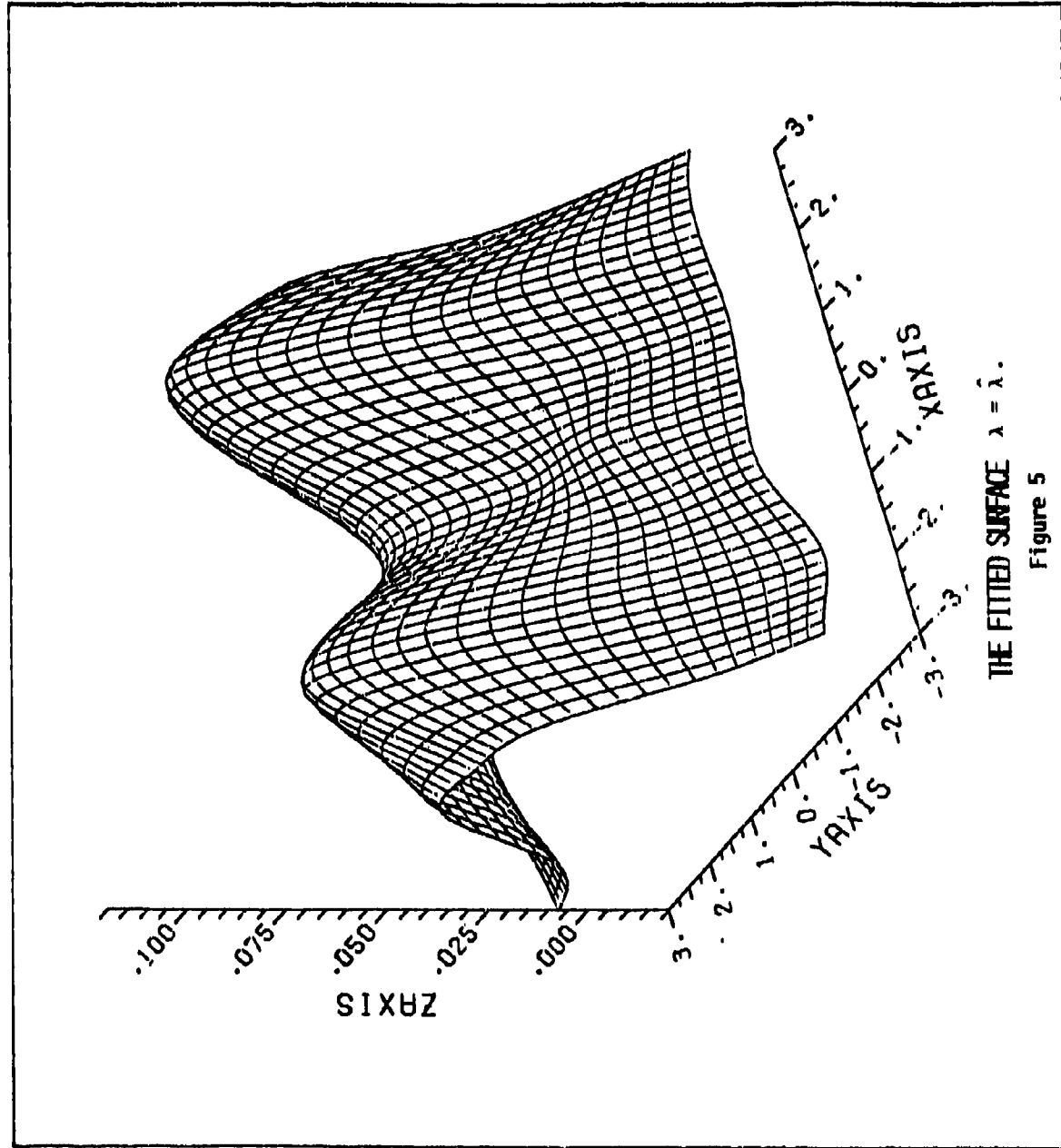
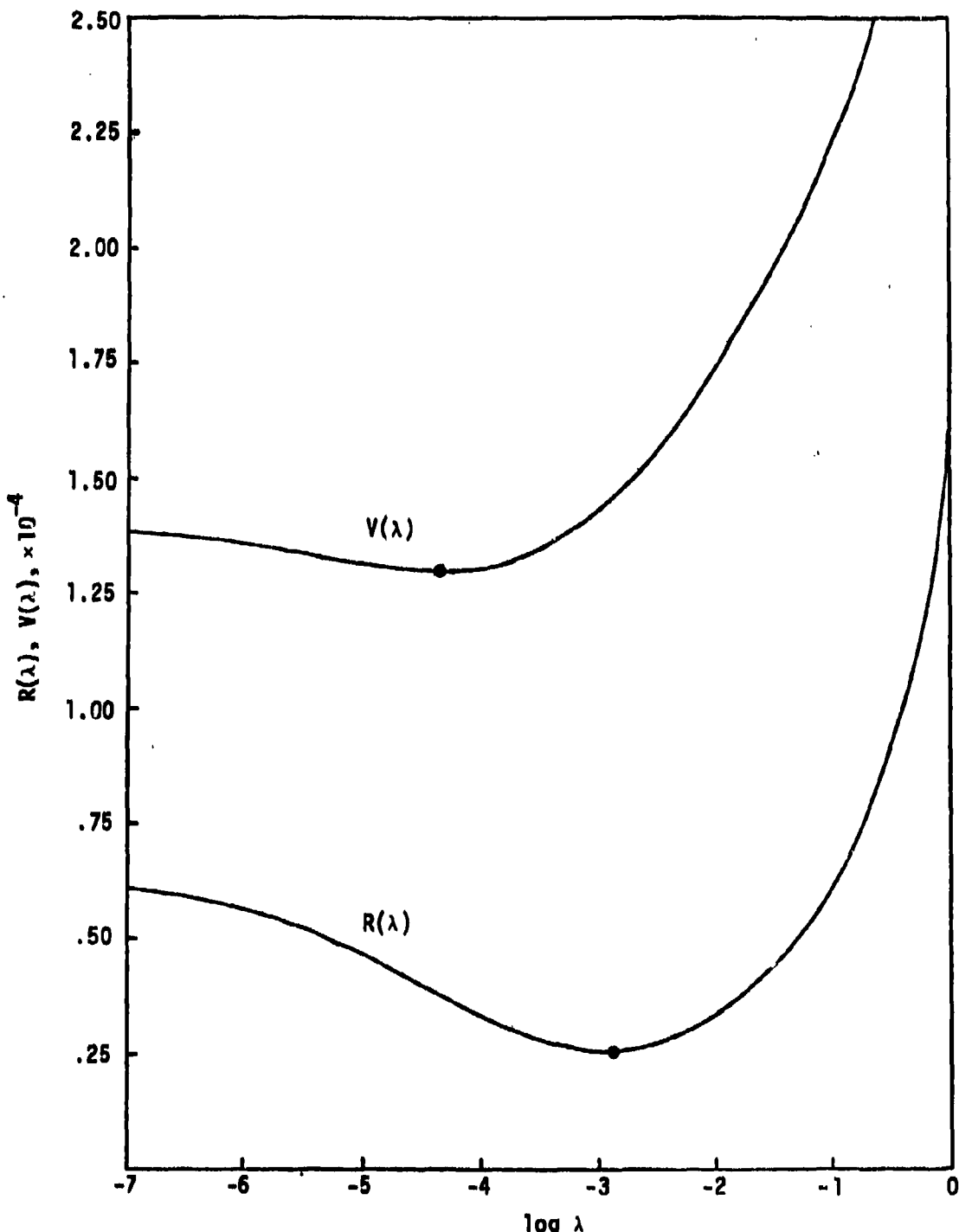


Figure 5



THE MEAN SQUARE ERROR $R(\lambda)$, AND THE
CROSS-VALIDATION FUNCTION $V(\lambda)$.

Figure 6
182

dimensional case for reasonably regular arrangements of data points indicate that $\min_{\lambda} R(\lambda) \simeq \text{const. } (\sigma^2/n)^p$ where p is some power slightly less than one. p depends on the rate of decay of eigenvalues of an appropriate reproducing kernel. See Wahba and Wold (1975), CW, and Wahba (1975b, 1977). If $u \in H^{2m}(R^2)$, $p = 2m/(2m+1)$. (In preparation).

Mr. Wendelberger's program is running for $n = 120$ and quite reasonable results have been obtained for this case, with randomly chosen points $\{t_i\}$. One cannot increase n with impunity, however. In the $n = 49$ case reported here the condition number of B , namely $\max_j b_j / \min_j b_j$ was around 200, and in the irregularly spaced $n = 120$ case this condition number was of the order of 4×10^5 . (Irregularly spaced points will increase the condition number.) For large n and a condition number somewhere around (we guess) 10^6 or 10^7 , the computation errors will begin to take over. Thus, in theory, a plot of $\log(\min_{\lambda} R(\lambda))$ vs. n should be approximately linear with slope $-p$, however, as roundoff error gets large, this plot will flatten out. Laurent and colleagues (1978) have developed a procedure for patching together surfaces of this type so that groups of points may be handled separately.

The cost of running a program designed just to produce Figure 5 from data, we estimate to be about \$4.00 at weekend rates at our computing center. To produce Figure 5 from a second set of data at the same points $\{t_i\}$, one would retain U , r and $\{b_i\}$, which depend on the $\{t_i\}$ but not z , and then the cost would be very small.

6. Miscellaneous Remarks

We hope to implement the $m = 3$ and $m = 4$ cases. n can then be selected from the data by comparing $V(\hat{\lambda})$ for each of the $m = 2, 3$ and 4 cases. For $m = 2$, the roughness penalty

$$\sum_{j=0}^2 \iint \left(\frac{\partial^2 u}{\partial x^j \partial y^{2-j}} \right)^2 dx dy$$

is the bending energy of a thin plate. For this reason, Duchon christened the solutions "plaqué mince" splines. We have reason to believe that the $m = 3$ case will be appropriate for the smoothing of certain meteorological data. In some cases the nature of the physical phenomena being smoothed may provide insight into a choice of m .

We note that the solutions $u_{n,m,\lambda}$ satisfy

$$\Delta^m u_{n,m,\lambda}|_t = 0, \quad t \notin t_1, \dots, t_n,$$

where Δ is the Laplacian operator $\Delta u = \frac{\partial^2 u}{\partial x^2} + \frac{\partial^2 u}{\partial y^2}$. The smoothing splines $f_{n,m,\lambda}$ satisfy $f_{n,m,\lambda}^{(2m)}(t) = 0$, $t \notin t_1, \dots, t_n$. For this reason, Prof. Iso Schoenberg has suggested to us that the functions $u_{n,m,\lambda}$ be called "Laplacian Smoothing Splines".

We have recently obtained what might be called the Laplacian histosplines, by analogy with Boneva, Kendall, and Stefanov (1971). These are functions which minimize the roughness penalty $\sum_{j=0}^m \iint_A \left(\frac{\partial^m u}{\partial x^j \partial y^{m-j}} \right)^2 dx dy$ subject to volume matching conditions of the form

$$\iint_{A_i} u dx dy = p_i, \quad i = 1, 2, \dots, n$$

where the A_i are n bounded areas in R^n whose union is A . These functions satisfy

$$\Delta^m u = \text{constant on each } A_i.$$

(Dyn, Wong, and Wahba (1979)), and, in preparation).

Various optimality properties of smoothing splines and histosplines in one dimension are known. For example, it can be shown from CW and Wahba (1975b) that

$$\begin{aligned} E \int_0^1 (f_{n,m,\lambda}(t) - f(t))^2 dt &= O(n^{-(2m)/(2m+1)}), \quad f \in H^m(0,1) \\ &= O(n^{-(4m)/(4m+1)}), \quad f \in H^{2m}(0,1) \end{aligned}$$

and f satisfies some boundary conditions. It is part of the folklore that these rates cannot be improved upon. Density estimates determined by the minimizer of $\int_0^1 (f^{(m)}(t))^2 dt$ subject to the area-matching conditions

$$\int_{t_i}^{t_{i+1}} f(t) dt = \text{fraction of observations in } [t_i, t_{i+1}]$$

are known to achieve the best possible convergence rates over $f \in H^m$ provided the t_i are chosen properly. See Wahba (1975c, 1976). Stone (1978) has given some results on best possible pointwise convergence rates in d dimensions. We conjecture that all the nice convergence properties of polynomial splines can be extended to the Laplacian smoothing splines and Laplacian histosplines.

APPENDIX

Outline of Proof of Theorem

Let r_1, r_2, \dots, r_M be a subset of M points selected from t_1, \dots, t_n with the property that the $M \times M$ matrix T with j^{th} entry $\phi_v(r_j)$ is of full rank. The space $H = \{u: u \in D^1, \frac{\partial^m u}{\partial x^j \partial y^{m-j}} \in L_2, j = 0, 1, \dots, m-1\}$ can be decomposed into the direct sum of two spaces:

$$H = \pi_{m-1} \oplus \underline{X},$$

where π_{m-1} is the M dimensional space of polynomials of total degree $m-1$ or less and $\underline{X} = \{u: u \in H, u(r_v) = 0, v = 1, 2, \dots, M\}$. It can then be shown that

$$\langle u, v \rangle_{\underline{X}} \equiv \iint \sum_{j=0}^m \binom{m}{j} \frac{\partial^m u}{\partial x^j \partial y^{m-j}} \frac{\partial^m v}{\partial x^j \partial y^{m-j}} dx dy$$

defines an inner product on \underline{X} . If an inner product is defined on π_{m-1} by $\langle u, v \rangle_{\pi_{m-1}} = \sum_{v=1}^M u(r_v)v(r_v)$, then π_{m-1} and \underline{X} are orthogonal subspaces. \underline{X} (and π_{m-1} , and hence H) are reproducing kernel spaces.

If the reproducing kernel $K(s, t)$ for \underline{X} can be found, then the solution $u_{n,m,\lambda}$ to the minimization problem of (4) will have a representation

$$u_{n,m,\lambda}(t) = \sum_{j=1}^n \tilde{c}_j K(t, t_j) + \sum_{v=1}^M \tilde{c}_v \phi_v(t). \quad (\text{A.1})$$

(See, e.g. Kimeldorf and Wahba (1971)). $u_{n,m,\lambda}$ will, of course, be independent of the choice of r_1, \dots, r_M . The reproducing kernel K has been found by Meinguet (1978, 1979) and is given by

$$\begin{aligned}
 K(s, t) &= E_m(s, t) - \sum_{\mu=1}^M p_\mu(s) E_m(t, r_\mu) \\
 &\quad - \sum_{v=1}^M p_v(t) E_m(s, r_v) \\
 &\quad + \sum_{\mu, v=1}^M p_\mu(s) p_v(t) E_m(r_\mu, r_v), \tag{A.2}
 \end{aligned}$$

where $\{p_\mu\}_{\mu=1}^M$ span π_{m-1} and are chosen so that $p_\mu(r_v) = 1$, $\mu = v$, $= 0$, $\mu \neq v$. Substituting (A.2) into (A.1), it is seen that a representation of the form (5) for $u_{n,m,\lambda}$ holds.

To show that K is the reproducing kernel for \underline{X} , it is necessary to show that

$$1) \quad K(s, \cdot) \in \underline{X}, \text{ each } s$$

$$11) \quad \langle K(s, \cdot), K(t, \cdot) \rangle_{\underline{X}} = K(s, t), \tag{A.3}$$

where

$$\langle u, v \rangle_{\underline{X}} = \sum_{j=1}^M \iint \binom{m}{j} \frac{\partial^m u}{\partial x^j \partial y^{m-j}} \frac{\partial^m v}{\partial x^j \partial y^{m-j}} dx dy. \tag{A.4}$$

Define

$$H_s(t) = E_m(s, t) - \sum_{\mu=1}^M p_\mu(s) E_m(r_\mu, t).$$

Then

$$K(s, t) = H_s(t) - \sum_{v=1}^M p_v(t) H_s(r_v). \tag{A.5}$$

The hard part is to show that $H_s \in H$. (Note that $E_m \notin H$.) Meinguet shows that $H_s \in H$, for each s , and we omit the proof. It then follows that $K(s, \cdot) \in H$, and, since $\sum_{v=1}^M p_v(\cdot) H_s(r_v)$ is the polynomial interpolating to H_s at r_1, \dots, r_M , $K(s, r_v) = 0$, $v = 0, 1, \dots, M$, and so $K(s, \cdot) \in \underline{X}$.

To establish (A.3), first note that

$$\frac{\partial^m}{\partial x^j \partial y^{m-j}} K(s, \cdot) = \frac{\partial^m}{\partial x^j \partial y^{m-j}} H_s(\cdot). \tag{A.6}$$

Consider the Green's formula

$$(-1)^m \sum_{j=0}^m \binom{m}{j} \iint \frac{\partial^m u}{\partial x^j \partial y^{m-j}} \frac{\partial^m v}{\partial x^j \partial y^{m-j}} dx dy = \iint \Delta^m u \cdot v dx dy \quad (A.7)$$

where $\Delta = \frac{\partial^2}{\partial x^2} + \frac{\partial^2}{\partial y^2}$. This formula holds provided, e.g. $v \in H \cap L_2$ and $u \in D$.

If $u \in D$, then the potential formula

$$\iint (\Delta^m u)(t) E_m(s, t) dt = u(s)$$

holds (see Schwartz (1966)) and in particular

$$\iint \Delta^m u \cdot H_s = u(s) - \sum_v^M p_v(s) u(r_v) . \quad (A.8)$$

Meinguet argues that, in fact (A.7) and (A.8) hold for $u = H_t$, $v = H_s$, giving

$$\begin{aligned} (-1)^m \sum_{j=0}^m \binom{m}{j} \iint \frac{\partial^m}{\partial x^j \partial y^{m-j}} H_t \frac{\partial^m}{\partial x^j \partial y^{m-j}} H_s \\ = H_t(s) - \sum_{v=1}^M p_v(s) H_s(r_v) \equiv K(s, t) , \end{aligned}$$

which, combined with (A.6), gives (A.3).

Equation (7) can be obtained as follows: Considering $K(t, t_j)$ as a function of t ,

$$\begin{aligned} K(t, t_j) = E_m(t, t_j) - \sum_{v=1}^M p_v(t_j) E_m(t, r_v) + \\ \text{a polynomial of degree } m-1 \text{ or less.} \end{aligned} \quad (A.9)$$

Now, if ϕ is any element of π_{m-1} , we have

$$\phi(t) - \sum_{v=1}^M p_v(t) \phi(r_v) \equiv 0 . \quad (A.10)$$

Letting $a_1(j), a_2(j), \dots, a_n(j)$ be the coefficients of $E_m(\cdot, t_1), E_m(\cdot, t_2), \dots, E_m(\cdot, t_n)$, in (A.9), it can be verified from (A.10) that

$$\sum_{k=1}^n a_k(j)\phi(t_k) = 0, \quad j = 1, 2, \dots, n,$$

which results directly in the conditions (7) on the coefficient vector \underline{c} in (5), namely, $T\underline{c} = 0$. Equation (6) is obtained as follows: One substitutes (A.1) into (4), and then uses (A.3) to evaluate the expression (4) to be minimized. By repeatedly using $T'\underline{c} = 0$, one obtains that \underline{c} and \underline{d} are chosen subject to $T'\underline{c} = 0$, to minimize

$$||\underline{z} - K\underline{c} - T\underline{d}||^2 + n \lambda \underline{c}' K \underline{c}.$$

Differentiating this expression with respect to \underline{c} and setting the result equal to zero, and using $T'\underline{c} = 0$, gives (6).

REFERENCES

- Athavale, M.L., and Wahba, G., (1978). Determination of an optimal mesh for a collocation - projection method for solving two point boundary value problems, University of Wisconsin-Madison, Statistics Department Technical Report #530, to appear, J. Approx. Theory.
- Benedetti, J., (1977). On the nonparametric estimation of regression functions, J. Roy. Stat. Soc. B., 39, 2, 248-253.
- Boneva, L., Kendall, D., and Stefanov, I., (1971). Spline transformations: Three new diagnostic aids for the statistical data-analyst (with Discussion), J. Roy. Stat. Soc. B., 33, 1-70.
- Craven, P., and Wahba, G., (1979). Smoothing noisy data with spline functions: estimating the correct degree of smoothing by the method of generalized cross-validation, Numer. Math. 31, 377-403.
- Duchon, Jean, (1976a). Interpolation des fonctions de deux variables suivant le principe de la flexion des plaques minces. R.A.I.R.O. Analyse numerique, 10, 12, pp.5-12.
- Duchon, Jean, (1976b). Fonctions spline du type "Plaque mince" en dimension 2. No. 231. Séminaire d'analyse numérique, Mathématiques Appliquées, Université Scientifique et Médicale de Grenoble.
- Dyn, N., Wahba, G., and Wong, W.H., (1979). To be submitted to J. Am. Stat. Soc. as comments on a paper by Tobler.
- Fleisher, J., (1979). Spline smoothing routines, Reference Manual for the 1110. Academic Computing Center, The University of Wisconsin-Madison.
- Golub, G., Heath, M., and Wahba, G., (1977). Generalized cross-validation as a method for choosing a good ridge parameter, University of Wisconsin-Madison, Department of Statistics Technical Report #491, to appear, Technometrics.
- Kimeldorf, G., and Wahba, G. (1971). Some results on Tchebycheffian spline functions. J. Math. Anal. Appl., 33, 82-95.
- Laurent, P.J., (1978). Seminar presented at the University of Wisconsin-Madison Statistics Department.
- Lucas, H., (1978). Estimation of smoothing parameters to smooth noisy data and confidence regions for the underlying function, Ph.D. Thesis, University of Wisconsin-Madison, Department of Statistics.
- Meinguet, Jean, (1978). Multivariate interpolation at arbitrary points made simple. Report No. 118, Institute de Mathématique Pure et Appliquée, Université Catholique de Louvain, to appear, ZAMP.
- Meinguet, Jean, (1979). An intrinsic approach to multivariate spline interpolation at arbitrary points. To appear in the Proceedings of the NATO Advanced Study Institute on Polynomial and Spline Approximation, Calgary 1978, B. Sahney, Ed.

- Merz, P., (1978a). Spline smoothing by generalized cross-validation, a technique for data smoothing. Chevron Research Company, Richmond, CA.
- Merz, P.M., (1978b). Determination of absorption energy distribution by regularization and a characterization of certain absorption isotherms, Chevron Research Company, Richmond, CA.
- Paihua Montes, Luis, (1978). Quelques methodes numeriques pour le calcul de fonctions splines a une et plusieurs variables. Thesis, Analyse Numerique Université Scientifique et Medicale de Grenoble.
- Schwartz, Laurent (1966). Theorie des distributions. Hermann, Paris.
- Smith, B.T., et al., (1976). Matrix Eigensystem Routines - EISPACK Guide. Springer-Verlag.
- Stone, C.J., (1978). Optimal rates of convergence for nonparametric estimates, Manuscript, Department of Mathematics, University of California, Los Angeles.
- Stutzle, Werner, (1977). Estimation and Parameterization of Growth Curves. Thesis, Swiss Federal Institute of Technology Zurich, Department of Mathematics.
- Utreras Diaz, F., (1978a). Sur le choix du parametre d'ajustement dans le lissage par fonctions spline, No. 296, Seminaire d'analyse numerique, Mathematiques Appliquees, Université Scientifique et Medicale de Grenoble.
- Utreras Dias, F., (1978b). Utilisation des programmes de calcul du parametre d'ajustement dans le lissage par fonctions spline. R.R. No. 121, Mathematiques Appliquees, Université Scientifique et Medicale de Grenoble.
- Wahba, G., (1971). On the regression design problem of Sacks and Ylvisaker, Ann. Math. Statist., 42, 3, 1035-1053.
- Wahba, G., (1974). Regression design for some equivalence classes of kernels, Ann. Statist., 2, 5, 924-934.
- Wahba, G., (1975a). A canonical form for the problem of estimating smooth surfaces, University of Wisconsin-Madison, Department of Statistics Technical Report #420.
- Wahba, G., (1975b). Smoothing noisy data with spline functions, Numer. Math., 24, 383-393.
- Wahba, G., (1975c). Interpolating spline methods for density estimation. I. Equispaced knots. Ann. Statist., 3, 30-48.
- Wahba, G., (1976). On the optimal choice of nodes in the collocation-projection method for solving linear operator equations, J. Approx. Theory, 16, 2, 175-186.
- Wahba, G., (1976). Histosplines with knots which are order statistics, J. Roy. Stat. Soc., Series B., 38, 2, 140-151.
- Wahba, G., (1977). Discussion to "Consistent nonparametric regression", by Charles J. Stone, Ann. Statist., 5, 637-640.

- Wahba, G., (1978a). Improper priors, spline smoothing and the problem of guarding against model errors in regression, University of Wisconsin-Madison, Department of Statistics Technical Report #508, to appear, J. Roy. Stat. Soc. B.
- Wahba, G., (1978b). Discussion to curve fitting and optimal design for prediction, A. O'Hagan, J. Roy. Stat. Soc. B., 40, 1, 1-42.
- Wahba, G., (1978c). Interpolating surfaces: High order convergence rates and their associated designs, with applications to X-ray image reconstruction, University of Wisconsin-Madison, Department of Statistics Technical Report #523, to appear, SIAM J. Numer. Anal..
- Wahba, G., and Wold, S., (1975). A completely automatic French curve: Fitting spline functions by cross-validation, Communications in Statistics, 4, 1, 1-17.
- Welch, J. (1979). Ph.D. dissertation, Dep't. of Chemical Engineering, University of Wisconsin, Madison, in preparation.

METHODOLOGY FOR ACCEPTANCE CRITERIA FOR TARGET
DISPERSION CHARACTERISTICS OF THE ARMOR PIERCING
DISCARDING SABOT (APDS) ROUNDS

Frank C. Hopkins
U. S. Army Materiel Systems Analysis Activity
Aberdeen Proving Ground, Maryland

ACRONYMS AND SYMBOLS

APDS	Armor Piercing Discarding Sabot
mm	Millimeter
OC	Operating Characteristics
PE	Probable Error
CPE_c	Characteristic Circular Probable Error
\hat{CPE}_c	Estimate of Characteristic Circular Probable Error
CPE_g	Level of Circular Probable Error which represents good lot quality
CPE_I	Inherent Circular Probable Error
CPE_L	Circular Probable Error which characterizes a lot
CPE_o	Observed Circular Probable Error
K	A Constant
λ	Ratio of CPE_o to CPE_c
n	Sample Size
N	Number of occasions
\hat{PE}	Estimate of Probable Error
σ^2	Population Variance
$\sigma_x^2, \sigma_y^2, \sigma_R^2$, etc.	Population Variance of a set of x, y and radial observations, etc.
$\hat{\sigma}^2$	Estimate of σ^2
$\hat{\sigma}_x^2, \hat{\sigma}_y^2, \hat{\sigma}_R^2$, etc.	Estimates of $\sigma_x^2, \sigma_y^2, \sigma_R^2$, etc.
S^2	Calculated variance of a sample
S_x^2, S_y^2, S_R^2 , etc.	Calculated variance of a set of x, y and radial observations, etc.

METHODOLOGY FOR ACCEPTANCE CRITERIA FOR TARGET DISPERSION CHARACTERISTICS OF THE ARMOR PIERCING DISCARDING SABOT (APDS) ROUNDS

1. INTRODUCTION

1.1 General

The estimation of target dispersion characteristics of Armor Piercing Discarding Sabot (APDS) ammunition in acceptance testing is accompanied by a number of difficulties. Test costs are high; therefore sample sizes are limited. Since dispersion patterns are subjected to relatively large variations, small sample sizes produce undesirable levels of inaccuracy in estimating dispersion characteristics. Control of test conditions throughout the test is limited to control of only a few factors such as tube aim point, cant, stability of the firing platform and tube condition, at the start of the test. Even with maximum possible control of such factors, they still exert a degree of error in round-to-round target impact points. In addition, there are several uncontrollable factors, such as wind and weather conditions, tube wear from round to round, droop, jump and other unknowns, which make it impossible to obtain uniform conditions throughout the test. These problems have accompanied every acceptance test conducted on APDS ammunition and have been exacerbated by two factors:

- o The lack of established test procedures designed to minimize the effects of uncontrollable test condition variations and
- o The lack of established acceptance criteria and estimation procedures designed to minimize consumer and producer risks.

The result has been that a large number of lots of APDS ammunition with very poor target dispersion characteristics have been accepted for use.

1.2 Purpose

This report develops methodology which can be used to derive acceptance plans for target dispersion characteristics of APDS rounds. In developing the methodology, the effect of test condition variations upon target dispersion patterns and the lack of established acceptance criteria and estimation procedures are addressed. Examples of inadequate firing procedures in accuracy tests of APDS rounds are presented, and corrective measures are proposed. Examples of acceptance criteria and estimation procedures which minimize consumer's and producer's risks are developed. Several acceptance plans, derived from the proposed methodology are presented.

2. TEST PROCEDURES

2.1 Background

The objective of an accuracy acceptance test of APDS rounds is to assess the dispersion pattern which characterizes a lot of ammunition and accept or reject the lot. The acceptance test requires firing a group of rounds at a vertical target some distance from the gun. The coordinates of the impact points of each round in the group are obtained, and estimates of the dispersion about the center of impact are determined.

When firing a group of rounds to assess dispersion characteristics, it is desirable to have identical test conditions for each round. In this manner, the differences in impact points of each round are the result only of inherent differences between the rounds. Inherent differences between rounds in a lot of APDS ammunition are due to chance variation within a stable pattern caused by manufacturing procedures and physical characteristics of the round and propelling charge. These inherent differences lead to different flight characteristics, and cause rounds to impact at different points on the target. If identical test conditions are obtained, the dispersion characteristics of the group of rounds fired reflect the degree of round-to-round uniformity in the manufacturing process and provide an estimate of quality control.

Unfortunately, test conditions from round to round are not identical. Gun elevation and deflection vary regardless of efforts to maintain a constant aim point. Weather conditions and other factors which effect accuracy also vary from round to round. Consequently, the dispersion pattern of a group of rounds on a target is not representative of the inherent round-to-round differences. The dispersion pattern consequently represents the combination of the inherent differences in rounds and the variability in test conditions from round to round.

2.2 Firing Procedures

The method of firing employed in an acceptance test of a lot of APDS ammunition must be conducted in a way that minimizes the effect of round-to-round variability in test conditions. In past acceptance tests, gun elevation and deflection settings have been controlled to a great extent, and severe weather conditions have been avoided. However, the method of firing in acceptance tests has not been one which minimized round-to-round variability in test conditions. The length of time required to fire a group of rounds has been as great as four hours. Test conditions such as tube droop, cant, ambient environmental conditions and other unknowns vary more over a long time interval than they do in a short one. Hence, as shown by an analysis of past acceptance tests of 105mm, APDS ammunition, a group of rounds fired over a long time period will tend to exhibit higher probable errors than would be observed over a short time period.

Figure 1 shows the accuracy results of an acceptance test of 105mm, APDS rounds conducted at Jefferson Proving Ground. Horizontal and vertical probable errors are presented as a function of time between rounds. The wind ranged from 2-10 knots and varied in direction from 140° to 180° during the course of the test. The probable errors for the entire 25 round group were calculated at 0.47 mils in the horizontal direction and at 0.29 mils in the vertical direction. Probable errors as a function of time between rounds were obtained by analyzing all combinations of two round groups in the test. The probable errors for each two round group were calculated and correlated with time between rounds fired. Although the trend in Figure 1 is linear, other shapes may be expected from the testing of other lots.

Figure 1 clearly illustrates that during an accuracy test the dispersion of impacts is greatly affected by the test conditions, which, in turn, vary with time.

The firing procedures employed in acceptance tests have not been designed to minimize the time over which a group of rounds is to be fired. In the past, as many as three different lots were often tested simultaneously, with rounds from each lot fired alternately, with reference rounds. The effect quadrupled the amount of time required to fire each test group of each lot. Consequently, the effect on dispersion due to variations in round-to-round test conditions, has been greater than that which could have been obtained if the time for firing each group were reduced.

In conducting an acceptance test, the individual groups of rounds from a test lot should be fired sequentially with no alternate firing of reference rounds or rounds from other test lots between rounds within a group. The time for firing each group of rounds can thus be minimized to the greatest extent possible. If reference rounds are to be fired, each group of reference rounds should be fired either before or after each group of test rounds. For example, if two ten round samples from a single lot are to be tested with fifteen reference rounds, the order of firing could be:

Five Reference Rounds

Ten Sample Rounds

Five Reference Rounds

Ten Sample Rounds

Five Reference Rounds

Estimates of probable errors for each group of rounds would then be calculated and pooled accordingly.

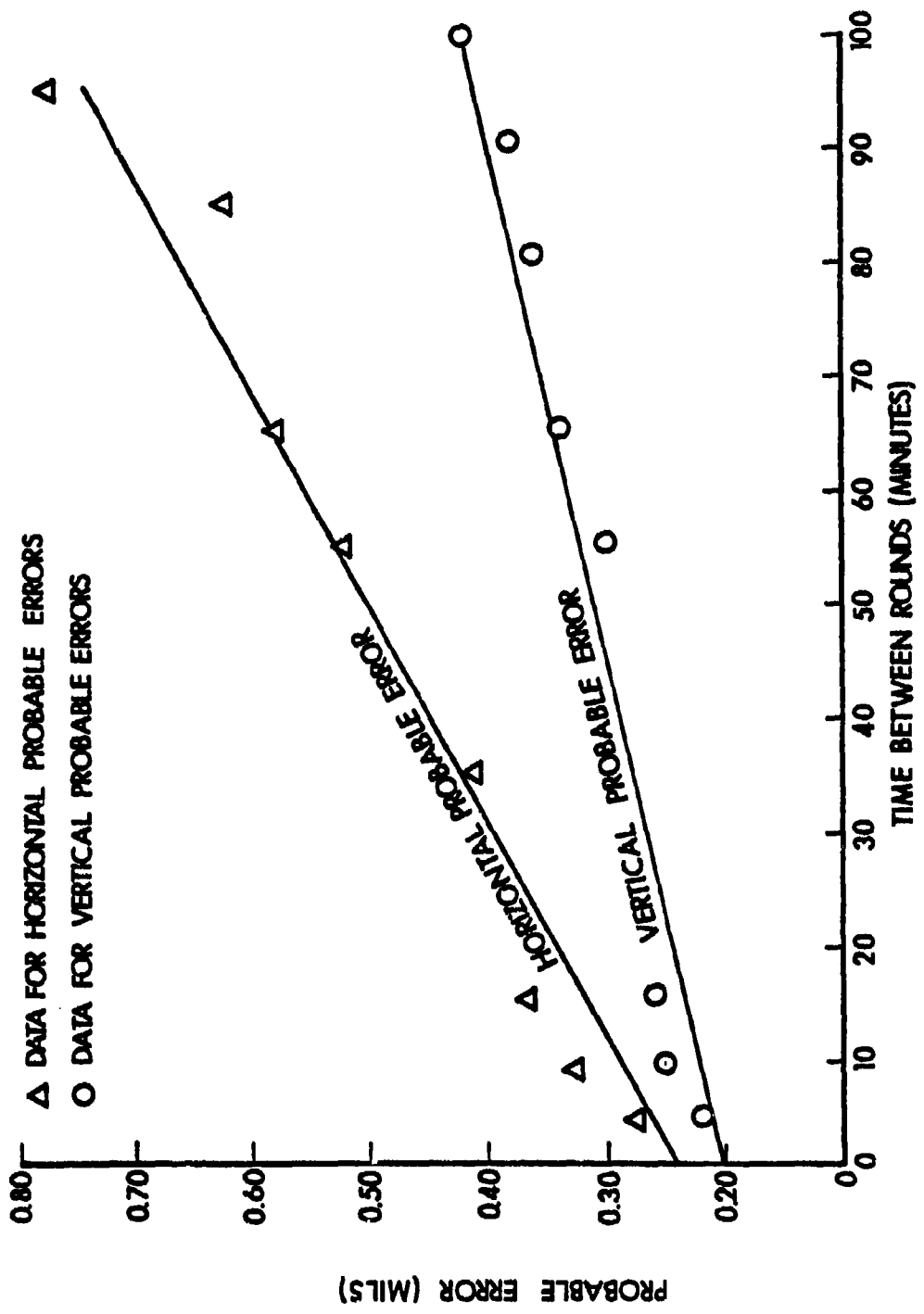


Figure 1. Probable Errors Observed During an Acceptance Test of a Single Lot of 105MM, M392, APDS as a Function of Time Between Rounds.

3. CALCULATION PROCEDURES

When a group of rounds is fired over a short time interval, the effect of nonuniform test conditions from round to round will still persist. Movement of the mean center of impact from round to round may occur, and, if so, the effect of this trend on calculated probable errors may be eliminated by the method of successive differences (Reference 1). For example, suppose the following impact coordinates, measured in inches, are obtained for a group of ten rounds fired at a vertical target 1000 meters from the gun:

<u>Round Number</u>	<u>Horizontal Coordinate (x)</u>	<u>Vertical Coordinate (y)</u>
1	65	110
2	70	120
3	60	115
4	75	100
5	70	105
6	85	95
7	80	90
8	95	95
9	90	85
10	100	75

Calculating probable errors in the usual manner for the entire ten-round group (References 2 and 3) yields,

$$\text{Horizontal probable error} = 0.23 \text{ mils}$$

$$\text{Vertical probable error} = 0.24 \text{ mils}$$

$$\text{Circular probable error} = 0.41 \text{ mils.}$$

Calculating probable errors using the method of successive differences yields,

$$\text{Horizontal probable error} = 0.13 \text{ mils}$$

$$\text{Vertical probable error} = 0.11 \text{ mils}$$

$$\text{Circular probable error} = 0.21 \text{ mils.}$$

The method of successive differences results in approximately a 50 percent reduction in probable error estimates in this particular example. The probable errors calculated by the standard method include the effects of test condition variability over the entire ten-round group, while the probable errors calculated by the method of successive

differences include only the test condition variability between successive rounds. Whenever the variation in test conditions is nonrandom, the result is a nonrandom dispersion pattern of shots about the center of impact. A trend of this type indicates that test condition variability over the entire group is greater than the variability between successive rounds. When this type of trend occurs, the use of the method of successive differences provides dispersion estimates which include only the effects of round-to-round test condition variability. In this manner, the effect of variability over the entire group is eliminated.

In determining the dispersion characteristics of a lot from a group of rounds, it is therefore desirable to limit the effect of test condition variability on the estimates of dispersion to that variability which occurs only between rounds.

It can be shown that the method of successive differences provides an unbiased estimate of the square of the probable error (PE). From statistical theory, an unbiased estimate of the variance (σ_x^2) in the x direction of a two-round sample is obtained by

$$\hat{\sigma}_x^2 = \frac{1}{2} (x_1 - x_2)^2, \text{ where}$$

x_1 and x_2 are the coordinates of impact on the x axis. If three rounds are fired and have coordinates of impact x_1 , x_2 and x_3 on the x axis,

$$S_{1x}^2 = \frac{1}{2} (x_1 - x_2)^2 \text{ and } S_{2x}^2 = \frac{1}{2} (x_2 - x_3)^2$$

provide two unbiased estimates of the variance, σ_x^2 . The sample variance calculated by the method of successive differences is $S_x^2 = 1/2 S_{1x}^2 + 1/2 S_{2x}^2$, and it is an unbiased estimate of σ_x^2 . Since

$$\begin{aligned} E(S_x^2) &= E(1/2 S_{1x}^2 + 1/2 S_{2x}^2) \\ &= E(1/2 S_{1x}^2) + E(1/2 S_{2x}^2) \\ &= 1/2 E(S_{1x}^2) + 1/2 E(S_{2x}^2) \\ &= \sigma_x^2/2 + \sigma_x'^2/2 \\ &= \sigma_x^2. \end{aligned}$$

Similarly, for a sample of size n

$$s_{1x}^2 = 1/2 (x_i - x_{i+1})^2, i = 1, 2, \dots, n-1.$$

Then $s_x^2 = \frac{1}{n-1} \sum_{i=1}^{n-1} s_{1x}^2$, the sample variance calculated by the method of successive differences, provides an unbiased estimate of σ_x^2 , because

$$\begin{aligned} E(s_x^2) &= E\left(\frac{1}{n-1} \sum_{i=1}^{n-1} s_{1x}^2\right) \\ &= \frac{1}{n-1} \sum_{i=1}^{n-1} E(s_{1x}^2) \\ &= \frac{1}{n-1} \sum_{i=1}^{n-1} \sigma_x^2 \\ &= \sigma_x^2. \end{aligned}$$

Since $(PE_x)^2 = K\sigma_x^2$,

where PE_x = probable error in the x direction and K is the appropriate constant,

$$E(\hat{PE}_x^2) = E(K\sigma_x^2) = K\sigma_x^2 = PE_x^2,$$

where $\hat{PE}_x^2 = K\sigma_x^2$ and $E(s_x^2) = \sigma_x^2$.

Hence, the method of successive differences gives an unbiased estimate of the square of the probable error between rounds in the x direction.

A similar proof shows that the method of successive differences also provides an unbiased estimate of the probable error squared between rounds in the y direction and also in the radial direction (circular probable error).

Consequently, the use of the method of successive differences provides unbiased estimates of the probable error squared and eliminates the effect of nonrandom test condition variation upon the dispersion results of an entire group of rounds.

Whenever the variation in test conditions is nonrandom and, thus, results in a dispersion pattern which is not random about the center of impact, the method of successive differences should be employed.

4. ACCEPTANCE CRITERIA

4.1 Applicable Parameters

In the development of acceptance criteria for dispersion characteristics of APDS rounds, parameters appropriate to an accept/reject decision must be selected. Horizontal and vertical probable errors could be the basis for a decision with independent criteria for each. This has the disadvantage, however, of not utilizing all available information. For example, the observed horizontal and vertical probable errors in a test could be 0.10 mils and 0.35 mils, respectively. The pooled average of these is 0.26 mils. If the reject criterion is to reject lots when either horizontal or vertical probable error is greater than 0.30 mils, this lot would be rejected. The problem with this type of accept/reject criteria is that it ignores good dispersion characteristics in one direction when dispersion in the other direction is poor.

Results of acceptance tests and life cycle evaluations of 105mm, M392, APDS rounds have shown that target dispersion patterns are approximately circular. In Reference 4, for example, horizontal and vertical probable errors were 0.19 mils and 0.21 mils, respectively for 803 rounds fired from a mid-life tube. Hence, the use of circular probable error, which effectively combines all dispersion information in both the horizontal and vertical directions, is appropriate. Use of this parameter simplifies the accept/reject criteria. Another advantage of using the circular probable error in estimating target dispersion rather than the present technique of computing independent horizontal and vertical probable errors, is that the sample size requirement is reduced significantly for the specified risk.

4.2 Distribution Of Circular Probable Errors

A lot has an inherent circular probable error, CPE_I , which describes its expected performance when random samples from the lot are fired under identical test conditions. If CPE_0 is the circular probable error observed for a random sample fired under identical test conditions, then

$$E(CPE_0) = CPE_I$$

Since circular probable error is a multiple of the radial standard deviation it follows that,

$$\frac{CPE_0^2}{CPE_I^2} = \frac{s_R^2}{c_R^2} .$$

where S_R is the observed radial standard deviation, and σ_R is the expected radial standard deviation for a random sample fired under identical conditions.

The distribution of $\frac{2(n-1)CPE_0^2}{CPE_I^2}$ will therefore be Chi-square, with $2(n-1)$ degrees of freedom for a random sample of size n fired under identical test conditions.

Identical conditions from round to round are not attainable during testing, however. Therefore, $\frac{CPE_0^2}{CPE_I^2}$ will not have a Chi-square distribution during tests. In fact, CPE_I cannot be adequately estimated from test results, since the effects of round-to-round variability in test conditions will always be included in circular probable error estimates.

To develop acceptance criteria for APDS rounds, it is necessary to know the form of the distribution of CPE_0 . It is also necessary to estimate a circular probable error, characterizing a lot, which can be determined from test data.

During acceptance testing, the effect of variation in test conditions from round to round on circular probable error estimates will vary from one occasion to another. On some days, test condition variability has little effect on dispersion patterns, while on other days, the effect of variable test conditions is comparatively large. Obviously, measurements which characterize a lot or its expected dispersion should not be based on days when test condition variability is unusually small or large. The measurement which adequately characterizes the performance of a lot should be based on the outcome expected on a randomly selected day, given that the day satisfies the meteorological requirement for conducting an acceptance test.

To define characteristic circular probable error, i.e., the probable error which is expected from a lot on a random day, we assume that a lot of infinite size is available. Let N random samples be selected from the lot and let each sample be tested on a random day. Let CPE_C denote the characteristic circular probable error of the lot. Then,

$$CPE_C = \lim_{N \rightarrow \infty} \left[\frac{1}{N} \sum_{i=1}^N (CPE_0^2)_i \right]^{1/2}$$

defines the characteristic circular probable error of the lot. In the above equation, $(CPE_0^2)_i$, is the square of the circular probable error observed on the i^{th} occasion. Since $\lim_{N \rightarrow \infty} \left[\frac{1}{N} \sum_{i=1}^N (CPE_0^2)_i \right]^{1/2}$ equals the expected value of the observed circular probable error on a randomly selected day, it is clear that CPE_C adequately defines the performance of the lot.

On some days, $E(CPE_0) \neq CPE_C$, since variability in test conditions such as wind and weather, tube wear from round to round, droop, jump, etc., may be unusually large or small. Suppose conditions on a given day are such that $E(CPE_0) = CPE_C$ for the random samples fired on that day. Call this an average day.

Now, looking only at tests conducted on average days (days for which $E(CPE_0) = CPE_C$), there is a characteristic radial standard deviation, σ_C , which describes the dispersion characteristics of the lot. Since circular probable error is a multiple of radial standard deviation, then,

$$\frac{CPE_0^2}{CPE_C^2} = \frac{s^2}{\sigma_C^2},$$

where CPE_0 is the circular probable error observed for a random sample tested on an average day, and s^2 is the estimate of the variance. The distribution of $\frac{2(n-1)}{CPE_C^2} CPE_0^2$ will therefore be Chi-square with $2(n-1)$ degrees of freedom for a random sample of size n tested on an average day.

Acceptance tests, however, are not usually conducted on average days, and

$$\frac{CPE_0^2}{CPE_C^2}$$

has in actuality greater variability than that predicted by the Chi-square distribution. To assess how this ratio varies during acceptance tests, the dispersion results of 176 groups of 105mm, APDS, M392 reference

rounds were analyzed. Eight of these groups had target misses and were excluded from further analysis. The remaining groups were tested on 168 different days over a twelve year period. Each group consisted of a ten round sample from one of two reference lots, and was fired at a target 2000 meters from the gun. There was no significant difference in the distribution of circular probable errors of each reference lot and results from the two lots were therefore combined. The estimate of the characteristic circular probable error of the reference lots, \hat{CPE}_C , was obtained from the following equation.

$$\hat{CPE}_C = \left[\frac{1}{168} \sum_{i=1}^{168} (CPE_0^2)_i \right]^{1/2},$$

where $(CPE_0^2)_i$ was the square of the circular probable error observed on the i^{th} occasion.

In order to facilitate the analysis, $\frac{CPE_0}{\hat{CPE}_C}$ was defined to be λ_i .

Assuming that CPE_C for the 168 reference groups was equal to the characteristic circular probable error of the reference lot, then

$$\lambda_i = \frac{CPE_0}{\hat{CPE}_C}.$$

For each of the 168 groups, λ_i was determined and the observed cumulative distribution of the λ_i 's was plotted. Figure 2 presents the observed cumulative distribution of λ_i and compares it to the cumulative distribution which would result if λ_i^2 were distributed as a Chi-square with 18 degrees of freedom.

From Figure 2, it is evident that if $2(n-1)\lambda_i^2$ were distributed as a Chi-square distribution with 18 degrees of freedom, 80 percent of the observations would be between 0.78 and 1.20. The observed cumulative distribution of the λ_i 's, however, shows that 80 percent of the observations were between 0.46 and 1.44, a considerably wider spread than that predicted by the Chi-square.

The Gamma distribution of the form $\text{Gamma}(X) = \frac{x^{\alpha-1}}{(\alpha-1)! \beta^\alpha} e^{-\frac{x}{\beta}}$ was fitted to the observed λ_i 's. With $\alpha = 7.4558$ and $\beta = 0.7261$, the Gamma distribution fits the data very well. The Chi-square, Cramer-Von Mises and Kolmogorov-Smirnov goodness of fit tests gave no reason to reject the Gamma distribution. A summary of the observed λ_i 's and of the fitted Gamma distribution are presented in Figure 3. Each data

point, denoted by a triangle, represents the number of observations within an interval of length 0.10. Points from the Gamma distribution were multiplied by 16.8 so that the data and fitted curve could be shown on the same scale. In Figure 4, the cumulative Gamma distribution is compared with the observed cumulative distribution of the λ_i 's. The data points, denoted by triangles, represent the observed cumulative probability that $\lambda_1 \leq \lambda$.

4.3 Criteria For Acceptance Plans

Assuming that λ follows the Gamma distribution with $a = 7.4558$ and $s = 0.1261$ for random samples of size 10, acceptance plans can be derived with various levels of consumer's risks (probability of accepting a lot with poor quality) and producer's risks (probability of rejecting a lot with good quality). The limitation of using this Gamma distribution is that it can only be used to calculate consumer's and producer's risks for acceptance plans with sample sizes which are multiples of ten. Derivations of distributions applicable to sample sizes other than multiples of ten are beyond the scope of this report. To develop an acceptance plan, it is necessary to specify the levels of characteristic circular probable errors associated with both good and poor quality. The sampling procedures and associated decision criteria must then be designated. Once this is done, the Gamma distribution can be used to derive the operating characteristics (OC), i.e., the probability of accepting a lot with a specified quality, associated with the plan. Comparisons of the OC of various plans can also be made, and the best plan can thereby be determined.

4.4 Development of Acceptance Plans

To develop the acceptance plans, CPE_g is defined as the level of circular probable error which represents good quality of a lot. Poor lot quality can be characterized by any multiple of CPE_g , as long as the multiple is greater than one. In order to develop examples of acceptance plans it is assumed in this report that poor quality is characterized by values of circular probable error greater than $2 CPE_g$. One possible acceptance plan is to test a ten round random sample from a lot and to calculate the observed circular probable error, CPE_0 , and then, decide to accept or reject the lot. One set of decision criteria includes accepting the lot, if $CPE_0 < 1.2 CPE_g$ or rejecting the lot, if $CPE_0 \geq 1.2 CPE_g$. This plan will be designated as Acceptance Plan A. Given a circular probable error, CPE_L , which characterizes the lot, $\frac{CPE_0}{CPE_L}$ is distributed as the Gamma distribution discussed in section 4.2, provided CPE_L is not very different from the pooled circular probable

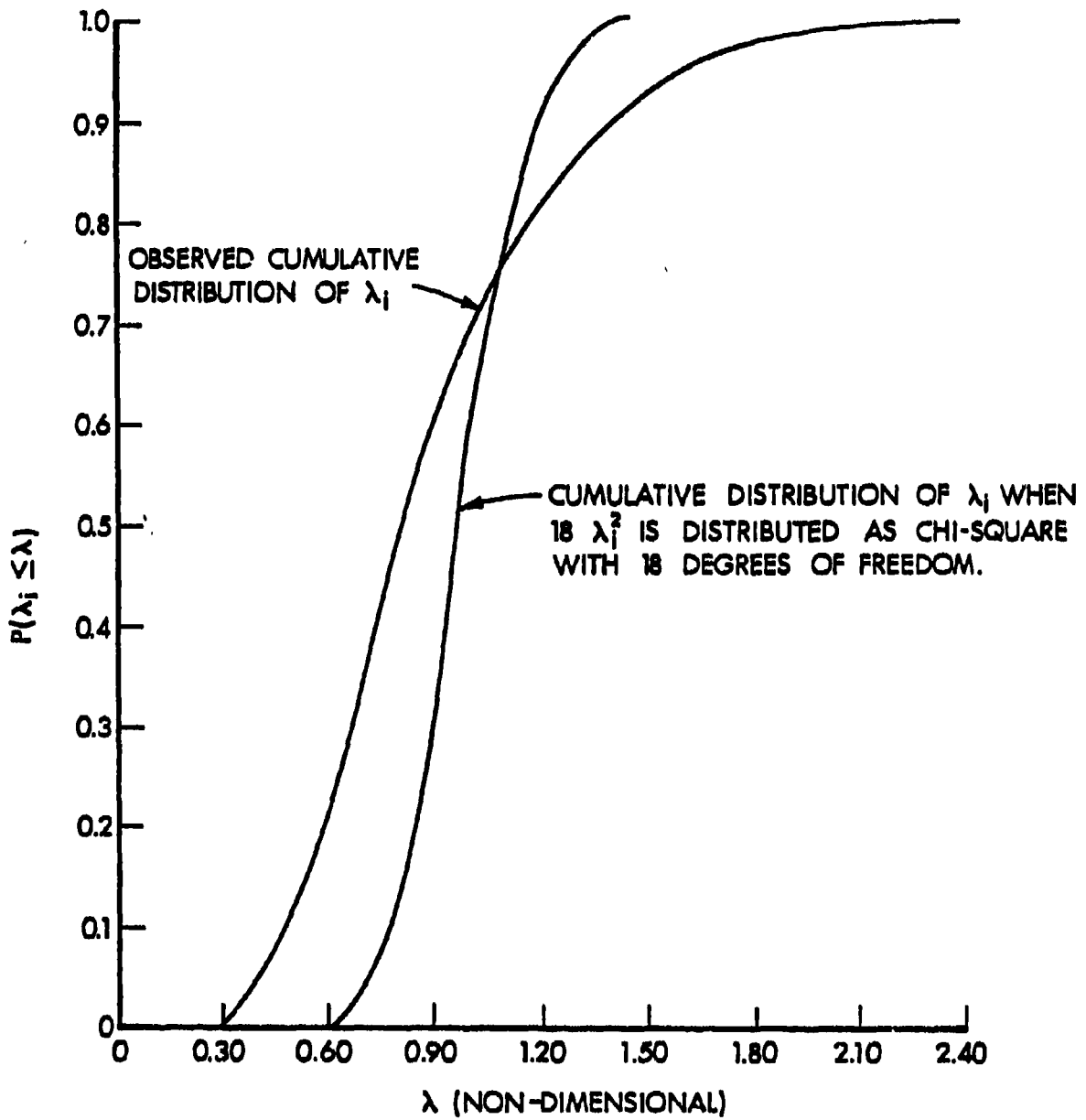


Figure 2. Cumulative Observed Distribution of λ_i 's Compared With That Predicted When $18 \lambda_i^2$ is Distributed as Chi-Square With 18 Degrees of Freedom.

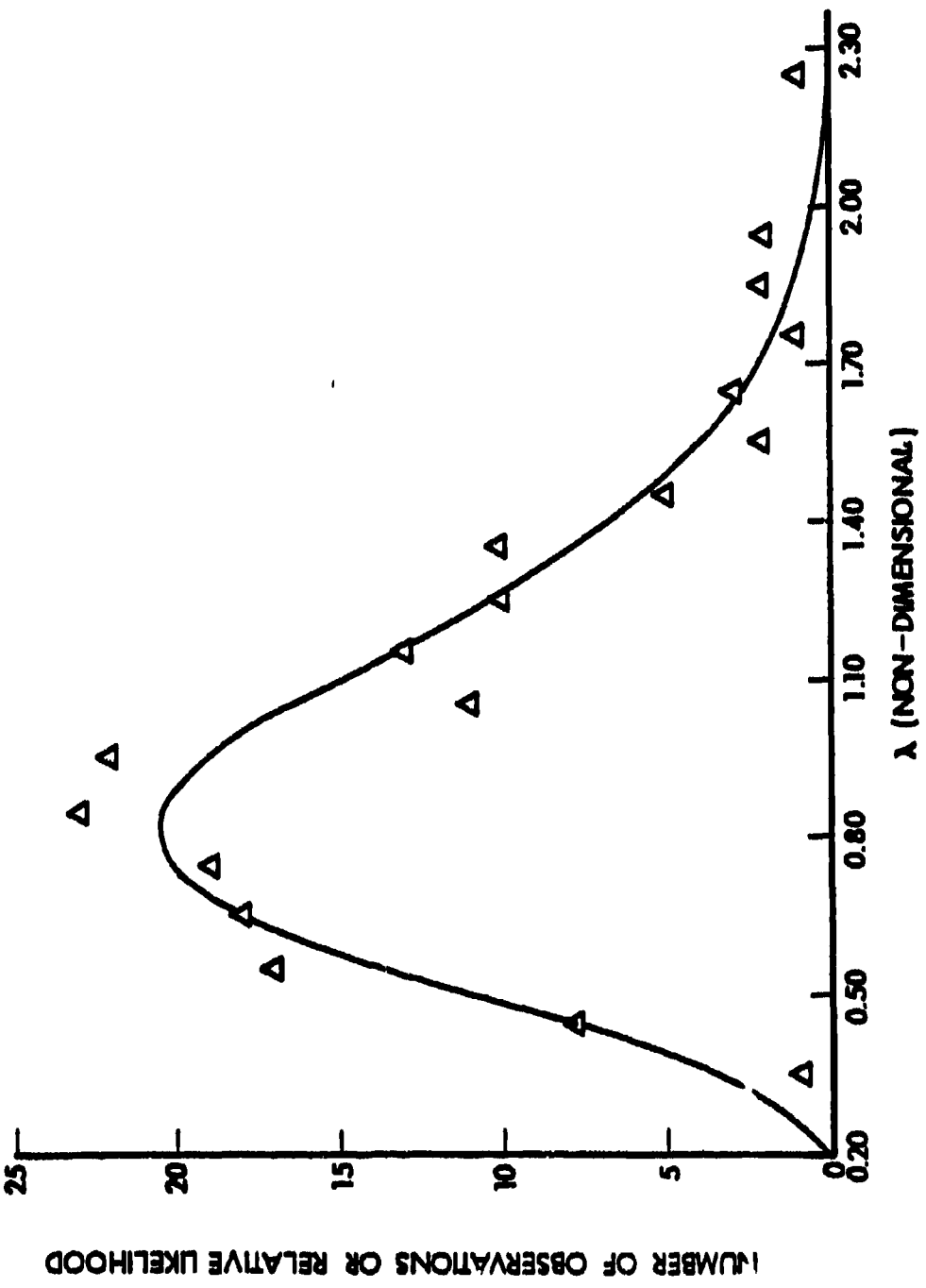


Figure 3. Gamma Distribution fitted to the Observed λ_i 's.

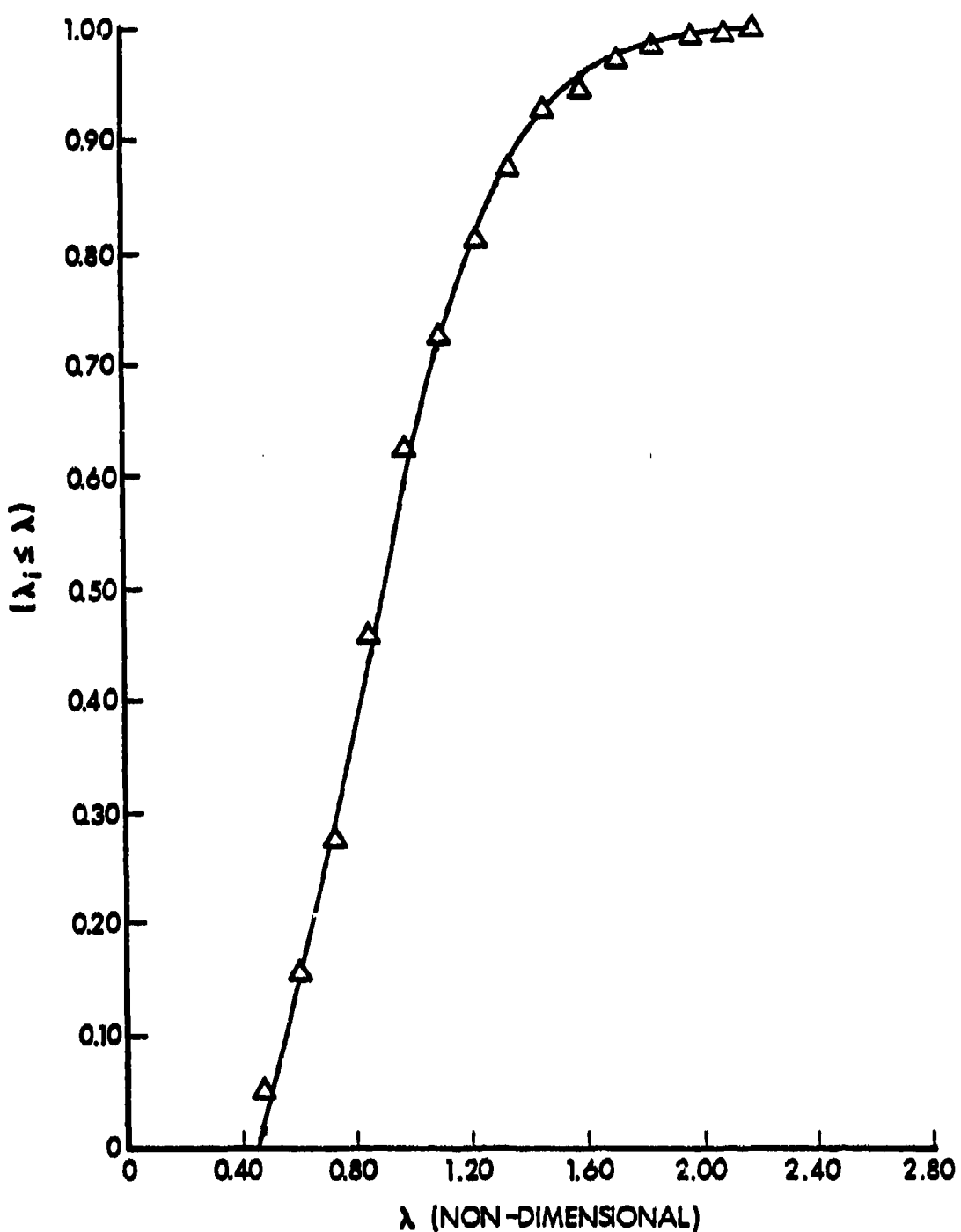


Figure 4. Cumulative Gamma Distribution Fitted to the Observed λ_i 's.

error of the 168 reference round groups. Further discussion of this point is presented later in this section. For now, it is assumed that CPE_0 is distributed as the Gamma distribution of section 4.2.

To derive the consumer's and producer's risks associated with this plan, first assume that $CPE_L = CPE_G$. Then, based on the cumulative Gamma distribution of Figure 4,

$$P(A/CPE_L = CPE_G) = P(CPE_0 < 1.2 CPE_L) = 0.80.$$

Based on the cumulative distribution of λ_1 when λ_1^2 is distributed as Chi-square with 18 degrees of freedom (Figure 2), the probability of accepting the lot, $P(A)$, is 0.90. Assuming that $CPE_L = 2CPE_G$, then based on the Gamma distribution, $P(A/CPE_L = 2CPE_G) = (PCPE_0 < 0.6 CPE_L) = 0.16$. Using the Chi-square of Figure 4, $P(A/CPE_L = 2CPE_G) = 0.00$. The consumer's and producer's risks for this plan are summarized in Table 1.

Table 1. Consumer's and Producer's Risk for Acceptance Plan A

Distribution Used	Consumer's Risk	Producer's Risk
Gamma	0.16	0.20
Chi-square	0.00	0.10

As noted in Table 1, the Gamma derived consumer's risk for Acceptance Plan A is 0.16 compared with the consumer's risk of 0.00 predicted by the Chi-square distribution. Thus, use of the Chi-square distribution for obtaining the consumer's risk for this plan would mislead one into thinking that Plan A is very good with respect to the consumer's risk, while the Gamma distribution shows that it is not.

Figure 5 presents the OC curves for Plan A based on the Gamma and Chi-square distributions. Note that the OC curve derived from the Chi-square distribution crosses the Gamma derived OC curve at the point where $CPE_L = 1.12 CPE_g$. When $CPE_L < 1.12 CPE_g$, the Chi-square derived OC curve overestimates the probability of acceptance the lot, misleading the manufacturer into believing that this risk is smaller than it actually is. When $CPE_L > 1.12 CPE_g$, the Chi-square derived OC curve underestimates the probability of accepting the lot. Therefore, for lots with poor circular probable error characteristics ($CPE_L > 2CPE_g$), the Chi-square derived OC curve misleads the consumer into believing that his risk is smaller than it actually is.

In Table 2 several acceptance plans are presented. It should be noted that these plans represent only a finite subset of an infinite set of acceptance plan strategies.

Table 2. Acceptance Plan Alternatives B Through H Based On Multiples Of Ten Round Samples

<u>Acceptance Plan Designation</u>	<u>Description of Acceptance Plan</u>
B	Test a single ten round random sample from a lot. Accept the lot if $CPE_0 < 1.4 CPE_g$. Otherwise reject the lot.
C	Test a single ten round random sample from a lot. Accept the lot if $CPE_0 < 1.6 CPE_g$. Otherwise reject the lot.
D	Test a single ten round random sample from a lot. Accept the lot if $CPE_0 < 1.8 CPE_g$. Otherwise reject the lot.
E	Test two ten round random samples from a lot. If the pooled $CPE_0 < 1.4 CPE_g$, accept the lot. Otherwise reject the lot.
F	Test a ten round random sample from a lot. Accept the lot if $CPE_0 < 1.4 CPE_g$. Reject the lot if $CPE_0 > 1.8 CPE_g$. Otherwise, test a second ten round random sample. Then, accept the lot if the pooled $CPE_0 < 1.4 CPE_g$. If the pooled $CPE_0 \geq 1.4 CPE_g$, reject the lot.
G	Test a ten round random sample from a lot. Accept the lot if $CPE_0 < 1.2 CPE_g$. Reject the lot if $CPE_0 > 1.54 CPE_g$. Otherwise, test a second ten round random sample. Then, accept the lot if the pooled $CPE_0 < 1.2 CPE_g$. If the pooled $CPE_0 \geq 1.2 CPE_g$, reject the lot.
H	Test a ten round random sample from a lot. Accept the lot if $CPE_0 < 1.6 CPE_g$. Reject the lot if $CPE_0 > 2.0 CPE_g$. Otherwise, test a second ten round random sample. Then, accept the lot if the pooled $CPE_0 < 1.6 CPE_g$. If the pooled $CPE_0 \geq 1.6 CPE_g$, reject the lot.

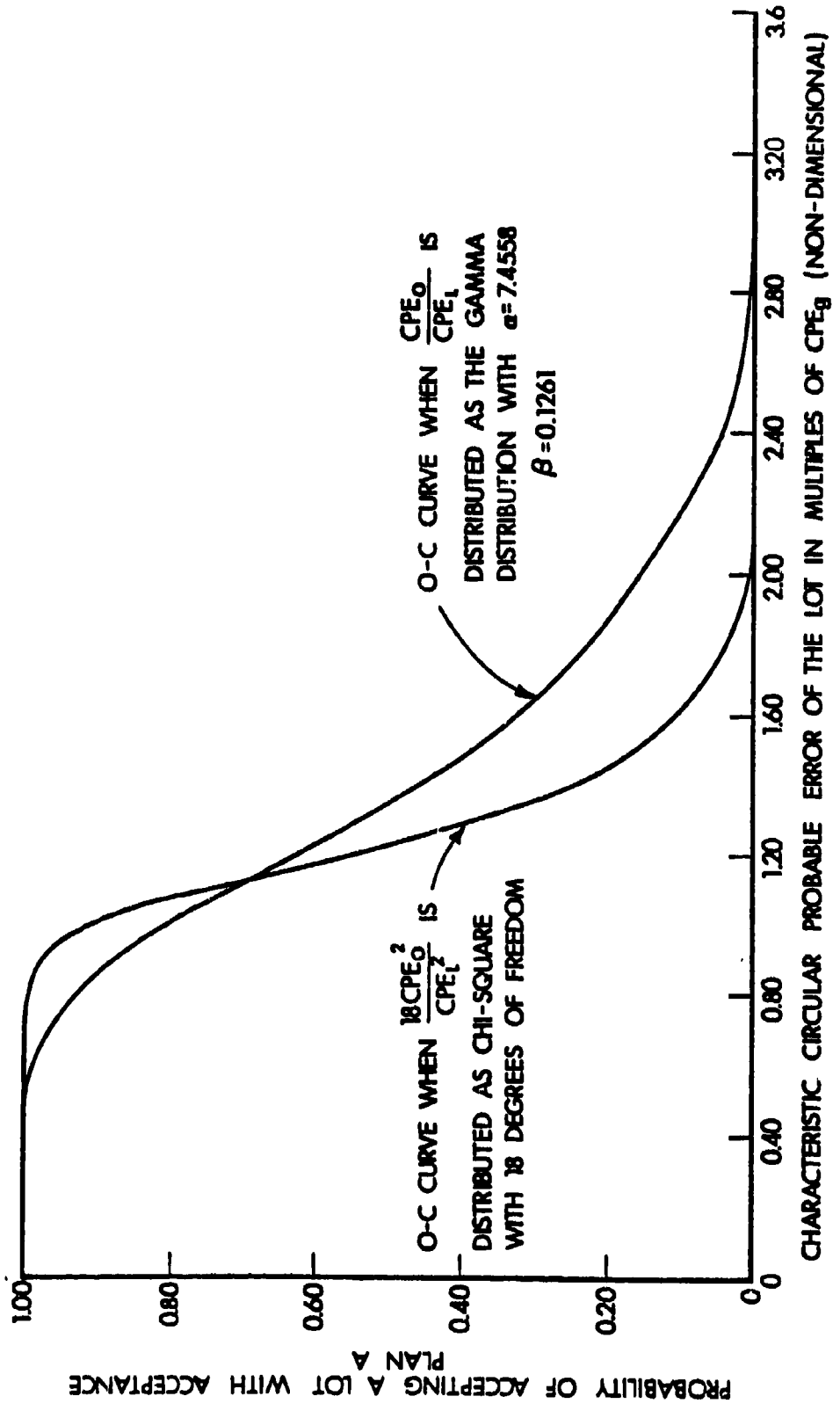


Figure 5. Operating Characteristics of Acceptance Plan A.

Figures 6 through 12 present the OC curves for acceptance plans B through H described in Table 2. In each figure, the consumer's risk is determined from the probability of accepting the lot when $CPE_L = 2CPE_g$. When $CPE_L = CPE_g$, the producer's risk is given by $1-P(A)$, where $P(A)$ is the probability of accepting the lot. The OC curves for all of the plans show that the Chi-square derived consumer's and producer's risks are lower than those derived from the Gamma distribution.

Table 3 summarizes the consumer's and producer's risk for acceptance plans A through H. The consumer's risks are presented as ranges. The lower bound in each case is obtained from the Chi-square derived OC curve, while the upper bound is obtained from the Gamma derived OC curve. The producer's risks are presented as point estimates and are obtained from the Gamma derived OC curves.

Table 3. Consumer's and Producer's Risks for Acceptance Plans A Through H

Acceptance Plan Designation	Consumer's Risk	Producer's Risk
A	0.00 - 0.16	0.20
B	0.04 - 0.25	0.10
C	0.14 - 0.40	0.13
D	0.32 - 0.50	0.07
E	0.00 - 0.09	0.07
F	0.03 - 0.28	0.04
G	0.00 - 0.16	0.11
H	0.17 - 0.55	0.02

It was previously assumed that $\frac{CPE_0}{CPE_L}$ would be distributed as the Gamma distribution with $\alpha = 7.4558$ and $\beta = 0.1261$. If CPE_L equals the characteristic circular probable error of the reference lot used to obtain the fitted Gamma distribution, the assumption is reasonable. The Gamma distribution was obtained from the actual distribution of observed circular probable errors over a twelve year period. It is reasonable to assume that this is representative of the distribution which will occur in the future. However, as CPE_L deviates from the characteristic circular probable error of the reference lots, the distribution of CPE_0 deviates from the Gamma distribution. The derived Gamma distribution represents the deviation in observed circular probable errors due to both inherent round-to-round differences and occasion-to-occasion test condition differences. As inherent round-to-round differences increase, which is the case for poor quality control during manufacturing, they tend to have an increasingly dominating effect on the distribution of CPE_0 relative

to the effect of occasion-to-occasion test condition variation. As the inherent differences increase without bound, the relative effect of occasion-to-occasion variation in test conditions upon CPE_0 tends towards

zero, and the distribution of $\frac{CPE_0^2}{CPE_L^2}$ approaches the Chi-square. On the

other hand, as inherent round-to-round differences decrease, the scatter of observed probable errors is increasingly dominated by the effect of

test condition variation, and $\frac{CPE_0}{CPE_L}$ will tend to have greater variation

than that predicted by the Gamma distribution. Consequently, as CPE_L increases towards poor lot quality, the true probability of accepting the lot lies somewhere between the probabilities obtained from the Chi-square and Gamma derived OC curves as shown in Figures 5 through 12. As CPE_L improves beyond good lot quality, the probability of accepting the lot decreases below that predicted by the Gamma derived OC curve. For these reasons, the consumer's risks in Table 3 are presented as ranges, with the Chi-square and Gamma derived risks being the lower and upper bounds, respectively. The producer's risk, since it is based upon lots of good quality, is presented as a point estimate based upon the Gamma derived OC curve. If CPE_g is approximately equal to the

characteristic circular probable error of the reference rounds, the Gamma derived risk is a reasonably good estimate of the producer's risk. However, if CPE_g is better than the characteristic circular probable error of the reference rounds, the Gamma derived producer's risk is a lower bound. This could happen if future APDS rounds are markedly more accurate than the reference rounds.

Reviewing the acceptance plans in Table 3, it is evident that Plan E provides the best combination of consumer's and producer's risks. However, twenty rounds are always needed for this plan. Plan G is the next best plan and is less costly than Plan E. If lots are produced with CPE_L equal to CPE_g , the average sample size for this plan is 11.5. This is due to the fact that retests would occur only 15 percent of the time.

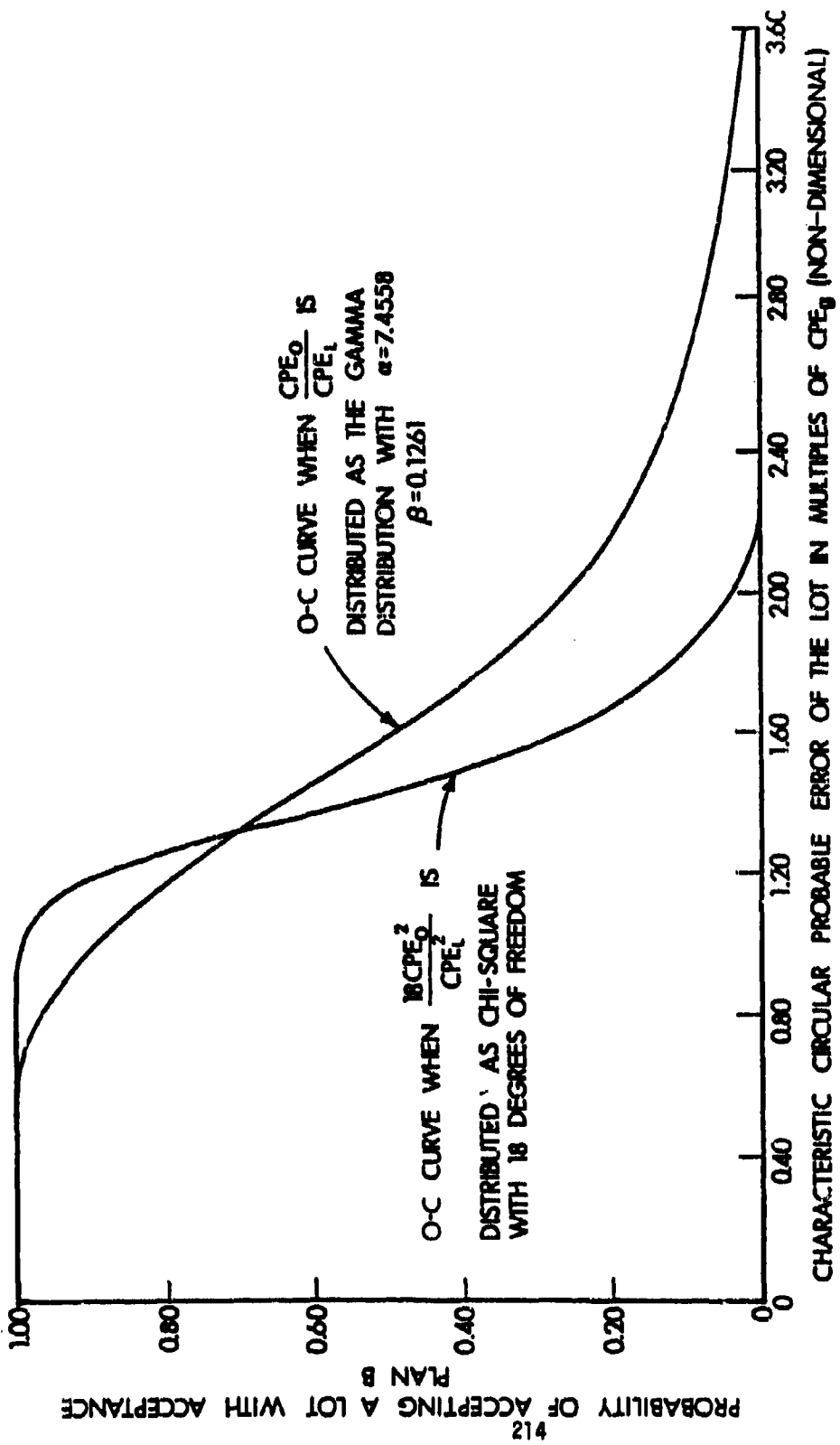


Figure 6. Operating Characteristic of Acceptance Plan B.

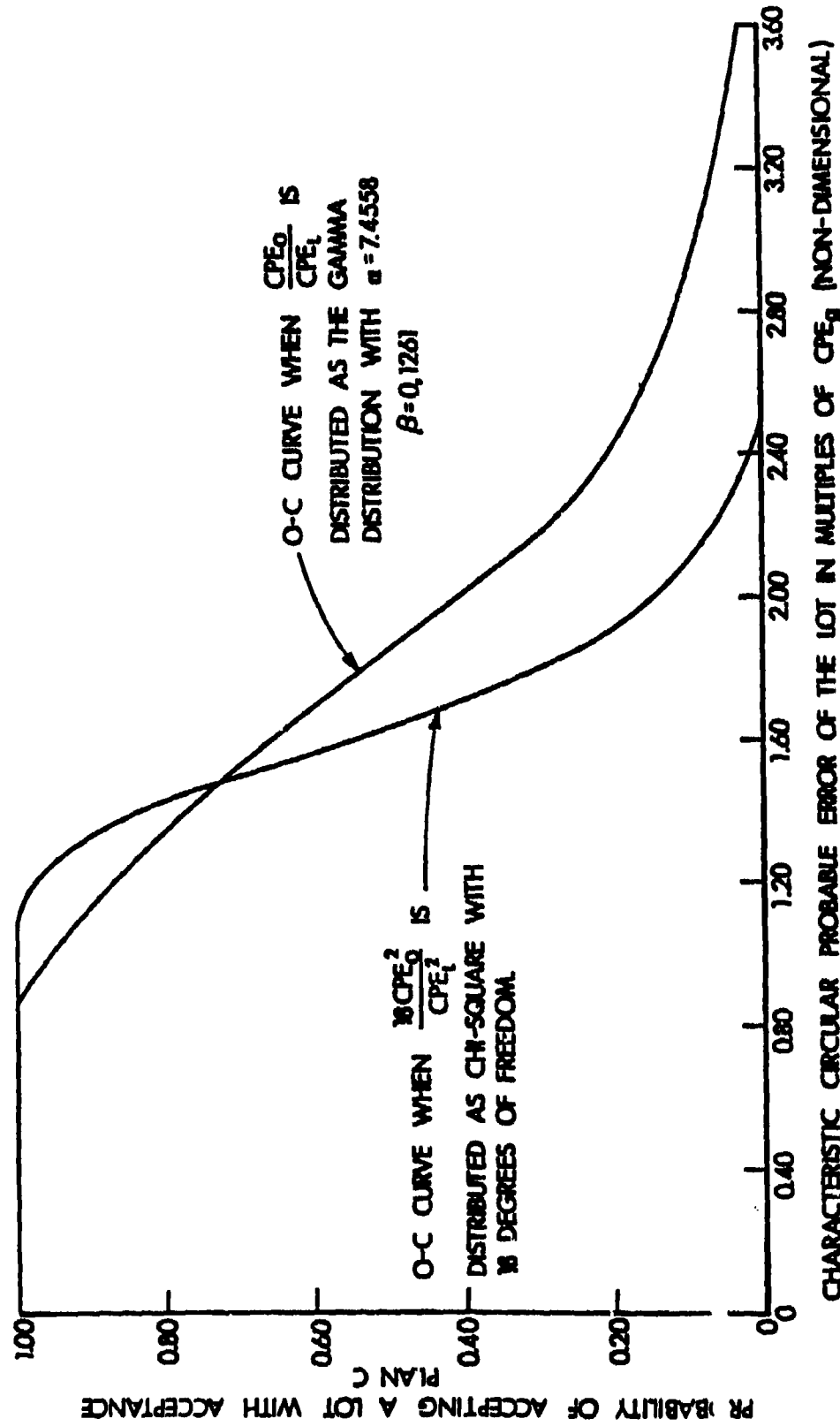


Figure 7. Operating Characteristic of Acceptance Plan C.

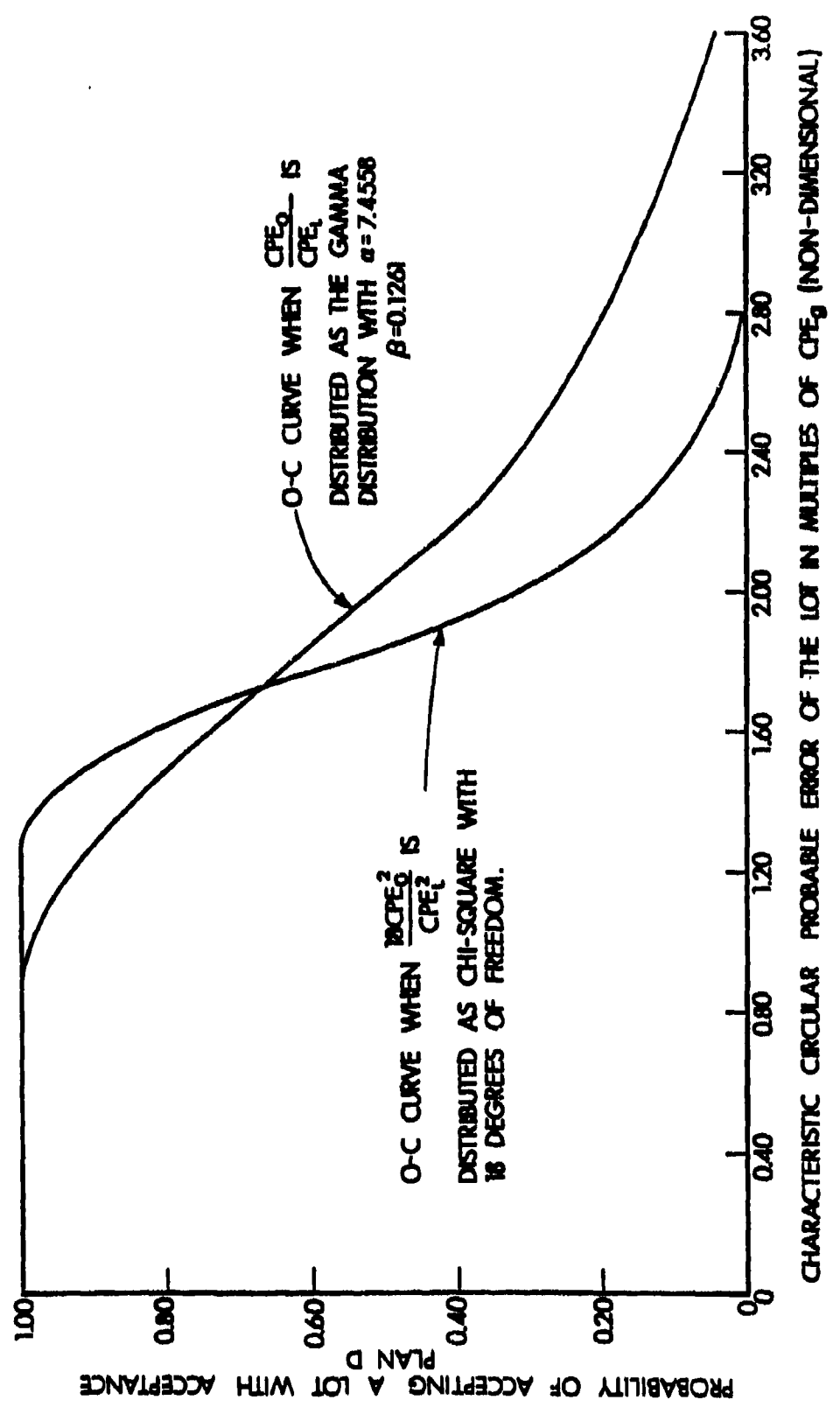


Figure 8. Operating Characteristic of Acceptance Plan D.

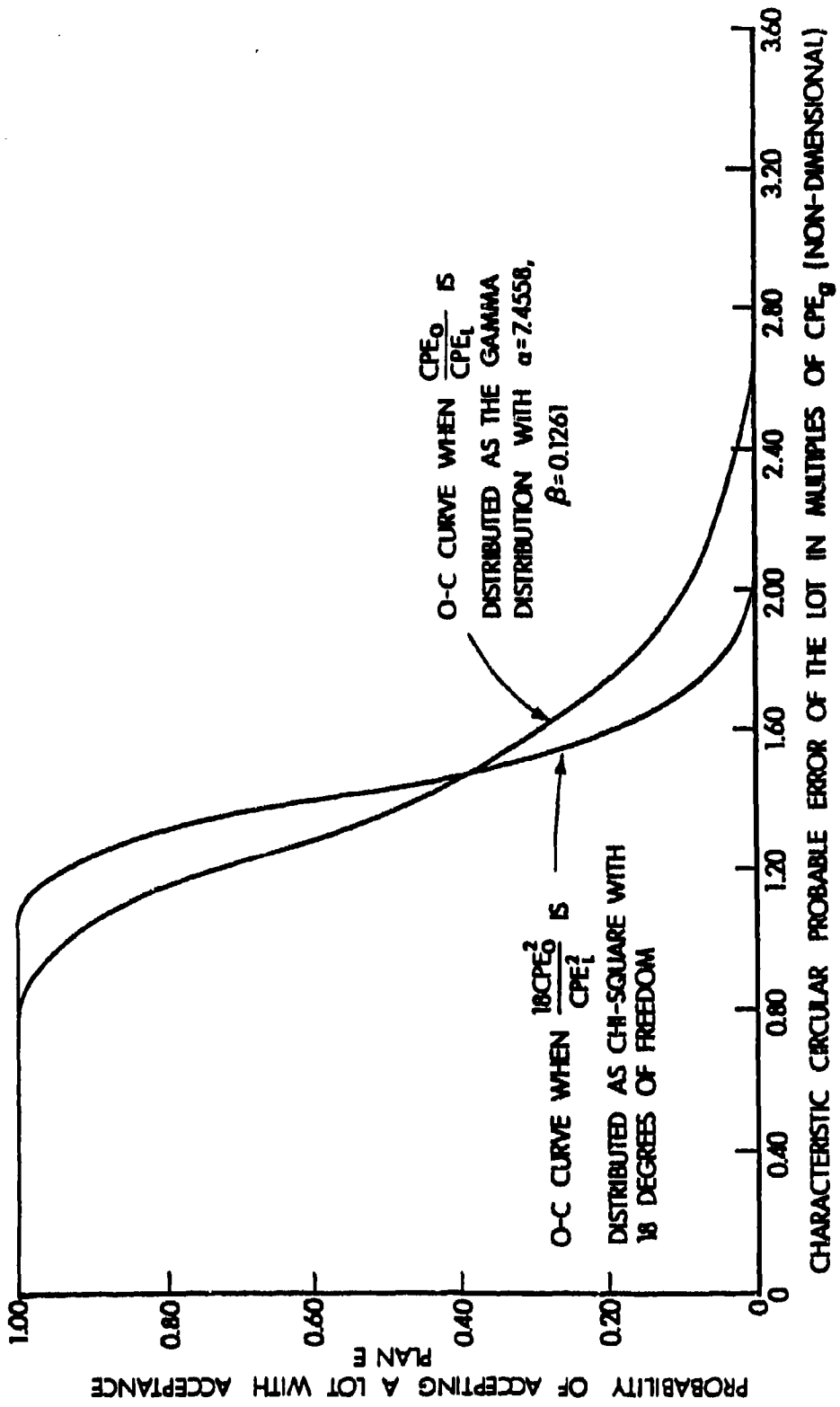


Figure 9. Operating Characteristics of Acceptance Plan E.

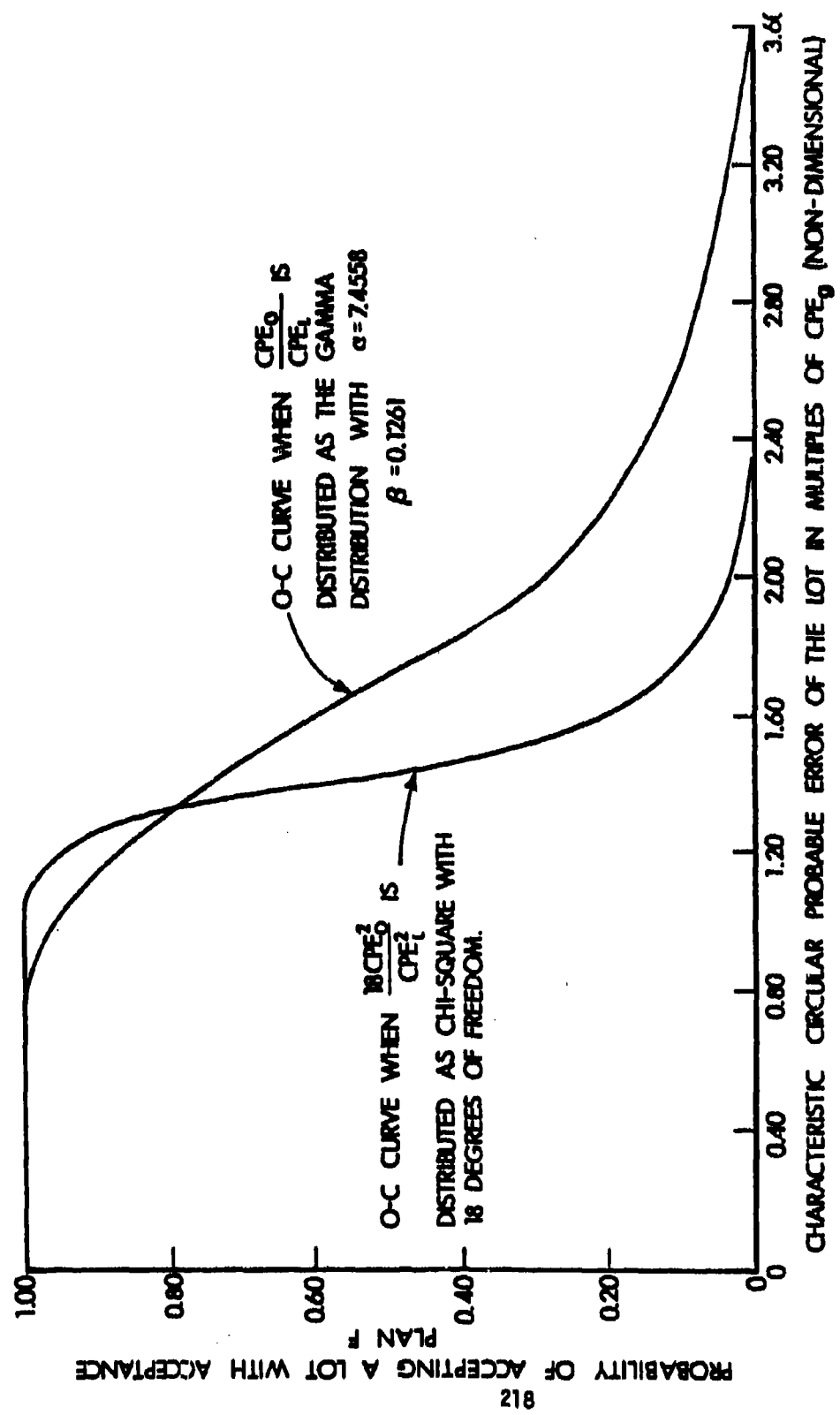


Figure 10. Operating Characteristics of Acceptance Plan F.

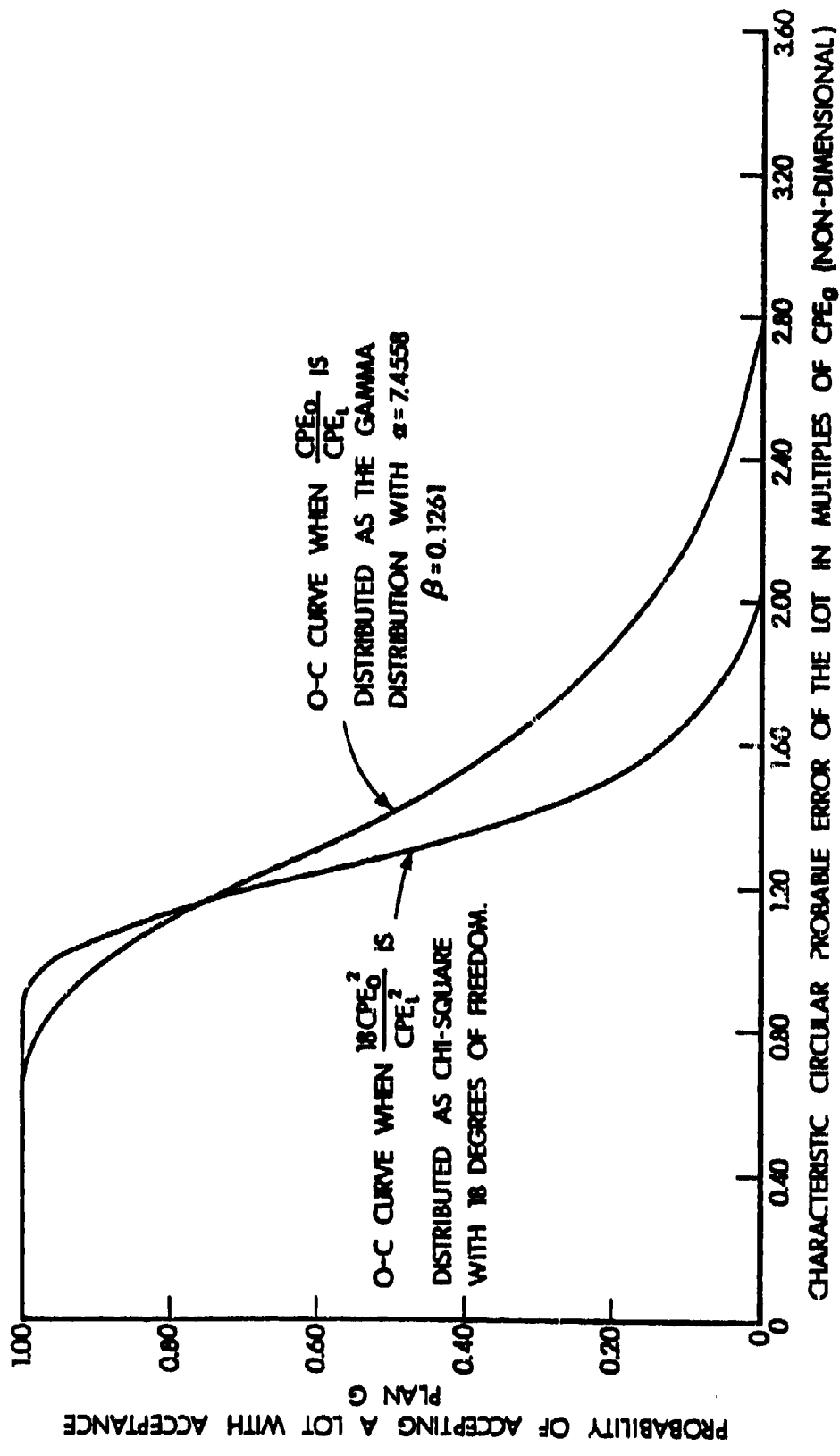


Figure 11. Operating Characteristics of Acceptance Plan G.

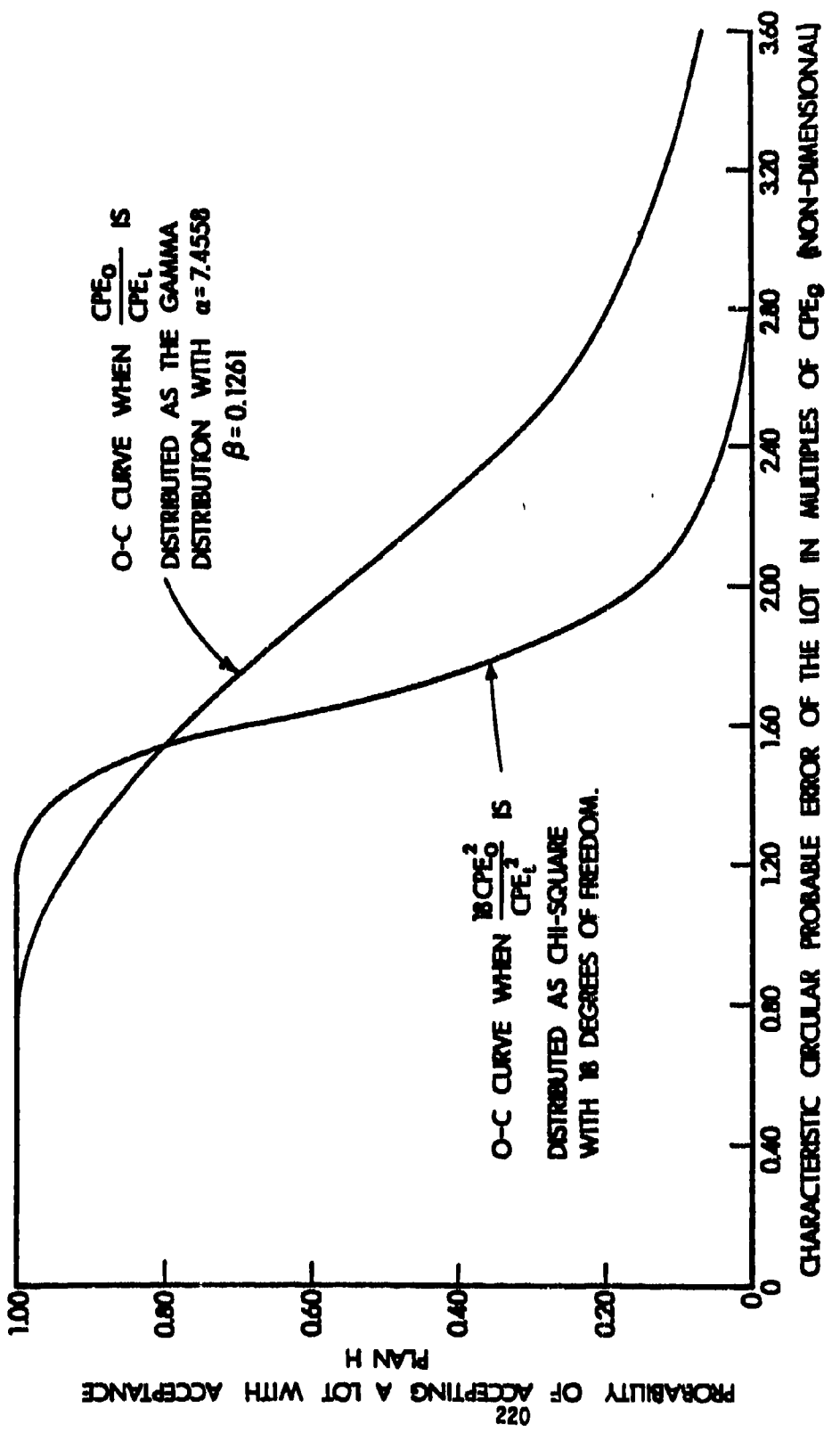


Figure 12. Operating Characteristics of Acceptance Plan H.

5. CONCLUSIONS AND RECOMMENDATIONS

In past acceptance tests, firing procedures have not been designed to minimize the effect of occasion-to-occasion variability in test conditions upon target dispersion characteristics. Future tests should be designed to minimize the time required to fire a group of rounds (see Section 2.2 for a detailed discussion).

Even when the time to fire a group of rounds is minimized, nonrandom dispersion patterns about the center of impact can occur. In this case the method of successive differences eliminates the effect of nonrandom trends on probable error estimates. This method of calculating probable errors should be employed whenever nonrandom trends in shot patterns occur (see Section 3 for a detailed discussion).

Decision criteria for acceptance plans, which are based on the use of circular probable error estimates, provide the optimum utilization of test data. Circular probable error estimates should therefore be used as the basis for decision criteria in future acceptance plans (see Section 4.1 for a detailed discussion).

The distribution of $\frac{CPE_0^2}{CPE_L^2}$ has not followed the Chi-square distribution

in the past. The ratio of observed circular probable error to the characteristic circular probable error of the two reference lots followed a Gamma distribution with $\alpha = 7.4558$ and $\beta = 0.1261$. This distribution was used to obtain the consumer's and producer's risks for several acceptance plans. These risks were then compared with the

corresponding consumer's and producer's risks obtained when $\frac{CPE_0^2}{CPE_L^2}$

follows the Chi-square distribution. It was shown that the actual consumer's risk of accepting poor lots is greater than the Chi-square derived risk and less than the Gamma derived risk. It was also shown that the Gamma derived producer's risk will provide a lower bound if the dispersion characteristics of future APDS rounds are superior to those of the reference rounds used in obtaining the Gamma distribution. From Table 3, it was evident that acceptance plan E provided the best combination of consumer's and producer's risks (see Section 4 for a detailed discussion).

The acceptance plans presented in this report represent only a small portion of the plans which could be developed for APDS type of ammunition. Undoubtedly it will be necessary to develop different acceptance plans for new types of APDS rounds undergoing development. These plans should be developed with recognition that the OC curves underestimate both the

consumer's and producer's risks, assuming that $\frac{CPE^2}{CPE_L^2}$ follows the Chi-square distribution.

distribution. The gamma distribution should be used for developing OC curves for the various plans. The consumer's and producer's risks associated with each plan can be compared and the best plan can then be selected (see Section 4.3 for a detailed discussion).

REFERENCES

1. Morse, Anthony P. and Grubbs, Frank E., "The Estimation of Dispersion From Differences," The Annals of Mathematical Statistics, Vol XVIII, No. 2., June 1947.
2. Groves, Arthur, "Handbook on the Use of the Bivariate Normal Distribution in Describing Weapon Accuracy," BRL Memorandum Report 1372, Sep 61.
3. Grubbs, Frank E., Statistical Measures of Accuracy, 1964.
4. Alexander, George D., "Stockpile Reliability Evaluation of Cartridge, 105mm: APDS-T, M392A2," AMSAA Technical Report 164, June 1976.

APPENDIX

Horizontal, vertical and circular probable errors observed for two reference lots of 105mm, APDS, M392 rounds on 168 occasions. A sample size of ten was used on each occasion.

Occasion	Probable Error In Mils		
	Horizontal	Vertical	Circular
1	0.47	0.20	0.62
2	0.14	0.29	0.39
3	0.25	0.24	0.42
4	0.28	0.23	0.44
5	0.28	0.18	0.41
6	0.12	0.13	0.22
7	0.19	0.15	0.30
8	0.16	0.13	0.25
9	0.35	0.25	0.53
10	0.21	0.15	0.32
11	0.10	0.18	0.25
12	0.21	0.13	0.30
13	0.13	0.06	0.18
14	0.26	0.12	0.35
15	0.20	0.16	0.31
16	0.14	0.24	0.34
17	0.20	0.15	0.31
18	0.30	0.17	0.42
19	0.23	0.16	0.34
20	0.09	0.16	0.22
21	0.25	0.15	0.36
22	0.19	0.10	0.26
23	0.30	0.14	0.40
24	0.05	0.12	0.16
25	0.14	0.11	0.22
26	0.14	0.23	0.33
27	0.22	0.28	0.44
28	0.10	0.12	0.19
29	0.08	0.16	0.22
30	0.14	0.17	0.27
31	0.16	0.13	0.25
32	0.23	0.33	0.49
33	0.11	0.08	0.17
34	0.16	0.21	0.32
35	0.32	0.18	0.45
36	0.13	0.14	0.23
37	0.10	0.18	0.25
38	0.18	0.16	0.29
39	0.26	0.29	0.48
40	0.24	0.15	0.35
41	0.37	0.15	0.49
42	0.47	0.20	0.62

Occasion	Probable Error In Mils		
	Horizontal	Vertical	Circular
43	0.24	0.33	0.50
44	0.26	0.33	0.51
45	0.22	0.18	0.35
46	0.14	0.29	0.39
47	0.39	0.17	0.52
48	0.26	0.16	0.37
49	0.18	0.20	0.33
50	0.10	0.23	0.31
51	0.20	0.20	0.35
52	0.18	0.22	0.35
53	0.18	0.15	0.29
54	0.12	0.08	0.18
55	0.30	0.14	0.40
56	0.22	0.20	0.36
57	0.25	0.25	0.43
58	0.12	0.13	0.22
59	0.17	0.18	0.30
60	0.20	0.14	0.30
61	0.15	0.15	0.26
62	0.33	0.30	0.55
63	0.37	0.30	0.58
64	0.29	0.29	0.50
65	0.38	0.23	0.54
66	0.20	0.18	0.33
67	0.20	0.14	0.30
68	0.25	0.15	0.36
69	0.31	0.13	0.41
70	0.16	0.12	0.24
71	0.18	0.33	0.46
72	0.21	0.15	0.32
73	0.22	0.19	0.36
74	0.33	0.27	0.52
75	0.14	0.07	0.19
76	0.15	0.09	0.21
77	0.10	0.27	0.35
78	0.11	0.09	0.17
79	0.10	0.13	0.20
80	0.06	0.09	0.13
81	0.26	0.17	0.38
82	0.16	0.13	0.25
83	0.12	0.11	0.20
84	0.14	0.21	0.31

Occasion	Probable Error In Mils		
	Horizontal	Vertical	Circular
85	0.32	0.14	0.43
86	0.20	0.14	0.30
87	0.19	0.18	0.32
88	0.11	0.08	0.17
89	0.15	0.11	0.23
90	0.30	0.14	0.40
91	0.13	0.18	0.27
92	0.12	0.18	0.26
93	0.22	0.19	0.36
94	0.11	0.12	0.20
95	0.21	0.16	0.32
96	0.09	0.11	0.17
97	0.15	0.22	0.33
98	0.24	0.13	0.33
99	0.30	0.17	0.42
100	0.12	0.11	0.20
101	0.11	0.11	0.19
102	0.26	0.09	0.34
103	0.25	0.15	0.36
104	0.18	0.15	0.29
105	0.26	0.17	0.38
106	0.10	0.19	0.26
107	0.22	0.16	0.33
108	0.20	0.07	0.26
109	0.22	0.32	0.48
110	0.17	0.15	0.28
111	0.20	0.16	0.31
112	0.25	0.19	0.38
113	0.30	0.21	0.45
114	0.14	0.10	0.21
115	0.18	0.09	0.25
116	0.09	0.16	0.22
117	0.15	0.18	0.29
118	0.21	0.20	0.35
119	0.20	0.53	0.69
120	0.16	0.16	0.28
121	0.21	0.18	0.34
122	0.19	0.13	0.28
123	0.11	0.06	0.15
124	0.10	0.13	0.20
125	0.12	0.18	0.26
126	0.18	0.16	0.29

Occasion	Probable Error In Mils		
	Horizontal	Vertical	Circular
127	0.22	0.15	0.33
128	0.13	0.11	0.21
129	0.34	0.17	0.47
130	0.22	0.27	0.43
131	0.29	0.31	0.52
132	0.40	0.17	0.53
133	0.50	0.34	0.74
134	0.43	0.32	0.66
135	0.54	0.44	0.85
136	0.10	0.17	0.24
137	0.33	0.31	0.55
138	0.30	0.27	0.49
139	0.27	0.27	0.47
140	0.38	0.14	0.50
141	0.43	0.42	0.74
142	0.40	0.31	0.62
143	0.17	0.43	0.57
144	0.18	0.14	0.28
145	0.33	0.26	0.51
146	0.25	0.14	0.35
147	0.20	0.28	0.42
148	0.07	0.18	0.24
149	0.18	0.11	0.26
150	0.19	0.13	0.28
151	0.16	0.23	0.34
152	0.29	0.24	0.46
153	0.19	0.24	0.37
154	0.35	0.32	0.58
155	0.18	0.14	0.28
156	0.15	0.22	0.33
157	0.24	0.08	0.31
158	0.25	0.22	0.41
159	0.25	0.15	0.36
160	0.31	0.23	0.47
161	0.21	0.14	0.31
162	0.26	0.23	0.42
163	0.23	0.37	0.53
164	0.29	0.21	0.44
165	0.16	0.23	0.34
166	0.35	0.44	0.69
167	0.28	0.18	0.41
168	0.17	0.25	0.37
Average	0.22	0.19	0.38

SEQUENTIAL ESTIMATION OF QUANTAL RESPONSE CURVES

R. Srinivasan
Temple University
Philadelphia, Pa.

R. M. Wharton
Trenton State College
Trenton, New Jersey

ABSTRACT

An approach to the sequential estimation of the fiftieth percentage point of a quantal response curve is discussed. A comparison of this method with some standard methods, using Monte Carlo simulation are presented and its ease of application and high efficiency demonstrated. The potential advantages of this scheme in the estimation of the slope of a response curve are also examined.

1. INTRODUCTION Experimental investigations often deal with quantal response variables conditioned on a continuous variable. For example, in testing the tolerance to a poison in a species of animal, we test animals at various drug levels. Here the response variable Y for a given animal will be survival ($Y=0$) or death ($Y=1$) and the conditioning variable X will be dosage of poison. Thus we are interested in the curve $P(Y(x)=1)$.

In this paper our primary concern is with the sequential estimation of the fiftieth percentage point of the response curve denoted $L_{.5}$ and the slope of the curve at $x=L_{.5}$. Section 2 discusses some sequential and non-sequential approaches to this

problem. Section 3 introduces a new sequential approach related to the Mood-Dixon Up-Down method (1948). It's goal is to allow more efficient estimation of $L_{.5}$ and the slope of the curve for a fixed small sample size n . The relative efficiency of this method compared to the Up-Down method and Wetherill's suggested "best" small sample technique for estimation of $L_{.5}$ are examined using Monte Carlo methods and the results summarized in Table 1.

Although our primary interest is in $L_{.5}$ we briefly discuss estimation of the p^{th} percentage point, L_p for arbitrary p in Section 4.

This paper represents only preliminary results. More extensive investigation of the relative merits of the methods suggested here are required and underway.

2. STANDARD DESIGNS For most applications the response curve is sigmoidal and two forms are commonly used to represent $P\{Y(x)=1\}$, the probit form

$$P\{Y(x) = 1\} = \int_{-\infty}^{\beta(x-a)} \exp(-\frac{1}{2}\pi t^2) / \sqrt{2\pi} dt$$

and the logit form

$$P\{Y(x) = 1\} = (1 + \exp(-\beta(x-a)))^{-1}$$

Since, in practice (Finney, 1952, p. 47), there is little to choose between the two forms, we will limit our discussion to the logit form because of its computational advantages.

Basically our problem is to take a sample $(x_1, y_1), (x_2, y_2)$, ..., (x_n, y_n) and estimate $L_{.5} = \alpha$ and the slope of the response curve at $x = L_{.5}$ which is β in the logit form. There are two important aspects to this problem. First, how do we select the x_i 's and second, what estimators to use for α and β . We are primarily interested in the first aspect.

The standard non-sequential experimental design for this case involves selecting k values of x_i hopefully about α and obtaining n_i observations at this x_i . The maximum likelihood estimators of α and β are easy to calculate for such a sample.

Sequential designs for this problem, which allow the choice of x_{i+1} after observing the result for the previous i observations, allow one to obtain a specified accuracy in estimation with a smaller sample size than that required with a non-sequential design. Thus sequential designs are useful when testing is expensive or when candidates for entry into the testing procedure are scarce.

In order to explore some of the difficulties encountered in sequential designs for the estimation of parameters of a response curve, we will briefly discuss some well known sequential designs.

Robbins and Monro (1951) introduced a method of stochastic estimation suitable for the general regression situation, and Chung (1954) considered the choice of parameters in the process

to obtain certain asymptotically optimum properties. Hodges and Lehmann (1955) extended Chung's work to cover the quantal response problem. If an estimate is required for L_p , the level of x at which $P(Y(x) = 1) = p$, then a series of observations $y_r(x_r)$ is taken at levels x_r such that

$$x_{r+1} = x_r - a_r(y_r(x_r) - p)$$

where the a_r 's are positive constants and after n observations, x_{n+1} is taken as the estimate of L_p . This method works best for $p = .5$.

Although this method has certain asymptotically optimal properties, it also has some practical drawbacks when applied with small to moderate sample sizes. First, it is usually difficult to apply the conditioning variable at arbitrary levels as required by this method. Secondly, if the starting value for the process is far from L_p , a substantial bias may be introduced in the estimate.

Another approach to the design problem, which alleviates the first of the drawbacks described above, was introduced by Dixon and Mood (1948). The method involves a grid of equally spaced values of the conditioning variable. A value x_0 is picked as close to $L_{.5}$ as possible and the response observed, if the response is positive at x_0 the next x value is taken one step lower and if the response is negative at x_0 the next x value is taken one step higher on the grid. The same process is utilized for each subsequent x_i . This design causes the sampled x_i 's to

cluster about $L_{.5}$, thus yielding a more accurate estimate of $L_{.5}$ whether the estimate is obtained by maximum likelihood, minimum chi-square or the Brownlee, Hodge approach (1953).

With the proper choice of starting value near $L_{.5}$ and step size near $1/8$, this scheme yields a highly efficient estimate of $L_{.5}$. However, if the step size is too large the efficiency decreases rapidly and if the starting value is chosen too far from $L_{.5}$ significant bias is introduced with small to moderate sample sizes. Thus with small sample sizes the mean square error of the estimate will increase with the size of the step and the difference between the starting value and $L_{.5}$. Another interesting observation noted by Wetherill (1963) is that for the joint maximum likelihood estimators of $\alpha = L_{.5}$ and β for the logistic curve, the efficiency of $\hat{\beta}$ increases with increased step size while as noted above the efficiency of $\hat{\alpha}$ decreases. The schemes presented in Section 3 represent an attempt to reduce these difficulties.

3. A MODIFIED UP-DOWN PROCEDURE There have been numerous modifications of the up-down method discussed in the literature, the purpose of which being to reduce the problems involved in estimating $L_{.5}$. A number of these modifications are considered by Wetherill (1963).

The modification we present here is motivated by a hope that it will yield improved estimates of the slope β as well

as $L_{.5}$. The rational for this scheme is that we use large steps in the beginning when searching for $L_{.5}$ and smaller steps as we narrow in on $L_{.5}$. The variable step size makes the estimate of $L_{.5}$ less sensitive to large errors in starting value and hopefully will increase the accuracy of our estimate for β .

A generalized Up-Down method can be described as follows:

1. Pick a minimum allowable step size δ .
2. Pick m such that the maximum allowable step size will be $m \cdot \delta$.
3. Pick a starting value x_0 .
4. If the response at any value x_i of the conditioning variable is positive, take the next x value $k_i \cdot \delta$ units lower. If the response is negative take the next x value $l_i \cdot \delta$ steps higher, where $1 \leq k_i \leq m$ and $1 \leq l_i \leq m$.

This generalized Up-Down method might be considered an Up-Down method with memory since k_i and l_i at any step are functions of the entire past history of the trial.

In order to investigate the effect of variable step size on the estimation of $L_{.5}$ two easily applied examples of the above scheme were considered:

METHOD I

In Method I, step size starts at one and increases by one as

long as the outcomes remain the same (i.e. all positive or negative) up to a maximum step size of 3. Once a sign change occurs, step size reverts back to one and the process continues for a predetermined number of steps. In the generalized scheme this would correspond to defining $m=3$, $k_0=l_0=1$

and

$$k_i = \begin{cases} \min[k_{i-1}+1, 3] & \text{if } y_i = y_{i-1} = 1 \\ 1 & \text{if } y_i = 1 \text{ and } y_{i-1} = 0 \end{cases} \quad i=1, 2, \dots, n$$

$$l_i = \begin{cases} \min[l_{i-1}+1, 3] & \text{if } y_i = y_{i-1} = 0 \\ 1 & \text{if } y_i = 0 \text{ and } y_{i-1} = 1 \end{cases} \quad i=1, 2, \dots, n$$

METHOD II

In Method II, step size starts at 3 and remains at three as long as the outcomes are the same. The step size is reduced by one for each change in outcome (down to a minimum of one) and increased by one whenever the outcome is the same as the previous one (up to a maximum of 3) and the process continues for a pre-determined number of steps. In the generalized scheme this would correspond to defining $m=3$, $k_0=l_0=3$ and

$$k_i = \begin{cases} \min[k_{i-1}+1, 3] & \text{if } y_i = y_{i-1} = 1 \\ \max[k_{i-1}-1, 1] & \text{if } y_i = 1 \text{ and } y_{i-1} = 0 \end{cases} \quad i=1, 2, \dots, n$$

$$l_i = \begin{cases} \min[l_{i-1}+1, 3] & \text{if } y_i = y_{i-1} = 0 \\ \max[l_{i-1}-1, 1] & \text{if } y_i = 0 \text{ and } y_{i-1} = 1 \end{cases} \quad i=1, 2, \dots, n$$

		$\alpha = 0$			$\beta = 1$			STEP = 0.5					
		UNMODIFIED			MODIFIED I			MODIFIED II			**		
n	start	$E(L_{50})$	RSE	$E(L_{50})$	RSE	$E(L_{50})$	RSE	$E(L_{50})$	RSE	$E(L_{50})$	RSE	$E(L_{50})$	RSE
34	0	-.012	.117	-.018	.146	-.014	.150	-.014	.159	-.014	.156	-.014	.156
	3	.374	.247	.130	.162	.069	.156	.069	.156	.069	.156	.069	.156
9	0	-.014	.231	.038	.454	.032	.533	.032	.533	.032	.533	.032	.533
	3	1.247	1.719	.497	.686	.324	.589	.324	.589	.324	.589	.324	.589
		$\alpha = 0$			$\beta = 1$			STEP = 1.0					
34	0	-.022	.129	-.026	.194	-.020	.187	-.020	.187	-.020	.187	-.020	.187
	3	.166	.152	.041	.189	.005	.197	.005	.197	.005	.197	.005	.197
9	0	-.014	.362	-.039	.665	-.057	.815	-.057	.815	-.057	.815	-.057	.815
	3	.587	.682	.135	.674	.006	.686	.006	.686	.006	.686	.006	.686
		$\alpha = 0$			$\beta = 1$			STEP = 1.5					
34	0	-.014	.148	-.035	.234	-.023	.226	-.023	.226	-.023	.226	-.023	.226
	3	.075	.156	-.005	.231	-.026	.221	-.026	.221	-.026	.221	-.026	.221
9	0	.013	.512	-.044	.846	-.070	1.062	-.070	1.062	-.070	1.062	-.070	1.062
	3	.310	.577	.053	.825	-.136	1.027	-.136	1.027	-.136	1.027	-.136	1.027

To compare these two modifications with the standard Up-Down method a Monte Carlo simulation was done assuming the population sampled was logistic with $\alpha=0$ and $\beta=1$. Starting values of $x_0=0,3$ and sample sizes $n=34$ and 9 were considered with a 1000 replications generated for each combination of x_0 and n . For ease of computation in this initial investigation, the following estimator of $L_{.5}$ due to Brownlee and Hodges (1953) was used.

$$\hat{L}_{.5} = \frac{\sum_{i=1}^n x_i}{n}$$

It should be noted that this estimator although easily calculated is asymptotically equivalent to the maximum likelihood estimator of $L_{.5}$. The basis for comparison between the modified and unmodified approaches was bias and mean square error. The results of this computer simulation are presented in Table 1.

The following observations should be made regarding Table 1:

1. The modified methods I and II reduce the bias for starting value $x_0=3$, for all three step sizes considered and do not substantially increase it for $x_0=0$.
2. The MSE is far more stable with respect to starting value for the modified methods as opposed to the unmodified method. (Recall, this was one of the major difficulties with the unmodified Up-Down method.)

3. The modified methods with step size = .5 are comparable to the unmodified method with step sizes 1.0 and 1.5 and to Wetherill's recommended technique (1963, p.34). The MSE's for this approach are given in the (**) column of Table 1 for a comparable set of parameters.

Thus the modified schemes allow estimation of $L_{.5}$, with small final step size, which is fairly stable with regard to starting value, even for relatively small sample sizes and comparable to Wetherill's "best" approach with regard to mean square error.

4. ESTIMATION OF GENERAL L_p . An extension of the generalized Up-Down method which might prove useful for estimation of general L_p can be described as follows: Steps 1,2 and 3 are the same as for the case $p=.5$ discussed in Section 3.

4. Pick an initial number n_0 of observations to be taken at x_0 .

5. After each trial estimate the proportion p' of positive responses at the level used for the current trial and consecutive with it, that is, back to the last change of level. If $p' > p$ and p' is estimated on n_0 trials or more decrease the level by $k_i \delta$ steps. If $p' < p$ increase the level $l_i \delta$ steps, where $0 \leq k_i \leq m$

and $0 \leq l_i \leq m$. Both l_i and k_i are usually set equal to zero if $p' = p$.

This scheme is a generalization of the inverse sampling rule described by Wetherill which was the most efficient approach he considered for the general L_p problem.

Empirical studies on this scheme and some possible alternatives will have to be done in order to justify its usefulness.

5. CONCLUSION. The two special cases of the generalized Up-Down method presented here are easily applied sampling schemes, which go a long way in reducing one of the main difficulties in the Up-Down method, that is the effect of starting value on efficiency and are themselves comparable in efficiency to Wetherill's "best" scheme for estimating $L_{.5}$.

A careful investigation of other special cases of the generalized scheme, the efficiency of such schemes in estimating the slope and the usefulness of the generalized scheme for general L_p are currently underway.

REFERENCES

- Brownlee, K.A., Hodges, J.L. and Rosenblatt, M. (1953), "The Up-Down Method with Small Samples", J. Amer. Statist. Assoc., 48, 262-277.
- Chung, K.L., (1954) "On a Stochastic Approximation Method", Ann. Math. Statist., 25, 463-483.
- Dixon, W.J. and Mood, A.M. (1948) "A Method for Obtaining and Analyzing Sensitivity Data", J. Amer. Statist. Assoc., 43 101-126.
- Finney, D.J., (1951), Statistical Methods in Biological Assay. London : Griffin.
- Hodges, J. L. and Lehmann, E. H. (1955), "Two Approximations to the Robbins-Monro Process", Proc. Third Berkeley Symp. I, 95-104.
- Robbins, H. and Monro, S. (1951) "A Stochastic Approximation Method", Ann. Math. Statist., 29, 400-407.
- Wetherill, G. B. (1963), "Sequential Estimation of Quantal Response Curves". J. Royal Statist. Soc. 1, 1-38.

A MONTE CARLO SIMULATION OF A
PROBABILITY RATIO SEQUENTIAL TEST (PRST)
PLAN FROM MILITARY STANDARD 781C

William J. Broemm
Reliability, Availability and Maintainability Division
U. S. Army Materiel Systems Analysis Activity
Aberdeen Proving Ground, Maryland 21005

I. INTRODUCTION

The topic of my presentation is a Monte Carlo Simulation of sequential test plans. The sequential test plans I am referring to are the Probability Ratio Sequential Test Plans, the PRST Plans, located in Military Standard 781C (Figure 1). In the literature, the PRST plans come under the category of the Reliability Design Qualification and Production Acceptance Tests (Exponential Distribution). Simply stated, these tests deal with items that have exponential times between failures.

The computer program discussed in this presentation is offered as an aid to test planners and those who are concerned with the application of the PRST plans. The utilization of the methodology proposed should permit the test planner, equipped with a reasonable amount of practical experience with the PRST plans, to make certain probabilistic statements regarding termination points in the plans, namely (1) the likelihood of reaching the last failure and (2) the likelihood of reaching the maximum test time.-

Historically, the PRST plans have no provision for estimating the true MTBF of an item of equipment, and therefore, the total test time expected to be consumed during testing may vary significantly (Figure 2). Consequently, program costs and schedules have to be planned to compensate for this range of uncertainty. However, with the help of the methodology delineated herein, one may be able to choose an appropriate test plan from MIL-STD 781C, select a lower test MTBF (θ_1), select a realistic range of true MTBF's for consideration, implement the simulation, and finally obtain measures of the two likelihood estimates aforementioned - all of this in order to reduce the range of uncertainty and therefore minimize program cost overruns.

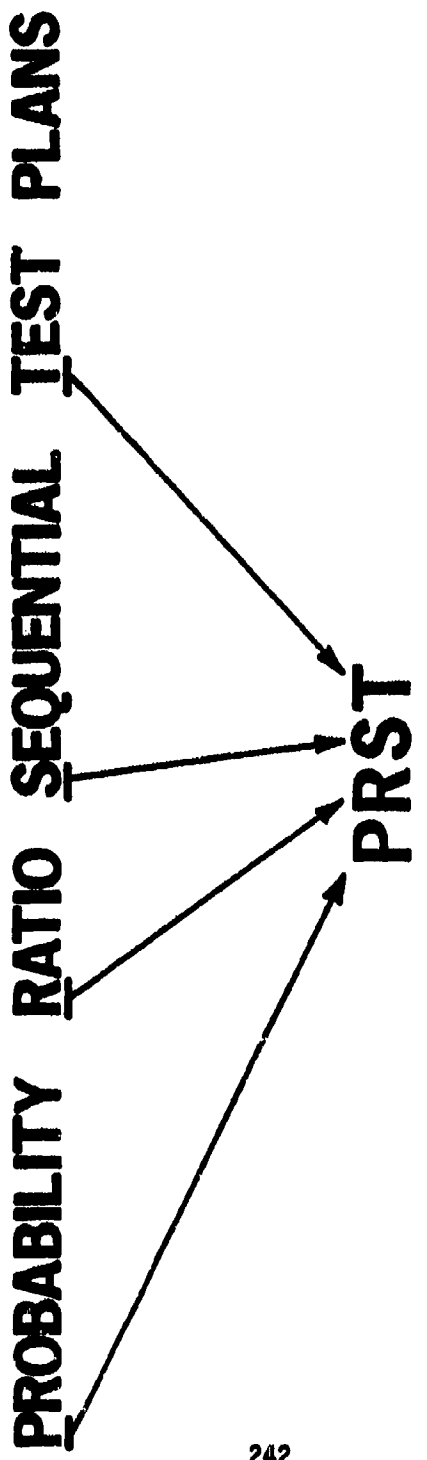


FIGURE 1. The Probability Ratio Sequential Test Plans

EXPECTED TEST TIME CURVE

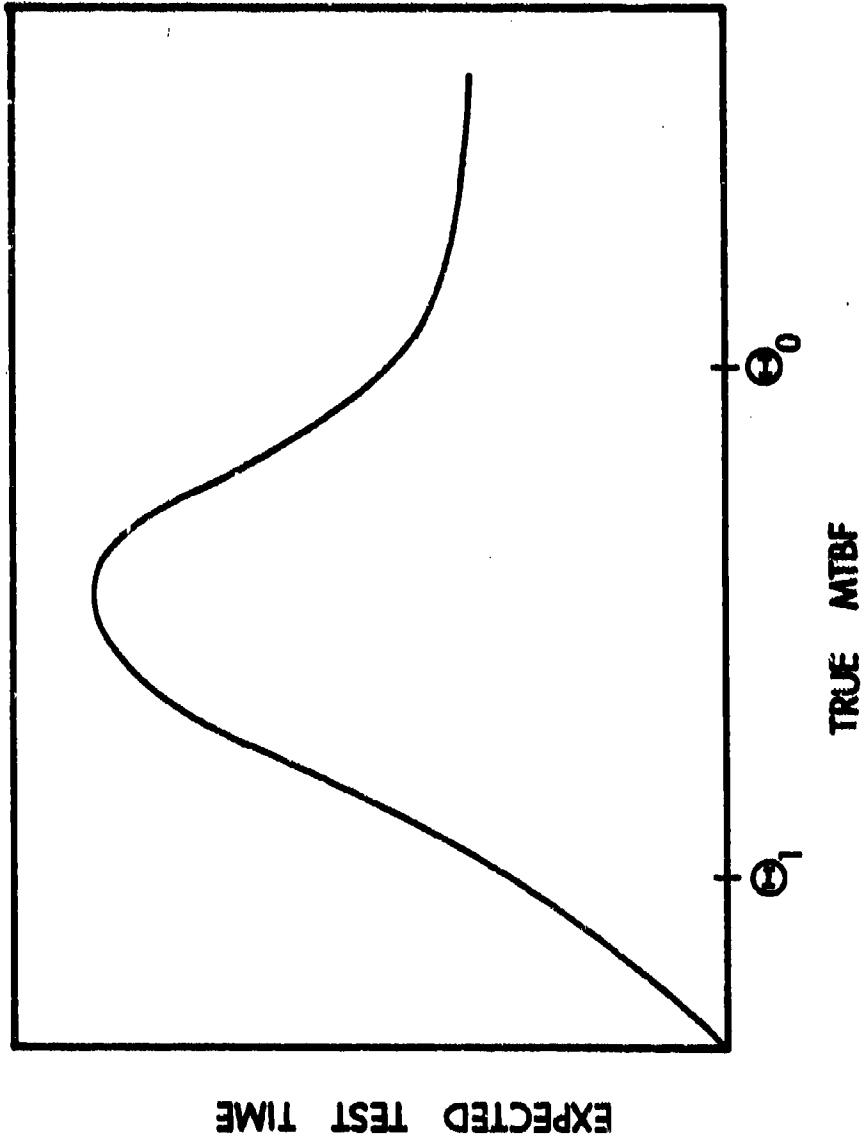


FIGURE 2. An Expected Test Time Curve

II. STATEMENT OF THE PROBLEM

A typical PRST plan from MIL-STD 781C, regardless of the total number of failures and the total test time in the plan, will basically assume an appearance as depicted in the following (Figure 3). Inherent in the design of the PRST arrow, if you will, are such things as decision risks, a discrimination ratio, and accept-reject criteria. Given that all of these things are in harmony, of concern is not the general shape or length of the PRST arrow but the two termination vectors located in the arrowhead. For simplicity, we may designate the last failure as F_L and the maximum total test time as T_M . The problem, then, becomes the following: When testing an item of equipment with the PRST plans, how often is the last failure reached (Figure 4)? In other words, what is the likelihood of reaching F_L (Figure 5)? In a similar manner, when testing an item of equipment with the PRST plans, how often is the maximum test time reached (Figure 6)? That is, what is the likelihood of reaching T_M (Figure 7)? These kinds of inquiries can be taken a step further and translated into probabilistic statements (Figure 8). Symbolically, we may ask: What is $P(F_L)$ and what is $P(T_M)$?

A GENERALIZED PRST PLAN

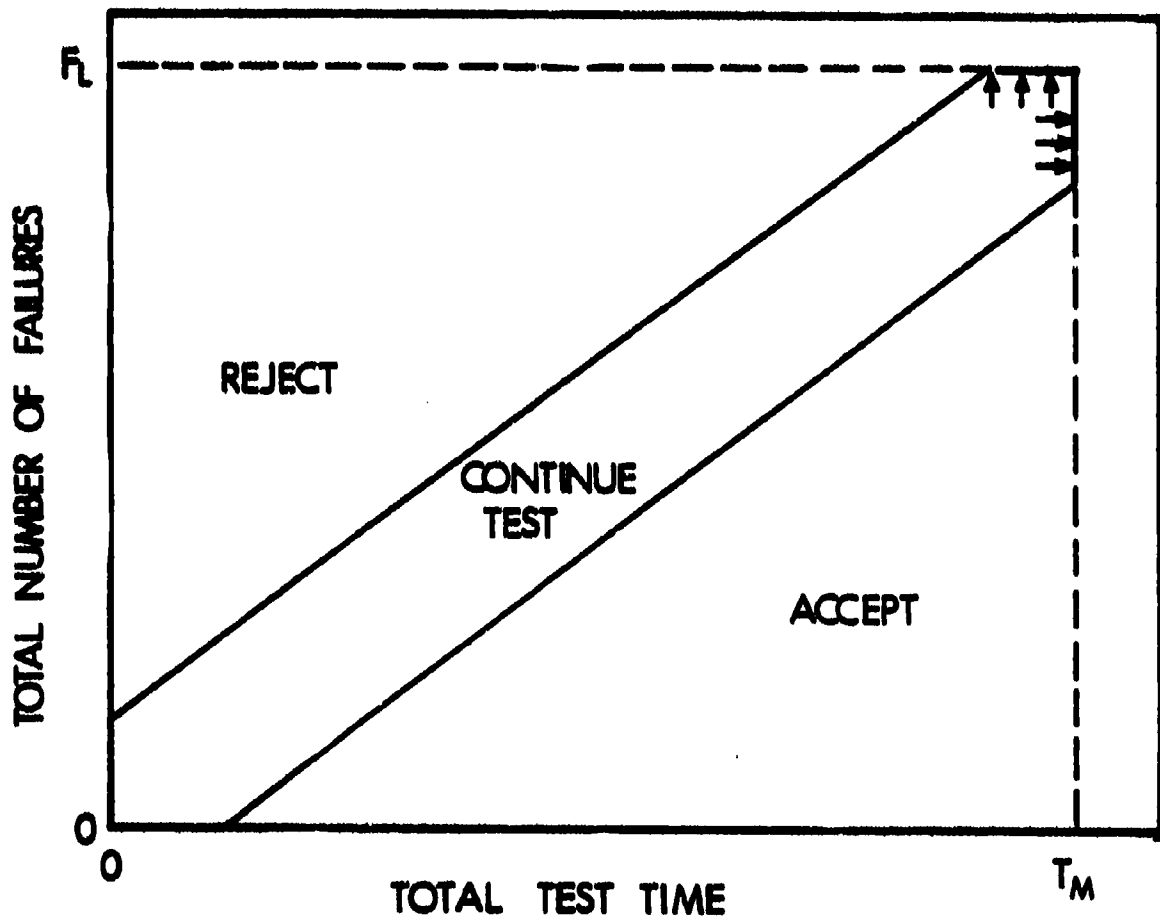


FIGURE 3. A Generalized PRST Plan

LAST FAILURE CONSIDERATION

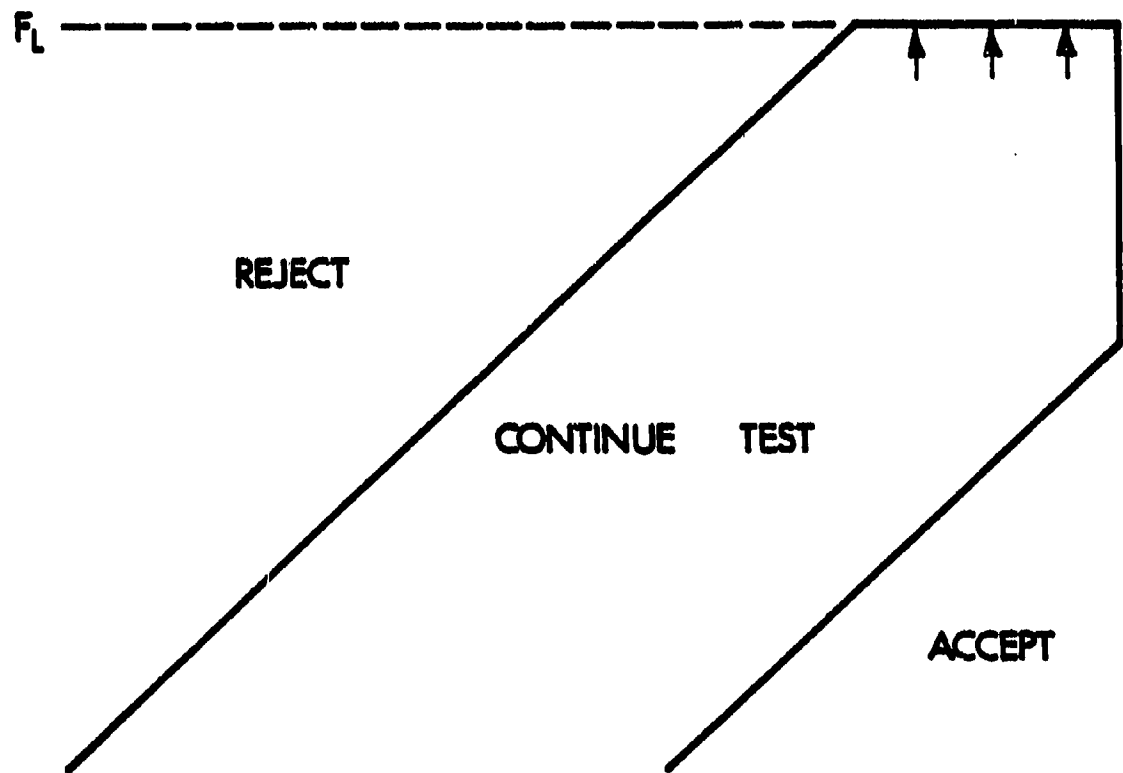


FIGURE 4. Last Failure Consideration

PROBLEM -

WHAT IS THE LIKELIHOOD OF REACHING F_L ?

FIGURE 5. The Likelihood of Reaching F_L

MAXIMUM TEST TIME CONSIDERATION

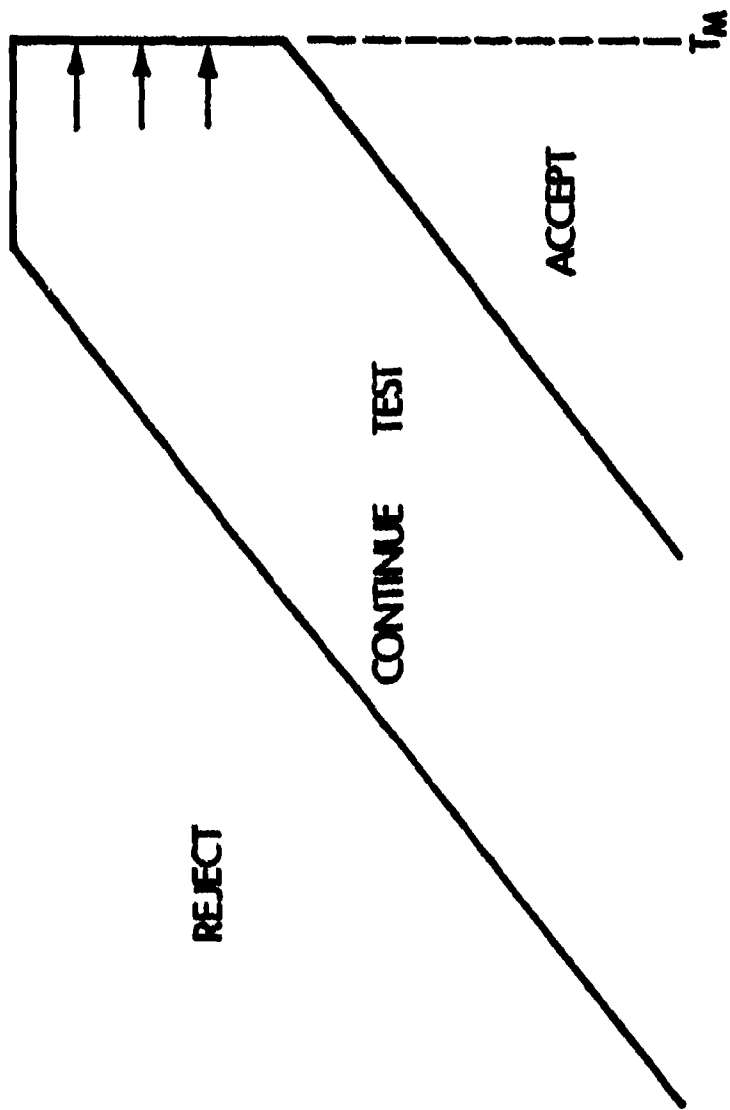


FIGURE 6. Maximum Test Time Consideration

FIGURE 7. The Likelihood of Reaching T_H

PROBLEM -
WHAT IS THE LIKELIHOOD OF REACHING T_H ?

PROBABILITY STATEMENTS

$P(F_L)$?

$P(T_M)$?

FIGURE 8. Probability Statements

III. A DESCRIPTION OF THE ALGORITHM

The purpose of the simulation, then, is to ascertain how often F_L and T_M are reached. The vehicle for doing this resides in the algorithm - a set of instructions that simulates the testing of an item of equipment using a typical PRST plan (Figure 9). The code, that is, set of instructions, makes use of two program counters. One counter corresponds to the last failure, F_L , and the other counter corresponds to the maximum test time, T_M . During each iteration of the simulation, an item of equipment can be either rejected, accepted or put to further test (as exemplified by the continue test strip). If the item is rejected or accepted prior to reaching truncation, then no counters are incremented, and a new iteration is begun. If the item fails within the continue strip without a rejection or an acceptance, then another failure time is called for, and the above process is repeated.

In order to test against the maximum test time value, a particular failure time is compared with the T_M value (Figure 10). If that particular failure time is greater than or equal to the T_M value, then the T_M counter is incremented by one and a new iteration is begun. If that particular failure time is less than the T_M value, then another failure time is called for and queried in the same manner.

Similarly, in order to test against the last failure, a particular failure number is compared with the maximum failure number, F_L , to determine equality. If equality exists, then the F_L counter is incremented by one and a new iteration is begun. If equality does not exist; that is, if the particular failure number is less than the F_L value, then another failure is called for and queried in the same manner.

Now, if we allow each iteration to be an independent event, and if we conduct a large number of these trials, then the F_L and T_M counters can be shown to be likelihood estimates for reaching the last failure and the maximum total test time, respectively. Furthermore, these likelihood estimates can be viewed in probabilistic terms, as stated previously.

A GENERALIZED PRST PLAN

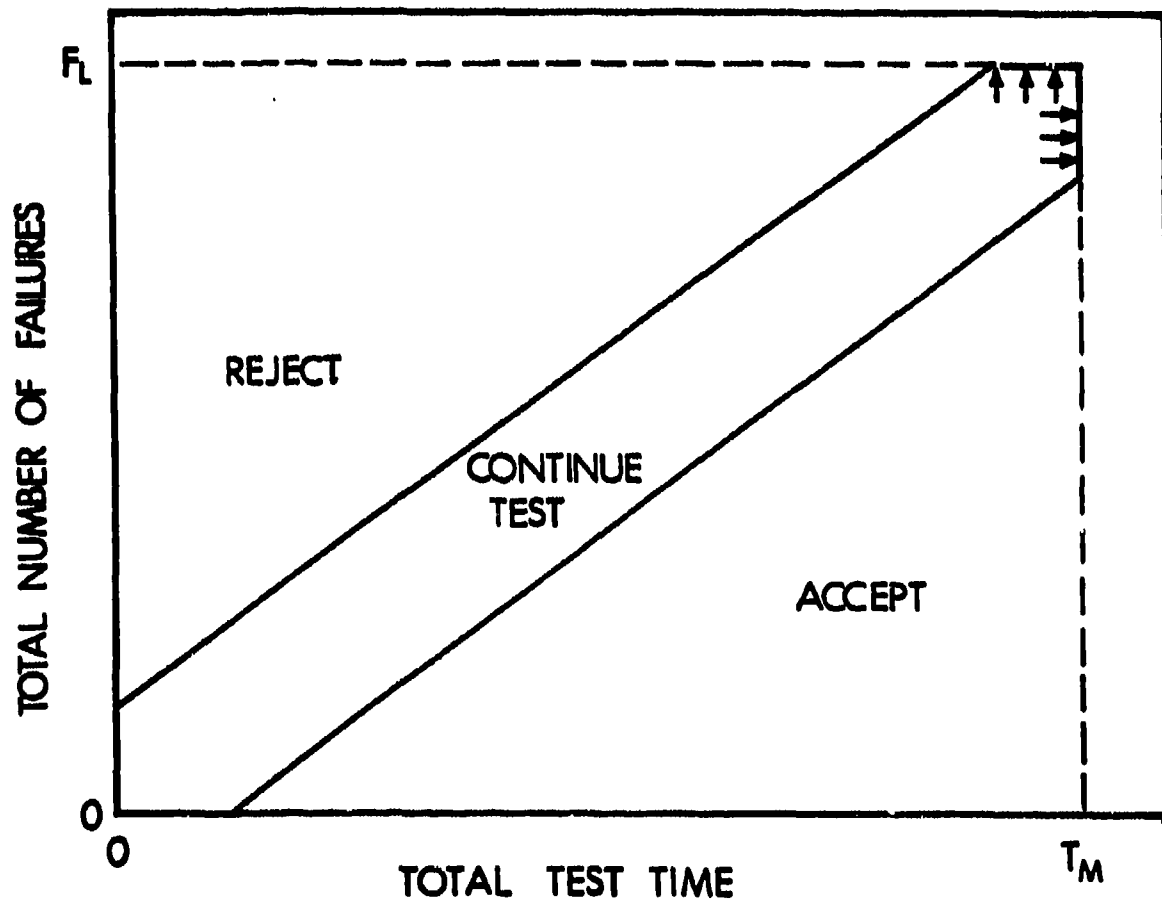


FIGURE 9. A Generalized PRST Plan

ALGORITHM CONSIDERATIONS

FAILURE TIME $\{ \begin{matrix} > \\ = \\ < \end{matrix} \}$ MAXIMUM TEST TIME, T_M

FAILURE NUMBER $\{ \begin{matrix} < \\ = \\ > \end{matrix} \}$ MAXIMUM FAILURE, F_L

FIGURE 10. Algorithm Considerations

IV. A PARTICULAR EXAMPLE FROM MIL-STD 781C

Upon selection of an appropriate PRST plan; that is, one that incorporates the desired decision risks, discrimination ratio, and accept-reject criteria, upon selection of a lower test MTBF value (θ_1), and upon specification of a range of true MTBF's for consideration, one is in a position to run the simulation in order to obtain likelihood estimates for reaching the last failure and the maximum total test time (Figure 11).

In order to demonstrate some of the results found, consider Test Plan III from MIL-STD 781C (Figure 12). Test Plan III is based on sixteen (16) failures, decision risks of 10 percent and a discrimination ratio of 2.0:1. If the lower test MTBF is chosen to be 100 hours, then the upper test MTBF will be 200 hours. If we select a range of true MTBF's between 60 and 300 hours, then this plot (Figure 13) demonstrates the likelihood of reaching the last failure. Consider an item of equipment with a true MTBF of 60 hours. More than likely that item of equipment will be rejected prior to reaching truncation. Consider an item of equipment with a true MTBF of 300 hours. More than likely that item of equipment will be accepted prior to reaching truncation. Clearly, it is when an item of equipment has a true MTBF between the lower test MTBF value, θ_1 , and the upper test MTBF value, θ_0 , that the item will most often be tested to truncation.

Similarly, this plot (Figure 14) demonstrates the likelihood of reaching the maximum total test time. The same set of arguments hold for this plot.

PROCEDURAL REMARKS

- 1 SELECT A PRST PLAN
- 2 CHOOSE A LOWER TEST MTBF, Θ_1
- 3 SELECT A RANGE OF TRUE MTBF'S
- 4 RUN THE SIMULATION
- 5 OBTAIN $P(F_L)$ AND $P(T_M)$

FIGURE 11. Procedural Remarks

MIL -STD 781C
TEST PLAN III

DECISION RISKS 10 PERCENT
DISCRIMINATION RATIO 2.0 : 1

FIGURE 12. Test Plan III from MIL-STD 781C

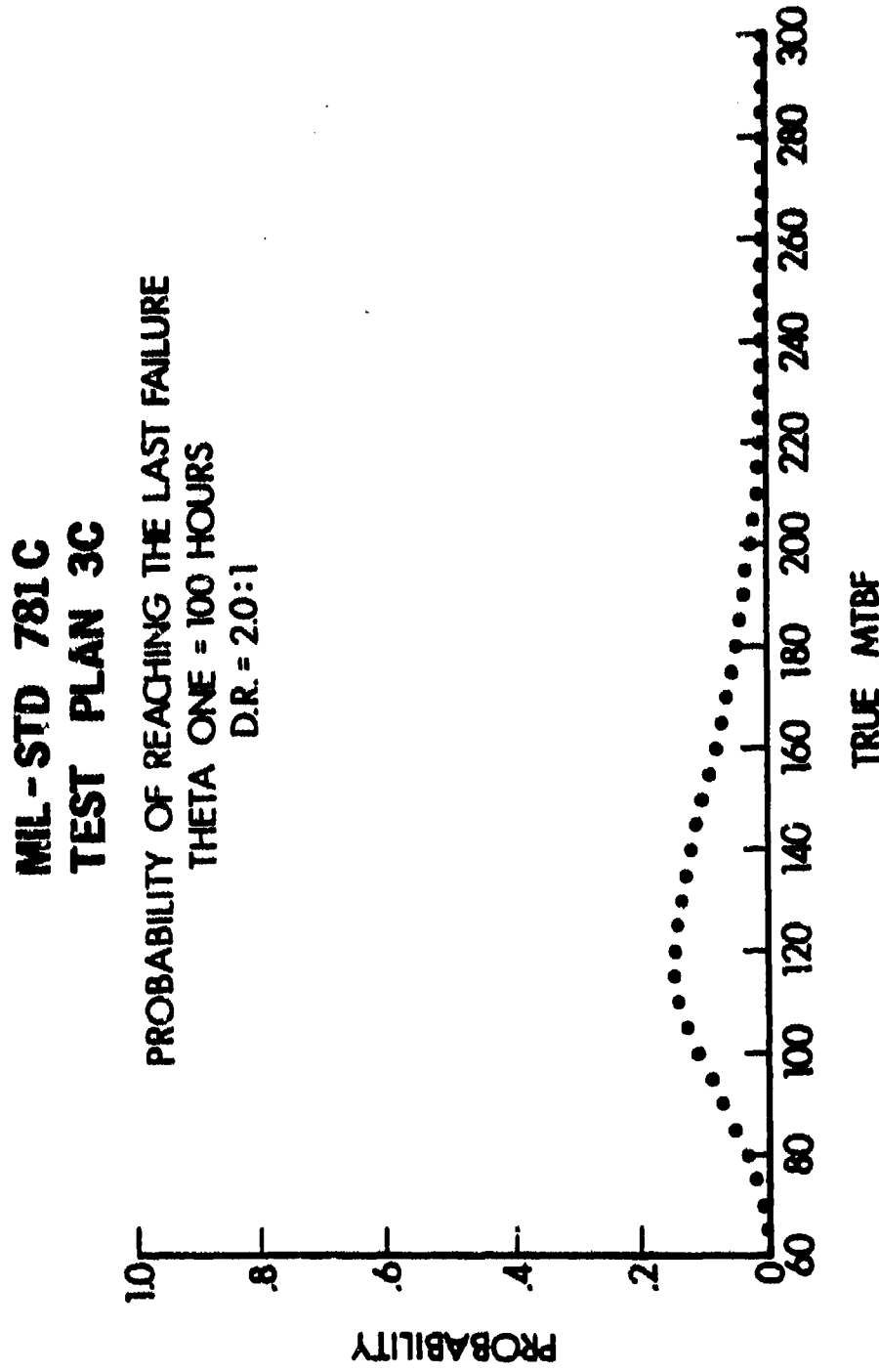


FIGURE 13. Probability of Reaching the Last Failure

MIL-STD 781 C
TEST PLAN 3C
PROBABILITY OF REACHING THE MAXIMUM TEST TIME
THETA ONE = 100 HOURS
D.R. = 2.0:1

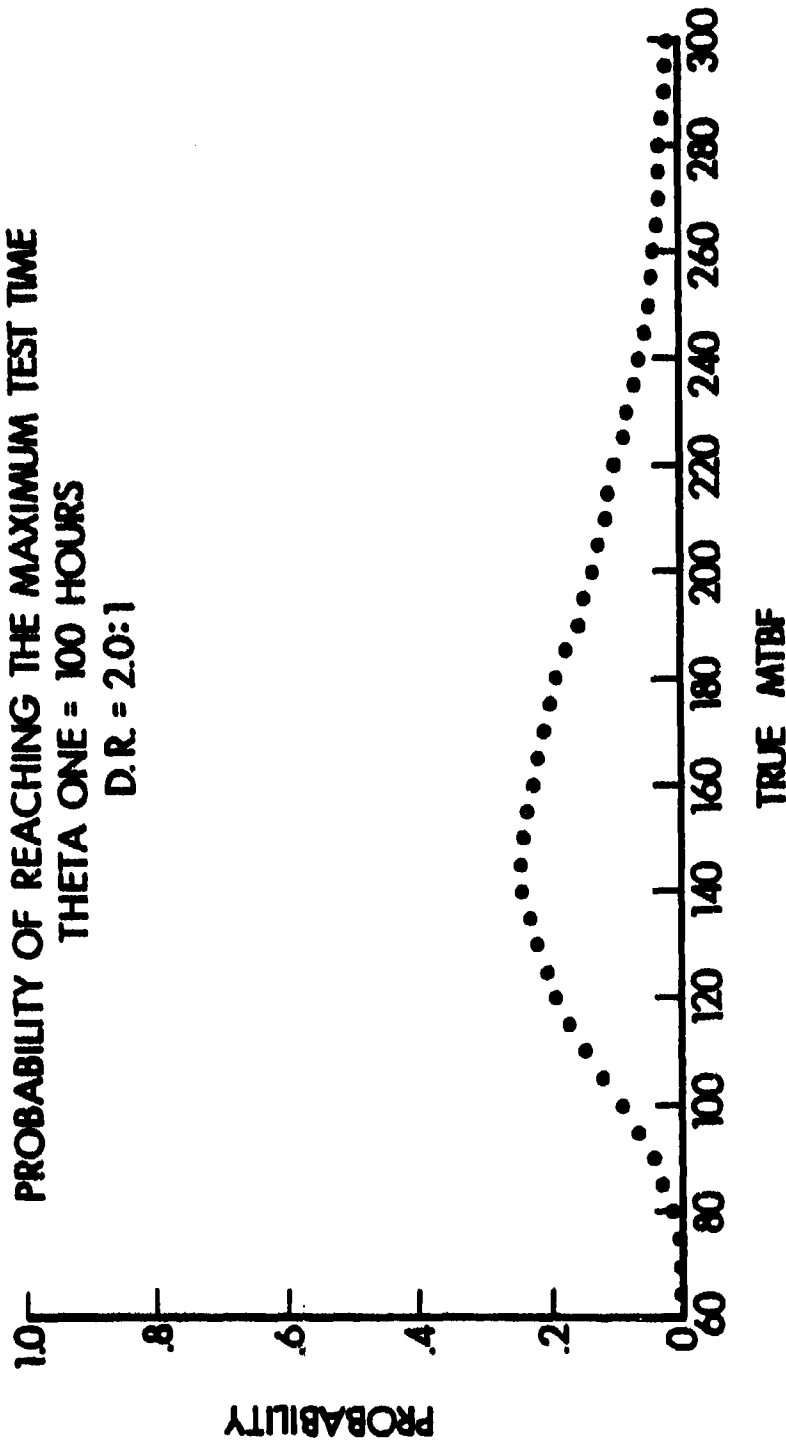


FIGURE 14. Probability of Reaching the Maximum Test Time

V. SUMMARY

In summary, the intent of my presentation has been to promulgate a methodology for determining the likelihood of reaching the truncation points in the family of PRST plans (Figure 15). With the knowledge of how often an item may be tested to truncation; that is, (1) the last failure in the plan and (2) the maximum total test time in the plan, a test planner may be in a better position to formulate and execute a well-conceived test plan package so that test costs and schedules can be reduced and so that program cost overruns can be kept to a minimum.

SUMMARY

LIKELIHOOD OF REACHING TRUNCATION IN THE PRST PLANS

- PROBABILITY OF REACHING THE LAST FAILURE
- PROBABILITY OF REACHING THE MAXIMUM TEST TIME

STRUCTURING OF BETTER TESTS

- TO REDUCE TEST COSTS
- TO FACILITATE SCHEDULING
- TO MINIMIZE PROGRAM COST OVERRUNS

FIGURE 15. Summary

STATISTICAL CONSULTING
OR
THERE ARE NO STANDARD PROBLEMS, ONLY STANDARD SOLUTIONS

Brian L. Joiner
Statistical Laboratory
University of Wisconsin-Madison
1210 W. Dayton Street
Madison, Wisconsin 53706

Abstract

Statistical consulting involves solving non-standard problems on a time scale such that optimal solutions are not feasible even if one could specify the problem concisely enough. One must seek to understand each problem properly and resist the temptation to slap it into the fold of an already existing solution. Here we give a small collection of examples where "standard" solutions, blindly applied would likely have proved worse than useless.

THE ITERATIVE NATURE OF ANALYSIS

Exhibit 1 is a schematic of the key steps in the iterative process of data analysis and model building. The importance of the core triangle of MODEL IDENTIFICATION, MODEL FITTING and DIAGNOSTIC CHECKING has been forcefully indicated by George Box and colleagues, especially in Box and Jenkins (1970). Additional key components illustrated in Exhibit 1 that all too often get overlooked in statistical practice are the need to pay careful attention to the data -- and its quality -- and to the underlying theory or structure of the problem.

Implicit in Exhibit 1 is the all important distinction between "assuming" and "pretending". The American Heritage Dictionary includes the following definitions.

- Assume: "To take for granted," and
- Pretend: "To play like, to make believe".

There is a subtle, but very important distinction between these two words. When doing statistical analysis our life is complicated by the fact that we must continually shift back and forth between these two concepts, and in the past have tended to rely on only one word -- assume -- to describe both.

When we tentatively define a plausible model INCLUDING THE NATURE OF THE DISTURBANCES, we put on our mathematicians hat and ask "What is an optimal, or at least defensible, way of fitting this model to data having the indicated error structure." To seek such answers, we must ASSUME that we know the nature of the model and the error structure perfectly. The mathematics takes us literally and treats the model as if it could "take for granted" everything we have said.

Having thus developed a fitting procedure, we proceed to apply it to the data at hand, but in so doing we switch from acting as mathematicians, and turn to being scientists. As scientists we can only PRETEND that the data can be completely described in the fashion ASSUMED in the mathematics. Of course, nature cares not at all about our play acting. Our pretending does not change the underlying model, nor the error structure. It will be what ever nature has chosen, and invariably nature has chosen a more complex structure than that described by the mathematics we have been able to accommodate.

We then move around the bend in Exhibit 1 to the analysis loop and begin DIAGNOSTIC CHECKING. There our role is to ask if there are serious DETECTABLE differences between nature and what we PRETENDED was true. Even while doing DIAGNOSTIC CHECKING we need to switch back and forth asking questions like, IF the disturbances were uncorrelated, what are the chances of observing a first order autocorrelation this high or higher.

Perhaps a useful way to sum this up is to say that it seems to be helpful to use two different words for the two different roles. Let us ASSUME when we're doing mathematics and let us PRETEND when we're fitting models to data. Using these two different words may help us keep from taking too seriously what we ordinarily ASSUME, but in fact can only PRETEND.

Vitamin B₂ in turnip greens

Another important feature of the Exhibit 1 is the need for continued data checking. The following two examples provide useful insight.

Both Anderson and Bancroft (1959, page 192) and Draper and Smith (1966, page 229 and 339) report analyses of some data on the effect of three variables on the amount of vitamin B₂ in turnip greens. The model given by D&S contains three terms X_2 , X_3 and X_2^2 and gives an (unadjusted) R^2 of 90% which is somewhat higher than the 75% given by A&B's model. Even relatively careful analyses of the residuals from the D&S model, such as the residual plots in Exhibit 2, reveals no serious problems with the fitted model.

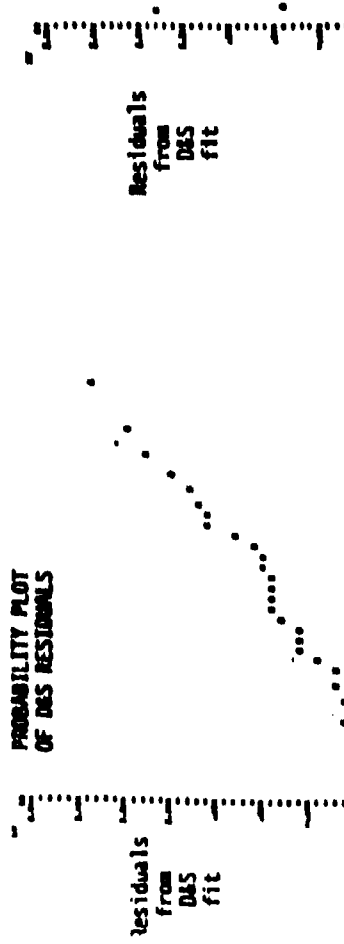
However, if one plots the original DATA in the ORDER they were presented in the textbook a very striking pattern can be seen. See

Exhibit 2

Residuals and data for Vitamin B₂ in turnips

PROBABILITY PLOT
OF THE RESIDUALS

RESIDUALS VS PREDICTED VALUES
FOR DLS FIT

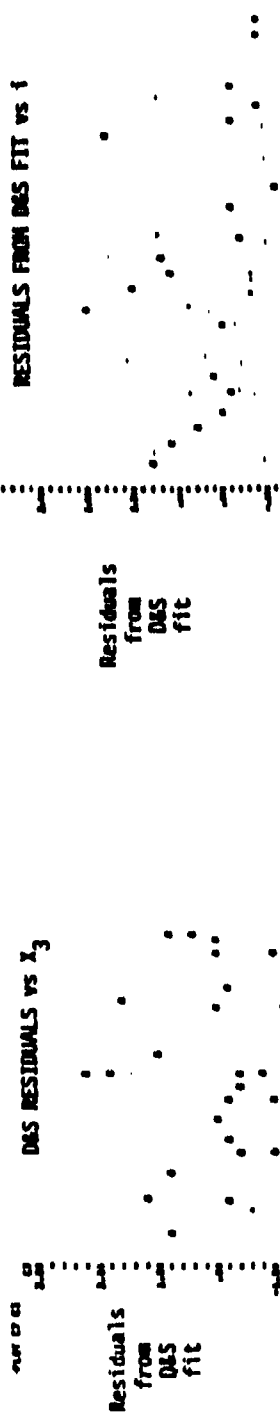


Probability Plot
(A)

264

Predicted Values
(B)

DLS RESIDUALS VS X₃



X₃ (Air temperature)

Order (i)

RESIDUALS FROM DLS FIT VS 1



Order (i)

Exhibit 2F. The data drop off nearly linearly. In fact, a simple straight line fitted to the plot in Exhibit 2F gives an R^2 of 90%! What is the explanation? The answer is not clear and attempts to get more details about the original experiment have not been successful. My conclusion is that there was some other factor not recorded that was the primary responsible party. It may have been that the values are reported in the order measured and that reagents or the greens themselves decayed over time. There is not other ready explanation. The Y values are not merely listed in decreasing order since a number of inversions are apparent in Exhibit 2F. The argument that X_2 is the most important factor loses credibility on at least two accounts. A quadratic is needed to fit the three levels of X_2 , and the Y values in Exhibit 2F seem to continually drop off unaffected by changes in X_2 . Careful data checking has opened serious questions about the quality of those data.

Oxygen in steel

Another example of important but not easily detectable time order decay of measurements is provided in Joiner and Campbell (1976). (Oxygen is there inadvertently misspecified as Nitrogen.) Two key plots are reproduced here as Exhibits 3A and 3B. Note again the serious data problems uncovered by careful checking. In this case a careful timely search for causes was made, but no explanation was found. At least the fact that the problem existed had been brought to light by the data checking.

This leads us to list the following caveats.

"Yet to calculate is not in itself to analyze."
Edgar Allan Poe, The Murders in the Rue Morgue.

"There's less there than meets the eye."
Joseph M. Cameron.

There are no standard problems, only standard solutions.

Checking residuals is not always enough, the data must also be checked.

Using least squares tells the mathematics to make the residuals orthogonal to all included terms, and to try to make them have a Gaussian distribution.

Beware of LURKING VARIABLES

- Operators change
- Analysts take breaks
- Reagents decay
- Voltages vary
- Connections are made
 - and broken
- Etc., etc., etc.

TIME ORDER is often a proxy for LURKING VARIABLES

RANDOMIZATION of time order often helps, but

- will still need to check data, residuals, for time order effects, and
- simple randomization may be too expensive in time consumed, materials used or complexity of organization, so
- compromises may be desirable

Even very similar plots often show quite different things.

There is no substitute for making a wide variety of plots.

One of the chief benefits of computers is the ability to make many plots, easily.

"The standard practice in which the mode of analysis determines the assumptions about the data must be avoided." David A. Kenny, Psychological Bulletin, 1975.

"We cannot expect certainty from data, only fallible information." David A. Kenny, Psychological Bulletin, 1975.

Using high powered statistical methods is seldom the most important contribution a good practicing statistician makes toward the solution of a problem.

A Non-standard design problem

How do you find out how much a wildlife preserve is worth? Exhibit 4 gives much of the background for a study designed to help find out. Randomly selected hunters who were successful in obtaining a goose hunting permit were to be offered varying amounts of cash for their permit. The responses from these actual offers were to be compared with those from another group to which hypothetical questions were posed of the form "If we were to offer you \$100 for your permit, would you take it?"

The design problem posed to us was how to distribute the actual cash offers over the range from \$1 to \$200. We had a dose-response curve to design for -- with the dose being \$. A novel feature was that higher doses were much more expensive than lower doses. Existing data from hypothetical questions suggested a standard logistic model. If P is fraction accepting offer, then

$$\log\left(\frac{P}{1-P}\right) = \alpha + \beta \log(\$)$$

seemed to be a reasonable model. However there was reason to believe that higher percentages would accept actual cash offers, than would accept hypothetical offers. However, the magnitude of the difference was unknown.

The problem was as usual non-standard. There were multiple objectives:

- Estimate area over curve (expected value of the resource to a Hunter),
- Compare this area with that obtained by two cheaper and more standard methods (hypothetical offers and travel costs),
- Compare the whole curves for the three methods,
- Compare some particular points on the curves.

There were multiple constraints:

- A maximum of \$16,000 in offers would be made,
- We would lose part of our fee for services if the actual payments to hunters totalled over \$12,000.
- There was a fixed cost of about \$5 per offer.
- A design was needed quickly - hunted season was about to open.

What we did

First we made several false starts, each time helping to clarify the problem. Other steps included:

- Identified "worse plausible case" (many people accept our \$),
- Identified "expected case",
- Under these and other scenarios we computed a wide variety of things of interest for a variety of designs.
- We selected two candidate designs to discuss with researchers,
- The desire to keep from going broke became one primary consideration.

The somewhat surprising answer was that the average selling price turned out to be \$160, for the permit alone. Even if every hunter got his limit of one goose, the cost per pound would be over 10 times that in local stores.

Another design problem

In another situation we sought to develop procedures for creating small fractions of $2^a 3^b 4^c 5^d 6^e$ designs "on the fly". One such example was to create a fraction of a $2^2 3^2 5^1 6^1$ design in about 60 runs. A careful search of the literature gave little useful information so we developed some ad hoc procedures. To see how well they worked we tried them on a $2^3 3^3$ design with 72 runs in which we wanted to estimate all interactions up through linear by quadratic. Here a Connor-Young (1961) design was available as a benchmark.

The most important practical conclusion we reached was that simple random sampling without replacement of the rows from the full design, gave designs with about 80% efficiency. Since this was a simple procedure and since no other procedure did markedly better without a lot of work, it was decided that simple random sampling was good enough.

Literature

Since we frequently need to locate articles on some new topics, we make extensive use of the Current Index to Statistics.* Volume 3 covering 1977, for example, gives convenient access to over 5000 journal articles, books and conference proceedings.

* Available from American Statistical Association, 806 15th St., N.W., Washington, D.C. 20005.

Teaching

Most students learn only how to solve text book problems--and worse yet--learn to think that all problems should be text book problems. Appendix A reproduces a syllabus from a course designed to counteract this shortcoming of our educational system.

Concluding remarks

Those of us who practice data analysis and design have an obligation to keep reminding those who teach and do statistical research that most problems do not fit into any standard mold. I hope that these brief descriptions help some, but I know that more detail on many more problems is necessary if the message is to be brought home, where it matters.

Acknowledgements

It is impossible at this stage to recall everyone who has contributed to the ideas expressed here. However, some that surely merit particular mention are Peter Piet, David Hall, Alison Pollack, Dennis Fryback, Tom Heberlein, David Gustafson, Cathy Campbell, Jessie Gwynne and Candy Smith.

References

- Box and Jenkins (1970) Time Series Analysis: Forecasting and Control.
Holden-Day, San Francisco, CA.
- Joiner and Campbell (1976). "Designing experiments when run order is
important", Technometrics 18, 249-259.
- Connor and Young (1961). "Fractional Factorial Designs for Experiments with
Factors at Two and Three Levels", NBS, Applied Mathematics Series 58
- Anderson and Bancroft (1952) Statistical Theory in Research. McGraw-Hill
Book Co., New York.
- Draper and Smith (1966) Applied Regression Analysis. John Wiley and Sons,
Inc., New York.

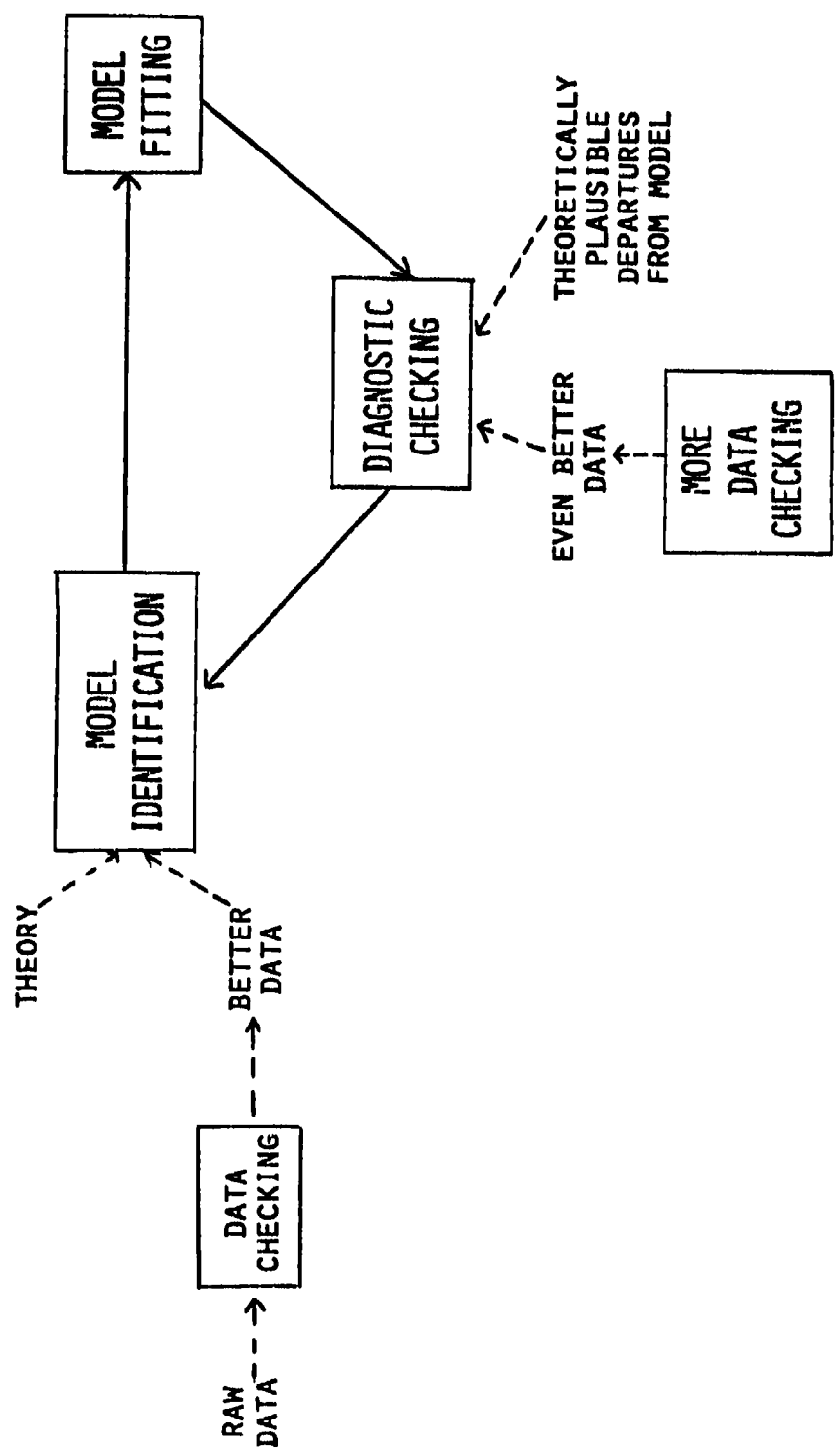


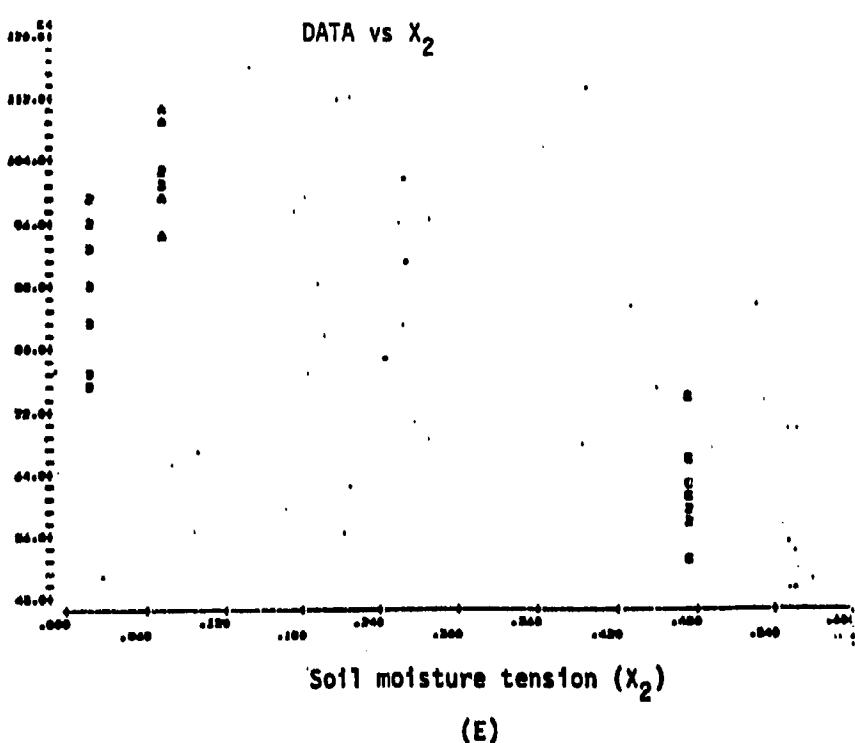
Exhibit 1

Key steps in the iterative process of data analysis and model building.

Exhibit 2 (continued)

Vitamin
B₂

DATA vs X₂



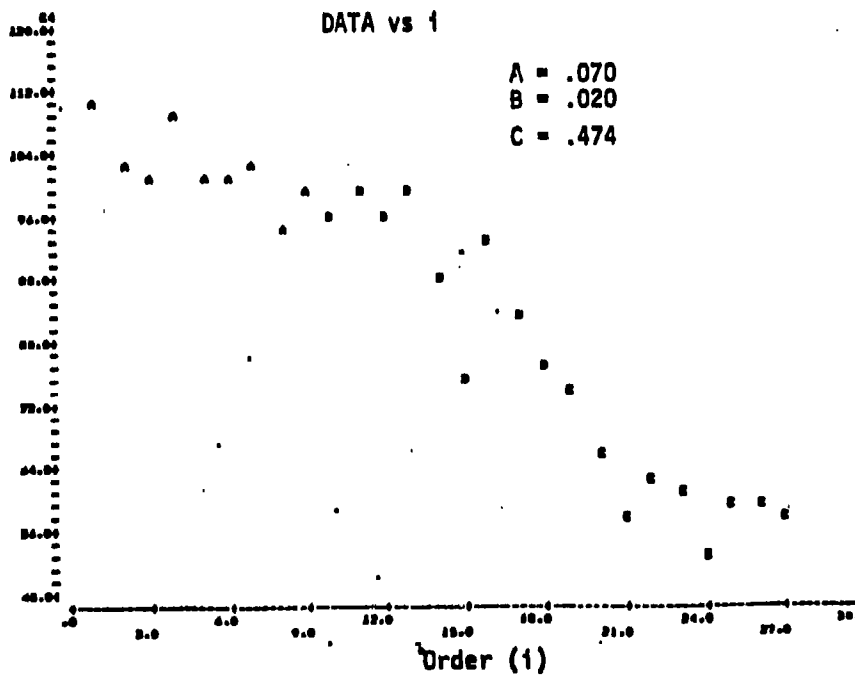
Soil moisture tension (X₂)

(E)

Vitamin
B₂

DATA vs 1

$$\begin{aligned} A &= .070 \\ B &= .020 \\ C &= .474 \end{aligned}$$



Order (1)

Letters denote values of X₂: A = 0.070, B = 0.020, C = 0.474.

Exhibit 3A
Measurements of oxygen content of steel rods, in order data taken.

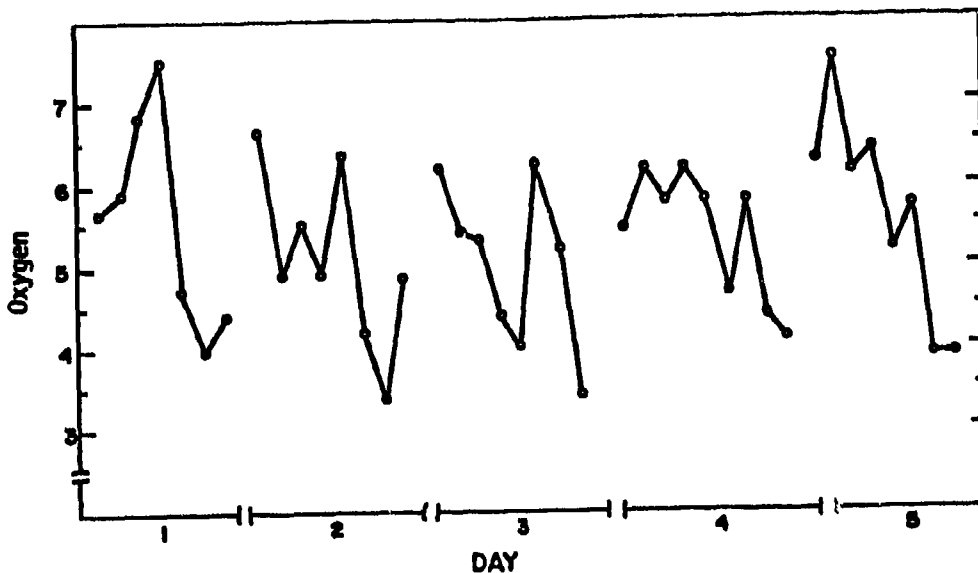
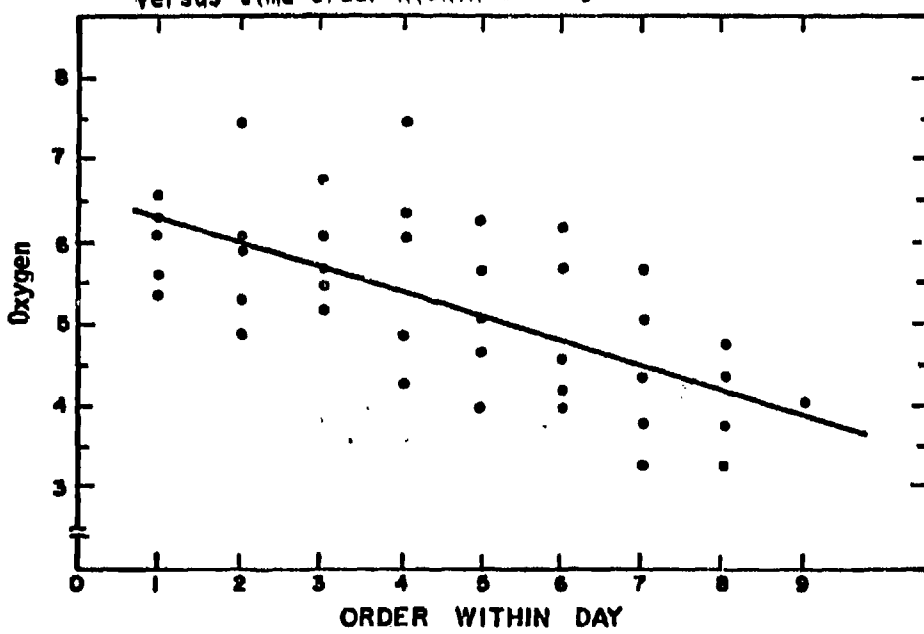


Exhibit 3B
Measurements of oxygen content of steel rods plotted versus time order within the day.



Chance to Shoot a Canada Goose Is Worth \$??? to a Hunter

By RALPH OLIVE
of the Journal Staff

HOW MUCH, in hard cash, is your hobby worth to you?

If you like to golf, would you be willing to forego the links for one summer if some mysterious benefactor paid you not to play? And if so, how much money would it take?

Two University of Wisconsin-Madison professors are trying to determine what financial value recreation has. They have taken goose hunters as their subject, and are putting the hunters to a test.

The project is being conducted by Richard C. Bishop and Thomas A. Heberlein, both associate professors in the Madison College of Agricultural and Life Sciences. Bishop explained the purposes of the research, and the way it is being conducted, in a telephone interview.

THE PROFESSORS obtained names of Wisconsin residents who were successful in obtaining the highly prized permits to hunt geese in the Horicon zone during the early season this year. The early season opens today and closes Oct. 18. A permit entitles a hunter to take one goose.

Letters and checks were sent to a number of hunters holding early season permits. The checks vary in amount. Bishop declined to reveal the range, but one person who contacted the Journal said he had been offered \$200, and another \$150. Each letter said, in part:

"Enclosed in this letter you will find a check from the University of Wisconsin. This check is negotiable and is made out in your name. We are offering to pay you this amount for foregoing the use of your early season Horicon Zone goose hunting permit . . .

"If you decide to forego the use of your permit at this price, you must put the permit and tag in the enclosed self-addressed stamped envelope and return it to us. If you decide not to forego the use of the permit, send us the check instead. If you return the check you should keep your permit."

Bishop said the transaction was legal, because the university will not use the permit. It will be returned when the hunting season is over.

Although depending on the honor system to some extent, Bishop said, if anyone tries to keep the permit and also cash the check, efforts will be made to recover the money.

A SECOND PART of the experiment involves sending a questionnaire to other goose hunters. Members of the second group are not being asked to give up their permits, but only to answer questions, such as how much they enjoy hunting, why they do it, and how long they have been interested in goose hunting. Each person who fills out a questionnaire will be paid \$5.

Altogether 900 persons are being contacted. Some are being asked to fill out the questionnaire, and others to give up their permits.

Bishop declined to discuss the amounts being offered the hunters to give up their permits, saying he was afraid that knowledge might affect the results. The amounts vary, because part of the object of the research is to determine how much money is required before a person will forego something he enjoys.

LAFTER IN the season, the two professors plan to interview a number of people who do participate in the goose hunt. They will ask the hunters how much they spent, and how valuable the hunt was to them as a recreational experience. Bishop and Heberlein received a grant of \$22,000 from the Wildlife Management Institute and Resources for the Future, both private groups with offices in Washington, D. C.

"We are not using any tax money," Bishop said.

The National Wildlife Federation's Conservation Directory lists the Wildlife Management Institute as a "national, nonprofit, private, membership organization, supported by industries, groups, and individuals, promoting better use of natural resources for the welfare of the Nation." Resources for the Future is listed as an organization that "works to advance the development, conservation, and use of natural resources and improvement of the quality of the environment through research and education programs."

Not all of the money is being used for payment to hunters. Bishop said there were other expenses, including clerical help and use of computers in compiling the results.

Bishop said the Wisconsin Department of Natural Resources was not involved in the study, although department officials know of it. Anthony Earl, DNR secretary, said the matter had been cleared with his office, and that the department, while not involved, had made no attempt to interfere.

Milwaukee Journal, Sunday, October 1

Discovery section (about page 5 or page 7)
Exhibit 4

APPENDIX A

Syllabus for
STATISTICAL CONSULTING
Fall 1978
Instructor: Brian Joiner

GOALS OF COURSE

Students will increase their knowledge of how one:

- A. analyzes data;
- B. gathers data;
- C. consults;
- D. uses the methodology literature;
- E. writes good reports.

GENERAL APPROACH

- We will tackle problems together, developing needed methodology as we go.
- We will work on:
 - old data sets;
 - live consulting data sets,
 - old data gathering situations;
 - live consulting data gathering situations.

BENEFITS OF APPROACH

- It could be a very exciting learning mode;
- It is well suited to my goals for the course.

CONCERNS OF MINE

- It will be a lot of continuous work for me;
- It will lead into areas that I know little about (could be embarrassing);
- Students may resent me not "teaching" them anything.

FALL BACK POSITION

- Like recent semesters
 - Hand out data sets for student analyses;
 - Talk about relevant methodology in class.

Implications:

- The specific techniques covered will not be considered as important as the general problem solving approach.
- We must assume students can cope with the literature under some guidance from me.
- It will be almost like "the real world", with attempts to maximize learning opportunities while working under my loose supervision.

MORE DETAILS

A. How to Analyze Data

- start from questions and data--not from statistical method;
- check data carefully and continually;
- formulate goals and questions precisely;
- formulate tentative models
 - mechanistic
 - empirical
- specify analytical approaches;
- use graphical techniques liberally
 - on data
 - on residuals
- organize hand work;
- use computers effectively, and intermix with hand work;
- bear in mind that summarizing and estimation should almost always be much more important than testing;
- finding the real uncertainty is often very difficult
 - multiplicity of procedures tried
 - complexity of structure of variation
- communicating results is an integral part of the analysis

Useful references (see below for details):

M&T; T; D&W; D; BH²; M-HB; FPP

B. How to gather data

- formulate goals precisely;
- quantify goals;
- specify variables precisely
- specify classes of candidate models
- describe blocking, realm of generalizability;
- consider alternative means of exposing true uncertainty;
- specify how you will seek to estimate
 - precision
 - bias
- describe plan for data gathering, in detail;
- describe randomization procedure in detail;
- describe data logging procedures in detail;
- if data will be computerized, describe process;
- specify ways that data will be checked;
- specify how data will tentatively be explored, summarized and otherwise analyzed;
- communicating alternative, tentative data gathering plans is an integral step.

Useful references:

BH²; S&C; Slonim; Williams; Kish; S²; C&S; Unobtrusive; FP? C&C; C.

C. How to consult

- how to interact productively;
- searching out the real problem;
- not limiting oneself to statistics
- helpful, resourceful attitude;
- sharing the work;
- proper level of sophistication of analyses/designs;
- communicating your understanding of problem;
- communicating your intended analysis/design strategy;
- communicating results of your analyses or plans for design;
- importance of good written communication;

References:

Schuchany; Joiner cryogenics

D. How to use methodology literature

- importance of not having to reinvent the wheel (especially square ones);
- how to find references of interest;

References:

Preface to CIS; CIS; NBS Index

E. Writing good reports

Good writing is a skill that can and must be learned. Practice and organization are key ingredients.

Some elements of a good report are often:

- executive summary
- description of problem; motivation; goals;
- description of data (and listing if appropriate);
- data checking procedures and results;
- non-technical overview of analysis strategy;
- results of analyses;
- recommendations for improvements in future data gathering;
- appendix: technical discussion of analyses
- appendix: data listing (if too long for body of report)

NOTE: In this class only 8 $\frac{1}{2}$ x11 inch paper can be used. Computer printout must be cut or xeroxed to this size; or if smaller, may be taped firmly to regular paper like part of the text of your report.

Some indicators of goal achievement

A. How to analyze data

- Reports of data analysis
 - data sets I hand out
 - data from consultations

B. How to gather data

- Reports of data gathering plans and results
 - situations handed out
 - consultations

C. How to consult

- diary-like reports of consultations (see Joiner Cryogenics)
- brief, one-half page personal reactions to consulting articles

D. How to use methodology literature

- brief annotated bibliography of key articles on some subject (e.g. errors in X's)
- brief review of 2 recent (appeared in last six months) methodology articles
- actual use of literature as evidenced in reports in A,B,C above.

E. How to write reports

- reports prepared for A,B,C and D above

Some work steps in learning to use computer effectively

On both UNIVAC 1110 and DEC 11/70 (WITS):

- enter data into a file and save;
- list file, edit some data and save corrected version;
- delete old file;
- on UNIVAC print TOC of:
 - Joiner*Data
 - MACC*MINITAB
- copy an element of JOINER*DATA or MACC*MINITAB and modify
 - delete one row
 - change several values
 - save modified version
- make Minitab runs using at least the following commands:
 - all types of plots; INDIC; EXECUTE; STORE K; LOG; NOBRIEF; ONEWAY; REGR; analyze residuals
- save a Minitab program, then execute it
- create an STJBANK using Minitab
- use Minitab to enter data from STJBANK & PRINT & PLOT
- use STATJOB to do regression and regression on logs
- use STATJOB to do BANKPRINT
- transfer data set from WITS->1110
 - " " " " 1110->WITS

References:

M-HB
M-RM
EDIT manual
STATJOB manuals
WITS manuals

To provide evidence of work you do in learning to use the computer:

- keep a diary, and write a report chronologizing your experience including listings of work steps, computer programs and output.

Some bench marks

By the end of the indicated week each student should have handed in documentation of the following:

<u>Week</u>	<u>Progress</u>
1	<ul style="list-style-type: none">- Proficiency on one computer (UNIVAC or DEC).- First data analysis or design report.
2	<ul style="list-style-type: none">- Brief annotated bibliography on some subject.- Second data analysis or design report.
3	<ul style="list-style-type: none">- Proficiency on second computer.- Brief summaries of two recent methodology articles.
4	<ul style="list-style-type: none">- Brief report on two papers on consulting- Should be able to use S&C and M&T (separate documentation not required)- Ideally should be involved as a consultant on some project (will depend on availability of projects).- Third data analysis or design report
5-15	<ul style="list-style-type: none">- At least four more reports on data analysis projects, design projects or consulting projects of increasing complexity.

A FEW IMPORTANT CONCEPTS IN ANALYSIS, AND KEY REFERENCES

Data checking: Critically important but no really good references.
See Daniel and D&W and Pollack & Joiner

Transformations(re-expression): M&T Ch. 4-6; ETA Ch. 3-6; Draper & Hunter (Tech. 1969); S&C; Box & Tiao.

Plotting data: M-HB; M&T; ETA.

Plotting and other analysis of residuals: D&S; M&T; Anscomb & Tukey.

Using computers: M-HB; M-RM; STATJOB manuals; BMDP manual; SPSS manual; SAS manual; Rummage manual; other special purpose programs.

Analysis of variance: Winer; BH²; M&T; Kirk; Hicks; Scheffe; Searle; MINITAB; Rummage; STATJOB; BMDP and other computer packages.

Outliers and seriously heavy tailed data; M&T; Denby & Mallows; Duter's computer program.

Missing Values: (See me and I'll get bibliography from Jock E.)

Categorical data: (...from Camil).

Non-independently distributed observations:

- Time series: B&J; BH²
- Components of variance situations: Anderson & McLean (3 places); Fuller & Battese;
- Other problems: Joiner & Campbell

Ethics: see 1977 CIS

Mechanistic model building: BH²

Empirical model building: D&W; BH²

Finding the real uncertainty: M&T; BH²

Variation in non-linearly transformed functions: BH²; Ku paper in Ku volume

GRADING

Each report (or other write-up) will be graded on three criteria

- quality of work,
- amount of work,
- quality of exposition.

Each criteria will be assessed on a three point scale

- + = well above average for course,
- / = as expected (average),
- = below expectation.

At the end of the semester you must return all of your work to me so I can review it and assign a grade for the course. You may pick up your materials after I have turned in the grades.

In assigning a final grade I consider all of the evidence you have submitted during the semester as to your potential as a practicing statistician. Grading is roughly as follows:

A = A very fine hiring opportunity for most anyone.

AB = Definitely above average. Would be well suited for some jobs but might have weaknesses in some others.

B = Average overall performance. Might be average in every respect or very good in some respects with critical weaknesses in others.

BC = Below average. Usually serious weaknesses in an important area, frequently due to low productivity, tardiness, poor exposition or repeated serious undetected "goofs" in analyses or designs.

C = Even further below average.

below C = ??

A few comments. I tend to reward hard creative work more than I punish the lack of. If you work hard and think a lot, you will probably get two benefits:

1. You will learn a lot, and
2. You will get a good grade.

If you don't work hard, you will surely suffer in the first and perhaps in the second. In short, you can gamble. In this course (and probably in others) the odds are probably about 50-50 of a decent grade with little effort. But if you choose to gamble, remember the possible loss in (2), and the sure loss in (1).

References

Probable extensive use

- M&T = Mosteller, F. and J.W. Tukey (1977). Data Analysis and Regression. Reading, Mass.: Addison Wesley Publ. Co.
- S&C = Snedecor, G.W. and W.G. Cochran (1967). Statistical Methods. Ames: Iowa State Univ. Press.

Other important references

- Anderson, Virgil L. and Robert A. McLean (1974). Design of Experiments. New York: Marcel Dekker, Inc.
- Anscombe, F.J. and J.W. Tukey (1963). "The Examination and Analysis of Residuals," Technometrics, V. 5, pp. 141-160.
- BH² = Box, George E.P., William G. Hunter and J. Stuart Hunter (1978). Statistics for Experimenters. New York: John Wiley and Sons.
- Box, G.E.P. and G.M. Jenkins (1970). Time Series Analysis. San Francisco: Holden-Day, Inc.
- Box, G.E.P. and G.C. Tiao (1973). Bayesian Inference in Statistical Analysis. Reading, Mass: Addison-Wesley Publ. Co.
- Campbell, Donald T. and Julian C. Stanley (1966). Experimental and Quasi-Experimental Designs for Research. Chicago: Rand-McNally.
- C = Cochran, W.G. (1963). Sampling Techniques. New York: John Wiley and Sons.
- C&C = Cochran, W.G. and G.M. Cox (1964). Experimental Designs. New York: John Wiley and Sons.
- D = Daniel, Cuthbert (1976). Applications of Statistics to Industrial Experimentation. New York: John Wiley and Sons.
- D&W = Daniel, C. and F.S. Wood (1971). Fitting Equations to Data. New York: John Wiley and Sons.
- Denby, L. and C.L. Mallows (1977). "Two Diagnostic Displays for Robust Regression Analysis," Technometrics, V. 19, pp. 1-14.
- Draper, N.R. and W.G. Hunter (1969). "Transformations: Some Examples Revisited," Technometrics, V. 11, pp. 23-40.

- D&S = Draper, N.R. and H. Smith (1966). Applied Regression Analysis. New York: John Wiley and Sons.
- Dutter, Rudolf (Jan. 1976). Computer Linear Robust Curve Fitting Program LINWDR, Rsr. Rept. No. 10. Zurich: Fachgruppe Fuer Statistik, Eidgenessische Technische Hochschule.
- FPP = Freedman, David, Robert Pisani and Roger Purves (1978). Statistics. New York: W.W. Norton and Co., Inc.
- Fuller, Wayne A. and George E. Battese (Sept. 1973). "Transformations for Estimation of Linear Models with Nested-Error Structure," J. Am. Stat. Assoc., V. 68, pp. 626-632.
- Hicks, Charles R. (1973). Fundamental Concepts in the Design of Experiments (2nd edn.). New York: Holt, Rinehart and Winston.
- CIS = Joiner, Brian L. (ed.) (published annually since 1975). Current Index to Statistics: Applications, Methods and Theory, Am. Stat. Assoc., Washington, D.C., and Inst. Math. Stat., San Carlos, Calif.
- Joiner, Brian L. (1977). "Evaluation of Cryogenic Flow Meters: An Example in Non-Standard Experimental Design and Analysis." Technometrics, V. 19, pp. 353-380.
- Joiner, Brian L. and Cathy Campbell (1976). "Designing Experiments When Run Order Is Important", Technometrics, V. 18, pp. 249-260.
- NBS Index = Joiner, Brian L., N.F. Laubscher, Eleanor S. Brown and Bert Levy (Sept. 1970). An Author and Permuted Title Index to Selected Statistical Journals. NBS Sp. Publ. 321, Washington, D.C.: Natl. Bur. Std.
- Kirk, R. (1968). Experimental Design: Procedures for the Behavioral Sciences. Brooks: Belmont, Calif.
- Kish, Leslie (1965). Survey Sampling. New York: John Wiley and Sons.
- Ku, H.H. (1969). "Notes on the Use of Propagation of Error Formulas. Precision Measurement and Calibration". NBS Sp. Publ. 300, V. 1. Washington, D.C.: Natl. Bur. Std.
- Natrella, Mary Gibbons (1966). Experimental Statistics. NBS Handbook 91. Washington, D.C.: Natl. Bur. Std.
- Pollack, Alison and Brian L. Joiner (June 1978). "All Data Sets Have Errors - Well, Almost All", to be published in proceedings of Electricity Pricing Res. Inst. Workshop on Modeling and Analysis, San Diego, Calif.

- M-HB = Ryan, Thomas A., Jr., Brian L. Joiner and Barbara F. Ryan (1976). MINITAB Student Handbook. North Scituate, Mass.: Duxbury Press.
- M-RM = (1978). MINITAB II, Reference Manual. Minitab Proj., Stat. Dept., Penn. State Univ., University Park.
- Scheffe, Henry (1959). The Analysis of Variance. New York: John Wiley and Sons.
- Searle, S.R. (1971). Linear Models. New York: John Wiley and Sons.
- Slonim, Morris James (1960). Sampling. New York: Simon and Schuster, Inc.
- S^2 = Sukhatme, Pandurang V. and Balkrishna V. Sukhatme (1970). Sampling Theory of Surveys with Applications (2nd edn.). Ames: Iowa State Univ. Press.
- T = Tukey, J.W. (1977). Exploratory Data Analysis. Reading, Mass.: Addison Wesley Publ. Co.
- Williams, William H. (1977). A Sampler on Sampling. New York: Academic Press.
- Winer, B.J. (1971). Statistical Principles in Experimental Design. New York: McGraw-Hill Book Co.
- W&S = Woodward, Wayne A. and William R. Schucany (1977). "Bibliography for Statistical Consulting," Biometrics, V. 33, pp. 564-565.

LASER BEAM WAR GAMES: DESIGN, ANALYSIS, AND MODELING CONSIDERATIONS

W.S. Mallios, R.D. Batesole, and D.R. Leal
The BDM Corporation

ABSTRACT. Concepts in classical design, analysis, and modeling require reexamination under force on force experimentation with real time casualty assessment. The degree of allowable free play between opposing sides must be prespecified in the design and conduct of encounters. Severely limiting free play can degrade whatever realism is achieved through such games, while maximizing free play leads to imbalances in the evaluation of treatment effects. Regarding analysis, adjustments are required for imbalances. However, adjustments through standard covariance analysis can be misleading since treatments affect many of the covariates. Regarding development of simulation models, a broad class of cause and effect relations can be estimated and evaluated in terms of the experimental data. Methods of structural regression are used in developing a data based simulation model for mounted combat.

1. Force on Force Experimentation.

"Hoping to add a touch of battlefield realism to its peacetime training exercises, the Army is developing a complex laser beam system that permits two forces to shoot at...each other without hurting anyone... When the system goes into operation...it will for the first time advance scorekeeping in war games significantly beyond the level of children shouting, 'Bang, bang, you're dead'." Los Angeles Times, 8/23/76.

In force on force experimentation, the trend is towards real time casualty assessment (RTCA). Opposing forces utilize weapons equipped with low intensity laser guns, laser-sensitive devices (sensors), and automatic telemetric links to and from a computer. When a combatant detects a target and engages it, he fires his weapon activating the laser gun. If he is on target, that target's sensors are activated. The physical parameters of the engagement (weapon type, target type, target exposure, range, etc.) are automatically transmitted to the computer which records the data, assesses the results, and, if a casualty is indicated, transmits that information to the target for attrition.

The objective of one such experiment was to evaluate the effectiveness of foxhole fortifications in dismounted combat. The scenario called for a threat force to attack and penetrate defense positions under a variety of conditions. Preliminary analyses indicated that threat tactics -- a free play variable -- had a major effect on threat penetration. The designator "free play" for tactics means that a threat team leader was free to choose tactics he thought best in the particular trial. Composed of 24 men -- 3 squads of 8 men each -- threat teams commonly employed two tactics with variations on each: (i) two maneuver squads and one fire squad, and (ii) one maneuver squad and two fire squads. The latter led to considerably greater threat success, a result which illustrates that serendipitous effects are a by-product of free play, force on force experiments.

Currently on the drawing board is an experiment planned to evaluate the effectiveness of a force guarding a nuclear facility to deter an attacking terrorist force. The scenario calls for a surprise attack by terrorists with the intent of securing and removing mock nuclear materials stored on site. The perimeter is brightly illuminated, open terrain. The terrorist force obscures its detection by attempted entry disguised as delivery vendors, innocuous travelers, or other deception. Engagement commences upon detection, identification, or overt act. A free play fire fight ensues until the terrorists are defeated or the terrorist mission is accomplished. Factors to be varied in this scenario include guard-terrorist forces sizes, weapons mixes, defense configuration (elevated guard tower, submerged pill box, or no special structure), and penetration distances from the outer perimeter to the storage area.

2. The Experiment Under Study. Data used in model building are drawn from TEMAWS*, an experiment on the effectiveness of scatterable mines on an attacking armor force. The tactical scenario was an attack by a Soviet tank company through a scatterable**, antitank minefield against a defending U.S. mechanized infantry team. Simulating the Soviet force were 15 M60 tanks reinforced by three APC TOWs. One M60 tank, two TOWs, and two Dragons simulated the U.S. force. A trial consisted on one complete attack through the minefield. The trial ended when the last attacking tank had penetrated the minefield or when all threat tanks had been killed. Figure 2.1 depicts a typical trial where the Cs denote the center of mass, in successive 30 second increments, of threat tanks advancing towards the defense. Minefield dimensions are 300 meters by 1000 meters. Threat configurations during minefield entry are illustrated for two trials in Figure 2.2. Figure 2.3 depicts an end of trial result where M denotes a mine or mobility kill, F denotes a direct fire kill on a threat tank, and I denotes a Dragon kill by threat artillery.

3. Statistical Design Considerations. In designing force on force experiments, there are constraints imposed by priorities, the budget, time, and the state of the art of the experimental technique. The constraints usually limit the number of treatments which can be evaluated in the experiment. Accordingly, there are two schools of thought regarding the conduct of the experiment once treatments are selected:

- (3.1) limit free play by controlling more of the uncontrolled variables; i.e., neutralize the effects of certain uncontrolled variables as opposed to expanding the number of treatments.;
- (3.2) allow free play to a maximum possible extent.

Those advocating (3.1) are usually motivated by imbalances arising from free play -- imbalances which complicate evaluation of treatment effects. Imbalances are illustrated by a partial listing of the TEMAWS design matrix in Table 3.1.

* TEMAWS is an acronym for tactical effectiveness of scatterable mines in the antiarmor weapons system.

** In tactical situations, mines may be scattered by artillery or helicopter

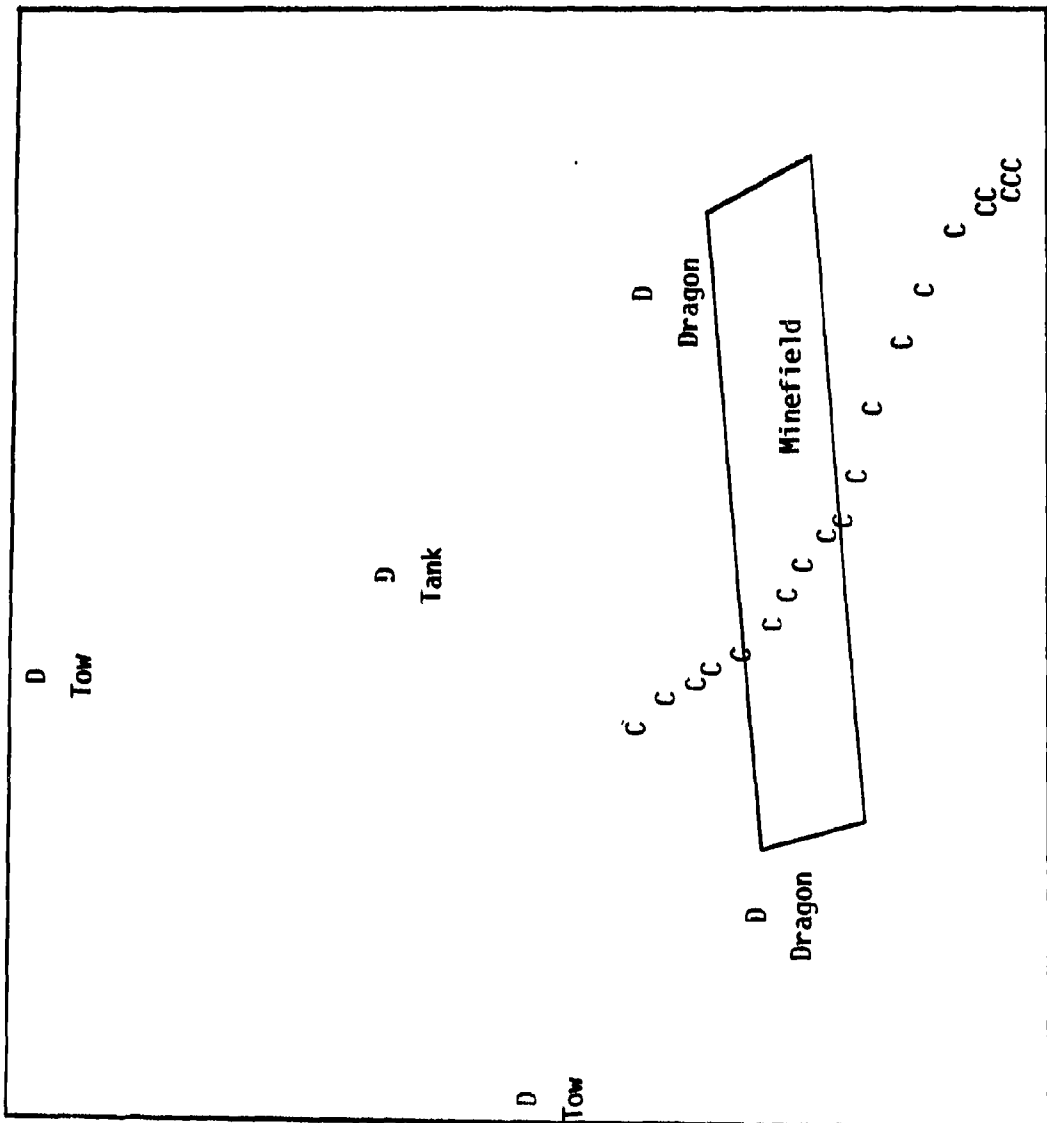


Figure 2.1 The Advancing Threat Force (excluding reinforcements)
Depicted in Terms of its Center of Mass (C) in successive
30 second Time Intervals.

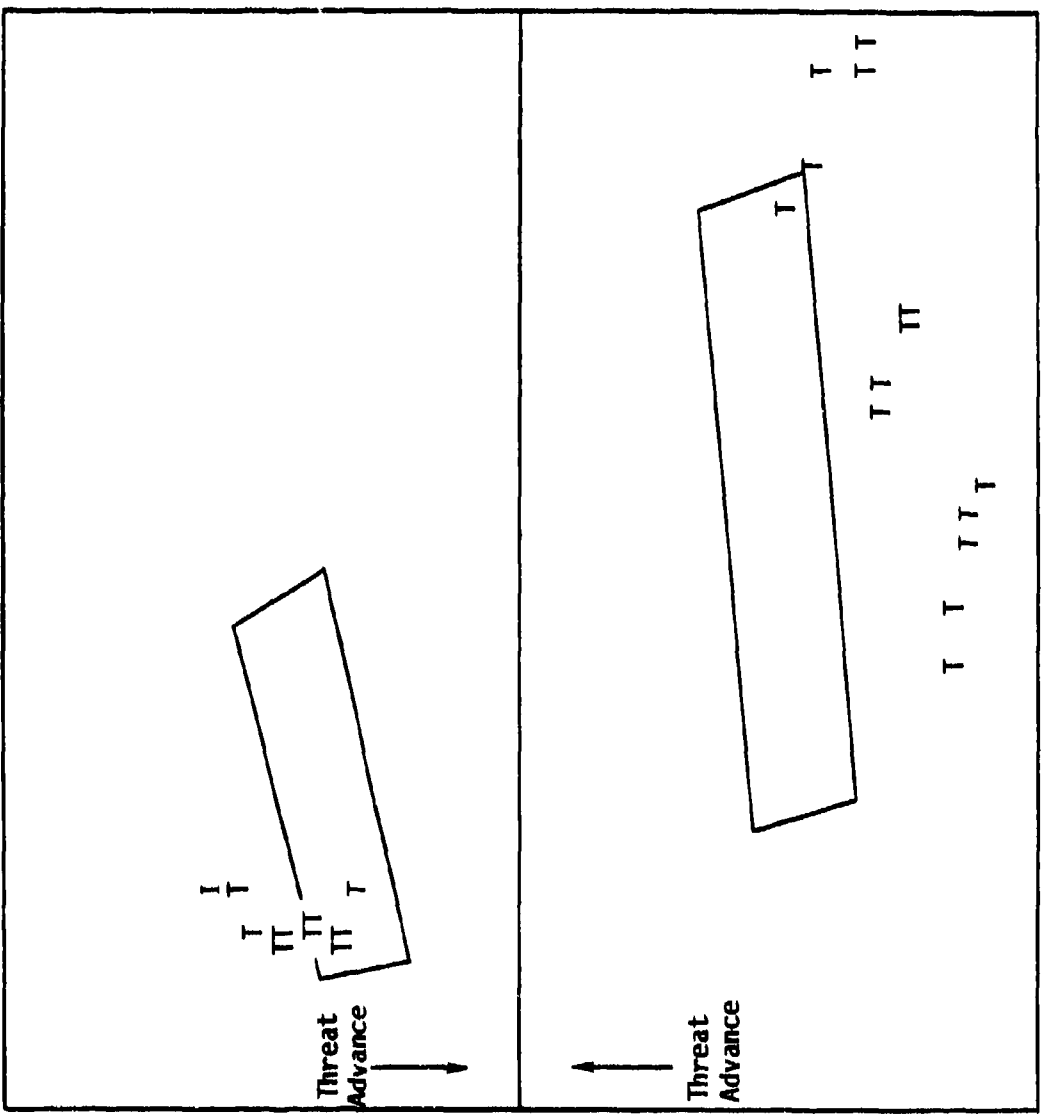


Figure 2.2 Threat Configurations During the 30 Second Interval
in Which the First Threat Tank Enters the Minefield.

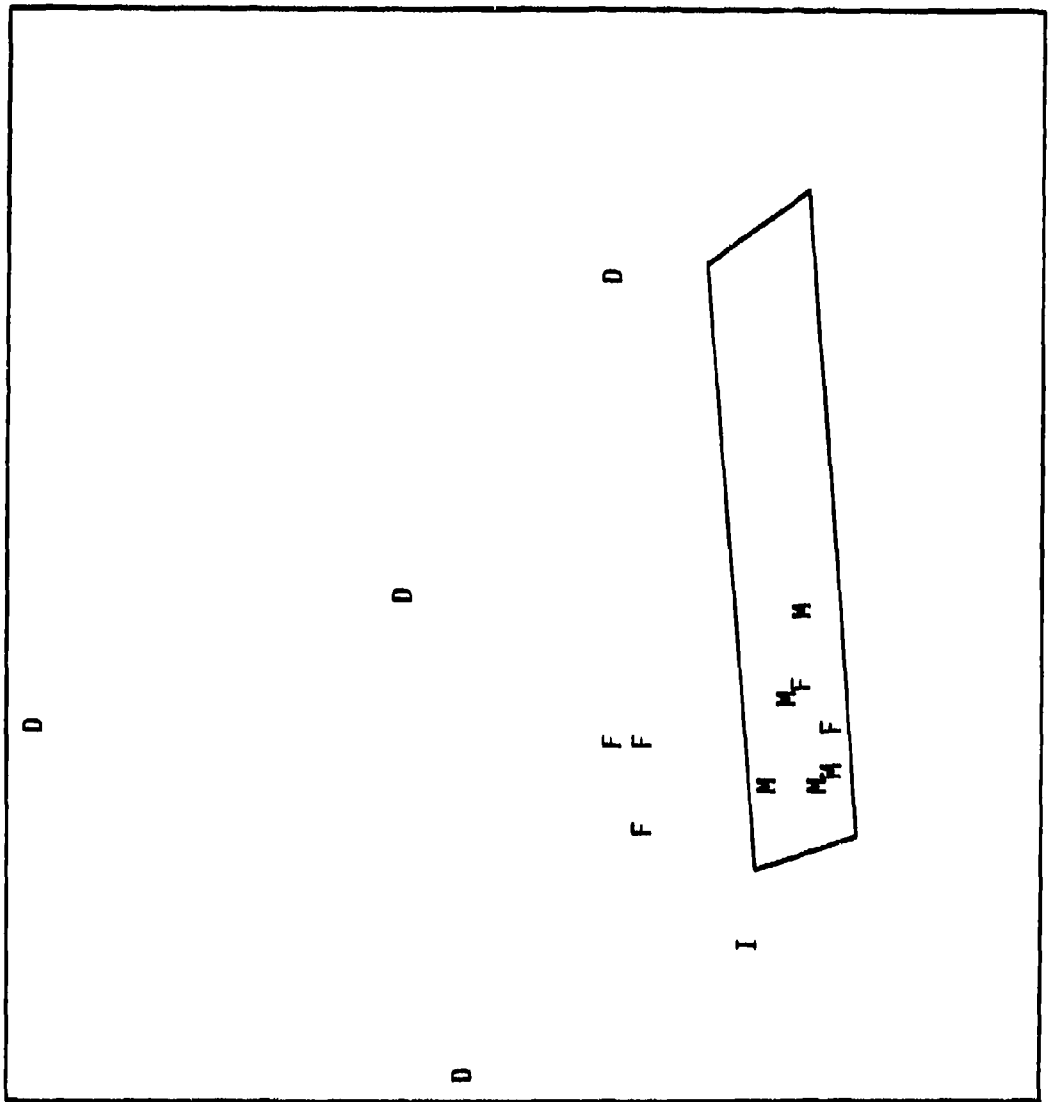


Figure 2.3 An End of Trial Result: D, Live Defense Weapon
 M, Mine Kill
 I, Artillery Kill
 F, Direct Fire Kill on Threat

Table 3.1 Summary Statistics for the Time Period Prior to When
the First Tank Enters the Minefield.

MINEFIELD DENSITY (Mines/Meter²)

Visibility	.00025	.0005	.001	.003	.0005	.01	BASELINE
Very Low	3, 1, 1 10-13						
Low	4 ⁽¹⁾ , 2 ⁽²⁾ , 0 ⁽³⁾ , 13-91 ⁽⁴⁾	5, 3, 0	6, 1, 1	5, 0, 5	4, 0, 1		8, 6 ⁽⁵⁾ , 1 ⁽⁶⁾
High	3, 3, 1 19-25	5, 2, 4 23-57	5, 1, 2 8-154	3, 3, 0 18-122	6, 2, 0 3-56		

(1) No. Trials

(2) No. Trials Where at Least One APC was Killed Before Minefield Entry

(3) No. Trials Where at Least One TOW was Killed Before Minefield Entry

(4) Range of Artillery Pairings Before Minefield Entry

(5) No. Trials Where at Least One APC Never Fired.

(6) No. Trials Where at Least One TOW Never Fired

Minefield density refers to the number of mines scattered uniformly over an area of 1000 meters by 300 meters. Visibility refers to the visibility of the mines to the oncoming threat force. Baseline trials are those for which there was no minefield. Numbers contained within the cells summarize events up to the time the first threat tank enters the minefield. In comparing, for example, low and high visibility at the .005 density, it is seen that for all five trials of low visibility, at least one TOW was killed before the first tank entered the minefield. Thus, for all trials of this treatment, the defense was one weapon short during the main part of the battle where synergistic effects of the minefield and defense fire on threat attrition were to be examined. Conversely, for all six trials of high visibility, both TOWs were available on first threat entry into minefield.

Without adjustment for imbalances, differences between the effects of these two treatments on end of trial dependent variables -- such as total threat casualties or casualty exchange ratios -- could be due to the difference in mine visibility, to the shortage on one TOW, to a combination of the two, or to other imbalances. With such complications brought on by imbalances, it is tempting to severely limit free play; e.g., conduct trials under the condition of no kills on either side prior to threat entry into the minefield. The difficulty with this recourse is that it runs counter to the purpose of RTCA -- attempted parity with realism. Sacrificing realism to attain greater balance is generally unacceptable since this recourse elevates the method of analysis to a higher level than the experimental objectives.

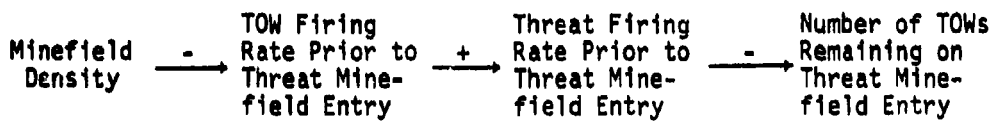
Aside from greater realism, an additional feature of (3.2) is the emergence of serendipitous effects. Notice, for example, the difference in threat configurations in Figure 2.2. One configuration shows a single cluster* of tanks and the other, three rather loose clusters. Entry and passage through the minefield in a single, tight cluster tends to reduce minefield kills but increases direct fire kills; i.e., a single, tight cluster draws more defense fire. Conversely, a highly scattered threat configuration, as quantified by a number of loose clusters, tends to increase minefield kills but reduce direct fire kills. Thus, there is a trade-off between minefield kills and direct fire kills on the threat which is dependent on threat clustering. This result was not anticipated in planning the experiment and would not have been uncovered had the configuration of threat tanks been prescribed and nearly constant between trials. In fact, it has become increasingly evident that, not only can serendipitous effects be expected to occur, but their effects on trial outcomes can be greater than that of treatments.

4. Analysis Considerations. When effects of treatments on end of trial dependent variables are analyzed without adjustment for free play variables, a common result is that treatments are insignificant. This result can be misleading since, under (3.2), effects of free play variables can dominate effects of treatments on trial outcomes; e.g., the loss of a defense weapon prior to threat minefield entry can have a greater effect on trial outcome than the visibility of mines. Moreover, adjustments for free play variables in terms of standard

* Threat force configuration, excluding reinforcements, is quantified in terms of clusters and non clusters within each of the areas prior to the minefield, within the minefield, and beyond the minefield. Clusters are updated every 30 seconds and are determined by the single link method (1). Within each area, a tank is part of a cluster if it is within 100 meters of a cohort. Also within each area, a tank is a non cluster if it is greater than 100 meters from the closest cohort.

covariance analysis are misleading when treatments affect the free play co-variables and treatment effects on the covariables are neglected*; see (4), (5).

An example of treatments affecting a covariate, say, the number of TOWs remaining on first threat entry into the minefield, is as follows. Suppose the TOW firing rate prior to threat entry into the minefield is negatively correlated with minefield density. Since the TOW firing signature is pronounced, its increased fire draws increased threat fire which decreases the TOW's chance of survival. Thus, minefield density has an indirect effect on the number of TOWs prior to threat minefield entry -- indirect in the sense that the effect of minefield density of TOW survival is through the TOW firing rate and the subsequent threat firing rate:



where $x \xrightarrow{+} y$ reads "x has a positive, direct effect on y". When the flow of events are characterized by this path diagram, a separate equation must be considered for each variable (other than minefield density) in evaluating treatment effects on dependent variables of interest.

The recourse to situations where treatments have possible effects on co-variables is the analysis of direct, indirect, and overall treatment effects as quantified through a structural regression system; see Appendix A. In such an analysis, each trial may be partitioned according to time intervals, whether fixed, random, or a combination thereof, and relevant variables are measured from each of successive intervals. To partition according to random time intervals is to partition according to events. For example, a scheme for event partitioning is the division of trials into before and after first threat entry into the minefield. A model for this scheme is as follows:

$$\sum_{h^*} \alpha_{bhh^*} y_{h^*}(b) = \sum_j \lambda_{bhj} x_j + \delta_{bh} \quad (4.1)$$

$$\sum_{h^*} \alpha_{ahh^*} y_{h^*}(a) = \sum_{h^*} \lambda_{ah^*} y_{h^*}(b) + \sum_j \lambda_{ahj} x_j + \delta_{ah}$$

where $y_{h^*}(b)$ and $y_{h^*}(a)$ denote the h^* -th endogenous variables during the before and after periods, respectively, $h, h^* = 1, \dots, p$; $\alpha_{fhh^*} = dy_h(f)/dy_{h^*}(f)$, the direct effect of $y_{h^*}(f)$ on $y_h(f)$, $f = a, b$; $\alpha_{fhh} = 1$; $\lambda_{ah^*} = dy_h(a)/dy_{h^*}(b)$,

* Even when treatments do not affect covariate, high correlations between co-variables can lead to poor treatment estimates; see (2), (3).

the direct effect of $y_{h*}(b)$ on $y_h(a)$; the x_j include treatment effects which are assumed constant within trials; $\lambda_{fhj} = dy_h(f)/dx_j$, the direct effect of x_j on $y_h(f)$; ϵ_{fh} is the model error. In evaluating treatment effects, note that x_j may have direct effects on both $y_h(a)$ and $y_h(b)$ and, hence, an indirect effect on $y_h(a)$ through $y_h(b)$. The overall x_j effect on $y_h(a)$ is the sum of the direct and all indirect effects of x_j on $y_h(a)$; see (5).

While simple, model (4.1) has the disadvantage that variables may be over aggregated which leads to a loss in information. For example, suppose a key factor in trial outcomes is the number of threat losses in the first minute after threat minefield entry. Aggregating this variable over the entire after period may obscure its importance. As such, the partitioning of TEMAWS trials employs both fixed and random time intervals. The random intervals (or event segments) are:

- (i) the time segment to t_0 , the time the first threat tank enters the minefield
 - (ii) t_0 to $t_0 + 150$ seconds
 - (iii) the time segment beyond $t_0 + 150$ seconds.
- (4.2)

The time line within each event segment is incremented into successive 30 second intervals from which relevant variables are measured:

$$\dots, \underbrace{[t_0 - 30, t_0]}, \underbrace{[t_0, t_0 + 30]}, \dots, \underbrace{[t_0 + 120, t_0 + 150]}, \underbrace{[t_0 + 150, t_0 + 180]}, \dots$$

First Event Segment Second Event Segment Third Event Segment

A model for this partitioning is as follows:

$$\sum_{h=1}^p \sum_{i=0}^{r_{hh*}} a_{ehh*i} y_{h*}(t-i) = \sum_{j=1}^q \sum_{i=0}^{r_{hj}} \lambda_{ehij} x_j(t-i) + \epsilon_{e*t}(t) \quad (4.3)$$

where $y_h(t)$ is the h -th endogenous variable in the t -th time interval and $y_h(t-i)$ is its i -th lag; $a_{ehh*i} = dy_h(t)/dy_{h*}(t-i)$, the direct effect of

$y_{h*}(t-1)$ on $y_h(t)$ in event segment e; e = 1, 2, 3 as defined in (4.2); $\alpha_{ehh0} = 1$; δ_{eh} (t) is the model error. Contrary to model (4.1), exogenous variables (other than lags of endogenous variables) are written as $x_j(t)$ to allow for variation in x_j within trials*; $\lambda_{ehij} = dy_h(t) / dx_j(t-i*)$, the direct effect of $x_j(t-i*)$ on $y_h(t)$, where $x_j(t-i*)$ is the value of x_j in time interval $t-i*$.

Treatment effects which are constant within trials tend to have decreasing direct effects on $y_h(t)$ with increasing time; i.e., as trial time increases, treatment effects on $y_h(t)$ are generally indirect and through $y_h(t-1)$ and $y_{h*}(t-1)$. Put simply, as the encounter progresses, performance variables tend to reflect the initial effects of treatments. Another reason for the decreasing effect, at least regarding minefield density, is that mines expended through encounters are not replaced. With a large threat force, the density would tend to decrease with increasing threat penetration. Effects of the decreasing density are reflected through, not only lagged variables for mine encounters, but through a variable measuring cumulative mine encounters.

The event segments in (4.2) are chosen such that coefficients in model (4.3) remain stable within segments for key uncontrolled variables**. The objective is to attain stability of coefficients with as few event segments as possible; i.e., since coefficients are unstable between event segments, a structural system is estimated for each segment. The 30 second intervals within event segments were chosen to prevent an over-aggregation of variables and to avoid causal feed backs whenever possible; i.e., the 30 second intervals are sufficiently small so that the structural system is largely recursive; see Appendix A.

5. Data Based Simulation Models. With the constant monitoring and RTCA of weapon systems throughout the encounter, laser beam war games have a major impact on modeling: (i) a broader class of cause and effect relations*** can be examined relative to non-RTCA experiments and (ii) cause and effects relations can be estimated in terms of the experimental data. The negative side of data based models is that there exist artificialities in field experiments.

* An example of x_j varying within trials is artillery fire which varies according to a prespecified rate for a portion of the encounter.

** It is not feasible to establish stability of coefficients for all endogenous variables due to their large number.

*** The term "A causes B" can be defined in terms of "A affects B", which implies that a change in the level of B is associated with a change in the level

These, however, can be largely mitigated through subjective adjustments of estimated relations. Thus, at the very least, sensitivity analyses can be performed on the mitigation of artificialities.

The alternative to data based models are non-data based models which were the only recourse prior to RTCA. These include deterministic models such as the original Lanchester model (6) and stochastic models which utilize data inputs (7), (8). Generally, these models do not or cannot address a number of relevant cause and effect relations. Take, for example, the number of mine encounters in the t -th time interval, say, ME (t). A non-data based model may predict ME (t) conditional on minefield density and, perhaps, on mine visibility. Under (4.3), the data based model predicts ME (t), not only in terms of density and visibility, but on the clustering of tanks in the minefield in $t-1$, on the dispersion of these clusters, on the rate of movement of tanks into and out of the minefield in $t-1$, on the firing rate of tanks in the minefield in $t-1$, and on cohort kills among threat tanks in the minefield in $t-1$. Moreover, ME (t) is affected by ME ($t-1$), ME ($t-2$),...; i.e., the data based model does not assume that the present is independent of the past as do many of the non-data based models; events which occur at one time interval can have a major effect on events occurring at subsequent time intervals.

Cause and effect relations comprising the data based model are estimated in terms of (4.3). There are advantages to this type of model. Firstly, structural regression is a well established, rigorous method of data based modeling as evidenced by its use in econometric modeling; see (9), (10). Secondly, when the linearity assumption is invalid (or when coefficients are not stable from one event segment to the next), a separate system can be fitted per event segment; i.e., rather than having to convert to a non-linear system, the time line is partitioned according to event segments such that response surfaces are adequately fitted by hyperplanes within segments*. Thirdly, (4.3) is a vehicle for evaluating treatment effects under the scenario of the experiment from which the data are drawn. This is an important feature in the presence of imbalances. Fourthly, (4.3) provides a solid foundation for excursions to other scenarios in evaluating treatments not considered in the experiment; e.g., weapon trade-off analyses can be performed, as in Section 8; or "dirty battlefield" scenarios can be simulated with varying degrees of obscuration and suppression. Finally,

(***cont'd) of A. There are two types of association. Either A is a mechanism through which B changes or A reflects (or is correlated with) some unknown, unmeasured, unused, or unavailable variable U which is a mechanism through which B changes. Note that only in the first type of association does A necessarily precede B in the sequence of events. Note also that knowledge of the type of association may be more likelihood than certainty.

* The transition from one event segment to the next or from one system of equations to the next is smooth due to the use of lag variables; i.e., lagged effects from the previous event segment are used in the equations for the current event segment.

this type of data based model provides a means of quantifying effects of player psychological profiles on encounter outcomes*.

6. A Path Diagram for TEMAWS. To avoid underidentification in (4.3), additional information is required on a number of parameters per equation. Usually, this information is derived from a subjective assessment that certain direct effects do not exist. In TEMAWS, this assessment is partially summarized by the path diagram in Figure 6.1 wherein all arrows denote direct effects. Threat configuration is t-1 affects threat fire, mine encounters, and defense fire in t. In listing the following variables which comprise threat configuration, P, W, and B denote, respectively, all threat positions prior to, within, and beyond the minefield:

- (6.1) the number of clusters** and non-clusters in each of P, W, and B at the end of each time interval
- (6.2) minimum ranges*** between each defense weapon and both clusters and non-clusters within each of P, W, and B
- (6.3) the dispersion*** of those clusters in (6.2)
- (6.4) the change in the number of clusters and non-clusters from t-2 to t-1 and from t-3 to t-2.

In model (4.3), these configuration variables are not only predictors in t-1, but are individually predicted in t.

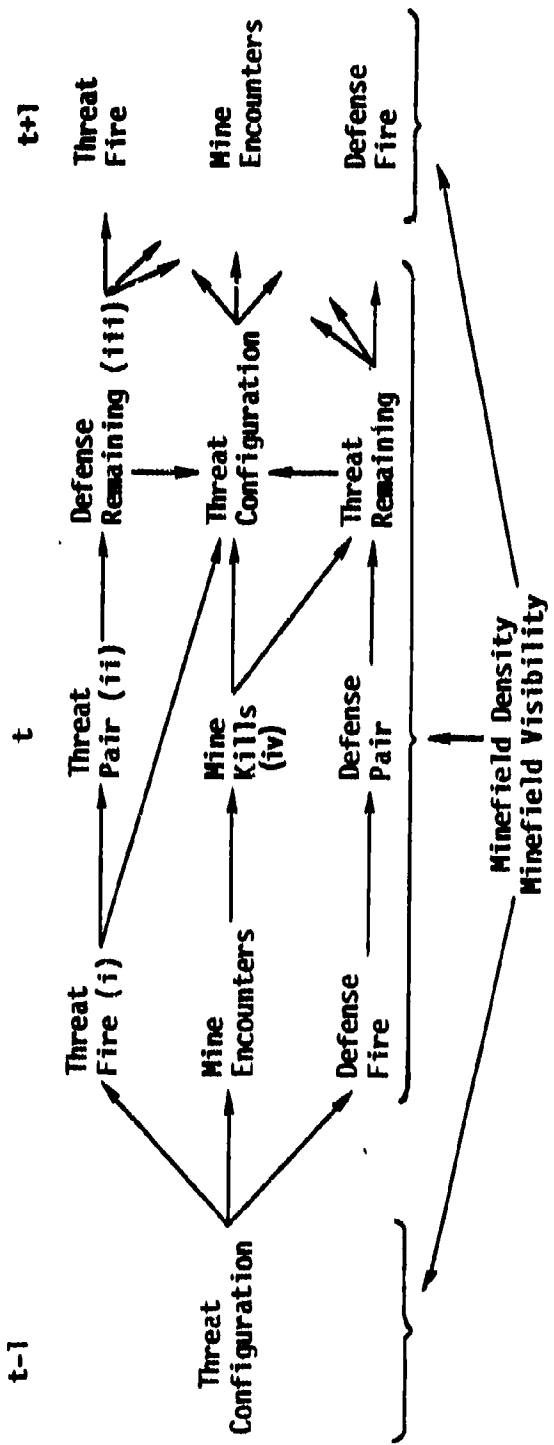
Within t, firings affect pairings, pairings affect attrition, and attrition affects threat configuration. In turn, configuration in t affects firings and mine encounters in t+1.

* In linear, reduced models, player or team effects are often quantified in terms of dummy variables whose coefficients are random effects. If, prior to the experiment, each participant responds to an appropriate psychological inventory, the responses can be converted to scores in terms of principal component or factor analysis; the scores become covariates which replace the dummy variables; see (1). In applying model (4.3) to TEMAWS data, player effects are reflected by performance data; i.e., dummy variables for player or team effects were not introduced and no psychological inventory was utilized in TEMAWS. Modeling in future RTCA experiments could be enhanced by utilizing an inventory, by quantifying players in terms of "psychological covariates", and by using these covariates as exogenous variables which are constant within trials. Proper rotation of personnel allows for these covariates to vary between trials.

** The threat reinforcements are not included in the threat tank clusters.

*** The reciprocals of the ranges and dispersion are used in the model; i.e., when a cluster or non-cluster is not present in P, or W, or B, the corresponding range and dispersion are set equal to zero.

Figure (6.1) A Path Diagram for TECWS



- (i) Threat fire includes firing by each threat tank and reinforcements include primary firings (by the 155mm main gun) and secondary firings (by the 7.62 coaxial mounted machine gun).
- (ii) A pairing occurs when a target becomes a candidate for attrition; i.e., the target has been fired on and its sensors have been activated.
- (iii) For defense weapons, attrition also includes personnel kills.
- (iv) Mine kills include both the mobility kill where the tank can fire but not move and the total kill where the tank can neither move nor fire.

Within t, mine encounters affect mine kills*. Each defense weapon is modeled individually regarding firings, pairings, and attrition**. Threat reinforcements and artillery are modeled individually regarding firings, pairings and attrition. For each t, threat tank firings*** are aggregated and modeled as an entity within each of P, W, and B, as are threat tank pairings and attrition.

The path diagram does not depict lagged effects. Lags of each variable extend back to at most five time intervals. Generally, the lags of $y_{eh^*}(t)$ do not have a direct effect on $y_{eh}(t)$, $h \neq h^*$. Exceptions to this are lags of mine kills affecting mobility kills and lags of pairings affecting firings for certain defense weapons.

The length of the interval t is sufficiently small such that causal feedbacks**** within t are largely avoided. Exception to this are feedbacks between firings of certain defense weapons which reflect position effects. Through adjustment of these coefficients, these feedbacks could also be used to simulate communications between defense weapons.

7.1 The Method of Simulation. Following estimation of parameters in (4.3), encounter outcomes are generated by converting predicted values in t to observed values in t which become predictors for other variables in t and lagged variables for predictions in t+1. For example, the predicted number of firings for a given defense weapon in t is taken as the expected value of a conditional Poisson distribution. Sampling therefrom provides an observed value which becomes (i) the first lag in predicting expected firings in t+1 and (ii) a predictor for expected pairings by this weapon in t. Observed pairings in t, obtained analogous to observed firings, become (i) the first lag in predicting expected pairings t+1 and (ii) a predictor for variables comprising threat attrition in t; these variables include individual threat reinforcements and threat tanks aggregated within each of P, W, and B.

Variables not following conditional Poisson distributions, such as ranges and cluster dispersions, are assumed to follow conditional normal distributions. For example, the predicted minimum range between a given defense weapon and all threat clusters within the minefield becomes the expected value of the conditional normal; the variance is taken as the estimated variance of the model errors (4.3). Sampling from this distribution provides the observed value for this particular range in t. This value, as an observed, threat configuration variable

* For mine kills in t, mobility kills are modeled separately from mine kills.

** Attrition on the weapon system is modeled separately from personnel kills.

*** Primary and secondary firings and pairings by the threat tanks are modeled separately.

**** A causal feedback between two variables A and B within t, denoted by $A \leftrightarrow B$, means that A affects B and B affects A sequentially over time within t.

in t , is a predictor for both mine encounters and firings in $t+1$.

This recursive procedure is followed in generating all predicted, observed, and lagged values for each $y_{eh}(t)$ in (4.3)*. Only initial conditions**, in terms of the earliest lags in the first event segment, must be prespecified.

Simulations are conducted under the following ground rules. Regarding end of trial criteria, the defense wins if the number of defense weapons remaining is greater than or equal to the number of live threat tanks plus the number of mobility killed tanks. The threat wins if the number of threat tanks penetrating the minefield is greater than three times the number of defense weapons remaining, excluding the Dragons. The threat also wins if all defense weapons are killed. The trial is termed no decision if 38 minutes have elapsed and neither side has won.

The following constraints are imposed on defense firings. After two firings from the same position, one Dragon moves to a new position; the other Dragon moves after one firing. Movement time is three minutes. One TOW will assume a new position after two firings, the other after three firings. Movement time is two minutes. If the tank fires as many as three rounds in one minute, its firing is deterred in the following thirty seconds***.

The firing constraint imposed on the defense tank reflects obscuration of its visibility due to its own firing. The present simulations do not account for obscuration occurring when a weapon has been paired. Nor do they account for suppressive reactions of personnel of a paired weapon. Moreover, the ground rules allow mobility killed tanks to continue firing. This creates a dual between

* For causal feedbacks, where $y_{eh}(t) \leftrightarrow y_{eh^*}(t)$, initial, observed values of $y_{eh}(t)$ and $y_{eh^*}(t)$ are obtained through the reduced system. These observed values become, then, predictors in the structural system where $y_{eh}(t) \rightarrow y_{eh^*}(t)$ and $y_{eh^*}(t) \rightarrow y_{eh}(t)$.

** These conditions include make-up and numbers of opposing forces, initial threat formations, and initial ranges.

*** Opinions regarding constraints on defense firings are varied and will be subject to future sensitivity analyses. Due to the pronounced firing signature of both Dragons and TOWs, there is general agreement that each will relocate "frequently". The consensus is that Dragon personnel will change positions usually after one or, at most, two firings and that relocation will take approximately three minutes. TOWs are said to relocate after two or, at most, three firings and that the relocation time is roughly two minutes.

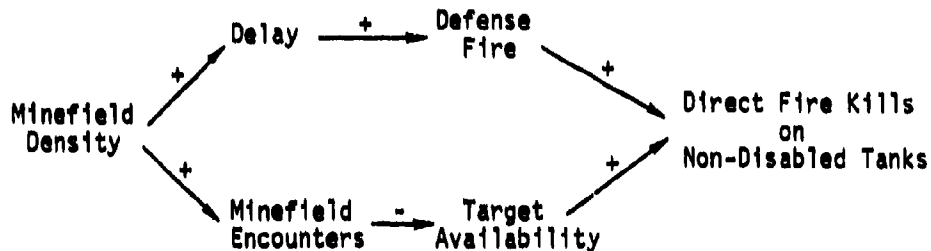
mobility killed tanks and defensive weapons, particularly for a large threat force in a high density minefield. The dual can lead to unrealistic results if, in fact, tank crews are likely to bail out of mobility killed vehicles. It should be recognized, however, that constraints can be imposed to deal with these situations based on the foundation provided by model (4.3).

Table 7.1 presents selected results from a simulated trial with double the average number of threat tanks employed in TEMAWS. The threat is declared a winner after seven minutes since threat tanks penetrated the minefield with a greater than 3 to 1 ratio; i.e., seven tanks penetrated against a remaining defense (excluding Dragons), of one tank and one TOW. Note that had the threat been declared a winner by penetrating the minefield with a ratio of at least 3 to 1, the trial would have terminated at the end of the thirteenth time interval.

8. Simulation Results. TEMAWS was intended to establish whether effects of the minefield and defense fire on the threat are additive or interactive. A means of resolution is through the relation between minefield density and the number of direct fire kills on non-disabled threat tanks. If there is a relation between the two, effects are interactive. No relation indicates additivity of effects.

In adjusting for imbalances, model (4.3) was exercised under the TEMAWS scenario with 100 simulated trials for densities of low visibility minefields. A plot of the average number of direct fire kills on non-disabled tanks versus minefield density is presented in Figure 8.1 for force sizes of 13, 26, 31, and 39 tanks. For 13 tanks, the average number* used in TEMAWS, the slope is negative. Positive slopes result for other force sizes.

These slopes can be explained through the following path diagram:



A positive effect of density on direct fire kills follows logically from the upper path: the greater the density, the more the evasive action by the threat and the greater the delay time; greater delays lead to more defense fire and, hence, to make more direct fire kills. Positive slopes in Figure 8.1 indicate that the upper path dominates; the lower path dominates with a negative slope. These

* Although 15 tanks were targeted for use, 13 were available, on the average.

Table 7.1 A Simulated Trial of Threat (26 Tanks, 3 APCs, Artillery)
Versus Defense (2 Dragons, 2 TOWs, 1 Tank);
Minefield Density = .0005 Mines/Meter²

Threat t ⁽¹⁾	Tanks Remaining ⁽²⁾			Firings ⁽³⁾			Defense Remaining ⁽⁴⁾			APCs Remaining ⁽⁴⁾			Artillery Pairings ⁽⁵⁾			Mine Attrition ⁽⁶⁾					
	P	W	B	Dr	Br	Ta	To	Dr	Br	Ta	To	A1	A2	A3	Dr	Br	Ta	To	E	M ₁	M ₀
0	26	0	0	0	0	0	0	1	1	1	1	1	1	1	0	0	0	0	0	0	0
1	26	0	0	0	0	0	1	0	1	1	1	1	1	1	0	0	0	0	1	0	0
2	26	0	0	0	0	1	0	1	1	1	1	1	1	1	0	0	0	0	0	0	0
3	26	0	0	0	1	0	0	1	1	1	1	0	1	1	0	1	1	0	1	0	0
4	26	0	0	0	0	1	0	1	1	1	1	0	1	1	1	0	1	2	1	0	0
5	26	0	0	0	0	0	0	1	1	1	1	0	1	1	1	0	0	1	0	0	0
6	26	0	0	0	0	0	0	1	1	1	1	0	1	1	1	0	0	1	0	0	0
7	26	0	0	0	0	0	0	1	1	1	1	0	1	1	1	0	0	1	0	0	0
8	26	0	0	0	0	0	0	1	1	1	1	0	1	1	1	0	0	1	0	0	0
9	25	1	0	0	0	0	0	1	1	1	1	0	1	1	1	0	0	1	0	0	0
10	22	3	0	0	0	1	0	0	1	1	1	0	1	1	1	0	0	1	0	0	0
11	15	7	1	1	0	1	1	0	1	1	1	0	1	1	1	0	0	1	0	0	0
12	10	6	4	0	1	2	0	0	1	1	1	0	1	1	1	0	0	1	0	1	0
13	4	7	6	1	0	0	1	0	1	1	1	0	1	1	1	0	0	1	0	1	0
14	1	7	7	0	0	2	0	0	1	1	1	0	1	1	1	0	1	0	1	0	0

(1) The t denote successive 30 second time intervals.

(2) P, W, and B denote, respectively, areas prior to, within, and beyond the minefield.

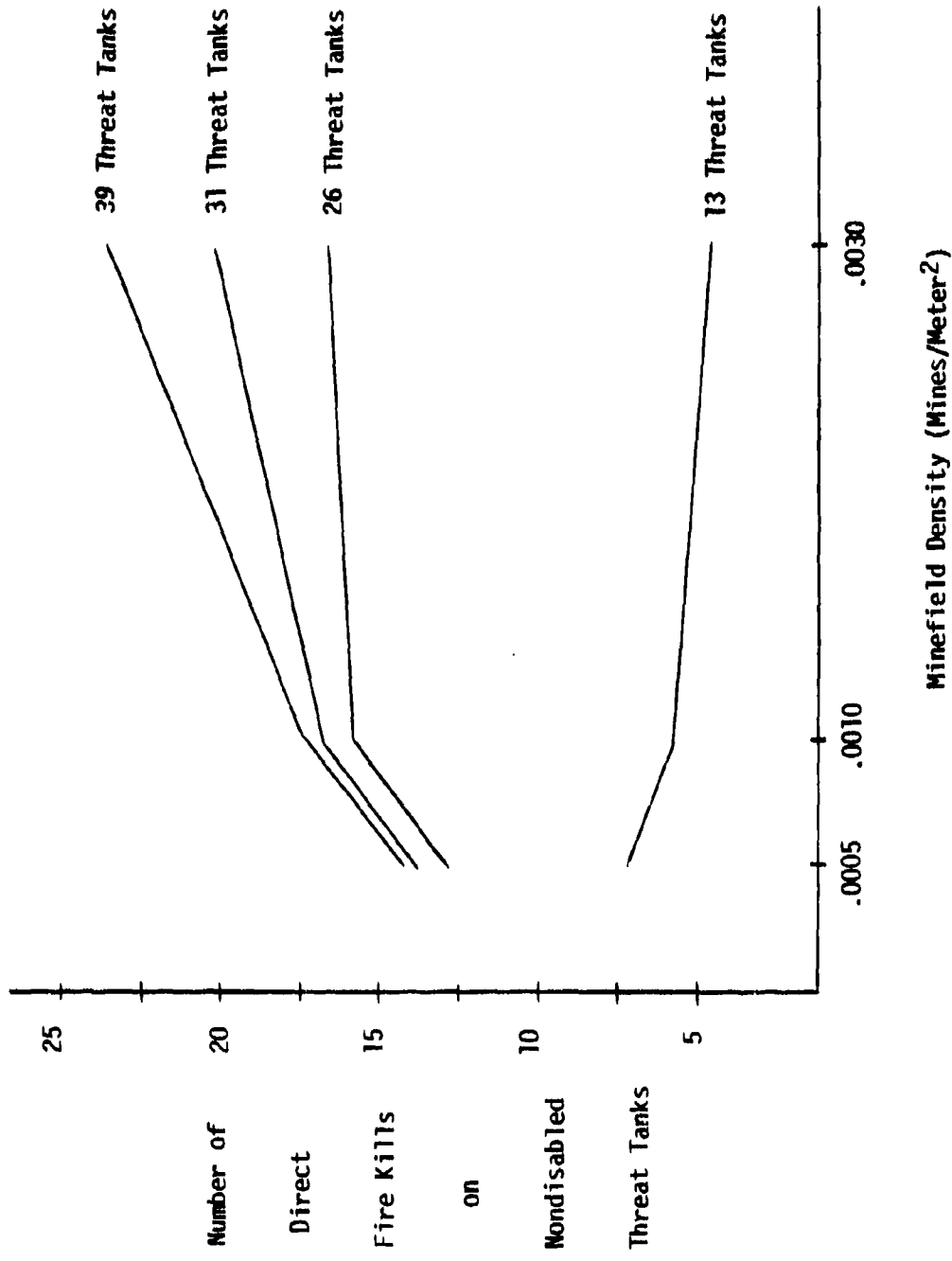
(3) Dr, Ta, and To denote, Dragon, Tank, and TOW, respectively.

(4) For defense and APCs remaining, 1 denotes continued participation and 0 denotes a kill on the particular weapon.

(5) Regarding artillery pairings, a defense weapon is paired and assessed for attrition if the weapon was sufficiently close to the point of impact.

(6) E, M₁ and M₀ denote, respectively, mine encounters, total mine kills, and mobility kills.

Figure 8.1 Effects of Minefield Density on Direct Fire Kills; Low Visibility Minefield.



results indicate that, given the force size in TEMAWS, target availability prevented the occurrence of a positive slope*. This illustrates the utility of a data based model such as (4.3). Excursions can be made to encounters with larger threat forces so as to remedy the problem of target availability. The slopes for these larger threat forces are positive indicating a synergistic effect between density and direct fire kills.

Simulation results in Table 8.1 summarize encounters of threat forces** matched against each of three defense forces: the TEMAWS force (2 TOWs, 2 Dragons, 1 tank), the TEMAWS force excluding Dragons, and the TEMAWS force including a second tank. It is seen, for example, that a threat force of 13 tanks wins in 33% of the encounters against (2 TOWs, 2 Dragons, 1 tank, density = .0005) and against (2 TOWs, 0 Dragons, 1 tank, density = .001). Since 150 mines were utilized for a density of .0005, there is a trade-off between the extra 150 mines required to achieve a .001 density and 2 Dragons. Other trade-offs are presented in Table 8.2***.

* At the time of the TEMAWS experiment, a larger number of tanks could not be instrumented for RTCA.

** Each threat force size includes the same reinforcements as in TEMAWS.

*** A word of caution is in order. Ground rules affect results of simulations. Results from a given set of ground rules should be held in abeyance until changes in ground rules are evaluated through sensitivity analyses.

**Table 8.1 Percent of Trials* in Which Threat Wins;
Low-Visibility Minefield.**

Minefield Density	0.0 (No Minefield)	.005	.001	.003									
Number of Threat Tanks	13 26 31 39	42 (1) 54 (2) 72 100	29 (3) 77 89 93	33 50 63 98	43 70 64 82	22 56 68 85	33 42 68 82	24 50 63 82	33 56 68 82	16 29 42 85	18 42 60 81	26 45 63 82	10 22 37 58

Defense Force	(1) 2 TOWs 2 Dragons 1 Tank	(2) 2 TOWs 0 Dragons 1 Tank	(3) 2 TOWs 2 Dragons 2 Tanks
---------------	-----------------------------------	-----------------------------------	------------------------------------

* Each percentage based on 100 simulated trials.

Table 8.2 Number of Threat Tanks Required for a Threat Win Probability of at least .50.

Minefield Density	No Minefield	.0005	.001	.003
Defense	2 TOWs, 2 Dragons 1 Tank	15	19	26
	2 TOWs, 0 Dragons, 1 Tank	12	16	23
	2 TOWs, 2 Dragons, 2 Tanks	22	27	34
				36

Appendix A. A number of assumptions are usually associated with model (4.3). Regarding $\delta_{eh}(t)$, it is assumed that $E(\delta_{eh}(t)) = 0$ and that

$$E \left[s_{eh}(t) \delta_{eh^*}(t') \right] = 0 \text{ for } t \neq t' \\ = c_{ehh^*} \text{ for } t = t' \quad (A.1)$$

Evaluation of residual crossproducts, based on ordinary least squares (OLS) estimation on a per equation basis in model (4.3), support (A.1). For tests of significance, normality of distribution is imposed on $\delta_{eh}(t)$.

The lagged variables in (4.3) serve the purpose of quantifying the dependence of the present on the past. In doing so, the lags also reinforce assumption (A.1). Regarding assumptions on the lags, let

$$\sum_{i=0}^{r_{hh^*}} a_{ehh^*i} \rho^{-i} = \theta_{ehh^*}(\rho),$$

and let the $p \times p$ matrix $\theta_e = (\theta_{ehh^*}(\rho))$.

It is assumed that all roots of the equation $\theta_e = 0$ are smaller than 1 in absolute value for each event segment e ; see (12). Estimated values of the a_{ehh^*i} support this assumption.

The structural system in (4.3) is rewritten as

$$a_e \underline{y} = \Gamma_e \underline{z} + \underline{\delta}_e, \quad (A.2)$$

where the $p \times 1$ vector $\underline{y} = (y_h(t))$; the $q^* \times 1$ vector \underline{z} contains all exogenous variables including $y_{h^*}(t-1)$ and $x_j(t-1)$, $i \neq 0$, $i^* \geq 0$;

$$q^* = q + \sum_{h,h^*} r_{hh^*} + \sum_{h,j} r_{hj} ;$$

the $p \times 1$ vector $\underline{\delta}_e = (\delta_{eh}(t))$; the $p \times p$ matrix $\alpha_e = (\alpha_{ehh^*})$, where α_{ehh^*} is the direct effect of $y_{h^*}(t)$ on $y_h(t)$ in event segment e ; $\alpha_{ehh} = 1$; the $p \times q^*$ matrix Γ_e contains direct effects of exogenous variables on endogenous variables. The structural system uniquely determines the reduced system and is given by

$$y = \alpha_e^{-1} \Gamma_e z + \alpha_e^{-1} \underline{\delta}_e = \beta_e z + \varepsilon_e,$$

where $\beta_e = \alpha_e^{-1} \Gamma_e$ and $\varepsilon_e = \alpha_e^{-1} \underline{\delta}_e$. From (A.1),

$$\underline{\delta}_e : (0, \sum_{e\delta}) \text{ where } E(\underline{\delta}_e \underline{\delta}_e') = \sum_{e\delta} = (\sigma_{ehh^*}).$$

$$\text{Thus, } \varepsilon_e : (0, \sum_{e\epsilon}) \text{ where } \sum_{e\epsilon} = \alpha_e^{-1} \sum_{e\delta} \alpha_e'^{-1}.$$

OLS estimation in the reduced system leads to consistent estimates of β_e and $\sum_{e\delta}$. Application of OLS estimation in the structural system yields inconsistent estimates unless the system is diagonally recursive*. In practice, however, assumptions underlying such a system are difficult to justify; see (13). As such, alternative structural estimation techniques, such as two stage least squares estimation** (9), (10), are applied in obtaining consistent estimates, assuming identification. The drawback of these estimation techniques is that the resulting estimates can be inefficient, especially when values of R^2 in the reduced system are low. For this reason, OLS estimation is applied in model (4.3) under the justification that mean square errors will be smaller relative to other estimation techniques.

* The structural system is termed diagonally recursive if α_e is triangular and $\sum_{e\delta}$ is diagonal.

** In experimental situations where the structural system is not well established, full information estimation techniques are risky; i.e., a bias in one equation is carried over to other equations. As such, only limited information techniques, such as two stage least squares estimation, were considered.

References

- (1) J. Hartigan (1975). Clustering Algorithms, Wiley and Sons, N.Y.
- (2) A. Hoerl and R. Kennard (1970). Ridge Regression: Biased Estimation for Non-Orthogonal Problems. *Technometrics*, 12, 55-68.
- (3) J. Webster, R. Gunst, and R. Mason (1974). Latent Root Regression Analysis. *Technometrics*, 16, 513-522.
- (4) W. S. Mallios (1967). A Structural Regression Approach to Covariance Analysis When the Covariable is Uncontrolled. *Journal of the American Statistical Association*, 62, 1037-49.
- (5) W. S. Mallios (1970). The Analysis of Structural Effects in Experimental Design. *Journal of the American Statistical Association*, 65, 808-827.
- (6) G. S. Hall (1971). Lanchester's Theory of Combat: The State of the Art in Mid-1970. Thesis, U.S. Naval Postgraduate School, Monterey, CA.
- (7) Models Review Committee, J. Honig, Chairman (1971). Review of Selected Army Models. Department of the Army.
- (8) War Gaming, Cosmagon, and Zigspiel. Operations Research Office, The Johns Hopkins University, (1960).
- (9) A. Goldberger (1964). Econometric Theory. Wiley and Sons, N.Y.
- (10) H. Theil (1971). Principles of Econometrics. Wiley and Sons, N.Y.
- (11) W. S. Mallios, R. D. Batesole, D. R. Leal and T. Tran (1978). Improved Quantification of Player Effects in Experimental Design. Proceedings of the 23rd Conference on the Design of Experiments in Army Research, Development, and Testing.
- (12) H. Mann and A. Wald (1943). On the Statistical Treatment of Linear Stochastic Difference Equations. *Econometrika*, 11, 173-220.
- (13) W. S. Mallios (1978). Resolving Under-Identification Through Replication in Experimental Design. Proceedings of the 23rd Conference on the Design of Experiments in Army Research, Development, and Testing.

DETERMINATION OF STRUCTURAL RELIABILITY USING A
FLAW SIMULATION SCHEME

Donald M. Neal and Donald S. Mason
Army Materials and Mechanics Research Center
Watertown, Massachusetts 02172

ABSTRACT

Reliability Calculations are made for both an anti-tank projectile and a fragmentation shell using fracture mechanics concepts in conjunction with the Monte Carlo method. Reliability estimates are evaluated and compared for both Weibull and Warner stress strength diagram definitions.

A probability density function representation of allowable stress (strength) is obtained from a fracture mechanics K_{IC} relationships where specific random form of the parameters is assigned. A normal density function is obtained for the structural element stresses by using results from a two-dimensional finite element solution.

In both Weibull and Warner diagram methods strength density distributions and parameters are the results of laboratory tensile tests. In the Weibull model the scale and shaped parameters were obtained from the Maximum Likelihood method. The Warner diagram method required a normal and best fit density function for stress and strength respectively.

Both the "weakest link" and series-parallel system are evaluated for desirability in estimating structural reliability. The "weakest link" approach which introduces reliability independence between elements will thereby describe a much more conservative reliability estimate than the series-parallel system which requires at least two adjacent elements to fail in order to have structural failure.

INTRODUCTION

This paper describes structural reliability from an idealized linear elastic fracture mechanics (F.M.) model. It is assumed that flaws exist in structural elements and are remote from any other flaws. These hypothetical flaws are described by random variations in size and orientation. Although these assumptions somewhat idealize the actual flaw distributions, they do provide a reasonable good qualitative analysis of failure probability as compared to the conventional deterministic approach which considers only one type of a singularly oriented crack (transverse to maximum applied stress) of a determined critical size.

Present fracture mechanics procedures as applied to structural reliability depend on determination of critical crack sizes by using proper K_{IC} relationships in conjunction with known stress distributions in the structure [1]. Once the critical crack sizes and locations are established a NDT (Non-Destructive Test) procedure is applied to the structure in order to establish if this crack exists. If a critical crack is located, the structure is rejected. It should be noted that an excessively large rejection rate can occur by applying this method since the probability of cracks oriented in this manner is very small [2]. One of the primary objection to the conventional (F.M.) procedure is the inability of NDT methods to detect cracks less than a certain size (e.g. .10 inch) [3]. If the critical size computed to be less than this size then the F.M. procedure will not be able to determine potential failure in the structures.

The uncertainties existing in the use of the analytic tools (such as Finite Element analysis) (F.E.) in obtaining the structural stress distribution can introduce considerable error in obtaining the critical flaw size. For example; the accuracy of the F.E. solution depends on the severity of stress gradients, mesh size, types of elements used and the effects of averaging stresses within the element.

The flaw simulation scheme (FSS) introduced in this paper attempts to provide alternatives to conventional methods described above, the authors do not consider this scheme as the ultimate answer in the application of F.M. to structural reliability but rather an alternative. When more knowledge is available regarding flaw types and their orientation in structures, this method can provide an excellent tool for establishing structural reliability.

In using the Monte Carlo method, [4] the flaw simulation scheme provides for variations in crack orientation and size in addition to computed stress values in the structure. Crack orientations are assumed to vary from 0° to 90° in a uniform random manner. The crack size variation is defined in exponential functional form where sizes vary from a large percent of very small cracks to a relatively small number of larger detectable cracks [5]. The stress values obtained for cracked structural element is assumed to be a normal distribution where Coefficient of Variation (CV) is varied in order to determine the effect of errors in the F.E. analysis.

The types of cracks and their locations are the through center crack, near cut-out edge, corner crack and surface crack (center). The structural configuration determines the types of cracks and their locations.

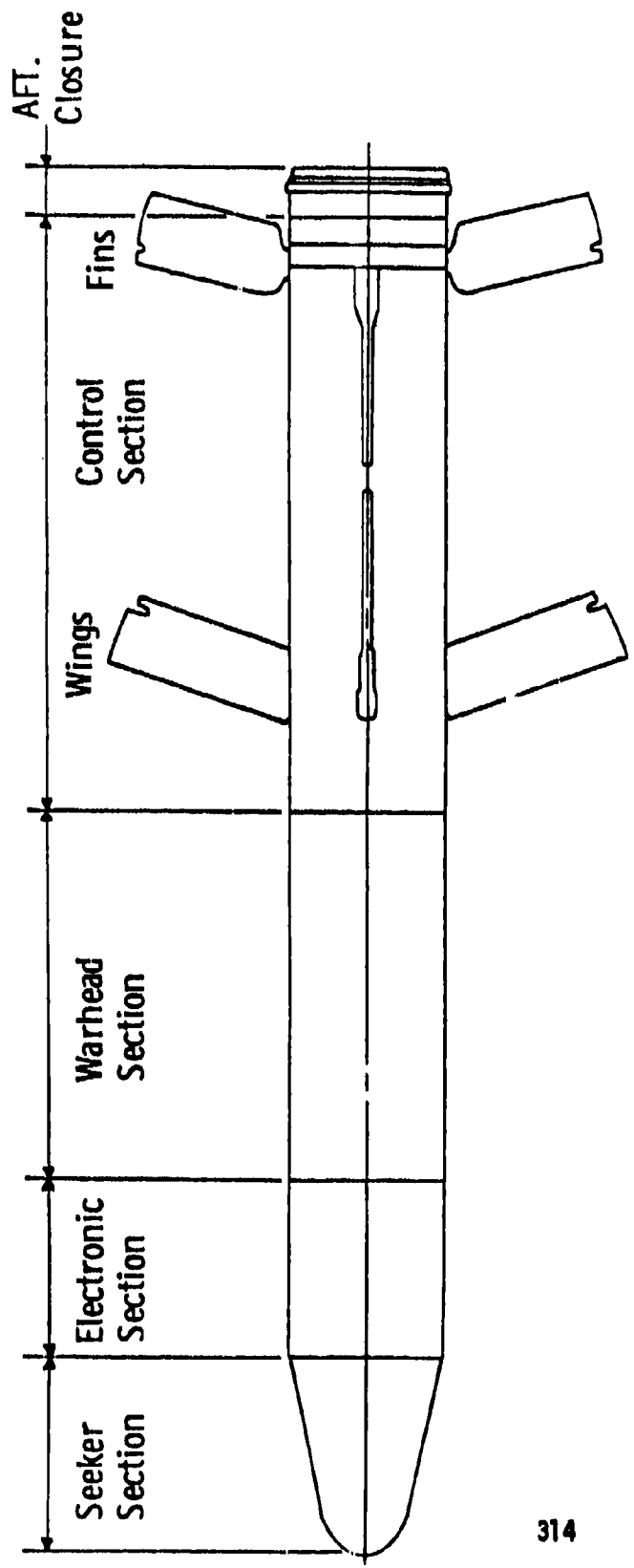
Types of Structures Considered

The model problems chosen to illustrate the technique proposed in this paper is the determination of structure reliability for an Anti-Tank Projectile control section (fig. 1) and a fragmentation shell (fig. 2). Both structures are made from relatively high strength brittle steel. The control section is subjected relatively large compressive loads at the aft section and tension stresses in the vicinity of the cut-out region where the fins are attached. The shell is internally loaded with a uniform pressure of 14KSI. This load represents a proof test used in evaluating shell quality. Reliability determination of the control section provided the opportunity to evaluate the series-parallel system approach because of the complex stress state introduced by the relatively large tension and compressive stresses in the structure. The weakest link approach is more readily adapted to the fragmentation shell loading state.

Statistic Evaluation of Variable Strength

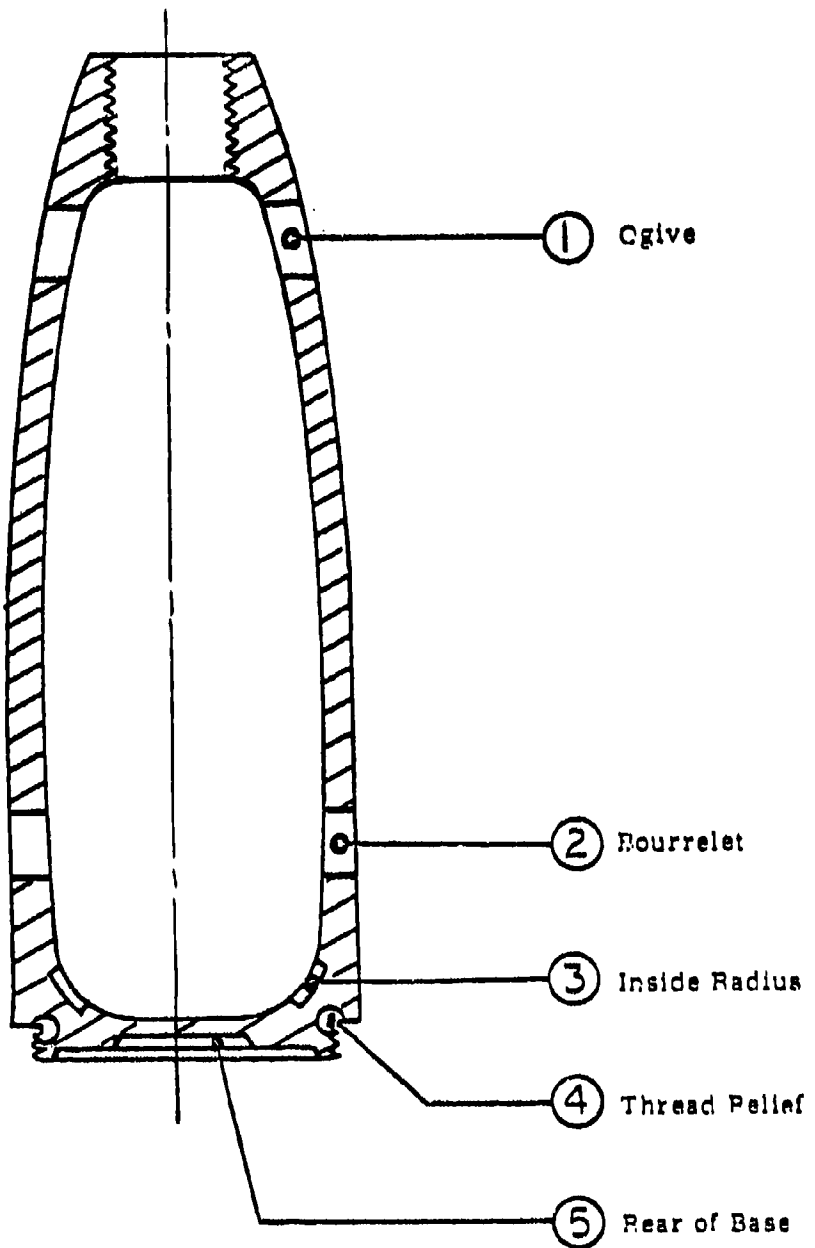
The lack of ductility characteristic of brittle materials has two undesirable consequences for the engineer. Firstly any misfit or miss-alignment produces local high stresses which cannot be relieved by plastic flow, unlike in ductile material. Brittle component designs differ from those for similar ductile components in that extra attention must be paid to detail, especially in highly stressed areas. The second consequence is more fundamental; all materials contain flaws such as microscopic cavities and dislocations and, in loaded brittle materials, these result in local stress concentration within the material. The strength of a component is governed by the chance that a severe stress concentration (c) will be subjected to a stress (σ) such that the local stress σ_c exceeds the material strength. The occurrence of this is a matter of chance and explains the marked variability generally observed in brittle material strengths. It also explains why brittle material failures may start away from the maximum continuum stress; if no severe flaws coincide with the maximum stress, failure may occur at a severe flaw subject to a lower stress at a position where σ_c is a maximum.

To overcome the strength variability by drastically reducing the applied loading is not an attractive engineering proposition. What is needed is an estimate of the likelihood of failure of the component under a specified load. This requires a detailed knowledge of the stresses in the structure, and the flaw distribution in the material. Well established techniques are available for the stress analysis, some of which are mentioned later.



ANTI-TANK PROJECTILE CONFIGURATION

Figure I



CROSS-SECTIONAL VIEW OF FRAGMENTATION SHELL

Figure 2

The variation in material strength due to the flaws in a particular material can be illustrated by fracture tests on a sample of specimens. A histogram of the fracture stresses of both brittle and ductile material subjected to uniform tension is shown in Fig. 3.1; the frequency of failure (F_f) is the fraction of the sample failing within the stress range σ to $\sigma + \delta\sigma$. In the limit, as the number of specimens (N) becomes large, the stress interval ($\delta\sigma$) in fig. 3.1 can be reduced to give a continuous distribution curve. Note the relatively large variation in strength of the brittle material as compared to the corresponding ductile material of similar test specimens. Structures with large variations in material strength, as shown for the brittle material, require a probabilistic approach in the design procedures.

A complementary form of fig. 3.1 is obtained if the data is presented in terms of the cumulative failure probability (P_f). This quantity is the fraction of the sample failing at or below the stress σ ; in the limit it is the integral of the frequency distribution with respect to stress, i.e.,

$$P_f(\sigma) = \int F_f d\sigma \quad (1)$$

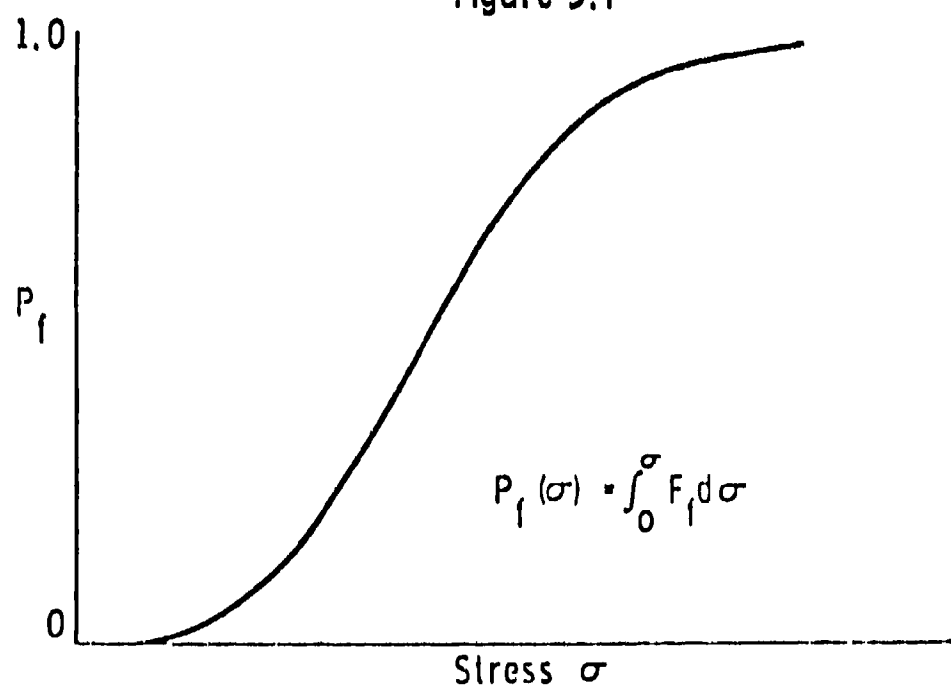
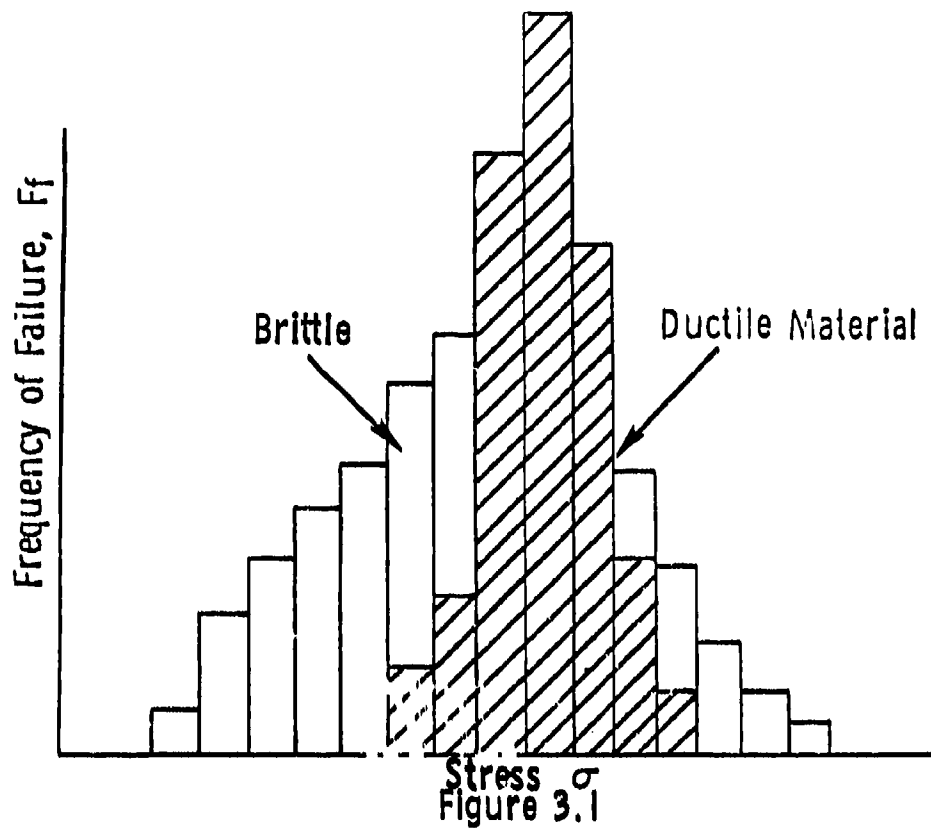
In practice the cumulative failure probability is usually found from the data using the "mean ranking" approach. The N failure stresses of the sample are arranged in ascending order: the cumulative failure probability associated with the i^{th} failure stress in the list is,

$$P_f(\sigma_i) = \frac{i}{N+1} \quad (2)$$

The probability distribution of the data can be plotted from this - see fig. 3.2.

Conventional Fracture Mechanic Approach to Structural Reliability

Fracture Mechanics in the design process requires the consideration of three factors: a stress analysis (F.E.), a measure of fracture toughness (K_{IC}) and the capability of inspecting for cracks. The stress analysis can require elaborate analysis using advanced F.E. or simpler closed form solutions depending on loading conditions and structural geometry. Since plane strain fracture toughness is a structure sensitive material characteristic similar to tensile and impact properties, it is dependent upon material condition, strain rate and temperature. In describing the fracture toughness of a material, determinations are necessary under a sufficiently wide variety of conditions to allow realistic assessment of the minimum value likely to be encountered in design conditions. Some of the crack detection techniques include ultrasonics, dye penetrants, magnetic particles and visual inspection.



PROBABILITY OF FAILURE DISTRIBUTION
Figure 3.2

Analytically, the critical flaw size is defined by an expression of the type shown below:

$$a_c = f \left[Q \left(\frac{K_{IC}}{\sigma} \right)^2 \right] \quad (3)$$

where:

a_c = critical flaw depth.

Q = a parameter which takes into account the shape of the flaw.

K_{IC} = plane strain fracture toughness of the material.

σ = the tensile component of stress acting normal to the plane of the flaw.

The depth a_c and orientation of flaws which, on the basis of the fracture toughness and stress factors, can result in catastrophic crack propagation. It should be noted that σ as defined above assumes flaw is normal to acting stress (see figure 4). This assumption rejects the possibility that flaw could be oriented in other directions, thereby neglecting obvious possibilities in favor of an unlikely one. This could result in incorrectly determining critical flaws size a_c . Present flaw detection methods in many instances are not capable of detecting critical flaws of a relatively small size. In fact, comments by [3] indicate flaws less than .1 inch of the time cannot be found in a structure. Of course the other difficulty involves not finding a detectable flaw size in a structure although it does exist.

Flaw Simulation Method

An alternative to the previously described conventional Fracture Mechanics approach is made by introducing variation in crack orientation and length by means of the Monte Carlo method. Initially four types of cracks are to be considered in an element (see fig. 5). The type and location of cracks depends on the structural configuration.

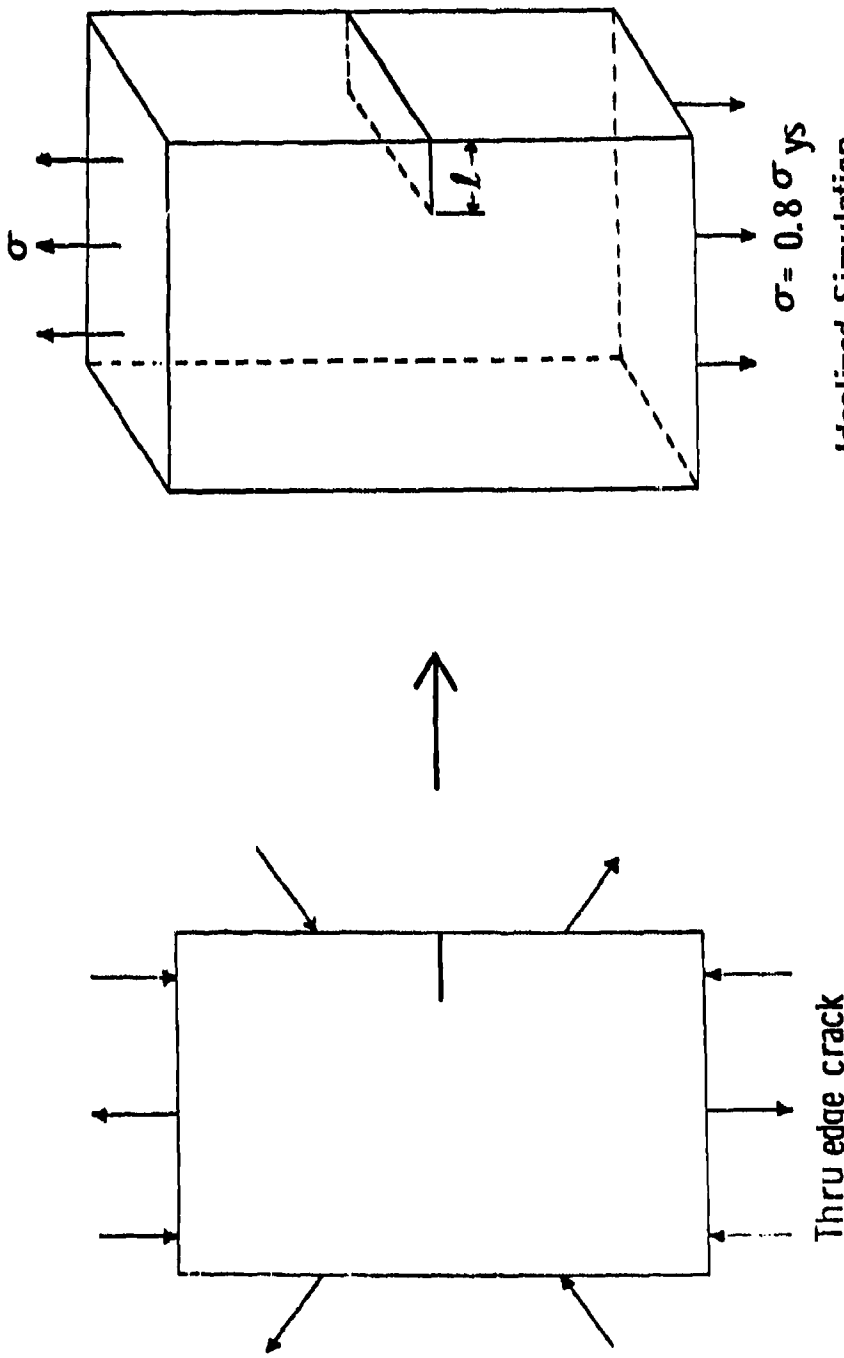
In the simulation scheme the allowable stress σ_c from K_{IC} relationships is written as:

$$\sigma_c = f(K_{IC}, l, \theta) \quad (4)$$

where:

l = crack length.

θ = angle of inclination of crack.



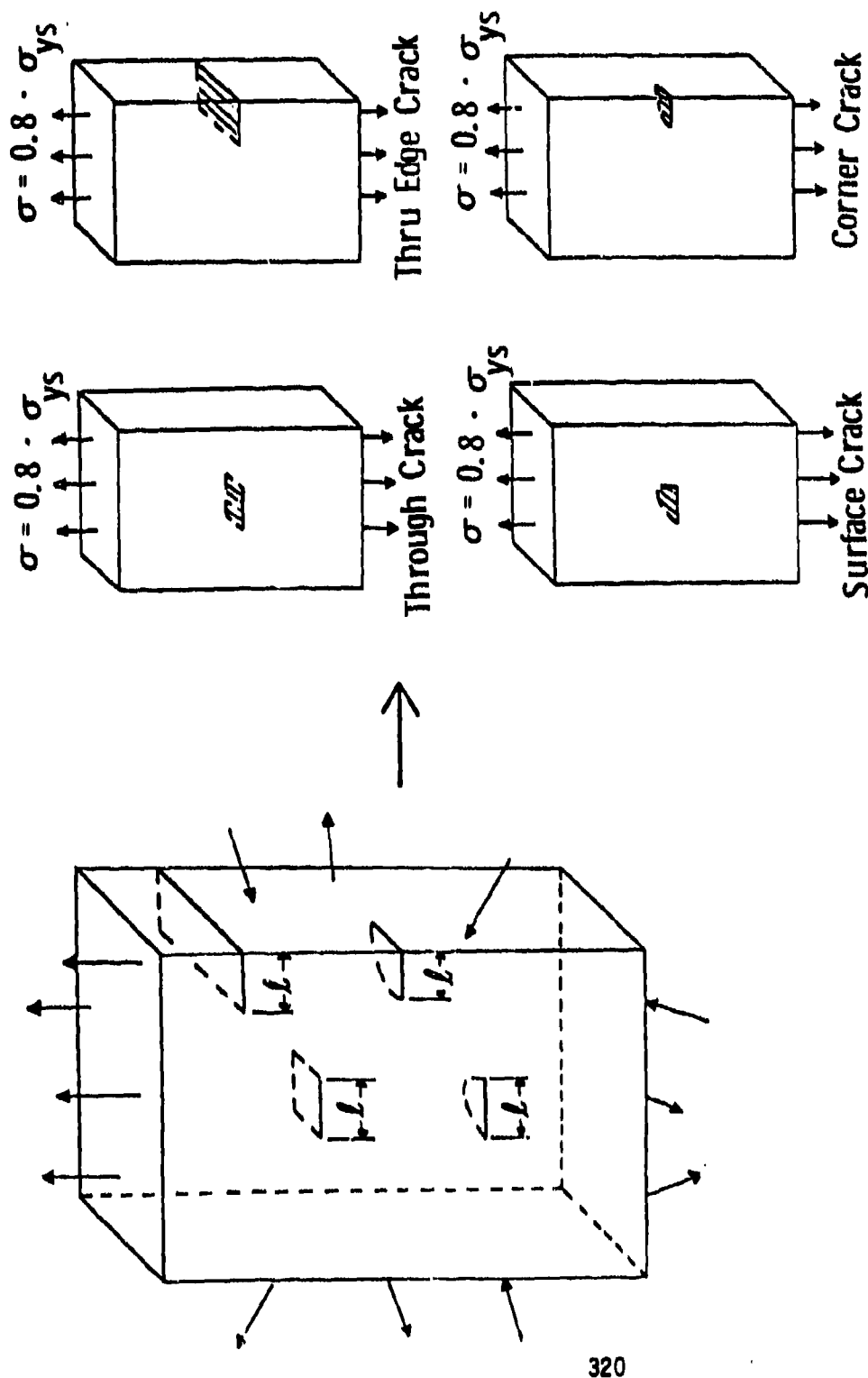
CONVENTIONAL SINGLE VALUED FOR CRACK ORIENTATION

Idealized Simulation

Figure 4

CRACK TYPES ASSUMED IN SIMULATION SCHEME

Figure 5



It is assumed that σ_c represents the material strengths and depends on the parameters K_{IC} , ℓ , θ . The variations in K_{IC} is represented by a normal probability density function (P.D.F) (fig. 6a). The angle θ is represented by uniform random numbers in range of 0 to 90° (fig. 6b). The distribution of sizes ℓ is of an exponential P.D.F. form shown in fig. 6c. The σ_c distribution is obtained from generating a set of uniform random numbers and solving for x in the relation,

$$\int_{-\infty}^x f_i = R, \quad (5)$$

where R = uniform random number and f_i corresponds to the desired type of frequency distribution. The K_{IC} distribution requires test results for material used in the structure in order to obtain the necessary mean and standard deviation values. In figure 6c the maximum crack length ℓ_2 is represented by the smallest detectable crack consistent with the capability of present available NDT methods. The assumed exponential form has been substantiated by [5,6] in laboratory tests.

A PDF can be obtained for the allowable stress σ_c by randomly selecting from K_{IC} , θ and ℓ distributions discreet sets of numbers and substituting them into equation 4. Note, there should be an equal amount of say N random numbers for each parameter in order to have N numbers representing the σ_c distribution.

The K_{IC} relationships for σ_c are written as:

(a) Through crack

$$\sigma_c = K_{IC} (2/\pi)^{1/2} (\ell \sin\phi)^{-1/2} \quad (6)$$

where $K_{IC} = K_I + K_{II}$,

$$K_I = \sigma (\ell \pi/2)^{1/2} \sin^2 \phi \text{ and}$$

$$K_{II} = \sigma (\ell \pi/2)^{1/2} \sin\theta \cos\theta.$$

(b) Corner crack

$$\sigma_c = 2/K_{IC} (1.28) (\ell/\pi)^{1/2}. \quad (7)$$

$$\sigma_c = f(K_{Ic}, \ell, \theta)$$

$$R_u = \int_{-\infty}^X f(t) dt$$

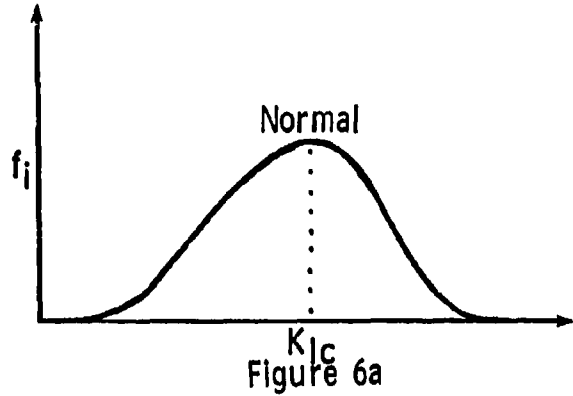


Figure 6a

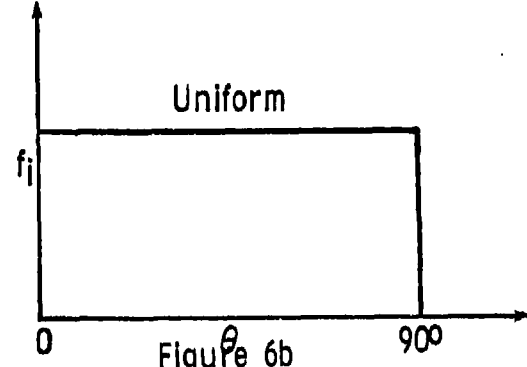


Figure 6b

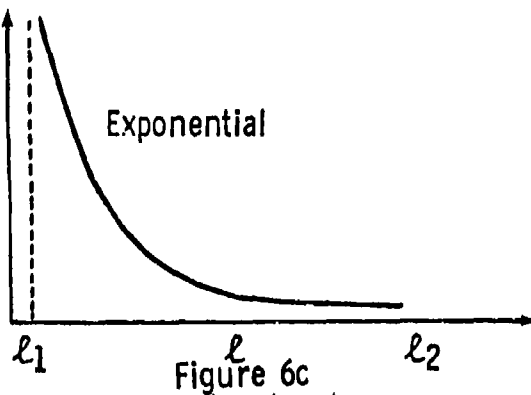
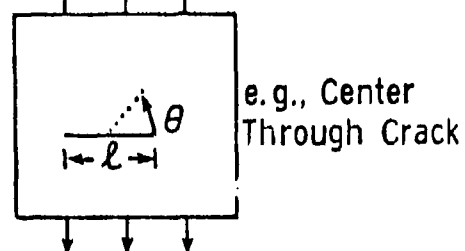


Figure 6c



e.g., Center
Through Crack

(c) Surface crack

$$\sigma_c = K_{IC} / 1.1(\pi a/Q)^{1/2}$$

where $Q = E(K)^2 - .212(\sigma/\sigma_{ys})^2$, (8)

$$K^2 = 1 - 4(a/l)^2$$

$$0 \leq a \leq .10 \text{ inches}$$

and

$$0 \leq l \leq .05 \text{ inches.}$$

In order to use σ_c relationship for the inclined edge crack a solution was obtained from [7], where a Modified Mapping Collocation scheme was used. The results are tabulated in Table 1. The appropriate interpolation procedure was applied in order to use Monte Carlo method as outlined in equation 4.

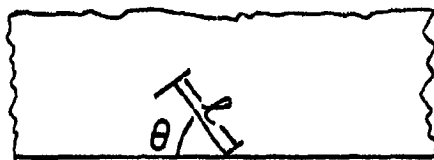
Structural Stress Analysis

In order to obtain the stress distributions in the Anti-Tank projectile (ATP) and fragmentation shell a finite element (F.E.) method was applied. As described previously the loading consists of a set-back type compressive load acting at a base of ATP and a internal pressure proof test load applied to the shell. Rectangular elements were used in the analysis for both structures where shell and ATP contains 693 and 601 elements respectively. The F.E. solution determines the average maximum and minimum principal stresses in each element. The maximum stress is used in the reliability determinations. These stresses should not be confused with critical stresses obtained from the K_{IC} relationships previously described. Having availability of element stresses and corresponding σ_c or strength values the reliability of the elements can be determined.

I. Element Reliability Calculation Methods

Element Reliability as related to the stress-strength (Warner) diagram [8] method (see Appendix A) assumes that the probability of survival (Reliability) is the probability that material strength will be greater than the stress in a given structural element over a range of stress values. The uncertainties in the F.E. solution are represented by a normal distribution f_2 , where calculated mean stress and assumed C.V. are the functional parameters. The distribution f_1 is obtained from known strength data (e.g. laboratory tests). This distribution does not necessarily have to be a

Inclined Edge Cracks (60%)



θ	$H_n = K_I / \sqrt{\pi l}$	$H_0 = K_{II} / \sqrt{\pi l}$
0	0.000	0.000
10	.160	.170
20	.296	.280
30	.461	.335
40	.680	.372
45	.705	.365
50	.781	.354
60	.920	.305
70	1.028	.224
80	1.098	.118
90	1.124	.000

$$\sigma_c = K_{Ic} / H_n \sqrt{\pi l}$$

Table I

normal function. It can be any P.D.F that accurately represents the empirical ranked data. In Appendix A, the probability of say s occurring is $f_2 ds$ while the probability of strength greater than S_1 is represented by the integral, with f_1 integrand and limits of S_1 and ∞ . Multiplication of these elements provides the necessary independence between the two conditions. Finally, integration over entire range of stress values defines probability of survival P_s of each element.

Element reliability numbers were obtained from a approach similar to the one previously described except that discreet values obtained from the Monte Carlo simulation were used to represent both σ and element stress density functions. This is a reasonable approach since distribution of strength values do not necessarily conform to any known density function. The tails of the two density functions are also more accurately represented than by some crude approximating function. This method is outlined in Appendix B where the probability of element survival is defined as follows; $a_i = 1$, when strength is greater than stress values otherwise it is zero. This process is completed when all combinations are considered. The relationship P_{s_k} therefore defines the Kth element reliability number.

Since the Weibull function is well adopted to brittle material subjected to uniform tension state it was included for comparison purposes in the probability of survival calculations of the fragmentation shell. The Weibull P.D.F. is common used in ceramics and other brittle materials evaluation. It uses the "weakest link" concept which is consistent with failure phenomenon of brittle materials which are subjected to tensile stresses primarily. A plot of strength vs cumulative density function (C.D.F.) for HFI steel used in the fragmentation shell construction is shown in fig. 7. Note the excellent correlation between emperical data and the Weibull function[9].

The Weibull probability of survival P_{s_i} for individual stressed components is written as,

$$P_{s_i} = \exp[-KV_i/V^*(\sigma_{max_i}/\sigma_o)^m] \quad (9)$$

where $K = 1$ for simple tensile stress, V_i = volume of element, V^* = volume of test specimen, σ_{max_i} = maximum principal stress in the element, σ_o and m are functional parameters obtained from test data using the maximum likelihood method.

It is obvious from equation 9 that P_{s_i} is functionally volume dependent. That is, larger volume smaller P_{s_i} numbers.

CUMULATIVE DENSITY FUNCTION VS. STRESS

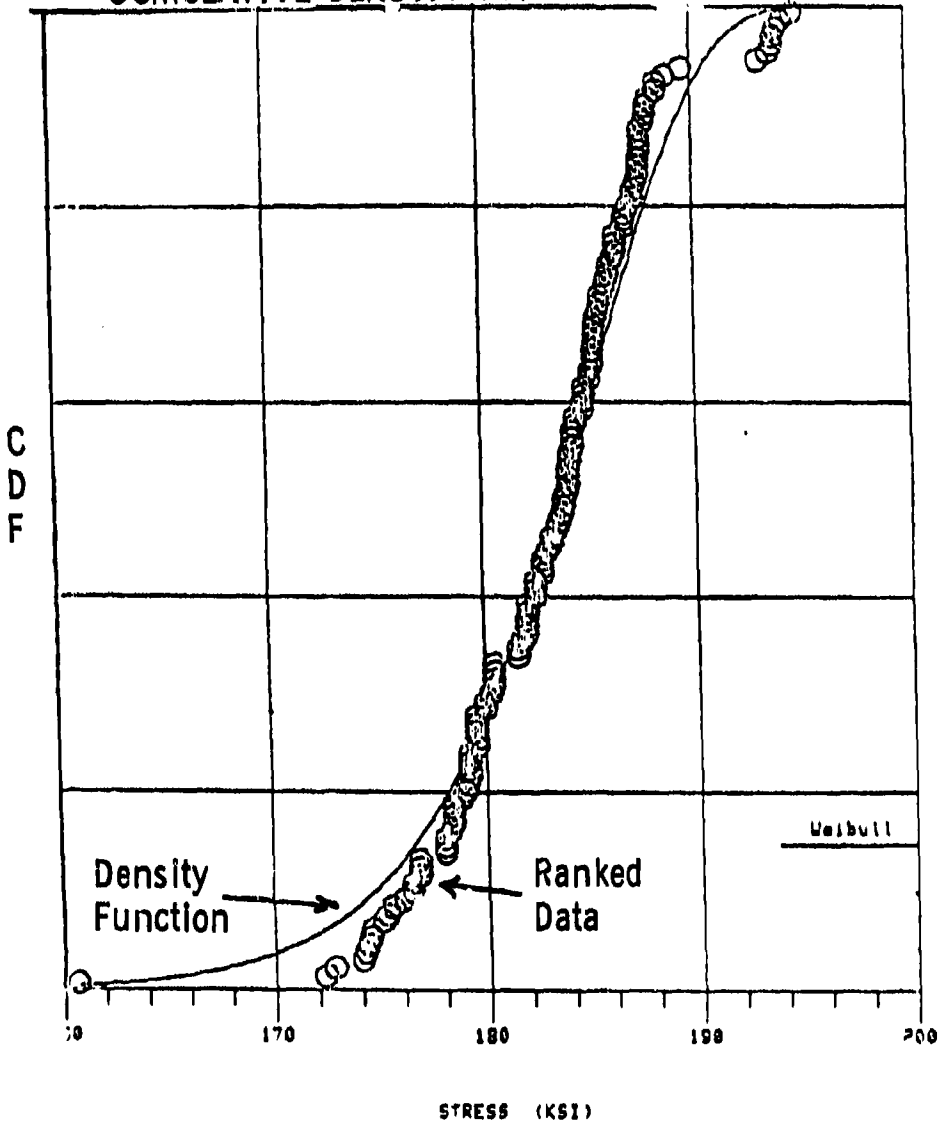


Figure 7

Structural Reliability

In order to obtain P_s of the entire structure the weakest link concept is applied, that is it assumed that each event or probability of survival of element is independent of any other one in the structure. Therefore the total P_s is written as

$$P_s = \prod_{K=1}^N P_{s_K}, \quad (10)$$

where N = number of elements in the structure and P_{s_K} is the Probability of Survival of the individual element. The corresponding probability of failure is defined as $P_f = 1 - P_s$.

A series-parallel approach is introduced in order to examine the case where more than one element is required to fail in order to have total structural failure. This method is described by examining a four element structure where two elements must fail (see Appendix C). The P_{s_i} values are determined for the elements by one of the methods previously described. The resultant P_s for the four elements is determined from application of the series approach. It should be noted that this method is somewhat less conservative than the conventional weakest link method. It is possibly more realistic, especially so for the complex states that exists in the ATP structure.

Numerical Results and Discussion

Numerical reliability (R) results are tabulated in Table II for the fragmentation shell subjected to an internal pressure of 14KSI (Proof test load) as a function of minimum detectable crack size. The Warner Diagram method as outlined in the text is represented by a normal stress-strength P.D.F. determined from F.E. solution and laboratory strength tests results respectively. The Monte Carlo Fracture Mechanics (F.S.S.) results are obtained from applying the scheme presented in the text where both stress and strength F.D.F. are the results of using the simulation scheme described in Appendix B. The Weibull R values were obtained from application of equation 9. It should be noted that both Warner and Weibull methods do not show variation due to changes in cracks sizes, which is expected.

Results from the Monte Carlo method indicate the importance of finding a crack of at least .025 inches or less in order to establish at least 92% probability of survival. The Warner Diagram and Weibull methods show much less conservative estimate of 1 and 22 failures in 1000 respectively. Since Warner and Weibull methods do not consider (F.M.), the R independency due to crack size is expected. Although it is assumed that cracks do exist in each element and the weakest link argument is used, a good qualitative measure of assessing the importance of finding cracks of a relatively small size is

Minimum Detectable Crack Size (in.)	Probability of Survival		Shell (Proof Test Load)
	Warner Diagram	Monte Carlo (F.M.)	Weibull
0.100	0.999	0.059	0.778
0.050	0.999	0.451	0.778
0.025	0.999	0.920	0.778

C.V. (Element Stress) 10%

$K_{IC} = 30 \text{ KSI} (\text{in})^{1/2}$, C.V. = 12%

Yield Strength = 140 KSI

Table II

available. Coefficient of Variation (C.V.) of 10% represents the variation in element stress values obtained from the finite element solution.

In table III Probability of survival estimates are for variation in crack size and element stress C.V. numbers. It should be noted that with crack sizes of .020 in. the effects of F.E. solution errors (e.g. C.V. values) are less than for larger cracks of .100 inch. Mean and C.V. values for K_{Ic} were obtained from laboratory test data. The material yield strength of 140 KSI provided an upper bound for calculated σ_c (allowable stress) obtained from the Monte Carlo Fracture Mechanics Method (F.S.S.).

Table IV provides a partial listing of reliability for the ATP system where crack sizes are .100 and .050 inches with variations in C.V. of 5% to 20%. The effects of F.E. errors are noted as in Tables III, small variation better reliability, large variation poorer reliability. The reliability numbers in parenthesis are results from application of the series-parallel method described in the text.

The series-parallel method which requires failure of all adjacent elements in order to have structural failure provides much less conservative estimate of reliability. It is possible that an upper and lower bound on reliability of this structure for the specified crack sizes could be a series-parallel system and the weakest link approach respectively. With tension and compressive stresses existing in this structure it does not seem advisable to consider structural failure in terms of any given element failure. It also unreasonable to assume that all adjacent elements must fail to have structural failure particularly if a bending stress exists in the structure.

Although the Monte Carlo (F.M.) is hypothetical method for estimating structural reliability, it does provide a desirable alternative to the present Fracture Mechanics approach which assumes cracks oriented transverse to maximum principal stress resulting in an unnecessarily high rejection rates. The ability of examining at least qualitatively the reliability of structures as related the ability of detecting flaws or cracks of various magnitudes can provide a guide for future NDT development procedures. If more information was known regarding structural flaw distributions the Monte Carlo method could provide an excellent reliability tool certainly superior to the present lab test procedures applied to brittle materials. In laboratory testing surface flaws are often removed from material thereby preventing an accurate representation of the materials strength as it is related to the structural component.

In application of the Monte Carlo method. Determination of proper number of simulation in Monte Carlo was obtained from examining the convergence rate for the calculated reliability numbers. Instead relying on some elaborate formulation for establishing proper number of simulations, a chart similar to the one shown in fig. 8 was used. All functional parameters were increased equally in number in order to examine over all

C.V. (Element Stress)

Minimum Detectable Crack Size (in.)	5%	10%	15%	20%
0.100	0.210	0.059	0.027	0.022
0.075	—	—	—	—
0.050	0.557	0.451	0.378	0.337
0.020	0.972	0.966	0.956	0.935
0.010	—	—	—	—

Structural Reliability of Shell (Proof Test Condition)

$K_{Ic}^1 = 30 \text{ ksi/in.}$, C.V. - 15%

Yield Strength - 160 ksi

Table III

Fracture Mechanics Method

C. V. (Element Stress)	5%	10%	15%	20%
Crack Size (in.)				
0.100	0.353 (0.960)	0.152 (0.841)	0.079 (0.744)	0.042 (0.569)
0.075	—	—	—	—
0.050	0.606 (0.976)	0.450 (0.970)	0.378 (0.965)	0.325 (0.954)
0.025	—	—	—	—

Structural Reliability

K_{IC} = 40 ksi/in., C.V. = 10%

Yield Strength = 215 Tension, Yield Strength = 240 Compression

Note: Numbers in Parenthesis are Series - Parallel System.
Others Weakest Link Concept.

Table IV

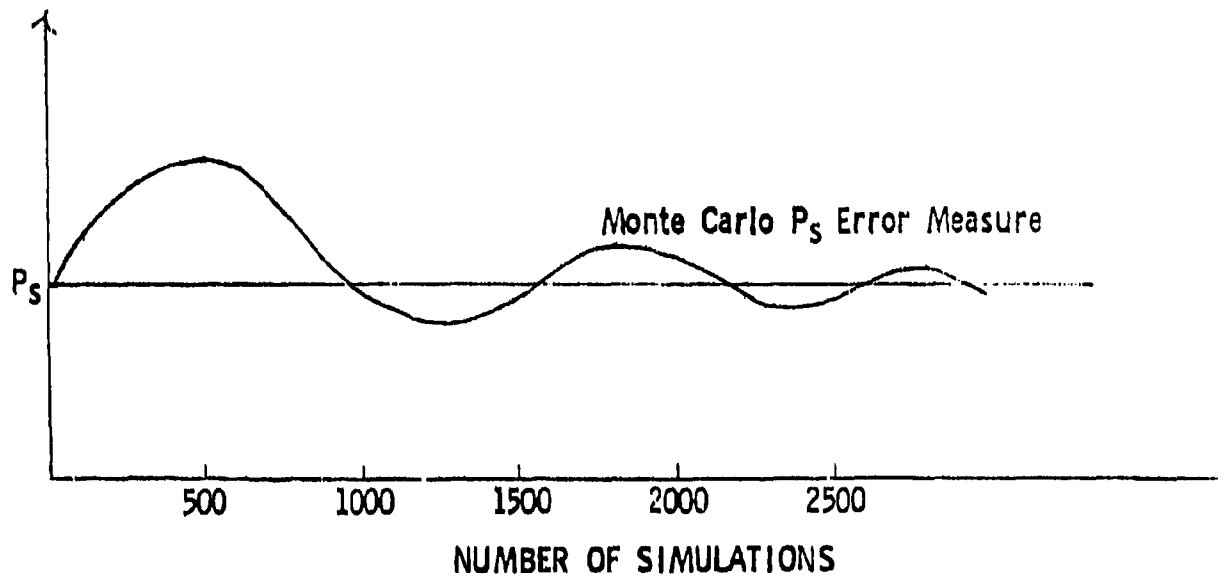


Figure 8

effects of the simulation. In order to examine the acceptability of this method, a comparison was made for R using the Warner diagram approach where normal-normal P.D.F.'s were calculated from a prescribed mean and S.D. for stress-strength values. Results show excellent agreement with Monte Carlo simulation method using the convergence rate approach.

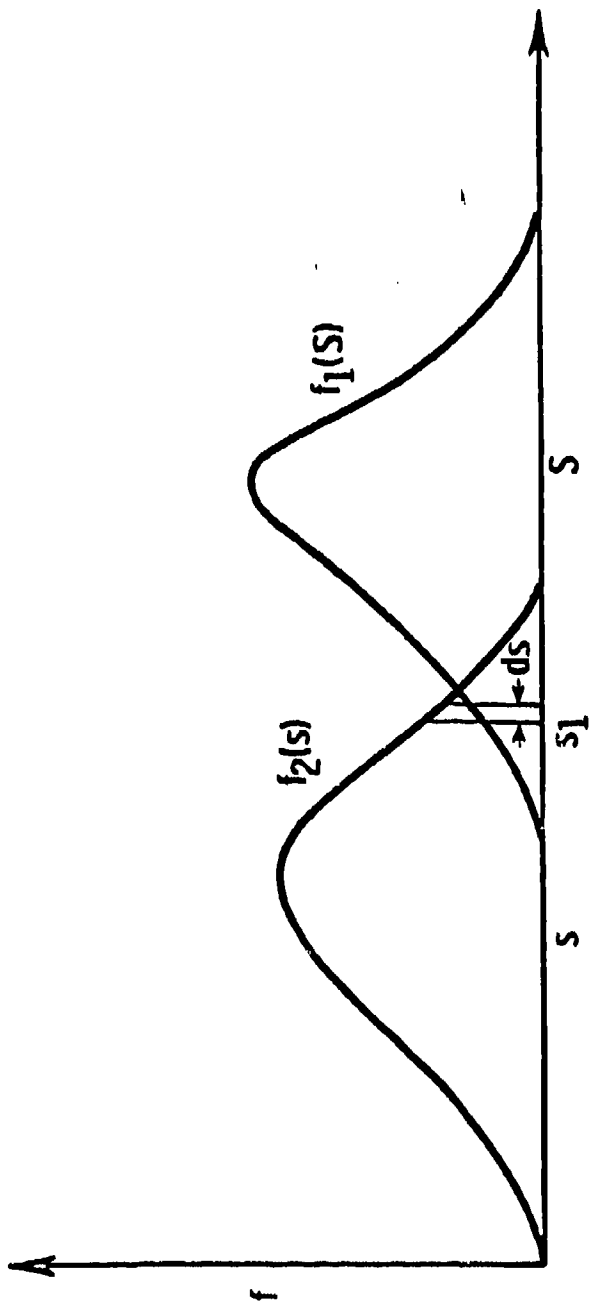
References

1. Bluhm, J. I., and Freese, C. E. "Crack Inspection Maps - An Application to Copperhead." Presented at Army Symposium of Solid Mechanics, Bass River, Mass., 3-5 October 1978
2. Tetalman, A. S. and Besuner, P. M. "The Application of Risk Analysis to the Brittle Fracture and Fatigue of Steel Structures." Proceedings of the Fourth International Conference on Fracture, Vol. 1, Waterloo Ontario, Canada, pp. 137-156, June 1977.
3. Hastings, C. H. AMMRC, Watertown, Mass., NDT Industrial Applications Branch, Private Conversation.
4. Shreides, Y. A. "The Monte Carlo Method," Pergamon Press, N.Y., Vol. 87, 197.
5. Smith, J. M. AMMRC, Watertown, Mass., NDT Branch, Private Conversation.
6. Ricca, J. J. AMMRC, Watertown, Mass., Polymer and Chemistry Div., Private Conversation.
7. Freese, C. E. Unpublished results.
8. Haugen, E. B. "Probabilistic Approach to Design," John Wiley and Sons, Inc., New York, 1968.
9. Weibull, W. "A Statistical Theory of the Materials." Proceedings of the Ingenjors Vetenskaps Akademien, Vol. 151, January 1939.

Acknowledgement

The authors acknowledge the support from Joseph I. Bluhm for providing inspiration and guidance and Lucy Channesian of AMMRC for typing and preparing the manuscript.

Appendix A



Warner Diagram

s = Calculated Stress

S = Materials Strength

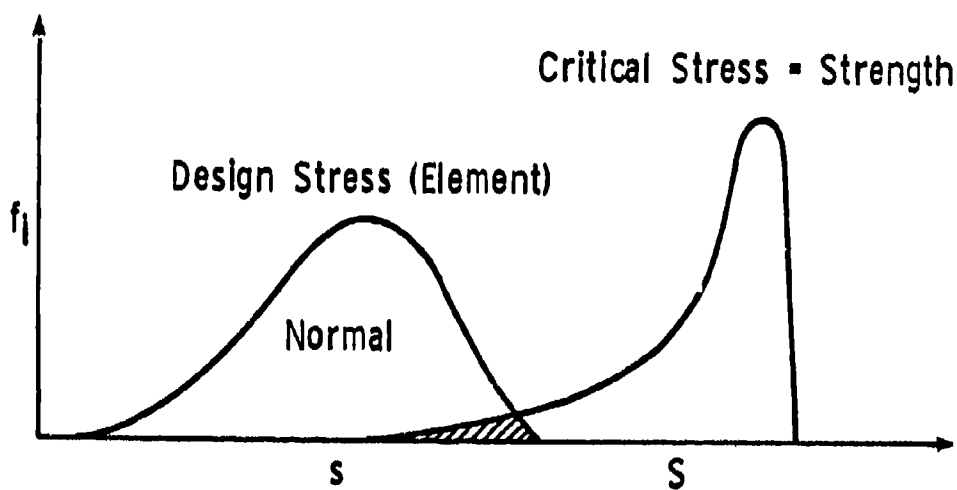
$$dP_s = f_2(s) \, ds \int_{s_1}^{\infty} f_1(S) \, dS$$

$$\text{And } P_s = \int dP_s = \int_{-\infty}^{\infty} f_2(s) \left[\int_s^{\infty} f_1(S) \, dS \right] \, ds$$

Where $f(s)$ and $f(S)$ are PDF representation for stress and strength values respectively.

PROBABILITY OF SURVIVAL DETERMINATION

Appendix B



$$Ps_K = 1/M^2 \sum_{j=1}^M \sum_{i=1}^M \alpha_i \quad \text{where } \alpha_i = \begin{cases} 1, & s_j > s_i \\ 0, & \text{Otherwise} \end{cases}$$

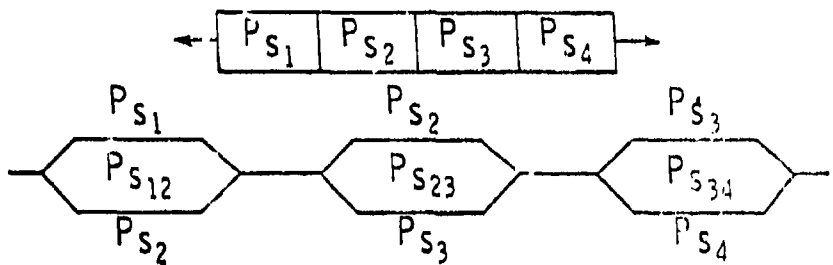
M = Number Simulations

Ps_K = Probability of Survival of Element K

Appendix C

Series - Parallel Concept (Tension-Compression)

Assume simply four element structure



$$\text{e.g., } P_{S12} = P_{S1} + P_{S2} - P_{S1} \cdot P_{S2}$$

Survival Probability for Structure

$$P_S = P_{S12} \cdot P_{S23} \cdot P_{S34}$$

For large structures all elements considered with their corresponding adjacent elements.

PREDICTED MECHANICAL BEHAVIOR OF MATERIALS WHEN SUBJECTED TO WEAPON SETBACK FORCES

Richard S. Simak
Munitions Development Branch
Munitions Division
Chemical Systems Laboratory
US Army Armament Research and Development Command
Aberdeen Proving Ground, Maryland 21010

ABSTRACT. Methods were investigated for estimating the mechanical behavior of various materials when subjected to weapon setback forces. A mathematical model was developed for predicting the dynamic behavior of the materials from which predictions concerning certain material-geometry combinations were made. Tests were carried out with aluminum and steel specimens and the resultant data were compared with results predicted by the mathematical model. The mathematical model selected was a viscoelastic model involving viscous, elastic, and, in one instance, plastic parameters.

I. INTRODUCTION. The design of chemical munitions involves several factors, among them is the structural behavior of the munition components when subjected to various loads. One important factor is the forces imposed by the launch environment which, for artillery rounds, is referred to as setback. At present, the developmental emphasis is on system testing which yields information on a specific configuration; and, if the configuration is changed, the system must be retested. In a few cases, bench testing supplements system testing and although the information obtained from the bench tests is more general than from system tests, it is limited to the geometry-material configurations tested. These two methods have resulted in increased project costs and, at times, in schedule slippages.

What is required is an alternate and somewhat more general method for analyzing the effects of the launch environment on munition components. Therefore, an investigation was undertaken to develop such a method and, thereby, reduce the amount of munition flight testing and/or dynamic testing required with its associated costs.

II. BACKGROUND. Although the plastic deformation of solids at high strain rates was commented on as early as 1904 by Hopkinson,¹ it was not until 1941 when Von Karman² and Taylor each independently established the theory of plastic propagation in metals that this phenomenon was seriously studied. Since the publication of this theory, a body of research data has grown. In general, these data can be summarized into four general statements which are: (1) The displacement mechanisms for metals subjected to impact loads are similar to those for statically applied loads but they have different distributions;³ (2) there exists a time delay between the application of impact loads and subsequent plastic yielding;¹ (3) materials' strength increases when subjected to impact loads, but by varying relative amounts for various materials, and the strain rate affects both the strength and ultimate elongation of a material;^{4,5} and (4) previous investigations showed that flow or viscous parameters are important.

III. MODELING EFFORT. Based on the information obtained during the above-mentioned literature search, a mathematical model has been developed to predict the time-dependent behavior of material. This model assumes that materials behave in an elastic manner

below the proportional limit (arbitrarily set at 2% elongation) and in a viscoelastic manner above the proportional limit. In addition, the viscoelastic element must have a time delay or, in this case, a viscous resistance feature which is known as a Voigt element. The mechanical analog of the model is given in figure 1.

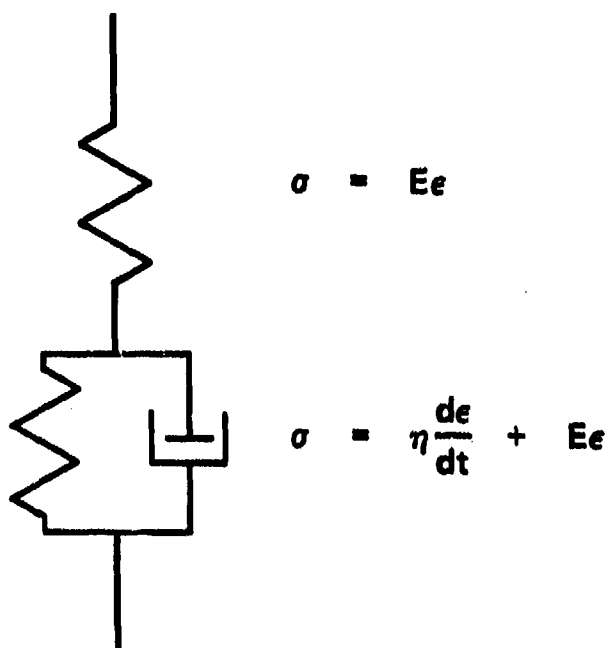


Figure 1. Mechanical Analog of Elastic-Viscoelastic Model

The response equation for this model is the sum of the two equations given to the right of figure 1. The time-dependent strain for this system is found by solving this equation for the model when excited by the forces due to the launch environment. Once the strain relationship is known, the other dynamic values can be determined. The dynamic values can, in turn, be substituted into the equations describing the specific geometry of interest which will yield predicted values. This methodology requires two types of data: first, an estimate of the forces imposed by the weapon system which can be obtained from acceleration/pressure histories of the weapons system and second the elastic and viscous constants of the material, which may be obtained from a statically obtained true stress-strain diagram by assuming that the material behaves elastically below the proportional limit and in a viscous manner above it. The graphical representation of this behavior is shown in figure 2.

IV. EXPERIMENTAL. To compare the model predictions with experimental data, a series of dynamic bench tests was performed involving two geometries (the thin flat plate as shown in figure 3 and the solid pin as shown in figure 4) and four materials (AISI 1018 and 1020 low carbon steel, type 316 austenitic stainless steel, and 6061-T6 aluminum alloy). The stress-strain diagrams for all four materials were generated to provide elastic and viscous material constants, as shown in figure 5.

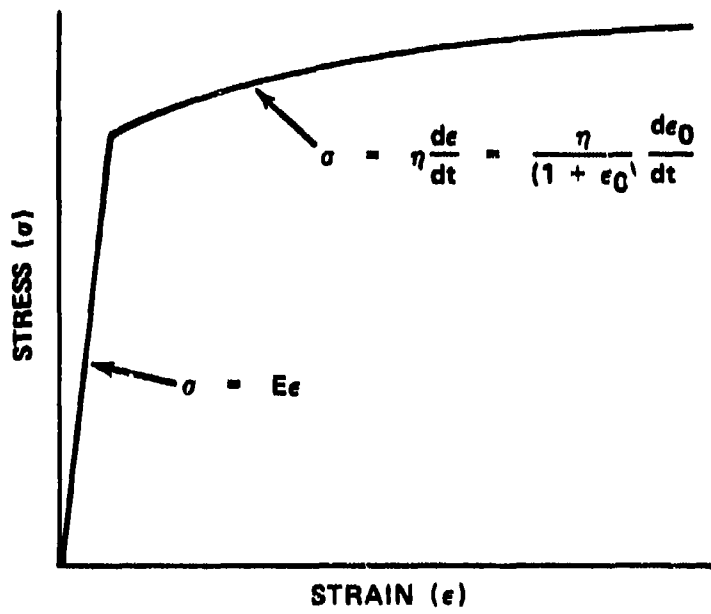


Figure 2. Idealized True Stress-Strain Diagram

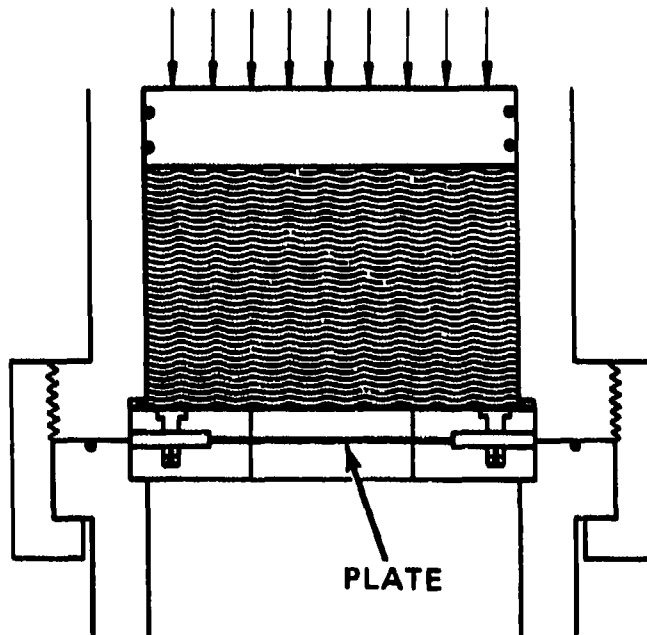


Figure 3. Flat-Plate Configuration

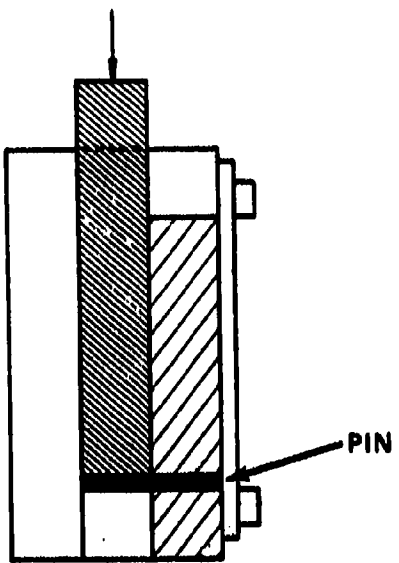


Figure 4. Solid-Pin Configuration

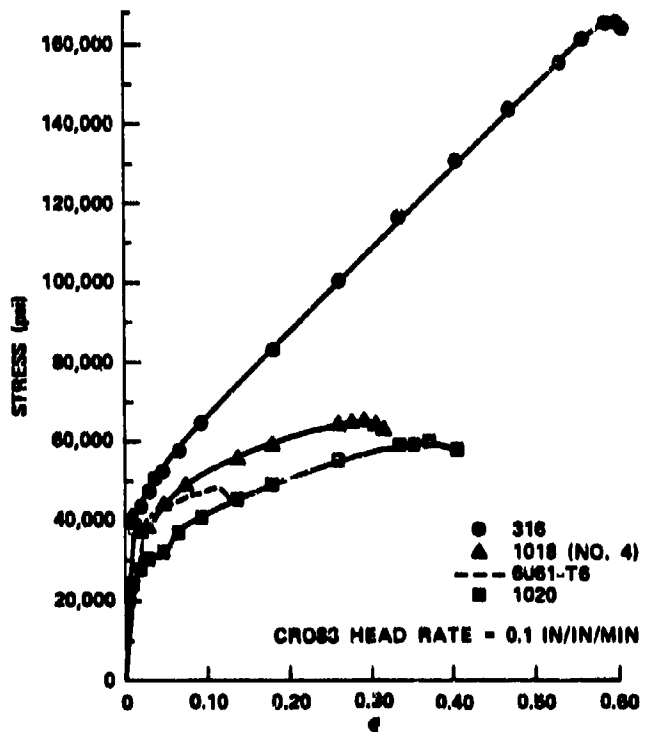


Figure 5. Statically Obtained True Stress-Strain Diagrams

The bench-test machine used in this work was a drop table shock machine which produces a controlled and reproducible acceleration at a constant pulse rate. The acceleration history for the bench-test machine used is a half sine wave pulse $[a(t) = a_p \sin(\frac{\pi}{T}t)]$. The response equation for this system is:

$$\eta \frac{de}{dt} + Ee = ma_p \sin\left(\frac{\pi}{T}t\right)$$

where the material response characteristics are on the left and the excitation forces are on the right side of the equal sign. The time dependent strain for this system is:

$$e(t) = \frac{ma_p}{\eta} \frac{\left[\frac{E}{\eta} \sin\left(\frac{\pi}{T}t\right) - \frac{\pi}{T} \cos\left(\frac{\pi}{T}t\right) + \frac{\pi}{T} e^{-\left(\frac{E}{\eta}\right)t} \right]}{\left(\frac{\pi}{T} \right)^2 + \left(\frac{E}{\eta} \right)^2}$$

which was obtained by solving the response equation. The dynamic modulus, that is, the stress divided by the strain, for this system is:

$$\phi = \frac{\left[\left(\frac{\pi}{T} \right)^2 + \left(\frac{E}{\eta} \right)^2 \right] \eta \sin\left(\frac{\pi}{T}t\right)}{\frac{E}{\eta} \sin\left(\frac{\pi}{T}t\right) - \frac{\pi}{T} \cos\left(\frac{\pi}{T}t\right) + \frac{\pi}{T} e^{-\left(\frac{E}{\eta}\right)t}}$$

In this work, the burst strength of a flat plate or the shear strength of a solid pin was to be measured; consequently, the system was evaluated at the peak stress ($t = \frac{T}{2}$). This occurs when the trigometric function in the numerator is equal to one. In addition, for these tests the pulse duration (T) was in the millisecond range which further simplifies the modulus to

$$\phi = \left(\frac{\pi}{T} \right) \eta .$$

The stress on a flat plate can then be found by solving the equation of motion for that geometry

$$\frac{\partial^2 w}{\partial t^2} = c_o^2 K^2 \Omega^2 \frac{\partial^4 w}{\partial x^4}$$

subject to the equation of continuity $v_o = \left(\frac{x}{t} \right) e$ which is:

$$\sigma = c_o v_o P \left(\frac{\Lambda}{4\pi K \Omega} \right)$$

where the stress wave propagation velocity, c_0 , equals $\left(\frac{\phi_0}{p}\right)^{\frac{1}{2}}$; radius of gyration, K , equals $\left(\frac{1}{\Lambda}\right)^{\frac{1}{2}}$; half wave length, Λ , equals $v_0 T$; and Ω equals $(1 + \frac{v}{2\pi})$, which accounts for radial and circumferential displacement. The stress on a solid pin can also be found by solving the equation of motion for that geometry, which is analogous to that for a flat plate.

V. RESULTS. The results of the dynamic bench-test effort are given in the table. This work involved five material-geometry combinations and because of the "go, no-go" nature of the test setup only upper and lower strength values are reported. Along with the test values are estimates of the precision of the shock machine, the elastic-viscoelastic model predictions, and, for comparative purposes, strength predictions based on statically obtained material properties using standard formulas.

VI. DISCUSSION. In comparing the elastic-viscoelastic model predictions with the bench-test values for low carbon steel and aluminum alloy, it is seen that the two-element model does adequately predict the behavior of these two metals. In comparing the two methods of predicting strength values, it is seen that the predictions based on the elastic-viscoelastic model are far superior to those made using standard strength values and formulas.

For the austenitic stainless steel type 316, the elastic-viscoelastic model predicted values considerably higher than the upper bench-test value for the solid-pin geometry (9,232 lb versus 2,552 lb). The most obvious explanation for this discrepancy is that the model as proposed does not adequately account for the behavior of 316 whereas it does so for low carbon steel and the aluminum alloy.

Both the low carbon steel and 6061-T6 aluminum alloy are basically pure metals doped with small percentages of other elements to achieve certain desirable mechanical properties. In the case of the aluminum alloy, the presence of these impurities in the crystal lattice tends to produce barriers to metal flow which can be modeled as a viscous drag element. In the case of low carbon steel, the presence of these impurities plus a susceptibility to strain hardening⁶ likewise tend to produce barriers to metal flow which can be modeled as a viscous drag element.

On the other hand, austenitic stainless steel type 316 is a mixture of iron, chromium, and nickel where the chromium and nickel atoms substitute for iron in the crystal lattice. Because of the high nickel content (10%-14%), this steel does not appreciably strain harden and is sometimes referred to as free spinning steel.⁷ This relative lack of strain hardening has been, in part, explained by an "easy glide" mechanism where the density of dislocations rises linearly with plastic strain.⁸ In fact, the presence of impurities would be the only serious barrier to metal flow and is overshadowed by the plasticity of the metal.

Since the austenitic stainless steel does not follow the elastic-viscoelastic model previously stated, a new and more general model which accounts for the behavior of this material must be postulated. Based on the above discussion, a three-element model shown in figure 6 is proposed. This model involves an elastic element to account for the behavior below the proportional limit, followed by a Voigt element to account for the impurities, followed by a friction element to account for the "easy glide" phenomenon. The response equation for this system is the sum of the three individual equations given in figure 6. The solution for the three-element model is analogous to that for the previously discussed elastic-viscoelastic model.

Table. Comparison Between Measured and Predicted Strengths

Material	Geometry	Batch-tested value	Estimated standard deviation	Model prediction	Static prediction
1018 Carbon steel	Flat plate (0.0153 inch thick)	647-693 psi	21.2 psi	698 psi	27 psi
1020 Carbon steel	Solid pin (0.125 inch diameter)	1,048-1,082 lb	49.0 lb	1,111 lb	388 lb
6061-T6 Aluminum	Flat plate (0.025 inch thick)	508-555 psi	21.2 psi	486 psi	59 psi
6061-T6 Aluminum	Solid pin (0.1875 inch diameter)	1,048-1,119 lb	49.0 lb	1,021 lb	714 lb
316 Austeritic steel	Solid pin (0.1875 inch diameter)	2,484-2,552 lb	78.0 lb	9,232 lb	1,898 lb

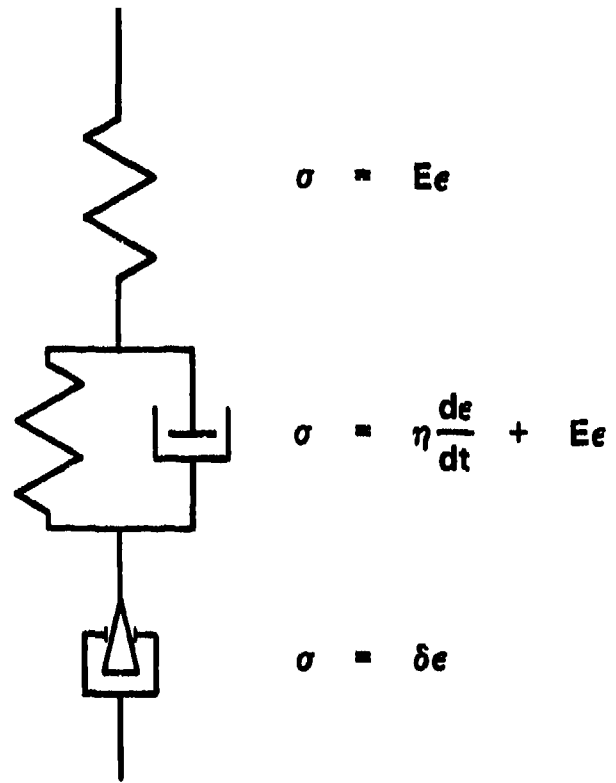


Figure 6. Mechanical Analog of Elastic-Viscoelastic-Plastic Model

In analyzing the true stress-strain diagram, three regions must be considered — elastic (0%–2% strain), viscoelastic (2%–3.9% strain) or transitional, and plastic (3.9%–59% strain) — instead of two regions as in the previous model. This, in effect, reduces the value of the viscous constant, thereby reducing the predicted shear strength from 9,232 to 2,833 lb. In comparing the three methods of predicting strength values for stainless steel, type 316, it is seen that the prediction based on the three-element model is superior to those made using both the standard formulas and the two-element model.

VII. SUMMARY. The mechanical behavior of materials subjected to impact loads can be predicted by using relatively simple mathematical models to describe their behavior, two of which have been discussed. The selection of model depends on the general form of the true stress-strain diagram of the candidate material. The model parameters can also be obtained from a true stress-strain diagram.

LITERATURE CITED

1. Clark, D. S. The Behavior of Metals Under Dynamic Loading. Met. Prog. 64(5), 67 (1953).
2. Von Karman, Theodore. OSRD No. 365. NDRC Report on the Propagation of Plastic Deformation in Solids. January 1942.
3. Rinehart, J. S., and Pearson, J. Behavior of Metals Under Impulsive Loads. Dover Publications, Inc., New York, New York. 1965.
4. Clark, D. S., and Wood, D. S. The Tensile Impact Properties of Some Metals and Alloys. ASM Trans. Q. 42, 45-74 (1950).
5. Wood, W. W., *et al.* Final Report. Advanced Theoretical Formability, Manufacturing Technology. Contract No. AF33 (657)-10823. USAF, Advanced Systems Manufacturing Technology Division. January 1965.
6. Guy, A. G. Introduction to Materials Science. McGraw-Hill Book Company, New York, New York. 1971.
7. Zapffe, C. A. Stainless Steel. American Society of Metals, Cleveland, Ohio. 1949.
8. McClintock, F. A., and Argan, A. S. Mechanical Behavior of Materials. Addison-Wesley Publishing Company, Reading, Massachusetts. 1966.

GLOSSARY

σ	Stress
ϵ	True strain = $\ln(1 + \epsilon_0)$
ϵ_0	Engineering strain
E	Modulus of elasticity
η	Viscous parameters
δ	Plastic modulus
ρ	Density
A	Shear area
I	Moment of inertia
ν	Poisson's ratio
ϕ	Dynamic tensile modulus
ϕ_s	Dynamic shear modulus = $\frac{\phi}{2(1 + \nu)}$
w	Displacement
t	Time
Λ	Half wave length = $v_0 T$
v_0	Impact velocity
a_p	Peak acceleration
T	Half sine wave period
x	Radial component of flat plate
c_0	Initial stress wave propagation velocity = $\left(\frac{\phi_s}{p}\right)^{1/2}$
K	Radius of gyration = $\left(\frac{I}{A}\right)^{1/2}$
m	Mass
Ω	Factor equal to $\left(1 + \frac{\nu}{2\pi}\right)$

SUCCESSFUL APPLICATION OF STEWARTSON'S LIQUID INSTABILITY/STABILITY CRITERIA TO THE DESIGN OF ARTILLERY PROJECTILES

John M. Ferriter
Munitions Development Branch
Munitions Division
Chemical Systems Laboratory
US Army Armament Research and Development Command
Aberdeen Proving Ground, Maryland 21010

ABSTRACT. The use of Stewartson's instability theory, in the design of liquid-filled projectiles, is a valuable tool for the munitions designer. A summary of Stewartson's theory, expanded to include viscous and liquid spin-up effects, is presented. Design procedures for applying the theory with an example are shown. Three examples, where the theory has been successfully applied, are also given.

I. INTRODUCTION. Early efforts in the design of liquid-filled projectiles gave engineers problems primarily because there was not a clear understanding of the liquid instability mechanism. When early projectile designs became unstable during flight, it was postulated that the failure of liquid to attain full spin (i.e., rigid body rotation) prior to shot exit was the chief cause for projectile instability. Longitudinal baffles were designed which effectively compartmentalized the projectile cavity. The baffles spun the liquid up as the projectile casing spun up in the tube; however, this was not sufficient to ensure that the projectile would be dynamically stable. Two problems encountered were: (1) Even though the liquid was completely spun up prior to shot exit, the baffles in the projectile could have been positioned so that asymmetries existed between the center axis of the projectile and the center of the baffles and because of this asymmetry, which could cause the projectile to be unstable, the designer could not predict whether or not two similar projectiles would be ballistically stable; (2) difficulties were also encountered in fabricating the transverse baffles due to projectile internal tolerances.

In an effort to observe the effect of liquids on the stability of projectiles, experiments were conducted in which lightweight projectiles were fired at low velocities. Low launch velocities enabled visual observations of projectile flight behavior. The problem encountered with this technique was that, unless flight behavior was dramatic, it could not determine if the wind and/or liquid caused the observed behavior.

The only theory explaining the effect of liquid in a spinning body was Greenhill's work related to spherical cavities. The theory showed that, if a spinning spherical top containing liquid was disturbed, the liquid was disturbed to a lesser degree. The liquid disturbance created natural oscillations which were characterized by discrete eigenfrequencies. The important aspect of the theory was that, if the natural frequency of the liquid coincided with a natural frequency of the top, the top could exhibit unstable motions. The coincidence of the two frequencies created a hydrodynamic couple, known as resonance. It turns out that, for a spinning spherical liquid-filled cavity, only one characteristic frequency causes resonance.

Stewartson's theory¹ analyzed the liquid effect on a spinning top. The interior geometry of the spinning top was a right circular cylinder. Stewartson found a double infinite number of modes of oscillation which would affect top stability unlike the sphere with only one mode. The modes are

characterized as radial (n) or axial (j) halfwaves. Resonance between the nutational frequency of the projectile and a natural frequency of the liquid causes dynamic instability. However, an important outcome of Stewartson's theory was that the designer could control resonance by varying the fill ratio and cavity fineness ratio (internal length/diameter ratio). Stewartson's theory has been a primary design tool in the design and development of liquid-filled munitions. The purpose of this paper is to show how the theory has been utilized for the design of liquid-filled projectiles. No mathematical derivation of Stewartson's theory will be provided as it is available in literature.

II. DYNAMICS OF LIQUID-FILLED PROJECTILES. The paper will not discuss in detail the dynamics of liquid-filled projectiles but will just mention a few key principles. The spinning liquid exerts pressure forces on the inner wall of the projectile and also is excited to a lesser degree when the projectile is subjected to an external disturbance. These two points show that there exists a complex interaction between the spinning projectile and internal liquid. The Navier-Stokes equations describe the perturbed fluid motion within the spinning projectile. The following boundary conditions are used with the Navier-Stokes equation: (1) Pressure is a constant on a free surface, (2) tangential components of the flow velocity and the velocity of the wall are equal, and (3) the normal components of the flow velocity and surface velocity are equal. A complete mathematical derivation can be found in literature.

III. STEWARTSON'S THEORY. When Stewartson's theory was applied to the design of liquid-filled projectiles, the results were twofold: (1) The theory provided the knowledge of the instability mechanism-resonance between the liquid eigenfrequency and projectile nutational frequency and (2) the theory provided designers a quantitative means for designing liquid-filled projectiles. The theory does not definitely predict the design will be stable but it does definitely state if a design is unstable.

Stewartson developed his theory using the following assumptions:²

1. The internal cavity is a right circular cylinder -- this limits the shape where the theory is applicable. However, in the case of binary projectiles, currently in development, right circular cylinders are used to contain the liquid.

2. The overturning moment is the only significant aerodynamic force. By neglecting the other aerodynamic moments, we can concentrate on the one force which will affect projectile stability with a liquid-filled payload.

3. The projectile flies with constant velocity and spin. In actuality, projectile spin decreases throughout flight where projectile velocity will decrease until apogee and then increase until impact. This assumption is chosen mainly for convenience (steady state).

4. The liquid is in rigid body rotation at shot exit with its spin identical to that of the projectile. This neglects liquid spin-up which does vary depending on liquid and launch conditions. However, it is a good assumption for first approximations.

5. The centrifugal force of the liquid is so much larger than the gravitational or drag forces -- the other forces can be neglected in the analysis.

6. The mass of liquid is small compared to the mass of the total projectile (this was taken for convenience). However, in actuality, it is a good assumption since most binary liquid payloads are approximately 10% of total projectile weight.

7. The liquid is incompressible and inviscid. Incompressibility is a good assumption for the liquids used; however, viscosity plays an important role in liquid spin-up.

8. External shell disturbances are restricted to small yaw amplitudes and the liquid experiences only small perturbations due to this external disturbance — the projectile can experience large yaw amplitudes. However, the assumption is acceptable to initial design procedures for liquid-filled projectiles.

Stewartson's theory provides the designer with two important facts:

1. The projectile yaw will grow without limit under certain conditions. Figure 1 depicts normal projectile yaw, whereas figure 2 shows yaw growth without limit.

2. The liquid conforms to cavity motions through excitation of small amplitude oscillations superimposed on the rigid body rotation.

Stewartson's instability criterion for minimizing resonance is:³

$$-1 < \frac{\tau_n - \tau_0}{\sqrt{S}} < 1$$

where τ_n = nutational frequency of projectile

τ_0 = natural frequency of liquid

S = Stewartson's parameter

$$= \frac{\rho [2R]^2 a^5}{I_x \sigma c/a}$$

where ρ = density of liquid

2R = pole value, Stewartson table

a = cavity radius

c = cavity length

I_x = axial moment of inertia

$$\sigma = (1 - 1/Sg)^{1/2}$$

Sg = gyroscopic stability

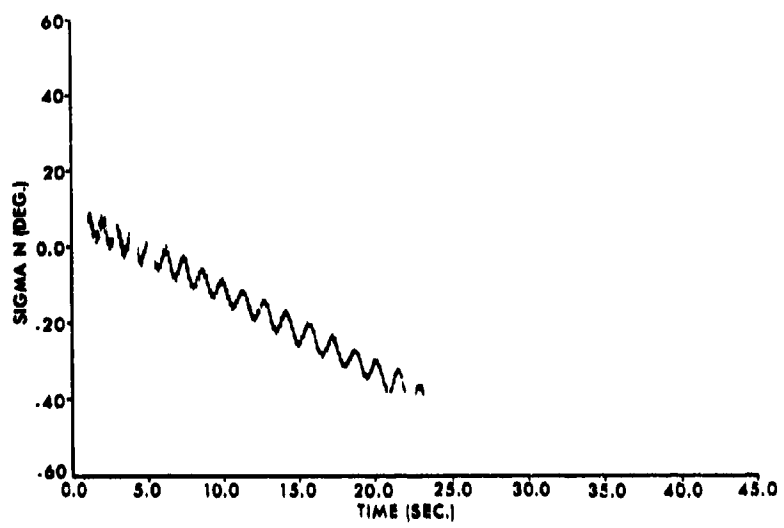


Figure 1. Normal Yaw History

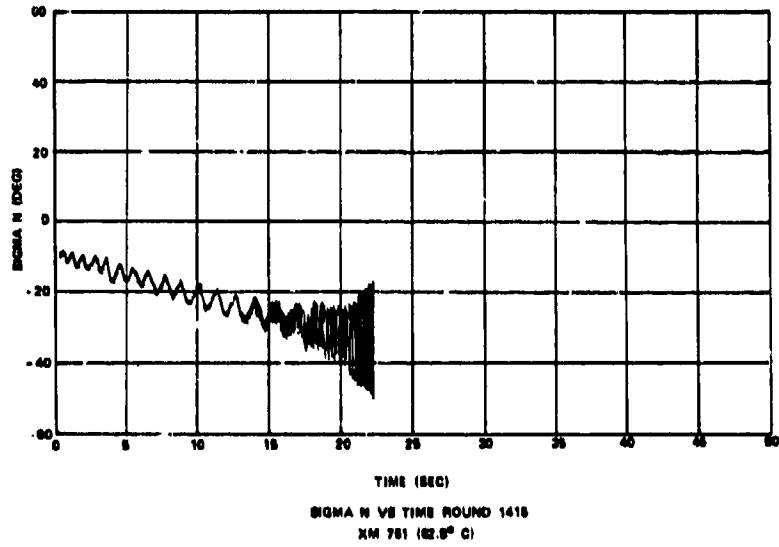


Figure 2. Yaw Growth without Limit History

IV. VISCOUS EFFECTS.⁴ Stewartson assumed the liquid to be inviscid. However, the viscosity of the liquid changes Stewartson's overall theory in the following ways: (1) The viscosity of the liquid will shift any liquid eigenfrequency slightly, and (2) the instability band for resonance is broadened. The inviscid eigenfrequency is

$$\tau = \frac{\tau_n + \tau_0}{2} \pm \left[\frac{(\tau_n - \tau_0)^2}{4} + \frac{|D|}{\sigma L} \right]^{.5}$$

When viscous effects are included, the eigenfrequency becomes

$$\tau = \frac{\tau_n + \tau_{0v}}{2} \pm \left[\frac{(\tau_n - \tau_{0v})^2}{4} + \frac{|D|}{\sigma L} \right]^{.5}$$

where

$$\tau_{0v} = \tau_0 + \frac{\partial \tau_0}{\partial c/a(2j+1)} \cdot \frac{c}{a(2j+1)} \left[\frac{\delta a}{a} - \frac{\delta c}{c} \right] + \frac{\partial \tau_0}{\partial b^2/a^2} \cdot \frac{2b^2}{a^2} \cdot \frac{\delta a}{a}$$

The difference of the viscous and inviscid liquid eigenfrequency, $\Delta\tau_0$, is composed of a real and an imaginary part [$\tau_{0v} - \tau_0 = \Delta\tau_0 = \epsilon - i\delta$]. The real part is added to the liquid eigenfrequency to shift it slightly where the imaginary part broadens the resonance band. Stewartson's instability criterion is modified to

$$-\left(1 + \frac{\delta}{\sqrt{S}}\right) < \frac{\tau_0 + \epsilon - \tau_n}{\sqrt{S}} < \left(1 + \frac{\delta}{\sqrt{S}}\right)$$

when viscosity is taken into account.

V. SPIN-UP. One of Stewartson's assumptions was that the liquid is at rigid body rotation at shot exit. This assumption has been experimentally shown (using on-board telemetry in projectiles) to be invalid. The liquid spin-up — defined as the process where the liquid acquires angular momentum — varies depending on liquid viscosity and projectile launch conditions. As the liquid spins up, the projectile casing spins down until liquid rigid body rotation is attained. The liquid close to the wall will spin up due to the frictional force between the liquid and the projectile casing. A second spin-up phenomenon exists which is defined as Eckman layers. An Eckman layer is formed when the canister ends act as centrifugal fans sucking the liquid from the nonrotating center core and throwing the liquid outward. The question is how to include liquid spin-up in the analysis of a liquid-filled projectile. Wedemeyer has shown that eigenfrequencies in a partially spinning fluid are the same as an equivalent cylinder having the same angular momentum. Knowing this, the designer can determine the stability of the projectile as liquid acquires angular momentum. The designer can evaluate spin-up at various stages; i.e., 10% spin-up, 20% spin-up.

The curves in figures 3 and 4 depict liquid spin-up.

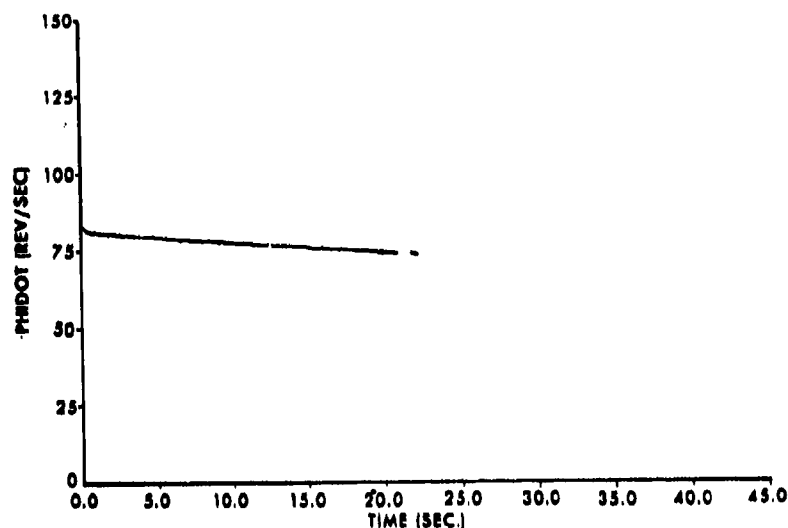


Figure 3. Liquid Spin-Up

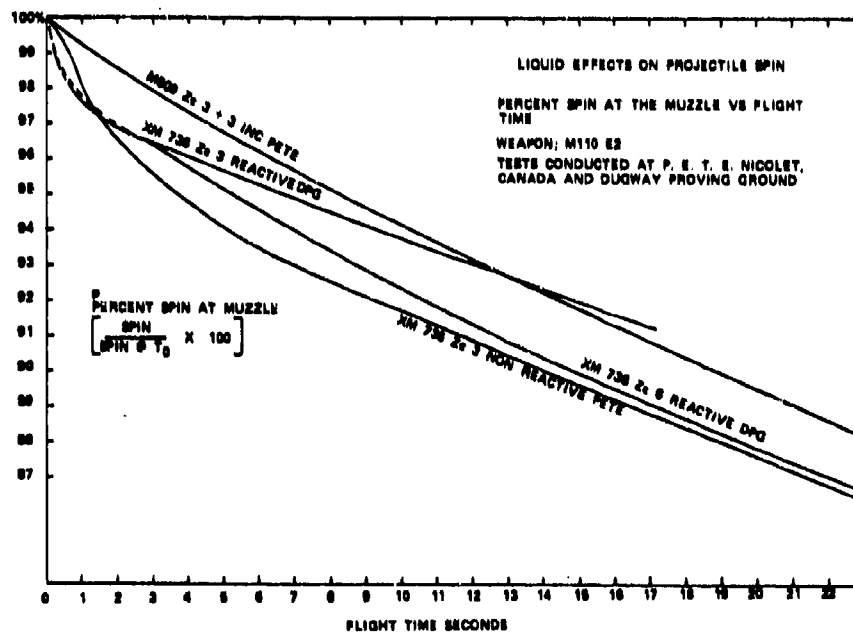


Figure 4. Liquid Effects on Projectile Spin

VI. APPLICATION OF STEWARTSON'S THEORY. The designer must apply Stewartson's theory modified for viscous effects to the steady state condition (no liquid spin-up) and then examine projectile stability during liquid spin-up. The following design steps may be used as a guide.

1. First a liquid fill must be chosen. The internal cavity dimensions will be designed dependent on the liquid chemistry and the fact that the liquid-filled projectile should weigh the same as conventional munitions of the same external shape.
2. The physical characteristics of the proposed design (moments of inertia, weight) are then used to calculate gyroscopic stability. Gyroscopic stability predicts projectile stability at shot exit.
3. The viscosity of the liquid should be checked to see if it is sufficient to produce viscous effects.
4. Determine Stewartson's instability criteria.
5. If the projectile is stable in steady state, the stability during liquid spin-up should then be examined.

The following example will illustrate the first four steps. The fifth step is lengthy due to the number of iterations needed to determine stability during liquid spin-up.

155-mm Projectile

Step 1: Determine the initial physical characteristics.

$$I_x = 19.525 \text{ slug}\cdot\text{ft}^2$$

$$I_y = 198.224 \text{ slug}\cdot\text{ft}^2$$

$$m = 3.20 \text{ slug}$$

$$n = 20 \text{ cal/turn}$$

$$\rho_a = 0.002378 \text{ slug}/\text{ft}^3$$

$$d = 0.51 \text{ ft}$$

$$a = 0.17 \text{ ft}$$

$$c/a = 4.65$$

$$C_{M\alpha} = 5.96$$

$$M_f = 0.236 \text{ slug}$$

The above constants are projectile physical characteristics calculated from step 1 or initial launch conditions; i.e., air density, bore rifling, and static moment coefficient.

Step 2: Next, calculate the rigid body gyroscopic stability.

$$Sg_r = \frac{p^2}{4M}$$

$$p = \frac{I_x}{I_y} \frac{2\pi}{n} = 0.0309$$

$$4M = 4 \left(\frac{\rho a S' d}{2n} \right) k_y^{-2} C_{Ma} = 0.00049$$

$$Sg_r = 1.95$$

The nutational frequency of the projectile is then calculated.

$$\tau_n = \frac{I_x}{I_y} (1 + \sigma)$$

$$\sigma = (1 - 1/Sg_r)^{.5} = 0.698$$

$$\tau_n = 0.167$$

The liquid gyroscopic stability is checked.

$$Sg_L = Sg_r \left(\frac{I_{x_0}}{I_{x_0} + i_{x_0}} \right)^2$$

$$i_{x_0} = 0.696 \text{ slug-ft}^2$$

$$I_{v_0} = I_x - i_{x_0} = 18.829 \text{ slug-ft}^2$$

$$Sg_L = 1.81$$

Step 3: Determine viscous effects.

$$v = \text{launch velocity} = 1027 \text{ ft/sec}$$

$$\Omega = \frac{2\pi}{nd} v = 632.6 \text{ radians/sec}$$

$$a = 5.2 \text{ cm}$$

$$\nu = 1.1 \times 10^2 \text{ stoke}$$

$$Re = 1.55 \times 10^6$$

$$\epsilon = 0.0003$$

$$\delta = 0.0007$$

ϵ & δ are sufficiently small that effects due to viscosity may be neglected.

Step 4: Calculate Stewartson instability at steady state.

Cavity is 90% full or $b^2/a^2 = 0.02$

$$c/a = 4.65$$

Construct the following table:

j	$4.65/2j + 1$	$r_0(n,j)$	$2R$
0	4.65	-	-
1	1.55	0.35 (1, 1)	1.359
2	0.93	0.45 (2, 2)	0.343
3	0.664	0.24 (2, 3)	0.119

Stewartson's table ($b^2/a^2 = 0.02$) is entered knowing columns 1 and 2 above, where radial modes $n = 1, 2, 3$ are checked to find r_0 (column 3) and $2R$ (column 4).

Stewartson's parameter is calculated

$$S = 0.38 \times 10^{-2} (2R)^2$$

for $n = 2, j = 3$

$$S = 5.38 \times 10^{-5} \quad \sqrt{S} = 7.33 \times 10^{-3}$$

$$-1 < \frac{r_0 - r_n}{\sqrt{S}} < 1$$

$$-1 < 9.96 < 1$$

The instability criteria show the projectile should be stable at steady state.

VII. PROJECTILES DESIGNED USING STEWARTSON'S THEORY. Designers must keep in mind that the chemical-filled round is normally required to be ballistically similar to a conventional round in the same family. This allows the use of conventional rounds as spotter rounds and also allows the use of the same firing tables with minor corrections. Projectiles are ballistically similar when the following are nominally the same: (1) external shape, (2) drag, (3) weight, and (4) internal ballistic characteristics. However, differences in physical characteristics may exist, provided that the effect of these differences on the means of the burst point distribution are predictable and can each be compensated for by the application of constant corrections for each charge.

A. M687 Projectile. The first binary round to apply Stewartson's theory was the M687 projectile. The advanced development round (see figure 5) was designed using a computer model of Stewartson's theory. Initial dispersion differences for impact points were attributed to miscalculation of range or the use of a faulty propellant or both. At the same time, failure of the burst disks to shear (which allows mixing of the liquids) and also changing the internal cavity from two to one right circular cylinder masked an instability problem. Increased instrumentation (on-board telemetry packages and high-speed tracking cameras) showed that the M687 round had stability problems. The M687 projectile used the same aerodynamic shape as the M483 improved conventional munition, a stable design. Therefore, the instability was attributed to the liquid payload. Analyses of the computer model revealed that liquid spin-up was neglected. The model predicted steady state behavior. The model was revised to incorporate the liquid spin-up phenomenon. The incorporation of the liquid spin-up resulted in the shortening of the internal cavity by 3.8 cm. Subsequent field trials showed the design to be stable under the severest launch conditions. Figure 6 shows the final design.

B. XM736 8-Inch Projectile. The XM736 8-inch projectile is currently in the development cycle. It has the same aeroballistic configuration as the M509 improved conventional munition. The computer model of Stewartson's theory, including viscous corrections and liquid spin-up, was used to arrive at the present design (figure 7). The use of Stewartson's theory minimized the possibility of a liquid stability problem. The XM736 projectile has a very stable aerodynamic shape; that fact, plus the adaptation of Stewartson's theory, produces a stable design even under the severest launch conditions.

C. 155-mm IVA Projectile. The 155-mm IVA projectile is currently in exploratory development. Stewartson's theory has been adapted for a number of liquid fills. All the designs have been successfully flight tested. A typical configuration is shown in figure 8.

Even though Stewartson's theory can only predict unstable rounds, the use of the theory has minimized costly testing by eliminating poor designs on the drawing board prior to fabrication. Tremendous success has been achieved in the design of liquid-filled projectiles by adapting Stewartson's theory. Currently, at Chemical Systems Laboratory, an independent laboratory in-house research project is in progress to expand Stewartson's theory for an internal step design. Stewartson's theory assumes a constant inside diameter. Current projectile designs may require a step design — two different inside diameters. The current approach for design of such projectiles is to assume a mean diameter. So far this has been successful. However, it is anticipated that a quantitative method will result from this research study.

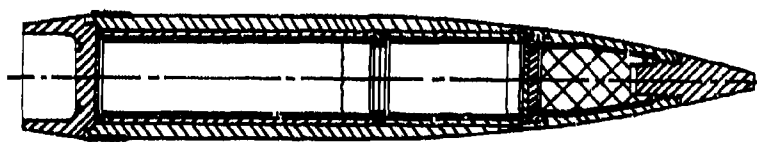


Figure 5. Advanced Development Round Design

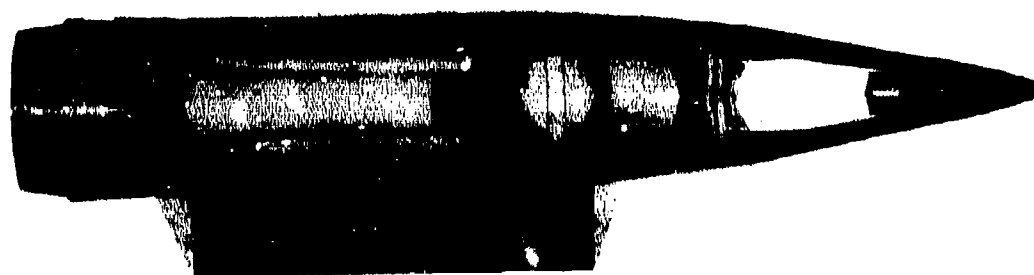


Figure 6. M687 Projectile Final Design

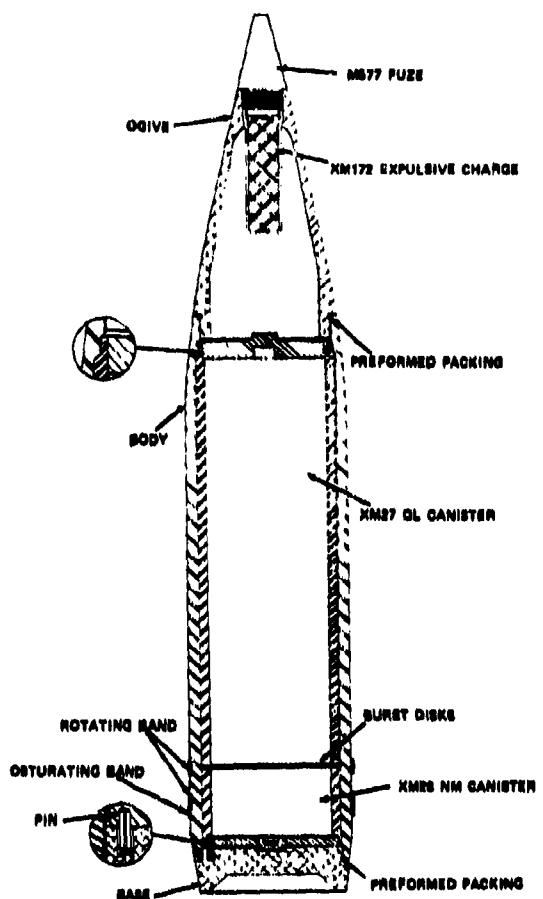


Figure 7. XM736 Projectile

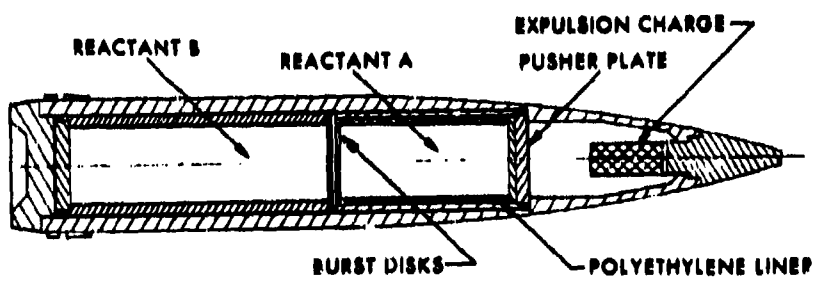


Figure 8. 155-mm IVA Projectile

VIII. CONCLUSION. Stewartson's instability/stability theory modified to include viscous effects and liquid spin-up provides the designer with a useful tool in liquid-filled projectile design. The use of Stewartson's theory in the design of binary chemical rounds has been very successful. The theory has reduced costly testing by computer modeling prior to fabrication and subsequent flight tests.

LITERATURE CITED

1. Stewartson, K. On the Stability of a Spinning Top Containing Liquid. *J. Fluid Mech.* 5, Part 4 (1959).
2. Karpov, B. G. BRL Report 1477. Dynamics of Liquid-Filled Shells - Aids for Designers. May 1963.
3. AMCP 706-165. Engineering Design Handbook. Liquid-Filled Projectile Design. April 1969.
4. Wedemeyer, E. H. BRL Report 1287. Dynamics of Liquid-Filled Shell: Theory of Viscous Corrections to Stewartson's Stability Problem. June 1965.

TOTAL TIME ON TEST PLOTS

Richard E. Barlow and Bernard Davis
 University of California, Berkeley
 Berkeley, California

I. INTRODUCTION

In this paper we present a particular graphical technique which is very useful in analyzing failure and survival data. The central concept in reliability theory is that of the failure rate. This is a feature of the life distribution. In fact, if the life distribution is continuous, which is very often the case, the failure rate uniquely determines the life distribution. Failure rate and aging are two very closely related concepts. For instance, if the unit which is being tested or is in service does not age with time, that is, its residual age is independent of its present age, we might say its life distribution has constant failure rate. This is the well-known characteristic property of the exponential distribution i.e.

$$F(x) = 1 - \exp \{-x/\theta\} \quad \theta > 0 \\ x \geq 0$$

Then,

$$\begin{aligned} \text{Prob } [X > x + y \mid X > x] &= \frac{\text{Prob } [X > x + y]}{\text{Prob } [X > x]} \\ &= \exp \{-(x + y)/\theta\}/\exp \{-x/\theta\} \\ &= \exp \{-y/\theta\} \\ &= \text{Prob } \{X > y\} . \end{aligned}$$

This research was supported by the Air Force Office of Scientific Research (AFSC), USAF, under Grant AFOSR-77-3179 with the University of California.

It can be shown quite easily that the only continuous life distribution with the non-aging property

$$\text{Prob } [X > x + y \mid X > x] = P[X > y]$$

is the exponential [3].

This is an ideal life distribution where the units of every age have the same residual life distribution as new units.

We have used the term "failure rate" earlier and we shall give a precise definition of the term below.

The conditional probability that a unit of age t will fail in the next interval of length x is

$$F(x/t) = \frac{F(t+x) - F(t)}{\bar{F}(t)}$$

where $\bar{F}(t) = 1 - F(t)$ is the survival function.

The failure rate $r(t)$ at time t is defined to be

$$\begin{aligned} r(t) &= \lim_{x \rightarrow 0} \frac{1}{x} \frac{F(x+t) - F(t)}{\bar{F}(t)} \\ &= \frac{f(t)}{\bar{F}(t)} \end{aligned}$$

where $f(t)$ is the density function of F . Note that $f(t)$ will exist if F is an absolutely continuous distribution. Most of the life distributions of interest are absolutely continuous, so, unless we specify otherwise, we shall assume that the density function exists for all the distributions under consideration.

If we integrate the failure rate function between 0 and x we get

$$\int_0^x r(t) dt = \int_0^x \frac{f(t)}{\bar{F}(t)} dt$$

$$= -\log \bar{F}(x)$$

i.e.

$$\bar{F}(x) = \exp \left\{ - \int_0^x r(t) dt \right\}.$$

So we see that the survival function \bar{F} , and hence the distribution function F , is uniquely determined by the failure rate function $r(t)$.

For the exponential distribution,

$$r(t) = \frac{1/\theta \exp \{-x/\theta\}}{\exp \{-x/\theta\}}$$

$$= 1/\theta$$

i.e. the exponential distribution has constant failure rate.

Other classes of life distributions of interest are the Increasing Failure Rate (IFR) distributions and the Decreasing Failure Rate (DFR) distributions. As the name suggests, a life distribution F is IFR if $r(x)$ is increasing and similarly, F is DFR if $r(x)$ is decreasing. Usually, items which during their life-span are subjected to wear tend to have life distributions which are IFR. The closest to a constant failure rate is exhibited by life distributions of electronic components which degrade very slowly and then only at the atomic level.

The interpretation of IFR is that as the item on test gets older, the distribution of the residual life tends to get closer to zero in some sense.

In terms of probabilities,

$$\text{Prob } [X > x + y \mid X > x]$$

decreases in x for all $y > 0$, assuming, of course, $\text{Prob } [X > x] > 0$.

A similar explanation applies to DFR distributions. For a rigorous treatment of the above see [8].

II. TOTAL TIME ON TEST

This classification of life distributions into IFR, DFR and constant failure rate distributions is of particular interest in reliability engineering and maintenance planning. For example, in formulating replacement policies, if it is known that the life distribution is either exponential or DFR, then clearly the optimal policy is to replace only upon failure.

Let us now suppose that we have a random sample

$$x_1, x_2, \dots, x_n$$

from a life distribution F .

$$\text{Let } x_{(1)} < x_{(2)} < \dots < x_{(n)}$$

be the ordered observations. Then,

$$T(x_{(i)}) = \sum_{j=1}^i x_{(j)} + (n - i) x_{(i)}$$

is defined to be the *total time on test* till the i th failure.

In general, if we denote by $n(u)$ the number of items on test at time u ,

$$T(x) = \int_0^x n(u) du$$

is the total time on test till x .

The total time on test we have defined above is not scale-independent so usually it is scaled by dividing by $T(X_{(n)})$.

Define

$$H_n(i/n) = \frac{T(X_{(i)})}{T(X_{(n)})}.$$

Then $H_n(i/n)$ is called the scaled total time on test till the i th failure and the plot of $(i/n, H_n(i/n))$ where adjacent points are joined by straight lines is known as the empirical scaled total time on test. We define $H_n(0) = 0$ so that the plot lies in the unit square and is 0 at 0 and 1 at 1.

If the underlying life distribution were really exponential it can be quite easily shown (see [2]) that $(H_n(\frac{1}{n}), \dots, H_n(\frac{n-1}{n}))$ are jointly distributed like the order statistics from a sample of size $n - 1$ from a Uniform $[0,1]$ distribution. Hence, we might expect $H_n(\frac{1}{n})$ to lie close to $1/n$ so that the plot would be quite close to the diagonal. Figure 1 shows an empirical scaled total time on test computed from a simulated exponential distribution with $n = 20$.

The theoretical basis for considering this plot as an exploratory tool for determining whether the underlying distribution is IFR, DFR or exponential is as follows:

Let $F_n(n)$ be the empirical distribution function determined by the sample.

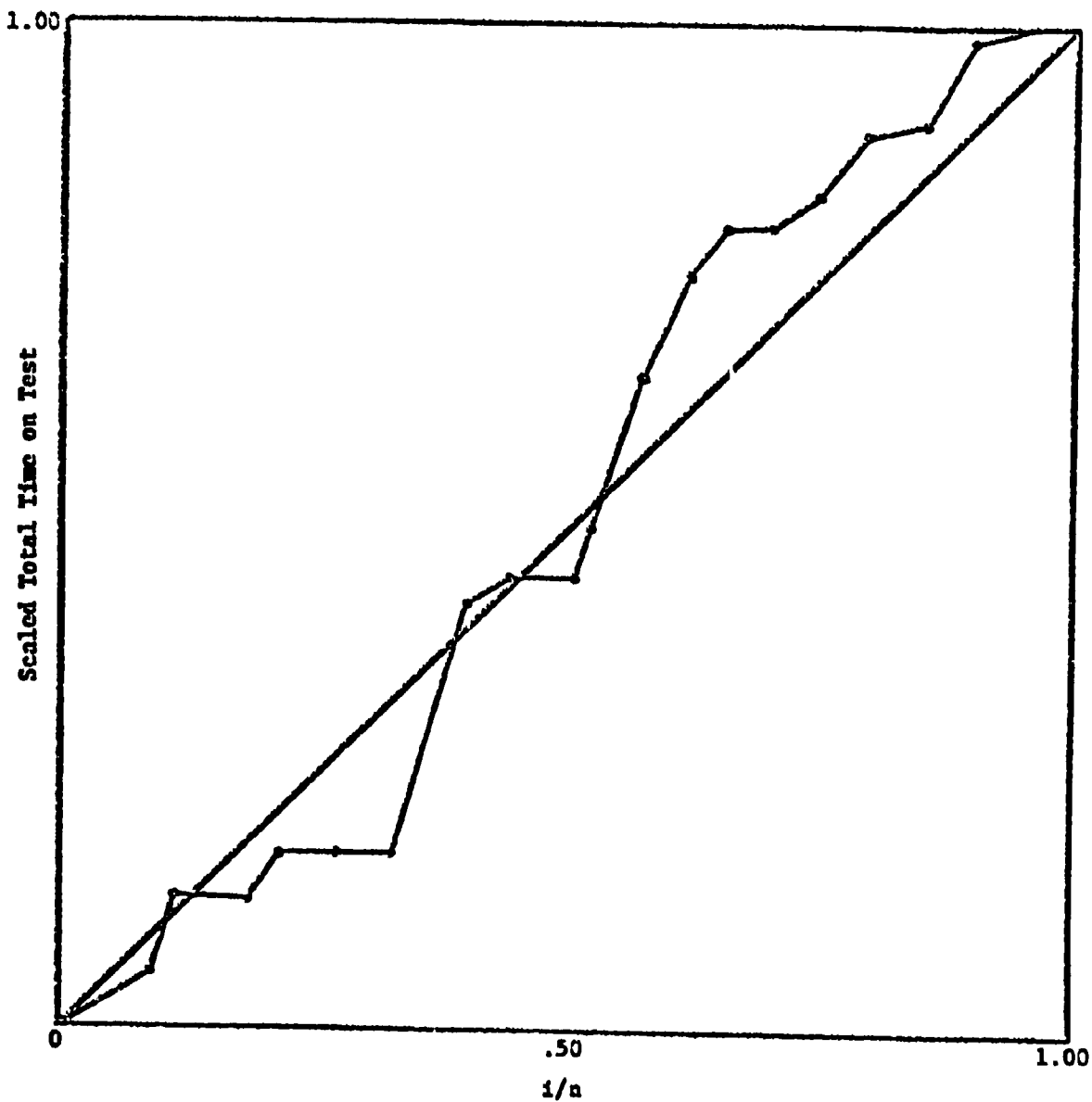


FIGURE 1

i.e.

$$F_n(x) = \begin{cases} 0 & \text{if } x < X_{(1)} \\ i/n & \text{if } X_{(i)} \leq x < X_{(i+1)} \\ 1 & \text{if } X_{(n)} \leq x . \end{cases}$$

Then it can be shown quite easily that

$$\frac{1}{n} T(X_{(i)}) = \int_0^{X_{(i)}} (1 - F_n(u)) dn .$$

Now define a transform of the actual distribution function as follows

$$H^{-1}(t) = \int_0^{F^{-1}(t)} (1 - F(u)) du \quad 0 \leq t \leq 1 .$$

The slope of $H_F^{-1}(t)$ at $t = F(x)$ can be shown to be $\frac{1}{r(x)}$.

Suppose that F has finite expectation, then the plot of

$(t, \frac{H_F^{-1}(t)}{H_F^{-1}(1)})$ is known as the scaled total time on test plot of F .

Figure 2 shows scaled total time on test plots of selected Weibull distributions. The significance of this plot is that the total time on test plot of an exponential distribution is the diagonal, that of an IFR distribution is a concave curve and that of a DFR distribution is a convex curve. Note that the Weibull family has both IFR and DFR members depending on the shape parameter.

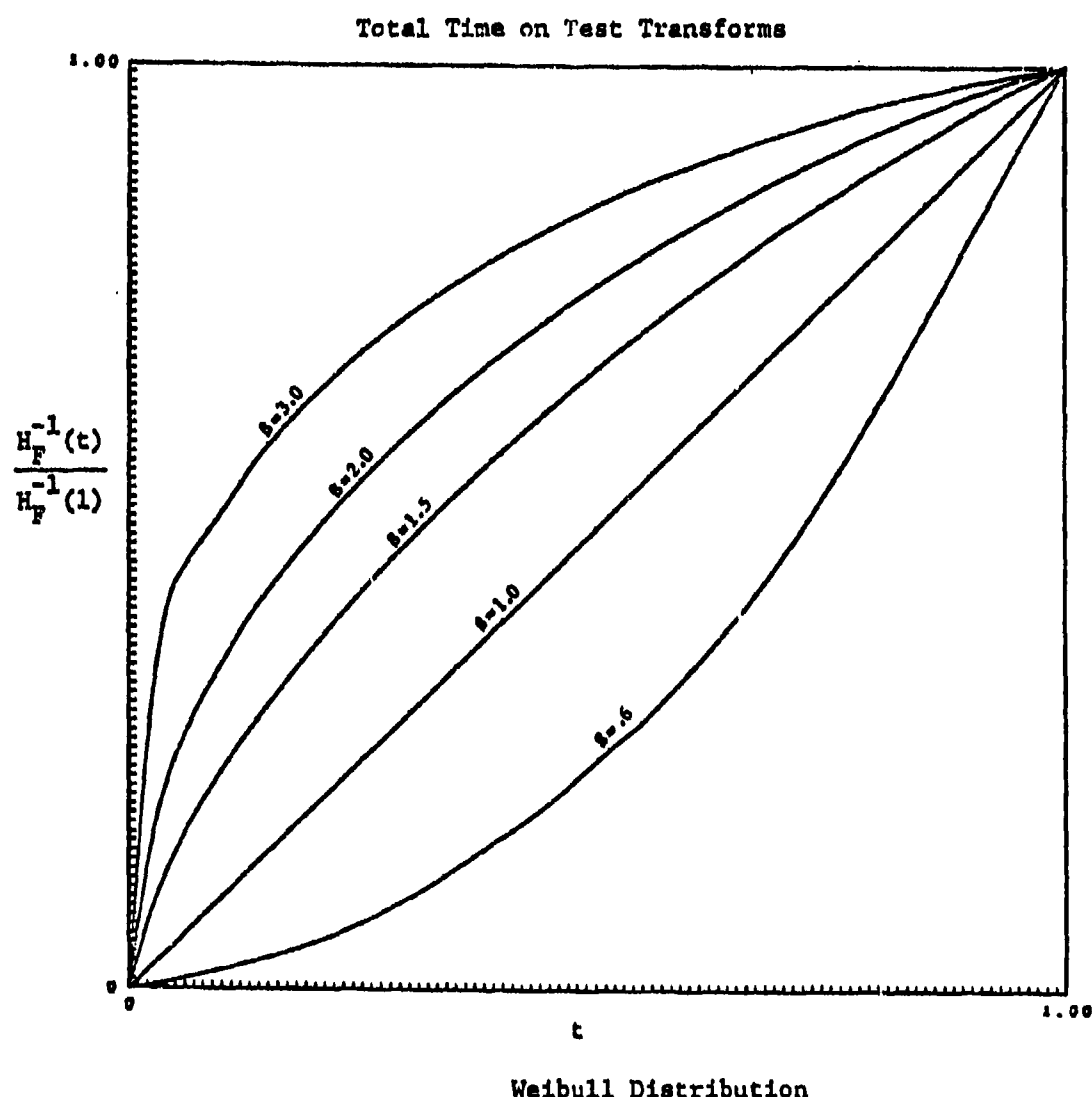


FIGURE 2

It has been proved (see [2]) that as the sample size increases the empirical plot converges to the total time on test plot of the actual distribution so that the empirical scaled total time on test is a very valid graphical tool to study the failure rate with.

Figure 3 is based on failures of engines of a certain model tractor. Data on 22 tractors were available and we had the times of failures of the tractors due to engine failure. When the original engine failed it was replaced by a reconditioned one and when it failed it was replaced by yet another reconditioned engine. An analysis of the life times of the engines showed that the original engines had life times which were quite IFR but the reconditioned engines were not quite as IFR (see [4]). For a related paper which contains several kinds of data see [1].

When the underlying life distribution is exponential we saw that the empirical scaled total time on test tends to lie close to the diagonal. This fact can be exploited to formulate a very simple test for exponentiality. If the plot were to follow the diagonal we might expect it to cross the diagonal a number of times. Then the number of crossings of the diagonal by the plot could be used as a test statistic. This was proposed by Barlow and Campo [2] and they computed the sampling distribution of the number of crossings when $n = 20$ using simulation. The exact distribution of the number of crossings has been computed by Bergman [5].

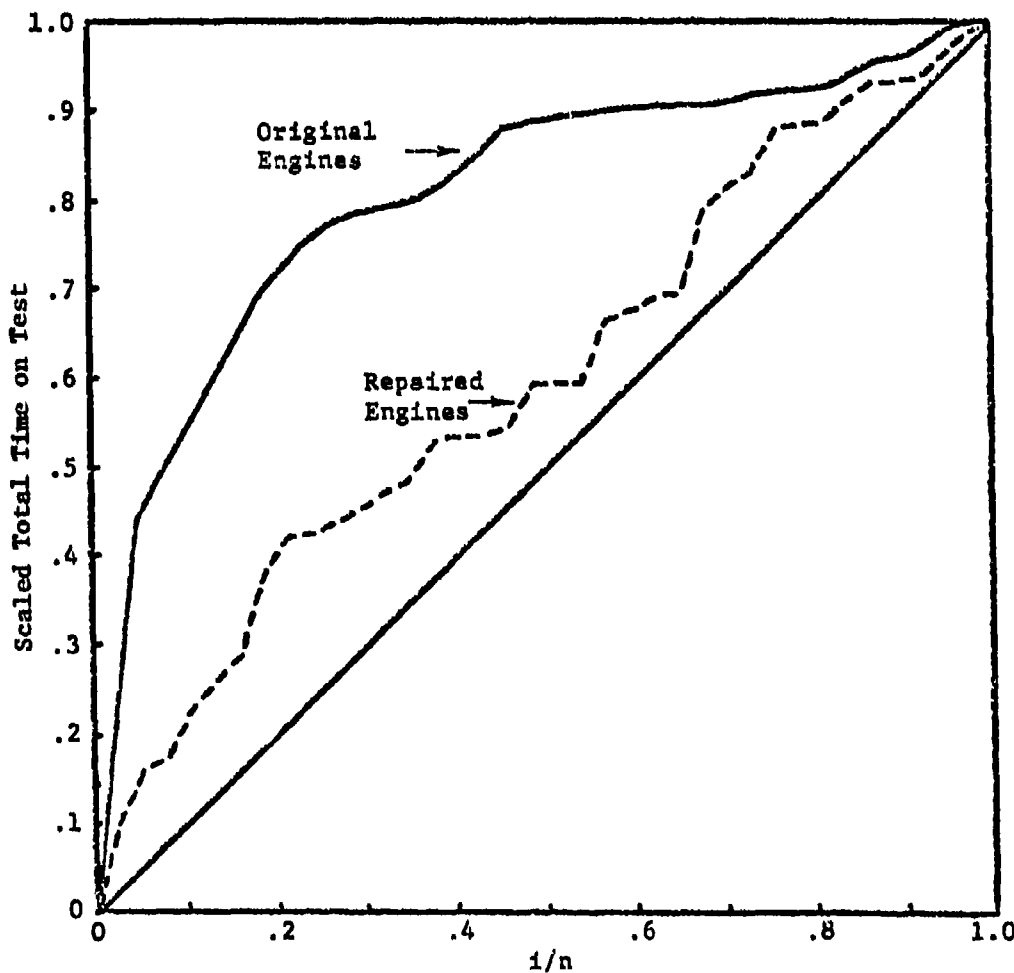


FIGURE 3

III. APPLICATIONS

One application of the total time on test plot is a method for determining graphically optimum replacement policies. We will use the tractor engine data for an example. Suppose c_1 is the cost of a tractor failing in service and c_2 is the cost of pulling out a tractor and replacing it during a planned maintenance period. We will assume that $c_1 > c_2$. Let F denote the underlying life distribution and let R be the planned operating time between overhauls of the engine. Then the expected long run cost of using the maintenance policy R is

$$C(R) = \frac{c_1 F(R) + c_2 (1 - F(R))}{R} \cdot \int_0^R (1 - F(u)) du$$

Since F is unknown we replace it with F_n , the empirical distribution function. Then, given c_1 and c_2 we want to determine the optimal R by minimizing

$$C(R) = \frac{c_1 F_n(R) + c_2 (1 - F_n(R))}{R} \cdot \int_0^R (1 - F_n(u)) du$$

Usually this is done numerically but we can use the total time on test plot to do it much more easily.

Recall that the total time on test till the i th failure was defined to be

$$T(X_{(i)}) = \int_0^{X_{(i)}} n(u) du$$

$$= n \int_0^{x_{(1)}} (1 - F_n(u)) du .$$

So that,

$$\left(\frac{1}{n}\right) \cdot T(x_{(1)}) = \int_0^{x_{(1)}} (1 - F_n(u)) du .$$

Now, minimizing $C(R)$ is equivalent to maximizing

$$\begin{aligned} \frac{1}{C(R)} &= \frac{(1/n) \cdot T(R)}{c_1 F_n(R) + c_2 (1 - F_n(R))} \\ &= \frac{(1/n) \cdot T(R)}{(c_1 - c_2) \left\{ \frac{c_2}{c_1 - c_2} + F_n(R) \right\}} \\ &= \frac{T(x_{(n)})}{n(c_1 - c_2)} \cdot \frac{T(R)/T(x_{(n)})}{\frac{c_2}{c_1 - c_2} + F_n(R)} . \end{aligned}$$

Clearly, maximizing the above is equivalent to maximizing

$$\frac{T(R)/T(x_{(n)})}{\frac{c_2}{c_1 - c_2} + F_n(R)} \quad (*)$$

To get the R which maximizes the above, draw the tangent from

$\frac{c_2}{c_1 - c_2}$ to the empirical scaled total time on test plot.

Let s denote the abscissa of the point of tangency. Then $F_n^{-1}(s)$ is the desired value of R . From the graph (Figure 4) it is seen that the slope of the tangent is the maximum value of (*).

This procedure can be implemented on an interactive computer graphics system to determine the sensitivity of R to different values of the costs c_1 and c_2 . Of course, the major drawback of this method is that if the empirical total time on test plot is based on a very unrepresentative sample then the resulting value of R may be worthless. On the other hand, if F were known we would use the transform of the actual distribution and the same method can be applied to the plot of the transform to compute R . In Figure 4 we have taken $c_1 = 3c_2$ and the optimum replacement policy is to overhaul the engines after 4815 operating hours. For related work see [4], [6].

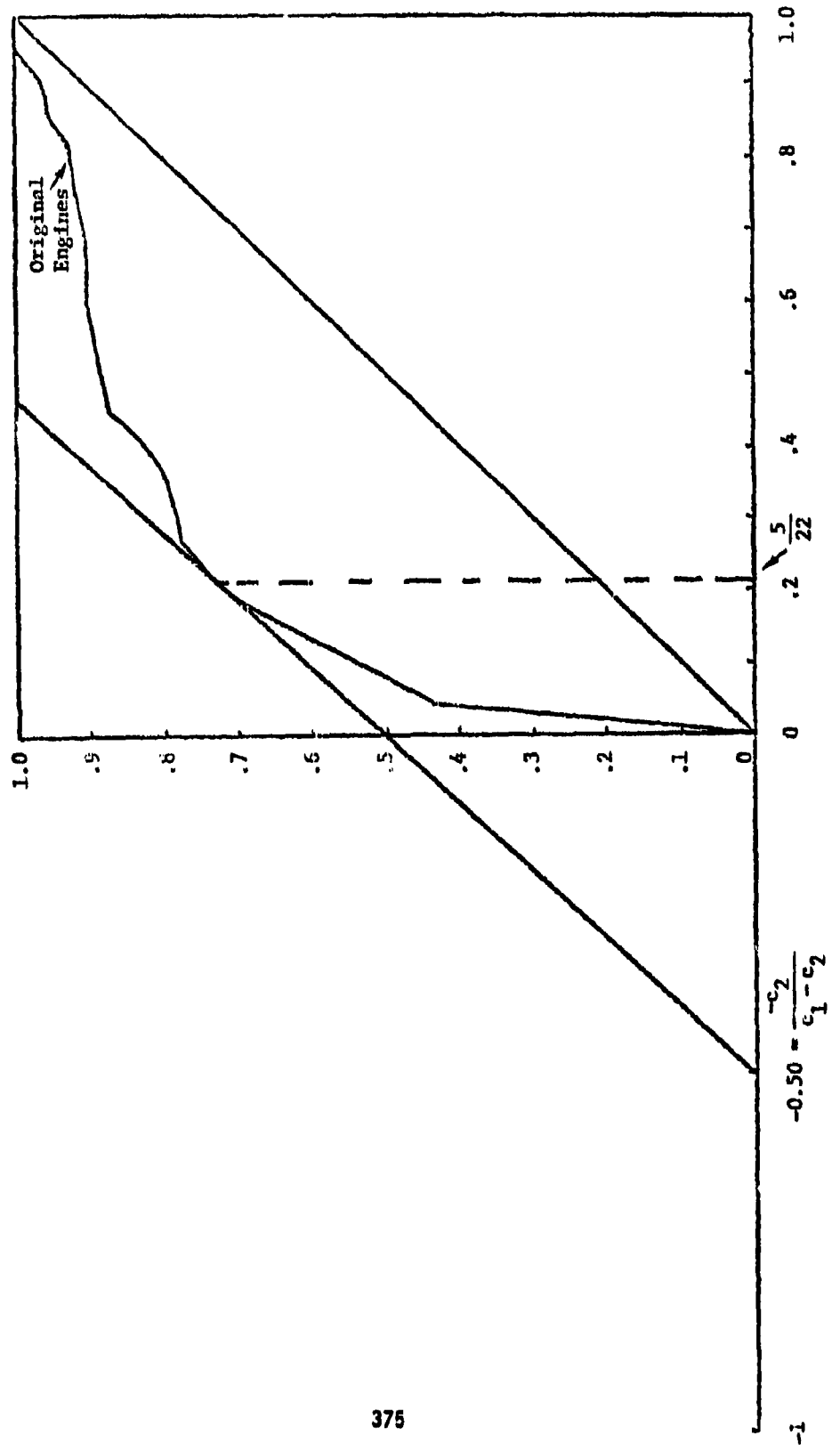


FIGURE 4

IV. THE BIVARIATE CASE

One area of reliability theory where not much work has been done is in graphical analysis of multivariate data. The problem has been to represent higher dimensional data or statistics on paper or any 2-dimensional medium. Some initial attempts have been made to tackle the problem in the bivariate case. We present below a technique for extending the total time on test concept to bivariate data.

In the univariate case the life distribution was completely determined by the failure rate function $r(x)$ and the total time on test plot was used to determine the behaviour of $r(x)$. In the bivariate case, in addition to aging we have the added complication of dependence. So instead of having just the failure rate we have a hazard gradient which is written as

$$g(x,y) = (r_1(x,y), r_2(x,y))$$

As in the univariate case, if the underlying life distribution $F(x,y)$ on $[0,\infty) \times [0,\infty)$ is absolutely continuous, then $r(x,y)$ determines $F(x,y)$ uniquely. In fact it can be shown [9] that

$$\bar{F}(x,y) = \exp \left\{ - \int_0^{(x,y)} r(g) dg \right\}$$

where $\bar{F}(x,y) = \text{Prob } \{X > x, Y > y\}$ and the line integral is path-independent.

The interpretation of the hazard gradient is as follows:

$r_1(x,y)$ = Conditional failure rate of
x given $Y > y$.

$r_2(x,y)$ = Conditional failure rate of
Y given $X > x$.

One of the properties of the hazard gradient is that the behaviour of $r_1(x,y)$ as y varies and the behaviour of $r_2(x,y)$ as x varies describe the nature of the dependence between X and Y . For instance, if $r_1(x,y)$ is decreasing in y then the conditional failure rate of X given $Y > y$ decreases as y increases, which is a form of positive dependence.

Now let us suppose we have a sample

$$(X_1, Y_1), \dots, (X_n, Y_n)$$

from absolutely continuous bivariate distribution F on $[0,\infty) \times [0,\infty)$.

Let

$$Y_{(1)} < Y_{(2)} < \dots < Y_{(n)}$$

be ordered Y-values. Let $X_{(\pi(i))}$ be the order statistic of the X-values associated with $Y_{(i)}$.

Now define a sequence of subsamples of the X-values as follows:

$$x^0 = \{X_{(\pi(1))}, \dots, X_{(\pi(n))}\}$$

$$x^1 = \{X_{(\pi(2))}, \dots, X_{(\pi(n))}\}$$

$$x^2 = \{X_{(\pi(3))}, \dots, X_{(\pi(n))}\}$$

$$\vdots \qquad \vdots$$

$$x^{n-1} = \{X_{(\pi(n))}\}$$

Define

$$T^k(j) = \left\{ \sum_{i=1}^j x_{(i)}^k + (n - k - j)x_{(j)}^k \right\} / \sum_{i=1}^n x_i \quad 0 \leq j \leq n - k \\ 0 \leq k \leq n - 1$$

where $\{x_{(1)}^k, \dots, x_{(n-k)}^k\}$ are the ordered observations in x^{n-k} .

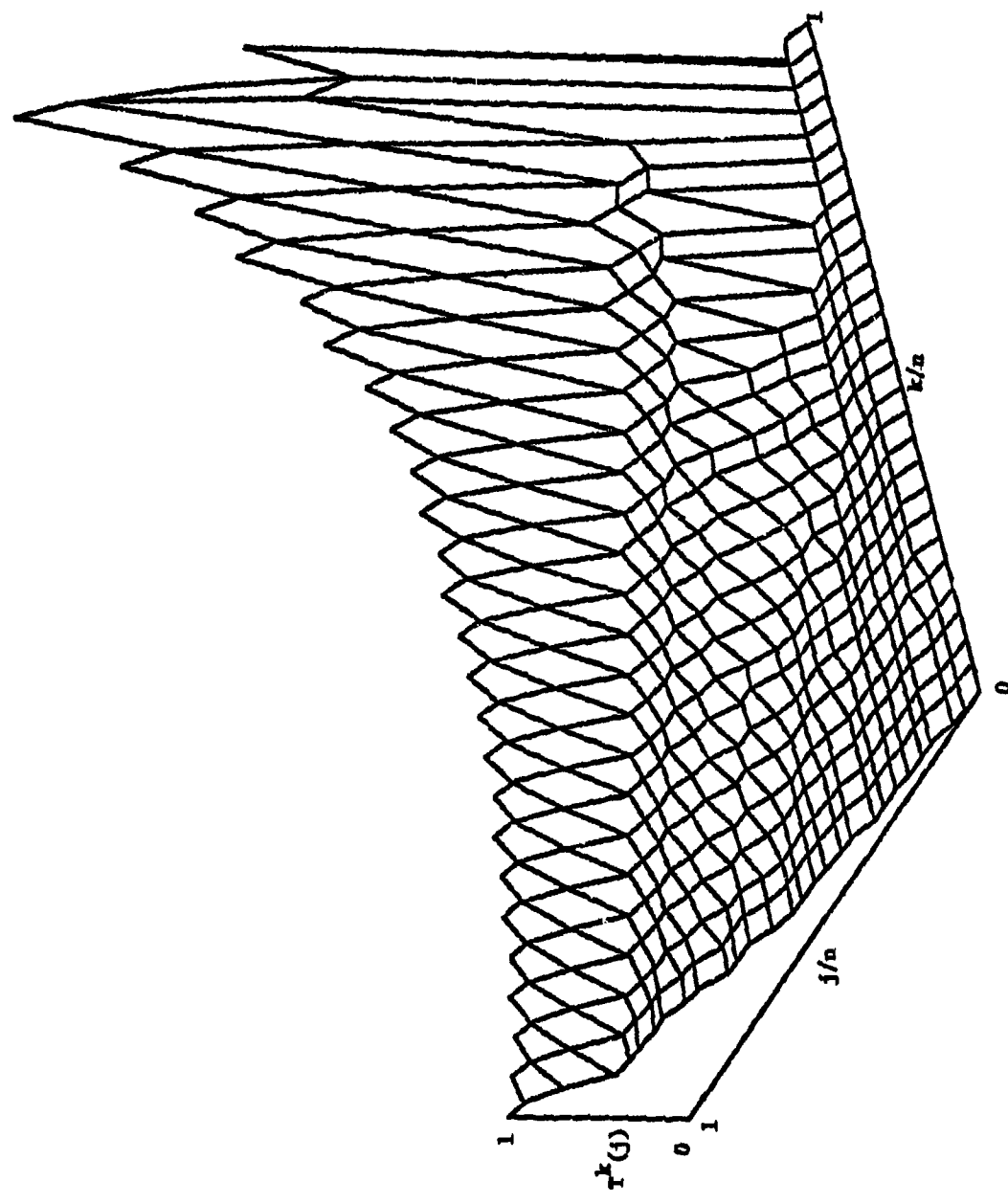
Now plot

$$\left\{ \left(\frac{j}{n}, T^k(j), \frac{k}{n} \right) : \begin{array}{l} 0 \leq k \leq n - 1 \\ 0 \leq j \leq n - k \end{array} \right\}.$$

We call this the empirical conditional scaled bivariate total time on test plot of X given Y . From this plot, as in the univariate case, we can determine the behaviour of $r_1(x,y)$. We do a similar plot with the Y 's in order to study $r_2(x,y)$.

Figure 5 shows a bivariate plot based on running and down times of the Yankee Nuclear Power Plant. We present the conditional plot of the down times given running times. The plot indicates that the down and running times are positively dependent and the down times are DFR. A Bivariate Weibull appears to be a likely model. The bivariate case is discussed in detail in [7].

FIGURE 5



REFERENCES

- [1] Ascher, Harold and Harry Feingold, "Is There Repair After Failure?," Proceedings 1978 Annual Reliability and Maintainability Symposium, (1978).
- [2] Barlow, Richard E. and Rafael A. Campo, "Total Time on Test Processes and Applications to Failure Data Analysis," Aerospace Research Laboratory Technical Report, (1975).
- [3] Barlow, Richard E. and Frank Proschan, STATISTICAL THEORY OF RELIABILITY AND LIFE TESTING, Holt, Rinehart and Winston, (1975).
- [4] Barlow, Richard E. and Bernard Davis, "Analysis of Time Between Failures for Repairable Components," Proceedings of SIAM Conference on Nuclear Systems Reliability Engineering and Risk Assessment, (1978).
- [5] Bergman, B., "Crossings in the Total Time on Test Plot," Scandinavian Journal of Statistics, (1977).
- [6] Bergman, B., "On Age Replacement and the Total Time on Test Concept," Technical Report, University of Lund, Sweden, (1978).
- [7] Davis, Bernard, "Graphical Techniques in Reliability Theory," Ph.D. Thesis, University of California, Berkeley, (1979).
- [8] Langbert, Naftali A., Ramón V. Léon and Frank Proschan, "Characterization of Nonparametric Classes of Life Distributions," Technical Report, Florida State University, (1978).
- [9] Marshall, A. W., "Some Comments on the Hazard Gradient," Stochastic Processes and Their Applications, (1975).

PITMAN-CLOSENESS EFFICIENCY OF ESTIMATORS
OF RELIABILITY WITH APPLICATION TO THE
EXPONENTIAL FAILURE MODEL

Danny Dyer
Department of Mathematics
University of Texas at Arlington
Arlington, Texas 76019

Jerome P. Keating
Bell Helicopter Textron
Fort Worth, Texas 76101

ABSTRACT

When there are available several point estimators of component or system reliability, it would be of interest to compare such estimators through some "closeness to the true value of reliability" criteria. Along these lines, the concept of Pitman-closeness efficiency is introduced. Essentially, when comparing two estimators of reliability for a given situation, Pitman-closeness efficiency gives the odds in favor of one of the estimators being closer to the true value of reliability than is the other. Theory is developed which provides a straightforward way to evaluate this measure of efficiency under fairly general conditions on the estimators. Based on this methodology, a comparison is made of several estimators of reliability based on Type II censored data from the one-parameter exponential failure model.

Key words: Pitman-closeness efficiency; Reliability function; Exponential failure model; Comparison of estimators.

This paper was presented (under a different title) at the 23rd Conference on the Design of Experiments in Army Research, Development and Testing.

PITMAN-CLOSENESS EFFICIENCY OF ESTIMATORS
OF RELIABILITY WITH APPLICATION TO THE
EXPONENTIAL FAILURE MODEL

Danny Dyer and Jerome P. Keating

1. INTRODUCTION

Point estimation of component or system reliability at time τ , $R(\tau) = \text{Prob}\{X > \tau\}$ where X is the failure time, is a frequently considered problem. Generally speaking, for the commonly assumed failure models, there are various methods by which an estimate may be obtained. When there are available several point estimators of $R(\tau)$, the traditional method of comparing such estimators is mean squared efficiency (i.e., the ratio of mean squared errors). However, except for a few cases (e.g., Zacks and Even 1966, Sinha 1972: exponential failure model; Zacks and Milton 1971: normal failure model), the determination of a closed-form expression for mean squared error can prove to be a difficult task. Furthermore, mean squared efficiency compares the average performance of an estimator relative to another; consequently, its usefulness isn't always clear, especially when a single estimate is to be made. Finally, mean squared efficiency can be misleading and unreliable (see, e.g., Dyer, Keating, and Hensley 1977; Box and Tiao 1973, p. 307).

We, therefore, propose another measure of efficiency motivated by the following idea due essentially to Pitman (1938). Let

$\hat{R}_1(\tau) = g_1(X; \tau, n)$, $i = 1, 2$, be two estimators of reliability $R(\tau) = h(\tau, \theta)$ based on a random sample X of size n from a given failure model with unknown parameter θ . Then $\hat{R}_1(\tau)$ is said to be a Pitman-closer estimator of $R(\tau)$ than is $\hat{R}_2(\tau)$ if

$$\text{Prob}\{|\hat{R}_1(\tau) - R(\tau)| < |\hat{R}_2(\tau) - R(\tau)|\} \geq .5 \quad (1.1)$$

for all (τ, θ, n) with strict inequality for some (τ_0, θ_0, n_0) . [Note: Under Pitman's original concept, $\text{Prob}\{|\hat{R}_1(\tau) - R(\tau)| < |\hat{R}_2(\tau) - R(\tau)|\}$ would be a fiducial probability statement. In this paper, however, $\text{Prob}\{|\hat{R}_1(\tau) - R(\tau)| < |\hat{R}_2(\tau) - R(\tau)|\}$ is determined in the classical sense and, therefore, has a relative-frequency interpretation.] We define the Pitman-closeness (PC) efficiency of $\hat{R}_1(\tau)$ relative to $\hat{R}_2(\tau)$ as

$$\begin{aligned} \text{rel.eff.}_{\text{PC}}(\hat{R}_1(\tau), \hat{R}_2(\tau); \tau, \theta, n) \\ = \frac{\text{Prob}\{|\hat{R}_1(\tau) - R(\tau)| < |\hat{R}_2(\tau) - R(\tau)|\}}{\text{Prob}\{|\hat{R}_2(\tau) - R(\tau)| < |\hat{R}_1(\tau) - R(\tau)|\}} \quad (1.2) \end{aligned}$$

Pitman-closeness efficiency gives the odds that one estimator is closer (in absolute value) to the true value of reliability than is the other estimator. For example, if $\text{rel.eff.}_{\text{PC}}(\hat{R}_1(\tau), \hat{R}_2(\tau); \tau, \theta, n) = 1.5$, then the odds are 3 to 2 in favor of $\hat{R}_1(\tau)$ being closer to $R(\tau)$ than is $\hat{R}_2(\tau)$. When $\text{rel.eff.}_{\text{PC}}(\hat{R}_1(\tau), \hat{R}_2(\tau); \tau, \theta, n) > 1$ for some (τ_0, θ_0, n_0) , we shall say that $\hat{R}_1(\tau)$ is more Pitman-closeness efficient than $\hat{R}_2(\tau)$ at (τ_0, θ_0, n_0) . If $\text{rel.eff.}_{\text{PC}}(\hat{R}_1(\tau), \hat{R}_2(\tau); \tau, \theta, n) \geq 1$ for all (τ, θ, n) with a strict inequality for

some (τ_0, θ_0, n_0) , then $\hat{R}_2(\tau)$ is said to be Pitman-closeness inadmissible relative to $\hat{R}_1(\tau)$.

In this paper, we develop theory which provides a straightforward way to evaluate (1.2) under fairly general conditions on the estimators. Through the use of Pitman-closeness efficiency, we then compare several estimators of reliability based on Type II censored test data from the (one-parameter), exponential failure model. The estimators considered are based on (a) the method of maximum likelihood, (b) minimum variance unbiasedness, and (c) the mean and median of Fraser's structural distribution of $R(\tau)$.

2. THEORY AND METHODOLOGY

Let $\hat{R}(T; n)$ be an estimator of reliability $R(\tau)$ which depends on (i) the sample size n , and (ii) τ and the life-test data only through a statistic T whose range is I . We shall say that $\hat{R}(T; n)$ is a non-decreasing full-range estimator of $R(\tau)$ if, for fixed n ,

- (i) $\hat{R}: I \xrightarrow{\text{onto}} [0,1]$ (it may be that one or both endpoints of $[0,1]$ are attained only by considering the extended range of T), and
- (ii) $\hat{R}(T; n)$ is a nondecreasing function of T on I but is strictly increasing on $I' \subset I$, where $0 < \hat{R}(T; n) < 1$ whenever $T \in I'$.
We assume $\text{Prob}\{T \in I'\} \neq 0$.

A nondecreasing full-range estimator of $R(\tau)$ is necessarily continuous on I .

Definition 2.1 Let $\hat{R}_i(T;n)$, $i=1,2$, be nondecreasing full-range estimators of $R(\tau)$. For fixed n , x_0 is said to be a point of intersection of $\hat{R}_1(T;n)$ and $\hat{R}_2(T;n)$ provided

$$(i) \quad \hat{R}_1(x_0;n) = \hat{R}_2(x_0;n);$$

(ii) for arbitrarily small $\epsilon > 0$, $\hat{R}_1(x_0 + \epsilon;n) - \hat{R}_2(x_0 + \epsilon;n)$ and $\hat{R}_1(x_0 - \epsilon;n) - \hat{R}_2(x_0 - \epsilon;n)$ have opposite signs.

Definition 2.2 Let $\hat{R}_i(T;n)$, $i=1,2$, be nondecreasing full-range estimators of $R(\tau)$. For fixed n , y_0 is said to be a switching point of $\hat{R}_1(T;n)$ and $\hat{R}_2(T;n)$ at $R(\tau)$ provided $\hat{R}_1(y_0;n) + \hat{R}_2(y_0;n) = 2R(\tau)$.

Note that x_0 depends only on the sample size n ; y_0 depends on n as well as $R(\tau)$. For fixed n , let $I_n \subset I$ be the set of points for which $\hat{R}_1(T;n)$ and $\hat{R}_2(T;n)$ are not both zero or both one. When $T \in I_n$, $\hat{R}_1(T;n) + \hat{R}_2(T;n)$ is continuous and increasing, thus the switching point of $\hat{R}_1(T;n)$ and $\hat{R}_2(T;n)$ at $R(\tau)$ is unique. We now prove the main result of this section.

Theorem 2.1 Let $\hat{R}_i(T;n)$, $i=1,2$, be nondecreasing full-range estimators of $R(\tau)$. In $I_n = (a,b)$, let y_0 be the unique switching point at $R(\tau)$ and suppose that $\hat{R}_1(t;n) = \hat{R}_2(t;n)$ only at a finite number of points of intersection, say, x_1, \dots, x_N . If $\hat{R}_1(t;n) > \hat{R}_2(t;n)$ whenever $t \in (a, \min(x_1, \dots, x_N))$, then

$$\text{Prob}(|\hat{R}_1(T;n) - R(\tau)| < |\hat{R}_2(T;n) - R(\tau)|)$$

$$= \sum_{k=0}^{[(N+1)/2]} \text{Prob}\{x_{(2k)} < T < x_{(2k+1)}\}, \quad (2.1)$$

where $x_{(0)} = a$, $x_{(1)} = \min(y_0, x_1, \dots, x_N), \dots, x_{(N+1)} = \max(y_0, x_1, \dots, x_N)$, $x_{(N+2)} = b$.

Proof. If $y_0 = x_i$ for some i , the result follows immediately by taking $x_{(j)} = x_{(j+1)} = y_0 = x_i$, where there are exactly $j-1$ of the x_i 's less than y_0 .

Assume that $y_0 \neq x_i$ for any i . Consider the partition of I_n determined by the distinct points $a = x_{(0)} < x_{(1)} < \dots < x_{(N+1)} < x_{(N+2)} = b$. We identify those open intervals $I_n(j) = (x_{(j)}, x_{(j+1)})$ such that whenever $t \in I_n(j)$, the inequality

$$|\hat{R}_1(t;n) - R(t)| < |\hat{R}_2(t;n) - R(t)| \quad (2.2)$$

holds. When $t \in (x_{(0)}, x_{(1)})$, (2.2) holds by hypothesis. Consequently, the theorem will follow by showing that (2.2) holds over exactly one of two adjacent open intervals, say, $I_n(i) = (x_{(i)}, x_{(i+1)})$ and $I_n(i+1) = (x_{(i+1)}, x_{(i+2)})$.

Case 1: $y_0 \leq x_{(i)}$. When $y_0 \leq x_{(i)}$, then $\hat{R}_1(t;n) + \hat{R}_2(t;n) > 2R(t)$; thus $\hat{R}_2(t;n) - R(t) > R(t) - \hat{R}_1(t;n)$, where $t \in I_n(i) \cup I_n(i+1)$. Suppose $\hat{R}_1(t;n) > \hat{R}_2(t;n)$, $t \in I_n(i)$. Then $\hat{R}_1(t;n) - R(t) > \hat{R}_2(t;n) - R(t)$, and $R(t) - \hat{R}_1(t;n) < \hat{R}_2(t;n) - R(t) < \hat{R}_1(t;n) - R(t)$. Consequently, $|\hat{R}_2(t;n) - R(t)| < |\hat{R}_1(t;n) - R(t)|$ since $\hat{R}_1(t;n) > R(t)$. Furthermore, $\hat{R}_1(t;n) < \hat{R}_2(t;n)$, $t \in I_n(i+1)$; hence $\hat{R}_1(t;n) - R(t) < \hat{R}_2(t;n) - R(t)$. It follows that $R(t) - \hat{R}_2(t;n) < \hat{R}_1(t;n) - R(t) < \hat{R}_2(t;n) - R(t)$ or, equivalently, $|\hat{R}_1(t;n) - R(t)| < |\hat{R}_2(t;n) - R(t)|$ since $\hat{R}_2(t;n) > R(t)$. On the other hand, if $\hat{R}_1(t;n) < \hat{R}_2(t;n)$, $t \in I_n(i)$, then (2.2) clearly holds over $I_n(i)$ but not over $I_n(i+1)$.

Case 2: $y_0 \geq x_{(i+2)}$. When $y_0 \geq x_{(i+2)}$, then $\hat{R}_1(t;n) + \hat{R}_2(t;n) < 2R(\tau)$; thus $\hat{R}_2(t;n) - R(\tau) < R(\tau) - \hat{R}_1(t;n)$, where $t \in I_n(i) \cup I_n(i+1)$. If $\hat{R}_1(t;n) > \hat{R}_2(t;n)$, $t \in I_n(i)$, then $\hat{R}_1(t;n) - R(\tau) > \hat{R}_2(t;n) - R(\tau)$. Thus $\hat{R}_2(t;n) - R(\tau) < \hat{R}_1(t;n) - R(\tau) < R(\tau) - \hat{R}_2(t;n)$, and $|\hat{R}_1(t;n) - R(\tau)| < |\hat{R}_2(t;n) - R(\tau)|$ since $R(\tau) > \hat{R}_2(t;n)$. Moreover, $\hat{R}_1(t;n) < \hat{R}_2(t;n)$, $t \in I_n(i+1)$; hence $\hat{R}_1(t;n) - R(\tau) < \hat{R}_2(t;n) - R(\tau)$. Consequently, $\hat{R}_1(t;n) - R(\tau) < \hat{R}_2(t;n) - R(\tau) < R(\tau) - \hat{R}_1(t;n)$, and $|\hat{R}_2(t;n) - R(\tau)| < |\hat{R}_1(t;n) - R(\tau)|$ since $R(\tau) > \hat{R}_1(t;n)$. On the other hand, if $\hat{R}_1(t;n) < \hat{R}_2(t;n)$, $t \in I_n(i)$, then (2.2) clearly holds over $I_n(i+1)$ but not over $I_n(i)$.

Case 3: $y_0 = x_{(i+1)}$. When $y_0 = x_{(i+1)}$, then $\hat{R}_1(t;n) + \hat{R}_2(t;n) < 2R(\tau)$, $t \in I_n(i)$; however, $\hat{R}_1(t;n) + \hat{R}_2(t;n) > 2R(\tau)$, $t \in I_n(i+1)$. If $\hat{R}_1(t;n) < \hat{R}_2(t;n)$, $t \in I_n(i)$, then $\hat{R}_1(t;n) < \hat{R}_2(t;n)$, $t \in I_n(i+1)$, and (see Cases 1 and 2) (2.2) holds over $I_n(i+1)$ but not over $I_n(i)$. If $\hat{R}_1(t;n) > \hat{R}_2(t;n)$, $t \in I_n(i)$, then $\hat{R}_1(t;n) > \hat{R}_2(t;n)$, $t \in I_n(i+1)$, and (see Cases 1 and 2) (2.2) holds over $I_n(i)$ but not over $I_n(i+1)$.

The proof is now complete. ■

If, for a given n , there are no points of intersection of $\hat{R}_1(T;n)$ and $\hat{R}_2(T;n)$ in I_n , we then have the following

Corollary 2.1. Let $\hat{R}_i(T;n)$, $i=1,2$, be nondecreasing full-range estimators of $R(\tau)$. Suppose there are no points of intersection of $\hat{R}_1(T;n)$ and $\hat{R}_2(T;n)$ in $I_n = (a,b)$. If $\hat{R}_1(t;n) > \hat{R}_2(t;n)$, $t \in I_n$, then

$$\begin{aligned} \text{Prob}\{|\hat{R}_1(T;n) - R(\tau)| < |\hat{R}_2(T;n) - R(\tau)|\} \\ = \text{Prob}\{a < T < y_0\}, \end{aligned} \tag{2.3}$$

where y_0 is the unique switching point of $\hat{R}_1(T;n)$ and $\hat{R}_2(T;n)$ at $R(\tau)$.

We point out, in passing, that if (in the theorem as well as the corollary) $\hat{R}_1(t;n) < \hat{R}_2(t;n)$ whenever $t \in (a, \min(x_1, \dots, x_N))$, then $\text{Prob}(|\hat{R}_1(T;n) - R(\tau)| < |\hat{R}_2(T;n) - R(\tau)|)$ clearly equals one minus the right hand side of (2.1) or, in the case of the corollary, (2.3).

3. ESTIMATORS OF RELIABILITY

We consider a specific failure model, namely, the one-parameter exponential. Let $x_{(1)} \leq x_{(2)} \leq \dots \leq x_{(k)}$ be the ordered first k failure times in a random sample of size n (i.e., a Type II censored sample) from $f_X(x;\theta) = (1/\theta) \exp(-x/\theta)$, $x > 0$. The reliability at time $\tau > 0$ is given by $R(\tau) = \text{Prob}(X > \tau) = \exp(-\tau/\theta)$. The statistic

$$T = \left[\sum_{i=1}^k x_{(i)} + (n-k)x_{(k)} \right] / \tau \quad (3.1)$$

is complete sufficient for $R(\tau)$. Furthermore, it is well known (Epstein and Sobel 1954) that T has a gamma distribution with shape parameter k and scale parameter $[-\ln R(\tau)]^{-1}$. We point out that, for a given k , the distribution of T depends on τ and θ only through $R(\tau)$. In other words, we need only specify the value of $R(\tau)$ and not that of τ and θ to index the distribution of T . Consequently, we henceforth write R instead of $R(\tau)$. It follows that $2(-\ln R)T$ has a chi-square distribution with $2k$ degrees of freedom.

By the invariance property of maximum likelihood estimators, the maximum likelihood estimator (MLE) of R is

$$\hat{R}_{MLE}(T;k) = \exp(-k/T), T > 0, k \geq 1. \quad (3.2)$$

Basu (1964) has shown that the minimum variance unbiased estimator (MVUE) of R is

$$\begin{aligned}\hat{R}_{MVUE}(T;k) &= 0, 0 < T \leq 1 \\ &= (1 - 1/T)^{k-1}, T > 1, k \geq 1.\end{aligned} \quad (3.3)$$

We now discuss two other estimators of R based on Fraser's (1968) structural inference (a group-theoretic approach to Fisher's fiducial theory). In the structural approach, as in the Bayesian approach, the given data induce a probability measure (called the structural density) on the parameter space. Unlike the Bayesian approach, however, this is achieved by assuming the existence of a structural model rather than a prior probability measure. The structural density of R , given $T = t > 0$, is (Maxwell 1973)

$$g(r|t) = t^k (-\ln r)^{k-1} r^{t-1} / \Gamma(k), 0 < r < 1, k \geq 1. \quad (3.4)$$

Expression (3.4) is also the Bayesian posterior density of R under Jeffreys' noninformative prior for a scale parameter (see Box and Tiao 1973, p. 44).

Measures of central tendency of the structural density of R would seem natural choices for point estimators of R . Since $E(R|t) = \int_0^1 g(r|t)dr = [1 - 1/(t+1)]^k$, an estimator of R based on the mean (SMN) of the structural density of R is

$$\hat{R}_{SMN}(T;k) = [1 - 1/(T+1)]^k, T > 0, k \geq 1. \quad (3.5)$$

In addition, by solving the equation $\int_0^m g(r|t)dr = .5$ for m , we obtain an estimator of R based on the median (SMD) of the structural density of R . The solution is

$$\hat{R}_{SMD}(T;k) = \exp(-m_{2k}/2T), T > 0, k \geq 1 \quad (3.5)$$

where m_{2k} is the median of a chi-square distribution with $2k$ degrees of freedom. For specified k , the value of m_{2k} can be found in Harter (1964). It is interesting to note that $\hat{R}_{SMD}(T;k)$ could also be obtained by a classical argument. Since $2(-\ln R)T$ has a chi-square distribution with $2k$ degrees of freedom, $\hat{R}_{SMD}(T;k)$ is a 50 percent lower (upper) confidence bound on R . Thus, $\hat{R}_{SMD}(T;k)$ is as likely to underestimate as to overestimate the true value of R . In this sense, $\hat{R}_{SMD}(T;k)$ is sometimes called a median unbiased estimator (Lehmann 1959, p. 83).

For $k \geq 1$, we note that $\hat{R}_{MLE}(T;k)$, $\hat{R}_{SMN}(T;k)$, and $\hat{R}_{SMD}(T;k)$ are each nondecreasing full-range estimators of R . Furthermore, $\hat{R}_{MVUE}(T;k)$ also has this property provided $k \geq 2$. When $k = 1$, $\hat{R}_{MVUE}(T;1)$ is a zero-one estimator of R and, as such, is of no practical interest. Henceforth, any discussion concerning $\hat{R}_{MVUE}(T;k)$ will assume $k \geq 2$.

4. PAIRWISE COMPARISON OF ESTIMATORS

The theory and methodology of Section 2 will now be applied to the estimators of Section 3.

4.1 $\hat{R}_{MLE}(T;k)$ and $\hat{R}_{MVUE}(T;k)$

We show that $\hat{R}_{MLE}(T;k)$ and $\hat{R}_{MVUE}(T;k)$ have a single point of

intersection in $I_k = (0, +\infty)$, $k \geq 2$. There is clearly no point of intersection in $(0, 1]$. When $t > 1$, $\hat{R}_{MLE}(t; k) = \hat{R}_{MVUE}(t; k)$ is equivalent to

$$h(t) = t \ln[t/(t-1)] = k/(k-1). \quad (4.1)$$

Since $\exp[1/(t-1)] > t/(t-1)$, $t > 1$, then $h'(t) < 0$; thus, $h(t)$ is decreasing. The existence of a unique root for (4.1) follows since $1 < h(t) < +\infty$ and $h(t)$ is continuous. By Theorem 2.1,

$$\begin{aligned} \text{Prob}(|\hat{R}_{MLE}(T; k) - R| < |\hat{R}_{MVUE}(T; k) - R|) \\ = \text{Prob}(0 < T < \min(x_0, y_0)) + \text{Prob}(T > \max(x_0, y_0)) \\ = \chi^2[2(-\ln R) \min(x_0, y_0); 2k] \\ + 1 - \chi^2[2(-\ln R) \max(x_0, y_0); 2k], \end{aligned} \quad (4.2)$$

where for specified $k \geq 2$, x_0 is the solution to $\exp(-k/x_0) = (1 - 1/x_0)^{k-1}$; y_0 is the solution to $\exp(-k/y_0) + (1 - 1/y_0)^{k-1} = 2R$ whenever $R > .5 \exp(-k)$, otherwise, $y_0 = -k/\ln(2R)$. We write $\chi^2(\cdot; m)$ as the chi-square distribution function with m degrees of freedom. When $k = 2, 3, 5, 7, 10$, and 20 , expression (4.2) has been evaluated numerically for $R = 0(0.01)1.0$. Based on these results, the graphs of $\text{rel.eff.}_{PC}\{\hat{R}_{MLE}(T; k), \hat{R}_{MVUE}(T; k); R, k\}$ versus R are given in Figure A.

4.2 $\hat{R}_{MLE}(T; k)$ and $\hat{R}_{SMD}(T; k)$

There are no points of intersection of $\hat{R}_{MLE}(T; k)$ and $\hat{R}_{SMD}(T; k)$ in $I_k = (0, +\infty)$, $k \geq 1$. This follows since the median is less than

the mean of a chi-square distribution (Groeneveld and Meeden 1977); consequently, $\hat{R}_{SMD}(t;k) = \exp(-m_{2k}/2t) > \exp(-k/t) = \hat{R}_{MLE}(t;k)$, $t > 0$. By Corollary 2.1,

$$\begin{aligned} \text{Prob}(|\hat{R}_{SMD}(T;k) - R| < |\hat{R}_{MLE}(T;k) - R|) \\ = \text{Prob}\{T < y_0\} = \chi^2[2(-\ln R)y_0; 2k], \end{aligned} \quad (4.3)$$

where for specified $k \geq 1$ and R , y_0 is the solution to $\exp(-m_{2k}/2y_0) + \exp(-k/y_0) = 1$.

For fixed $k \geq 1$, $\hat{R}_{SMD}(t;k) > \hat{R}_{MLE}(t;k)$, $t > 0$; furthermore, $\hat{R}_{SMD}(T;k)$ underestimates R , on the average, 50 percent of the time. It follows that $\hat{R}_{SMD}(T;k)$ is closer to the true value of R than is $\hat{R}_{MLE}(T;k)$, on the average, at least 50 percent of the time. It will be instructive to prove

Theorem 4.1 $\hat{R}_{MLE}(T;k)$ is Pitman-closeness inadmissible relative to $\hat{R}_{SMD}(T;k)$.

Proof For fixed k and R ,

$$\begin{aligned} [\exp(-k/y_0) \exp(-m_{2k}/2y_0)]^{1/2} \\ < [\exp(-k/y_0) + \exp(-m_{2k}/2y_0)]/2 \\ < \exp(-m_{2k}/2y_0), \end{aligned}$$

since the geometric mean of two unequal positive real numbers is less than their arithmetic mean. By simplification,

$$m_{2k} < 2(-\ln R)y_0 < (m_{2k} + 2k)/2.$$

Hence, for $k \geq 1$ and $0 < R < 1$,

$$.5 < \chi^2[2(-\ln R)y_0; 2k] < \chi^2[(m_{2k} + 2k)/2; 2k]$$

$$\leq \chi^2[(m_2 + 2)/2; 2] = \int_0^{1+\ln 2} (1/2) \exp(-x/2) dx \approx .571.$$

By (4.3), it follows that

$$1 < \text{rel.eff.}_{PC}\{\hat{R}_{SMD}(T;k), \hat{R}_{MLE}(T;k); R, k\} < 1.331. \blacksquare$$

From the proof of Theorem 4.1, the odds in favor of $\hat{R}_{SMD}(T;k)$ being closer to R than is $\hat{R}_{MLE}(T;k)$ range from slightly better than even to approximately 4 to 3. The exact extent of this efficiency can be determined from the graphs (based on numerical evaluation of (4.3)) of $\text{rel.eff.}_{PC}\{\hat{R}_{SMD}(T;k), \hat{R}_{MLE}(T;k); R, k\}$ versus R given in Figure B.

4.3 $\hat{R}_{SMD}(T;k)$ and $\hat{R}_{MVUE}(T;k)$

We use an argument similar to that of Subsection 4.1 to show that $\hat{R}_{SMD}(T;k)$ and $\hat{R}_{MVUE}(T;k)$ have a single point of intersection in $(1, +\infty)$. When $t > 1$, $\hat{R}_{SMD}(t;k) = \hat{R}_{MVUE}(t;k)$ is equivalent to

$$h(t) = t \ln[t/(t-1)] = m_{2k}/2(k-1). \quad (4.4)$$

However, $h(t)$ is continuous and decreasing; furthermore, $1 < h(t) < +\infty$. Since $2(k-1)$ is the mode of a chi-square distribution with $2k$ degrees of freedom and is less than m_{2k} (Groeneveld and Meeden 1977), it follows that a unique root for (4.4) exists. By Theorem 2.1,

$$\begin{aligned} \text{Prob}(|\hat{R}_{SMD}(T;k) - R| < |\hat{R}_{MVUE}(T;k) - R|) \\ = \chi^2[2(-\ln R) \min(x_0, y_0); 2k] \\ + 1 - \chi^2[2(-\ln R) \max(x_0, y_0); 2k], \end{aligned} \quad (4.5)$$

where for specified $k \geq 2$, x_0 is the solution to $\exp(-m_{2k}/2x_0) = (1 - 1/x_0)^{k-1}$; y_0 is the solution to $\exp(-m_{2k}/2y_0) + (1 - 1/y_0)^{k-1} = 2R$ whenever $R > .5 \exp(-m_{2k}/2)$, otherwise, $y_0 = -m_{2k}/2\ln(2R)$.

For fixed $k \geq 2$, $\hat{R}_{SMD}(t;k) > \hat{R}_{MVUE}(t;k)$ if and only if $t \in (0, x_0)$. Consequently, a conclusion similar to that which immediately preceded Theorem 4.1 cannot be made. Nevertheless, we have the following

Theorem 4.2 $\hat{R}_{MVUE}(T;k)$ is Pitman-closeness inadmissible relative to $\hat{R}_{SMD}(T;k)$.

Proof For fixed k , let x_0 be the unique point of intersection and $R_0(k) = \exp(-m_{2k}/2x_0) = (1 - 1/x_0)^{k-1}$. When $R > R_0(k)$, then $1 < x_0 < y_0$, where y_0 is the switching point at R . Thus, $\exp(-m_{2k}/2y_0) < [\exp(-m_{2k}/2y_0) + (1 - 1/y_0)^{k-1}]/2$ or, equivalently, $m_{2k} > 2(-\ln R)y_0$. From (4.5),

$$\begin{aligned} \text{Prob}(|\hat{R}_{SMD}(T;k) - R| < |\hat{R}_{MVUE}(T;k) - R|) \\ = x^2[2(-\ln R)x_0; 2k] + 1 - x^2[2(-\ln R)y_0; 2k] \\ > x^2[2(-\ln R)x_0; 2k] + 1 - x^2(m_{2k}; 2k) > .5. \end{aligned}$$

When $R < R_0(k)$, then $y_0 < x_0$ and $\exp(-m_{2k}/2y_0) > [\exp(-m_{2k}/2y_0) + \hat{R}_{MVUE}(y_0;k)]/2$. Thus, $m_{2k} < 2(-\ln R)y_0$. From (4.5),

$$\begin{aligned} \text{Prob}(|\hat{R}_{SMD}(T;k) - R| < |\hat{R}_{MVUE}(T;k) - R|) \\ = x^2[2(-\ln R)y_0; 2k] + 1 - x^2[2(-\ln R)x_0; 2k] \\ > x^2(m_{2k}; 2k) = .5 \quad \blacksquare \end{aligned}$$

While Theorem 4.2 says that $\hat{R}_{SMD}(T;k)$ is to be preferred over

$\hat{R}_{MVUE}(T;k)$ from a Pitman-closeness efficiency point of view, the extent of this efficiency can be determined from the graphs (based on numerical evaluation of (4.5)) of $\text{rel.eff.}_{PC}(\hat{R}_{SMD}(T;k), \hat{R}_{MVUE}(T;k); R, k)$ versus R given in Figure C.

4.4 $\hat{R}_{SMD}(T;k)$ and $\hat{R}_{SMN}(T;k)$

We show that $\hat{R}_{SMD}(T;k)$ and $\hat{R}_{SMN}(T;k)$ have a single point of intersection in $I_k = (0, +\infty)$, $k \geq 1$. When $t > 0$, $\hat{R}_{SMD}(t;k) = \hat{R}_{SMN}(t;k)$ is equivalent to

$$\lambda(t) = t \ln(1 + 1/t) = m_{2k}/2k. \quad (4.6)$$

Since $\exp(-x) > 1 - x$, $0 < x < 1$, $\lambda'(t) = \ln(1 + 1/t) - 1/(t+1) > 0$ and $\lambda(t)$ is continuous and increasing. For fixed $k \geq 1$, it follows that a unique root for (4.6) exists since $0 < \lambda(t) < 1$, $t > 0$, and $m_{2k} < 2k$. Denote the root by x_0 . When $t < x_0$, $\lambda(t) < m_{2k}/2k$; consequently, $\hat{R}_{SMN}(t;k) > \hat{R}_{SMD}(t;k)$. By Theorem 2.1,

$$\begin{aligned} \text{Prob}(|\hat{R}_{SMN}(T;k) - R| < |\hat{R}_{SMD}(T;k) - R|) \\ = x^2[2(-\ln R) \min(x_0, y_0); 2k] \\ + 1 - x^2[2(-\ln R) \max(x_0, y_0); 2k], \end{aligned} \quad (4.7)$$

where for specified $k \geq 1$ and R , x_0 is the solution to

$$\exp(-m_{2k}/2x_0) = [1 - 1/(x_0 + 1)]^k; \quad y_0 \text{ is the solution to}$$

$$\exp(-m_{2k}/2y_0) + [1 - 1/(y_0 + 1)]^k = 2R. \quad \text{The graphs (based on}$$

numerical evaluation of (4.7)) of $\text{rel.eff.}_{PC}(\hat{R}_{SMD}(T;k), \hat{R}_{SMN}(T;k); R, k)$ versus R are given in Figure D.

4.5 $\hat{R}_{SMN}(T;k)$ and $\hat{R}_{MLE}(T;k)$

There are no points of intersection of $\hat{R}_{SMN}(T;k)$ and $\hat{R}_{MLE}(T;k)$ in $I_k = (0, +\infty)$, $k \geq 1$. Since $\exp(1/t) > 1 + 1/t$, then $\hat{R}_{MLE}(t;k) = \exp(-k/t) < [1 - 1/(t+1)]^k = \hat{R}_{SMN}(t;k)$, $t > 0$. By Corollary 2.1,

$$\begin{aligned} \text{Prob}(|\hat{R}_{SMN}(T;k) - R| < |\hat{R}_{MLE}(T;k) - R|) \\ = \text{Prob}(T < y_0) = \chi^2[2(-\ln R)y_0; 2k], \end{aligned} \quad (4.8)$$

where for specified $k \geq 1$ and R , y_0 is the solution to $\exp(-k/y_0) + [1 - 1/(y_0+1)]^k = 2R$.

Theorem 4.5 $\hat{R}_{SMN}(T;k)$ is more Pitman-closeness efficient than $\hat{R}_{MLE}(T;k)$ if and only if $R > R'_0(k) = \exp(-m_{2k}/2x'_0)$, where for specified $k \geq 1$, x'_0 is the solution to $\exp(-m_{2k}/2x'_0) = \{\exp(-k/x'_0) + [1 - 1/(x'_0+1)]^k\}/2$. Furthermore, $.199 < R'_0(k) < e^{-1} \approx .368$, $k \geq 1$.

Proof The average of $\hat{R}_{MLE}(T;k)$ and $\hat{R}_{SMN}(T;k)$ is a nondecreasing full-range estimator of R . We first show that $\hat{R}_{SMD}(T;k)$ and $[\hat{R}_{MLE}(T;k) + \hat{R}_{SMN}(T;k)]/2$ have a single point of intersection in $(0, +\infty)$. When $t > 0$, $\hat{R}_{SMD}(t;k) = [\hat{R}_{MLE}(t;k) + \hat{R}_{SMN}(t;k)]/2$ is equivalent to

$$\begin{aligned} h(t;k) &= t \ln 2 - t \ln \{\exp(-k/t) + [1 - 1/(t+1)]^k\} \\ &= m_{2k}/2. \end{aligned} \quad (4.9)$$

For fixed $k \geq 1$, $h(t;k)$ is continuous and increasing over $(0, +\infty)$.

Furthermore, $\lim_{t \rightarrow \infty} h(t;k) = k$; thus $0 < h(t;k) < k$, $t > 0$. Since $m_{2k} < 2k$, the existence of a unique root, say x'_0 , for (4.9) is established. Let $R'_0(k) = \exp(-m_{2k}/2x'_0)$. When $t < x'_0$, $h(t;k) < m_{2k}/2$;

thus, $\hat{R}_{SMD}(t;k) < [\hat{R}_{MLE}(t;k) + \hat{R}_{SMN}(t;k)]/2$. For specified R , let y_0 be the switching point of $\hat{R}_{MLE}(T;k)$ and $\hat{R}_{SMN}(T;k)$ at R . When $R > R_0(k)$, $\hat{R}_{SMD}(y_0;k) > [\hat{R}_{MLE}(y_0;k) + \hat{R}_{SMN}(y_0;k)]/2 = R$ or, equivalently, $m_{2k} < 2(-\ln R)y_0$. By (4.8),

$$\begin{aligned} \text{Prob}\{|\hat{R}_{SMN}(T;k) - R| < |\hat{R}_{MLE}(T;k) - R|\} \\ = x^2[2(-\ln R)y_0; 2k] > x^2(m_{2k}; 2k) = .5. \end{aligned}$$

The last inequality is reversed when $R < R_0(k)$.

For fixed $k \geq 1$, $\exp(-2k/m_{2k}) + [m_{2k}/(m_{2k}+2)]^k < 2e^{-1}$; thus, $h(m_{2k}/2;k) > m_{2k}/2$. Since $h(t;k)$ is increasing in t , then $x_0 < m_{2k}/2$ and $R_0(k) < e^{-1} \approx .368$, $k \geq 1$. Furthermore, $m_{2k}/2x_0^k$ decreases with increasing k . The solution to $h(x_0^k;1) = m_2/2$ is $x_0^k = .4289$; thus, $\min_k R_0(k) = R_0(1) = \exp[-m_2/2(.4289)] \approx .199$. ■

Although the true value of R is unknown, most situations of interest would presuppose that reliability is at least 37 percent. In these situations, $\hat{R}_{SMN}(T;k)$ would be preferred over $\hat{R}_{MLE}(T;k)$ from a Pitman-closeness efficiency point of view. The extent of this efficiency may be determined from the graphs (based on numerical evaluation of (4.8)) of $\text{rel.eff.}_{PC}\{\hat{R}_{SMN}(T;k), \hat{R}_{MLE}(T;k); R, k\}$ versus R given in Figure E.

4.6 $\hat{R}_{SMN}(T;k)$ and $\hat{R}_{MVUE}(T;k)$

For specified $k \geq 2$, we show there is exactly one point of intersection of $\hat{R}_{SMN}(T;k)$ and $\hat{R}_{MVUE}(T;k)$ in $(1, +\infty)$. There is clearly no point of intersection in $(0, 1]$. When $t > 1$, $\hat{R}_{SMN}(t;k) = \hat{R}_{MVUE}(t;k)$ is equivalent to

$$\mu^{k-1}(\mu + 2)^k = (\mu + 1)^{2k-1}, \quad (4.10)$$

where $\mu = t-1 > 0$. Equation (4.10) may be written as a polynomial equation in μ of degree $2k-2$, i.e.,

$$\sum_{j=1}^k \left[2^j \binom{k}{j} - \binom{2k-1}{j} \right] \mu^{2k-1-j} - \sum_{j=k+1}^{2k-1} \binom{2k-1}{j} \mu^{2k-1-j} = 0. \quad (4.11)$$

Let a_j be the coefficient of μ^{2k-1-j} . For $j = 1, \dots, k$,

$$a_j = 2^j \binom{k}{j} - \binom{2k-1}{j} = \frac{(2k-2j+2)}{j} 2^{j-1} \binom{k}{j-1} - \frac{(2k-1)}{j} \binom{2k-1}{j-1},$$

for $j = k+1, \dots, 2k-1$,

$$a_j = -\binom{2k-1}{j}.$$

Then $a_1 = 1$; $a_2 = k-1$; and since $a_3 = -(k-1)$, it follows that $a_j < 0$, $j = 3, \dots, 2k-1$. Consequently, by Descartes' rule of signs there is exactly one positive root for (4.11), and thus for (4.10).

By Theorem 2.1,

$$\begin{aligned} \text{Prob}\{|\hat{R}_{SMN}(T;k) - R| < |\hat{R}_{MVUE}(T;k) - R|\} \\ = x^2 [2(-\ln R) \min(x_0, y_0); 2k] \\ + 1 - x^2 [2(-\ln R) \max(x_0, y_0); 2k], \end{aligned} \quad (4.12)$$

where for specified $k \geq 2$, x_0 is the solution to $[1 - 1/(x_0+1)]^k = (1 - 1/x_0)^{k-1}$; y_0 is the solution to $[1 - 1/(y_0+1)]^k + (1 - 1/y_0)^{k-1} = 2R$ whenever $R > (1/2)^{k+1}$, otherwise, $y_0 = [1 - (2R)^{1/k}]^{-1} - 1$.

As previously mentioned, when the true value of reliability is at least 37 percent, $\hat{R}_{SMN}(T;k)$ would be preferred over $\hat{R}_{MLE}(T;k)$ from a Pitman-closeness efficiency point of view. A similar statement can

be made with regard to $\hat{R}_{SMN}(T;k)$ and $\hat{R}_{MVUE}(T;k)$.

Theorem 4.4 When $R > e^{-1}$, $\hat{R}_{SMN}(T;k)$ is more Pitman-closeness efficient than $\hat{R}_{MVUE}(T;k)$.

Proof For specified $k \geq 2$, let $R_0(k) = \hat{R}_{SMN}(x_0;k) = \hat{R}_{MVUE}(x_0;k)$, where x_0 is the point of intersection of $\hat{R}_{SMN}(T;k)$ and $\hat{R}_{MVUE}(T;k)$. By a Padé rational approximation of index 2 to the binomial series (i.e., $(1+x)^n \approx [2 + (n+1)x]/[2 - (n-1)x]$, Ralston 1955, pp. 278-280), $x_0 \leq k - .5$; thus, $R_0(k) \leq e^{-1}$, $k \geq 2$. Let y_0 be the switching point of $\hat{R}_{SMN}(T;k)$ and $\hat{R}_{MVUE}(T;k)$ at R . Note that when $R > e^{-1}$, then $x_0 < y_0$.

The average of $\hat{R}_{SMN}(T;k)$ and $\hat{R}_{MVUE}(T;k)$ is a nondecreasing full-range estimator of R . When $k \geq 4$, there are no points of intersection of $\hat{R}_{SMD}(T;k)$ and $[\hat{R}_{SMN}(T;k) + \hat{R}_{MVUE}(T;k)]/2$ in $(0,+\infty)$ since $\hat{R}_{SMD}(t;k) < [\hat{R}_{SMN}(t;k) + \hat{R}_{MVUE}(t;k)]/2$, $t > 0$. Thus, $\hat{R}_{SMD}(y_0;k) < [\hat{R}_{SMN}(y_0;k) + \hat{R}_{MVUE}(y_0;k)]/2 = R$ or, equivalently, $m_{2k} > 2(-\ln R)y_0$, $k \geq 4$. From (4.12), for $k \geq 4$ and $R > e^{-1}$,

$$\begin{aligned} \text{Prob}\{|\hat{R}_{MLE}(T;k) - R| < |\hat{R}_{SMN}(T;k) - R|\} \\ = x^2[2(-\ln R) \max(x_0, y_0); 2k] \\ - x^2[2(-\ln R) \min(x_0, y_0); 2k] \\ = x^2[2(-\ln R)y_0; 2k] - x^2[2(-\ln R)x_0; 2k] \\ < x^2(m_{2k}; 2k) - x^2[2(-\ln R)x_0; 2k] < .5. \end{aligned} \quad (4.13)$$

When $k = 2$ or 3, there is a unique point of intersection, say x_0^* , of $\hat{R}_{SMD}(T;k)$ and $[\hat{R}_{SMN}(T;k) + \hat{R}_{MVUE}(T;k)]/2$ in $(0,1)$. However, the inequality $\hat{R}_{SMD}(t;k) < [\hat{R}_{SMN}(t;k) + \hat{R}_{MVUE}(t;k)]/2$ still holds

for $t \geq 1$. Since $x_0^k < 1 < x_0$, then (4.13) holds for $k \geq 2$. ■

Theorem 4.4 is somewhat conservative in the following sense. For a given $k \geq 2$, it is quite likely that $\hat{R}_{SMN}(T;k)$ is more Pitman-closeness efficient than $\hat{R}_{MVUE}(T;k)$ for values of R considerably less than .368. The extent of this efficiency is shown in the graphs (based on numerical evaluation of (4.12)) of rel.eff. $_{PC}(\hat{R}_{SMN}(T;k), \hat{R}_{MVUE}(T;k); R, k)$ versus R given in Figure F.

5. DISCUSSION OF RESULTS

Pitman-closeness efficiency is inherently dependent upon the probability that an estimator underestimates (or overestimates) the true value of the parametric function being estimated. Since $\text{Prob}(\hat{R}_{MLE}(T;k) < R) = x^2(2k; 2k) > .5$, $k \geq 1$, then $\hat{R}_{MLE}(T;k)$ tends to underestimate R . On the other hand, $\hat{R}_{MVUE}(T;k)$ tends to overestimate R whenever $R > e^{-1} \approx .368$. To see that this is so, first note that $m_{2k} > 2k - .7$, $k \geq 1$; thus $[m_{2k}/(m_{2k} - 2)]^{k-1} \leq [1 - 1/(k-1.35)]^{k-1} < e$ or, equivalently, $2\{1 - \exp[-1/(k-1)]\}^{-1} < m_{2k}$. For fixed k , $q(R;k) = 2(-\ln R)[1 - R^{1/(k-1)}]^{-1}$ is a decreasing function of R . Thus, for fixed $k \geq 2$ and $R > e^{-1}$, $q(R;k) < q(e^{-1};k) = 2\{1 - \exp[-1/(k-1)]\}^{-1} < m_{2k}$. The result now follows since $\text{Prob}(\hat{R}_{MVUE}(T;k) > R) = 1 - x^2[q(R;k); 2k]$. Moreover, as R decreases from e^{-1} to 0, both $\hat{R}_{MVUE}(T;k)$ as well as, of course, $\hat{R}_{MLE}(T;k)$ tend to underestimate R . Generally speaking, from Figure A, $\hat{R}_{MLE}(T;k)$ is more Pitman-closeness efficient than $\hat{R}_{MVUE}(T;k)$. For

low to moderate reliability, the odds in favor of $\hat{R}_{MLE}(T;k)$ being closer to the true value of R are quite high. For high reliability, the odds still favor $\hat{R}_{MLE}(T;k)$ but are only slightly better than even. This result is somewhat consistent with a mean squared efficiency comparison given by Zacks and Even (1966, Figure 3). They show graphically that $\hat{R}_{MLE}(T;k)$ is more mean squared efficient than $\hat{R}_{MVUE}(T;k)$ over the interval $.03 < R < .61$ ($n = k = 4, 8$). Maximum mean squared efficiency is reached at approximately $R = .22$. And although $\hat{R}_{MVUE}(T;k)$ is more mean squared efficient than $\hat{R}_{MLE}(T;k)$ when $R \gg .61$, the mean squared error of $\hat{R}_{MVUE}(T;k)$ is only slightly less than that of $\hat{R}_{MLE}(T;k)$.

When $R > e^{-1}$, Fraser's structural inference provides estimators which fall between the maximum likelihood estimator (which tends to underestimate R) and the minimum variance unbiased estimator (which tends to overestimate R). In other words, when $R > e^{-1}$ (i.e., $t \geq k - .5$), either (a) $\hat{R}_{MLE}(t;k) < \hat{R}_{SMD}(t;k) < \hat{R}_{SMN}(t;k) < \hat{R}_{MVUE}(t;k)$ or (b) $\hat{R}_{MLE}(t;k) < \hat{R}_{SMN}(t;k) < \hat{R}_{SMD}(t;k) < \hat{R}_{MVUE}(t;k)$ holds. It is the latter inequality, i.e., (b), that is true if reliability is high. When $R \ll e^{-1}$, the structural estimators give estimates of R which are larger than those given by the maximum likelihood or minimum variance unbiased estimators both of which tend to underestimate R .

In any event, by Theorems 4.1 and 4.2, $\hat{R}_{MLE}(T;k)$ and $\hat{R}_{MVUE}(T;k)$ are both Pitman-closeness inadmissible relative to $\hat{R}_{SMD}(T;k)$. Consequently, from a Pitman-closeness efficiency point of view, the preference among the estimators $\hat{R}_{MLE}(T;k)$, $\hat{R}_{MVUE}(T;k)$, $\hat{R}_{SMD}(T;k)$, and

$\hat{R}_{SMN}(T;k)$ reduces to comparing only the latter two except in the following relatively minor situation. When $k = 2$ and $.17 < R < .22$, $\hat{R}_{SMN}(T;k)$ is more Pitman-closeness efficient than $\hat{R}_{SMD}(T;k)$; in turn, $\hat{R}_{SMD}(T;k)$ is more Pitman-closeness efficient than $\hat{R}_{MLE}(T;k)$; yet, $\hat{R}_{MLE}(T;k)$ is more Pitman-closeness efficient than $\hat{R}_{SMN}(T;k)$. A similar statement can be made when $k = 3$ and $.20 < R < .22$. Fortunately, this circular paradox vanishes when $k \geq 4$. It is because of this apparent absence of a general transitivity property that pairwise comparisons of the estimators were made in Section 4.

For fixed k , a preference set for $\hat{R}_{SMD}(T;k)$ ($\hat{R}_{SMN}(T;k)$) is the subinterval(s) of the R -interval, i.e., $[0,1]$, over which $\hat{R}_{SMD}(T;k)$ ($\hat{R}_{SMN}(T;k)$) is more Pitman-closeness efficient than $\hat{R}_{SMN}(T;k)$ ($\hat{R}_{SMD}(T;k)$). Preference sets as well as the specific odds in favor of being closer to the true value of reliability may be determined from Figure D. Regardless of the number of failures, $\hat{R}_{SMD}(T;k)$ is preferred when reliability is high or low. The odds are slightly better than even, in this case, that $\hat{R}_{SMD}(T;k)$ will be closer to the true value of reliability. On the other hand, regardless of the number of failures, $\hat{R}_{SMN}(T;k)$ is preferred for the middle values of reliability, i.e., the component is about as reliable as it is unreliable. In this case, the odds favoring $\hat{R}_{SMN}(T;k)$ being closer to the true value of reliability are, generally speaking, quite high.

FIGURE A. EFFICIENCY OF MAXIMUM LIKELIHOOD
RELATIVE TO MINIMUM VARIANCE

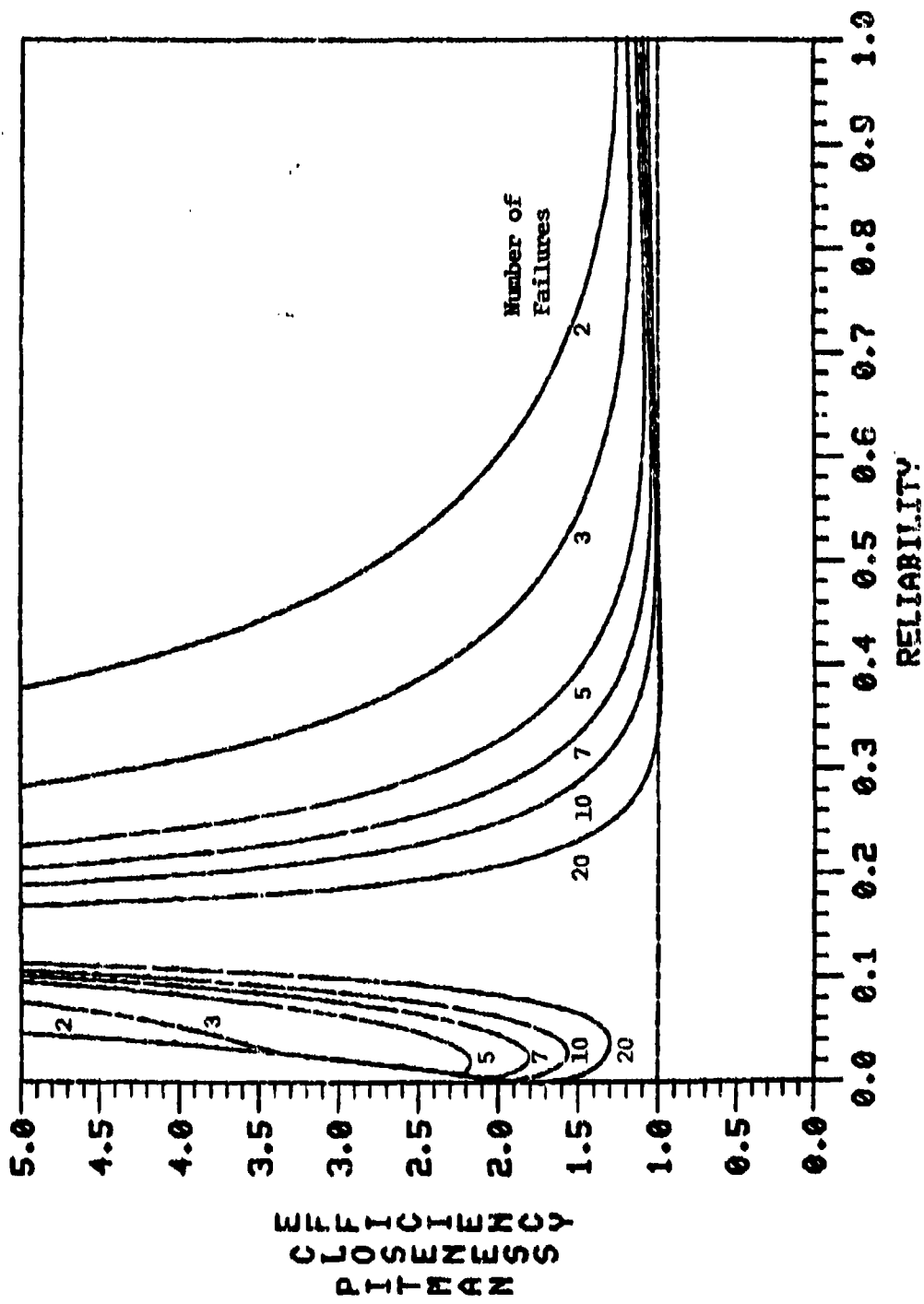
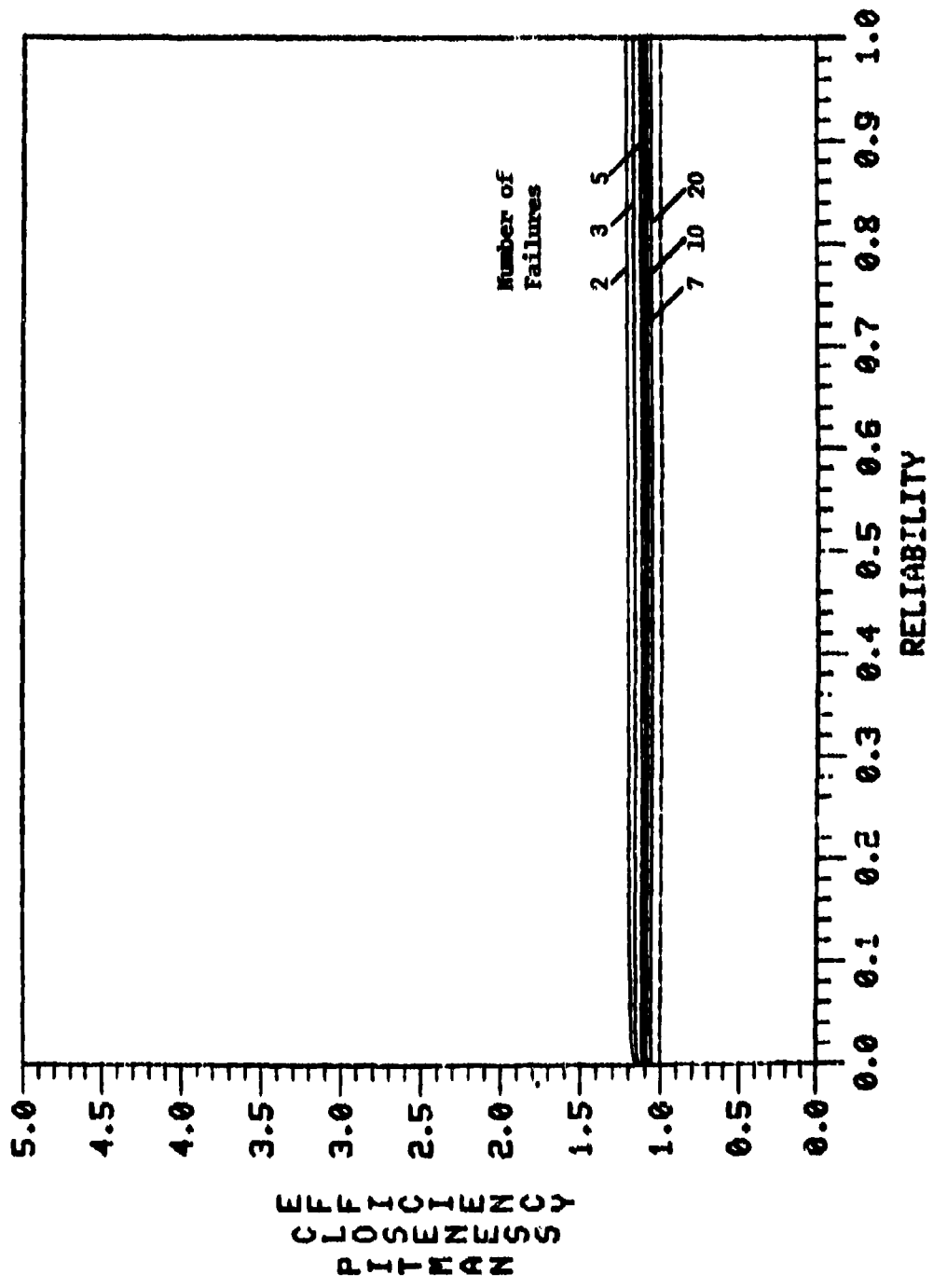
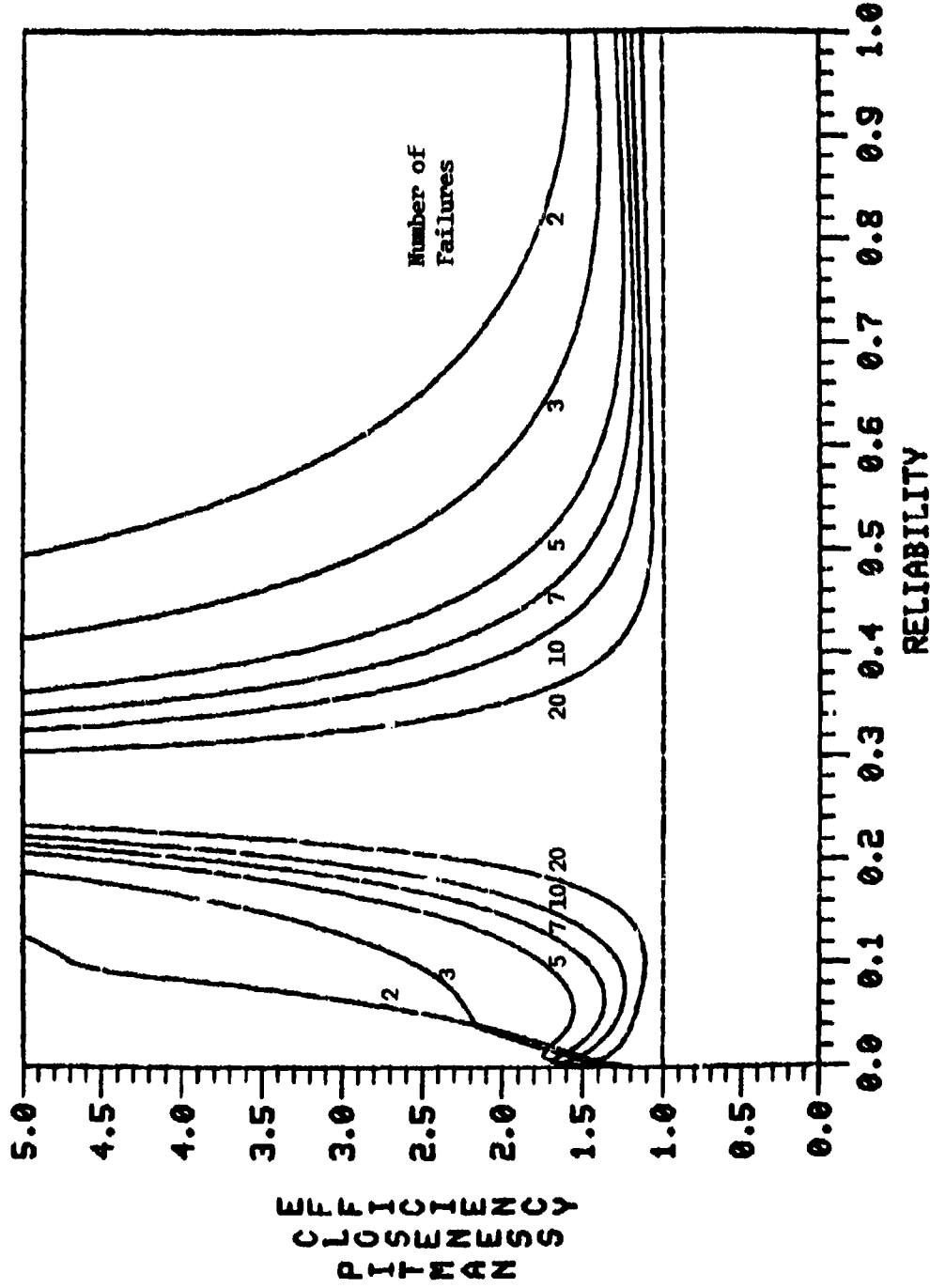


FIGURE B. EFFICIENCY OF STRUCTURAL MEDIAN
RELATIVE TO MAXIMUM LIKELIHOOD



**FIGURE C. EFFICIENCY OF STRUCTURAL MEDIAN
RELATIVE TO MINIMUM VARIANCE**



**FIGURE D. EFFICIENCY OF STRUCTURAL MEDIAN
RELATIVE TO STRUCTURAL MEAN**

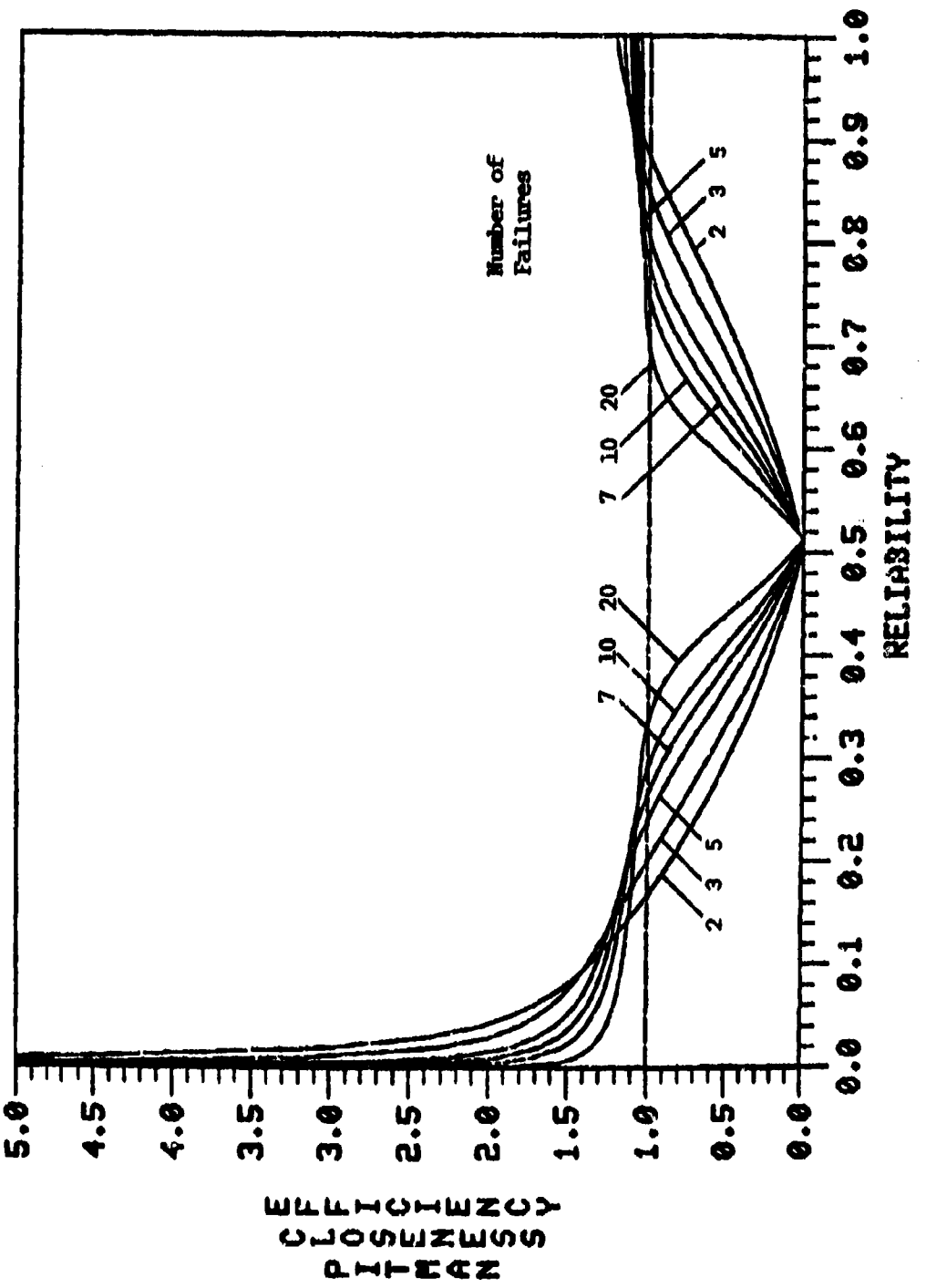


FIGURE E. EFFICIENCY OF STRUCTURAL MEAN
RELATIVE TO MAXIMUM LIKELIHOOD

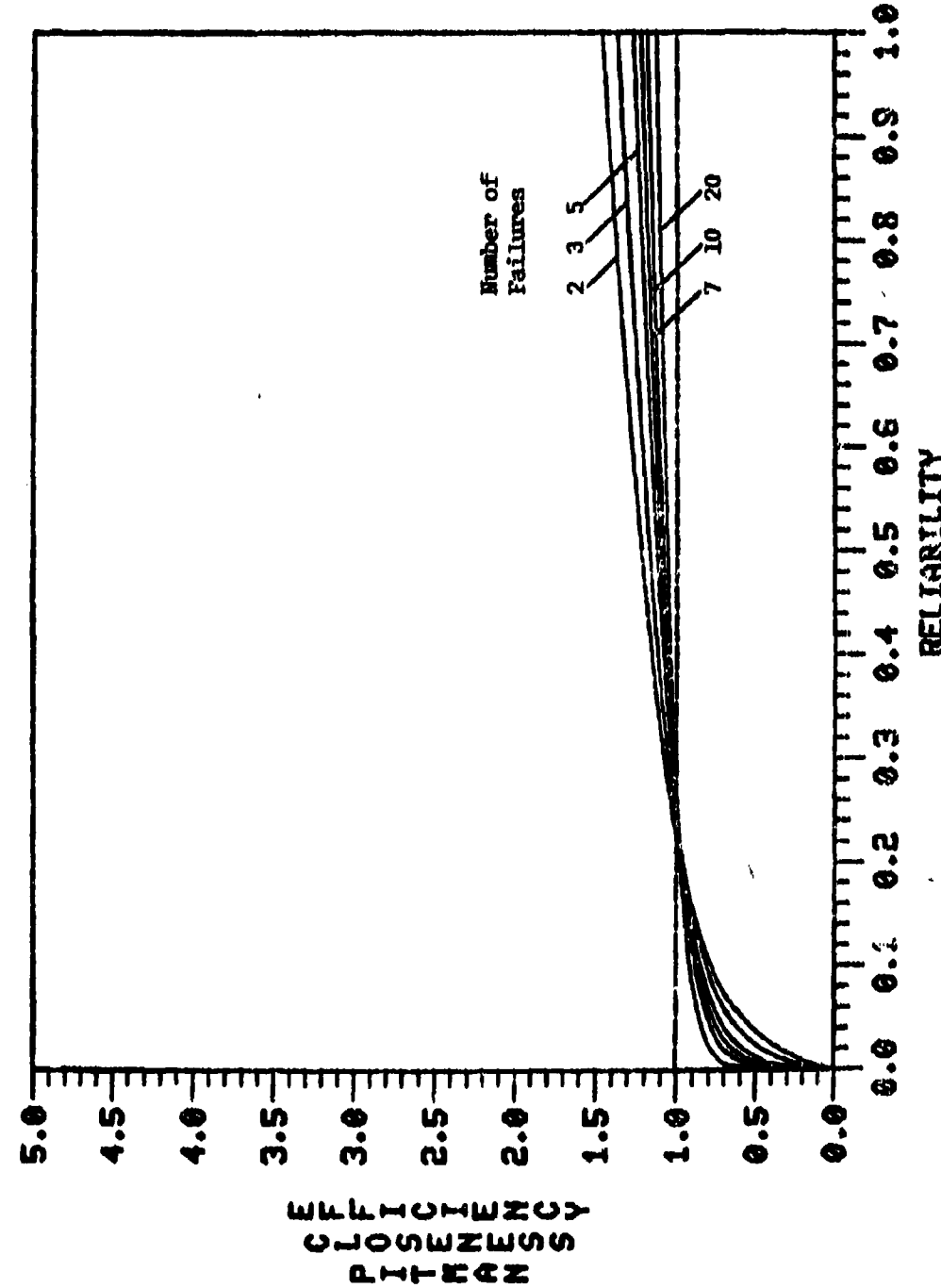
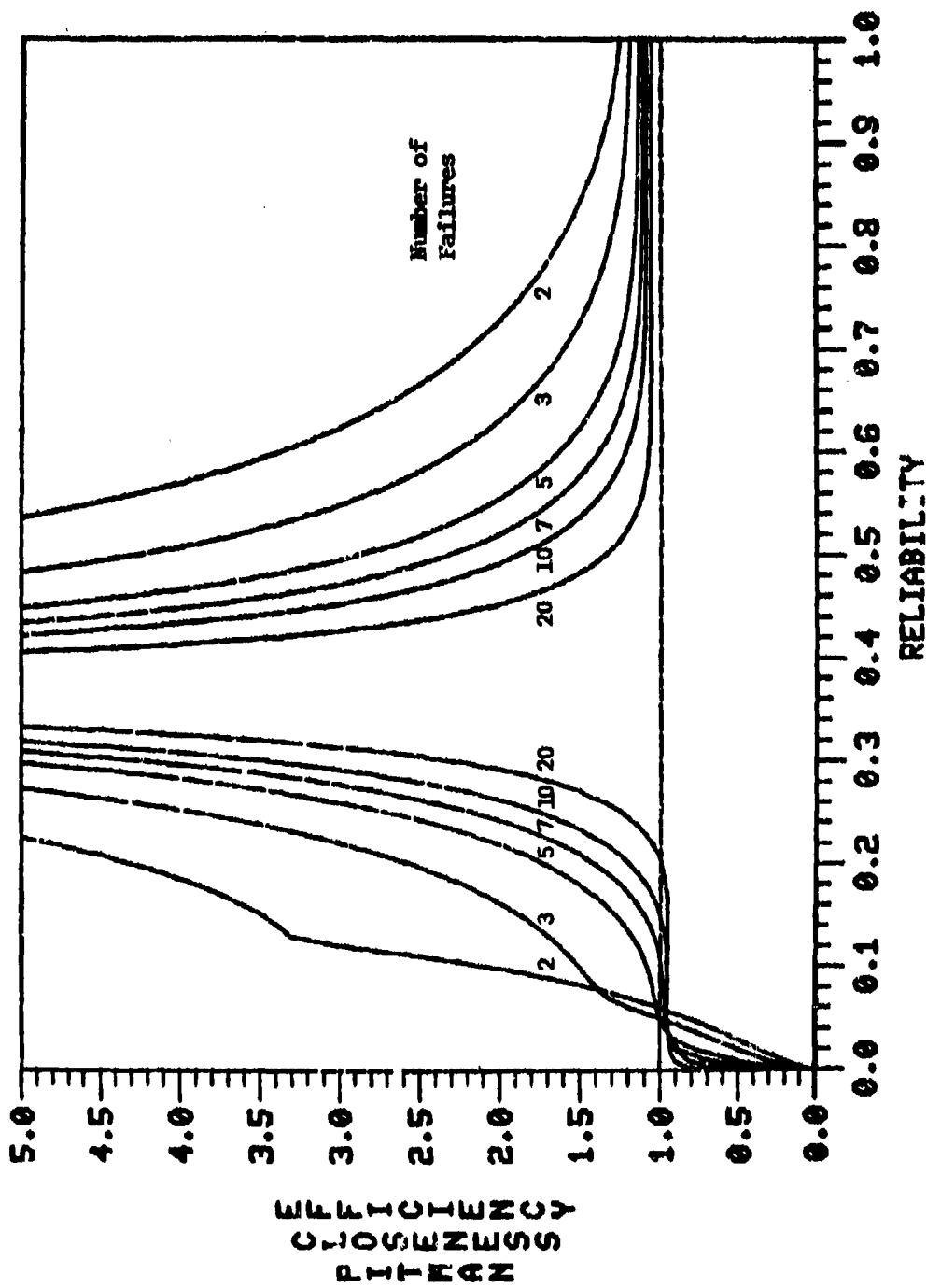


FIGURE F. EFFICIENCY OF STRUCTURAL MEAN
RELATIVE TO MINIMUM VARIANCE



REFERENCES

- Basu, A. P. (1964), "Estimates of Reliability for Some Distributions Useful in Life Testing", Technometrics, 6, 215-219.
- Box, George E. P., and Tiao, George C. (1973), Bayesian Inference in Statistical Analysis, Reading, Mass.: Addison-Wesley Publishing Co.
- Dyer, Danny D., Keating, Jerome P., and Hensley, Onas L. (1977), "Comparison of Point Estimators of Normal Percentiles", Communications in Statistics, B6(3), 269-283.
- Epstein, Benjamin, and Sobel, Milton (1954), "Some Theorems Relevant to Life Testing from an Exponential Distribution", Annals of Mathematical Statistics, 25, 373-381.
- Fraser, D. A. S., (1968), The Structure of Inference, New York: John Wiley and Sons.
- Groeneveld, Richard A., and Meeden, Glen (1977), "The Mode, Median, and Mean Inequality", American Statistician, 31, 120-121.
- Harter, H. Leon (1964), New Tables of the Incomplete Gamma-Function Ratio and of Percentage Points of the Chi-Square and Beta Distributions, Washington, D.C.: U.S. Government Printing Office.
- Lehmann, E. L. (1959), Testing Statistical Hypotheses, New York: John Wiley and Sons.
- Maxwell, E. A. (1973), "Applications of the Structural Model to Censored Data", Journal of the American Statistical Association, 68, 440-444.
- Pitman, E. J. G. (1938), "The Estimation of the Location and Scale Parameters of a Continuous Population of any Given Form", Biometrika, 30, 391-421.
- Ralston, Anthony (1965), A First Course in Numerical Analysis, New York: McGraw-Hill Book Co.
- Sinha, S. K. (1972), "Reliability Estimation in Life Testing in the Presence of an Outlier Observation", Operations Research, 20, 888-894.
- Zacks, S., and Even, M. (1966), "The Efficiencies in Small Samples of the Maximum Likelihood and Best Unbiased Estimators of Reliability Functions", Journal of the American Statistical Association, 61, 1033-1051.
- Zacks, S., and Milton, Roy C. (1971), "Mean Square Errors of the Best Unbiased and Maximum Likelihood Estimators of Tail Probabilities in Normal Distributions", Journal of the American Statistical Association, 66, 590-593.

THE TWENTY-FOURTH CONFERENCE ON THE DESIGN OF EXPERIMENTS IN
ARMY RESEARCH, DEVELOPMENT AND TESTING

4-6 October 1978

Host: The Mathematics Research Center

Roster of Registrants

William Agee
Analysis & Computation Division
White Sands Missile Range
New Mexico 81002

Harold Ascher
Naval Research Laboratory
Code 1434
Washington, D. C. 20375

John C. Atkinson
Bureau of Foods, FDA HFF-110
200 "C" St. S.W.
Washington, D. C. 20204

Steven P. Bailey
Statistics Department
University of Wisconsin-Madison

Robert Batesole
BDM Services Company
P.O. Box 100, Bldg. 2871
Fort Ord, CA 93941

Dr. H. Boussus von Luetzow
U. S. Army Engineer Topographic Labs.
Ft. Belvoir, Virginia 22060

G. K. Bhattacharyya
Department of Statistics
University of Wisconsin-Madison

John W. Bond
U. S. Army Mobility Equipment
Research & Development Command
Ft. Belvoir, Virginia 22060

G. E. P. Box
Mathematics Research Center
University of Wisconsin-Madison

Ralph A. Bradley
Department of Statistics
Florida State University
Tallahassee, Florida 32306

William Broemm
Aberdeen Proving Ground
U. S. Army Materiel Systems
Analysis Activity
Aberdeen, Maryland 21005

Dr. Mark Brown
Memorial Sloan-Kettering Cancer
Center and City College
CUNY
1275 York Avenue
New York, NY 10021

Annette Bruno
Department of Revenue
State of Wisconsin

John Robert Burge
Walter Reed Army Institute of
Research
Washington, D.C. 20012

Evan E. Chen
Department of Statistics
University of Wisconsin-Madison

Gina G. Chen
Department of Statistics
University of Wisconsin-Madison

Herbert Cohen
Army Materiel Systems Analysis
Activity
Aberdeen Proving Ground,
Maryland 21005

Eugene E. Coppola
Benet Weapons Laboratory
Watervliet Arsenal
Watervliet, NY 12189

Bernard Davis
Department of Statistics
University of California
Berkeley, CA 94720

Douglas DePriest
Office of Naval Research
Statistics & Probability Program
Arlington, Virginia 22217

Lorraine DeRobertis
Department of Statistics
University of Wisconsin-Madison

Norman R. Draper
Department of Statistics
University of Wisconsin-Madison

Lt. Holly S. Erwin
Hq. U. S. Army Combat
Development Experimentation Command
Ft. Ord, CA 93941

Oskar Essenwanger
MIRADCOM
ATTN: DRDMI-TRA
Bldg. 7770
Redstone Arsenal, Alabama 35809

Michael Farrell
U. S. Army Waterways Experiment
Station
Vicksburg, Mississippi 39180

Osvaldo N. Ferreiro
Department of Statistics
University of Wisconsin-Madison

Dr. John M. Ferriter
Chemical Systems Laboratory
Aberdeen Proving Ground,
Maryland 21005

Walter D. Foster
AFIP
Rm. M-127
Washington, D. C. 20306

Arthur Fries
Department of Statistics
University of Wisconsin-Madison

C. Maxson Greenland
Chemical Systems Laboratory
Aberdeen Proving Ground,
Maryland 21005

T. N. E. Greville
Mathematics Research Center
University of Wisconsin-Madison

Paul Griffith
BDM Services Company
P.O. Box 100, Bldg. 2871
Fort Ord, CA 93941

Dr. Frank E. Grubbs (Retired)
U. S. Army Ballistic Research Lab.
Aberdeen Proving Ground,
Maryland 21005

Bernard Harris
Mathematics Research Center
University of Wisconsin - Madison

Lawrence Hatch
National Security Agency
Columbia, Maryland 21044

Raymond F. Hojnacki
U. S. Army Aviation Engineering
Flight Activity
Edwards Air Force Base, CA 93523

Craig Hopkins
U. S. Army Material Systems
Analysis Activity
Aberdeen Proving Ground,
Maryland 21005

Gregory B. Hudak
Department of Statistics
University of Wisconsin-Madison

George R. Humfeld
David W. Taylor Naval Ship
R&D Center
Code 187
Bethesda, Maryland 20084

Dr. Edmund Inselmann
Commander, U. S. Army
Combined Arms Center
ATTN: ATCA-CAA-2
Fort Leavenworth, Kansas 66027

Peter J. Jacobs
Department of Statistics
University of Wisconsin - Madison

Paul Jankowski
Picatinny Arsenal
Bldg. 353
Dover, N.J. 07801

Rodney L. Johnson
U. S. Army Mobility Equipment
R&D Command
Ft. Belvoir, Virginia 22060

Brian L. Joiner
Department of Statistics
University of Wisconsin - Madison

S. K. Katti
Department of Statistics
University of Wisconsin - Madison

Thomas J. Kitchell
U. S. Army Concepts Analysis Agency
8120 Woodmont Avenue
Bethesda, Maryland 20014

Lawrence Klimko
Department of Statistics
University of Wisconsin - Madison

William Kruskal
Department of Statistics
University of Chicago
1118 E. 58th St.
Chicago, IL 60637

P. S. Ladouceur
Directorate of Mathematics &
Statistics
Operational Res. & Analysis
Establishment
Department of National Defence
Ottawa, Ontario, Canada K1A 0K2

Robert L. Launer
Army Research Office
P.O. Box 12211
Research Triangle Park,
North Carolina 27709

Sue Leurgans
Department of Statistics
University of Wisconsin - Madison

Kevin Little
Department of Statistics
University of Wisconsin - Madison

Richard Martin
Statistical Laboratory
University of Wisconsin - Madison

Arthur D. Mason, Jr., M.D.
Chief, Laboratory Division
U. S. Army Institute of Surgical Research
Brooke Army Medical Center, Bldg. 2653
Fort Sam Houston, Texas 78234

Dr. Walter S. McAfee
U. S. Army Electronics
R&D Command
Office of the Scientific Advisor
ATTN: DRDEL-SA
Fort Monmouth, N.J. 07703

Robert Miller
Department of Statistics
University of Wisconsin - Madison

L. David Minsk
U. S. Army Cold Regions
Research & Engineering Laboratory
Hanover, New Hampshire 03755

Frank Montfort
Department of Sociology
University of Wisconsin - Madison

Dr. Richard Moore
U.S. Army Ballistics Research Lab
Aberdeen Proving Ground,
Maryland 21005

Vedula N. Murty
Penn State University
Capitol Campus
Room E-258
Middleton, PA. 17057

Donald Neal
Army Materials & Mechanics
Research Center
Arsenal Street
Watertown, Massachusetts 02172

Paul Newbold
Mathematics Research Center
University of Wisconsin - Madison

Ben Noble
Mathematics Research Center
University of Wisconsin - Madison

Dr. John Overdeck
National Security Agency
Columbia, Maryland 21044

Cpt. Oliver J. Ozment, Jr.
HQ. U. S. Army Combat Developments
Experimentation Command
Ft. Ord, CA 93941

Carl Pace
Waterways Experiment Station
P.O. Box 631
Vicksburg, Mississippi 39180

Charles Palit
Wis. Surv. Res. Lab
University of Wisconsin - Madison

Harold C. Pasini, Jr.
U. S. Army Materiel Systems
Analysis Activity
ATTN: DRXSY-RW
Aberdeen Proving Ground,
Maryland 21005

Aubrey W. Presson
USAMIRADCOM Eng. Lab., T&ED
ATTN: DRDMI-ETP
Redstone Arsenal, Alabama 35809

Carol D. Rose
TARADCOM
ATTN: DRDTA-ZSS
Warren, Michigan 48090

Edward W. Ross
Natick R&D Command
Kansas Street
Natick, MA 01760

Rodney Russell
U.S. Army Materiel Systems
Analysis Activity
Aberdeen Proving Ground
Maryland 21005

Seymour M. Selig
Office of Naval Research
Operations Res. Program
800 N. Quincy Street
Arlington, Virginia 22217

Ralph E. Shear
U. S. Army Ballistics Research Lab.
Aberdeen Proving Ground,
Maryland 21005

Richard S. Simak
Chemical Systems Lab.
ATTN: DRDAR-CLN-D
Aberdeen Proving Ground,
Maryland 21010

Jill (House) Smith
U. S. Army Ballistic Research Lab.
Aberdeen Proving Ground,
Maryland 21005

Dr. Andrew P. Soms
Mathematics Research Center
University of Wisconsin - Madison

Douglas B. Tang
Walter Reed Army Institute of Research
Washington, D. C. 20012

Dr. Malcolm Taylor
U. S. Army Ballistic Research Lab.
Aberdeen Proving Ground,
Maryland 21005

Joseph M. Tessmer
U. S. Army Concepts Analysis Agency
8120 Woodmont Avenue
Bethesda, M.D. 20014

Jerry Thomas
U. S. Army Concepts Analysis Agency
8120 Woodmont Avenue
Bethesda, Maryland 20014

Walter Thomson
Commander, U. S. Army Combined Arms
Center
ATTN: ATCA-CAT-D
Fort Leavenworth, Kansas 66027

Dr. Bruce Trumbo
National Science Foundation
Washington, D. C. 20550

Steve Verrill
Department of Statistics
University of Wisconsin - Madison

Joseph G. Vaelkel
Department of Statistics
University of Wisconsin - Madison

Grace Wahba
Department of Statistics
University of Wisconsin - Madison

Robert L. Wardrop
Mathematics Research Center &
Department of Statistics
University of Wisconsin - Madison

Edward J. Wegman
Office of Naval Research
Code 436
800 N. Quincy Street
Arlington, Virginia 22217

Robert M. Wharton
301 North Bellevue Avenue
Langhorne, PA. 19047

Dean W. Wichern
Mathematics Research Center
University of Wisconsin - Madison

Lang Withers
U. S. Army Operational Test &
Evaluation Agency
5600 Columbia Pike
Falls Church, Virginia 22041

Frank Womack
NSWC - Code C34
Dahlgran, Virginia 22448

Ralph Woratscheck
U. S. Army Aviation Engineering
Flight Activity
Edwards Air Force Base, CA 93523

C. J. (Jeff) Wu
Department of Statistics
University of Wisconsin - Madison

Unclassified

(14) ARO-79-2

SECURITY CLASSIFICATION OF THIS PAGE (When Data Entered)

REPORT DOCUMENTATION PAGE		READ INSTRUCTIONS BEFORE COMPLETING FORM
1. REPORT NUMBER ARO Report 79-2	2. GOVT ACCESSION NO.	3. RECIPIENT'S CATALOG NUMBER
4. TITLE (Include Subtitle) PROCEEDINGS OF THE TWENTY-FOURTH CONFERENCE ON THE DESIGN OF EXPERIMENTS IN ARMY RESEARCH, DEVELOPMENT, AND TESTING (24th)		5. TYPE OF REPORT & PERIOD COVERED Interim Technical Report
6. AUTHOR(s) Held at Mathematics Research Center, University of Wisconsin, Madison, Wisconsin on 4-6 October 1978.	7. CONTRACT OR GRANT NUMBER(S) 11 JUN 79	
8. PERFORMING ORGANIZATION NAME AND ADDRESS	9. PROGRAM ELEMENT, PROJECT, TASK AREA & WORK UNIT NUMBERS 12 407 p	
10. CONTROLLING OFFICE NAME AND ADDRESS Army Mathematics Steering Committee on Behalf of the Chief of Research, Development and Acquisition	11. REPORT DATE JULY 1979	
12. MONITORING AGENCY NAME & ADDRESS (if different from Controlling Office) U. S. Army Research Office P. O. Box 12211 Research Triangle Park, NC 27709	13. NUMBER OF PAGES 415	
14. SECURITY CLASS. (of this report) Unclassified		
15. DECLASSIFICATION/DOWNGRADING SCHEDULE		
16. DISTRIBUTION STATEMENT (of this Report) Approved for public release; distribution unlimited. The findings in this report are not to be construed as official Department of the Army position, unless so designated by other authorized documents.		
17. DISTRIBUTION STATEMENT (of the abstract entered in Block 20, if different from Report) This report contains most of the papers presented at the 24th		
18. SUPPLEMENTARY NOTES This is a technical report resulting from the Twenty-Fourth Conference on the Design of Experiments in Army Research, Development and Testing. It contains most of the papers presented at that meeting. These treat various Army statistical and design problems. Topics included:		
19. KEY WORDS (Continue on reverse side if necessary and identify by block number) weather experiments, sequential designs, environmental quality problems, red noise, small sample behavior, rapid geodetic survey system, analysis of variance, partial factorial experiments, experiments in sorptivity, pseudo-random number generators, point and interval estimation, regression on Bernoulli random variables, smoothing curves and surfaces, acceptance criteria, quantal response curves, Monte Carlo simulation of a probability ratio sequential test, statistical consulting, laser beam war games, structural reliability, mechanical behavior of materials, Stewartson's liquid instability/stability criteria, graphical technique for analyzing failure and survival data, and efficiency of estimators of reliability		